

JMC 2018

Journées de
la matière
condensée



du 27 au 31 août
2018 à GRENOBLE

site web : jmc2018.sciencesconf.org



Graphisme : CNRS Alpes - service communication - LRF
© Julien BOBROFF - CNRS Physique / Adrien Orthlieb / aron / Nicolas / Marina Scarpis / Sergey Labath / Vasily Smirnov / Mikaz

Livre de Résumés

— Par ordre alphabétique des auteurs présentateurs —

Book of Abstracts

— In alphabetical order of the presenting authors —

Les partenaires



Stripe domains in thin magnetic films for spin waves channeling

K. AIT-OUKACI^{a,b}, D. LACOUR^a, S. PETIT-WATELOT^a, R. BELKHOUB^b,
M. HEHN^a

- a. Institut Jean Lamour, Campus Artem, 2 allée André Guinier, BP50840 - F-54011 Nancy
- b. Synchrotron SOLEIL, L'Orme des Merisiers, Saint-Aubin, BP 48, 91192 Gif-sur-Yvette Cedex, France
- * Mail : kosseila.ait-oukaci@univ-lorraine.fr

The possibility to channel spin waves in domain walls has been first shown by numerical calculations in materials with perpendicular to film plane magnetization in 2009 [1]. This concept is particularly interesting since domain walls can reach lateral sizes of several nanometers (so with ultra-high integration capabilities) and are reprogrammable (the channel can be erased and rewritten through an appropriate magnetic field history). The aim this work is the development of new spin-waves guides and devices based on the use of magnetic domain walls to channel spin waves. To achieve a first experimental demonstration in perpendicular to film plane magnetized films materials with low magnetic damping and control magnetic textures have to be synthesized.

I will present in detail the domain structures in two magnetic systems, high (111) textured [Co/Ni] Multilayers of thicknesses varying from 10 nm to 200 nm and amorphous CoFeB with thicknesses varying from 200 nm to 300 nm. The domain sizes and domain shapes have been studied as a function of thickness, magnetic history and annealing temperature. In [Co/Ni], a quality factor around 0.7 and a damping parameter of 1.5×10^{-2} could be measured. We observed by magnetic force microscopy (MFM) that the stabilization of straight stripe patterns is more difficult to obtain in comparison to epitaxial Co layers [2]. In the sample with the optimum thickness of 50nm, straight stripe patterns could be stabilized. Amorphous CoFeB shows weak stripes domains and a damping parameter of 7×10^{-3} could be measured. From the domain pattern and damping point of view, this material appears to be the most promising for spin wave channeling.

[1] F. Garcia-Sanchez et al., Phys. Rev. Lett. 114, 247206 (2015)S. Author, Journal 100, 101101 (2009)

[2] M. Hehn, S. Padovani, K. Ounadjela, and J. P. Bucher, Phys. Rev. B 54,3428 (1996).

Unravelling Dzyaloshinskii-moriya interaction and chiral nature of graphene/cobalt interface

F. AJEJAS^{1,2,*}, A. GUDÍN², R. GUERRERO², M. A. NIÑO², S. PIZZINI⁴, J. VOGEL⁴, M. VALVIDARES⁵, P. GARGIANI⁵, M. VARELA⁶, JULIO CAMARERO^{2,3}, RODOLFO MIRANDA^{2,3}, AND PAOLO PERNA²

¹ *Unité Mixte de Physique, CNRS, Thales, Univ. Paris-Sud, Université Paris-Saclay, Palaiseau, France.*

² *IMDEA Nanociencia, 28049 Madrid, Spain*

³ *DFMC, Instituto “Nicolás Cabrera” & IFIMAC, Universidad Autónoma de Madrid, 28049 Madrid, Spain.*

⁴ *CNRS, Institut Néel Université Grenoble Alpes, , 38000 Grenoble, France.*

⁵ *ALBA SYNCHROTRON LIGHT SOURCE, Cerdanyola del Vallès, 08290 Barcelona, Spain.*

⁶ *DFM, IMA & Instituto Pluridisciplinar, Universidad Complutense de Madrid, 28040, Madrid, Spain.*

* Corresponding autor email: fernando.ajejas@cnrs-thales.fr

The development of room temperature graphene-based spintronic devices requires that, in addition to its passive capability to transmit spins over long distances and spin lifetime [1], other active properties are incorporated to graphene. Long range magnetic order and spin filtering in graphene can be achieved by molecular functionalization [2,3] as well as by the introduction of giant spin-orbit coupling (SOC) in the electronic bands of graphene by intercalation of adequate metals [4].

Here, we report on high quality, gr/Co(111)/Pt(111) stacks grown epitaxially on MgO(111) crystals, characterized by XPS-UPS, LEED, STEM, Kerr Magnetometry, XMCD and Kerr Microscopy, that exhibit enhanced perpendicular magnetic anisotropy (PMA) for Co layers up to 4 nm thick and left-handed Néel-type chiral DWs stabilized by interfacial Dzyaloshinskii–Moriya interaction (DMI) localized at both graphene/Co and Co/Pt interfaces with opposite sign [6]. While the DMI at Co/Pt side is due to the intrinsic SOC, the sizeable DMI experimentally found at the gr/Co interface has Rashba origin [5]. The active magnetic texture is protected by the graphene monolayer and stable at 300 K in air, and, since it is grown on an insulating substrate, amenable to transport measurements [5].

The discovery of a strong DMI at the Graphene/Cobalt interface is a crucial step to promote 2D materials spinorbitronics based on the electrical control of the transport and manipulation of topologically protected magnetic structures, such as chiral domain walls and skyrmions [6].

[1] W. Han, R.K. Kawakami, M. Gmitra and J. Fabian, *Graphene Spintronics*, Nat. Nanotech. 9, 794 (2014).

[2] M. Garnica *et al.*, *Long range magnetic order in a purely organic 2D layer adsorbed on epitaxial graphene*, Nature Phys. 9, 368–374 (2013).

[3] D. Maccariello, *et al.*, *Spatially resolved, site-dependent charge transfer and induced magnetic moment in TCNQ adsorbed on graphene*, Chemistry of Materials 26 (9), 2883–2890 (2014).

[4] F. Calleja *et al.*, *Spatial variation of a giant spin-orbit effect induces electron confinement in graphene on Pb islands*, Nature Physics 11, 43–47 (2015).

[5] F. Ajejas, P. Perna, *et al.*, submitted (2018).

[6] A. Fert, V. Cros and J. Sampaio, *Skyrmions on the track*, Nat. Nanotech. 8, 152–156 (2013).

Simulation of tip-sample heat transfer due to air conduction

A. Alkurdi^{a,*}, A.M. Massoud^{a,b}, E. Guen^a, C. Lucchesi^a, R. Vaillon^a, S. Gomes^a,
J.-M. Bluet^b and P.-O. Chapuis^a

- a. Univ Lyon, CNRS, INSA-Lyon, Université Claude Bernard Lyon 1, CETHIL UMR5008, F-69621, Villeurbanne, France.,
b. Univ Lyon, Institut des Nanotechnologies de Lyon (INL), CNRS, INSA de Lyon, F-69621 Villeurbanne, France

* ali.alkurdi@insa-lyon.fr

Scanning thermal microscopy (SThM), where a micro to nanometer-scale probe tip measures the temperature close to a surface, is a key thermal characterization tool. The spatial and temperature resolutions of this technique are limited by the size of the tip, the sample properties, and the various tip-sample heat transfer mechanisms [1] depending on the operation conditions. In the most common cases, heat transfer due to air conduction dominates all other mechanisms.

In this communication, we present a study of heat transfer through air between a sample surface and a heated probe brought close to contact. We consider two types of probes: a platinum/rhodium alloy (Pt/Rh) filament of the Wollaston tip and a silica sphere attached to a doped silicon tip. The sphere has a diameter of $\sim 40 \mu\text{m}$. We study the lateral spreading of the heat exchange, the amplitude of the power as a function of the distance and the impact of roughness. For large distances of the order of $100 \mu\text{m}$, there is no interaction between the probe and the sample, and the probe temperature remains constant. At intermediate distances, the temperature decreases when decreasing the distance. This is the typical behavior of heat diffusion through air, which is simulated by means of the Finite Element Method (FEM). For nanometric distances, when the distance is comparable with the mean free path of air molecules ($\sim 65 \text{ nm}$), the latter regime of heat transfer overestimates the tip-sample exchanged thermal flux. We take the deviation of the diffusive regime into account by adding a thermal resistance corresponding to the ballistic regime in air, which allows us to reproduce numerically the ballistic leveling off seen experimentally.

We conclude that this simple model describes well the tip-sample heat transfer through air and is an alternative to the complexity of the Boltzmann transport equation for configurations with large aspect ratios.

Further probe types are being studied to obtain an optimized probe with improved sensitivity.

[1] S. Gomès et al., Scanning thermal microscopy: A review, *Phys. Status Solidi A* **212**, No. 3, 477–494 (2015)

Acknowledgements: We thank the support of projects ANR TIPTOP, ANR Demo-NFR-TPV, Nano 2017, and EU FP7 IP QuantiHeat.

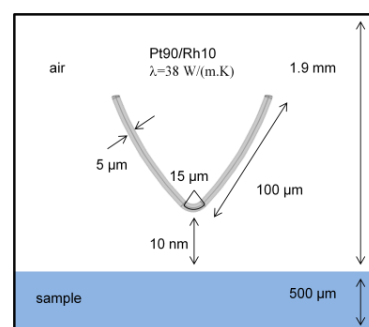


Figure 1: Hot probe close to the contact with sample surface.

Split gate devices in silicon CMOS : Tunable coupling and Gate-coupled radiofrequency reflectometry

A. Amisse^a, H. Bohuslavsky,^{a,b} R. Ezzouch^a, A. Crippa^a, R. Maurand^a, M. Urdampilleta^b, T. Meunier^b, C. Bauerle^b, B. Bertrand^c, L. Hutin^c, M. Vinet^c, S. de Franceschi^a, M. Sanquer^a, X. Jehl^a

a. Univ. Grenoble Alpes, CEA, INAC-PHELIQS, 38000 Grenoble

b. Institut Néel, F-38042 Grenoble, France

c. CEA, LETI, Minatec Campus, F-38054 Grenoble, France

* anthony.amisse@cea.fr

Since the proposal of D.Loss and D. P. DiVincenzo in 1997 [1], semiconductor-based quantum dots have been widely studied as promising platform for Quantum computing. In Grenoble, the Quantum Silicon Group [2] is pursuing the development of silicon-based spin qubits relying on industrial-scale CMOS technology. To this aim, we leverage the expertise in microelectronics at Leti and the expertise in cryogenic transport and high-frequency measurements at the INAC and Néel institutes. Recently, we reported the first silicon spin qubit issued from a 300-mm CMOS fab line [3].

In this work, we address the problem of controlling the coupling between two neighboring quantum dots. Simultaneously, we employ and improve a specific technique for the charge (and spin) state read-out, which is known as gate-coupled radiofrequency reflectometry [4]. Our experiments are performed on double-gate nanowire transistors with a split-gate geometry [5].

The poster is organized in two parts : the first one is dedicated to the tunable coupling between two quantum dots in a silicon nanowire thanks to a backgate voltage while the second part presents new results on gate radiofrequency reflectometry for the readout of the quantum dot charge and spin states.

[1] Loss, D. et al. Quantum computation with quantum dots.
PRA 57, 120, doi: 10.1103/PhysRevA.57.120 (1998)

[2] <https://www.quantumsilicon-grenoble.eu/>

[3] Maurand, R. et al. A CMOS silicon spin qubit.
Nat. Commun. 7, 13575 doi: 10.1038/ncomms13575 (2016)

[4] Gonzalez-Zalba, M.F. et al. Probing the limits of gate-based charge sensing.
Nat. Commun. 6, 6084 doi: 10.1038/ncomms7084 (2015)

[5] Roche, B. et al. A two-atom electron pump.
Nat. Commun. 4, 2544 doi : 10.1038/ncomms2544 (2013)

Désordre de solitons dans un système Onde de Densité de Charge

Gilles Abramovici^{a*}, David Le Bolloc'h^a

a. LPS, Université Paris Sud, CNRS UMR 8502, 91405 Orsay France

* abramovici@lps.u-psud.fr

La diffraction cohérente de rayons X dans des systèmes à Onde Densité de Charges (ODC) génère des pics de réflexion satellites autour de chaque pic de Bragg, ces satellites (situés à $q=\pm 2k_F$) proviennent de la période de l'ODC. Lorsque ces échantillons sont soumis à un champ électrique, deux « super-satellites » apparaissent autour de chaque satellite $\pm 2k_F$; ils sont interprétés comme provenant de l'apparition d'un réseau périodique de solitons, qui se superpose au réseau de l'ODC. Lorsque qu'on augmente le courant, les super-satellites s'éloignent de $q = \pm 2k_F$ et s'affinent en largeur. Cette observation s'explique par le fait que le réseau de soliton a une période plus grande pour de faibles courants et devient plus dense et mieux ordonné pour des courants plus forts.

Nous proposons un modèle statistique où les solitons ont une probabilité d'exister en chaque point de l'espace ; ce modèle reproduit l'expérience et semble confirmer l'interprétation des résultats en terme de solitons. Plus précisément, dans ce modèle statistique, à partir une distribution de probabilité uniforme, qui donne une loi binomiale dans un ensemble microcanonique, on ajoute un poids $\exp(-S)$, où S diminue avec l'ordre et est, par ailleurs, proportionnelle à la force électrique qE et on calcule dans le nouvel ensemble adéquat la diffraction d'un faisceau réfracté par le réseau de solitons.

Effect of chemical pressure on the metal-insulator transition and Dirac points in the quasi-2D BaCoS₂ system

H. Abushammala^{a*}, P. Toulemonde^b, Y. Klein^a, and A. Gauzzi^a

a. IMPMC - Sorbonne Université, CNRS, MNHN, IRD – 4 place Jussieu, 75005 PARIS

b. Institut Néel – 25 Avenue des Martyrs, 38042 Grenoble

* Email : haneen.abushammala@upmc.fr

The 2D BaCo_{1-x}Ni_xS₂ (BCNS) system has attracted a great deal of interest due to a metal-insulator transition (MIT) controlled by doping [1], similar to that found in cuprates and Fe-based superconductors. In BCNS, doping is achieved by partially substituting Co for Ni in a peculiar network of puckered edge-sharing (Co/Ni)S₅ pyramids forming a square lattice (Fig 1a). In spite of several studies, the mechanism of the MIT remains little understood. Recently, it was found that the semimetallic endmember (x=1) displays a unique electronic structure characterised by Dirac nodes arising from the non symmorphic crystal symmetry. The question arises whether this property is preserved across the MIT. In order to address this issue, we have attempted to stabilise the semimetallic phase by applying chemical pressure to the insulating phase (x = 0). Indeed, chemical pressure is expected to increase the bandwidth without introducing any disorder in the electronically active Co site.

To the best of our knowledge, only aliovalent substitution at the Ba site has been hitherto reported. With such substitutions, one can not separate the effect of the bandwidth control parameter from that of the filling control parameters.

In this context, we have synthesised Ba_{1-x}Sr_xCoS₂ using high pressure. Different substitution levels (x) have been tested in order to determine the solubility limit of Sr. We found that the unit cell volume of BaCoS₂ is progressively reduced with x. Concomitant to this effect, the magnetic order temperature also decreases from the value, T_N = 300 K for x = 0, down to T_N = 240 K for x = 0.07 (Fig. 1.b).

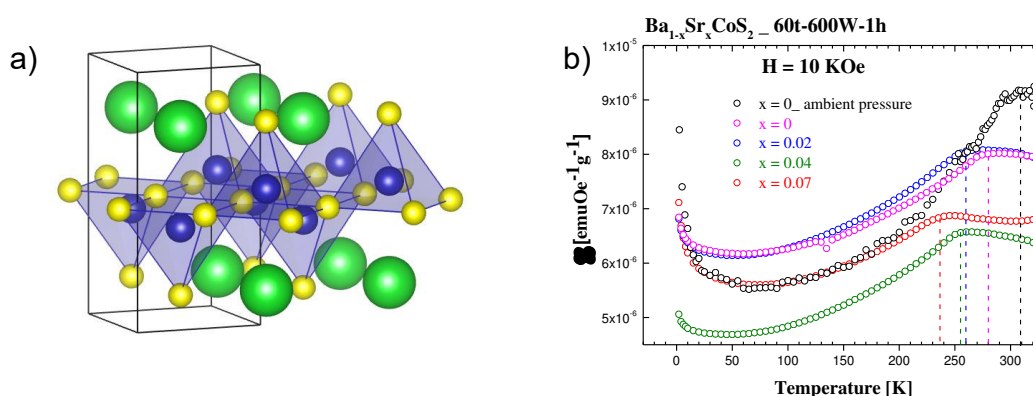


Figure 1: a) Structure of BCNS system, b) Magnetic susceptibility of polycrystalline Ba_{1-x}Sr_xCoS₂ with x = 0, 0.02, 0.04 and 0.07.

[1] Takeda, J. *et al.* (1995). *Journal of the Physical Society of Japan*, 64(7), 2550-2557.

Breakdown of superfluidity and extreme value statistics in a one dimensional Bose gas

Mathias Albert^{a*} et Cord Müller^b

a. Université Côte d'Azur, CNRS, Institut de Physique de Nice

b. Fachbereich Physik, Universitat Konstanz, Konstanz, Germany

* mathias.albert@inphyni.cnrs.fr << Mathias Albert >>

Phase coherence is a key ingredient of many characteristic quantum effects in transport phenomena, some of the most striking ones being superfluidity, conductance quantization, or the quantum Hall effect. In particular, interference effects have a prominent role in presence of disorder, resulting in weak or strong Anderson localization.

In this talk I will discuss statistical properties of a one dimensional Bose-Einstein condensate at rest or moving through a disordered region of finite extent. I will focus on the superfluid fraction and the critical velocity and demonstrate their connections to extreme value statistics of the random environment.

Language: English.

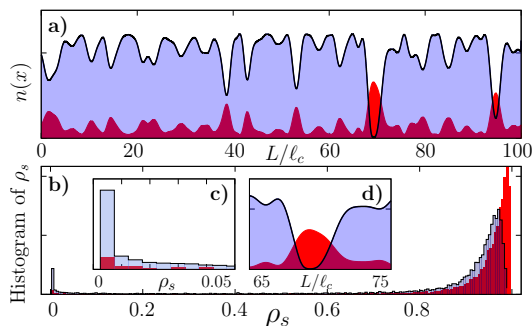


Figure 1: **a)** Spatial density of a disordered one dimensional Bose-Einstein condensate (blue) and the corresponding speckle potential (red). **b)** Histogram of the superfluid fraction for two different system size.

Memristive devices: from bio-inspired computing to artificial neural networks

Fabien Alibart^{a,b*}

a. LN2-CNRS, Boulevard de l'université, Sherbrooke, Canada

b. IEMN-CNRS, Boulevard Poincaré, Villeneuve d'Ascq, France

* fabien.alibart@iemn.univ-lille1.fr

One of the biggest challenge for future information and communication technologies would be to replicate the brain computing capacity to learn, adapt and evolve in a complex environment. The emergence of memristive devices is currently driving an increasing interest in neuromorphic computing to complement and to provide enhanced functionalities to existing CMOS/Von Neumann processors with the aim to realize low-power bio-mimetic hardware systems. Indeed, this technology appears as a realistic solution for the implementation of synaptic functions, one of the most critical component to be realized in such circuits. Two main streams are now driving research efforts: (i) from one hand, the quest for ultra high-density, low power and analog programmability memory devices would offer promising solution for artificial neural networks implementation. (ii) In the other hand, the bio-mimetic approach aims at replicating and implementing in emerging memory technologies synaptic features observed in biology that would revolutionize our way of building computing systems. In this talk, I will present how different memristive technologies can be used with respect to this two approaches and how innovative circuits can be built based on this elementary devices.

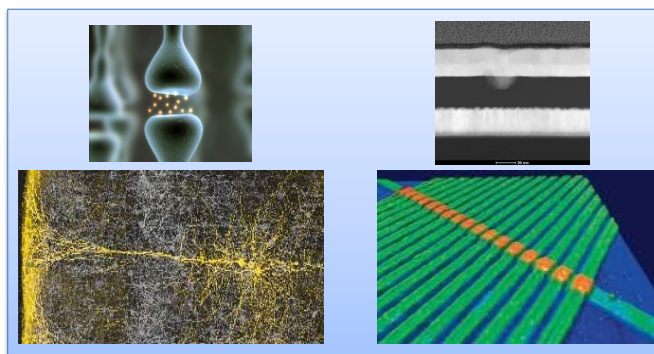


Figure 1 : *Illustration of the artificial neural network concept. From biological synapse to neuron (left), and from memristive devices to high density memory circuits (right).*

Polariton black-hole horizons

H.-S. Nguyen^a, M. Milicevic^a, D. Gerace^b, I. Carusotto^c, E. Galopin^a, A. Lemaître^a,
I. Sagnes^a, J. Bloch^a, A. Amo^{a,d*}

- a. Centre de Nanosciences et de Nanotechnologies, CNRS, Univ. Paris-Sud, Université Paris-Saclay, C2N-Marcoussis, 91460 Marcoussis, France
- b. Dipartimento di Fisica, Università di Pavia, via Bassi 6, I-27100 Pavia, Italy
- c. INO-CNR BEC Center and Dipartimento di Fisica, Università di Trento, I-38123 Povo, Italy
- d. Univ. Lille, CNRS, UMR 8523 -- PhLAM -- Physique des Lasers Atomes et Molécules, F-59000 Lille, France

* alberto.amo@univ-lille1.fr

Photonic systems have appeared in the past few years as excellent candidates to study analogue gravity phenomena [1]. Microcavity polaritons are particularly well suited for this task. They combine long propagation distances with interparticle interactions that can largely exceed their linewidth, putting polaritons in the hydrodynamic regime with metrics in close analogy to that of space-time around the event horizon of a black hole [2].

Here we present the realization of an acoustic black hole using polaritons in a 1D semiconductor microcavity with an engineered obstacle [3]. At high excitation power, we show a transition at the position of the obstacle between regions of subsonic and supersonic flow, giving rise to an acoustic black hole horizon: sonic excitations of the fluid are unable to propagate back from the supersonic region to the horizon, analogous to what happens to light trying to escape from astrophysical black holes.

Our black hole presents interesting assets in views of observing Hawking radiation. The abruptness of the transition, results in a high analogue surface gravity, with an expected effective Hawking temperature on the order of a few Kelvin, much larger than the cavity lifetime, the relevant energy scale in our system [4].

We will discuss other configurations based on type-II Dirac points in engineered honeycomb lattices of polaritons, which present single particle dispersion relations mimicking those of light close to a black hole [5].

[1] T. G. Philbin, C. Kuklewicz, S. Robertson, S. Hill, F. König, and U. Leonhardt, *Fiber-Optical Analog of the Event Horizon*, *Science* **319**, (2008).

[2] D. Gerace and I. Carusotto, *Analog Hawking radiation from an acoustic black hole in a flowing polariton superfluid*, *Phys. Rev. B* **86**, 144505 (2012).

[3] H. S. Nguyen, D. Gerace, I. Carusotto, D. Sanvitto, E. Galopin, A. Lemaître, I. Sagnes, J. Bloch, and A. Amo, *Acoustic Black Hole in a Stationary Hydrodynamic Flow of Microcavity Polaritons*, *Phys. Rev. Lett.* **114**, 36402 (2015).

[4] P. Grišins, H. S. Nguyen, J. Bloch, A. Amo, and I. Carusotto, *Theoretical study of stimulated and spontaneous Hawking effects from an acoustic black hole in a hydrodynamically flowing fluid of light*, *Phys. Rev. B* **94**, 144518 (2016).

Lasing in topological photonic lattices

Alberto Amo^{a*}

a. Univ. Lille, CNRS, UMR 8523 -- PhLAM -- Physique des Lasers Atomes et Molécules, F-59000 Lille, France

* alberto.amo@univ-lille1.fr

The implementation of topological effects in photonics has recently emerged as a promising research avenue for the manipulation of photons at the micron-scale [1]. The possibility of engineering the on-site energy and hopping makes polariton lattices an excellent platform to study this type of phenomena. In this presentation we will review our recent experiments on the topological properties of polariton lattices etched in semiconductor microcavities. In 2D, we have implemented honeycomb lattices in which polaritons behave as electrons in graphene, and we have studied the edge states that emerge from the topological properties of the lattice [2,3]. In 1D, we have fabricated lattices that implement the orbital version of the Su-Schrieffer-Heeger Hamiltonian. These lattices show lasing in topological edge states with resilience to disorder [4].

The implementation of these properties in the world of photonics opens new opportunities in the fabrication of micrometric scale photonic chips with properties intrinsically robust to noise, disorder and defects.

[1] T. Ozawa, H. M. Price, A. Amo, N. Goldman, M. Hafezi, L. Lu, M. Rechtsman, D. Schuster, J. Simon, O. Zilberberg, and I. Carusotto, *Topological Photonics*, arXiv:1802.04173 (2018).

[2] M. Milićević, T. Ozawa, P. Andreakou, I. Carusotto, T. Jacqmin, E. Galopin, A. Lemaître, L. Le Gratiet, I. Sagnes, J. Bloch, and A. Amo, *Edge states in polariton honeycomb lattices*, *2D Mater.* **2**, 34012 (2015).

[3] M. Milićević, T. Ozawa, G. Montambaux, I. Carusotto, E. Galopin, A. Lemaître, L. Le Gratiet, I. Sagnes, J. Bloch, and A. Amo, *Orbital Edge States in a Photonic Honeycomb Lattice*, *Phys. Rev. Lett.* **118**, 107403 (2017).

[4] P. St-Jean, V. Goblot, E. Galopin, A. Lemaître, T. Ozawa, L. Le Gratiet, I. Sagnes, J. Bloch, and A. Amo, *Lasing in topological edge states of a one-dimensional lattice*, *Nat. Photonics* **11**, 651 (2017).

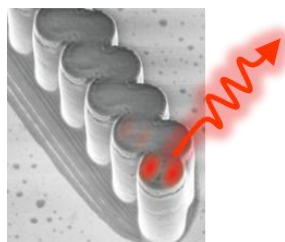


Figure 1: Zigzag lattice of polariton micropillars implementing the Su-Schrieffer-Heeger Hamiltonian and showing lasing in a topological edge state.

Competition between growth kinetic and thermodynamic effect in the atomic arrangements of Ag-Co nanoalloys

P. Andreazza^{a*}, C. Andreazza-Vignolle^a, Y. Garreau^{b,c}, A. Coati^b, R. Ferrando^d, J. Creuze^e, A. Lemoine^a

- a. Interfaces, Confinement, Matériaux et Nanostructures, ICMN, Université d'Orléans, CNRS, Orléans, France
- b. Synchrotron Soleil, Gif-sur-Yvette, France
- c. MPQ, Université Paris Diderot, CNRS, Paris, France
- d. Università di Genova, Department of Chemistry and Industrial Chemistry, Italy
- e. SP2M, ICMMO, Université Paris-Sud, CNRS, Orsay, France

* pascal.andreazza@univ-orleans.fr

As lot of Ag-based binary metallic alloys, Ag-Co system is a very weakly miscible system in wide ranges of temperature and composition. Since Ag presents lower surface energy and larger size (to minimize elastic energy), a surface segregation of silver is expected at the equilibrium in Ag-based bimetallic alloy surface. To the nanometer scale, the size reduction favors exotic segregation behavior by surface and/or core contraction effects that can be opposed to kinetic trapping effects induced by the growth mode. In our works, atom mobility during the formation of Ag-Co supported nanoalloys were studied through in situ investigations of the structural arrangement evolution. Obtained by sequential atom deposition for each type of atoms (Ag and Co), the different configurations: Co deposition on Ag core and Ag deposition Co core were investigated during the growth.

Morphological and structural evolutions are followed by in situ and real time wide and small angle X-ray scattering obtained simultaneously in X-ray grazing incidence geometry (GISAXS and GIWAXS) in single or multi-wavelength (anomalous) mode. In addition, the quantitative structural analysis of experimental data was facilitated and consolidated using Monte Carlo (MC) simulations of Co-Ag nanoalloys in a semi-empirical tight-binding approach. Furthermore, atomistic simulations of the cluster growth by molecular dynamics (MD) were done to reveal the atom migration leading to phase separation or core-shell formation (Fig.1). In a metastable deposition mode, i.e. by depositing Co above an Ag core, the configuration is complex: Co atoms incorporate the initial Ag core in sub-layer position leading to janus then core-shell configuration with the Co content. In the more stable reverse deposition mode, unexpected, Ag nucleate in domains on Co core, rather than in shell.

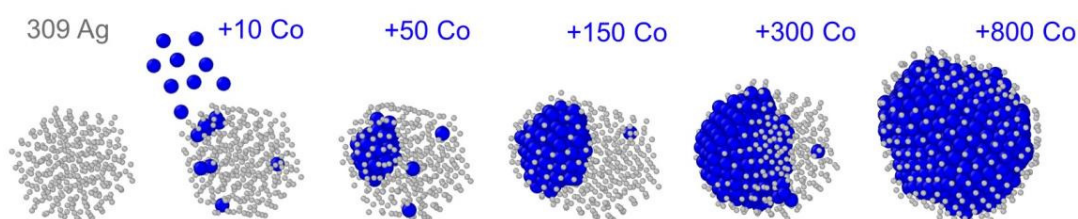


Figure 1 : Molecular dynamics simulation of atom migration during Co atom deposition on Ag icosahedral cluster (Ag in grey and Co in blue, Ag atoms in a reduced size for better observation).

Computation of the ground-state energy of a chemical Hamiltonian using a noisy quantum processor model

Valentin Anfray^{a*}, Thomas Ayril,^a

a. Atos Quantum Lab, Les Clayes-sous-Bois, France

* valentin.anfray@atos.net

Determining the ground-state energy of a chemical Hamiltonian is a complex problem because the dimension of the Hilbert space grows exponentially in the number of orbitals. One way to find this energy is to use a quantum computer, where the computation in principle scales linearly in the number of orbitals. However, current quantum computers are nonideal due to imperfections and environmental noise. A solution is to generate short circuits in order to minimize noise and decoherence effects. To quantify this using numerical simulation of quantum processor, we implemented and compared the phase estimation algorithm [1] and the variational quantum eigensolver (VQE) for ideal and non-ideal quantum processors in terms of result accuracy and gate number for a spin and a Hubbard model. We detailed the VQE by comparing different optimizers and implementing two different preparations; one involving the unitary coupled cluster theory [2] and the other called “hardware-efficient” [3].

- [1] James D. Whitfield, Jacob Biamonte, and Al an Aspuru-Guzik. Simulation of electronic structure hamiltonians using quantum computers. *Molecular Physics*, 109(5):735–750, 2011.
- [2] Alberto Peruzzo, Jarrod McClean, Peter Shadbolt, Man-Hong Yung, Xiao-Qi Zhou, Peter J. Love, Al an Aspuru-Guzik, and Jeremy L. O’Brien. A variational eigenvalue solver on a photonic quantum processor. *Nature Communications*, 5:4213 EP –, Jul 2014.
- [3] Abhinav Kandala, Antonio Mezzacapo, Kristan Temme, Maika Takita, Markus Brink, Jerry M. Chow, and Jay M. Gambetta. Hardware-efficient variational quantum eigensolver for small molecules and quantum magnets. *Nature*, 549:242 EP –, Sep 2017.

Atomic and electronic structure of transition-metal doped LaAlO₃/SrTiO₃ interfaces

M. Lee,^{a,b} R. Arras,^{*,a} B. Warot-Fonrose,^a T. Hungria,^c M. Lippmaa,^d H. Daimon^b and M. J. Casanove^a

- a. Centre d'Elaboration des Matériaux et d'Etudes Structurales (CEMES), CNRS UPR 8011 and Université de Toulouse, 29 rue Jeanne Marvig, F-31055 Toulouse, France
- b. Nara Institute of Science and Technology (NAIST), 8916-5 Takayama, Ikoma 630-0192, Japan
- c. Centre de MicroCaractérisation Raimond Castaing, Université de Toulouse, 3 rue Caroline Aigle, F-31400 Toulouse, France
- d. Institute for Solid State Physics, University of Tokyo, 277-8581 Chiba, Japan

* remi.arras@cemes.fr

In 2004, the discovery of a two-dimensional electron gas (2DEG) at the interface between two insulating perovskites LaAlO₃/SrTiO₃(001) [1] has motivated a large research effort, which has led to the discovery of new interfacial properties (magnetism, superconductivity, tunable Rashba effect...), offering consequently a new playground to investigate condensed-matter fundamental mechanisms and new opportunities for proposing alternatives concepts for future electronic devices. Among the different possibilities to tune these properties, doping the interface may be considered as an efficient way to modify the electronic properties either directly or via induced modifications in the atomic structure.

The present study participates to this effort by exploring LaAlO₃/SrTiO₃ interfaces doped with transition-metal atoms, namely iridium or cobalt atoms. Cobalt was chosen as a dopant because of its role in developing a dilute magnetic semiconductor state in TiO₂ [2], whereas novel properties arising from an interplay between strong spin-orbit interaction and electron correlations could be expected in the case of Ir doping. Besides, the 5d electronic structure of Ir doping could increase the carrier mobility at the interface compared to 3d electrons [3].

High quality nanostructures, typically LaAlO₃(5u.c.)/doped-SrTiO₃(1u.c.)/SrTiO₃ (substrate), were grown by pulsed laser deposition (PLD). Atomically resolved high-angle annular dark field scanning transmission electron microscopy (HAADF-STEM) was implemented to probe the local structure at the interface and quantify the level of strain near the interface, whereas the electronic structure was investigated by electron energy loss spectroscopy in a STEM. We will report the evolution of the electronic and atomic structure of the doped LaAlO₃/SrTiO₃ interface as a function of the doping level [4], and its consequence on the transport properties. A special emphasis will be put on the location of the dopant atoms (preferred atomic site, cationic inter-diffusion, state of strain...) using a combination of experimental techniques and first-principles calculations.

[1] A. Ohtomo and H. Y. Hwang, *A high-mobility electron gas at the LaAlO₃/SrTiO₃ heterointerface*, Nature **427**, 423 (2004).

[2] Y. Matsumoto *et al*, *Room-temperature ferromagnetism in transparent transition metal-doped titanium dioxide*, Science **291**, 854 (2001).

[3] S. Nazir *et al*, *Nb and Ta layer doping effects on the interfacial energetics and electronic properties of LaAlO₃/SrTiO₃ heterostructure: first-principles analysis*, Phys. Chem. Chem. Phys. **18** (2016), 2379–2388.

Quantum Cellular Automata

Pablo Arrighi^{a*}

a. Aix-Marseille Univ, LIS, Marseille, France

* pablo.arrighi@univ-amu.fr

In order to simulate quantum systems efficiently, we ought to use quantum systems. The framework of Quantum Cellular Automata (QCA), including Quantum Walks, is a strategic for quantum simulation. First, because QCA constitute a privileged mathematical setting in which to discretize the quantum system to be simulated. Secondly, because they constitute a promising architecture for quantum simulation devices. Last, because the imperfections of the quantum simulation devices are more likely to map onto the natural noise models of the simulated quantum phenomena. I will review a number of theoretical results on quantum simulation with QCA.

STM observation of topological defects and chaos in graphene on a metal

Alexandre Artaud^{a*}, Benjamin Canals^b, Philippe David^b, Valérie Guisset^b, Claude Chapelier^c et Johann Coraux^b

- a. Institut für Experimentelle und Angewandte Physik, Christian-Albrechts-Universität, D-24118 Kiel, Germany
- b. Univ. Grenoble-Alpes, CNRS, Inst NEEL, F-38042 Grenoble, France
- c. Univ. Grenoble-Alpes, CEA, INAC-PHELIQS, F-38000 Grenoble, France

* artaud@physik.uni-kiel.de

Order emerges in physical systems as their temperature lowers and symmetries break. Vis-à-vis the concept of order lies that of topological defects. They are low dimensionality objects where order vanishes, and cannot be removed by a continuous transformation of the system. Dislocations for instance are topological defects relative to the translational long range order, and can only be removed by bringing them to the sample edge.

When graphene is supported by a crystalline substrate, their superposition gives rise to a periodic modulation of order (called a moiré lattice). It is usually assumed graphene that this modulation is commensurate with the substrate, so the moiré displays translational long-range order and is said to be superperiodic.

To investigate possible topological defects, scanning tunneling microscopy (STM) is insightful, as it can visualize them at the atomic scale. Here, we exploit a complementary tool known as geometric phase analysis (GPA) [1] to extrapolate local strain fields from our STM images and highlight topological defects.

In graphene on a Re(0001) surface, this analysis reveals domains of moiré slightly shifted and rotated with respect to each other, and separated by domain walls that constitute topological defects in the moiré long-range order. Secondly, within a moiré domain, carbon atoms undergo a non-periodic static distortion wave. This means that in this system, long-rang order does not occur and instead a metastable phase develops, which can be described in an analogy with chaotic dynamic systems [2].

[1] M.J. Hÿtch *et al.*, Quantitative measurement of displacement and strain fields from HREM micrographs, *Ultramicroscopy*, **74**, 3, 131-146 (1998)

[2] P. Bak, Commensurate phases, incommensurate phases and the devil's staircase, *Rep. Prog. Phys.*, **45**, 6, 587-629 (1982)

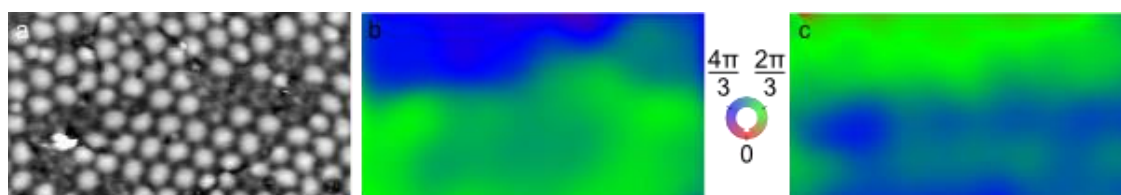


Figure 1 : GPA analysis of graphene on Re(0001). (a) STM topograph with atomic resolution revealing the moiré lattice as well as defective structures. (b-c) Corresponding geometric phase maps of graphene: the color code corresponds to the shift of carbon atoms with respect to a reference position. The contrast between the top left corner and the rest of the image then translates a significant shift between two domains.

Energetic and entropic footprints of quantum noise

A. Auffèves^{a*}, Maxime Clusel, Cyril Elouard^b, David Herrera-Martí^c, Benjamin Huard^{d,e}

- a. Univ. Grenoble Alpes, CNRS, Grenoble INP, Institut Néel, 38000 Grenoble, France
- b. Department of Physics and Astronomy and Center for Coherence and Quantum Optics, University of Rochester, Rochester, New York 14627, USA
- c. ProbaYes S.A.S., Grenoble, France
- d. Université Lyon, ENS de Lyon, Université Claude Bernard, CNRS, Laboratoire de Physique, F-69342, Lyon France
- e. Laboratoire Pierre Aigrain, Département de Physique de l'ENS, Ecole Normale Supérieure, PSL Research University, Université Paris Diderot, Sorbonne Paris Cité, Sorbonne Universités, UPMC Univ Paris 6, CNRS, 75000 Paris, France

* alexia.auffeves@neel.cnrs.fr

Despite its strategic interest for the development of scalable computing architectures, the question of the energetic cost of quantum information processing is still in its infancy. Such energetic cost is expected to be tightly related to the amount of quantum noise that should be overcome to perform the computation. A proper framework to conduct these investigations is provided by stochastic thermodynamics, which has analyzed for years the fundamental relations existing between energy, information, and noise. It is a major challenge of quantum thermodynamics to extend these relations in the quantum realm where noise is of purely quantum origin, e.g. stems from quantum measurement and decoherence.

In this talk we will present a new framework for quantum stochastic thermodynamics, that ultimately aims at answering these questions [1,2]. After recalling the general tools of stochastic thermodynamics, we will present the new concept of quantum heat. Quantum heat corresponds to the energetic fluctuations experienced by a quantum system, that are induced by measurement back-action and decoherence. We show that quantum heat provides the proper energy scale to estimate the cost of quantum control and feedback [2]. Finally, we evidence that quantum heat can become a resource in new kinds of genuinely quantum engines, extracting work from quantum measurement [1].

[1] C. Elouard, D. Herrera-Martí, B. Huard, and A. Auffèves, [Phys. Rev. Lett. 118, 260603 \(2017\)](#), featured in [Nature Research Highlights](#) and [Phys.org](#).

[2] C. Elouard, D. Herrera-Martí, M. Clusel, A. Auffèves, [npjQI 3:9 \(2017\)](#).

Bistability and displacement fluctuations in a quantum nanomechanical oscillator

R. Avriller^{a*}, B. Murr^a, and F. Pistolesi^a

a. Université de Bordeaux, CNRS, LOMA, UMR 5798, F-33405 Talence

* remi.avriller@u-bordeaux.fr

Remarkable features have been predicted for the mechanical fluctuations at the bistability transition of a classical oscillator coupled capacitively to a quantum dot [1,2]. These results have been obtained in the regime $\hbar\omega_0 \ll k_B T \ll \hbar\Gamma$ where ω_0 , T and Γ are the mechanical resonating frequency, the temperature, and the tunneling rate, respectively. A similar behavior could be expected in the quantum regime of $\hbar\Gamma \ll k_B T \ll \hbar\omega_0$.

We thus calculate the energy and displacement fluctuation spectra and study their behavior as a function of the electro-mechanical coupling constant when the system enters the Frank-Condon regime. We find that, in analogy with the classical case, the energy fluctuation spectrum and the displacement spectrum widths show a maximum for values of the coupling constant at which a mechanical bistability establishes [3].

- [1] G. Micchi, R. Avriller and F. Pistolesi, *Mechanical Signatures of the Current Blockade Instability in Suspended Carbon Nanotubes*, Phys. Rev. Lett. **115**, 206802 (2015).
 [2] G. Micchi, R. Avriller and F. Pistolesi, *Electro-Mechanical Transition in Quantum dots*, Phys. Rev. B. **94**, 125417 (2016).
 [3] R. Avriller, B. Murr and F. Pistolesi, *Bistability and Displacement Fluctuations in a Quantum Nano-mechanical Oscillator*, Phys. Rev. B. **97**, 155414 (2018).

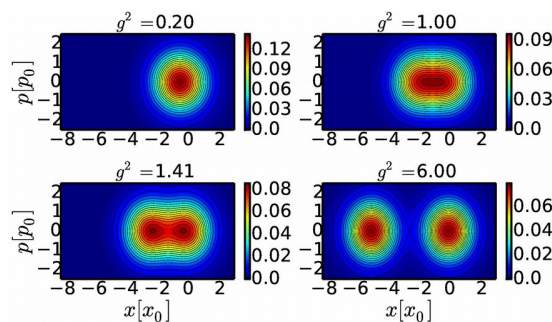


Figure 1 : The Wigner distribution of a quantum nanomechanical oscillator coupled to tunneling electrons while increasing electromechanical coupling g^2 . Extracted from [3].

Fluides supercritiques et développement durable : de l'élaboration au recyclage des matériaux

Cyril Aymonier^{a*}, Gilles Philippot^a, Michael Tsang^b, et Guido Sonnemann^b

a. CNRS, Univ. Bordeaux, Bordeaux INP, ICMCB, UMR 5026, F-33600 Pessac

b. Univ. Bordeaux, CNRS, ISM, UMR 5255, F-33400 Talence

* cyril.aymonier@icmcb.cnrs.fr

Cette contribution porte sur la présentation d'une technologie considérée comme durable, la technologie « fluides supercritiques », pour l'élaboration et le recyclage des matériaux [1]. Cette technologie offre aujourd'hui la possibilité de produire en continu, très rapidement (quelques secondes), de façon durable à grande échelle un certain nombre de nanostructures. Ces nanostructures ont généralement des propriétés différentes de celles préparées à partir de voies plus conventionnelles. Au cours des 10 dernières années, la technologie fluides supercritiques a également été développée pour apporter une alternative dans le domaine du recyclage des matériaux [2].

Suite à une brève introduction sur les propriétés spécifiques des milieux fluides supercritiques, une description des différents outils expérimentaux et numériques, aujourd'hui disponibles pour la communauté scientifique, sera proposée ; ces outils donnent accès à une meilleure compréhension, mais aussi à un meilleur contrôle sur la synthèse des nanomatériaux. La versatilité de la voie fluides supercritiques permet la synthèse de différentes natures de matériaux inorganiques, notamment par l'utilisation de différents couples solvants / précurseurs et aux chimies associées. Pour finir, nous discuterons des performances de ces matériaux, notamment suite à leur intégration dans des microsystèmes.

Années après années, cette technologie a trouvé de nouvelles applications, notamment dans le domaine du recyclage des matériaux. Pour cette application recyclage, deux solvants sont principalement utilisés, à savoir l'eau et le dioxyde de carbone en conditions supercritiques. L'intérêt et les potentialités de cette technologie de pointe dans le domaine du recyclage seront illustrés par les exemples suivants: i) le recyclage des fibres de carbone des matériaux composites et des aimants permanents dans l'eau sous- et supercritique et ii) la récupération de l'électrolyte dans les batteries Li ions, la récupération des métaux lourds et la délamination de multimatériaux par la technologie CO₂ supercritique.

Pour finir, nous discuterons de la problématique « fluides supercritiques et développement durable » sur la base d'évaluations réalisées par analyses de cycle de vie, sur les procédés d'élaboration et de recyclage des matériaux en milieux fluides supercritiques [3,4].

[1] C. Aymonier, G. Philippot, A. Erriguible, S. Marre, Playing with solvents in supercritical conditions and the associated technologies for advanced materials by design, *J. Supercrit. Fluids* **134**, 184 (2018)

[2] C. Aymonier, G. Philippot, A. Erriguible, S. Marre, Material processing and recycling with near- and supercritical CO₂-based solvents, *RSC*, in press (2018)

[3] M. Tsang, G. Philippot, C. Aymonier, G. Sonnemann, Anticipatory life-cycle assessment of supercritical fluid synthesis of barium strontium titanate nanoparticles, *Green Chem.*, **18**, 4924 (2016)

[4] M. Tsang, E. Kikuchi-Uehara, G. Sonnemann, C. Aymonier, M. Hirao, Evaluating nanotechnology opportunities and risks through integration of life-cycle and risks assessment, *Nature Nanotechnology* **12**, 734 (2017).

Towards a realistic simulation of trapped-ion and superconducting quantum bits and gates

Olivier Allègre^a, Emmanuel Lilette^a, and Thomas Ayrat^{a*}

a. Atos Quantum Lab, Les Clayes-sous-Bois, France

* thomas.ayral@atos.net

As academic and industrial laboratories announce the experimental implementation of quantum chips with a growing number of quantum bits, simple algorithms can be turned from theoretical proposals to actual computations. Despite this progress, the experimental results reveal deviations from the theoretical predictions. These discrepancies stem from the fact that most predictions are based on ideal models for the building blocks of quantum algorithms: quantum bits and gates. In reality, these building blocks are implemented using e.g trapped ions or superconducting Josephson junctions, both of which have intrinsic imperfections, while being subjected to external perturbations.

In this work, we model both quantum platforms, using Hamiltonian models of the qubit and its environment. This allows us to compute the quantum channels corresponding to gate operations using numerical quantum process tomography. We check our assumptions by comparing our results to experimental characterizations of these two quantum platforms.

Crystal growth mechanism and ferroelectric domains in BiFeO₃ nanoparticles

Xiaofei Bai^{a*}, Pavan Nukala^b, Jie Wei^c, Maria Varela^d, Nicolas Guiblin^b,
Brahim Dkhil^b, Ingrid Canero-Infante^a

- a. CNRS, Institut des Nanotechnologies de Lyon, CNRS UMR5270 ECL INSA UCBL CPE, 7, Avenue Jean Capelle, 69621, Villeurbanne, France
- b. Laboratoire Structures, Propriétés et Modélisation des Solides (SPMS), CentraleSupélec, CNRS-UMR8580, Université Paris-Saclay, Gif-sur-Yvette, France
- c. Electronic Materials Research Laboratory, Key Laboratory of Ministry of Education & International Center for Dielectric Research, Xi'an Jiaotong University, Xi'an 710049, People's Republic of China
- d. Departamento de Física de Materiales & Instituto Pluridisciplinar, Universidad Complutense de Madrid, Madrid 28040, Spain

* xiaofeibxf@gmail.com

Abstract: BiFeO₃, as a promising multiferroic material, has attracted strong interest for acoustics, optical, electrical and magnetic study. Here we systematically designed a wet-chemical synthesis process with two optimizing thermal treatment steps to obtain single-phase BiFeO₃ nanoparticles via Differential Scanning Calorimetry. The pure phase is confirmed from powder X-ray diffraction. Further, ferroelectric domains in nanoparticles are observed by high resolution transmission electron microscopy, with Fe displacements of 35 pm contributing to the polarization and ferroelectricity in our nano BiFeO₃. Through Electron Energy Loss Spectroscopy, a local octahedral ligand environment around Fe³⁺ is confirmed, which character of *R3c* in BiFeO₃ nanoparticles. Finally, we thoroughly analysed the growth kinetics via Johnson-Mehl-Avrami thermal kinetic model and deduced that the crystallization mechanism of our nano BiFeO₃ is surface nucleation from precursor powders. Our findings therefore furnish a practical method for synthesizing high quality nano BiFeO₃ and highlight the ferroelectricity in BiFeO₃ nanoparticles which rely on the interface coupling.

Intégration de techniques innovantes dans un MEB-FIB TESCAN

TESCAN FRANCE est née suite à la fusion de TESCAN, entreprise tchèque, leader mondial de la fabrication de microscopes électroniques à balayage (MEB), et ORSAY PHYSICS, société française réputée pour sa capacité d'innovation et d'industrialisation dans le domaine des colonnes à faisceaux d'ions (FIB) et des systèmes d'injection de gaz (GIS).

Toujours à la recherche d'innovation, TESCAN intègre aujourd'hui de multiples techniques d'analyses au sein de la plateforme DualBeam (MEB - FIB). Plus que les traditionnels systèmes de microanalyse EDS, WDS et EBSD, un TOF -SIMS spectromètre de masse en temps de vol qui permet de faire des analyses chimiques ou isotopiques sur des traces en 2D et 3D sera présenté.

De plus en combinaison avec différents accessoires tels que platine Cryo, platine de traction chauffante ou nanoindenteur il est possible d'avoir une meilleure compréhension de nos matériaux sous contraintes.

Après un rappel de ces différentes techniques d'analyses et des limites de chacune nous présenterons des applications dans divers domaines d'application.



Development of the unique UHV instrument allowing correlation FIB-SEM-SIMS analysis

J. Silvent¹, A. Houel¹, E. Verzeroli¹, A. Delobbe¹

¹Orsay Physics, Fuveau, France

Corresponding author: jeremie.silvent@orsayphysics.com;

Benefiting from its extensive knowledge and its in-depth expertise in dual beam FIB/SEM (Focused Ion Beam/ Scanning Electron Microscope) systems and UHV (Ultra High Vacuum) environment, Orsay Physics has developed a convenient versatile and customizable instrument called NanoSpace allowing correlation of FIB-SEM with SIMS (Secondary Ions Mass Spectrometry) analyses. The SIMS is a label-free technique that not only reveals the chemical composition of a biological sample providing an excellent metabolite and lipid detection, but also cell phenotype discrimination.

The SIMS analysis is performed by the combination of a new secondary ion extraction column and an OTOF (Orthogonal Time Of Flight) detector which has the advantage of a simultaneous detection of all the masses and a dynamic range of 10^6 - 10^7 . Both have been completely optimized in order to enhance the collection of the secondary ions and increase the mass resolution ($M/\Delta M$) of above 5,000. In addition, as the NanoSpace is working in UHV, surface analysis and imaging are all the more reliable in a contaminant-free environment (pressure condition below $5 \cdot 10^{-10}$ mbar inside the chamber). A very wide range of ion species can be chosen as the primary ion beam according to the user needs, including Xe^+ , Ar^+ , O^{2+} , Si^+ , Au^+ , and even gold clusters. Finally, the SEM instrument allows to obtain high resolution imaging (<2 nm).

The development of this new tool is an instrument of interest in biology to obtain both *in situ* chemical analysis and 3D tomography of a biological sample at the nanometric scale. The sample preparation could require a washing using a volatile salt solution to maintain the osmotic pressure, *e.g.* ammonium formate, and then a freeze drying in liquid propane or nitrogen or high pressure freezing. Thus, no special sample preparation technique (dehydration, fixation, etc...) are necessary making the NanoSpace an easy and versatile instrument.

Keywords: SIMS, FIB, SEM, correlative analyses, *in-situ* analyses, Cryo mode

Synthesis and characterization of nanocrystalline FeCu alloys prepared by high energy ball milling process

N. Boudinar^{a,*}, A. Djekoun^a, A. Otmani^a, B. Bouzabata^a, J. M. Greneche^b

^a Laboratoire de Magnétisme et de Spectroscopie des Solides Université Badji Mokhtar, Faculté des sciences B. P: 12 (23000) ANNABA -Algérie

^{*} Ecole Préparatoire aux Sciences et Techniques Annaba – Algérie

^b Laboratoire de Physique de l'Etat Condensé, UMR CNRS 6087 Université du Maine Faculté des Sciences 72085 LEMANS Cedex 9 –France

E-mail : n_boudinar@yahoo.fr

Nanocrystalline FeCu alloys were prepared by mechanical alloying of Fe and Cu elemental powders using a planetary ball mill under protection atmosphere. The powders were characterized by X-ray powder diffraction (XRD), scanning electron microscopy (SEM) and vibrating sample magnetometry (VSM). Rietveld analysis of the X-ray diffraction data reveals a decrease in the grain size down to 12 nm and a value of lattice parameter was reached to 0.36327 nm, after 48 h of milling time. The magnetic hysteresis measurements revealed that the FeCu alloy nanostructures display ferromagnetic behavior with enhanced magnetic properties at room

temperature. The coercive field, determined from the hysteresis curves, ranges from 117 to 147 G, and the saturation magnetization shows a maximum as a function of milling time.

Keywords: Fe–Cu alloy, mechanical alloying, nanocrystalline structure, magnetic properties.

Caractéristiques morphologiques des calculs de l'arbre urinaire à l'échelle mésoscopique

A. BOUTEFNOUCHET^{a*}, B. HANNACHE^b, A. LEKOUGHET^c, K. GHENAIET^d, R. MECHER^e, M. DAUDON^f

- a. Faculté de Médecine d'Annaba Algérie
- b. Université de Constantine Algérie
- c. Institut des Sciences Vétérinaires, Souk-Ahras, Algérie.
- d. Département de Biochimie, Faculté des sciences Université Annaba
- e. Département de Pharmacie, Faculté de Médecine Annaba
- f. Service des explorations fonctionnelles, hôpital Tenon, AP—HP, 4, rue de la Chine, 75020 Paris, France

delatif@yahoo.fr

Résumé :

But : Etude de la lithogénèse des calculs de l'arbre urinaire par l'observation au microscope électronique à balayage (MEB) de leurs structures intimes à l'échelle mésoscopique et l'identification, par fluorescence X, des oligoéléments qu'ils renferment.

Matériel et méthodes : Dans cette étude on a considéré des calculs de l'arbre urinaire à différentes compositions dont les oxalates de calcium, les phosphates de calcium, les purines, et la cystine. Ces calculs se présentent sous une morphologie ayant trait au processus de leur lithogénèse (figure 1). A partir d'une étude préalable selon une approche morphologique et constitutionnelle associant les observations par loupe binoculaire et l'analyse par spectrométrie infrarouge à transformée de Fourier, nous avons considéré un ensemble de calculs urinaires présentant des profils pathologiques particuliers dont les calculs formés sur une plaque de Randall, les calculs d'infection avec ou sans germes uréasiques et des calculs d'hypercalciurie primaire. Ces calculs ont été observés au Microscope électronique à balayage pour déterminer leur structure intime à l'échelle mésoscopique et ensuite analysés par fluorescence X.

Résultats : Les observations à l'échelle mésoscopique ont révélé que les composants lithiasiques présentent des cristallites à morphologie particulière pouvant non seulement faciliter leur identification mais aussi déterminer les conditions particulières de leur formation. D'un autre côté l'analyse des éléments de lithiase urinaire par fluorescence X a pu mettre en évidence la présence de huit éléments dont les plus abondants sont le Zn et Sr. Cependant les composants lithiasiques oxalo et phospho-calciques sont relativement plus riches en oligoéléments.

Conclusion : L'utilisation de technique physique telles que la microscopie électronique à balayage et la fluorescence X nous a permis de récolter des éléments déterminants dans l'étude des processus de la lithogénèse des calculs de l'arbre urinaires.

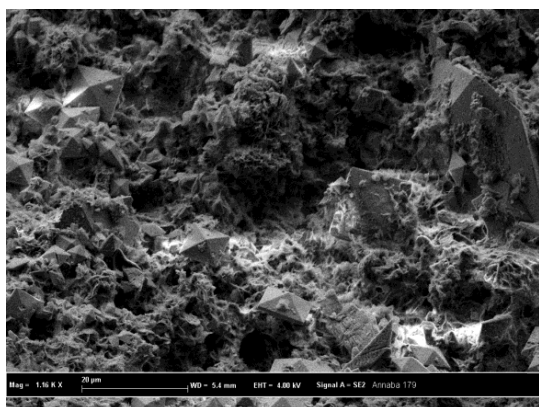


Figure 1: Micrographie MEB d'un calcul rénal mettant en évidence des Cristaux octaédriques d'oxalate de calcium dihydraté (Weddellite) sur fond de cristallites d'oxalate de calcium monohydraté (Whewellite) et orientant vers un contexte étiologique d'hyperoxalurie associée à une hypercalciurie intermittente

Microscopie électronique operando pour la catalyse hétérogène

Mounib Bahri^{a*}, Walid Baaziz^a, Kassioyé Dembélé^{a,b}, Anne-Sophie Gay^b, Charles Hirlimann^a, Ovidiu Ersen^{a*}.

- a. Institut de Physique et Chimie des Matériaux de Strasbourg (IPCMS), UMR 7504 CNRS – Université de Strasbourg, 23 rue du Loess, 67034 Strasbourg, cedex 2, France.
 - b. IFP– Énergies Nouvelles (IFPEN), 69360 Solaize, France.
- * mounib.bahri@ipcms.unistra.fr, ovidiu.ersen@ipcms.unistra.fr

Durant ces dernières années, la microscopie électronique environnementale en milieu gaz à haute température est devenue un outil indispensable pour étudier en temps réel les modifications structurales dans les matériaux nanostructurés. La dynamique des processus physico-chimiques activés à l'interface solide/gaz par la présence d'un environnement de gaz particulier ou par la température est devenue également accessible par l'observation directe de changements induits dans la phase solide. Dans le domaine de la catalyse hétérogène, l'une des contraintes d'analyse est de pouvoir étudier les nano-catalyseurs à des pressions représentatives des processus à étudier qui sont de l'ordre de 1 atmosphère pour un grand nombre de réactions d'intérêt. Ceci est possible aujourd'hui en utilisant des cellules fermées par deux membranes, avec les grains catalytiques insérés à l'intérieur et traversés par le gaz, qui peuvent être utilisés comme porte-objet dans le microscope [1]. La possibilité d'analyser les produits de réaction à la sortie de cette cellule en utilisant un analyseur de gaz résiduel permet de corréler les changements structuraux aux niveaux de catalyseurs à leurs performances catalytiques et ouvre une multitude de possibilités d'études à travers ce mode d'analyse qui fait partie des techniques in-situ operando.

Pour illustrer les possibilités de cette méthodologie de suivi *in operando* des processus catalytiques, nous présentons ici trois types d'études. Le premier se propose de suivre en temps réel la croissance des nanotubes de carbone multi-parois catalysée par des nanoparticules de ruthénium dans des conditions proches de celles utilisées dans les réacteurs : les résultats obtenus nous ont permis de proposer un nouveau modèle de croissance basé sur une oscillation de relaxation entre la phase carbure et la phase métallique qui se traduit par une variation cyclique de la cinétique de croissance. Le deuxième exemple concerne l'étude in-situ de la réaction de méthanation du CO₂ en considérant comme catalyseur des particules de Ni supportées sur de l'alumine ; l'étude *in operando* de ce système a permis d'obtenir deux informations fondamentales du point de vue de la mécanistique du processus catalytique: *i*) la détection du CO comme produit de réaction dont la concentration augmente avec la consommation du CO₂, ce qui signifie que la réaction se produit en deux étapes, et *ii*) l'augmentation progressive de la production du méthane avec la température simultanément à l'apparition de particules de taille plus petite et de clusters, ce qui conduit à une augmentation de la surface « active » des nanoparticules.

Comme dernier exemple, la stabilité thermique de nanostructures Pd@SiO₂ a été étudiée pour la première fois par microscopie électronique en utilisant une approche de type « étude d'objet unique » qui combine le mode environnementale à pression atmosphérique à la tomographie électronique. Ceci nous a permis de corréler les informations sur la stabilité thermique des particules (diffusion, fragmentation, coalescence) à l'évolution de leur forme 3D et cristallographie de surface.

[1] L. F. Allard, S. H. Overbury, W. C. Bigelow, M. B. Katz, D. P. Nackashi, J. Damiano, *Microsc. Microanal.* 2012, 18, 656 - 666.

Velocity waves in large-scale human crowds

Nicolas Bain^{a*}, Denis Bartolo,^a

a. Univ Lyon, Ens de Lyon, Univ Claude Bernard, CNRS, Laboratoire de Physique, F-69342 Lyon, France

* nicolas.bain@ens-lyon.fr

I will discuss the propagation of velocity waves in large-scale human crowds. Firstly, I will present a set of measurements performed on a number of different pedestrian crowds. I will demonstrate and quantitatively characterise longitudinal and non dispersive velocity waves propagating upstream the average pedestrian flow and show that transverse velocity fluctuations are strongly over damped. Secondly, I will show how to infer a predictive hydrodynamic description of some human crowds from their velocity wave spectra.



Figure 1: The starting line of the 2017 Bank of America Chicago Marathon

Conformation of grafted polymer chains in nanoporous membrane

Erigene Bakangura^a, Nicolas Jouault^b, Anastasia Christoulaki^b, Alexis Chennevière^{a*}

- a. Laboratoire Léon Brillouin, UMR12 CEA-CNRS, Bât. 563 CEA Saclay, 91191 Gif sur Yvette Cedex
 b. Laboratoire PHENIX, Sorbonne Université, 4 place Jussieu — 75252 Paris Cedex 5, FRANCE
 * alexis.chenneviere@cea.fr

Nanoporous anodized aluminum oxide membrane (AAO) is one of the most popular nanomaterial because of its simple, cheap and well controlled fabrication process. For example, several studies showed that grafting or adsorbing polymer chains within the pores can influence significantly the flow of simple liquids, translocation rate of polymer chains or even ionic conductivity[1]. On the fundamental point of view, several studies managed to characterize the brush extension on flat and convex surfaces[2]–[4]. These studies highlighted a very good agreement between the experimental studies and the scaling law model developed by Alexander, De Gennes, Daoud and Cotton. However, regarding concave polymer brush, there is still a theoretical debate on the validity of the Daoud-Cotton model for such systems [5]. Here, we used small angle neutron scattering in order to probe the conformation of end-grafted polystyrene chains within AAO nanopores with diameter ranging from 20 to 60 nm. We show that the molecular weight of grafted chains and their grafting density influence the form factor of the pores.

As a complementary characterization, we determined the hydrodynamic radius of the grafted nanopores by measuring the flow rate at constant pressure drop. The comparison of both SANS and flow permeability experiment allows to couple molecular insight and transport properties of grafted nanoporous membrane.

1. Md Jani, et al. . Prog. Mater. Sci. 58, 636–704 (2013).
2. Lal, J., et al., J. Phys. II 7, 19 (1997).
3. Auroy, P. et al., . J. Phys. II 3, 227–243 (1993).
4. Marzolin, C. et al. . Macromolecules 34, 8694–8700 (2001).
5. Manghi, M., et al., Eur. Phys. J. E 5, 519–530 (2001).

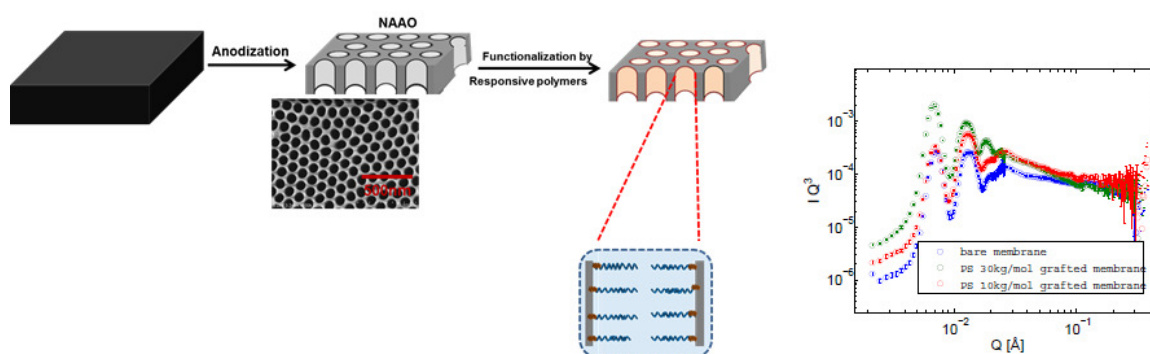


Figure 1 : (left) : Synthesis scheme of polymer grafted aluminum oxide nanoporous membrane (right) : SANS spectra of bare membrane and grafted PS-NH₂ which molecular weights are 10kg/mol and 30 kg/mol immersed in a mixture of THF-h and THF-d (31.1 %/ 69.9 %)

Operating Quantum States in Single Magnetic Molecules: Implementation of Quantum Gates and Algorithm

C. Godfrin,^a R. Ballou,^a E. Bonet,^a S. Klyatskaya,^b M. Ruben,^b W.
Wernsdorfer,^b F. Balestro ^{a,c*}

- a. Univ. Grenoble Alpes, CNRS, Grenoble INP, Institut Néel, 38000 Grenoble, France.
- b. Institute of Nanotechnology, Karlsruhe Institute of Technology, 76344 Eggenstein-Leopoldshafen, Germany.
- c. Institut Universitaire de France, 103 boulevard Saint-Michel, 75005 Paris, France.

* franck.balestro@neel.cnrs.fr

The application of quantum physics to the information theory turns out to be full of promises. The first step is to realize the basic block that encodes the quantum information, the qubit. Among all existing qubits, spin based devices are very attractive since they reveal electrical read-out and coherent manipulation. Beyond this, the more isolated a system is, the longer its quantum behavior remains, making of the nuclear spin a serious candidate for exhibiting long coherence time and consequently high numbers of quantum operation.

In this context I will present experimental results based on a TbPc₂ single molecular magnet spin transistor. This setup enabled us to read-out electrically both the electronic and the nuclear spin states and to coherently manipulate the nuclear spin[1,2]. I will present the study of the dynamic of a single 3/2 nuclear spin under the influence of a microwave pulse. After the energies difference measurement between these states I will show the coherent manipulation of the three nuclear spin transitions up to 10MHz, using only a microwave electric field, exhibiting coherence time higher than 1ms.

More than demonstrating the qubit dynamic, these measures demonstrate that a nuclear spin embedded in a molecular magnet transistor is a four quantum states system that can be fully controlled. Theoretical proposal demonstrated that quantum information processing could be implemented using a 3/2 spin such as quantum gates [3] and algorithm [4]. I will present the implementation of the Grover algorithm [5] to then show the implementation of the iSWAP gate and the measurement of its phase.

[1] Thiele S. et al. Science 344, 1135 (2014)

[2] Godfrin C. et al. ACS Nano 11, 3984 (2017)

[3] Kiktenko E. O. et al. Phys. Rev. A 91, 042312 (2015)

[4] Leuenberger M. et al. Phys. Rev. Lett. 89, 207601 (2003)

[5] Godfrin C. et al. Phys. Rev. Lett. 119, 187702 (2017)

The specific heat of Herbertsmithite under high magnetic fields

Q. Barthélemy,^{a*} E. Kermarrec,^a F. Bert,^a A. de Muer,^b P. Mendels^a

- a. Laboratoire de Physique des Solides, UMR 8502, Univ. Paris-Sud, Université Paris-Saclay, FR-91405 Orsay, France
- b. Laboratoire National des Champs Magnétiques Intenses, CNRS-UGA-UPS-INSA-EMFL, FR-38042 Grenoble, France

* quentin.barthelemy@u-psud.fr

It is now well-established that the ground state of the quantum kagome Heisenberg antiferromagnet (QKHA) is a spin liquid. Yet which class of quantum spin liquid (QSL) and elementary excitations is stabilized is still an heavily debated issue. While DMRG studies initially pointed to the existence of a singlet-triplet gap favoring a short-range resonating valence bond model “à la Anderson”, recent tensor network states techniques conclude on the contrary that the excitations are gapless. A spinon ($S = 1/2$ excitations) Fermi sea could be stabilized among all the numerous possibilities for the ground state. Probing experimentally the low-energy spectrum is therefore a key strategy in unveiling the nature of the ground state. For this purpose, specific heat appears as an invaluable tool, especially in the low-energy range beyond neutron techniques sensitivity. In this field of research, the emblematic Herbertsmithite $\text{ZnCu}_3(\text{OH})_6\text{Cl}_2$ compound is close to be a perfect realization of the QKHA and harbors a well-established QSL state: it features $S = 1/2$ Cu^{2+} kagome planes decoupled by diamagnetic Zn^{2+} with a small inter-site mixing. This mixing originates in a few quasi-free Cu^{2+} spins between the planes, sufficient to screen the low-temperature macroscopic measurements of the kagome physics. For instance, it results in a Schottky anomaly in the specific heat which prevents from an accurate determination of the T-dependence of the looked for specific heat originating from the kagome planes for usual lab-fields. We present data taken on single crystals of Herbertsmithite for magnetic fields up to 34T and temperatures down to 0.5K which open an experimental window where the kagome specific heat is measured in isolation. Indeed, for such high fields, the Schottky anomaly is shifted to relatively high temperatures so that the antisite contribution turns to be negligible. We will discuss the relevance of its variation with (high) fields and temperature to the various proposed models.

- [1] P. Mendels *et al.*, Phys. Rev. Lett. 98, 077204 (2007)
- [2] S. Yan *et al.*, Science 332, 1173 (2011)
- [3] M. R. Norman *et al.*, Rev. Mod. Phys. 88, 041002 (2016)
- [4] H. J. Liao *et al.*, Phys. Rev. Lett. 118, 137202 (2017)

Spin Liquid Ground State in $\text{Y}_3\text{Cu}_9(\text{OH})_{19}\text{Cl}_8$: A μSR Study

Q. Barthélemy,^{a*} P. Mendels,^a P. Puphal,^b K. M. Zoch,^b C. Krellner,^b F. Bert^a

a. Laboratoire de Physique des Solides, UMR 8502, Univ. Paris-Sud, Université Paris-Saclay, FR-91405 Orsay, France

b. Physikalisches Institut, Goethe-University Frankfurt, DE-60438 Frankfurt am Main, Germany

* quentin.barthelemy@u-psud.fr

Recent theoretical work supported by DFT calculations stressed the possibility to merge strong correlations, metallicity and Dirac fermions with electron doping in the emblematic Herbertsmithite compound $\text{ZnCu}_3(\text{OH})_6\text{Cl}_2$ [1, 2]. Indeed, for any electronic structure model that respects the hexagonal symmetry on the kagome lattice, protected Dirac points are located at the Fermi level for a filling $n = 4/3$. We explored the possibility to meet this challenge by replacing Zn^{2+} ($n = 1$) with trivalent Y^{3+} . The syntheses of $\text{YCu}_3(\text{OH})_6\text{Cl}_3$ (non-hydrothermal conditions) and of its sister compound $\text{Y}_3\text{Cu}_9(\text{OH})_{19}\text{Cl}_8$ (hydrothermal conditions) were successfully completed in the past two years [3, 4] but the charge of kagome layers is still balanced by boundings between Y^{3+} and the additional anions. The Kapellasite-type structures of these two cuprates are closely related, with no antisite disorder. While $\text{YCu}_3(\text{OH})_6\text{Cl}_3$ presents perfect kagome planes with partial disorder in the two Y sites, the full occupancy in $\text{Y}_3\text{Cu}_9(\text{OH})_{19}\text{Cl}_8$ makes the kagome lattice slightly distorted inducing two Cu sites (Fig. 1). This small release of frustration may be responsible for the weak singularities in thermodynamic measurements around 2K, when no sign of freezing is found in $\text{YCu}_3(\text{OH})_6\text{Cl}_3$ down to 400mK. Nonetheless, our μSR experiments discard the development of bulk long range order of frozen magnetism in $\text{Y}_3\text{Cu}_9(\text{OH})_{19}\text{Cl}_8$ down to 40mK, a first requirement for a spin liquid ground state.

[1] I. I. Mazin *et al.*, Nature Communications 5, 4261 (2014)

[2] D. Guterding *et al.*, Scientific Reports 6, 25988 (2016)

[3] W. Sun *et al.*, J. Mater. Chem. C 4, 8772 (2016)

[4] P. Puphal *et al.*, J. Mater. Chem. C 5, 2629 (2017)

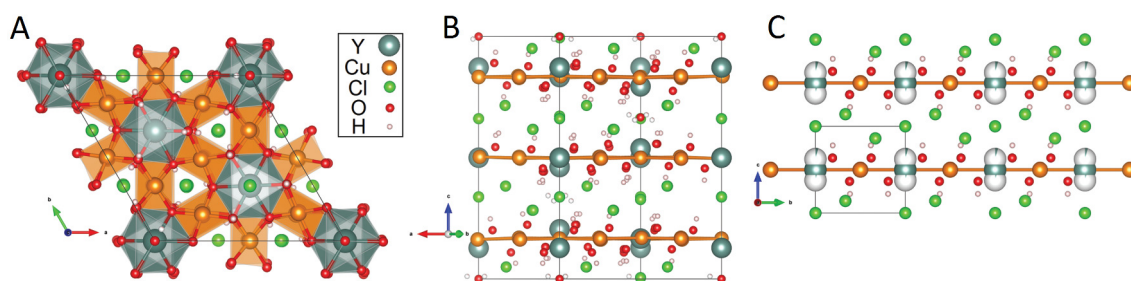


Figure 1: The structures of $\text{Y}_3\text{Cu}_9(\text{OH})_{19}\text{Cl}_8$ (A, B) and $\text{YCu}_3(\text{OH})_6\text{Cl}_3$ (C). Adapted from [4].

Nested sampling for high-throughput computational thermodynamics

Livia Bartók-Pártay^{a*}, Robert J. N. Baldock^b, Albert Bartók-Pártay^c, Noam Bernstein^d, and Gábor Csányi^e

- a. Department of Chemistry, University of Reading, Reading, UK
- b. École Polytechnique Fédérale de Lausanne, Lausanne, Switzerland
- c. STFC Scientific Computing Department, Rutherford Appleton Laboratory, Didcot, UK
- d. Department of Engineering, University of Cambridge, Cambridge, UK
- e. US Naval Research Laboratory, Washington, US

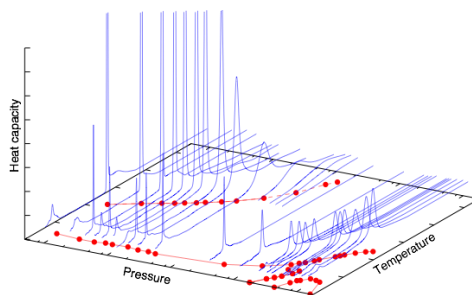
* l.bartokpartay@reading.ac.uk

In recent years we have been working on adapting a novel computational sampling technique, called nested sampling, to study the potential energy surface of atomistic systems [1]. Nested sampling automatically generates all the relevant atomic configurations, unhindered by high barriers, and one of its most appealing advantages is that the global partition function can be calculated very easily as a simple post-processing step, thus thermodynamic properties become accessible. Nested sampling explores the potential energy surface starting from the high energy region, hence no prior knowledge of the potentially stable structures is needed. This means that unlike other methods, nested sampling may be fully automated, allowing high-throughput calculations of phase transformations and phase diagrams of different materials [2,3,4].

[1] L. B. Pártay, A. P. Bartók, and G. Csányi, *J. Phys. Chem. B* **114**, 10502 (2010)

[2] R. J. N. Baldock, L. B. Pártay, A. P. Bartók, M. C. Payne, and G. Csányi, *Phys. Rev. B* **93**, 174108 (2016)

[3] R. J. N. Baldock, N. Bernstein, K. M. Salerno, L. B. Pártay, and G. Csányi, *Phys. Rev. E* **96**, 043311 (2017)



[4] L. B. Pártay, *Comp. Mat. Sci.* **149**, 153 (2018).

Figure 1 : Calculating the phase diagram with Nested Sampling: calculations can be performed at a series of pressures, and phase transitions are located by peaks of the heat capacity curves (blue). Red lines show the evaporation, melting and solid-solid transition lines.

The non-linear mechanics of slender deformable bodies

Basile Audoly^{a*}

a. LMS, École Polytechnique, CNRS, Université Paris-Saclay, 91128 Palaiseau, France

* baudoly+jmc18@gmail.com

We discuss some challenges arising in the mechanics of slender (quasi-1D) deformable bodies, such as a thin thread of a viscous fluid [1,2], curly hair [3,4,5], or a carpenter's tape for example. Slender bodies can exhibit a number of complex and intriguing behaviors that are accessible through simple experiments. The analysis of slender bodies exposes one to many of the fundamental concepts of 3D non-linear mechanics, albeit in a simpler setting where explicit analytical solutions and fast numerical methods can be proposed. Based on examples, we review some problems arising in the analysis of deformable bodies, including the derivation of accurate 1D mechanical models by dimensional reduction, the solution of non-linear 1D models by analytical or numerical methods, and the analysis of material or geometrical instabilities.



- [1] P.-T. Brun, N. M. Ribe, and B. Audoly. A numerical investigation of the fluid mechanical sewing machine. *Physics of fluids*, 24(4):043102, 2012.
- [2] B. Audoly, N. Clauvelin, P.-T. Brun, M. Bergou, E. Grinspun, and M. Wardetzky. A discrete geometric approach for simulating the dynamics of thin viscous threads. *Journal of Computational Physics*, 253:18–49, 2013.
- [3] F. Bertails, B. Audoly, M-P. Cani, B. Querleux, F. Leroy, and J.-L. Lévêque. Super-helices for predicting the dynamics of natural hair. In *ACM Transactions on Graphics*, pages 1180–1187, August 2006.
- [4] M. Bergou, M. Wardetzky, S. Robinson, B. Audoly, and E. Grinspun. Discrete elastic rods. *ACM Transactions on Graphics*, 27(3):63:1–63:12, 2008.
- [5] J. T. Miller, A. Lazarus, B. Audoly, and P. M. Reis. Shapes of a suspended curly hair. *Physical Review Letters*, 112:068103, 2014.

A graphene Zener-Klein transistor cooled by a hyperbolic substrate

E. Baudin^{a,*}, W. Yang^a, S. Berthou^a, X. Lu^b, Q. Wilmart^a, A. Denis^a, M. Rosticher^a, T. Taniguchi^c, K. Watanabe^c, G. Fève^a, J.M. Berroir^a, G. Zhang^b, C. Voisin^a, and B. Plaçais^a

- a. Laboratoire Pierre Aigrain, 24 rue Lhomond, 75231 Paris Cedex 05, France
 b. Beijing National Laboratory for Condensed Matter, Beijing 100190, China
 c. Advanced Materials Laboratory, National Institute for Materials Science, Tsukuba, Japan

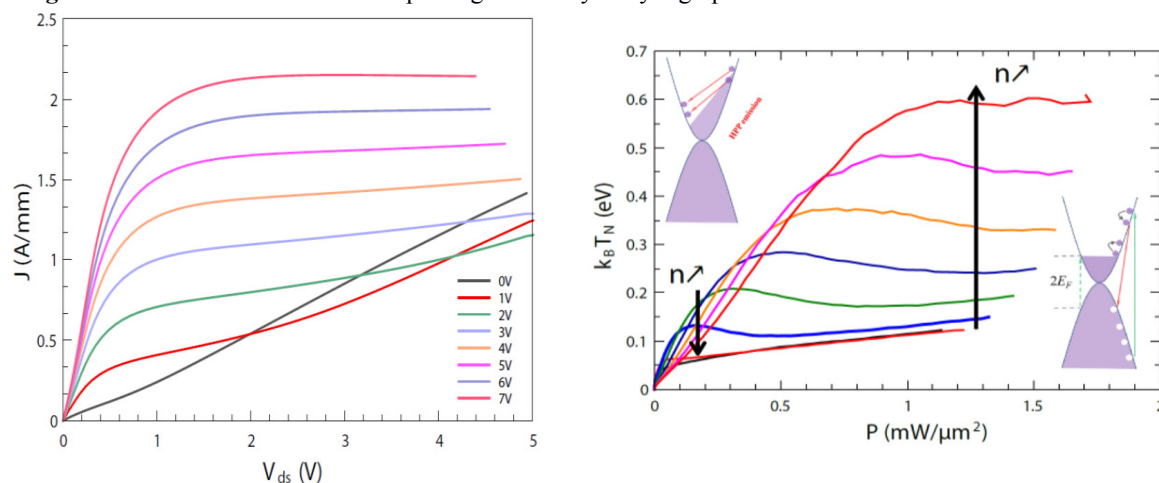
* baudin@lpa.ens.fr

Engineering of cooling mechanisms is a bottleneck in nanoelectronics. Whereas thermal exchanges in diffusive graphene are driven by defect-assisted supercollisions [1], the case of high-mobility graphene on hBN is radically different with a prominent contribution of remote phonons from the substrate. Here, we show that a bilayer graphene on hBN transistor can be driven in the Zener-Klein tunneling regime where current is fully saturated (Figure 1 left). Using sensitive GHz noise thermometry [2], we show that ZK-tunneling triggers a new cooling pathway due to the emission of hyperbolic phonons polaritons (HPPs) in hBN by out-of-equilibrium electron-hole pairs (Figure 1 right). The most obvious consequence is a reversal of this mechanism is by far the most efficient in graphene and promotes graphene Zener-Klein transistors as a valuable route for power RF amplification.

[1] A. Betz et al., Nat. Phys., 9 (2013) 109

[2] W. Yang et al., Nat. Nanotechnology 13 (2018) 47

Figure 1 : Current saturation in n-doped high-mobility bilayer graphene on hBN transistor with a channel



length of 4 μm . At charge neutrality transport is dominated by Zener-Klein tunnelling. (right) Electronic noise temperature function of the deposited Joule power. The noise temperature saturates when entering the Zener-Klein tunnelling regime indicating a new efficient cooling pathway switches on.

Role of Yttrium addition on the improvement of the plasticity in the Cu-Zr-Ti metallic glass system

Oriane Baulin^{a*}, Damien Fabrègue^a, Sébastien Gravier^b, Jean-Marc Pelletier^a

a. Université de Lyon, INSA-Lyon, Université Claude Bernard Lyon 1, CNRS, Laboratoire MATEIS, 7 avenue Jean Capelle, 69621 Villeurbanne Cedex, France

b. Science et Ingénierie des Matériaux et Procédés, Univ. Grenoble Alpes CNRS/Grenoble INP, 38302 Saint-Martin d'Hères, France

* Corresponding author: oriane.baulin@insa-lyon.fr

Yttrium is known to exhibit a high atomic radius, contributing to the maximum disorder principle. It also shows a strong affinity with oxygen. This reaction contributes to stabilize the liquid phase and delay the crystallization in metallic glasses. Moreover increasing the GFA, micro-alloying of Y is also responsible of an improvement of a lot of properties, as for example, corrosion resistance, thermal stability, biocompatibility and also the plasticity of the sample. However no clear explanations have been presented about this beneficial effect.

In this work, after determining the optimum quantity of Yttrium to add, the characterization of this material was conducted. 1 at. % of Y in the Cu-Zr-Ti leads to an increase of 2% of plastic strain. The microstructure was precisely studied using Transmission Electron Microscopy (TEM) observations and some explanation about this improvement can be discussed. Yttrium nano-precipitates with a core-shell structure were observed. This leads to an improvement of the ductility of the material, due to the nano-crystallized areas induced by the precipitates. EDX and EELS analysis were also used to confirm that they correspond to yttria.

Corrosion behaviour was also investigated in several electrolyte mediums and 1 at. % Y increases the corrosion potential to -0.23 V/SCE which is close to the Ti-6Al-4V alloy. NaCl solution and NaCl solution with 4g/L of albumin were used. These proteins adsorbed on the sample surface to create a passive level and avoid the immediate dissolution due to the main Cu content. They drastically change the material corrosion behaviour.

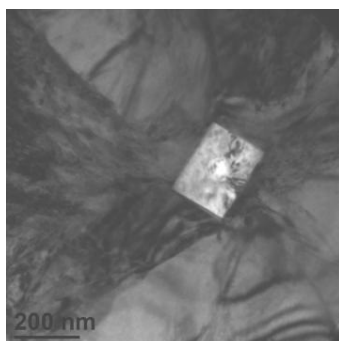


Figure 1 : TEM observations of an Yttria precipitate

Structural and dynamical properties of water confined in highly ordered mesoporous silica in presence of electrolytes

Markus BAUM^a, Diane REBISCOUL^a, Fanni JURANYI^b Francois RIEUTORD^c

- a. CEA, ICSM – UMR 5257 CEA-CNRS-UM-ENSCM, 30207 Bagnols-sur-Cèze Cedex, France
 b. Paul-Scherrer-Institute, 5232 Villigen, Switzerland
 c. CEA, INAC, Minatec Campus, 38000 Grenoble, France

Presenting author email: markus.baum@cea.fr

The understanding and the prediction of materials behavior regarding their interactions with aqueous solutions is of great interest in various fields, such as geochemistry, catalysis and nuclear wastes. Most of these materials are completely or partially nanoporous such as cementitious materials, clay materials, and amorphous nanoporous alteration layer of glasses. They consist of a set of confined media having a complex form and filled with water and ions. For instance, under confinement, the solvent behavior can be modified due to strong interactions between water molecules and pore surfaces, structuring water and slowing down its dynamics, from nanoscale to macro-scale.¹ Several parameters play a major role on this behavior changes such as pore size, surface composition, roughness and curvature.² Also, the presence of ions is expected to have a slow-down effect on the water mobility perturbing the hydrogen bond network through solvation and sorption.^{3,4} The determination of the consequences of such modifications on dissolution is a scientific challenge since the characterization of these processes in nanoconfinement is sophisticated.

In this study, we propose an innovative approach. We relate the surface ion excess with the water structure determined by Infrared spectroscopy and the water dynamics at a picosecond scale characterized by QENS (FOCUS, $T = 300$ K, $\lambda = 4.32$ Å) in highly ordered nanoporous silica (SBA-15; pore size 6.6 nm) filled with electrolyte solutions XCl_2 ($X = Ba^{2+}$, Ca^{2+} and Mg^{2+}) at various concentrations (see Figure). Depending on the present ions and with increasing electrolyte concentration, we found a decrease of water dynamics and an increase of less coordinated water population.

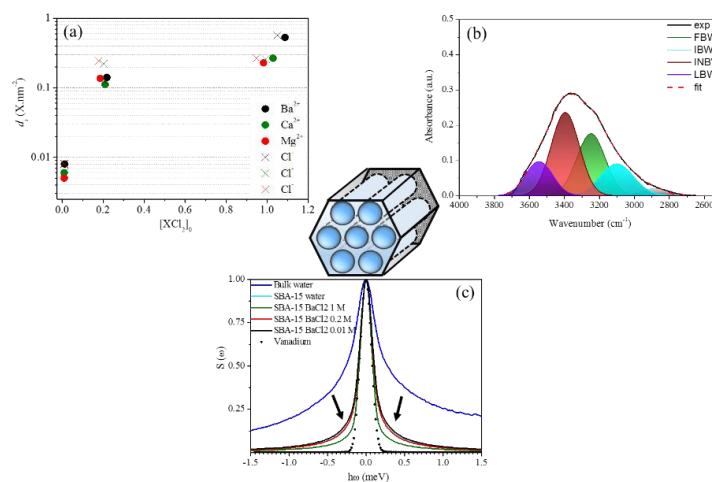


Figure: Sorption isotherms of XCl_2 electrolytes ($X = Ba^{2+}$, Ca^{2+} and Mg^{2+}) at various concentrations in SBA-15 (a). Sum over Q of QENS spectra of SBA-15 filled of $BaCl_2$ electrolytes at various concentrations obtained at 300 K and $\lambda = 4.32$ Å (b). Decomposition of O-H stretching band of $BaCl_2$ solution at 1 M in nanoconfinement (c).

- [1] Chiavazzo E. et al., Scaling behavior for the water transport in nanoconfined geometries. *Nature communications*. **2014**, 5, 1-11.
 [2] Briman, I. M. et al., Impact of Pore Size and Pore Surface Composition on the Dynamics of Confined Water in Highly Ordered Porous Silica. *Journal of Physical Chemistry C*. **2012**, 116, 7021-7028.
 [3] Ishai, P. B. et al., Influence of Ions on Water Diffusion - A Neutron Scattering Study, *The Journal of Physical Chemistry C*. **2013**, 117, 7724-7728.
 [4] Mamontov, E. et al., Dynamics of Water in LiCl and CaCl₂ Aqueous Solutions confined in Silica Matrices: A Backscattering Neutron Spectroscopy Study. *Chemical Physics*, **2008**, 352, 117-124.

Magnetic interactions in the frustrated pentagonal compound $\text{Bi}_2\text{Fe}_4\text{O}_9$

K. Beauvois^{a*}, V. Simonet^b, E. Ressouche^a, S. Petit^c, M. Gospodinov^d and V. Skumryev^e

- a. CEA, INAC/SPSMS-MDN, Grenoble, France
- b. Institut Néel-CNRS, Grenoble, France
- c. CEA-CNRS, LLB Saclay, France
- d. Institute of Solid State Physics, Bulgarian Academy of Sciences, Bulgaria
- e. Universitat Autònoma de Barcelona, Spain

ketty.beauvois@neel.cnrs.fr

The Fe^{3+} ions in $\text{Bi}_2\text{Fe}_4\text{O}_9$ materialize the first analogue of a magnetic pentagonal lattice [1]. The unit cell contains two different sites of four iron atoms each, which have different connectivities with the other irons (three or four neighbours for Fe_1 and Fe_2 respectively), and that form a lattice of pentagons. Because of its odd number of bonds per elemental brick, this lattice is prone to geometric frustration. The compound magnetically orders around 240 K: the resulting spin configuration on the two sites is the same, i.e. two orthogonal pairs of antiferromagnetic spins in a plane, with a global rotation between the two sites Fe_1 and Fe_2 . This peculiar magnetic structure, which is the result of the complex connectivity, has opened new perspectives in the field of magnetic frustration.

Here, we present the work in progress concerning the understanding and the consequences of the peculiar magnetic interactions in this original system. First, magnetization distribution maps have been measured at the Institut Laue Langevin (ILL) using polarized neutrons under an applied magnetic field. Remarkably, the magnetic moments of the Fe_1 sites, contrary to those of Fe_2 , are extremely weakly (or even not) polarized by the field both in the paramagnetic phase and in the ordered one. This indicates a paramagnetic liquid of classical spin dimers that condensate into a long-range arrangement below the Néel temperature. These dimers are stabilized by a strong antiferromagnetic coupling between pairs of Fe_1 atoms combined with a high degree of frustration. In a second step, the magnetic excitations have been investigated by inelastic neutron scattering using triple axis spectrometers at the LLB and the ILL. The confrontation of the experimental results with spinwave calculations confirms the hierarchy of the interactions between the iron sites in the lattice, and therefore the validity of the classical spin dimer picture.

Our new experimental results on $\text{Bi}_2\text{Fe}_4\text{O}_9$ open interesting perspectives in the field of frustrated pentagonal lattices.

- [1] E. Ressouche, V. Simonet, B. Canals, M. Gospodinov, V. Skumryev, Phys. Rev. Lett. 103, 267204 (2009).

3D self-assembly using DNA as programmable molecules

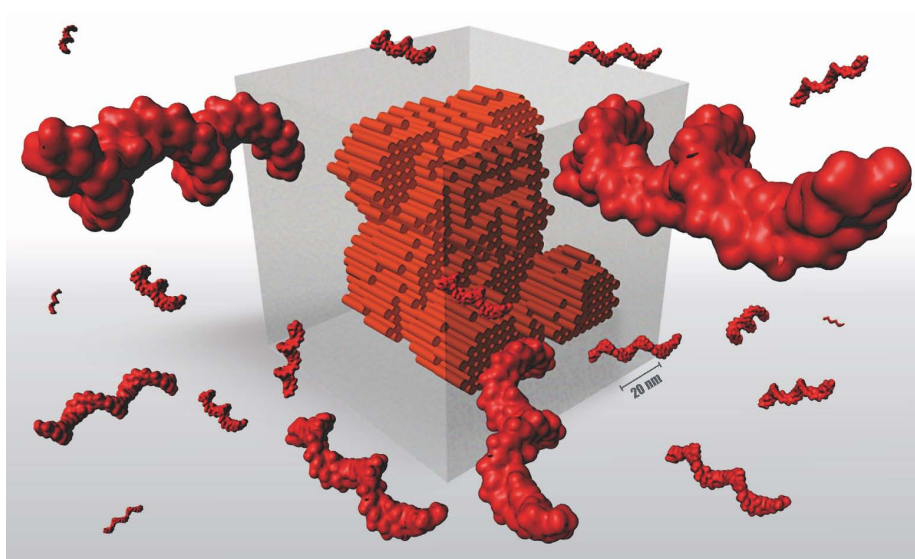
Allan Mills^a, Nesrine Aissaoui^a, Yonggang Ke^b, Peng Yin^c and Gaëtan Bellot^{a*}

- a. Centre de Biochimie Structurale, CNRS 5203, INSERM U1191, Montpellier, France.
- b. Department of Biomedical Engineering, Georgia Institute of Technology, Atlanta, USA.
- c. Wyss Institute for Biologically Inspired Engineering, Harvard University, Boston, USA.

* gaetan.bellot@cbs.cnrs.fr

Our goal is to build artificial molecular systems and machines sufficiently sophisticated to recapitulate and decipher fundamental aspects of biology and to help solve problems of medical interest. We use a DNA self-assembly method called DNA origami, which represents a landmark as the first practical method to self assemble megadalton scale nanostructures with arbitrarily-defined morphology and programmable actuation. I will first present an overview of the field of DNA origami nanotechnology and next present several applications of this method [1-3]. At the end, I will report the ability to engineer DNA nanostructures up to 1 gigadalton by using a new method called DNA Lego [4]. This recent work introduces the practical one-pot construction of fully addressable nanostructures containing 1.7 million nucleotides, comparable to the size of an entire genome of some bacteria. Collectively, these methods may offer a 'bottom-up' route to scale programmable morphology and create opportunities for *de novo* fabrication of high-performing functional molecular systems previously inaccessible.

- [1] Salas D, Angular reconstitution-based 3D reconstructions of nanomolecular structures from super resolution light-microscopy images. PNAS. 2017, doi: 10.1073/pnas.1704908114.
- [2] Vasiliauskaite-Brooks I, Structural insights into adiponectin receptors suggest ceramidase activity. Nature. 2017, doi: 10.1038/nature21714.
- [3] Ke Y, Regulation at a distance of biomolecular interactions using a DNA origami nanoactuator. Nature Comm. 2016, doi: 10.1038/ncomms10935.
- [4] Ont LL, Programmable self-assembly of three-dimensional nanostructures from 10,000 unique components. Nature. 2017, doi: 10.1038/nature24648.



Characterisation of as deposited and annealed CuIn_3Se_5 thin films

S. Rahal¹, M. Benabdeslem*¹, N. Benslim¹, L. Bechiri¹, T. Touam², A. Djekoun³, P. Decorse⁴

¹Laboratoire LESIMS. Département de physique. Université d'Annaba. Algeria.

²Laboratoire LSC. Département de physique. Université d'Annaba. Algeria.

³Laboratoire LM2S. Département de physique. Université d'Annaba. Algeria.

⁴UMR7086 Interfaces, Traitements, Organisation et Dynamique des Systèmes (ITODYS)
Université DIDEROT. Paris, FR 75000

Abstract

Among the I-III-VI chalcopyrite semiconducting materials, CuInSe_2 and the related ordered vacancy compounds (OVC) CuIn_3Se_5 , etc have become in the last few decades a suitable alternative as photovoltaic absorbers for highly efficient and low-cost solar cells. The result of extensive research on these materials was the achievement of over 20.3% solar cell conversion efficiency in laboratory [1] while the reported value for large-scale devices is 12% . The presence of this OVC compound was detected as a secondary phase in In-rich CuInSe_2 thin films and was found to play an important role in the performance of the CuInSe_2 -based solar cells. Herein, we report engineering of thin films of CuIn_3Se_5 obtained from ball milled powder. The powder of the ordered vacancy compound (OVC) has been successfully synthesized by mechanical milling from elemental pure Cu, In and Se precursors. The thin films of CuIn_3Se_5 were deposited onto glass substrates at room temperature by thermal evaporation technique and then annealed in vacuum. Powder XRD characterization and chemical bounding (XPS) confirm the formation of the tetragonal ordered defect compound phase (OVC) with lattice constants $a = 5.83 \text{ \AA}$ and $c = 11.71 \text{ \AA}$. The obtained thin layers were characterised and the changes in structural, optical and morphological properties have been studied using a range of techniques. The optical properties (absorption, gap, refraction index) of the films were analysed in the spectral range of 300-1800 nm. The absorption coefficient \rightarrow exhibits high values in the visible range and reaches a value of 10^5 cm^{-1} . The band gap energy E_g of the annealed thin films was estimated to be approximately 1.75 eV.

***THEORETICAL AND EXPERIMENTAL STUDY OF $\text{Cu}_2\text{ZnSnS}_4$
COMPOUND FOR SOLAR CELLS***

N. Benslim, M. Chaouche, S. Rahal, K. Hamdani, M. Benabdeslem, L. Bechiri

Laboratoire d'Etude de Surfaces et Interfaces de la Matière Solide (LESIMS), Département de Physique, Faculté des Sciences, Université Badji Mokhtar, BP 12 Sidi Amar – Annaba 23000, Algérie.

E-mail : benslimc8@gmail.com

Abstract

In this work we focus on the synthesis of the precursor materials as well as on deposition of thin $\text{Cu}_2\text{ZnSnS}_4$ (CZTS) films on corning substrates. This absorber can be obtained by substituting the toxic selenium by sulfur and the rare and cost element indium by zinc and tin in CuInSe_2 ternary compound. The nanocrystalline CZTS powder used for evaporation of thin films was obtained by mechanical alloying process from Cu_2SnS_3 and ZnS initial mixtures following two steps. Structural and optical properties of CZTS films have been studied. Powder X ray diffraction measurements showed that the semiconductor has the Kesterite structure in the tetragonal space group ($I\bar{4}$). A preferential orientation along (112) was observed for all compounds with lattice constants both powders and layers of $a = 5.40 \text{ \AA}$ and $c = 10.93 \text{ \AA}$. Transmittance and reflectance spectra were recorded in the wavelength range of 250-3000 nm using Shimadzu spectrophotometer. The direct band gap of the CZTS was estimated to be about 1.54 eV, which is the optimal band gap for the absorber of solar cells. The structural and optical properties of Kesterite CZTS, studied by using the full potential linearized augmented plane wave method (FP-LAPW) within the density functional theory (DFT), showed good agreement with our experimental results.

Simulation par dynamique moléculaire de la translocation d'une poly-cytosine dans une protéine d'alpha-hémolysine confinée dans un nanopore.

Bentin Jérémie^{a*} et Fabien Picaud^a

a. Nanomedecine, Imagerie, Thérapeutique, 16 route de Gray, 25030 Besançon cedex, France

* jeremy.bentin@edu.univ-fcomte.fr

Le biomimétisme est un nouveau champ de recherche visant à transposer les propriétés intrinsèques remarquables du vivant vers le monde solide. Dans ce cadre, transférer des protéines transmembranaires sélectives dans des pores nanométriques, tout en les laissant parfaitement opérationnelles, apparaît comme un challenge novateur et plein d'espoir. L'alpha-hémolysine est une protéine du staphylocoque doré qui a la capacité de créer des pores lors de son insertion dans des membranes lipidiques. Ces pores, liés à la présence de la protéine, ont alors la capacité de trier sélectivement de grosses molécules, et notamment les brins d'ADN, selon leur arrangement. Utiliser cette protéine dans un nanopore hydrophobe permettra donc de développer un nouveau type de séquenceur d'ADN, naturel et à bas cout de revient.

Le principe de fonctionnement de ce séquenceur d'ADN est le suivant : après avoir calibré les dimensions du nanopore afin que la protéine ne soit pas dénaturée en son sein et conserve donc ses propriétés, un courant ionique est crée en imposant une tension de part et d'autre de la membrane. Puis les brins d'ADN que l'on souhaite séquencer, traverseront le pore sous l'effet de cette tension, et bloqueront partiellement le courant le temps de la traversée. De par leurs différences structurelles, chaque nucléotide modifiera le courant différemment, et l'observation des variations du courant ionique durant le passage du brin d'ADN dans l'alpha-hémolysine pourra permettre de remonter à la séquence de nucléotide imposée.

Nous présenterons ici nos résultats, obtenus grâce à des simulations de dynamique moléculaire, sur le passage d'un brin de poly-cytosine au travers d'une protéine d'alpha-hémolysine insérée dans un pore de néo-pentane. Après avoir décrit l'état du système natif, nous étudierons notamment le temps de traversée et le blocage de courant ionique induit par le passage du brin d'ADN, et les comparerons avec des résultats obtenus expérimentalement sur des systèmes similaires. Ces résultats numériques permettent d'espérer une généralisation du séquençage, tout comme il l'avait été dans une membrane biologique par le biais d'autres simulations.

- [1] Tom Z. Butler, Ionic current blockade from DNA and RNA molecules in the Alpha-Hemolysine nanopore, *Biophysical Journal* **93**, 3229-3240 (2007)
- [2] Simon Cabello-Aguilar, and Sebastien Balme, Slow translocation of polynucleotides and their discrimination by alpha-hemolysin inside a single track-etched nanopore designed by atomic layer deposition, *Nanoscale* **5**, 9582 (2013)

Kinetic energy spectra in a vibrated 2D granular medium with magnetic dipolar interactions.

Michael Berhanu^{a*}, Simon Merminod,^b Eric Falcon^a and Gustavo Castillo^c

a. Université Paris Diderot, MSC, UMR 7057 CNRS, Paris, France

b. School of Physics, Brandeis University, Waltham, Massachusetts 02453, USA

c. Instituto de Ciencias de la Ingeniería, Universidad O'Higgins, Rancagua, Chile

* michael.berhanu@univ-paris-diderot.fr

Using a 2D out-of-equilibrium system of magnetized and vibrated granular particles, a transition from a granular gas towards a hexagonal crystal has been reported, when magnetic field is increased at constant agitation [1]. By extracting the longitudinal and transverse current correlations in dynamical regime, the spectrum of excitations can be measured in the Fourier space to characterize how kinetic energy is distributed through the scales. In the granular phase, we show that energy transfers between particles are mediated by compression longitudinal waves. In contrast, in the hexagonal solid phase, energy transfers occur by the macroscopic equivalent of phonons, whose dispersion relations for longitudinal and transverse waves can be analytically computed. Moreover, for the granular gas phase, we quantify the out-of-equilibrium character. The fluctuating hydrodynamic theory [2] explains indeed well the deviation from energy equipartition due to dissipative collisions. A moderate increase of magnetic field, induces a repulsion between particles. The rate of collision is thus reduced and the distance to thermal equilibrium is decreased.

- [1] S. MERMINOD, M. BERHANU & E. FALCON, Transition from a dissipative to a quasi-elastic system of particles with tunable repulsive interactions, *EPL*, **106** 44005 (2014).
 [2] A. PUGLISI, A. GNOLI, G. GRADENIGO, A. SARRACINO & D. VILLAMAINA, Structure factors in granular experiments with homogeneous fluidization, *J. of Chem. Phys.*, **136** 014704 (2012).

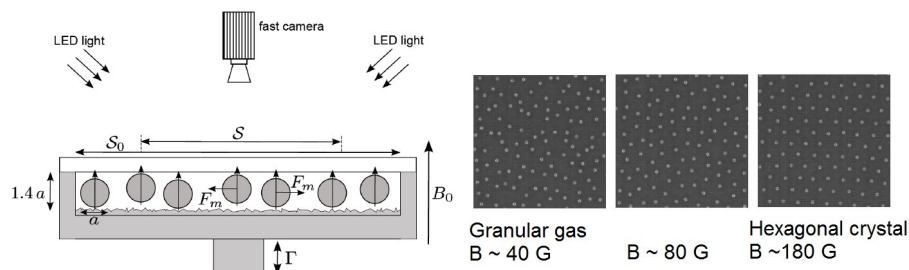


Figure 1: Left, Experimental setup. 2000 soft magnetic spheres of diameter $a = 1$ mm are confined in a square cell (9×9 cm). Right, Snapshots of the experiment for various values of imposed magnetic field B for a constant agitation.

The theory of optical black hole lasers

Jose L. Gaona-Reyes^a, David Bermudez^{a*}

a. Department of Physics, Cinvestav, A.P. 14-740, 07000 Mexico City, Mexico

* dbermudez@fis.cinvestav.mx'

The event horizon of black holes and white holes can be achieved in the context of analogue gravity. It was proven for a sonic case that if these two horizons are close to each other their dynamics resemble a laser, a black hole laser, where the analogue of Hawking radiation is trapped and amplified. Optical analogues are also very successful and a similar system can be achieved there. However, the conditions in the optical case are different than those in the sonic one.

In this work, we present a theoretical description of the optical black hole laser (OBHL) following the approach of Corley and Jacobson [1], that is, by providing a WKB description of the evolution of frequency modes through a cavity and allowing mode conversion processes at the horizons. In the optical context, the cavity is formed by a pair of light pulses. In particular, we study the Hawking process also for a bosonic field, in this case photons, but in the normal dispersion regime. This fact forces an inverse order of the horizons (a BH–WH order) to get the proper kinematic behavior. Moreover, the change of velocity is now due to dispersion, and not as a consequence of modifications in the fluid flow. Hence, is Hawking radiation amplified in the optical analogue? And if so, under what conditions?

In addition, we derive the forward propagation of modes and, in this way, the heuristic argument for the amplification is easier to follow. Furthermore, it is known that the amplification depends mainly on the phase difference of the modes in both horizons. Here, we develop a method to approximate this phase difference and study its behavior. Finally, we present some numerical simulations of the OBHL based on the nonlinear Schrödinger equation (NLSE) including negative frequencies, which are usually not considered in this kind of simulations but that are necessary to obtain the correct modes of the black hole laser and its amplification [2].

[1] S. Corley, T. Jacobson. “Black hole lasers”, Phys. Rev. D **59**, 124011 (1999).

[2] J.L. Gaona-Reyes, D. Bermudez. “The theory of optical black hole lasers”, Ann. Phys. **380**, 41–58 (2017).

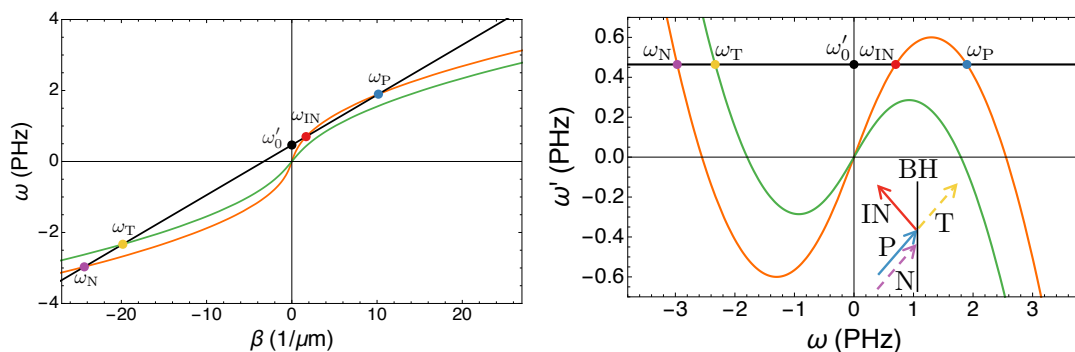


Figure 1 : Modes corresponding to a fixed value of the co-moving frequency ω' in the laboratory frame (left) and in the co-moving frame (right). The three modes IN, P, and N are found for the dispersion relation with $\delta n = 0$ (orange line) and the T mode for $\delta n = \delta n_{\text{max}}$ (green line).

Fully unsupervised online spike sorting based on an artificial spiking neural network

Marie Bernert^{a,b,c}, Blaise Yvert^{a,b*}

- a. INSERM, Braintech Laboratory U1205, F-38000 Grenoble, France
- b. Univ Grenoble Alpes, Braintech Laboratory U1205, F-38000 Grenoble, France
- c. CEA, Léti, F-38000 Grenoble, France

* blaise.yvert@inserm.fr

Sorting the spiking activity of individual neurons from extracellular recordings remains a challenging issue in neuroscience. Traditional spike-sorting methods rely on an action potential detection combined with a clustering algorithm, and often require offline processing. Here we present a fully unsupervised online spike sorting method based on a spike-timing dependent plasticity (STDP) artificial neural network, a type of network able to perform unsupervised pattern learning. Our STDP network is organized into layers connected by feedforward synapses implementing various plasticity rules. The input signal, band-pass filtered, is continuously fed into the input layer. After a short learning period, the spike trains of the output layer directly reflect the detected and sorted action potentials present in the input signal (Fig 1). This method shows good performances on single electrode compared to classical spike-sorting methods, and can be adapted to process several channels simultaneously. Such STDP network applied to spike sorting opens perspectives to embed neuromorphic hardware in intelligent brain implants, and more generally to achieve complex pattern recognition with neuromorphic architectures.

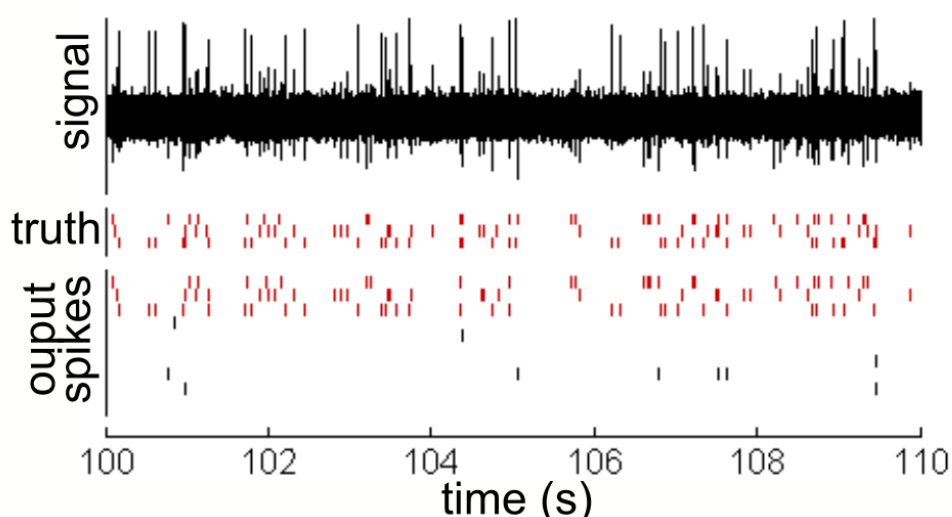


Figure 1 : Activity of the network's output layer compared to ground truth activity on a simulated signal.

Doubly-dressed states for near-field trapping and subwavelength lattice structuration

S. Bernon^{a*}, M. Bellouvet^a, R. Veyron^a, A. Hillico^a, J. Cayssol^b, P. Lalanne^a, and P. Bouyer^a

- a. Laboratoire Photonique, Numérique et Nanosciences (LP2N), UMR 5298, CNRS - IOGS - Univ. Bordeaux, Institut d'Optique d'Aquitaine, 33400 Talence, France
- b. LOMA (UMR-5798), CNRS and University Bordeaux 1, F-33045 Talence, France

* simon.bernon@institutoptique.fr

Atomic physics and solid-state devices have developed on nearly parallel tracks for several years, merely regarding each other as a source of inspiration. Over the last decade, however, the concept of hybrid systems where the quantum mechanical properties of coupled systems cannot be disentangled has spurred a blossoming research activity. Here, I will discuss a novel hybrid quantum system that engineers Bose and Fermi quantum gas dynamics in close proximity, and strongly interacting with, nano-structured surfaces capable of generating sub-wavelength lattice potentials with tailored electromagnetic properties. Such experimental platform belongs to the class of optical lattice quantum simulators. Compared to the state of the art, nano-structured lattices could strongly reduce lattice size and therefore enhance the relevant energy scale (tunneling, interaction) to enter more deeply into strongly correlated regimes. It would then bridge the gap between solid state (0.1 nm) and optical (500 nm) crystals to exploit simultaneously regimes free of far field fundamental limitations and cold atom controllability. The experimental challenge for such platform is to control the quantum gas in the close vicinity of the surface where tremendous Casimir Polder (CP) force apply on atoms. In this presentation, I will detail a novel trapping method (Doubly Dressed State) [1] capable to overcome the CP force at short distance and to generate optical lattice potentials with sub-wavelength period and controllable lattice depth and trap to surface distance (see Figure 1).

[1] M. Bellouvet, C. Busquet, J. Zhang, P. Bouyer and S. Bernon, arXiv:1710.05696.

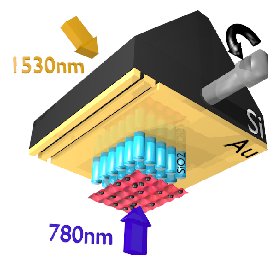


Figure 1: Hybrid quantum simulator: atoms (black balls) are trapped in the DDS near field trap (red) periodically modulated by the dielectric surface (blue cylinders).

Opposites attract in Soft Matter: Mechanisms and Applications

Fanny Mousseau, Evdokia Oikonomou, Victor Baldim and Jean-François Berret

Matière et Systèmes Complexes, UMR 7057 CNRS Université Denis Diderot Paris-VII, Batiment Condorcet, 10 Rue Alice Domon et Léonie Duquet, F-75205 Paris, France

jean-francois.berret@univ-paris-diderot.fr

Recent studies have pointed the importance of electrostatic assembly in the elaboration of innovative nanomaterials [1]. Beyond their structures, many important questions on the thermodynamics of association remain to be answered. Here, we investigate the complexation between oppositely charged polymers chains using a combination of different techniques, isothermal titration calorimetry (ITC), static and dynamic light scattering and electrophoresis. Upon addition of polycation to polyanion the results obtained by the different techniques reveal a two-step process [2]. The primary process is the formation of highly charged polyelectrolyte complexes of sizes 100 nm. The secondary process is the transition towards a coacervate phase made of rich and poor polymer droplets. The binding isotherms measured are accounted for using a phenomenological model that provides the thermodynamic parameters for each reaction. Small enthalpies and large positive entropies consistent with a counterion release scenario are found throughout this study. Applications of the above strategy to other charged nanosystems, including inorganic nanoparticle [3], natural organic matter [4] or phospholipids [5] have shown strong similarities with polymer complexation. Beyond, this work stresses the importance of the underestimated formulation pathway or mixing order in charged systems [1].

[1] J.-P. Chapel and J.-F. Berret, *Curr. Opin. Colloid Interf. Sci.* **17**, 97-105 (2012)

[2] L. Vitorazi, N. Ould-Moussa, S. Sekar, J. Fresnais, W. Loh, J.-P. Chapel and J.-F. Berret, *Soft Matter* **10**, 9496-9505 (2014)

[3] F. Mousseau, L. Vitorazi, L. Herrmann, S. Mornet and J.-F. Berret, *J. Colloid Interf. Sci.* **475** 36-45 (2016)

[4] F. Loosli, L. Vitorazi, J.-F. Berret and S. Stoll, *Water Research* **80**, 139-148 (2015)

[5] F. Mousseau, E. Seyrek, R. Le Borgne and J.-F. Berret, *Langmuir* **31**, 7346-7354 (2015)

Large scale fluctuating motion in confluent cell monolayers: particle-based model and normal mode analysis

Eric Bertin (CNRS, LIPhy, Grenoble)

Collaboration with :

S. Henkes, K. Kostanjevec, J.M. Collinson (U. Aberdeen), R. Sknepnek (U. Dundee)

Long-range displacement and velocity correlations in epithelial cell monolayers have been linked to active nematics [1], glassy dynamics [2], and active or passive cell intercalation events, i.e., T1 transitions [3]. Here we show that simple uncoordinated, but persistent cell motility coupled with the collective elastic modes of the cell sheet is sufficient to produce characteristic swirl-like correlations, leading to a divergent correlation length in the limit of infinite persistence time. We derive this result using both continuum elasticity and a normal modes formalism, and test our derivation with numerical simulations of a simple soft agent-based model. Finally, we compare our results to the in-vitro experiments of confluent corneal epithelial cell sheets.

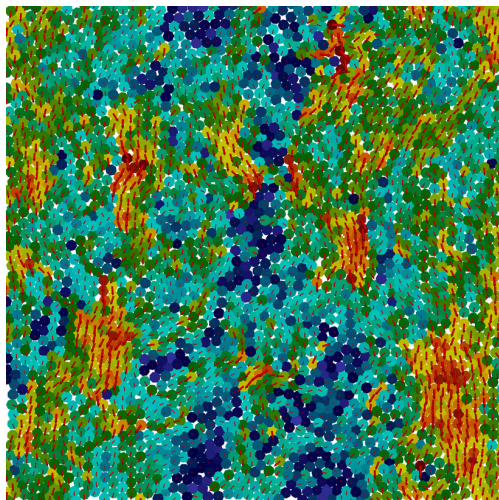


Figure: Velocity map in the particle-based model, showing spatially correlated displacements

- [1] A. Doostmohammadi et.al., *Soft Matter* **11**, 7328 (2015).
- [2] O. Chepizhko et.al., *PNAS* **113**, 11408 (2016).
- [3] M. Popovic et.al., *New Journal of Physics* **19**, 033006 (2017).

Band Filling Control of the Dzyaloshinskii-Moriya Interaction in Weakly Ferromagnetic Insulators

G. Beutier^{a,*}, S. P. Collins^b, O. V. Dimitrova^c, V. E. Dmitrienko^d, M. I. Katsnelson^{e,f}, Y. O. Kvashnin^g, A. I. Lichtenstein^{f,h}, V. V. Mazurenko^f, A. G. A. Nisbet^b, E. N. Ovchinnikova^c, D. Pincini^{i,b}

- a. Univ. Grenoble Alpes, CNRS, Grenoble INP, SIMaP, France
- b. Diamond Light Source, United Kingdom
- c. Lomonosov Moscow State University, Russia
- d. A. V. Subnikov Institute of Crystallography, FSRC "Crystallography and Photonics" RAS, Russia
- e. Radboud University Nijmegen, Institute for Molecules and Materials, The Netherlands
- f. Department of Theoretical Physics and Applied Mathematics, Ural Federal University, Russia
- g. Department of Physics and Astronomy, Uppsala University, Sweden
- h. Institut für Theoretische Physik, Universität Hamburg, Germany
- i. London Centre for Nanotechnology and Department of Physics and Astronomy, University College London, United Kingdom

* guillaume.beutier@grenoble-inp.fr

The antisymmetric exchange interaction, a.k.a Dzyaloshinskii-Moriya interaction (DMI), is responsible for the stabilisation of various exotic noncollinear magnetic ground states, such as spin spirals and skyrmions. It was first introduced to explain the spontaneous magnetisation in weak ferromagnets, in which spins are slightly canted away from the collinear antiferromagnetic order.

We re-examined four isostructural weak ferromagnets, FeBO_3 and MCO_3 ($M = \text{Mn, Co, Ni}$), by means of a novel X-ray diffraction method providing the sign of the DMI [1], and discovered a spectacular reversal of the sign of DMI with the filling of the 3d band of the transition metal [2].

[1] Dmitrienko, Ovchinnikova, Collins, Nisbet, Beutier, Kvashnin, Mazurenko, Lichtenstein, and Katsnelson, *Nat. Phys.* **10**, 202 (2014).

[2] Beutier, Collins, Dimitrova, Dmitrienko, Katsnelson, Kvashnin, Lichtenstein, Mazurenko, Nisbet, Ovchinnikova, and Pincini, *Phys. Rev. Lett.* **119**, 167201 (2017).

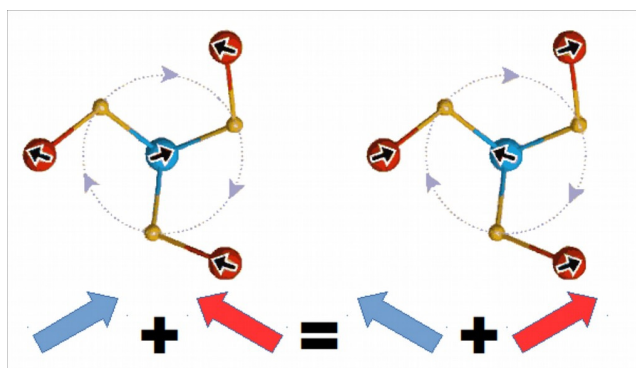


Figure: The two possible magnetic structures in the isostructural weak ferromagnets FeBO_3 and MCO_3 ($M = \text{Mn, Co, Ni}$). Both have the same net magnetization, yet opposite signs of DMI.

Modeling wurtzite-phase InGaAs/GaAs single-quantum-dot nanowire emitters

Saranath Seshadri^a, Daria Beznasyuk^a, Eva Monroy^b, Moira Hocevar^{a*}

a. Univ. Grenoble Alpes, CNRS-Institut Néel, 38000 Grenoble, France

b. Univ. Grenoble Alpes, CEA, INAC, PHELIQS, 38000 Grenoble, France

* moira.hocevar@neel.cnrs.fr

Nanowires can host a broad range of material combinations with different lattice parameters, since the strain caused by lattice mismatch can be elastically released at the side walls. Such capacity of deformation allows the synthesis of dislocation-free heterostructures that are not feasible in traditional planar films, which pushes forward the possibilities for quantum device engineering.

As an example, InGaAs/GaAs quantum dot nanowires are promising candidates for single photon emission at telecommunication wavelengths. This material combination is very relevant in optoelectronics. For example, InGaAs/GaAs Stransky Krastanov quantum dots have shown superior device properties in lasers, optical amplifiers and high-efficiency solar cells. The nanowire geometry allows extending the range of feasible material combinations. However, homogeneous GaAs nanowires generally present $\langle 0001 \rangle$ -oriented wurtzite crystalline structure. Therefore, piezoelectric and spontaneous polarization becomes important and need to be taken into account to understand the electronic band structure.

Here, we develop a model of wurtzite-phase InGaAs/GaAs single-quantum-dot nanowires using the Nextnano³ software [1]. The InGaAs/GaAs quantum dot structure is simulated in three dimensions (3D). The nanowire is modeled as a hexahedral prism on a GaAs substrate, to provide a reference in-plane lattice parameter, and is embedded in a rectangular prism of air which allows elastic strain relaxation. In a first stage, the 3D strain distribution is calculated by minimization of the elastic energy assuming zero stress at the nanowire surface. Then, the band profile is calculated by solving the Poisson-Schroedinger equation self-consistently, using the effective mass approximation. The model takes into account the piezoelectric fields resulting from the strain distribution, as well as the spontaneous polarization associated with wurtzite III-As materials. As an output, we obtain the 3D band profiles, the energy eigenvalues with the wavefunction distribution, and the interband wavefunction overlap.

The results of the 3D simulations are compared to 1D calculations, concluding that 3D modeling is necessary to describe the band structure of heavily strained quantum dot nanowires, since the strain distributes non-uniformly in the quantum dot. Additionally, the wavefunctions of the electron and hole must overlap radially and axially to ease the process of recombination. Fig.2 demonstrates the probability of occupation of electrons and holes in an $\text{In}_{0.6}\text{Ga}_{0.4}\text{As}$ dot, where the probability of emission is relatively low since the wavefunction overlap is minimum.[2]

From these results, we identify the optimum quantum dot dimensions, compositions and interface gradings for efficient emission at the telecommunication wavelengths.

[1] S. Birner, *et al.*, *IEEE Transactions on Electron Devices* **54**, 2137 (2007).

[2] Y.M. Niquet, *Physical Review B* **74**, 155304 (2006).

Strain induced defects at InAs/GaAs nanowire interfaces.

Daria Beznasyuk^{a*}, Marcel Verheijen^{b,c}, Julien Claudon^d, Moïra Hocevar^a

- a. University Grenoble Alpes, CNRS-Institut Néel, 38000 Grenoble, France
- b. Department of Applied Physics, Eindhoven University of Technology, 5600 MB Eindhoven, the Netherlands
- c. Philips Innovation Services Eindhoven, High Tech Campus 11, 5656AE Eindhoven, the Netherlands
- d. University Grenoble Alpes, CEA, INAC-Pheliqs, 38000 Grenoble, France

* dariabeznasyuk@gmail.com

Nanowires can host material combinations of very different lattice parameters owing to their small lateral size and high aspect ratio. Such geometry promotes elastic relaxation of mismatch strain on the nanowire sidewalls and allows to create dislocation free interfaces with no equivalent in traditional thin film epitaxy. Yet, strain affects the band structure of the final nanowire device and thus its electronic and optical properties. In this regard, it is important to understand how the strain distributes at the vicinity of the interface in axial nanowire heterostructures.

We use transmission electron microscopy to investigate the strain distribution in $\text{In}_{0.85}\text{Ga}_{0.15}\text{As}/\text{GaAs}$ nanowires, which theoretical lattice mismatch is 6% [1]. We study nanowires with diameters below and above the theoretical critical diameter for dislocation free interfaces [2]. To do so, we combine high-resolution scanning transmission electron microscopy (HRSTEM) together with image processing (Geometrical Phase Analysis (GPA)). We observe that nanowires with diameters below 40 nm at the interface are free of misfit dislocations (Figure 1 a). A 20 nm-long region in the vicinity of the interface is 6% compressed. The strain is fully elastically released via crystalline planes bending close to the side walls. On the other hand, we found that nanowires with diameters above 95 nm at the interface exhibit strain relaxation both elastically and plastically, via plane bending close to the nanowire sidewalls and formation of misfit dislocations, respectively (Figure 1 b). Experimental results are compared with theoretical simulations.

[1] D. V. Beznasyuk et al., *Nanotechnology*, **28**, 365602 (2017)

[2] F. Glas, *Phys. Rev. B* **74**, 121302 (2006)

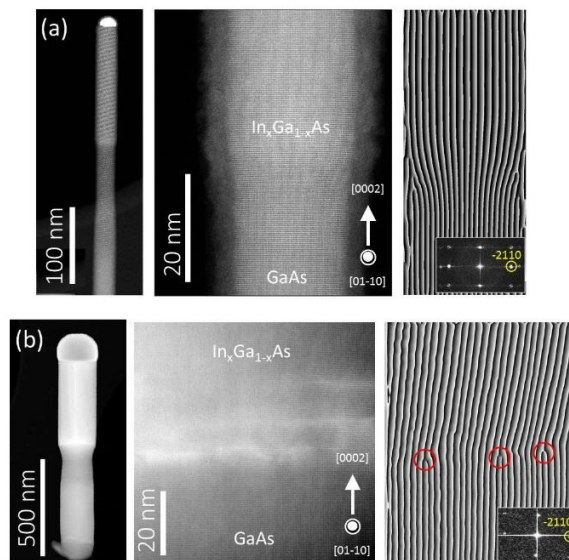


Figure 1: HRSTEM images of the wurtzite $\text{In}_{0.85}\text{Ga}_{0.15}\text{As}$ -on-GaAs nanowires with (a) 22 nm and (b) 190 nm at the interface. HRSTEM images after Fourier filtering of (-2110) Bragg-reflection, displaying banding of planes. Misfit dislocations are marked with red circles.

"Electronic read-out of 2 nuclear spins in a single-molecule magnets"

Hugo Biard^{1*}, Wolfgang Wernsdorfer¹², Franck Balestro¹³

1. Univ. Grenoble Alpes, CNRS, Grenoble INP, Institut Néel, 38000 Grenoble, France
2. Physikalisches Institut, Karlsruhe Institute of Technology, D-76131 Karlsruhe, Germany
3. Institut Universitaire de France, 103 Boulevard Saint-Michel, 75005 Paris, France

* hugo.biard@neel.cnrs.fr

« The realization of an operational quantum computer is one of the most ambitious technological goals of today's scientists. In this regard, the basic building block is generally composed of a two level quantum system (a quantum bit). Such quantum system must be fully controllable and measurable, which requires a connection to the macroscopic world. In this context, solid state devices, which establish electrical connections to the qubit, are of high interest. Among the different solid state concepts, spin based devices are very attractive since they already exhibit long coherence times.

Electrons possessing a spin 1/2 are conventionally thought as the natural carriers of quantum information, but alternative concepts propose the use of molecular magnets as building blocks for nanospintronics devices and quantum computing, materials whose magnetic quantum states are well defined. Their magnetic moment, or the nuclear spin carried by a single atom, benefit from longer coherence times compared to purely electronic spins, because of a better isolation from the environment. In this context, our team combines the different disciplines of spintronics, molecular electronics, and quantum information processing. In particular, the objective is to fabricate, characterize and study molecular devices (molecular spin transistor, molecular spin-valve and spin filter, molecular double dot devices, carbon nanotube nano-SQUIDs, etc.) in order to manipulate[1] and read-out individual spins[2,3,4] and to perform quantum operations like the Grover algorithm[5].

I will present the first read-out of two nuclear spins, coupled inside the Tb₂Pc₃ single-molecule magnets. It is the first step to achieve two qubit quantum operations using a molecular spin transistor. »

[1] S. Thiele, F. Balestro, R. Ballou, S. Klyatskaya, M. Ruben, W. Wernsdorfer, *Science* **2014**

[2] M. Urdampilleta, S. Klyatskaya, J-P. Cleuziou, M. Ruben, W. Wernsdorfer, *Nature Materials* **2011**.

[3] R. Vincent, S. Klyatskaya, M. Ruben, W. Wernsdorfer, F. Balestro. *Nature* **2012**.

[4] M. Ganzhorn, S. Klyatskaya, M. Ruben, W. Wernsdorfer. *Nature Nanotechnology* **2013**.

[5] C. Godfrin, A. Ferhat, R. Ballou, S. Klyatskaya, M. Ruben, W. Wernsdorfer, F. Balestro. *PRL* **2017**

Pressure-driven flow focusing in a microfluidic cross junction

Ilyesse Bihi^a, Doriane Vesperini^a, Badr Kaoui^a and Anne Le Goff^a

a. Sorbonne Universités, Université de Technologie de Compiègne, CNRS, Biomechanics and Bioengineering Laboratory (UMR 7338), 60200 Compiègne, France

* ilyesse.bihi@utc.fr

Flow focusing consists in injecting a core liquid into another surrounding flowing sheath liquid (Figure 1.A). This can be used, for example, to align micro particles or cells [1]. Here, we investigate experimentally the influence of the imposing pressure to generate co-flow in a cross-junction microfluidic device. We inject water in the central inlet and different mixtures of glycerol-water in the two lateral inlets. We vary the concentration of the added glycerol in order to tune the viscosity contrast between the core and the sheath liquids. A pressure generator is used to control the flows and the established flow rates are measured by flow-meters. We draw a state diagram that delimits the regions of the co-flow, the inner backflow and the outer backflow (Figure 1.B). A model, based on the electric circuit analogy, is proposed to predict the boundaries in the state diagram. We characterize in detail the width of the jet as a function of different parameters: the inlet pressures, the flow rates the viscosity contrast and the channel aspect ratio. This study defines the conditions needed to create a co-flow regime with a specific jet width using a pressure driven flow.

- [1] D. Vesperini, O. Chaput, N. Munier, P. Maire, F. Edwards-Lévy, A. V. Salsac, & A. Le Goff. Deformability- and size-based microcapsule sorting. *Medical Engineering and Physics*, **48** 68-74. (2017).

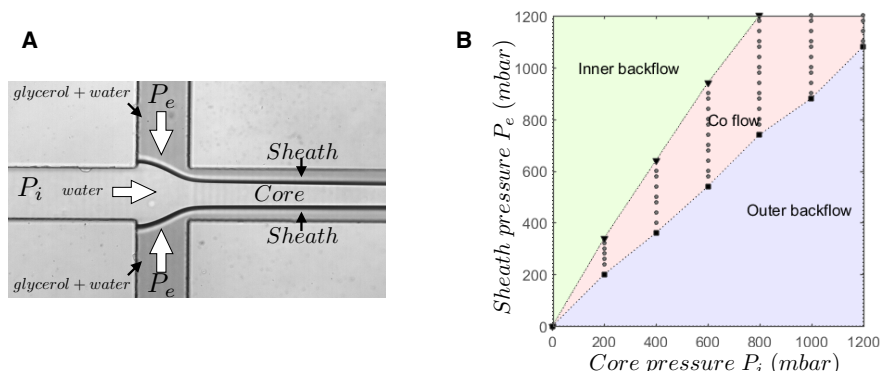


Figure 1: A) Image of a flow focusing of two liquids in a microfluidic device. B) State diagram in a $55 \mu\text{m}$ wide channel and $23 \mu\text{m}$ height, with a viscosity contrast $\mu_e/\mu_i=60$

Quantum fluids of light in semiconductor lattices

Jacqueline Bloch

Centre de Nanoscience et de Nanotechnologies, CNRS, Universités Paris Sud et Paris Saclay, Route de Nozay, 91460 Marcoussis, France

Jacqueline.bloch@c2n.upsaclay.fr

Semiconductor microcavities appear today as a powerful platform for the study of quantum fluids of light. They enable confining both light and electronic excitations (excitons) in very small volumes. The resulting strong light-matter coupling gives rise to hybrid light-matter quasi-particles named cavity polaritons. Polaritons propagate like photons but strongly interact with their environment via their matter part: they are fluids of light and show fascinating properties such as superfluidity or nucleation of quantized vortices. Sculpting microcavities at the micron scale, we fabricate at C2N lattices of various geometries and use this photonic platform for the emulation of various Hamiltonians.

After a general introduction, I will illustrate with a few examples how we can imprint on photons physical properties originating from the geometry and topology of the considered lattice: - A photonic benzene molecule present spin-orbit coupling and allows building a microlaser emitting chiral photons. - A photonic polyacetylene chain presents robust topological edge states. - A honeycomb lattice allows emulating Dirac physics with s or p orbitals and manipulating Dirac cones.

When controlling the interplay between pump, on-site nonlinearity and dissipation, this photonic platform opens the way to the exploration of complex non-linear dynamics, non-linear topological physics and in a near future quantum many body physics with light.

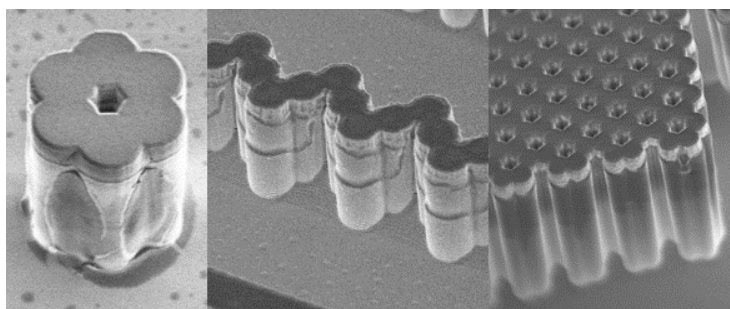


Figure 1 : Scanning electron microscopy image of semiconductor lattices where quantum fluids of light can be manipulated. (left) a photonic benzene molecule, (center) a zigzag chain of coupled resonators, (right) a honeycomb lattice of coupled resonators also named photonic graphene.

Accurate deep neural network potential for predicting properties of solids

Anton Bochkarev, Ambroise van Roekeghem and Natalio Mingo

CEA, LITEN, 17 Rue des Martyrs, 38054 Grenoble, France

Density Functional Theory is a very versatile tool which allows to compute multiple properties of materials. Nowadays, it is routinely applied for predicting, e.g., binding and cohesive energies of molecules and solid, electronic band structures, vibrational properties at 0K. Nevertheless, as the computational complexity of the DFT calculations scales non-linearly with the system size, the applications are often limited to the systems containing at maximum a few hundreds of atoms. It is therefore difficult to apply DFT for studying, e.g., solids with defects, properties of the materials at finite temperature, dynamical effects. To overcome these issues, the “classical” interatomic potentials are applied. Usually, these potentials approximate the energy of interaction between atoms by some kind of analytical function with the parameters which are adjusted to match experimentally known properties. The main disadvantage of these potentials is the lack of accuracy and transferability. The machine-learning technics provide the way to produce the interatomic potentials which are addressing deficiencies of the “classical” interatomic potentials while staying computationally efficient.

We present an interatomic machine-learning potential trained on DFT calculations using artificial neural networks (ANN). Our algorithm simultaneously trains on the DFT data for energies and atomic forces. This leads to the more efficient utilization of the DFT data as well as an increased accuracy of the potential. Our machine-learning potential is also universal in terms of the size of the system and its chemical composition. We demonstrate its versatility and accuracy via computing various properties of solids and compare the results with direct DFT calculations.

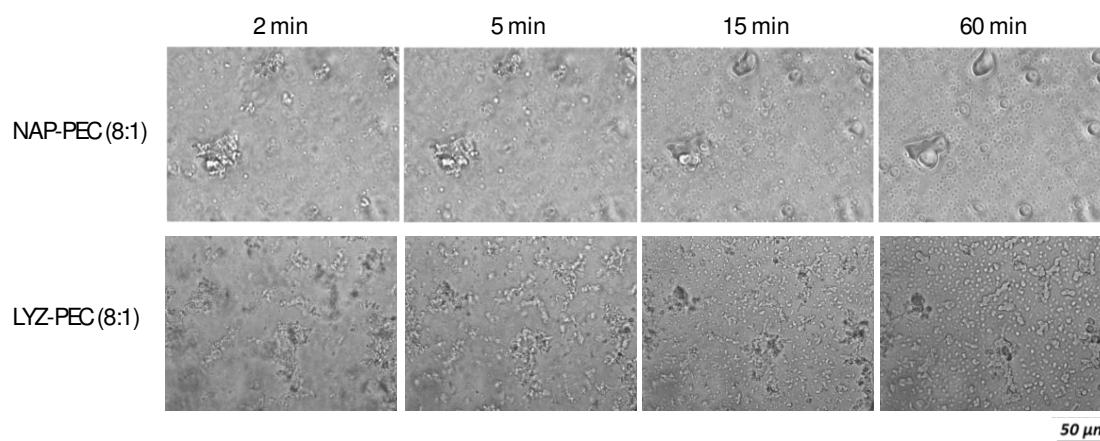
Associative properties of rapeseed napin and pectin: a solid-to-liquid transition during complex coacervation.

Adeline Boire^{*}, Chloé Amine & Denis Renard

UR1268 Biopolymères Interactions Assemblages, INRA, 44300 Nantes, France

* adeline.boire@inra.fr

Using a droplets-based millifluidic device [1], we successfully map, through turbidity measurements, the phase behavior of a plant protein, rapeseed napin (NAP), mixed with a plant polysaccharide, pectin (PEC). The optimum pH for NAP-PEC interactions was found at pH 4, corresponding to the highest electrostatic contribution between the two biopolymers. Additional optical microscopy performed at pH 4 highlighted a solid-to-liquid phase transition overtime. We showed that charge neutralization is a requisite for the transition as no rearrangement was observed when residual charges remain. In addition, this transition was found to be temperature-dependent suggesting that secondary interactions, such as hydrogen bonds, may play a role in this phenomenon. To the best of our knowledge, such solid-to-liquid transition has never been reported for protein-polysaccharide mixtures. We question the role of protein flexibility in this phenomenon as NAP is predicted to be partially disordered. To test this hypothesis, we used lysozyme (LYZ) which is similar to NAP in terms of size, molecular weight and charge density but more rigid. We showed that kinetics of rearrangement were slowed down in the case of LYS. The polysaccharide rigidity (i.e. persistence length) could also influence time and temperature-dependence of the solid-to-liquid transition even though it was not investigated here.



[1] C. Amine, A. Boire, J. Davy, M. Marquis and D. Renard, Droplets-based millifluidic for the rapid determination of biopolymers phase diagrams, *Food Hydrocolloids* **70**, 234 (2017)

Cells and humans bodies motion and self-organization in architected environments

Maxime Bonnefoy^{a,b,*}

- a. Laboratoire interdisciplinaire de Physique, CNRS – UGA Grenoble
- b. Digital RDL (research by design laboratory), CRESSON – AAU – UGA Grenoble

* bonnefoy.m@univ-grenoble-alpes.fr

I do this communication proposal for the mini-symposium « active fluids and crowd motions » as a PhD student working on a transdisciplinary research in architecture and biology, a research lead at two scales : cells behaviour is studied at the biological scale, and humans behaviour at the architectural scale. What links these two different fields is the intricate relations between a living being and its environment.

We aim to study how a pattern impacts the behaviour of the living beings, based upon three hypothesis: First, we forecast that the observation of the living beings motor expression allows us to identify and to qualify these living – environment links. Then we assume that these behaviours witness the living beings abilities and qualities to perceive their environment and to carry out associated actions. Finally, we propose that from these two scale observations we can establish criteria of how these environments may be qualified by the morphology.

The numerical transition in the midst of which our society is provides new processes useful in both biology and architecture: firstly, to design micro-environments substrates for the mechanical study of cells and secondly, to design and produce computationally complex morphologies. These technological are renewing research thinking toward a collaborative and fruitful work between the two disciplines. Architecture offers to the field of biology a new approach to morphologies and the way they are perceived and experienced (threshold perception, corporal appropriation of space...). In return biology provides to architecture a rigorous protocol to observe spontaneous and self-organising living beings.

As the PhD project started only few month ago, the purpose of this short contribution would be more about sharing ideas and concepts than presenting final results.

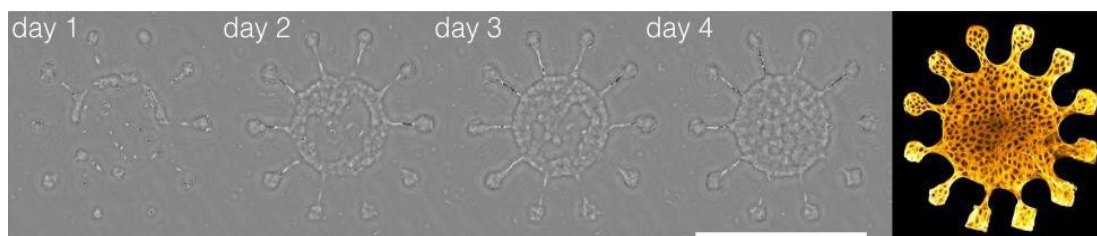


Figure 1 : Illustration of cell population dynamics in micro-architectures. Lenless microscopy give an unprecedented access to the dynamics of population of cells over days. Scale = 2mm.

Electrical conduction properties of diamond nanoneedles, studied by ion spectroscopy in field ion microscopy.

M.Borz¹, I.Blum¹, L.Arnoldi¹, A.Obraztsov^{2,3} and A.Vella¹

Corresponding author : laurent.arnoldi@univ-rouen.fr

¹. Groupe de Physique des Matériaux UMR CNRS 6634, Université et INSA de ROUEN, Université Normandie 76801 SAINT ETIENNE DU ROUVRAY CEDEX France

². University of Eastern Finland, Department of Physics and Mathematics, Joensuu 80101, Finland

³. M. V. Lomonosov Moscow State University Department of Physics, Moscow 119991, Russia

Mono-crystalline diamond needles are quite attractive samples for field emission applications, mainly used as point electron source[1]. Even though the CVD production process of this kind of sample is now quite efficient and reproducible, the performances of these electrons sources can change from one needle to another. These changes could be related to a change in the electrical conduction therefore we used a new experimental setup to study the conduction properties of diamond nanoneedles in a large range of emission currents and under femtosecond laser illumination.

The experimental setup is a field ion microscopy (FIM), equipped with an energy analyzer and a pico-ampere meter, used to measure the emitted ion current at the needle apex and the energy of these emitted ions.

Changing the voltage applied to the nanoneedle, we exhibited two different conduction behaviors: a first regime, at low emission current, which corresponds to the ohmic conduction and a second regime, at high emission current, which corresponds to a Poole-Frenkel (PF) conduction mechanism[2]. The PF effect occurs when a high field is applied inside the material ($\sim 10^5$ - 10^6 V/m) and is strong enough to activate the trapped carriers. As it increases the free carrier density, the resistivity becomes itself a function of the applied field. We discuss the transition between these two conduction mechanisms and its dependence as a function of the emitted current and the needle geometry.

Under femtosecond laser illumination, the resistivity changes and the transition from the ohmic conduction regime to the PF regime is observed at higher emission currents. The study of the changes of the conduction parameters under illuminations allows us to draw conclusion on the optical absorption process of these nanoneedles and on their heating induced by laser illumination.

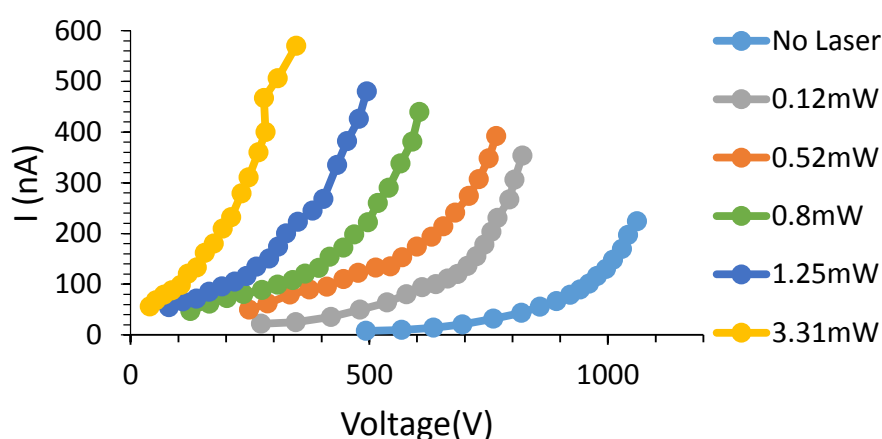


Figure 1: FIM emitted current from a diamond needle as function of the applied voltage. Values measured at 80K for different laser illumination at $\lambda=515$ nm, Neon pressure of $4 \cdot 10^{-5}$ mbar.

[1] V.I.Kleshch et al., "Single Crystal Diamond Needle as Point Electron Source", *Scientific Reports* **6**, Article number: 35260 (2016)

Deposition of hafnium/zirconium oxides solid solution by reactive magnetron sputtering for fast and low power ferroelectric devices

Jordan Bouaziz^{a,b}, Bertrand Vilquin^a, Pedro Rojo Romeo^a, Nicolas Baboux^b,
Bruno Masenelli^b

- a. Université de Lyon, Ecole Centrale de Lyon, Institut des Nanotechnologies de Lyon, CNRS UMR5270, 36 avenue Guy de Collongue, 69134 Ecully cedex, France
- b. Université de Lyon, INSA de Lyon, Institut des Nanotechnologies de Lyon, CNRS UMR5270, 7 avenue Capelle, 69621 Villeurbanne cedex, France

* jordan.bouaziz[a]insa-lyon.fr

IoT sensor node requires edge computing which means processing data at the source. These systems need highly energy efficient microprocessor units (MCU) using embedded non-volatile memories (eNVM). However eFLASH technology is limited by low write speed, high power and low endurance. Alternative fast, low power and high endurance eNVM could greatly enhance energy efficiency. FeRAM has the highest endurance of all emerging NVMs. However perovskite based eFeRAM is incompatible with Si CMOS, it does not easily scale and has manufacturability and cost issues. Recently discovered, doped HfO₂ [1] is a promising candidate to solve these problems. HfO₂ processes are already integrated in Si CMOS industry and its ferroelectric properties are adequate for using oxide layer thinner than 10nm. Nevertheless some of its properties should be improved for industrial applications.

As a consequence, the nucleation and stabilization of the ferroelectric phase (f-phase) has to be understood; the nucleation of the f-phase is attributed to the polar orthorhombic phase (o-III phase), but other phases are generally present inside the oxide after the growth due to stabilization issues [2]. Particularly, the formation of the monoclinic phase has to be avoided to enhance ferroelectricity. The presence of the f-phase has often been studied by Atomic Layer Deposition (ALD) [3].

However, the electrodes are most of the time made by sputtering, and industrial processes to separate Hf and Zr are usually expensive. It could be interesting to have only one process where the separation of Hf and Zr is not needed. Also, sputtering using only one target like Hf/Zr or HfO₂/ZrO₂ could ease co-sputtering for the realization of 1% La-doped Hf_{0.5}Zr_{0.5}O₂ as it shows a low annealing temperature and a very promising endurance and remanent polarization [4].

In 2015, Park et al. [3] wrote: “So far, it seems critical that the dielectric layer is deposited in the amorphous phase and crystallized in a later annealing step.” However, to our knowledge, there was no clear evidence of the phenomenon as films are generally grown amorphous by ALD. In this work, we grow ferroelectric (Hf,Zr)O₂ solid solutions made by reactive RF magnetron sputtering at room temperature and by using only one target. Changing the conditions in the sputtering chamber lead to crystalline or amorphous films at room temperature. We characterize the films by different technics such as X-rays Diffraction and Positive Up Negative Down (PUND) electrical characterization and we give details about the properties of our films and how one can improve their properties.

[1] T.S. Böske, et al., Appl. Phys. Lett. 99, 102903 (2011).

[2] M.H. Park, et al., Nanoscale. 10, 716–725 (2018).

[3] M.H. Park, et al., Adv. Mater. 27, 1811–1831 (2015)

[4] A.G. Chernikova et al., ACS Appl. Mater. Interfaces. 10 (2018) 2701–2708.

Experimental evidences of light superfluidity in a bulk nonlinear crystal

O. Boughdad^a, M. Albert^a, P.É. Larré^b, C. Michel^a and M. Bellec^a

a. Institut de Physique de Nice, Université Côte d'azur, CNRS,

b. Laboratoire de Physique Théorique et Modélisation, Université de Cergy-Pontoise, CNRS

omar.boughdad@unice.fr; claire.michel@unice.fr; bellec@unice.fr

Superfluidity, the ability of a fluid to move without friction along a pipe or past an obstacle is one of the most striking manifestations of the quantum nature of matter. In the few last years quantum hydrodynamics behaviors have been also studied with polaritons in semiconductor microcavities and with photons in nonlinear optics, leading to the emergent research field of quantum fluids of light [1]. Among the various ways of tracking light superfluidity, we propose here to experimentally study how light propagation is affected by the presence of an optical obstacle [2].

We make use of a photorefractive crystal with controllable nonlinear response. A local drop of the optical index is photo-induced by a narrow beam in the crystal and creates the obstacle. Simultaneously, a second, larger monochromatic beam is sent into the crystal and creates the fluid of light. In this configuration, the transition from a nonsuperfluid regime to a superfluid regime is mediated by the ratio v/c_s which is experimentally controlled by the incidence angle θ_{in} and by the input intensity of the fluid-of-light beam. Figure 1 presents spatial distribution of the intensity of the fluid of light measured at the output face of the crystal for various v/c_s . At large v/c_s , diffraction appears in the transverse plane, and progressively manifests as a characteristic cone of fringes upstream from the obstacle. At very low v/c_s , long-range radiation upstream from the obstacle is no longer present, indicating a superfluid motion of light. In this cavityless all-optical system, we extract a direct optical analog of the drag force exerted by the fluid of light and measure the associated displacement of the obstacle. Both quantities drop to zero in the superfluid regime.

The experimental capability to shape both the flow and the potential landscape paves the way for simulation of quantum transport in complex systems.

- [1] I. Carusoto and C. Cuiti, "Quantum fluids of light", Rev. Mod. Phys. **85**, 299 (2013).
 [2] C. Michel, O. Boughdad, M. Albert, P.É. Larré and M. Bellec "Superfluid motion and drag-force cancellation in a fluid of light", accepted in Nature Commun., arXiv:1710.03081 (2017)

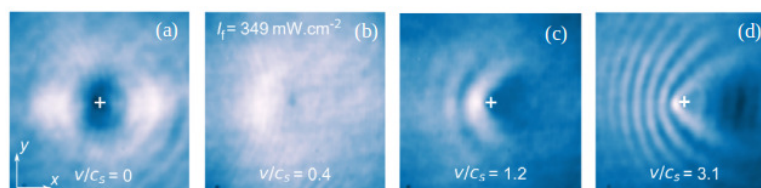


Figure 1: Spatial distribution of the output intensity of the fluid-of-light for various v/c_s

HeteroProtein Complex coacervates: mechanisms and potential applications

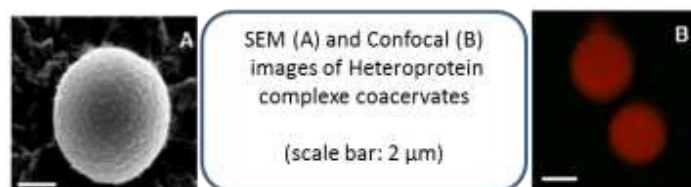
Saïd Bouhallab^{a*}, Thomas Croguennec^a

a. UMR1253, INRA, Agrocampus-Ouest, STLO, 65 rue de Saint-Brieuc, F-35042 Rennes, France

* said.bouhallab@inra.fr

The application of fundamental physicochemical concepts for rational design of functional assemblies from food proteins constitute a response to the growing trend toward the development of new and innovative food products and also an opportunity to generate new protein-based supramolecular structures with new applications. Because of their omnipresence in food systems and their biodegradability, proteins are the focus of many attempts for their use as building blocks for such supramolecular structures. Controlled self- co-assembly of proteins can generate a variety of supramolecular structures that vary in shape, size and density (fibrils, spherulites, nanotubes, etc). For instance, well-defined microspheres called heteroprotein complex coacervates (HPCC) can be formed by control mixing of oppositely charged proteins.¹ The objective of our research is to understand the mechanisms behind HPCC process from initial spontaneous molecular interaction to micro-scale characterization. In this communication, we will summarize our results on several binary protein systems and will show that co-assembly of proteins into complex coacervates (Figure) is a generic process that is, de facto, independent of the protein amino-acid sequence. We will report on the requirements that drive such spontaneous co-assembly: protein conformational state and flexibility, molar stoichiometry, total protein concentration, charge anisotropy, etc. The Research challenges and the promising uses of HPCC in food and non-food sectors (encapsulation of bioactives, design of edible films) will be discussed.

[1] T. Croguennec, G. Miranda-Tavares, S. Bouhallab, S., Heteroprotein complex coacervation: A generic process, *Adv. Colloid Interface Sci.*, 2017, **239**, 115-126.



A single Cr spin in a quantum dot: an efficient spin qubit for hybrid spin mechanical systems

H. Boukari^{a*}, A. Lafuente-Sampietro^{a,b}, M. Sunaga^b, K. Makita^b, S. Kuroda^b, L. Besombes^a

a. Univ. Grenoble Alpes, CNRS, Grenoble INP, Institut Neel - 38000 Grenoble, France

b. University of Tsukuba, Institute of Materials Science - Tsukuba, 305-8573 Japan

* herve.boukari@neel.cnrs.fr

Incorporating single magnetic atoms in semiconducting quantum dots (QDs) is a promising route to fabricate hybrid spin-mechanical systems where the optical properties of the QDs are coupled to the spin states of the magnetic atoms through exchange interaction. The incorporation of Chromium (Cr) in II-VI compounds is of particular interest because Cr enters the II-VI matrix as a Cr^{2+} ion with a spin $S=2$ and an angular momentum $L=2$. In this case, the spin-orbit interaction connects the spin of the Cr to its local strain environment through the modification of the crystal field. Optical probing and some optical control of the spin of a single Cr atom incorporated in a CdTe/ZnTe QD was recently demonstrated [1,2]. There, the spin to strain coupling is more than two orders of magnitude larger than for elements without orbital momentum like NV centers in diamond or Mn atoms in II-VI QDs. Thus, strain induced by mechanical excitations such as surface acoustic waves (SAW) are seen as a very efficient way to coherently drive the spin of single Cr atoms. Before that, one has to develop optical technique to control single spins and deeply understand the dynamics of those spins.

We analyze here the source of spin relaxation for a single Cr atom inserted in a CdTe/ZnTe QD. We demonstrate that the spin of a Cr atom can be prepared by resonant optical pumping. Using this preparation technique, we show that efficient hole-Cr flip-flops dominate the exciton-Cr spin dynamics [3]. This spin flip mechanism appears in the excitation power dependence of the photoluminescence (PL) intensity distribution of the exciton at zero field and under a longitudinal magnetic field. A model confirm that hole-Cr flip-flops in the nanosecond range are induced by the interplay of the hole-Cr exchange interaction and the coupling to the strain field of acoustic phonons.

We also present resonant PL experiments that directly evidence this spin-flip process. The distribution of the PL intensity under resonant excitation shows that there is an efficient transfer from the Cr spin states $S_z=+1$ to $S_z=0$. We show that this transfer, responsible for the optical pumping of the Cr spin under resonant excitation, is induced by the hole-Cr flip-flops. Monitoring the time dependence of the resonant PL intensity under modulated excitation permits to probe the dynamics of the optical initialization of the Cr spin, which takes place in a few tens of nanoseconds.

In addition to the dynamics induced by carrier-Cr exchange coupling, we finally demonstrate, using a spatially resolved two-wavelength pump-probe experiment, that a Cr spin significantly interacts with non-equilibrium acoustic phonons generated during the optical excitation inside or near the QD.

[1] A. Lafuente-Sampietro, H. Utsumi, H. Boukari, S. Kuroda, L. Besombes, Phys. Rev. B 93, 161301(R) (2016).

[2] A. Lafuente-Sampietro, H. Utsumi, H. Boukari, S. Kuroda, and L. Besombes, Phys. Rev. B 95, 035303 (2017).

[3] A. Lafuente-Sampietro, H. Utsumi, M. Sunaga, K. Makita, H. Boukari, S. Kuroda, L. Besombes, Physical Review B. 97, 155301 (2018).

Neutron Resonance Spin Echo or how to get a high-energy resolution in a triple-axis spectrometer.

F. Bourdarot^{a*}

a. Université Grenoble Alpes, CEA, INAC, MEM MDN, F-38000 Grenoble, France France

* bourdaro@ill.fr

Neutron scattering spectroscopy is an advanced method for studying the dynamics of condensed matter. In physics, the study of dispersive excitations such as phonons and magnons is an important experimental data in many materials (HTc superconductors, thermoelectric, magnetic systems). These dispersive excitations are traditionally studied by inelastic neutron scattering on three-axis spectrometer (TAS), as well their lifetime which is given by the inverse of the width of the measured excitation. Accessible widths are typically of the order of 0.5 to 1 meV, which corresponds to lifetimes of a few picoseconds, i.e relatively short lifetimes. In order to measure much longer lifetimes, a new method, combining the neutron resonance spin-echo technique (NRSE) and TAS, has been developed over the past fifteen years. This method of spin-echo focusing, proposed by F. Mezei[1], makes possible to measure the widths of the dispersive excitations in the solids throughout the Brillouin zone with a resolution of a few μeV , thus improving the typical TAS resolution of about 2 orders a magnitude. On IN22, it has made possible to improve the energy resolution from 1.1meV to $1\mu\text{eV}$ for non-dispersive excitations and to $10\mu\text{eV}$ for dispersive excitations, thus allowing access to lifetimes on the order of one hundred pico-second, much more interesting for the physics of condensed matter. During the presentation, we will show what it has been possible to measure by this technique that can not be achieved by other techniques. In particular, the measurement of acoustic phonon lifetimes in an intermetallic clathrate $\text{Ba}_{7.81}\text{Ge}_{40.67}\text{Au}_{5.33}$, finding large values of phonon lifetime which spectacularly falsify the theoretical expectation[3].

- [1] F. Mezei ed. Neutron Spin Echo, Lecture Notes in Physics, Volume **128**, Berlin Heidelberg New York, Springer Verlag, (1980)
- [2] Direct measurement of individual phonon lifetimes in the clathrate compound $\text{Ba}_{7.81}\text{Ge}_{40.67}\text{Au}_{5.33}$, P.-F. Lory et al., Nat. Commun. **8**, 491 (2017)

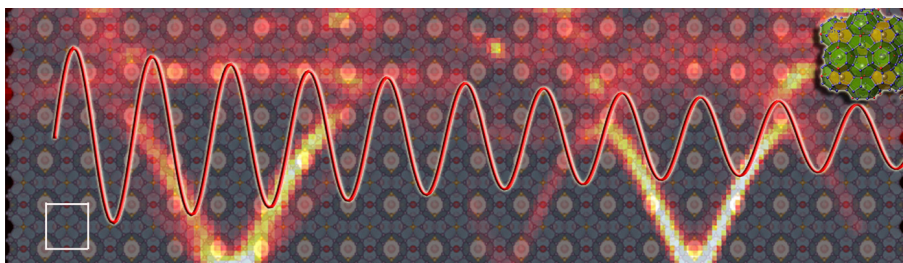


Figure 1: Illustration of the phonon lifetime in a Clathrate. The red-white colour illustrates the measured phonon dispersion relationship, whereas the red sinusoid illustrates an acoustic phonon decaying with time for a mean free path of 25 nm

Tunable spin-valley physics in a silicon quantum bit

Léo Bourdet^{a*} and Yann-Michel Niquet^a

a. *University Grenoble Alpes, CEA, INAC-MEM, 38000 Grenoble, France*

* leo.bourdet@cea.fr

The electron spin in silicon has shown to be a prime candidate for quantum computing thanks to its excellent coherence properties due to the magnetic-free environment and the low spin-orbit coupling (SOC) in the conduction band. However recent experiments [1] have demonstrated electrical manipulation of the electron spin in a silicon nanowire CMOS device using SOC. Here comes a difficult challenge: how to keep the coherence properties and still be able to couple the spin to the electric field?

We propose an answer that relies on the spin-valley mixing which is controlled by tuning the valley splitting with the potential applied on the back electrode (Fig 1.). This allows to adiabatically go from a spin qubit, where quantum coherence is long, to a valley qubit, where manipulation is efficient. We will review our model for SOC and electrical manipulation and validate it against realistic tight-binding simulations and experimental data. Then to assess the validity of the approach we study the effect of noise (charge and phonon) and surface roughness variability in both modes. This approach can be implemented in other type of devices, provided that they respect specific criteria, opening new possibilities for the design of robust and electrically addressable silicon qubits.

- [1] A. Corna *et al*, Electrically driven electron spin resonance mediated by spin-valley-orbit coupling in a silicon double quantum dot, *npj Quantum Information* **4**, 6 (2018)
- [2] L. Bourdet and Y.-M. Niquet, All-electrical manipulation of silicon spin qubits with tunable spin-valley mixing, arXiv:1802.04693 (2018)

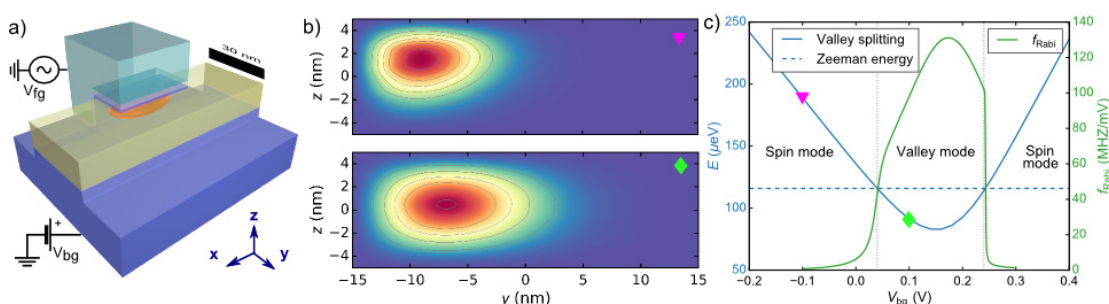


Figure 1: (a) 3D geometry of the device included in the simulations with schematic of the wavefunction. (b) Wavefunction density computed in tight-binding in the spin (up) and valley (bottom) modes. (c) Rabi frequency between the two lowest states and valley splitting as a function of potential. Manipulation is efficient only in the valley mode i.e when the valley splitting is lower than the Zeeman energy.

Building a biodegradable implant out of silk fibroin to support neuro-regeneration after severe brain injuries

Antoine Bourrier^{a*}, Benoit Charlot^b, Frederic Saudou^c David Kaplan^d

- a. Laboratoire des Technologies de la Microelectronique - CNRS/UGA/CEA, Grenoble
- b. Grenoble Institut des Neurosciences, Inserm/UGA, Grenoble
- c. Institut d'Electronique des Systèmes, CNRS, Montpellier.
- d. Department of Biomedical Engineering, Tufts University, Medford, MA, USA.

*antoine.bourrier@cea.fr

Hospitals daily face the tremendous number of strokes or large brain trauma victims that suffer from blood brain barrier disruption, causing large disturbances in brain tissue. Once stabilized, those patients face motor disorder with a low rehabilitation rate.

Today progresses in neurons regeneration understanding [1] and recent advances in that field at GIN Grenoble demonstrate the positive incidence of light, mechanical and biochemical stimulation on the speed and success of axonal regrowth.

Used for centuries as a stitching material, silk fibroin is a natural protein, extracted from bombyx mori cocoons, that can be assembled into films, hydrogels or sponges. It's an FDA approved biocompatible and biodegradable material, that is thus a material of growing interest to build implantable devices carrying physical and biological functions [2].

By gathering light stimulation, mechanical guidance and biochemical activity on a rolled-up fibroin film/hydrogel 3D implant, we aim at building and testing an axonal highway to support large network rehabilitation in vivo. By reconnecting disturbed brain layers together, this technology might improve patients recovery after dramatic brain injuries.

[1] B.Zhou, Facilitation of axon regeneration by enhancing mitochondrial transport and rescuing energy deficits. *J Cell Biol.* 2016 Jul 4;214(1):103-19

[2] DL Kaplan, Silk as a Biomaterial, *Prog Polym Sci.* 2007; 32(8-9): 991–1007

Superconductivity in boron-doped diamond. Phase diagram revisited by thickness-dependent transport studies

J. Bousquet^{a,b*}, M. Solana^{a,b}, F. Jomard^c, L. Saminadayar^{a,b}, C. Marcenat^{d,e}, E. Bustarret^{a,b} and T. Klein^{a,b}

- a. Univ. Grenoble Alpes, Inst NEEL, F-38042 Grenoble, France
- b. CNRS, Inst. NEEL, F-38042 Grenoble, France
- c. GEMaC, UVSQ and CNRS, 45 avenue des Etats-Unis, 78035 Versailles, France
- d. Univ. Grenoble Alpes, INAC-SPSMS, F-38000 Grenoble, France
- e. CEA, INAC-SPSMS, F-38000 Grenoble, France

* jessica.bousquet12@gmail.com

Since its discovery [1], the superconductivity of boron-doped diamond has been intensively investigated and a large number of experimental studies reported results suggesting the standard electron-phonon coupling mechanism to be at the origin of the superconducting state. However, all the studies [2-4], carried out on different crystalline orientation, reports an electronic phase diagram with a square root dependence of the critical temperature T_c with the boron content $T_c \propto ([B]/[B]_{c,s} - 1)^{0.5}$. This behaviour, which is far from the exponential law expected from the BCS theory, has been tentatively attributed to the proximity of the Metal-to-Insulator-Transition (MIT) which coincides with the superconducting onset $[B]_{c,s} = [B]_{c,MIT}$ in this system.

In 2010 [5], a similar square root dependence of T_c has been observed in boron-doped silicon films but, in this latter one, $[B]_{c,s}$ is almost 1000 times higher than $[B]_{c,MIT}$ and T_c strongly depends on the thickness of the Si:B layers [6].

Motivated by the similarity between the two systems, we have undertaken a new detailed study of the electronic properties of boron-doped diamond at the vicinity of the Superconducting-to-Insulator transition (SIT). Magneto-transport measurements were carried out on series of samples with a boron content ranging from 1.10^{20} to 3.10^{21} cm⁻³ and thickness varying from 5 nm to 3 μ m. By using a well-defined mesa-structured Hall-bar geometry, we have been able to reduce the parasitic currents induced by local doping fluctuations, and to obtain a new phase diagram differing from the one so far [6]. In this latter one, a new metallic and non-superconducting state has been unveiled between the MIT and the onset of superconductivity and the dependence of T_c with the doping content was found to be more consistent with the BCS theory, assuming however a reduced value of the Coulomb pseudopotential μ^* .

- [1] E. A. Ekimov et al., Superconductivity in diamond, *Nature* **425**, 6982 (2004)
- [2] E. Bustarret et al., Dependence of the Superconducting transition temperature on the doping level in Single-crystalline Diamond films, *Phys. Rev. Lett.* **93**, 237005 (2004)
- [3] T. Klein et al., Metal-Insulator transition and superconductivity in Boron-doped diamond, *Phys. Rev. B.* **75**, 165313 (2007)
- [4] A. Kawano et al., Superconductor-to-Insulator transition in Boron-doped diamond films grown using Chemical Vapour Deposition, *Phys. Rev. B.* **81**, 085318 (2010)
- [5] C. Marcenat et al., Low-temperature transition to a superconducting phase in boron-doped silicon films grown on (001)-oriented silicon wafers, *Phys. Rev. B.* **81**, 020501 (2010)
- [6] A. Grockowiak et al., Thickness dependence of the superconducting critical temperature in heavily doped Si:B epilayers, *Phys. Rev. B.* **88**, 064508 (2013)
- [7] J. Bousquet et al., Phase diagram of boron-doped diamond revisited by thickness-dependent transport studies, *Phys. Rev. B(R)*, **95**, 161301 (2017)

High harmonic generation in 2D and 3D semiconductors

Willem BOUTU

Ultrafast Nanophotonics Group
LIDYL/Attophysics Laboratory
CEA Saclay, France

Ultrafast nano-photonics science is emerging thanks to the extraordinary progresses in nano-fabrication and ultrafast laser science. Nanotechnology enables the engineering of photonic structures at the nanometer scale for enhancing light-matter interaction, which can be exploited in a number of photonic applications. Our research is motivated by the novel fundamental processes occurring while a semiconductor is submitted to a strong laser field. Electrons start to oscillate in coherence and are accelerated by the laser field in the Brillouin zone. After recombination, high order harmonics are emitted, carrying with them precious information about the fundamental process¹⁻³. Strategies to boost and control at a nanoscale this coherent phenomenon are of recent focus⁴⁻⁶. We propose new routes in boosting the non-linear response using nanostructured photonic crystals. Here, we demonstrate field amplification through light confinement in ZnO nano-structured 3D waveguides. Using our novel “nano-amplifiers”, we have observed the amplification of high harmonics from mi-infrared laser-crystal interaction by up to 2 orders of magnitude. Compared to previous works⁶, we extend enhancement of high harmonic to the highly non-perturbative regime. Amplification of up the 15th harmonic order is reported⁷. Nanostructuring semiconductors offers also the possible to control the high harmonic generation light properties. We will present strategies to manipulate the orbital angular momentum of light.

Finally, we investigate high harmonic generation in 2D semiconductors. Graphene has attracted significant attention in recent years due to its extraordinary mechanical, electronic and optoelectronic properties. High harmonic generation from graphene on substrate has been reported for the first very recently⁸. Here, we report for the first time on the generation of high harmonics from free-standing graphene. We study the laser polarization dependence of the harmonics to reveal the impact of the band-gap opening induced by the substrate.

1. Ghimire, S. *et al.* Observation of high-order harmonic generation in a bulk crystal. *Nat. Phys.* **7**, 138–141 (2011).
2. Luu, T. T. *et al.* Extreme ultraviolet high-harmonic spectroscopy of solids. *Nature* **521**, 498–502 (2015).
3. Ndabashimiye, G. *et al.* Solid-state harmonics beyond the atomic limit. *Nature* **534**, 520–523 (2016).
4. Han, S. *et al.* High-harmonic generation by field enhanced femtosecond pulses in metal-sapphire nanostructure. *Nat. Commun.* **7**, 13105 (2016).
5. Vampa, G. *et al.* Plasmon-enhanced high-harmonic generation from silicon. *Nat. Phys.* **13**, 659–662 (2017).
6. Sivis, M. *et al.* Tailored semiconductors for high-harmonic optoelectronics. *Science* **357**, 303–306 (2017).
7. Franz *et al.* submitted to Science Advances [arXiv:1709.09153](https://arxiv.org/abs/1709.09153)
8. Naotaka Yoshikawa, Tomohiro Tamaya, Koichiro Tanaka, *Science* **356**, 736–738 (2017).

Dimensionality driven enhancement of ferromagnetic superconductivity in URhGe

Daniel Braithwaite^{*a}, Dai Aoki^{a,b}, Jean-Pascal Brison^a, Jacques Flouquet^a, Georg Knebel^a, Ai Nakamura^b, Alexandre Pourret^a.

a. Univ. Grenoble Alpes and CEA, INAC-PHELIQS, F-38000 Grenoble, France

b. Institute for Materials Research, Tohoku University, Oarai, Ibaraki 311-1313, Japan

* daniel.braithwaite@cea.fr

We report an experimental study applying uniaxial stress and magnetic field at very low temperature on the ferromagnetic superconductor URhGe. This system is famous for the co-existence of superconductivity and ferromagnetism at ambient pressure, but also for its remarkable phase diagram under magnetic field. When a field is applied along the b-axis, transverse to the easy magnetization c-axis, two separate pockets of superconductivity exist, one at low field, and a re-entrant superconducting phase appearing under field. Here we show that uniaxial stress can spectacularly modify the phase diagram, pushing the high field superconductivity pocket to lower fields so that it reconnects to the low-field superconducting phase. This implies that the field H_R where the magnetic moments rotate from the easy axis to align with the field is strongly suppressed by stress. Simultaneously superconductivity is significantly enhanced and the critical temperature at high field reaches 1K, twice higher than at ambient pressure, while the critical temperature at zero field also increases. This enhancement of superconductivity is directly related with the increase of the magnetic susceptibility perpendicular to the easy axis, and to a reduction of the ferromagnetic anisotropy. This provides novel input for theories of superconductivity in correlated ferromagnetic materials and many perspectives for future experimental studies.

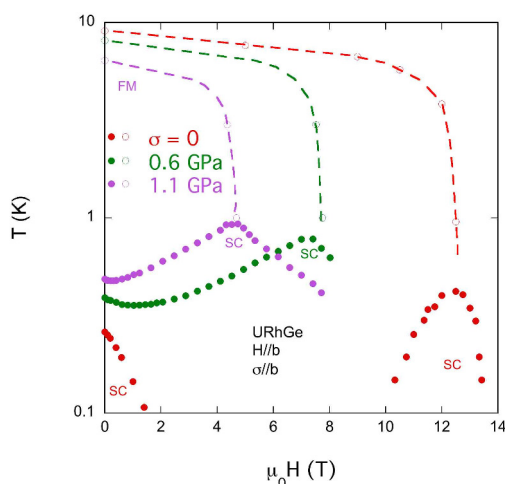


Figure 1 : Ferromagnetic and superconducting T-H phase diagram of URhGe for different values of uniaxial stress applied along the b-axis

Le GN-MEBA : le réseau des utilisateurs de MEBs et Microsondes et de leurs accessoires.

François Brisset^{a*}, Florence Robaut^b, et Philippe Jonnard^c

- a. ICMMO, CNRS – Université Paris-Saclay, 91400 Orsay.
- b. SIMAP - Grenoble INP, BP75, 38402 Saint-Martin d'Hères
- c. LCPMR, CNRS – Sorbonne Université, 75005 Paris

* francois.brisset@u-psud.fr

A la demande de la SFP et pour renforcer les liens entre les 2 communautés, le GN-MEBA [1], Groupement National de Microscopie Electronique à Balayage et Microanalyses, division thématique de la SFP, propose un mini-colloque. Au cours de cette présentation, un état des activités du GN-MEBA sera proposé. Cela ira des journées pédagogiques, permettant de présenter les connaissances de base mises à jour en microscopie électronique à balayage et microanalyses, aux journées thématiques, permettant de présenter les avancées dans un domaine donné, en passant par les écoles d'été organisées par le groupement. Un point sera fait sur les ouvrages publiés par les experts du domaine et édités par le GN-MEBA [2]. Les enquêtes et les échantillons tests (grands moments concernant la maîtrise des équipements) seront évoqués. Enfin, quelques exemples de réalisations mettant en avant les capacités des équipements seront également présentés avant les conférences spécialisées qui suivront.

[1] www.gn-meba.org

[2] www.gn-meba.org/ouvrages.htm



Figure 1 : Photo de groupe de l'école d'été du GN-MEBA ayant eu lieu à Bordeaux en 2017. Environ 200 personnes ont assisté aux cours en amphi et aux TD à l'aide de 23 colonnes électroniques (http://www.gn-meba.org/ec_ete/ec_ete.htm).

Microswimmer's motion in a complex environment

Marvin Brun-Cosme-Bruny^{a*}, Philippe Peyla, et Salima Rafai

a. LIPhy, 140 Rue de la Physique, 38402 Saint-Martin-d'Hères

* marvin.brun-cosme-bruny@univ-grenoble-alpes.fr

The microalga *Chlamydomonas Reinhardtii* is used here as a model system to study the effect of complex environments on microswimmer's motion. Its motion can be modeled by Runs & Tumbles so that it describes a persisted random walk where we can extract an analogous diffusion coefficient. To model a complex medium in our experiments, series of pillars are designed in a regular lattice by means of soft lithography microfabrication where cells are introduced. Their swimings are then tracked and analysed within the pillars.

Relevant statistical observables allowed us to quantify the bias involved by the presence of pillars for which we only varied the inter-pillar distance or pillars density. Particularly, as the interpillar-distance is shortened, the mean persistence length gets shorter, so does the diffusion coefficient. This provides the first bases of understanding on active matter in complex environments.

Moreover, their collective motion can be used as a model of wet crowd, where hydrodynamic interactions are predominant, unlike most of crowd usual models (humans, sheeps, hants) mostly interacting by contact and "social" forces. Further more, phototaxis is a specific characteristic of *Chlamydomonas* that allows us to mimic a crowd in a panic and observe collective rushes towards a light source, inducing clogging near constrictions. These experiments on chip give new means of comparison (hydrodynamic versus contact interactions) to get a better understanding of crowd motion in a panic.

Quantitative study of the adsorption / desorption of CO₂ molecules at {100} ceria surfaces *via* atomic scale Environmental Transmission Electron Microscopy (ETEM) and Diffuse Reflectance FT-IR Spectroscopy (DRIFTS)

Matthieu Bugnet^{a*}, Steven H. Overbury^b, Zili L. Wu^b, Francisco Cadete Santos Aires^c, Frederic Meunier^c, Thierry Epicier^a

^a University of Lyon, INSA-Lyon, UCBL Lyon 1, MATEIS, UMR 5510 CNRS, 69621 Villeurbanne Cedex, France.

^b Chemical Science Division, Center for Nanophase Materials Science, Oak Ridge National Laboratory, Oak Ridge, Tennessee 37831, USA.

^c University of Lyon, UCBL Lyon 1, IRCELYON, UMR 5256 CNRS, 69100 Villeurbanne, France.

* matthieu.bugnet@insa-lyon.fr

Transmission electron microscopy (TEM) is a well-established characterization technique to combine bulk and surface analysis of solids at the nanoscale. With a dedicated Environmental TEM (ETEM), the effect of the atmosphere on the reactivity of surfaces exposed to gas and temperature can be investigated *in situ*.

Our work focuses on ceria (CeO₂), a fundamentally interesting and technologically important catalyst and catalyst support [1]. With a strong tendency to be reduced under the electron beam, CeO₂ is also a challenging material in a High Vacuum (HV) TEM column, and offers a perfect field of play for redox state control in the ETEM. Whereas the redox properties of CeO₂ have been widely studied in the TEM using electron energy-loss spectroscopy (EELS), in-depth atomic scale surface analysis under environmental conditions is lacking and is now addressed here.

CeO₂ nanocubes [3] were observed in a dedicated Cs-corrected FEI Titan ETEM, equipped with a high-speed CMOS Gatan OneViewTM camera. In situ diffuse reflectance FT-IR spectroscopy (DRIFTS) was also performed using a setup described elsewhere [4].

The mobility of Ce and O atoms is monitored using high resolution TEM under various atmospheres, i.e. HV, O₂ and CO₂. A home-made image processing routine was developed to track and quantify the intensity of Ce columns, then the atomic mobility directly evidenced using video recording of atomic resolution 4Kx4K images at 25 fps [5]. The Ce mobility in HV is significantly higher on {001} surfaces than on other low-index {110} and {111} facets appearing at the edges of the nanocubes. Furthermore, the mobility decreases when the atmosphere changes from HV to O₂, then decreases even further when CO₂ is adsorbed on the surface as confirmed by EELS. The effect of temperature on the surface mobility under HV, O₂ and CO₂ is also investigated *in situ*. Significant differences in carbonate desorption temperatures were observed by DRIFTS between unreduced and reduced ceria, which are compared to ETEM results.

These findings open a field of study for direct visualization and control of atomic scale phenomena at surfaces such as adsorption and desorption of molecular species.

[1] A. Trovarelli, *Catalysis by Ceria and Related Materials*, Imperial College Press, London (2002).

[2] R. Wang et al., *Nano Lett.* **8** 962 (2008).

[3] Z. Wu et al., *Langmuir*, **26** 16595-16606 (2010).

[4] D. Lorito et al., *Appl. Catalysis B*, **197** 56-61 (2016).

[5] M. Bugnet et al., *Nano Letters*, **17** 7652-7658 (2017).

Integrated motions of molecular machines and motors: Small-angle scattering studies

Giacomo Mariani^a, Nicolas Jouault^a, Antoine Goujon^b, Jean-Rémy Colard-Itté^b, Emilie Moulin^b, Nicolas Giuseppone^b, and Eric Buhler^{a*}

- a. Matière et Systèmes Complexes Laboratory (MSC), UMR 7057, University Paris Diderot-Paris 7, Bâtiment Condorcet, 75205 Paris Cedex 13, France
 b. Institut Charles Sadron (ICS), University of Strasbourg, 23 rue du Loess, BP 84047, 67034 Strasbourg Cedex 2, France

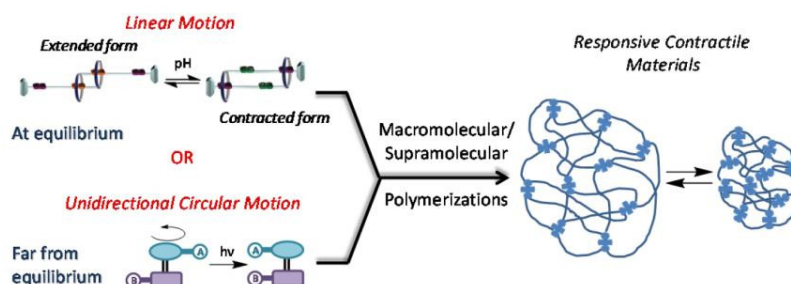
* eric.buhler@univ-paris-diderot.fr

Switchable functional molecules capable of producing mechanical work constitute an active focus in nanotechnologies as they can be a source of components for molecular-based devices and materials. In particular, the dynamic nature of mechanically interlocked molecules allows their components to undergo relative internal movements, which can be exploited in translation and circumrotation. When it comes to using molecular machines to facilitate the creation of materials on the macro-scale, the primary concern is whether the nano-sized machines will be able to amplify their mechanical behavior to create a response in the bulk material. Hence, one of the most fundamental and challenging objectives associated to nano-machines rests on their coupling (in space and time) in order to transfer controlled motions from the molecular arena to the supramolecular and macroscopic scale.

In the present work, we have developed two kinds of responsive contractile polymeric materials: i) The first one concerns nano-machines linked into a supramolecular polymer in which we produced micrometric motions (contraction/extension) by the integration of thousands of single contractile nano-switches by altering the pH of the solution; just like myofibrils do when packed in bundles in muscles. ii) The second one is based on the connection of light-driven rotary motors with the possibility to make them functioning far from equilibrium and acting as reticulation units in an entangled polymer network.

Small-angle neutron scattering (coupled with light and X-ray scattering) has been used to investigate the structure of the supramolecular self-assemblies of nano-machines before and after the induced structural changes as well as the dynamics of the contraction process at different length and time scales. We discuss here the relation between the local and overall structure of the self-assemblies and the properties of the materials [1]. We show that these findings open up new possibilities of using molecular machines in smart responsive materials.

[1] G. Mariani, A. Goujon, E. Moulin, M. Rawiso, N. Giuseppone, E. Buhler *Nanoscale* **2017**, *9*, 18456–18466, Integration of molecular machines into supramolecular materials: actuation between equilibrium polymers and crystal-like gels



Gold nanoparticles SPRi enhanced signal for small molecules detection with split aptamers

Arnaud Buhot^{a*}, Ferial Melaine^a, Clothilde Coihlac^a and Yoann Roupioz^a

a. Univ. Grenoble Alpes, CEA, CNRS, INAC-SyMMES, F-38000 Grenoble, France

* arnaud.buhot@cea.fr

Aptamers are single-stranded DNA or RNA molecules capable of binding to target molecules like proteins, metal ions or drugs. Due to their specific binding affinities and other advantages compared to antibodies (higher stability, lower cost, easy chemical modification...), they provide a great opportunity to produce sensing surfaces for effective and selective detection of small molecules.

Surface Plasmon Resonance imaging (SPRi) has become one of the most widely used label-free method for the study of bio-recognition events on surfaces. This technique provides a rapid approach, however, limited in sensitivity by low refractive index changes occurring when small molecules (<500 Da) are captured on the biosensor. Whereas significant reflectivity variation are observed upon the interaction of large molecules like proteins to the sensing interface, for small targets such as adenosine, the reflectivity variation is often too small to be detected by SPRi. Thereby, only few studies have been reported SPRi-based biosensor for small molecules detection using aptamers.

We developed a bioassay based on three different but compatible and complementary strategies [1, 2]: 1/ the engineering of split aptamer sequences adapted from the adenosine model aptamer, 2/ the use of gold nanoparticles for Surface Plasmon Resonance amplification signal and 3/ the thermodynamic stability of the complex formed to quantify the small molecule adenosine.

The experimental results have demonstrated that the combined strategies allow us to obtain state-of-the-art detection limit below 50nM. Furthermore, the determination of the melting temperatures of the complex formed by the split aptamers and the adenosine targets open the door for an access to the thermodynamical parameters.

[1] F Melaine, Y Roupioz, A Buhot, **Microarrays** **4**, 41-52 (2015).

[2] F Melaine, C Coihlac, Y Roupioz, A Buhot, **Nanoscale** **8**, 16947-16954 (2016).

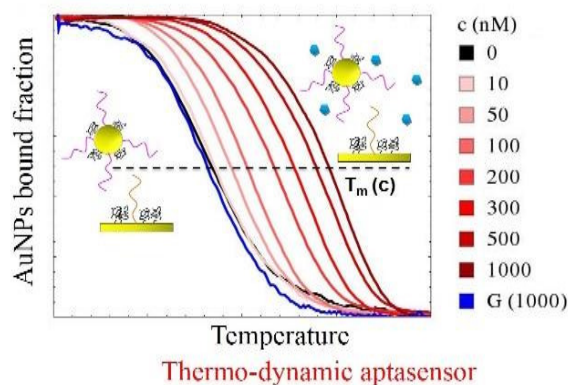


Figure 1: Adenosine detection from melting temperature shift of split-aptamer functionalized AuNP.

Anisotropic Kondo pseudo-gap and Hidden Order in URu₂Si₂

J. Buhot^{a,b,*}, X. Montiel^c, Y. Gallais^b, M. Cazayous^b, A. Sacuto^b, G. Lapertot^d, D. Aoki^{e,d}, N. E. Hussey^a, C. Pépin^f, S. Burdin^g, M.-A. Méasson^{h,b}

- a. High Field Magnet Laboratory (HFML-EMFL), Institute for Molecules and Materials, Radboud University Nijmegen, Toernooiveld 7, 6525 ED Nijmegen, The Netherlands.
- b. Laboratoire Matériaux et Phénomènes Quantiques, UMR 7162 CNRS, Université Paris Diderot, Bât. Condorcet 75205 Paris Cedex 13, France.
- c. Department of Physics, Royal Holloway, University of London, Egham, Surrey TW20 0EX, UK.
- d. Université Grenoble Alpes, CEA, INAC, PHELIQS, F-38000 Grenoble, France.
- e. Institute for Materials Research, Tohoku University, Oarai, Ibaraki 311-1313, Japan.
- f. Institut de Physique Théorique, CEA-Saclay, 91191 Gif-sur-Yvette, France.
- g. Université Bordeaux, CNRS, LOMA, UMR 5798, F 33400 Talence, France.
- h. Institut NEEL CNRS/UGA UPR2940, MCBT, 25 rue des Martyrs BP 166, 38042 Grenoble cedex 9, France.

* jonathan.buhot@ru.nl

While the Kondo effect is well understood for single Kondo impurity systems, for Kondo lattice systems containing rare-earth elements (for which the Kondo impurities are realized by local f electron orbitals), it remains more puzzling and exhibits surprising phenomena [1, 2]. For instance, anisotropic orbital-dependent hybridization may have significant consequences for the entire phase diagram of these systems [3]. The heavy fermion URu₂Si₂ that exhibits one of the most mysterious quantum states of matter below 17.5 K, the so-called “hidden order” (HO) state, is a relevant example of metallic Kondo lattice systems for which exotic Kondo effects may play a significant role in the appearance of the HO. Despite over three decades of intensive research, no consensus has yet been found regarding the microscopic nature of the HO. Recent efforts have revealed important information on this problem, including the A_{2g} signatures of the HO state as seen by Raman spectroscopy [4, 5]. While the URu₂Si₂ “story” appears close to being resolved, some key issues remain, such as the inter-relation between the Kondo coherent regime and the HO state.

Here, we present a Raman polarized study of the Kondo physics of single crystalline URu₂Si₂ [6]. We observe a symmetry dependence of the electronic Raman response through the Kondo crossover (100K), with a Kondo pseudo-gap developing mainly in the E_g symmetry, highlighting the presence of strong anisotropy. Thanks to Raman vertex calculations (in agreement with our observations), we provide the k -space dependence of the Kondo pseudo-gap showing a d -wave like geometry. Such anisotropy has not been predicted and has never been taken into account in theoretical models until now. Moreover, the Kondo pseudo-gap opening is found to be reinforced at low temperatures, within the HO state, suggesting that Kondo physics may play an important role as a precursor to the HO state. Finally, the anisotropy of the pseudo-gap is similar in form to that proposed for the chiral d -wave (E_g) superconducting state that appears below $T_c = 1.5$ K.

[1] Yang et al., PNAS 109, E3060 (2012)

[2] Lonzarich et al., ROPP 80, 024501 (2017)

[3] Weber et al., PRB 77, 125118 (2008)

[4] Buhot, et al., PRL 113, 266405 (2014)

[5] Kung et al., Science 347, 1339 (2015)

[6] Buhot et al., submitted (2018)

High fidelity qubit readout using a V-shaped transmon in a 3D cavity

R. Dassonneville, L. Planat, J. Puertas, S. Leger, K. Bharadwaj, F. Foroughi, C. Naud, W. Guichard, N. Roch, O. Buisson^{a,b}

^aUniversity Grenoble Alpes, Institut Néel, F-38000 Grenoble, France.

^bCNRS, Institut Néel, F-38000 Grenoble, France.

* olivier.buisson@neel.cnrs.fr / nicolas.roch@neel.cnrs.fr

Using the transverse dispersive coupling between a qubit and a microwave cavity is the most common read-out technique in circuit-QED. However, despite important progresses, implementing a fast high fidelity readout remains a major challenge. Indeed, inferring the qubit state is limited by the trade-off between speed and accuracy due to Purcell effect and unwanted transitions induced by readout photons in the cavity. To overcome this, we introduce a circuit with a V-shaped energy spectrum coupled to a 3D-cavity [1,2]. This circuit presents one transmon qubit with a large intrinsic longitudinal coupling to an anharmonic mode, called ancilla mode. This ancilla mode results from the hybridization between the microwave cavity and the V-shape circuit. Longitudinal coupling is a key point to our readout scheme since such a coupling is immune to Purcell effect. We will present qubit readout performance using this 3D V-shaped transmon inserted in a cavity with fidelity as high as 97%. We will also discuss the quantum non-demolition properties of this novel readout as function of the readout photons number.

R. Dassonneville is supported by the CFM recherche foundation. This work is supported by the French Agence Nationale de la Recherche (ANR-CE24-REQUIEM).

[1] É. Dumur, et al, Phys. Rev. B 92, 020515(R) (2015).

[2] É. Dumur, et al, IEEE Trans. On Appl. Supercond. 26, 1700304 (2016).

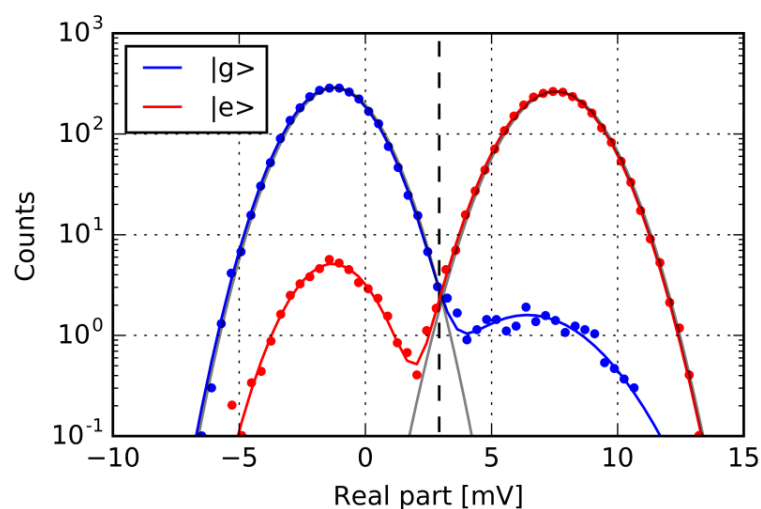


Figure 1: Histograms of single shot readout signal measured during 500ns when the qubit is prepared in the ground (blue) or excited state (red). Here the fidelity of this readout is about 97%.

Biomimetic approaches to blood cells/vascular walls interactions

Lionel Bureau^{a*}, Daria Tsvirkun^b, Mehdi Inglebert^a, Alain Duperray^c, Chaouqi Misbah^a, Heather S. Davies^a, Nouha El Amri^a, Claude Verdier^a, Delphine Débarre^a, and Ralf P. Richter^d

- a. Laboratoire Interdisciplinaire de Physique, Grenoble, France
- b. Research Center for Obstetrics, Gynecology and Perinatology, Moscou, Russie
- c. Institut pour l'Avancée des Biosciences, Grenoble, France
- d. Schools of Biomedical Sciences & Physics and Astronomy, University of Leeds, UK

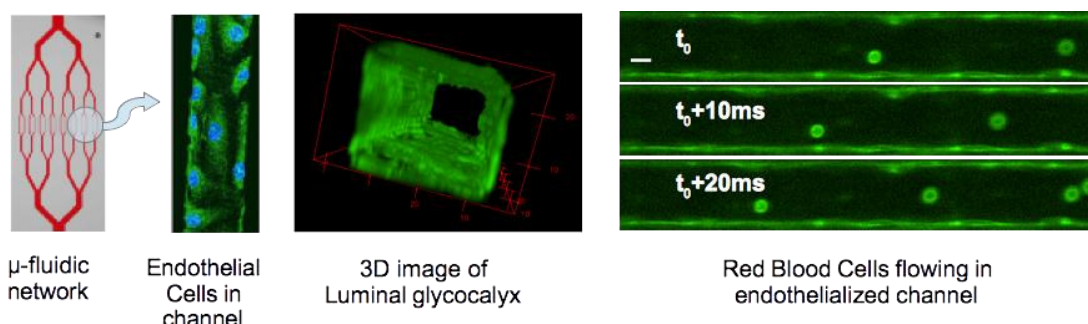
* lionel.bureau@univ-grenoble-alpes.fr

Interactions between circulating cells and blood vessel walls are central to many physiological processes such as the early stages of the immune or inflammatory response, gas exchanges with tissues, or vascular remodeling. A key player in regulating such processes is the so-called endothelial glycocalyx, a soft and μm -thick layer of biomacromolecules lining the lumen of blood vessels. While the glycocalyx is recognized as the primary « gatekeeper » of the vascular walls, its mechanical role in controlling the adhesive and hydrodynamic interactions with flowing cells is far from being elucidated.

In this talk, I will present the biomimetic strategies developed at LIPhy to address this issue. Combining microfluidics with endothelial cell culture, we create microvasculatures-on-a-chip, which we have shown to recapitulate in vitro the nature of the blood vessel surface and some of the salient features of microconfined flow of red blood cells [1]. In a complementary approach, we use well-controlled biopolymer layers in order to mimic the glycocalyx and study how such layers affect the motion of particles flowing nearby [2]. I will discuss how these experimental strategies help us to better understand the physics of cell/wall interactions in blood flows.

[1] D. Tsvirkun et al. Microvasculature on a chip: study of the Endothelial Surface Layer and the flow structure of Red Blood Cells, *Sci. Rep.* **7**, 45036 (2017)

[2] H. S. Davies et al. Elastohydrodynamic lift at a soft wall, *Phys. Rev. Lett.* **120**, in press (2018)



Dispersive charge density wave excitations in $\text{Bi}_2\text{Sr}_2\text{CaCu}_2\text{O}_{8+\delta}$

L. Chaix^{a,b,*}, G. Ghiringhelli^{c,d}, Y. Y. Peng^c, M. Hashimoto^e, B. Moritz^a, K. Kummer^f, N. B. Brookes^f, Y. He^g, S. Chen^g, S. Ishida^h, Y. Yoshida^h, H. Eisaki^h, M. Salluzzoⁱ, L. Braicovich^{c,d}, Z.-X. Shen^{a,g}, T. P. Devereaux^{a,g} and W.-S. Lee^a

- a. Stanford Institute for Materials and Energy Sciences, SLAC National Accelerator Laboratory and Stanford University, 2575 Sand Hill Road, Menlo Park, California 94025, USA.
- b. Institut Néel, CNRS-UGA, F-38042 Grenoble, France.
- c. Dipartimento di Fisica, Politecnico di Milano, Piazza Leonardo da Vinci 32, I-20133 Milano, Italy.
- d. CNR-SPIN, CNISM, Politecnico di Milano, Piazza Leonardo da Vinci 32, I-20133 Milano, Italy.
- e. Stanford Synchrotron Radiation Lightsources, SLAC National Accelerator Laboratory, 2575, Sand Hill Road, Menlo Park, California 94025, USA.
- f. European Synchrotron Radiation Facility (ESRF), BP 220, F-38043 Grenoble Cedex, France.
- g. Geballe Laboratory for Advanced Materials, Stanford University, Stanford, California 94305, USA.
- h. National Institute of Advanced Industrial Science and Technology (AIST), Japan.
- i. CNR-SPIN, Complesso Monte Sant'angelo, Via Cinthia, I-80126 Napoli, Italy.

* laura.chaix@neel.cnrs.fr

Uncovering the mechanism of high temperature superconductivity in cuprates remains an important question in condensed matter physics. While spin fluctuations may be crucial for forming superconductivity in cuprates [1], abundant experimental observations also demonstrate a strong electronic coupling to the lattice [2, 3]. It is still debating whether the phonons also play a role in the pairing mechanism. Resonant inelastic X-ray scattering (RIXS) measurements on cuprate compounds provide opportunities to probe both magnetic and charge excitations in the energy and momentum space, which may shed new light on the cuprate problems [4, 5, 6].

In this study, we performed ultrahigh energy resolution RIXS in the soft x-ray regime on the heavily underdoped cuprate superconductor $\text{Bi}_2\text{Sr}_2\text{CaCu}_2\text{O}_{8+\delta}$ (Bi-2212). In the quasi-elastic region, an incommensurate charge density wave (CDW) was confirmed. Importantly, this RIXS study revealed signatures of dispersive CDW excitations that emanate from the CDW wavevector and intersect with bond-stretching phonons, causing an anomalously enhanced phonon intensity at a wavevector away from the CDW wavevector [7]. Temperature dependent measurement will be also shown.

- [1] – D. J. Scalapino, *Rev. Mod. Phys.* **84**, 1383–1417 (2012)
- [2] – A. Lanzara, *et al.*, *Nature* **412**, 510 (2001)
- [3] – W. Meevasana, *et al.*, *Phys. Rev. Lett.* **96**, 157003 (2006)
- [4] – M. Le Tacon, *et al.*, *Nature Phys.* **7**, 725–730 (2011)
- [5] – W. S. Lee, *et al.*, *Nature Phys.* **10**, 883–889 (2014)
- [6] – W. S. Lee *et al.*, *Phys. Rev. Lett.* **110**, 265502 (2013)
- [7] – L. Chaix, *et al.*, *Nature Phys.* **13**, 952–956 (2017)

Structural and optical properties of $\text{Sr}_x\text{Cd}_{1-x}\text{F}_2$ mixed fluoride: an ab-initio study

Z. Chouahda, L.Tairi , R. Khemissi, H. Meradji and S. Ghemid

Laboratoire de Physique des Rayonnements
Université Badji Mokhtar, Annaba, Algérie.

Keywords: Mixed fluorides $\text{Sr}_x\text{Cd}_{1-x}\text{F}_2$, Insulators, Wide band gap, DFT, FP-LAPW, Optical properties.

The first-principle calculations are performed to study the structural and optical properties of $\text{Sr}_x\text{Cd}_{1-x}\text{F}_2$ mixed fluoride using the full potential-linearized augmented plane wave method (FP-LAPW) [1,2] implemented in the code WIEN2K within the density functional theory (DFT) [3]. In this approach the Wu-Cohen generalized gradient approximation (WC-GGA) [4-6] was used for the exchange-correlation potential. The supercell is generated with the parent fluoride structure of CdF_2 . The ground-state properties have been calculated. Equilibrium lattice constant and bulk modulus are estimated. The optical properties such as the real and imaginary parts of dielectric function, optical reflectivity, absorption coefficient, optical conductivity, refractive index, extinction coefficient and electron energy loss are performed for the energy range of 0-40 eV. The studied properties are reported for the first time for $\text{Sr}_x\text{Cd}_{1-x}\text{F}_2$.

References

- [1] P. Blaha, K. Schwarz, P. Sorantin, S.B. Trickey, *Comput. Phys. Commun.* **59** (2), 399 (1990)
- [2] P. Blaha, K. Schwarz, G.K.H. Madsen, D. Kvasnicka, J. Luitz J, *WIEN2K, an augmented planewave plus local orbitals program for calculating crystal properties.* Vienna (2008)
- [3] J.P. Hohenberg, *Phys. Rev.* (1964), **B36**, 864
- [4] Z. Wu., R.E. Cohen, *Phys. Rev. B*, **73**(23), 2116 (2006)
- [5] E. Engel, S.H. Vosko, *Phys. Rev. B*, **47**(20), 13164 (1993)
- [6] F. Tran, P. Blaha, *Phys. rev. letter*, **102**(22), 226401(2009)

Rheology of a Gold Meniscus of Few Atoms

J. Comtet^{a*}, A. Lainé,^a A. Niguès,^a L. Bocquet,^a A. Siria,^a

a. Laboratoire de Physique Statistique, ENS, Paris, France

* jean.comtet@gmail.com

In this talk, we probe plasticity at the individual atomic level by measuring the viscoelastic rheological response of a gold neck of few atoms radius, submitted to picometric oscillations. Shearing the bridge with increasing amplitude, we uncover a dramatic transition from a purely elastic regime to a plastic flow regime, up to the complete shear-induced melting of the bridge. Varying the lateral junction size through a change in conductance, we study the dependence of those distinct rheological regimes on the junction geometry. In those molecular objects, plastic flow seems to be limited by the sliding of atomic planes under shear, as predicted for dislocation free systems, while the dissipative regime is well-described by a viscous-like frictional force, distinct from traditional plasticity models.

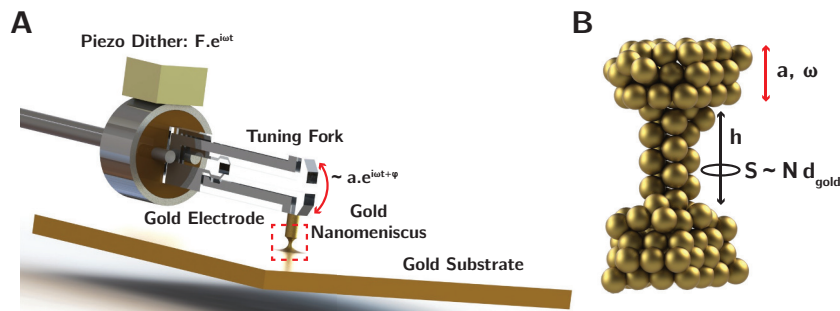


Figure 1: (A) Schematic of the experimental set-up. A gold junction (red dashed box) is formed between a gold electrode, attached to the tuning fork and the gold substrate. A piezo dither excites the tuning fork with an oscillatory force $F^* = F \cdot e^{i\omega t}$, leading to an oscillation amplitude $a^* = a \cdot e^{i\omega t + \phi}$ of the the gold electrode and tuning fork. (B) Schematic representation of the idealized junction geometry, for $N = G/G_0 \approx 4$. The junction is assumed to have a rod-like shape with height h and surface area $S \sim N d_{\text{gold}}$.

Modeling the thermal stability of core-shell Iron-Gold nanoparticles

Florent Calvo^{a*}, Magali Benoit,^b Nicolas Combe,^b and Joseph Morillo^b

a. LiPhy, CNRS and University Grenoble Alpes

b. CEMES, Toulouse

florent.calvo@univ-grenoble-alpes.fr

Iron and gold do not easily mix in bulk phases. At the nanoscale, core-shell iron-gold nanoparticles are potentially useful owing to the magnetic properties of iron and the biocompatibility of surrounding gold. In this contribution we explore the stable structures of small iron-gold nanoparticles at finite temperature by means of computational modeling. A many-body empirical potential of the embedded-atom family was designed using ingredients for the individual metals, and fitted to reproduce density-functional theory data for impurities in bulk or clusters materials as well as surface energies and intermetallics.

Core-shell nanoparticles containing a few thousand atoms were modeled assuming a cubic iron core with bcc symmetry surrounded by a gold shell of fcc symmetry, keeping an epitaxial relationship at the (100) contact between the two metals. Using exchange Monte Carlo simulations, the thermal stability of so prepared nanostructures was investigated and the core-shell phase segregation found to prevail even beyond the melting range.¹

In contrast, using the alternative potential previously proposed by Zhou and coworkers² we find that the nanoparticles readily transform into randomly mixed cubic structures already at room temperature.

[1] F. Calvo, M. Benoit, N. Combe and J. Morillo, *J. Phys. Chem. C* **121**, 4680-4891 (2017).

[2] X. W. Zhou, R. A. Johnson, J. N. G. Walley, *Phys. Rev. B* **69**, 144113 (2004).

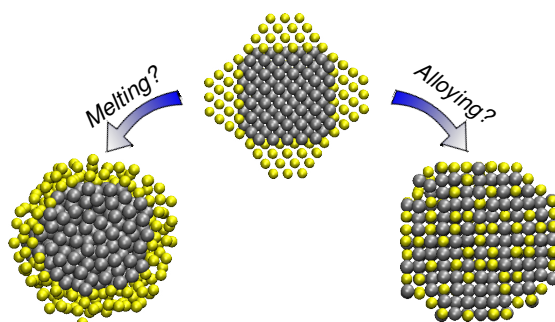


Figure 1: How do core-shell iron-gold nanoparticles melt in the computer?

Reconstituting *in vitro* the remodeling of membrane nanotubes by actin dynamics

Antoine Allard^{a,b}, Guillaume Lamour^a, Sid Labdi^a, Cécile Sykes and Clément Campillo^{a*}

a. Université Evry Val d'Essonne, LAMBE, Boulevard F Mitterrand, Evry 91025, France

b. Institut Curie, PSL Research University, CNRS, UMR 168, 75005 Paris, France

* clement.campillo@univ-evry.fr

Inside living cells, the remodeling of membrane nanotubes by the dynamics of acto-myosin networks is crucial for processes such as intracellular traffic or endocytosis. However, the mechanisms by which acto-myosin dynamics affect nanotube morphology are largely unknown. How much radial and axial forces are generated on the tube by acto-myosin dynamics? Can these forces lead to nanotube scission? How do they relate to the structure of the acto-myosin network? To address these questions, we perform *in vitro* experiments to decipher the physics of nanotube remodeling in biochemically controlled assays recapitulating key aspects of cellular membranes and actin dynamics. We use two complementary techniques to form membrane nanotubes on which we reconstitute acto-myosin networks from purified proteins. By using optical tweezers, we will measure the forces implied in nanotube formation and maintenance in presence of acto-myosin. In parallel, we develop a novel assay to image supported nanotubes and acto-myosin networks polymerizing on such nanotubes at the nanometric scale by using Atomic Force Microscopy. By combining these two techniques, we investigate how the structure of the acto-myosin network at the nanometric scale dictates tube reshaping at the micrometric scale and how this explains the results obtained in cells. This will shed new light on nanotube shape regulation and deepen our understanding of cellular functions.

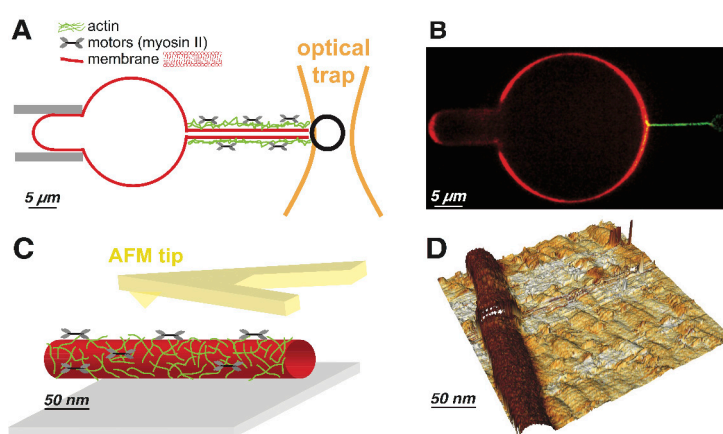


Figure 1 A) Sketch of an acto-myosin network surrounding a membrane nanotube extruded from a liposome with an optical tweezer. B) Fluorescent micrograph of a nanotube on which actin polymerizes C) Scheme of the AFM observation of nanotubes able to trigger a reconstituted acto-myosin network D) AFM imaging of a membrane nanotube formed close to a substrate.

The Neurophysics of Ion Channels : Merging Cutting-Edge Imaging techniques with Computational Neuroscience to Disclose Ion Channel Functioning in Neurons

Marco Canepari^{a,b,c*}

- a. Laboratory for Interdisciplinary Physics, UMR 5588 CNRS and Université Grenoble Alpes, 38402 Saint Martin d'Hères, France.
- b. Laboratories of Excellence, Ion Channel Science and Therapeutics, France.
- c. Institut National de la Santé et Recherche Médicale (INSERM), France.

* marco.canepari@univ-grenoble-alpes.fr

The function of neuron in its multiple compartments is governed by several biophysical parameters including morphology and the expressed proteins in the membranes and in the cytoplasm. These factors determine the generation of action or synaptic potentials and their propagation, as well as the underlying chemical signaling. Yet, dedicated experimental and theoretical methods are necessary to disclose the complexity of electrical and chemical signals and to understand the activity of individual channels cooperating to generate a global function in neuronal compartments. Here I will present a cutting-edge imaging approach, based on combined electrophysiology, membrane potential imaging and ultrafast calcium imaging, which allows tracking the activity of voltage-gated calcium channels in neuronal dendrites from ex-vivo preparations, as well as their biophysical regulation by membrane potential changes [1,2]. I will then show some optical recordings of fast calcium currents, associated with backpropagation of action potentials in the apical dendrite of the CA1 hippocampal pyramidal neuron, and I will illustrate how the resulting calcium signals are finely regulated by the synergy of different types of voltage-gated calcium channels [3]. This pure experimental analysis of calcium currents reveals only a part of the physiological scenario since also other channels, in particular potassium channels, participate to the cooperation that shapes both the membrane potential and the calcium signal. To overcome this limitation we use a computational framework based on NEURON (<https://www.neuron.yale.edu/neuron/>) to analyse our experimental data and disclose the kinetics of all ion channels underlying a given physiological signal. Thus, I will finally present an unpublished research in which we used this novel approach of combining our advanced imaging methods with computational tools based on NEURON modelling to precisely reconstruct the kinetics of all dendritic calcium and potassium associated with the climbing fibre synaptic potential in the cerebellar Purkinje neuron.

- [1] N. Jaafari, M. De Waard, and M. Canepari, Imaging Fast Calcium Currents beyond the Limitations of Electrode Techniques. *Biophys. J.* **107**,1280-1288 (2014)
- [2] N. Jaafari, E. Marret, and M. Canepari, Using simultaneous voltage and calcium imaging to study fast Ca²⁺ channels. *Neurophotonics* **2**, 021010 (2015)
- [3] N. Jaafari, and M. Canepari, Functional coupling of diverse voltage-gated Ca(2+) channels underlies high fidelity of fast dendritic Ca(2+) signals during burst firing. *J. Physiol.* **594**, 967-983 (2016)

FeSi : a novel building-block for iron-based superconductivity

F. Bernardini,^a G. Garbarino,^b A. Sulpice,^c M. Núñez-Regueiro,^c E. Gaudin,^d
B. Chevalier,^d M.-A. Méasson,^c A. Cano,^{c,d} and S. Tencé^d

- a. Dipartimento di Fisica, Università di Cagliari, IT-09042 Monserrato, Italy
- b. European Synchrotron Radiation Facility, 6 rue Jules Horowitz, 38043 Grenoble, France
- c. CNRS, Université Grenoble Alpes, Institut Néel, 38042 Grenoble, France
- d. CNRS, Univ. Bordeaux, ICMCB, UPR 9048, F-33600 Pessac, France

* andres.cano@cnrs.fr

Iron-based materials provide the latest platform for high-temperature unconventional superconductivity [1]. In these superconductors, the Fe atom is invariably associated to pnictogen (As, P) or chalcogen (Se, S, Te) elements, with the only and intensively debated exception of YFe₂Ge₂ [2,3]. This circumstance raises the important fundamental question about the link between Fe-based superconductivity and the apparent need of these pnictogens and chalcogens [3]. At the same time, to escape from such harmful and/or comparatively scarce As- or Se-like elements is highly desirable for applications.

In the talk I will introduce the new material LaFeSiH [4], which is first silicide that surpasses traditional pnictide and chalcogenide compounds as Fe-based superconductors, and discuss some of its physical properties. These include superconductivity with onset at 11 K, and its coexistence with antiferromagnetic order and orthorhombic distortion already in the parent phase.

- [1] See e.g. H. Alloul and A. Cano (Guest Editors), Iron-based superconductors, C. R. Physique 17, 1 (2016) ; and the references therein.
- [2] J. Chen et al., Unconventional Superconductivity in the Layered Iron Germanide YFe₂Ge₂, PRL 116, 127001 (2016).
- [3] H. Kim et al., Crystal growth and annealing study of fragile, non-bulk superconductivity in YFe₂Ge₂, Phil. Mag. 95, 804 (2015) ; D. Guterding et al., Nontrivial Role of Interlayer Cation States in Iron-Based Superconductors, PRL 118, 017204 (2017).
- [4] F. Bernardini, G. Garbarino, A. Sulpice, M. Núñez-Regueiro, E. Gaudin, B. Chevalier, A. Cano, and S. Tencé, Iron-based superconductivity extended to the novel silicide hydride LaFeSiH, PRB 97 100504(R) (2018).

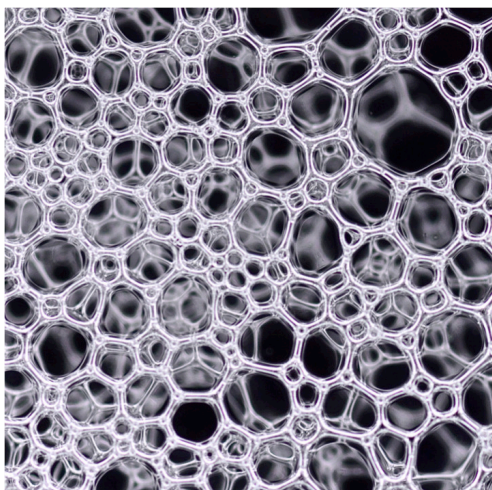
Marangoni effects and foam films

Isabelle Cantat

Univ Rennes, CNRS, IPR (Institut de Physique de Rennes) - UMR 6251, F- 35000
Rennes.

isabelle.cantat@univ-rennes1.fr

Surface tension gradients induce flows, known as Marangoni flows. They play an enhanced role in systems with a large amount of free interfaces, such as foams, emulsions and thin liquid films. In such systems, the interfaces are deformable and the stress at the interface is usually unknown, making the prediction of the flow difficult. We produce controlled deformations of a liquid structure made of few films connected to each other by menisci, and measure films thickness maps and velocity fields to determine the nature of the flow in the structure. This is an important step to understand the origin of the especially high effective viscosity of liquid foams.



- [1] *Extension of a suspended soap film: A homogeneous dilatation followed by new film extraction.*
J. Seiwert, M. Monloubou, B. Dollet, I. Cantat. *Phys. Rev. Lett* **111**, p. 094501 (2013).
- [2] *Theoretical study of the generation of soap films: role of interfacial visco-elasticity.*
J. Seiwert, B. Dollet, I. Cantat. *J. Fluid. Mech.* **739**, pp. 124-142 (2014).
- [3] *Velocity field in a vertical foam film.*
J. Seiwert, R. Kervil, S. Nou, I. Cantat. *Phys. Rev. Lett.* **118** p. 048001 (2017).

Numerical Quality Control for DFT-based Materials Databases

Christian Carbogno^{a*}, Kristian Sommer Thygesen^b, Björn Bieniek^a, Claudia Draxl^{c,a},
Luca Ghiringhelli^a, Andris Gulans^c, Oliver T. Hofmann^d, Karsten W. Jacobsen^b,
Sven Lubeck^c, Jens Jørgen Mortensen^b, Mikkel Strange^b, Elisabeth Wruss^d,
and Matthias Scheffler^a

- a. Fritz-Haber-Institut der Max-Planck-Gesellschaft,
Faradayweg 4–6, D-14195 Berlin, Germany
- b. Center for Atomic-scale Materials Design (CAMD), Department of Physics,
Technical University of Denmark. Fysikvej 1 2800 Kgs. Lyngby, Denmark
- c. Physics Department and IRIS Adlershof,
Humboldt-Universität zu Berlin, Zum Großen Windkanal 6, D-12489 Berlin, Germany
- d. Institute of Solid State Physics,
Graz University of Technology, NAWI Graz, Petergasse 16, 8010 Graz, Austria

* carbogno@fhi-berlin.mpg.de

Density-functional theory (DFT) has become an invaluable tool in materials science. Recently, the precision of different approaches has been scrutinized for the PBE functional using extremely accurate numerical settings [1]. However, little is yet known about code- and method-specific errors that arise under more commonly used numerical settings, e.g. in *high-throughput* calculations. This constitutes a severe issue, since it prevents repurposing DFT data created using different settings and/or codes, for instance the calculations stored in the NOMAD [2] or other repositories [3,4,5].

To overcome this, we study the convergence of different properties (geometries, total and relative energies) in four conceptually-different DFT codes (exciting, FHI-aims, GPAW, and VASP) for typical settings used in production calculations. Specifically, we discuss relative and absolute errors as a function of the numerical settings, e.g., basis sets and **k**-grids, for 71 elemental solids [1]. Using this data, we propose an analytical model that allows for error estimates for *any* compound, as we explicitly demonstrate for 73 binary and ternary solids. We show how the developed formalism can be incorporated into electronic structure theory databases so that data created using different settings and/or codes becomes quantitatively comparable [6], e.g., so to use it in machine-learning approaches. Eventually, we discuss the extensibility of our approach towards more complex materials properties.

- [1] K. Lejaeghere, *et al.*, *Science* **351**, aad3000 (2016).
- [2] L. M. Ghiringhelli, *et al.*, *NPJ Computational Materials* **3**, 46 (2017).
- [3] C. E. Calderon, *et al.*, *Comput. Mater. Sci.* **108**, 233 (2015).
- [4] A. Jain, *et al.*, *APL Materials* **1**, 011002 (2013).
- [5] J. E. Saal, *et al.*, *JOM* **65**, 1501 (2013).
- [6] <https://analytics-toolkit.nomad-coe.eu/>

Analogue quantum simulation of wormholes and exotic spacetimes

Carlos Sabín^{a*}

a. Instituto de Física Fundamental, Consejo Superior de Investigaciones Científicas, Serrano 113-bis 28006 Madrid (Spain)

* csl@iff.csic.es

Quantum simulators are becoming increasingly popular as non-universal quantum computers with the potential of proving the long-sought quantum supremacy. An alternate approach is to consider them as useful tools to explore the frontiers of physics, ranging from open problems in well-established theories such as quantum field theory to untested physics whose observability is hard or dubious.

Wormholes or Einstein-Rosen bridges are compelling mathematical objects appearing in some solutions of Einstein's General Relativity equations. Since they provide a bridge between distant regions of spacetime, they have attracted a great deal of attention from a foundational viewpoint as well as at a pedagogical level. They might contain closed timelike curves (CTCs), which are also interesting for Quantum Computing applications, since they would boost the capabilities of quantum computers. Moreover, wormholes can be "black hole mimickers".

We present several schemes for analog quantum simulation of spacetimes containing traversable wormholes. First, a suitable spatial dependence in the external bias of a dc-SQUID array mimics the propagation of light in a 1D wormhole background. The impedance of the array places severe limitations on the type of spacetime that we can implement. However, we find that wormhole throat radius in the sub-mm range are achievable. The quantum fluctuations of the phase due to the impedance might be seen as an analogue of Hawking's chronology protection mechanism. We will discuss as well possible applications of these techniques to different spacetime metrics of interest such as Gödel, Alcubierre and Kerr.

Alternatively, we propose a recipe for the simulation in a Bose-Einstein condensate, both in $1+1$ D and $3+1$ D. While in the former case it is enough to modulate the speed of sound along the condensate, in the latter case we need to choose particular coordinates, namely generalized Gullstrand-Painlevé coordinates. For weakly interacting condensates, in both cases we present the spatial dependence of the external magnetic field which is needed for the simulation, and we analyze under which conditions the simulation is possible with the experimental state-of-the-art.

- [1] C. Sabín, Quantum simulation of traversable wormhole spacetimes in a dc-SQUID array Phys. Rev. D. **94**, 081501(R) (2016).
- [2] J. Mateos, C. Sabín Quantum simulation of traversable wormhole spacetimes in a Bose-Einstein condensate Phys. Rev. D. **97**, 044045 (2018).
- [3] C. Sabín, One-dimensional sections of exotic spacetimes with superconducting circuits arXiv: 1707.07439.

High-throughput studies in computational solid-state physics: a review

Jesús Carrete^{a*}

a. Institute of Materials Chemistry, TU Wien, A-1060 Vienna, Austria

* jesus.carrete.montana@tuwien.ac.at

While high-throughput studies are a relatively recent development in the context of materials science as a whole, they are also mature enough that a set of defining traits can be identified. This contribution aims to provide an overview of the field including its history, features, main achievements and most important open challenges.

The starting point is a review of the earliest attempts at high-throughput studies of solid-state systems, but more importantly of their notable predecessors in theoretical chemistry. This is followed by an analysis of the factors that made the current wave of high-throughput research possible.

On this background, the talk then presents a sketch of the main ingredients that define high-throughput studies in our field today. Special emphasis is put on the largest international projects that have emerged as a natural consequence of those general ideas. A small survey of studies showcasing the implementation and consequences of this approach are discussed in some detail.

The last part of the talks deals with the main barriers to further development of high-throughput studies, from both a scientific and a technical perspective, and with the sometimes tense relationship with conventional attitudes in material science.

Analog models of gravity: quantum simulating fundamental theories in condensed matter and optical systems

Iacopo Carusotto*

INO-CNR BEC Center and Università di Trento, 38123 Povo, Italy

* iacopo.carusotto@unitn.it

In this introductory talk I will review the basic concepts underlying the physics of the so-called analog models of gravity and, more in general, the recent developments in the use of condensed matter and optical systems to quantum simulate problems of high energy and gravitational physics [1,2].

After a brief historical review of the general concept of analog model, I will summarize the most promising systems that are presently under experimental investigation in this context, among which surface waves on classical fluids, sonic excitations in superfluids of ultracold atoms and of photons, and nonlinear optical systems. For each of these systems, I will illustrate my view on the main recent achievements and the most challenging open questions.

A special attention will be paid to the analog Hawking radiation, that is the emission of correlated pairs of quanta by the horizon of an analog black hole out of the zero-point quantum fluctuations. The mathematical analogy with quantum field theory of curved space-times will be highlighted, as well as the rich new features that are characteristic of condensed matter and optical systems.

I will conclude with a sketch of the most exciting new perspectives of the field. On one hand, I will show how analog models are suggesting new configurations where quantum hydrodynamics effects can be experimentally investigated and entanglement of macroscopic hydrodynamic degrees of freedom generated and manipulated. On the other hand, I will illustrate the latest advances in the investigation of the back-reaction effects of quantum fluctuations onto the underlying space-time metric and I will present simple toy-models of this physics that may provide some new insight into very challenging black hole evaporation phenomena.

[1] C. Barceló, S. Liberati, M. Visser, *Liv. Rev. Relativity* **14**, 3 (2011)

[2] I. Carusotto and R. Balbinot, *Nat. Phys. News & Views*, Aug. 2016

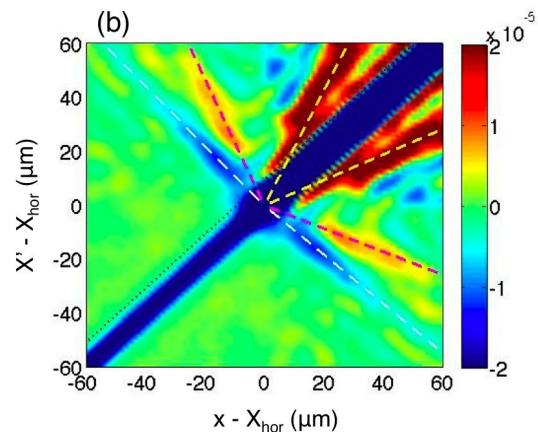


Illustration 1: Light intensity correlations in the emission from a quantum fluid of light displaying an analog black hole horizon. Signatures of analog Hawking radiation are highlighted. Figure from Gerace and Carusotto, PRB 86, 144505 (2012)

Efficient approach for a fully quantum dynamics from first principles: application to protonated water clusters

Michele Casula^{a*}, F. Mouhat^a, S. Sorella^b, R. Vuilleumier^c, and M. Saitta^a

- a. IMPMC, Sorbonne Universités, CNRS UMR7590, IRD UMR206, MNHN, 4 Place Jussieu, 75252 Paris, France
- b. International School for Advanced Studies (SISSA), Via Bonomea 26, 34136 Trieste, Italy
- c. PASTEUR, Département de chimie, École normale supérieure, Sorbonne Université, CNRS, PSL Research University, 75005 Paris, France

* michele.casula@upmc.fr

We introduce [1] a novel and efficient approach for a fully quantum description of coupled electron–ion systems from first principles. It combines the very accurate quantum Monte Carlo solution of the electronic part with the path integral formalism for the quantum nuclear dynamics. In order to cope with the intrinsic noise due to the stochastic nature of quantum Monte Carlo methods, we generalize the path integral molecular dynamics using a Langevin thermostat correlated according to the covariance matrix of quantum Monte Carlo nuclear forces. Our general algorithm relies on a Trotter breakup between the dynamics driven by ionic forces and the one set by the harmonic interbead couplings. The latter is exactly integrated, even in the presence of the Langevin thermostat, thanks to the mapping onto an Ornstein–Uhlenbeck process. This framework turns out to be very efficient in the case of noiseless (deterministic) ionic forces as well. The new implementation is validated on the Zundel ion (H_5O_2^+) and applied to the protonated water hexamer [2], showing unexpected quantum nuclear features, expected to be relevant also for liquid water.

[1] Félix Mouhat, Sandro Sorella, Rodolphe Vuilleumier, Marco Saitta, and Michele Casula, Fully Quantum Description of the Zundel Ion: Combining Variational Quantum Monte Carlo with Path Integral Langevin Dynamics, *Journal of Chemical Theory and Computation* **13**, 2400 (2017)

[2] article in preparation

Dynamiques de spin dans les pyrochlores iridates $\text{Ho}_2\text{Ir}_2\text{O}_7$ et $\text{Dy}_2\text{Ir}_2\text{O}_7$

V. Cathelin^{a*}, E. Lefrançois^{a,b,c}, E. Lhotel^a, J. Robert^a, P. Lejay^a, F. Damay^d,
L.C. Chapon^{b,e}, R. Ballou^a, V. Simonet^a

- a. Institut Néel-CNRS, Grenoble, France
- b. Institut Laue-Langevin, Grenoble, France
- c. Institut Max Planck, Stuttgart, Allemagne
- d. Laboratoire Léon Brillouin, Saclay, France
- e. Diamond Light Source, Didcot, UK

* vadim.cathelin@neel.cnrs.fr << V. Cathelin >>

Les oxides de pyrochlore iridates sont des matériaux de formule $R_2\text{Ir}_2\text{O}_7$. Ces composés sont formés de deux réseaux pyrochlores interpénétrés, l'un de ces réseaux portant les ions iridium, l'autre les ions terre-rare (R). Pour la plupart des ions terre-rare, le réseau iridium s'ordonne dans un arrangement magnétique "all-in all-out" à environ 100 K, et engendre un champ moléculaire orienté selon les directions locales $\langle 111 \rangle$ sur le réseau terre-rare (voir [1]). Quand $R = \text{Ho}$ ou Dy , ce champ magnétique entre en compétition à très basse température avec les interactions ferromagnétiques R - R .

Nous avons montré que dans $\text{Ho}_2\text{Ir}_2\text{O}_7$ cette compétition génère de la fragmentation magnétique, phase dans laquelle les moments magnétiques fragmentent, conduisant à la superposition d'une phase magnétique ordonnée et d'une autre fluctuant continûment (voir [2]). De cette phase émergent des excitations, appelées monopoles magnétiques, qui évoluent dans un potentiel périodique, induit par le réseau iridium. Cela aboutit à une dynamique non conventionnelle qui diffère des spin-ice canoniques.

Lors de ma présentation, je montrerai que $\text{Dy}_2\text{Ir}_2\text{O}_7$ stabilise aussi une phase fragmentée et j'accentuerai sur les dynamiques lentes à très basse température mesurées en susceptibilité alternative entre 80 mK et 4 K. En effet, les temps de relaxation peuvent être décrits par une loi d'Arrhenius dans chacun des systèmes présentés mais avec différents temps caractéristiques et barrières d'énergies.

- [1] Anisotropy-Tuned Magnetic order in Pyrochlore Iridates, E. Lefrançois, V. Simonet, R. Ballou, E. Lhotel, A. Hadj-Azzem, S. Kodjikian, P. Lejay, P. Manuel, D. Khalyavin, and L. C. Chapon, Phys. Rev. Lett. **114**, 247202 (2015);
- [2] Fragmentation in spin ice from magnetic charge injection, E. Lefrançois, V. Cathelin, E. Lhotel, J. Robert, P. Lejay, C. V. Colin, B. Canals, F. Damay, J. Ollivier, B. Fåk, L. C. Chapon, R. Ballou and V. Simonet, Nature Commun. **8**, 209 (2017).

Single-atom-resolved probing of lattice gases in momentum space

H. Cayla¹, C. Carcy², Q. Bouton¹, R. Chang¹, G. Carleo², M. Mancini¹ and D. Clement^{1*}

¹*Laboratoire Charles Fabry, IOGS, CNRS,
Universite Paris-Saclay, 91127 Palaiseau cedex, France*

²*Institute for Theoretical Physics,
ETH Zurich, 8093 Zurich, Switzerland*

Measuring the full distribution of individual particles is of fundamental importance to characterize many-body quantum systems through correlation functions at any order. Real-space probes of individual quantum objects – ions, superconducting qubits, Rydberg atoms or neutral atoms through a quantum gas microscope – have indeed paved the way to unprecedented investigations of many-body physics. Here I will present an experiment that provides the possibility to reconstruct the momentum-space distribution of three-dimensional interacting lattice gases atom-by-atom [1]. This is achieved by detecting individual metastable Helium atoms [2, 3] in the far-field regime of expansion, when released from an optical lattice. We benchmark our technique with Quantum Monte-Carlo calculations, demonstrating the ability to resolve momentum distributions of superfluids occupying 10^5 lattice sites. It permits a direct measure of the condensed fraction across phase transitions, as we illustrate on the superfluid-to-normal transition. Our single-atom-resolved approach opens a new route to investigate interacting lattice gases through momentum correlations.

-
- [1] H. Cayla, C. Carcy, Q. Bouton, R. Chang, G. Carleo, M. Mancini and D. Clement, submitted (2017).
[2] Q. Bouton, R. Chang, L. Hoendervanger, F. Nogrette, A. As-

- pect, C. Westbrook and D. Clement, Phys. Rev. A 91, 061402(R) (2015).
[3] F. Nogrette, D. Heurteau, R. Chang, Q. Bouton, C. Westbrook, R. Sellem and D. Clement, Rev. Scient. Instrum 86, 113105 (2015).

* david.clement@institutoptique.fr

Supraconductivité : point sur les différents mécanismes - théorie et expérience

Hervé Cercellier^{a*}

a. Université Grenoble Alpes et CNRS, Institut Néel, F-38000 Grenoble, France

* herve.cercellier@neel.cnrs.fr

(ENGLISH BELOW) Depuis la découverte de la supraconductivité en 1911 jusqu'à aujourd'hui, de nombreux matériaux supraconducteurs ont été identifiés et différents mécanismes de couplage ont été proposés. Après un rappel de la théorie BCS (Bardeen, Cooper, et Schrieffer) expliquant la supraconductivité à partir d'un mécanisme de couplage électron-phonon, une liste non exhaustive de supraconducteurs suggérant l'existence de nouveaux mécanismes sera établie et discutée.

Since the discovery of superconductivity in 1911 until today, many superconducting materials have been identified and different coupling mechanisms have been proposed. After a review of the BCS theory (Bardeen, Cooper, and Schrieffer) explaining superconductivity from an electron-phonon coupling mechanism, a non-exhaustive list of superconductors suggesting the existence of new mechanisms will be established and discussed.

Deciphering biomineralization pathways with new x-ray Bragg microscopy

Virginie Chamard^{a*}

a. Aix-Marseille Université, CNRS, Centrale Marseille, Institut Fresnel, Marseille, France

* virginie.chamard@fresnel.fr

Biomineralization processes result in the production of outstandingly complex mineralized structures in living organisms (e. g., teeth, bones, shells, etc.). While they are still poorly understood to date, deciphering these mechanisms is of crucial importance: in materials science, it should provide bio-inspired strategies for the synthesis of nanostructured inorganic materials using soft chemistry and environmentally friendly processes; in paleoclimatology, strong impacts are also expected due to the use of biomineral proxies to perform paleoclimate reconstructions. On the contrary to the classical crystallization theory scheme, the production of most calcareous crystalline biominerals integrates several complex processes, likely based on the generic formation of a submicrometric granular structure. Hence, gaining access to the crystalline architecture at the mesoscale, *i. e.*, over a few granules, is key to building realistic biomineralization scenarios. This is hindered by the difficulty to image complex crystalline materials at the nanoscale, one of today's major challenges of nanoscience.

Answering this need would require a microscopy method combining sensitivity to the crystalline properties, 3D imaging capability, in situ compatibility and high spatial resolution. In this context, the recent advents of x-ray lensless imaging methods, based on Bragg coherent diffraction at third generation synchrotron sources, have opened promising perspectives, filling the gap between direct microscopies (AFM, SEM, TEM) and reciprocal-space based x-ray Bragg diffraction analysis. The decisive answer has been brought by 3D Bragg ptychography microscopy [2], which merges concepts developed in inverse microscopy and crystallography. This x-ray Bragg microscopy fully meets the requirements imposed by the structural investigation of biominerals.

In this presentation, the general concepts of Bragg ptychography will be detailed, illustrated by recently proposed developments [2-7]. I will further describe how Bragg ptychography can be exploited to bring new insights on the biomineral crystalline structure. Perspectives with respects to the understanding of the biomineralization mechanisms will be finally presented [8].

This project has received funding from the European Research Council (ERC) under the European Union's Horizon H2020 research and innovation program grant agreement No 724881.

- [1] M. A. Pfeifer, *et al.*, Nature **442**, 63 (2006). A. Ulvestad, *et al.*, Science **348**, 1344-1347 (2015).
- [2] P. Godard, *et al.*, Nature Communications **2**, 568 (2011).
- [3] P. Godard, *et al.*, Optics Express **20**, 25914 (2012).
- [4] F. Berenger, *et al.*, Physical Review B **88**, 144101 (2013).
- [5] A. I. Pateras, *et al.*, Physical Review B **92**, 205305 (2015).
- [6] V. Chamard, *et al.*, Scientific Reports **5**, 9827 (2015).
- [7] S. O. Hruszkewycz, *et al.*, Nature Materials **16**, 244 (2017).
- [8] F. Mastropietro, *et al.*, Nature Materials **16**, 946 (2017).

Phase space representation of the quantum electron motion in a magnetic field

Thierry Champel^{a*} et Serge Florens^b

- a. Univ. Grenoble Alpes, CNRS, LPMMC, 25 avenue des Martyrs, 38042 Grenoble, France
- b. Univ. Grenoble Alpes, CNRS, Institut Néel, 25 avenue des Martyrs, 38042 Grenoble, France

* thierry.champel@grenoble.cnrs.fr

In disordered two-dimensional electron gases, the electronic motion at high magnetic fields is essentially decomposed into a fast orbital motion and a slow drifting motion of the orbit center along equipotential lines of the potential landscape. This motion decomposition can be encapsulated in the quantum mechanical language by using a specific basis of semi-coherent states within a Green's function formalism.

We present a generalization of this phase space method suitable to incorporate Landau level mixing processes in a nonperturbative manner. As a result, we derive a generic quantum solution in the phase space embracing all possible cases of electronic motions in quadratic potential landscapes at arbitrary magnetic field strength. This solution allows one to precisely define under which conditions on the magnetic field and the potential landscape the (effective) orbital motion remains related to a discrete quantization.

ÉGALITÉ DES CHANCES

UN ENJEU POUR TOUS ET TOUTES, FEMMES ET HOMMES

**TABLE RONDE PLÉNIÈRE OUVERTE À TOUS
SUIVIE D'UN BUFFET**

JOURNÉES DE LA MATIÈRE CONDENSÉE

<https://jmc2018.sciencesconf.org>

CAMPUS UNIVERSITAIRE ST MARTIN D'HÈRES - AMPHI WEIL

30 AOÛT 2018 DE 11H00 À 12H30

THÈMES ABORDÉS :

- VISIBILITÉ DES FEMMES DANS LA RECHERCHE ET L'ENSEIGNEMENT SUPÉRIEUR
- HARCÈLEMENT MORAL ET SEXUEL

INTERVENANT-E-S :

NATHALIE COULON MAÎTRESSE DE CONFÉRENCES EN PSYCHOLOGIE, LILLE - HARCÈLEMENT

FRANÇOISE LE MOUËL SOPHIA CONSULTING - VISIBILITÉ

SÉVERINE LOUVEL MAÎTRESSE DE CONFÉRENCES EN SOCIOLOGIE, GRENOBLE - VISIBILITÉ

CHRISTOPHE RIBUOT VICE-PRÉSIDENT RH, UNIVERSITÉ GRENOBLE-ALPES - HARCÈLEMENT

DISCUSSION ANIMÉE PAR **DOMINIQUE CHANDESRIS** AVEC :

CATHERINE PICART, MATHIEU GIBERT, CATHERINE LANGLAIS, MICHÈLE LEDUC ET ALAIN SCHUHL

COMITÉ D'ORGANISATION : NEDJMA BENDIAB, MIREILLE BAURENS, DOMINIQUE CHANDESRIS, GIOVANNA FRAGNETO, MATHIEU GIBERT, CLAUDINE LACROIX, MIREILLE LAVAGNA, LAËTITIA MARTY, VALÉRIE REITA, ANNE SCHUHL.

Design - dutillo-cusani.com



Etude des propriétés structurales optiques et électroniques du composé $\text{Cu}_2\text{ZnSnS}_4$ de type Kesterite par la DFT pour les applications photovoltaïques

M. Chaouche, K. Hamdani, N. Benslim, M. Benabdeslem, L. Bechiri

Laboratoire d'Etude de Surfaces et Interfaces de la Matière Solide (LESIMS), Département de Physique, Faculté des Sciences, Université Badji Mokhtar –Annaba, Algérie

mouna_chaouche@yahoo.com

Résumé

Le quaternaire $\text{Cu}_2\text{ZnSnS}_4$ (CZTS) attire l'attention des chercheurs depuis une décennie, il a confirmé ses potentialités dans les applications photovoltaïques. Celui-ci est considéré en tant que matériau prometteur dans la fabrication et l'amélioration de la couche absorbante des cellules solaires. Il est constitué d'éléments non toxiques et abondants sur la croûte terrestre. Nous avons étudié les propriétés structurales, optiques et électroniques du composé quaternaire de type Kesterite ($\text{Cu}_2\text{ZnSnS}_4$) par la méthode des ondes planes augmentées et linéarisées FP-LAPW bases sur le formalisme de la théorie de la fonctionnelle de la densité (DFT) implémentée dans le code Wien2K. Le potentiel d'échange et de corrélation est traité dans le cadre de l'approximation de la densité locale (LDA) et pour le calcul des propriétés optiques et électroniques nous avons également utilisé l'approche d'échange modifiée de Becke-Johnson (mbj), qui sert à optimiser le potentiel correspondant pour les calculs de structure de bande électronique. Cette étude nous a permis de déterminer les valeurs des paramètres cristallins ($a= 5.36 \text{ \AA}$ et $c = 10.74 \text{ \AA}$) à l'équilibre qui sont proche de celles obtenues expérimentalement. Par ailleurs, les propriétés optiques de ce composé, plusieurs grandeurs ont été calculées à savoir ; l'indice de réfraction (n), le coefficient d'extinction (K) et la partie réelle et imaginaire de la fonction diélectrique (ϵ_1, ϵ_2). L'analyse de la structure électronique du CZTS confirme son caractère de structure de bande à gap direct égale à 1.3 eV. L'analyse de la densités d'états totales (T-DOS) et partielles (P-DOS) obtenues par la LDA-mbj pour le composé CZTS nous a permis d'étudier l'hybridation des états atomiques et leurs contributions dans la structure de bande du composé KS-CZTS.

Mots clés : $\text{Cu}_2\text{ZnSnS}_4$, Wien2K, FP-LAPW, DFT.

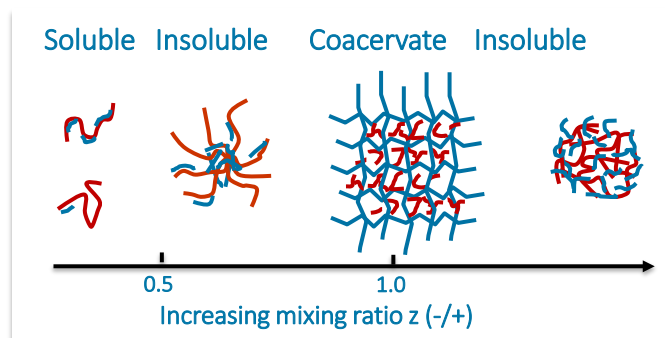
The three possible states of polyelectrolyte complex coacervates: soluble, dispersed & macroscopic phase.

J.-P. Chapel^{a*}, X. Liu^{a,b.}, M. Haddou^{a,b.}, C. Pucci^{a,b.}, J. Giermanska^{a.}, Ch. Schatz^{b.}

- a. CRPP, CNRS - Univ. Bordeaux, 115 Av. A. Schweitzer 33600 Pessac.
b. LCPO, CNRS- ENSCPB - Univ. Bordeaux, 16 Av. Pey-Berland 33607 Pessac.

*chapel@crpp-bordeaux.cnrs.fr

Complex coacervation is a well-known liquid-liquid phase separation resulting from the electrostatic interaction of oppositely charged polyelectrolytes (PEs) or colloids. We put forward SANS evidences of the local structures of the three distinctive association states found in a model PANA/PDADMAC [1] coacervating system, i.e., soluble and dispersed PECs together with the coacervate phase. We show the unambiguous presence of the very controversial soluble complexes between PEs with a large chain length asymmetry. Indeed, with just few short guest chains, the long host chain holds the characteristic of a charged PE, that is, its water solubility in a thermodynamic sense. With more short chains, the hydrophobic segments start to associate and microphase separate generating dispersed PECs. The core-shell structure evolves into compact sphere as the mixing charge ratio Z approach 1. Soluble PECs are absent for more symmetric systems or in the presence of salt where only dispersed PECs are obtained. At stoichiometry ($Z=1$) complex coacervation occurs. This dense phase can be regarded as a network of random mixed polyion chains with a mesh size much smaller than the R_g of PE chains. An additional scattering maximum is found in our system at high q arising from the relatively stiff PDADMAC cylinders (non-electrostatic persistence length ~ 3 nm), randomly distributed in the concentrated network as anticipated by the “jammed state” proposed by the Rawiso’s group. [2]



- [1] Liu et al. *Soft Matter* (2016), 12, 9030 & *Adv. Col. Int. Sci.* (2017), 239, 178.
[2] Lorchat et al. *EPL*, **106** (2014) 28003.

Lipid Membranes in an Electric Field

Thierry Charitat^{a*}, Arnaud Hemmerle^b, Giovanna Fragneto^c et Jean Daillant

- a. UPR 22/CNRS, ICS, Université de Strasbourg, 23 rue du Loess, F-67034 Strasbourg
- b. CINaM, Campus de Luminy, Case 913, F-13288 Marseille
- c. Institut Laue-Langevin, 71 av. des Martyrs, BP 156, F-38042 Grenoble
- d. Synchrotron SOLEIL, L'Orme des Merisiers, Saint-Aubin, F-91192 Gif-sur-Yvette Cedex

* charitat@unistra.fr

Electric fields have a strong influence on lipid membrane behavior and are used in many applications in cell biology, biotechnology and pharmacology [1]. High electric field can lead to cell hybridization, electroporation, electrofusion and electropermeabilization, opening wide applications in tissue ablation and gene therapy. Lower electric fields can also induce shape deformation of the lipid bilayer and under certain conditions its destabilization. This electroformation process has become one of the classical methods to form large unilamellar vesicles. The effect of electric fields on membrane elasticity has been investigated using synchrotron grazing incidence x-ray scattering [2]. Using a recently developed method, we are able to precisely determine membrane tension, rigidity and interaction potentials. We show that membrane tension is decreased, possibly down to negative values and that the membrane rigidity is increased. A full analysis of our data as a function of applied potential and frequency shows that it is possible to decouple simple electrokinetic effects from the bilayer elasticity which is affected by the local electric field. The effects on the membrane itself and Debye electrical double bilayer could be fully analysed leading to a fine understanding of AC fields effects.

- [1] U. Zimmermann. Electrical breakdown, electropermeabilization and electrofusion. In *Reviews of Physiology*, volume 105, pages 175-256. Springer Berlin Heidelberg, 1986.
- [2] A. Hemmerle, G. Fragneto, J. Daillant and T. Charitat, *Physical Review Letters*, 116, 228101 (2016).

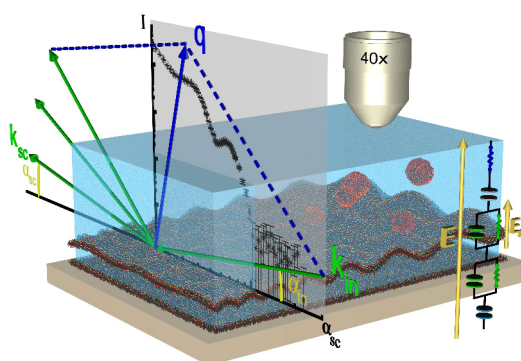


Figure 1: Schematic view of a model supported double bilayers under an electric field investigated by x-rays off-specular reflectivity.

Integrated microelectrode array and microfluidic platform for stimulating and recording reconstructed neuronal networks

B. Charlot^{*,a,d}, E. Moutaux^{b,c}, E. Malyshev^{a,d,f}, F. Bardin^{a,e},
F. Saudou^{b,c}, and M. Cazorla^{b,c}

- a. IES, Institut d'Electronique et des Systèmes, CNRS UMR 5214
 - b. GIN, Grenoble Institute of Neuroscience, INSERM U1216
 - c. Université Grenoble Alpes, Grenoble, France
 - d. Université de Montpellier, Montpellier, France
 - e. Université de Nîmes, Nîmes, France
 - f. Saint Petersburg Academic University, Saint Petersburg, Russia.
- * benoit.charlot@umontpellier.fr

Compartmentalized microfluidics are devices that allow the in-vitro reconstitution of neuronal circuits using primary cultures of different neuronal populations. This configuration allows the reconstruction of axono-dendritic contacts between two cortical populations such as those found between cortical layers in vivo. In order to extend the functional analysis of reconstructed cortico-cortical networks, we developed a specific Micro Electrode Array (MEA) substrate that fits to the microfluidic geometry to stimulate and record pre- and post-synaptic neurons (Figure1). Presynaptic electrodes were disposed at the entrance of axonal channels in order to stimulate the axon initiation segment that will generate physiological action potentials and trigger release of neurotransmitter in the synaptic chamber. Postsynaptic electrodes are located under postsynaptic neuronal cell bodies. Combined with high-resolution fluorescence videomicroscopy and fast calcium imaging, this system allows monitoring intracellular dynamics, Calcium responses and synaptic transmission to different forms of neuronal activity. By combining space-time compartmentalization of neuronal populations with high-resolution videomicroscopy and electrophysiological stimulation and recording, our platform allows to decipher the cellular events that are involved in synaptic transmission and plasticity within neuronal networks. This device can be applied to virtually any type of neuronal circuits but also neuromuscular junctions.

- [1] A. Virlogeux, E. Moutaux, W. Christaller, A. Genoux, J. Bruyère, B. Charlot, M. Cazorla, F. Saudou, "Reconstituting Corticostriatal Network On-a-Chip Reveals the Contribution of the Presynaptic Compartment to Huntington's Disease", *Cell Reports* 22-1 (2018)
- [2] J.M. Peyrin et al. "Axon diodes for the reconstruction of oriented neuronal networks in microfluidic chambers", *Lab Chip* 11, 3663-3673 (2011).
- [3] A.M. Taylor, D.C. Dieterich, H.T. Ito, S.A. Kim, E.M. Schuman, "Microfluidic local perfusion chambers for the visualization and manipulation of synapses", *Neuron* 66, 57-68 (2010)

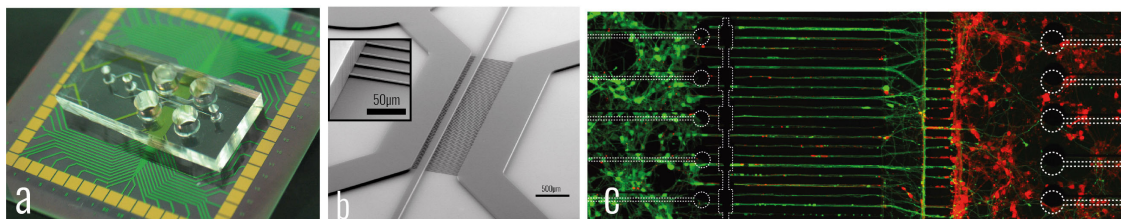


Figure 1 : Integrated multi-electrode array and microfluidics. a, Photographs of the microfluidics connected to the multi-electrode array substrate and details of the post synaptic electrodes. b, Dual thickness SU-8 mold of the microfluidic culture chamber. c, Design of the system showing the different compartments and their respective electrodes (Green, GFP- expressing cortical neurons; Red, mCherry-expressing cortical neurons).

Effet de la pression hydrostatique et de la non-parabolicité de la bande de conduction sur les propriétés optoélectroniques dans un puits quantiques à base de GaAs / Ga_xAl_{1-x}As

Y.Chrafi^{a*}, K.Rahmani^b, L.Moudou^a et I.Zorkani^c,

- Laboratoire du Développement Durable, LDD, Faculté des Sciences et Techniques, Université Sultan Moulay Slimane, Béni Mellal -Maroc.
- Equipe de Recherche en Physique Théorique et Matériaux, ERPTM, Faculté Polydisciplinaire, Université Sultan Moulay Slimane, Béni Mellal -Maroc.
- Groupe des Nanomatériaux et Energies Renouvelables, LPS, Faculté des Sciences Dhar El Mehraz, Université Sidi Mohamed Ben Abdellah, Fès -Maroc.

*younescharafih@gmail.com ---- kh.rahmani@hotmail.fr

Dans le présent travail, nous avons étudié, dans le cas de la bande de conduction non-parabolique, l'effet de la pression hydrostatique sur les propriétés optoélectroniques d'un puits quantique (QW) à base du matériau GaAs dopé par le Si et entouré en sandwich par Ga_{1-x}Al_xAs où le taux d'aluminium est fixé à 30%. Nos calculs sont effectués dans le contexte de l'approximation du formalisme de la fonction d'enveloppe, et en utilisant la méthode de la différence finie.

Nos résultats montrent que les transitions d'énergie diminuent avec l'augmentation de la pression hydrostatique ce qui entraîne des fortes modifications sur les propriétés optiques de la nanostructure (QW).

L'augmentation de la pression crée un déplacement du coefficient d'absorption optique vers les basses énergies et une diminution de la valeur du pic d'absorption. En revanche, l'indice de réfraction se déplace vers les hautes énergies. Nous avons montré qu'en présence d'une pression hydrostatique et suite à son effet sur les transitions intersousbandes, ces propriétés optiques dépendent aussi du taux de concentration du dopant et de la largeur du puits quantique. L'étude réalisée peut être intéressante dans les nanofabrications des puits quantiques et en particulier pour ceux qui sont utilisés dans le domaine optique et électronique.

- [1] R. Khordad, S. Kheirzadeh Khaneghah, M. Masoumi. Superlatt. Microstruct. 47 (2010) 538.
- [2] F. Urgan, U. Yesilgul, S. Sakiroglu, M.E. Mora-Ramos, C.A. Duque, E. Kasapoglu, H. Sari, I. Sökmen, Opt. Commun.309 (2013) 158.
- [3] B. Akbarnavaz Farkoush, Gh. Safarpour, A. Zamani. Superlatt. Microstruct. 59 (2013) 66.
- [4] H. Akabli, A. Almagoussi, A. Abounadi, A. Rajira, K. Berland, and T. G. Andersson, Superlattices and Microstructures 52, 70 (2012).

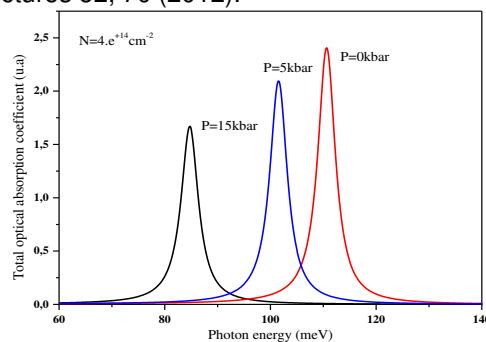


Figure 1 : L'évolution du coefficient d'absorption total en fonction de l'énergie du photon incident pour trois valeurs de la pression hydrostatique (P=0, 5 et 15kbar).

Probing the structure and composition of nanoporous alumina by SANS. From measurement to implementation for polyelectrolytes in a charged confining medium.

Anastasia Christoulaki^{a*}, Alexis Chennevière^b, Nicolas Jouault^a, and Emmanuelle Dubois^a

- a. Sorbonne Université, CNRS, Laboratoire PHENIX, Case 51, 4 place Jussieu, F-75005 Paris, France
 b. Laboratoire Léon Brillouin CEA-CNRS, Saclay 91191 Gif-sur-Yvette Cedex, France

* anastasia.christoulaki@sorbonne-universite.fr

Nanoporous materials can be used as media for studying confinement of soft matter. Among them nanoporous alumina membranes (nPAM) are promising model systems for such studies. The nPAMs are synthesized by electrochemical anodization of aluminum and consist of parallel nanochannels with monodispersed diameters that are arranged in a hexagonal lattice and whose size is directly tunable by the synthesis conditions. Moreover, nPAM is an amphoteric material whose charge behavior depends on the pH, thus providing both geometrical and electrostatic confinement.

The conformation and dynamics of soft matter can be addressed by Small Angle Neutron Scattering (SANS). However, before studying the behavior of guest species inside a host medium, it is essential to characterize the confining medium. For this reason, the nPAM were characterized by SANS by utilizing the well-known method of contrast variation from which information on the structure and chemical composition can be extracted. The characterization of such highly dense ordered structures is non-trivial and a detailed strategy will be proposed in order to avoid multiple scattering effects and “match” the nPAM since there is no contrast matching point where the nPAM scattering intensity “eliminates”. Our results show that the nPAM contains two layers with different composition and are radially distributed around the pore axis, forming a contamination shell. Fitting of the SANS experimental data provides the basic geometrical characteristics such as the pore diameter, interpore distance and the extent of the contamination shell. The fitting model that includes a hexagonal structure factor with a form factor of a core-shell cylinder will be detailed (see Figure 1).

Finally, we will present some SANS data to study the behavior of sodium polystyrene sulfonate (NaPSS) inside nPAM having different pore sizes and charges.

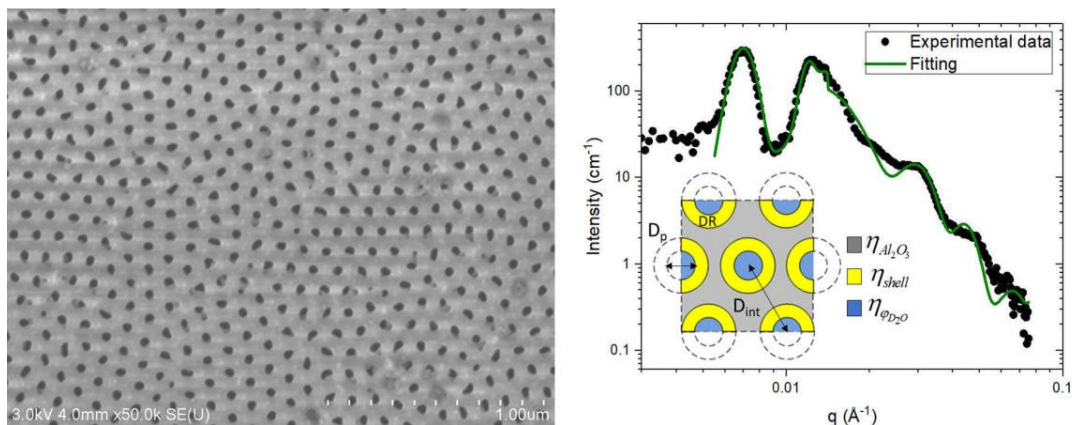
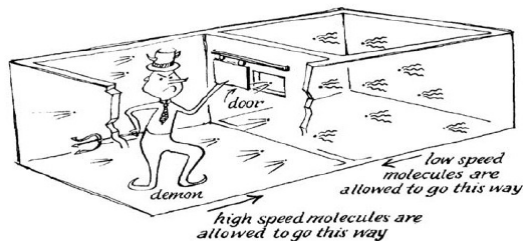


Figure 1 : Left: SEM image of a nPAM. Right: SANS data of a nPAM and the corresponding fitting with a core-shell cylinder model.

The Maxwell demon and Landauer's principle: from gedanken to real experiments

S. Ciliberto

Laboratoire de Physique de l'ENS de Lyon, CNRS UMR5672
46 Allée d'Italie- 69364 Lyon- France



During this talk we will recall the connections between information and thermodynamics. We will then discuss a specific example of the measure of the Landauer's bound.

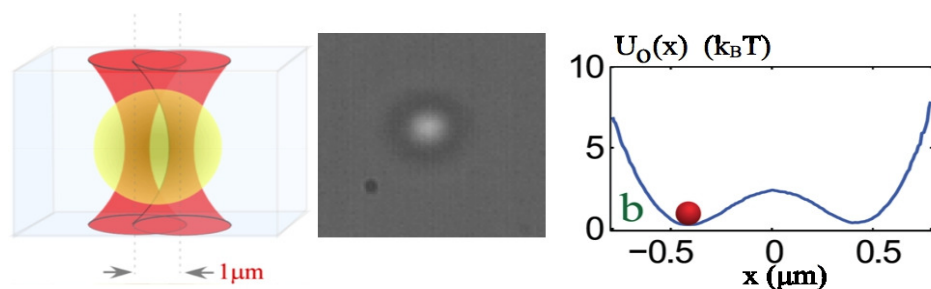
Rolf Landauer argued that the erasure of information is a dissipative process. A minimal quantity of heat, proportional to the thermal energy, is necessarily produced when a classical bit of information is deleted. A direct consequence of this logically irreversible transformation is that the entropy of the environment increases unavoidably by a finite amount. We experimentally show the existence of the Landauer bound in a generic model of a one-bit memory. Using a system of a single colloidal particle trapped in a modulated double-well potential, we establish that the mean dissipated heat saturates at the Landauer bound in the limit of long erasure cycles. This result demonstrates the intimate link between information theory and thermodynamics. For a memory erasure procedure, which is a logically irreversible operation, a detailed Jarzynski Equality is verified, retrieving the Landauer limit independently of the work done on the system.

References :

Experimental verification of Landauer's principle linking information and thermodynamics, A. Bérut, A. Arakelyan, A. Petrosyan, S. Ciliberto, R. Dillenschneider, E. Lutz, Nature, 483, 187–189 (08 March 2012).

Detailed Jarzynski Equality applied to a Logically Irreversible Procedure, A. Bérut, A. Petrosyan, S. Ciliberto, EPL, 103 (2013) 60002

Information: From Maxwell's demon to Landauer's eraser, Eric Lutz, Sergio Ciliberto, Physics Today 68 (9), 30 (2015)



Controlling symmetry and localization properties with an artificial gauge field in a disordered Floquet system

J.-F. Clément^{a*}, C. Hainaut^a, I. Manai^a, JC Garreau^a, P. Szriftgiser^a, G. Lemarié^{b,c},
N. Cherroret^d, D. Delande^d et R. Chicireanu^a

- a. Université de Lille, CNRS, UMR 8523, Laboratoire de Physique des Lasers Atomes et Molécules, F-59000 Lille, France
- b. Laboratoire de Physique Théorique, IRSAMC, Université de Toulouse, CNRS, 31062 Toulouse, France
- c. Department of Physics, Sapienza University of Rome, P.le A. Moro 2, 00185 Rome, Italy
- d. Laboratoire Kastler Brossel, UPMC-Sorbonne Universités, CNRS, ENS-PSL Research University, Collège de France, 4 Place Jussieu, 75005 Paris, France

* jean-francois.clement@univ-lille.fr

Anderson localization, which has long been a paradigm of condensed matter physics [1], has been observed and studied in the last decades in many different disordered systems, both classical and quantum. The symmetry characteristics of the disordered system are expected to greatly affect its localization and transport properties, yet few experiments are available in this direction. Here we report upon the experimental realization of an artificial gauge field in a synthetic (temporal) dimension of a disordered, periodically driven (Floquet) quantum system [2]. Our remarkably simple technique is used to control the Time-Reversal Symmetry (TRS) properties, and leads to two experimental observations representing smoking-gun signatures of this symmetry breaking. The first consists in the first observation of the Coherent Forward Scattering (CFS), a novel genuine interferential signature of the onset of the (strong) Anderson localization, recently predicted [3]. The second is a measurement of the celebrated $\beta(g)$ function [4], with a direct test of the one-parameter scaling hypothesis, and its universality in two different symmetry classes.

- [1] P. W. Anderson, Absence of Diffusion in Certain Random Lattices, *Phys. Rev.* **109**, 1492 (1958)
- [2] C. Hainaut, I. Manai, J.-F. Clément, JC Garreau, P. Szriftgiser, G. Lemarié, N. Cherroret, D. Delande and R. Chicireanu, Controlling symmetry and localization with an artificial gauge field in a disordered quantum system, *Nature Communications*, **9**, 1382 (2018)
- [3] T. Karpiuk, N. Cherroret, K. L. Lee, B. Grémaud, C. A. Müller and C. Miniatura, Coherent Forward Scattering Peak Induced by Anderson Localization, *Phys. Rev. Lett.* **109**, 190601 (2012)
- [4] E. Abrahams, P. W. Anderson, D. C. Licciardello, and T. V. Ramakrishnan, Scaling Theory of Localization: Absence of Quantum Diffusion in Two Dimensions, *Phys. Rev. Lett.*, **42**, 673 (1979)

Adsorption and Transport in Hierarchical Nanoporous Media

Benoit Coasne^{a*}

a. Laboratoire Interdisciplinaire de Physique, CNRS/Univ Grenoble Alpes, Grenoble, France

* benoit.coasne@univ-grenoble-alpes.fr

Hierarchical nanoporous materials, which combine several porosity scales, are widely used in industry (adsorption, separation, catalysis) to overcome slow diffusion and enhance access to the large surface area in microporous solids (< 2 nm). The benefits of adding meso (2-50 nm) and macro (> 50 nm) pores to the existing microporosity was demonstrated but engineering of such solids, which are heterogeneous in size, shape, and connectivity, still relies on trial and error strategies. Available modeling approaches, even when based on a physical ground, are limited to empirical parameters which cannot be derived from molecular adsorption/transport coefficients. In particular, none of the existing approaches offers the ground for a bottom up model of adsorption/transport in multiscale materials as (1) they describe empirically the interplay adsorption/transport and (2) they do not account for the breakdown of hydrodynamics at the nm scale.

I will present a multiscale model of adsorption and transport in hierarchical nanoporous materials (Figure 1) [1]. I will first show how adsorption, permeance, and transport in such media can be described without having to rely on macroscopic concepts such as hydrodynamics [2,3]. Using fundamental parameters and coefficients available to simple experiments, we will see how transport coefficients can be rigorously obtained from simple models in the framework of Statistical Mechanics. Then, I will present a multiscale model of adsorption and transport in hierarchical materials [4]. Thanks to the use of atom-scale simulations, which capture the different adsorption and transport regimes upon varying the temperature, pore size, pressure, etc. this bottom-up model does not rely on hydrodynamics and, hence, does not require assuming a given adsorption or flow type. I will also discuss NMR experimental results on transport in hierarchical zeolites [5].

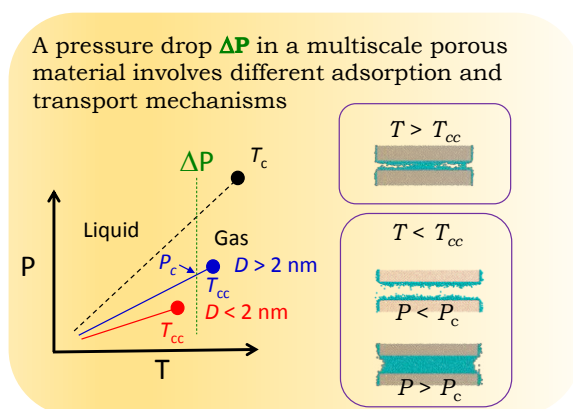


Figure 1 : P-T phase diagram of a fluid confined in micro and mesopores. For a pore size D , the bulk critical temperature T_c is shifted to $T_{cc}(D)$. Pore filling is reversible for $T > T_{cc}$, and irreversible for $T < T_{cc}$. In the latter case, the pore is partially filled for $P < P_c$ and completely filled for $P > P_c$.

- [1] B. Coasne, A. Galarneau, C. Gerardin, F. Fajula, F. Villemot, *Langmuir* 29, 7864 (2013).
 [2] K. Falk, B. Coasne, F. J. Ulm, R. Pellenq, L. Bocquet, *Nature Comm.* 6, 6949 (2015).
 [3] T. Lee, L. Bocquet, B. Coasne, *Nature Comm.* 7, 11890 (2016).
 [4] A. Botan, F. J. Ulm, R. Pellenq, B. Coasne, *Phys. Rev. E* 91, 032133 (2015).
 [5] A. Galarneau, F. Guenneau, A. Gedeon, D. Mereib, J. Rodriguez, F. Fajula, B. Coasne, *J. Phys. Chem. C* 120, 1562 (2016).

Disentangling electronic & structural dynamics with X-ray lasers for shining new light on ultrafast photoinduced transitions

E. Collet^{a*}, G. Azzolina^a, S. Zerdane^a, R. Bertoni^a, C. Mariette^a,
E. Trzop^a, H. Cailleau^a, M. Lorenc^a, M. Cammarata^a

a. Univ Rennes 1, CNRS, Institut de Physique de Rennes, UMR 6251, F-35042 Rennes

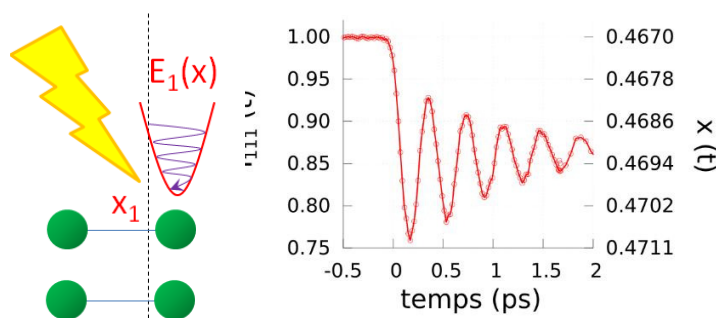
* eric.collet@univ-rennes1.fr

The advent of control science for directing matter and energy represents an important challenge for material science. It is now possible to control materials by light for generating remarkable properties on ultrafast timescale (ferroelectricity, conductivity, magnetism, photochromism...). These result from complex correlations between electronic and atomic constituents of matter. X-ray free electron lasers (X-FEL) open new possibilities for probing ultrafast photoinduced phenomena in order to disentangle, understand and control electronic and structural dynamics [1,2] (Figure 1). Ultrafast photoswitching in bistable molecular crystals is associated with a complex transformation pathway, multiscale in nature, where both molecular photo-switching (100 fs) and macroscopic elastic (ns) or thermal (μ s) transformation of the crystal play their role [3]. We have studied the basic mechanisms allowing light to switch molecular materials between different magnetic states, by using femtosecond x-ray diffraction & absorption and optical spectroscopy. The stabilization of the photoinduced magnetic state results from the activation and damping of a molecular breathing mode. We gained experimental insights of this process, beyond the Born–Oppenheimer approximation, by disentangling the electronic charge-transfer excitation decay from the structural trapping dynamics [4-6]. We have demonstrated that in the active crystalline medium cooperative elastic effects can drive self-amplified and coherent response to light excitation [3]. The self-amplification process results from the elastic field induced by light and coupled to the molecular volume change, allowing the transformation of several molecules from a single photon.

X-ray free electron lasers broaden the range of methods for investigating ultrafast dynamics in mater, which will boost our capabilities to gather new insight into electronic and structural changes involved during light-induced phenomena.

- [1] E. Collet et al, *Reflète phys.* **44-45**, 44 – 49 (2015)
 [2] M. Chergui and E. Collet, *Chem. Rev.* **117**, 11025–11065 (2017)
 [3] R. Bertoni et al, *Nature Materials* **15**, 606-610 (2016)
 [4] M. Cammarata, et al, *Physical Review Letters* **113**, 227402 (2014)
 [5] H.T. Lemke et al, *Nature Communication* **8**, 15342 (2017)
 [6] S. Zerdane, *Chemical Science* **8**, 4978 (2017).

Figure 1 : Femtosecond laser excitation of Bi modifies instantaneously its potential energy surface and the equilibrium distance x between atoms, launching so coherent phonon. Ultrafast X-ray diffraction allows monitoring atomic motions in real time [1].



Two-boson correlations in three weakly coupled Bose-Einstein condensates

Enrico Compagno^{a*}, Denis Feinberg^a, Anna Minguzzi^b, Luigi Amico^{c,d}

- a. Institut Néel, CNRS and Université Grenoble Alpes, Grenoble, France
- b. LPMMC, Université Grenoble Alpes and CNRS, Grenoble, France
- c. Dipartimento di Fisica e Astronomia, Via S. Sofia 64, 95127 Catania, Italy
- d. LANEF 'Chaire d'excellence', Université Grenoble-Alpes and CNRS, Grenoble

* enrico.compagno@neel.cnrs.fr

Three weakly coupled Bose-Einstein condensates (BECs) are studied with large symmetrical offsets of their chemical potentials. This results in two canonical (Josephson) density and phase modes behaving very differently. The first mode is rapidly oscillating. The second one is a slow mode featuring an effective Josephson effect between one of the BECs and the two others altogether. It involves correlated two-boson fluctuations between the BECs and entails squeezing and two-mode entanglement. The solution of a Bose-Hubbard model is explored both in the classical limit and by exact diagonalization for small atom numbers. The two-boson correlation function is calculated and a representation in terms of coherent states is put forward.

Optical study of vibronic coupling in the quantum spin liquid candidate $Tb_2Ti_2O_7$

Evan Constable^{a,b,*}, L. Bergen^a, R. Ballou^b, J. Robert^b, C. Decorse^c, J.-B. Brubach^d, P. Roy^d, E. Lhotel^b, V. Simonet^b, S. Petit^e and S. deBrion^b

- a. Institute of Solid State Physics, Vienna University of Technology, Vienna, Austria
- b. Institut Néel, CNRS and Université Grenoble Alpes, Grenoble, France
- c. ICMMO, Université Paris-Sud, Orsay, France
- d. Synchrotron SOLEIL, Gif-sur-Yvette, France
- e. Laboratoire Léon Brillouin, CEA, CNRS, Université Paris-Saclay, Gif-sur-Yvette, France

* evan.constable@tuwien.ac.at

In the study of geometrically frustrated magnetism, the precise nature of the ground state in $Tb_2Ti_2O_7$ has remained a long-standing conundrum. In this pyrochlore material, no conventional spin-ice or long-range magnetic order is stabilized, even at very low temperatures. Quantum fluctuations are suspected of being at the origin of an exotic phase, yet so far they have lacked conclusive evidence. Using high-resolution synchrotron-based terahertz spectroscopy, we have probed the lowest energy excitations of $Tb_2Ti_2O_7$. It is revealed that a double hybridization of crystal-field-phonon modes is present across a broad temperature range. This so called vibronic process affects the electronic ground state that can no longer be described solely by electronic wave functions. Rather, a collective state prevails, built on the ground and first excited crystal-field states mixed with two different phonon modes. This provides a crucial path for quantum spin-flip fluctuations to inhibit the stabilization of conventional magnetic states. The study is further complimented by recent ultrafast terahertz-pump/optical-probe measurements on the ELBE free electron laser that confirm the presence of the vibronic coupling.

[1] E. Constable, R. Ballou, J. Robert, C. Decorse, J.-B. Brubach, P. Roy, E. Lhotel, L. Del-Rey, V. Simonet, S. Petit, and S. deBrion 2017 Physical Review B Vol 95, 020415(R).

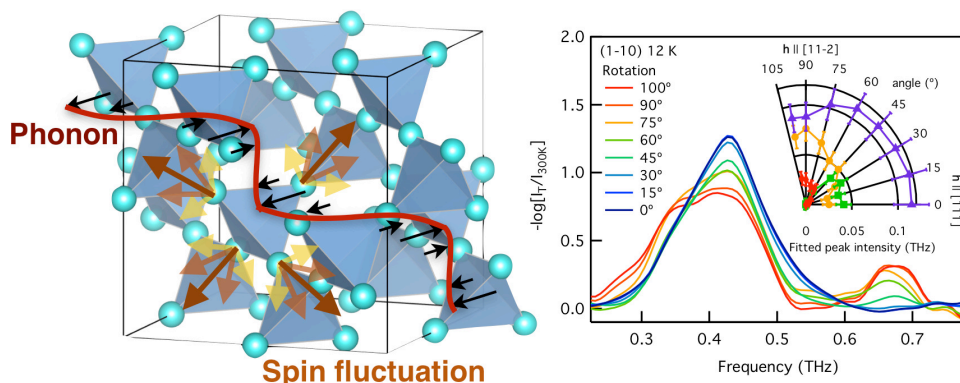


Figure 1 : (left) Tb^{3+} Pyrochlore network and graphical description of the vibronic process that involves the hybridization between a phonon and a crystal field excitation. (Right) Angular dependence of the THz spectra.

***In-Situ* X-Ray Diffraction Studies On Piezoelectric Thin Films**

T.W. Cornelius^{a,*}, C. Mocuta^b, S. Escoubas^a, E.B. Araujo^c, E.C. Lima^d, A.L. Kholkin^{e,f}, O. Thomas^a

- a. Aix-Marseille Univ, Univ de Toulon, CNRS, IM2NP (UMR7334), Marseille, France
- b. Synchrotron SOLEIL, L'Orme des Merisiers Saint-Aubin, BP 48, Gif-sur-Yvette France
- c. Departamento de Física e Química, Universidade Estadual Paulista, Ilha Solteira, Brazil
- d. Universidade Federal do Tocantins, Porto Nacional, TO, Brazil
- e. Department of Physics & CICECO – Aveiro Institute of Materials, University of Aveiro, Portugal
- f. ITMO University, St. Petersburg 197101, Russia

* thomas.cornelius@im2np.fr

Within the last decade, the properties of ferroelectrics have been extensively studied. Several important devices, such as Ferroelectric Random Access Memories (FeRAMs) and Dynamic Random Access Memory (DRAM), are manufactured based on ferroelectric thin films [1, 2]. With the crescent and continuous demand for portability in consumer electronics, the understanding of the effects of miniaturization on the properties of ferroelectric thin films becomes increasingly important. Although continuous improvements in conventional semiconductor designs are implemented, the basic physics of the size effects is, however, poorly understood. It is well known that the crystallite size plays an important role in tailoring ferroelectric properties.

The piezoelectric properties of $\text{Pb}(\text{Zr}_{1-x}\text{Ti}_x)\text{O}_3$ (PZT) and $\text{Pb}_{1-y}\text{La}_y(\text{Zr}_{1-x}\text{Ti}_x)\text{O}_3$ (PLZT) thin films of different compositions consisting of few tens of nanometer sized grains were studied by *in-situ* local probe X-ray diffraction at the DiffAbs beamline at Synchrotron SOLEIL [3]. For this purpose, gold electrodes of 0.3 mm in diameter were deposited on top of the thin film of which one was contacted electrically with a thin wire. A Pt layer was used as back electrode. Constant electric fields as well as alternating ones with frequencies ranging from 0.01 Hz to 31 kHz were applied. The diffraction signal from an area beneath the electrically contacted electrode was monitored as a function of the applied electric field. From the shift of the position of the Bragg peak induced by the applied potential, the piezoelectrically generated strain was determined revealing “butterfly loops” [4] which are a clear signature of the piezoelectric hysteresis. Asymmetric butterfly loops found for PZT thin films with $x = 0.5$ indicate the presence of a self-polarization which tends to disappear for PZT thin films with $x = 0.47$ [5]. These findings are supported by piezoelectric force measurements revealing an asymmetry of the hysteresis loops towards positive electric fields which are a clear signature of a macroscopic self-polarization effect in the studied PZT films. For PLZT thin films the piezoelectric coefficient was found to be increased with a maximum for films with 3% La. For both PZT and PLZT films the butterfly loops are less pronounced for AC frequencies > 1 Hz and the piezoelectric response was found to be smaller than for DC electric fields. In addition, a linear behavior of the piezoelectrically induced strain as a function of the applied electric field was found for PLZT thin films instead of butterfly loops.

This work was partially funded by the CAPES-COFECUB project Ph801-14.

- [1] J.F. Scott and C.A. Araujo, *Science* 246, 1400 (1989).
- [2] J.F. Scott, *Ferroelectric Memories* (Springer, Heidelberg, Germany, 2000).
- [3] A. Davydok, T.W. Cornelius et al., *Thin Solid Films* 603, 28 (2016)
- [4] M.C. Ehmke et al., *J. Am. Ceram. Soc.* 96, 2913 (2013).
- [5] T.W. Cornelius et al., *J. Appl. Phys.* 122, 164104 (2017)

Buckling instability and swimming of elastic spherical shells

A. Djellouli^a, P. Marmottant,^a H. Djeridi,^b C. Quilliet,^a and G. Couplier^{a*}

a. Université Grenoble Alpes, CNRS, LIPhy, F-38000 Grenoble, France

b. Université Grenoble Alpes, Grenoble INP, CNRS, LEGI, F-38000 Grenoble, France

* gwennou.couplier@univ-grenoble-alpes.fr

Under pressure, a hollow elastic sphere becomes unstable and collapses. It reinflates back when the pressure is decreased. The shape hysteresis associated to this deformation cycle makes this simple object a good candidate for becoming a microswimmer, that is, a swimmer able to move at low Reynolds number.

We explore this possibility through a macroscopic experiment in fluids of varying viscosities so as to explore different flow regimes [1]. We show that not only the shape sequence hysteresis leads to swimming (Fig. 1) but the asymmetry in the deformation velocity makes the fast buckling phase an efficient mechanism for propulsion that implies inertial effects and subtle coupling between shape post-buckling oscillations and fluid flow patterns. Our modeling shows that such an inertial regime could even be reached at microscopic scale.

We anticipate that a conveyor made of a few of microbubbles with different shell thicknesses, would constitute a microrobot whose 3D displacement can be remotely controlled by an echographic device - a relatively cheap and widely available tool in the hospitals.

- [1] A. Djellouli, P. Marmottant, H. Djeridi, C. Quilliet and G. Couplier, *Buckling Instability Causes Inertial Thrust for Spherical Swimmers at All Scales*, Phys. Rev. Lett. 119, 224501 (2017)

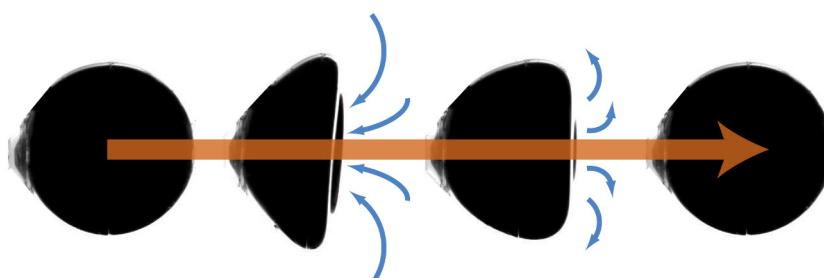


Figure 1: Deformation sequence of an elastic shell under increasing then decreasing external pressure. The blue arrows schematize the flow patterns during resulting deflation and re-inflation. This flow sequence results in a net motion for the shell. See video [here](#).

Optical spectroscopy of excited exciton states in MoS₂ monolayers in van der Waals heterostructures

E. Courtade^{a*}, C. Robert^a, M. Manca^a, B. Urbaszek^a, B. Lassagne^a, T. Amand^a, P. Renucci^a, X. Marie^a, M. Semina^b, M.M. Glazov^b, T. Taniguchi^c, K. Watanabe^c

- a. Université de Toulouse, INSA-CNRS-UPS, LPCNO, 135 Av. Rangueil, 31077 Toulouse, France
- b. Ioffe Institute, 194021 St. Petersburg, Russia
- c. National Institute for Materials Science, Tsukuba, Ibaraki 305-0044, Japan

The optical properties of MoS₂ monolayers are dominated by excitons, but for spectrally broad optical transitions in monolayers exfoliated directly onto SiO₂ substrates detailed information on excited exciton states is inaccessible.

Encapsulation in hexagonal boron nitride (hBN) allows approaching the homogenous exciton linewidth [1,2], but interferences in the van der Waals heterostructures make direct comparison between transitions in optical spectra with different oscillator strength more challenging. We have performed reflectivity and photoluminescence excitation experiments which reveal the presence of excited states of the A exciton in MoS₂ monolayers encapsulated in hBN layers of calibrated thickness, allowing us to extrapolate an exciton binding energy of ≈ 220 meV [3].

We theoretically reproduce the energy separations and oscillator strengths measured in reflectivity by combining the exciton resonances calculated for a screened two-dimensional Coulomb potential with transfer matrix calculations of the reflectivity for the van der Waals structure.

Our analysis shows a very different evolution of the exciton oscillator strength with principal quantum number for the screened Coulomb potential as compared to the ideal two-dimensional hydrogen model.

- [1] F. Cadiz et al, Physical Review X **7**, 021026 (2017).
- [2] E. Courtade, Physical Review B **96**, 085302 (2017)
- [3] C. Robert *et al*, Phys. Rev. Mat. **2**, 011001(R) (2018)

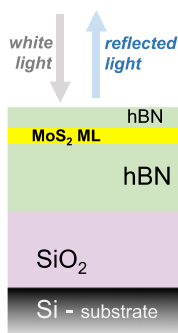


Figure 1 : Schematic of the investigated Van der Waals heterostructure

Gate reflectometry for hole spin qubit readout

A. Crippa^{a*}, R. Maurand^a, R. Ezzouch^a, A. Aprà^a, A. Amisse^a, X. Jehl^a,
M. Sanquer^a, M. Urdampilleta^b, C. Bauerle^b, T. Meunier^b, B. Bertrand^c,
H. Bohuslasvki^{a,c}, L. Hutin^c, S. Barraud^c, M. Vinet^c, L. Bourdet^d, Y.M.
Niquet^d, and S. De Franceschi^a

- a. CEA, INAC-PHELIQS, F-38054 Grenoble, France
- b. CNRS, Institut Néel, F-38042 Grenoble, France
- c. CEA, LETI, Minatec Campus, F-38054 Grenoble, France
- d. CEA, INAC-MEM, F-38054 Grenoble, France

* alessandro.crippa@cea.fr

Considerable progress has been made in the recent years toward the development of quantum processors in silicon (see, e.g., Refs. [1-5]). Research efforts were so far focused mainly on electron spin qubits. Confined holes, as opposed to electrons, may offer an attractive alternative, owing to an intrinsically strong spin-orbit coupling and to a reduced susceptibility to the nuclear-spin environment, which is known to be a major limiting factor to electron spin coherence. Our team has carried out pioneering work in this direction, reporting a first demonstration of spin-qubit functionality in p-type Si transistors issued from an industry standard fabrication line [6]. Following this proof-of-concept results, hole spin qubits have been gaining interest in the scientific community. A significant amount of work needs to be done in order move ahead, both at the technological and fundamental level. We have recently carried out systematic work to acquire a better understanding of the mechanism for electrically-driven hole spin control [7]. In this talk, we will present our progress toward the implementation of dispersive readout via gate-coupled radio-frequency reflectometry [8]. This technique does not require any locally fabricated charge-sensing device, which is an advantage in the prospect of future large-scale integration

- [1] Veldhorst, M. *et al.* A two-qubit logic gate in silicon, *Nature* **526**, 410–414 (2015).
- [2] Watson, T. F. *et al.* A programmable two-qubit quantum processor in silicon. *Nature* **555**, 633–637 (2018)
- [3] Zajac, D. *et al.* Resonantly driven CNOT gate for electron spins. *Science* **359**, 439-442 (2018)
- [4] Yoneda, J. *et al.* A quantum-dot spin qubit with coherence limited by charge noise and fidelity higher than 99.9%. *Nature Nanotech.* **13**, 102-106 (2018)
- [5] Mi, X. *et al.* Strong coupling of a single electron in silicon to a microwave photon. *Science* **355**, 156–158 (2017).
- [6] Maurand, R. *et al.* A CMOS silicon spin qubit. *Nat. Commun.* **7**, 13575 (2016).
- [7] Crippa, A. *et al.* Electrical Spin Driving by g-Matrix Modulation in Spin-Orbit Qubits. *Phys. Rev. Lett.* **120**, 137702 (2018).
- [8] Crippa, A. *et al.* Level spectrum and charge relaxation in a silicon double quantum dot probed by dual-gate reflectometry. *Nano Letters* **17**, 1001 (2017).

Nano-mechanics of ionic liquids at dielectric and metallic interfaces

Léo Garcia^a, Elizabeth Charlaix^a and Benjamin Cross^{a*}

a. Laboratoire Interdisciplinaire de Physique
Université Grenoble Alpes, Centre National de la Recherche Scientifique,
140 Av. de la physique, BP 87 38402 Saint Martin d'Hères - France

* benjamin.cross@univ-grenoble-alpes.fr

Using a dynamic surface force apparatus, we investigate the nano-mechanics and the nano-rheology of an ionic liquid at dielectric and metallic solid surfaces. On smooth dielectric Pyrex surfaces, we find an ordered interfacial phase extending over less than 3 nm away from the top of the layer, with a compression modulus of 15 MPa extracted from the profile of the oscillatory forces. We discuss the boundary flow of the Newtonian bulk phase on this ordered interfacial layer. On metallic platinum surfaces, our hydrodynamic measurements evidence an interfacial soft solid layer extending up to 20 nm away from the top of the layer. The elastic modulus of this interfacial layer, derived from elasto-hydrodynamic measurements, is similar to the one found on Pyrex surfaces. Both on the dielectric and on the metal surfaces, the thickness of the interfacial phases is not found to change upon approach of the opposite surface, and does not exhibit a capillary-freezing transition.

MASQ Tools: Simple software for Multi-Atomic Structure Factor Calculations

Gabriel J. Cuello^{a*}

a. Institut Laue Langevin, 71 av des Martyrs, 38042 Grenoble, France

* cuello@ill.fr

The total scattering experiments allow the determination of the structure factors for mono- and multi-atomic systems. In the former case, the extraction of the correlation functions is straightforward. For the latter the situation becomes complex due to the overlapping of different correlation functions. In fact, in a system with n atomic species, the total signal is composed of $n(n+1)/2$ partial structure factors, each one with a different weighting factor that depends on the composition and the scattering power of the involved atoms [1].

This program use as input the chemical formula (including isotopes) and gives as outcome the weighting factors for numerical simulations, X-ray scattering and neutron scattering. It gives these factors for three different formalisms: Faber-Ziman [2], Ashcroft-Langreth [3] and Bathia-Thorton [4] (the latter only valid for binary systems). The program also gives the neutron scattering lengths and cross sections (coherent and incoherent, free and bound) per scattering unit, as well as the absorption cross sections.

This non-commercial software has been developed in python and in PHP for its web-based version. The program includes the most recent data compilation of neutron scattering lengths and neutron scattering cross sections [5]. This allows its use also to consult information about neutron scattering data for a given atom/isotope.

[1] G. J. Cuello, *J. Phys. Cond. Matter* **20**, 244109 (2008).

[2] T. E. Faber and J. M. Ziman, *Phil. Mag.* **11**, 153 (1965).

[3] N. W. Ashcroft and D. C. Langreth, *Phys. Rev.* **156**, 685 (1967) ; *Phys. Rev.* **159**, 500 (1967) ; *Phys. Rev.* **166**, 934 (1968).

[4] A. B. Bathia and D. E. Thornton, *Phys. Rev. B* **2**, 3004 (1970).

[5] J. Dawidowski, J. R. Granada, J. R. Santisteban, F. Cantargi and L. A. Rodríguez Palomino, p. 471 in *Neutron Scattering – Fundamentals*, F. Fernández-Alonso and D. Price (Eds.), (Elsevier, Amsterdam, 2013).

Frustrated magnetism vs. glassiness

Leticia F. Cugliandolo^{a,b*}

a. Sorbonne Université, Laboratoire de Physique Théorique et Hautes Energies, France

b. Institut Universitaire de France

* leticia@lpthe.jussieu.fr

Frustrated magnets are systems in which the interactions in combination with the lattice structure impede the spins to order in an optimal configuration at zero temperature. Spin glasses are materials with random exchange interactions that induce frustration but also disorder. In this talk I will review some salient features of these two families of magnets, and I will focus on the main similarities and differences that have been identified so far in experimental, numerical and analytic studies.

Force-strain study of 2D soap bubbles

Damien Cuvelier^{a*}

a. UMR 144 Institut Curie/IPGG, 6 rue Jean Calvin 75005 Paris

* damien.cuvelier@curie.fr

An original set-up is used to study the mechanics of soap bubbles. Soap bubbles are squeezed between two parallel surfaces and punctually deformed by two needles. The force measurement is carried out by the deflection of a micro-plate. We performed the stretching from single bubbles to multiple bubbles.

For one 2D bubble, we experimentally and theoretically show that its rigidity is inversely proportional to the radius. This allows us to determine the interfacial properties.

For two bubbles in contact, the rigidity of the system under strain is the rigidity of a single bubble with a double radius.

We study experimentally the dynamics of strain-induced T1 neighbor switching in clusters of 2D bubbles (fig 1). At a quasi-static time scale, we show that the T1 transition occurs at the same value of force and strain for different cluster sizes of 4 identical bubbles. The force deformation curves are superposed on a single master curve. The T1 transition for asymmetrical clusters composed of bubbles of various sizes occurs at different values of force and strain whereas the rigidity observed remains the same as for the case of symmetrical clusters. The time scale of rearrangement is set by the surface tension, the surface viscous forces and the sizes of the bubbles.

In order to approach to a 2D foam situation, we stretched bigger clusters. After an elastic deformation of these clusters we observed the successive rearrangements at a quasi-constant force value as it had already been observed for a sheared 2D soap bubbles foam [1].

[1] (1) Kabla, A., Scheibert, J., & Debregeas, G. (2007). Quasi-static rheology of foams. Part 2. Continuous shear flow. *Journal of Fluid Mechanics*, 587, 45-72.

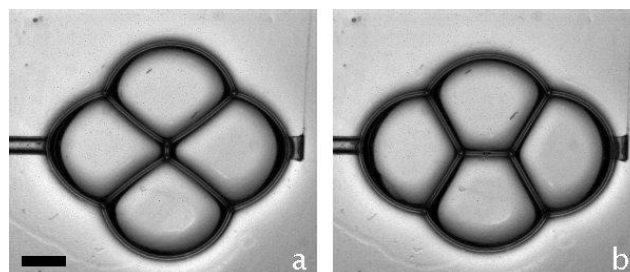


Figure 1 : T1 transition of 4 identical bubble (a. before b. after). The scale bar represents 2cm

Rhenium epitaxial nanowires

C. Naud^{a*}, K. Bharadwaj^a, A. Kapoor^a, B. Gilles^b, R. Kramer^a, O. Buisson^a

a. Institut Neel CNRS/UGA BP 166 38042 GRENOBLE Cedex 9

b. SIMAP BP 75 38402 Saibt Martin d'Hères

* Cécile.naud@neel.cnrs.fr

This work has been performed in the frame of the realization of superconducting quantum circuits based on Josephson junctions. Currently, the superconducting quantum circuits are realized with Aluminium which is easily evaporated. Nevertheless, the thin films of Aluminium are polycrystalline and have a poor crystallographic quality. This gives rise to limitations of the characteristics of the circuits. In order to obtain better performances, we are preparing our superconducting thin films by molecular beam epitaxy. The rhenium has been chosen because the lattice mismatch between rhenium and sapphire [0001] is small. The quality of the layer as well as the interface between sapphire and the rhenium is very high. Moreover, the rhenium does not oxidise, leading to clean interfaces.

We present the epitaxial growth and the structural characterizations of the rhenium thin film. Starting from these epitaxial films, we have realized the fabrication of nanowires down to 50 nm using electron beam lithography. Critical temperature, critical current and fluctuations around the superconducting transition measurements have been performed as function of their widths.

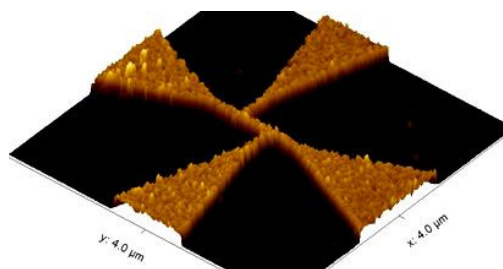


Figure 1 : Rhenium nanowire onto a sapphire substrate.

High temperature superconducting oxchlorides: a light element model for cuprates

Matteo d'Astuto^{a*}

a. Institut NEEL CNRS/UGA UPR2940, 25 rue des Martyrs BP 166, 38042 Grenoble cdx 9, France

* matteo.dastuto@neel.cnrs.fr

The copper oxchloride cuprate $\text{Ca}_2\text{CuO}_2\text{Cl}_2$ (CCOC) system, with vacancy or Na doping on the Ca site, is unique among the high temperature superconducting cuprates (HTSCs) since it: lacks high Z atoms; has a simple I4/mmm 1-layer structure, typical of 214 (LSCO) cuprates, but which is stable at all doping and temperatures; and has a strong 2D character due to the replacement of apical oxygen with chlorine [1]. It also shows a remarkable phase diagram, with a superconducting T_c growing to the optimal doping without any minimum around 1/8 doping, despite the observation of charge modulations by near-field spectro-microscopy [2]. Due to the reduced number of electrons, advanced calculations that incorporate correlation effects, such as quantum Monte Carlo [3], are easier, but relatively little is known about CCOC (for a cuprate) from an experimental point of view. We are now filling this gap by a comprehensive experimental study covering the whole phase diagram, in particular of the (para)magnon [4] and phonon dispersion [5].

- [1] Z. Hiroi, N. Kobayashi, M. Takano, *Nature* **371**, 139 (1994); Y. Kohsaka et al. *JACS* **124**, 12275 (2002)
- [2] T. Hanaguri et al. *Nature* **430**, 1001 (2004); K. Fujita et al. *PNAS* **111**, E3026 (2014)
- [3] K. Foyevtsova et al., *Phys. Rev. X* **4**, 031003 (2014); L. K. Wagner, *Phys. Rev. B* **92**, 161116(R) (2015)
- [4] B. W. Lebert, et al. *Phys. Rev. B* **95** 155110 (2017); B. Lebert et al., in preparation
- [5] M. d'Astuto et al. *Phys. Rev. B* **88**, 014522 (2013); B. Lebert et al., in preparation

Unveiling the mysterious magnetic state of superconducting iron under pressure

B. W. Lebert^{a,b}, T. Gorni^a, M. Casula^a, J.-P. Rueff^b, S. Klotz^a, F. Baudalet^b, J. M. Ablett^b, T. Straessle^c, T. Hansen^d, A. Juhin^a, A. Polian^{a,b}, P. Munsch^a, G. Le Marchand^{a,b}, Z. Zhang^{a,b}, M. d'Astuto^{e*}

- a. IMPMC UMR7590, Sorbonne Université, 4, pl. Jussieu, BC 115, 75252 Paris cdx 5
- b. Synchrotron SOLEIL, Saint-Aubin, BP 48 91192 Gif-sur-Yvette cdx
- c. Paul Scherrer Institut, Villigen, Switzerland
- d. Institut Laue-Langevin, 71 av. des Martyrs, CS 20156, 38042 GRENOBLE cdx 9, France
- e. Institut NEEL CNRS/UGA UPR2940, 25 rue des Martyrs BP 166, 38042 Grenoble cdx 9, France

* matteo.dastuto@neel.cnrs.fr

Compressed iron undergoes a transition from bcc to hcp crystal structure with a loss of ferromagnetism. The magnetic state of the hcp phase has been debated for many decades and experiments give seemingly contradictory results. Mössbauer measurements find no magnetism, however x-ray emission spectroscopy finds remnant magnetism and Raman mode splitting suggests symmetry breaking due to antiferromagnetism. These paradoxical results are consistent with either a paramagnetic state with spin fluctuations faster than Mössbauer timescales or an antiferromagnetic state, afmII, which is undetectable with Mössbauer spectroscopy. We performed neutron powder diffraction measurements in the hcp phase and do not observe afmII order down to 1.8 K, while confirming the existence of a local magnetic moment in the hcp phase with x-ray emission spectroscopy and find it is intrinsic to this phase (1). This local magnetic moment disappears at 30-40 GPa, exactly the same pressure region where superconductivity disappears. To solve the paradox, we derived an antiferromagnetic spin Hamiltonian modelled from *ab initio* calculations, where we allowed for spin fluctuations in both direction and magnitude. We found that the frustration inherent in the hcp lattice implies the existence of a complex texture of stripe patterns, compatible with the experimental results.

- [1] B. W. Lebert, T. Gorni, M. Casula, J.-P. Rueff, S. Klotz, F. Baudalet, J. M. Ablett, T. Straessle, T. Hansen, A. Juhin, A. Polian, P. Munsch, G. Le Marchand, Z. Zhang, M. d'Astuto, *article in preparation*.

A tunable two-dimensional electron system created at the surface of SnO₂(110)

J. Dai^a, E. Frantzeskakis,^a F. Fortuna,^a P. Le Fèvre,^b F. Bertran,^b R. Yukawa,^c
H. Kumigashira,^c P. Lömker,^d M. Müller,^{d,e} and A. F. Santander-Syro^{a*}

- a. CSNSM, Université Paris-Sud, CNRS/IN2P3, Université Paris-Saclay, 91405 Orsay Cedex, France
- b. Synchrotron SOLEIL, L'Orme des Merisiers, Saint-Aubin-BP48, 91192 Gif-sur-Yvette, France
- c. Photon Factory, Institute of Materials Structure Science, High Energy Accelerator Research Organization (KEK), 1-1 Oho, Tsukuba 305-0801, Japan
- d. Peter Grünberg Institut (PGI-6), Forschungszentrum Jülich GmbH, D-52428 Jülich, Germany
- e. Fakultät Physik, Technische Universität Dortmund, D-44221 Dortmund, Germany

* andres.santander@csnsm.in2p3.fr

Tin oxide (SnO₂) is an important transparent binary oxide widely used as a gas sensor material and believed to remain insulating even in the presence of oxygen vacancies [1]. We report that a new 2D electron system (2DES) can be created and controlled at the (110) surface of SnO₂, see Figure 1. We characterize its electronic structure using angle resolved photoemission spectroscopy (ARPES), and show that it is formed out of the bulk *s*-like conduction band minimum of SnO₂ confined at the surface. The carrier density of such 2DES increases by an order of magnitude when cooling down from room temperature to 15 K, and can be further enhanced to $n_{2D} = (2.15 \pm 0.04) \times 10^{13} \text{ cm}^{-2}$ after thermal deposition of an atomic layer of Eu, linking the origin of this 2DES to the oxygen vacancies created at the SnO₂ surface after the redox reaction with Eu.

[1] L. R. Merte, et al., Phys. Rev. Lett. **119**, 096102 (2017).

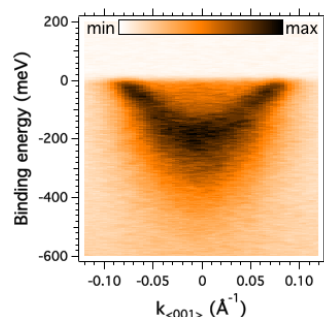


Figure 1: Energy-momentum ARPES intensity map at the SnO₂(001) surface, along the in-plane $k_{\langle 001 \rangle}$ direction. The measurement temperature is $T = 15 \text{ K}$.

Smart Discrete Elements based on the A-CD2 approach

S. Dal Pont*

a. Université Grenoble Alpes, Laboratoire 3SR, France

* stefano.dalpont@3sr-grenoble.fr

This paper focuses on the enhancement of a discrete-elements approach to model the evolution of a crowd of people in emergency evacuation situations.

The selected discrete element model is based on the non-smooth mechanics principles [1]. The application of the principle of virtual work in association with appropriate constitutive laws relating internal stress and velocities, result in a set of equations of motion, valid both for smooth and for non-smooth evolutions. The atomized efforts contact dynamics approach respecting the Clausius–Duhem inequality (A-CD2) [2] provides the numerical framework of the approach and guarantees the existence and the uniqueness of the solution without the need of penalty formulations.

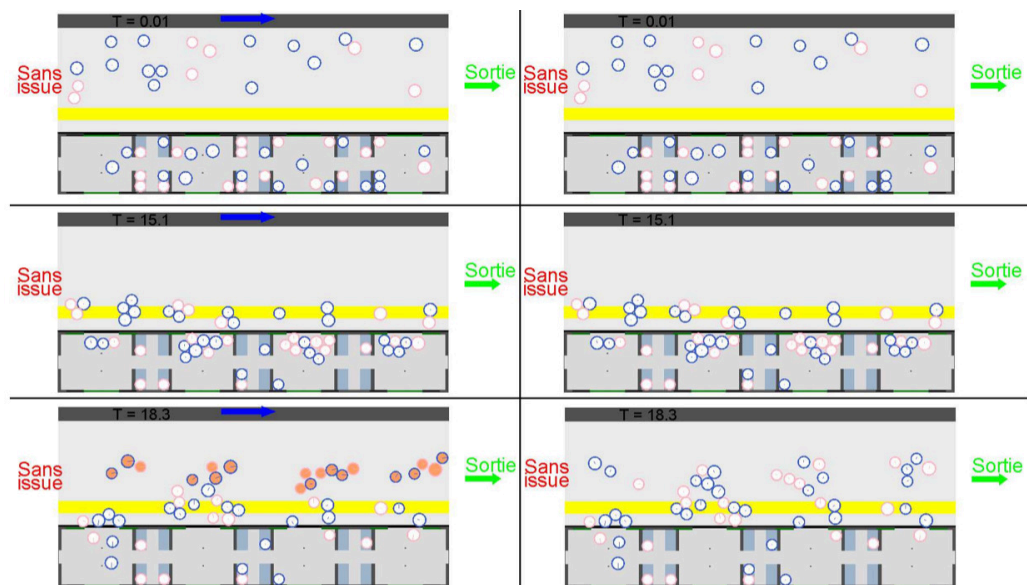
As a further step, the method has been enhanced to develop « smart » particles, i.e. pedestrians. Level-sets have been introduced to provide to each grain a desired velocity or, in other terms, « willingness ». Each particle representing a human being has specific and unique properties such as its own velocity, mass, reactivity, etc. and actively interacts through « social » forces with the external environment (i.e. other pedestrians and/or obstacles). The system evolves naturally, thus simulating pedestrian traffic and the behavior of a crowd of people.

Some typical situations are finally illustrated and compared, when possible, with real safety exercises in configurations such as the presence of a bottle-neck, emergency evacuations and platform-train exchange.

[1] M. Frémond, Rigid bodies collisions. Phys Lett A 204:33–41 (1995)

[2] S. Dal Pont, E. Dimnet, A theory for multiple collisions of rigid solids and numerical simulation of granular flow. Int J Solids Struct., 43/20:6100–6114 (2006)

Figure 1 : Signage system proposed at RATP : photograms of one typical simulation of the platform/train passenger interchange with (on the left) and without (on the right) signage



Size effects for amorphous crystallization kinetics: Constraints imposed by nucleation and growth specificities

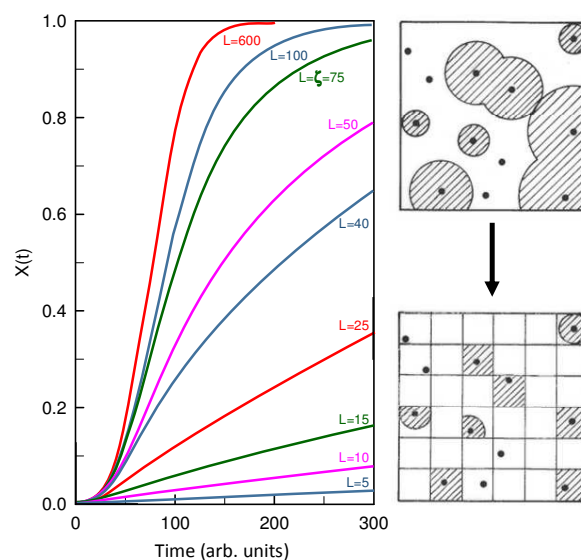
Marc Descamps^{*}, Jean-François Willart

Université de Lille, CNRS UMR 8207 – UMET – Unité Matériaux et Transformations,
F-59000, Lille

* marc.descamps@univ-lille1.fr.

The main purpose of the presentation is to highlight the intrinsic link between the nucleation rate and growth rate with a temperature dependent characteristic transformation time $\tau(T)$, and a characteristic size $\xi(T)$. The consequences on the influence of the sample size on kinetics of crystallization is considered. The expression of the kinetic crystallization rate, $X(t)$, of a nucleation and growth transformation is fundamentally dependent on the position of the sample size (L) with respect to ξ . It changes from an Avrami like behavior for $L \gg \xi$ to a size dependent exponential regime for $L \ll \xi$. The significance of size effect and confinement for amorphous stabilization in the pharmaceutical sciences is discussed.

Marc Descamps, Jean-François Willart *International Journal of Pharmaceutics* 542
(2018) 186–195



2-Dimensional simulation of the time evolution of the transformed fraction $X(t)$ for different grain sizes (from above to below ξ).

Emission d'électrons induite par irradiation d'une nanopointe avec un laser ultrarapide

Maxime DUCHET*, Sorin PERISANU, Eric CONSTANT, Anthony AYARI, Vincent LORIOT, Franck LEPINE, Stephen PURCELL

Univ Lyon, Université Claude Bernard Lyon 1, CNRS, Institut Lumière Matière, F-69622, VILLEURBANNE, France

*maxime.duchet@univ-lyon1.fr

La dynamique électronique quantique dans des atomes, des molécules et des solides excités par laser est responsable de nombreux processus tel que la photoémission, la photoémission assistée par émission de champ (*Photofield emission*) [1], la ionisation au-dessus du seuil (*Above Threshold Ionisation, ATI*) pour les gaz, la photoémission au-dessus du seuil (*Above Threshold Photoemission, ATP*) pour les solides [2] et l'émission de champ optique (*Optical Field emission*) [3-4]. L'excitation d'une pointe de taille nanométrique par un laser femtoseconde permet d'avoir à la fois une très bonne résolution spatiale et temporelle afin d'étudier puis de contrôler les dynamiques électroniques.

Je montrerai dans un premier temps les résultats des émissions électroniques observées en irradiant une pointe de tungstène de 40 nm de rayon avec un oscillateur femtoseconde opérant à la cadence de 80 MHz et délivrant des impulsions de 14 fs. Je détaillerai les étapes importantes réalisées pour les obtenir, incluant le taillage de la pointe par électrolyse, la caractérisation des impulsions lasers par la méthode FROG (frequency resolved optical gating), l'alignement et la focalisation du laser sur la pointe, et la mesure des spectres en énergie. Enfin, je présenterai nos derniers résultats utilisant le champ électrique du laser et l'effet de pointe en vue d'extraire des informations sur les propriétés quantiques des atomes se trouvant au bout de la pointe.

[1] Yanagisawa H, Hafner C and Doná P. *Laser-induced field emission from a tungsten tip: Optical control of emission sites and the emission process*. Physical Review B, **81** (11): 115429 (2010).

[2] Schenk M, Krüger M and Hommelhoff P. *Strong-Field Above-Threshold Photoemission from Sharp Metal Tips*. Physical Review Letters, **105** (25): 257601 (2010).

[3] M. Uiberacker, Th. Uphues, M. Schultze, A. J. Verhoef, V. Yakovlev, M. F. Kling, J. Rauschenberger, N. M. Kabachnik, H. Schröder, M. Lezius, K. L. Kompa, H.-G. Müller, M. J. J. Vrakking, S. Hendel, U. Kleineberg, U. Heinzmann, M. Drescher & F. Krausz. *Attosecond real-time observation of electron tunnelling in atoms*. Nature, **446** : 627-632 (2007).

[4] Bormann R, Gulde M, Weismann A, Yalunin SV and Ropers C. *Tip-Enhanced Strong-Field Photoemission*. Physical Review Letters, **105** (14): 147601 (2010).

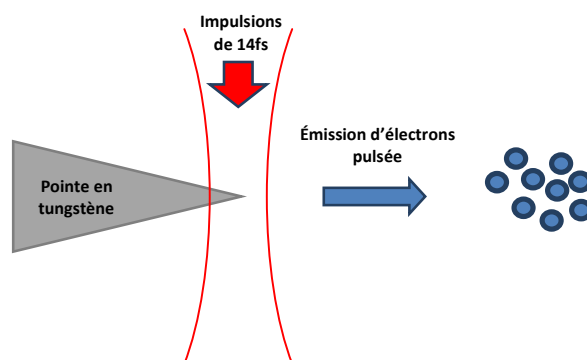


Figure 1 : Schéma de l'émission électronique d'une pointe de tungstène irradiée par un laser femtoseconde

Towards Single Spin detection using microwaves

**J.F. Silva Barbosa¹, P. Campagne-Ibarcq¹, P. Jamonneau^{1,2}, S. Probst¹, Y. Kubo¹,
A. Bienfait¹, T. Teraji³, S. Pezzagna⁴, D. Vion¹, R. Heeres¹ and P. Bertet¹**

¹Quantronics Group, SPEC, CEA-Saclay, France, ²LPQM, ENS de Cachan, France, ³NIMS, University of Tsukuba, Japan, ⁴Department of Nuclear Solid State Physics, Leipzig University, Germany

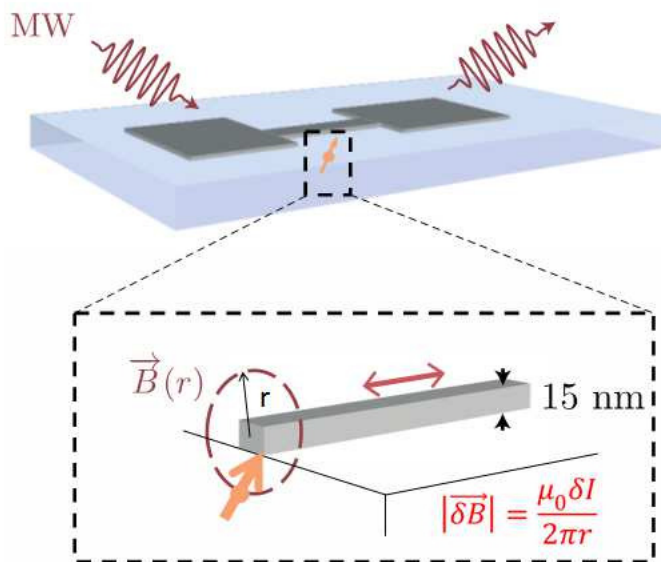


Figure.1: Sketch of our method

Our project aims at detecting a single spin using magnetic resonance techniques by coupling it to a high quality factor superconducting resonator. The electron spins of choice are shallow (~15 nm) implanted single Nitrogen-vacancy (NV) centers in an ultrapure isotopically-enriched C12 diamond layer. After characterization at room temperature using a confocal microscopy, an Aluminium microwave resonator is fabricated on top with a nanometric constriction (width ~40 nm) carefully aligned to a pre-selected NV center.

The constriction enhances the magnetic field generated by the microwave frequency current, and therefore allows to increase the spin-resonator coupling strength to a range of 1 – 5 kHz. Microwave-only measurements in a dilution refrigerator at 20mK should then allow to observe a spin-echo signal from a single spin.

Magnetic order, slow dynamics and possible magnetic fragmentation in rare earth spinels CdYb_2S_4 and CdYb_2Se_4

P. Dalmas de Réotier^{a*}, A. Yaouanc^a, C. Ritter^b, A. Maisuradze,^c B. Roessli,^d
A. Bertin,^a P.J. Baker,^e and A. Amato^f

- a. Université Grenoble Alpes and CEA, Institut Nanosciences et Cryogénie, Pheligs, F-38000 Grenoble, France
- b. Institut Laue Langevin, F-38042 Grenoble cedex 9, France
- c. Tbilisi State University, Department of Physics, GE-0128 Tbilisi, Georgia
- d. Paul Scherrer Institute, Laboratory for Neutron Scattering and Imaging, CH-5232 Villigen-PSI, Switzerland
- e. STFC Rutherford Appleton Laboratory, ISIS facility, Chilton, OX11 0QX. United Kingdom
- f. Paul Scherrer Institute, Laboratory for Muon-Spin Spectroscopy, CH-5232 Villigen-PSI, Switzerland

* pierre.dalmas-de-reotier@cea.fr

For the last two decades, geometrically frustrated magnetism has been an active field of condensed matter research which has unveiled new concepts in the physics of interacting systems. The pyrochlore series of compounds has been at the forefront of the activity in the domain. Here we report on a study of the spinels CdYb_2S_4 and CdYb_2Se_4 [1] in which the Yb^{3+} rare earth ions sit at the same sublattice of corner-sharing regular tetrahedra as in the pyrochlores. The difference in the local environment of the rare earth ions in the pyrochlores and spinels gives a new perspective that we illustrate by a discussion of the magnetic order, slow dynamics and possible magnetic fragmentation found for these two spinels.

[1] P. Dalmas de Réotier *et al*, Phys. Rev. B **96**, 134403 (2017).

New insights into the magnetic textures of MnSi

P. Dalmas de Réotier^{a*}, A. Maisuradze,^b A. Yaouanc^a, B. Roessli,^c A. Amato^d,
D. Andreica^e, and G. Lapertot^a

- a. Université Grenoble Alpes and CEA, Institut Nanosciences et Cryogénie, Pheliqs, F-38000 Grenoble, France
- b. Tbilisi State University, Department of Physics, GE-0128 Tbilisi, Georgia
- c. Paul Scherrer Institute, Laboratory for Neutron Scattering and Imaging, CH-5232 Villigen-PSI, Switzerland
- d. Paul Scherrer Institute, Laboratory for Muon-Spin Spectroscopy, CH-5232 Villigen-PSI, Switzerland
- e. Babes-Bolyai University, Faculty of Physics, 400084 Cluj-Napoca, Romania

* pierre.dalmas-de-reotier@cea.fr

The non-centrosymmetric compound MnSi was the first system in which a magnetic skyrmion lattice has been identified a decade ago. Although skyrmions and skyrmion lattices have been observed in numerous other compounds, MnSi remains a model system for a study of the interplay of the magnetic interactions which are at the origin of the skyrmions. Here, from a quantitative interpretation of muon spin rotation spectra, we revisit its magnetic structure in the helical and conical phases [1,2] and find subtle deviations from the structures taken for granted. These results point to the need of a microscopic model for the description of the interactions at play. Preliminary results in the skyrmion phase are finally presented.

[1] P. Dalmas de Réotier *et al*, Phys. Rev. B **93**, 144419 (2016).

[2] P. Dalmas de Réotier *et al*, Phys. Rev. B **95**, 180403 (2017).

Berezinskii-Kosterlitz-Thouless crossover for Dipolar excitons

Suzanne Dang ^{a*}, Romain Anankine ^a, Carme Gomez ^b, Aristide Lemaître ^b, Markus Holzmann ^c et François Dubin ^a

- a. Institut des Nanosciences de Paris, Sorbonne University, 4 place Jussieu, 75005 Paris.
- b. C2N, University Paris-Saclay, Route de Nozay, 91460 Marcoussis, France.
- c. Laboratoire de Physique et Modélisations des Milieux Condensés, 25 avenue des Martyrs, 38042 Grenoble, France.

* suzanne.dang@insp.upmc.fr

Indirect excitons confined in GaAs double quantum wells (DQW) constitute a model system to investigate the quantum phases accessible to dipolar gases. Indirect excitons result from the Coulomb attraction between spatially separated electrons and holes, a situation which is directly achieved by applying an electric field perpendicular to the plane of a DQW. In recent experiments we have reported signatures of quantum coherence and quantized vortices in the photoluminescence radiated by indirect excitons confined in a two-dimensional trap [1]. Here we show that in this geometry the excitons quantum phase transition obeys the Berezinskii-Kosterlitz-Thouless (BKT) mechanism, as expected theoretically. We show that the crossover occurs in a very unique way, due to strong dipolar interactions between excitons and also their underlying four-component spin-structure.

In our experiments, the BKT transition is accessed by unveiling the exciton equation of state, at thermal equilibrium, together with its scale invariance (Fig. 1). Using Monte-Carlo simulations we quantify this behavior and then localize the crossover, precisely its critical temperature and density. These physical parameters are then confirmed quantitatively by analyzing the excitons quantum spatial coherence and the spatial distribution of density fluctuations. The latter analysis allows us to reveal the expected defect-driven nature of the excitonic superfluid transition at two-dimensions [2].

[1] R. Anankine et al. , Phys. Rev. Lett. , 2017, 118, 127402.

[2] S. Dang et al., submitted

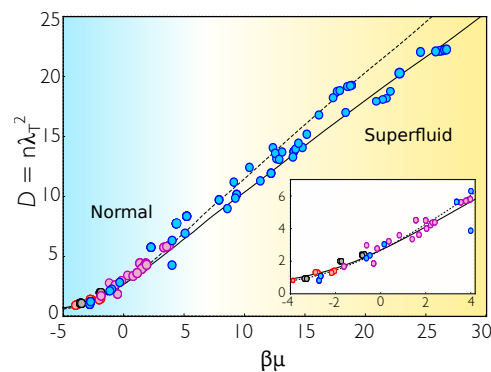


Figure 1: Phase space density $D=n\lambda_T^2$ as a function of the scaled chemical potential $\beta\mu = \mu/k_B T_b$ measured at $T=0.33, 1.2, 2.5$ and 3.5 K (blue, pink, black and red respectively).

Development of a multi-band magnetic material by coating oxide in fluid processing

Marie Darcheville^{a*}, Christophe Boscher^a, Karine Vallé^a, Anne-Lise Adenot-Engelvin^a, Clément Sanchez^b and André Thiaville^c

- a. CEA, DAM Le Ripault, F-37260 Monts, France
- b. Laboratoire Chimie de la Matière Condensée de Paris, UPMC – Tour 44 – 43/Et 4, 4 Place Jussieu, 75252 Paris Cedex 05, France
- c. Laboratoire de Physique des Solides, UMR 8502 Université Paris-Sud bât 510, 91405 Orsay Cedex, France

* marie.darcheville2@cea.fr

The goal of the thesis is to develop micro-pattern networks of magnetic oxides by fluid processing, in order to create a framework with magnetic domains. The purpose is to realize new materials with perfectly controlled magnetic properties. In this way, we would like to study the potential of inkjet printing to produce these structured materials. The formulation $Zn_xFe_{3-x}O_4$ has been chosen because it allows to modify and to control the magnetic and dielectric properties of the final product by changing the ratio between Fe and Zn quantities.

The development of these new materials requires the synthesis of an ink made of magnetic nanoparticles dispersed in a liquid media. This ink will be ejected by inkjet printing in order to obtain the final material.

Thus, the first step of the project is to synthesize magnetic nanoparticles. At least two size ranges are intended (< 30 nm, and between 30 and 70 nm) to analyze the influence of the size of the particles on the structure and on the magnetic properties of the coating. Different methods of synthesis have been tested like the thermal decomposition in a conventional way and by means of microwave assistance. The aim is to control the size and morphology spread of the obtained nanoparticles. An experimental study has been realized to optimize the synthesis conditions and to choose the most appropriate synthesis to launch the dispersion step.

The results introduced in this poster show the capability of developing a synthesis method with a good control of particle size and morphology, and above all adaptable and repeatable.

The dispersion of these nanoparticles in a liquid media and the optimization of the rheology are currently going on to make these formulations compatible with the inkjet printing process.

Synthèses sous hautes pressions – hautes températures de nouveaux composés multiferroïques NaLnCoWO_6

Céline Darie^a, Peng Zuo^a, Claire V. Colin^a, Holger Klein^a, Pierre Bordet^a, Céline Goujon^a, Murielle Legendre^a, Eric Elkaim^b, Emmanuelle Suard^c

- a. Institut Néel, Université Grenoble-Alpes and Institut Néel, CNRS, Grenoble F_38042, France
- b. Synchrotron SOLEIL, L'Orme des Merisiers, Saint Aubin — BP 48, F-91192 Gif-sur-Yvette, France
- c. Institut Laue-Langevin, BP 156, F- 38042 Grenoble, France

* celine.darie@neel.cnrs.fr

Récemment des concepts théoriques ont prédit la possibilité de générer de la ferroélectricité par la rotation des octaèdres d'oxygènes dans des structures dérivées de la structure pérovskite : c'est la « Ferroélectricité Hybride Impropre ». Parmi les structures prédites nous nous sommes intéressés à la classe des doubles pérovskites ordonnées $\text{AA}'\text{BB}'\text{O}_6$. [1,2]

Nous avons synthétisé la série des composés NaLnCoWO_6 avec $\text{Ln} = (\text{La}, \text{Pr}, \text{Nd})^{\text{A}}, (\text{Sm}, \text{Eu}, \text{Gd}, \text{Tb}, \text{Dy}, \text{Ho}, \text{Er}, \text{Yb and Y})^{\text{B}}$. Les trois premiers membres de la série ont été obtenus par une méthode A type céramique à 900°C sous air. Les membres de la série correspondant aux terres rares plus petites ont été obtenus pour la première fois par stabilisation sous Hautes Pressions - Hautes Températures (HP-HT) : méthode B. Les caractérisations structurales obtenues par diffraction des rayons X haute résolution et diffraction des neutrons seront présentées ainsi que les premières mesures magnétiques et électriques [3].

[1] King, S. Thimmaiah, A. Dwivedi, and P.M. Woodward, Chem. Mater. 19, 6451 (2007).

[2] M. Retuerto et al., Inorg. Chem. 52, 12482 (2013).

[3] P. Zuo, C. V. Colin, H. Klein, P. Bordet, E. Suard, E. Elkaim and C. Darie Inorg. Chem., **56**, 8478 (2017)

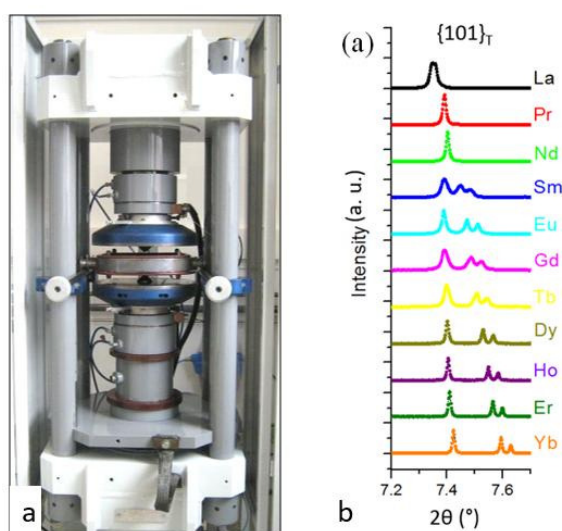


Figure 1 : (a) dispositif HP-HT de l'Institut Néel – Belt (b) diffractogrammes de la série NaLnCoWO_6 : évolution des raies $\{101\}_r$.

Nouvelle phase trigonale $\text{Ba}_3\text{NiSb}_2\text{O}_9$ obtenue par synthèse Haute Pression/ Haute Température

Céline Darie^{a*}, Christophe Lepoittevin^a, Holger Klein^a, Stéphanie Kodjikian^a, Pierre Bordet^a, Claire V.Colin^a, M. Legendre^a, C. Goujon^a, Catherine Deudon^b, Christophe Payen^b

- a. Institut Néel, Université Grenoble-Alpes and Institut Néel, CNRS, Grenoble F_38042, France
 b. Institut des Matériaux Jean Rouxel (IMN), UMR6502, Université de Nantes, CNRS ,Nantes Cedex 3 F_44322, France

* celine.darie@neel.cnrs.fr

Dans le cadre de la recherche de composés présentant un comportement de Liquide de Spin Quantique (LSQ) nous nous sommes intéressés à la synthèse du composé $\text{Ba}_3\text{NiSb}_2\text{O}_9$. Les propriétés LSQ semblent liées à la présence d'un réseau 2D triangulaire du nickel, avec frustration géométrique des interactions antiferromagnétiques, au sein de la structure cristalline, dite 6H-B (hexagonale groupe d'espace P63mc) qui est constituée de bi-octaèdres NiSbO_9 . Les premières études physiques, conduites jusqu'à 0,35 K, montrent que la phase 6H-B se comporte comme un LSQ sans gap de spin [1]. Du point de vue de la synthèse, des échantillons polycristallins de $\text{Ba}_3\text{NiSb}_2\text{O}_9$ 6H-B sont obtenus par traitement haute pression haute température (HPHT, 3GPa et 600 °C) d'une phase $\text{Ba}_3\text{NiSb}_2\text{O}_9$ dite 6H-A, préparée à pression ambiante, contenant des bioctaèdres Sb_2O_9 .

Nous présenterons tout d'abord l'originalité et la particularité des synthèses sous hautes pressions et hautes températures (HP-HT) ainsi que les études structurales fines effectuées pour caractériser le composé $\text{Ba}_3\text{NiSb}_2\text{O}_9$ obtenu dans nos dispositifs [2].

La mise en évidence d'une nouvelle forme cristallographique conservant l'empilement des réseaux triangulaires de Ni ont permis de valider ce composé comme une réalisation expérimentale d'un composé de type Liquide de spin [3].

- [1] J. G. Cheng, G. Li, L. Balicas, J. S. Zhou, J. B. Goodenough, C. Xu, and H. D. Zhou, Phys. Rev. Lett. **107**, 197204 (2011).
 [2] C. Darie, C. Lepoittevin, H. Klein, S. Kodjikian, P. Bordet, C. V. Colin, O. I. Lebedev, C. Deudon, and C. Payen, J. Solid State Chem. **237**, 166 (2016).
 [3] J. A. Quilliam, F. Bert, A. Manseau, C. Darie, C. Guillot-Deudon, C. Payen, C. Baines, A. Amato, and P. Mendels, Physical Review B **93**, 214432 (2016).

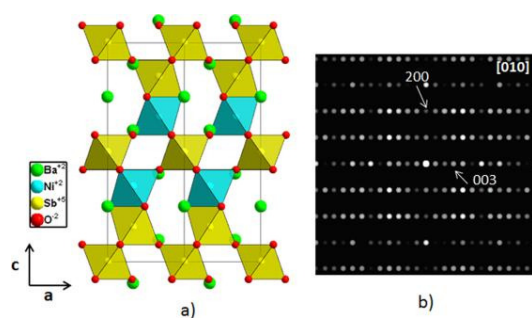


Figure 1 : (a) Modèle structural proposé dans le groupe d'espace P3. Projection selon l'axe b. (b) Simulation du cliché de diffraction électronique en précession pour l'axe de zone [0 1 0].

Mapping Local Resistance of Sidewall Graphene Nanoribbons

A. De Cecco^{1,2}, V. Prudkovskiy², D. Deniz³, Y. Hu³, Y. Hu³, J.-P. Turmaud³, J. Gigliotti³,
L. Ma⁴, C. Berger^{2,3}, W. A. de Heer^{3,4}, H. Courtois^{1,2}, C. B. Winkelmann^{1,2}

¹ Université Grenoble Alpes, Institut Néel, 25 Avenue des Martyrs, 38042 Grenoble, France

² CNRS, Institut Néel, 25 Avenue des Martyrs, 38042 Grenoble, France

³ School of Physics, Georgia Institute of Technology, Atlanta, USA

⁴ TICNN, Tianjin University, China

Epitaxial graphene on SiC represents one of the most promising candidates for large-scale integration of graphene-based electronics. In particular, epitaxial graphene sidewall nanoribbons (GNRs) are nanostructures of fundamental interest which can provide direct and controllable access to charge neutral graphene [1]. High-temperature epitaxial growth methods can provide exceptionally homogeneous and pure GNRs samples [2]. Due to quantum confinement effects, exceptional ballistic transport at room temperature was recently observed in these systems [3]. Ballistic transport in graphene close to the Dirac point has been the subject of several theoretical studies, but its fundamental aspects are not yet fully understood. Using a cryogenic combined AFM/STM setup, we measure the local resistance and potential of GNR-based devices with nm-scale spatial resolution and μV -scale voltage resolution. Local potential and resistance, measured at room temperature both in the invasive and non-invasive probe regimes, show plateaus and non-constant slopes which provide clear indication of non-diffusive transport.

References:

- [1] Palacio *et al.*, *Nano Lett.* **15** (1), pp. 182–189 (2014)
 [2] Sprinkle *et al.*, *Nature Nanotechnology* **5**, pp. 727–731 (2010)
 [3] Baringhaus *et al.*, *Nature* **506**, pp. 349–354 (2014)

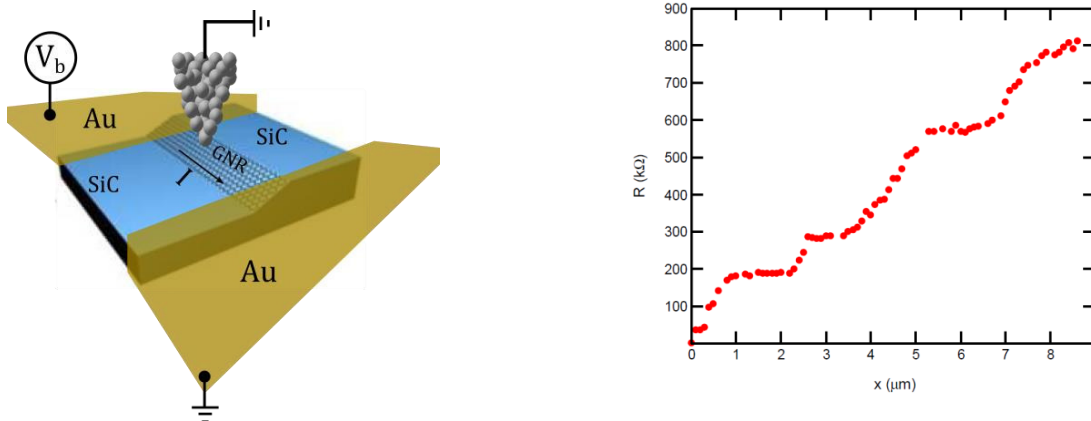


Fig. (left) Schematic representation of a sidewall GNR between two metallic contacts explored by a scanning probe tip. (right) Local resistance to nearest contact as a function of distance showing plateaus and varying slopes.

Simulating spin models on a Rydberg platform

S. de Leseleuc, V. Lienhard, D. Barredo, T. Lahaye and A. Browaeys

Laboratoire Charles Fabry, UMR 8051, Institut d'Optique, CNRS, Univ Paris Sud 11, 2 Avenue Augustin Fresnel, 91127 Palaiseau cedex, France
sylvain.leseleuc@institutoptique.fr

I will present our effort to control the dipole-dipole interaction between single Rydberg atoms to implement various spin Hamiltonians that could be useful for the quantum simulation of various condensed matter problems. Our platform is based on single atoms trapped in an array of optical tweezers generated by holography. With our atom assembler technique, we overcome the random loading of the traps to prepare fully loaded, 2 or 3d, arrays of single atoms [1].

As a first example of spin Hamiltonian, we can implement the quantum Ising model by coupling ground-state atoms to one Rydberg state and use the van der Waals interaction between two Rydberg atoms. I will describe the evolution of the system after a sudden quench of the Hamiltonian, or contrarily after an adiabatic change of the parameters, where we observed the build-up of anti-ferromagnetic correlations between the spins [2].

I will also briefly show how we can control the resonant dipole-dipole interaction between Rydberg states of different parities, which leads to a spin excitation hopping from one atom to another [3]. We have recently developed optical tools to locally control this interaction which opens exciting prospects for the simulation of XY Hamiltonians and topological problems.



Figure 1 : Atom assembly of an atomic array (before / after). This technique, together with the excitation of atoms to Rydberg states, allows the simulation of spin models on systems of various geometries and size.

[1] D. Barredo *et al.*, Science **354** 1021 (2016)

[2] V. Lienhard *et al.*, arXiv :1711.01185

[3] S. de Leseleuc *et al.*, Phys. Rev. Lett. **119** 053202 (2017)

Current-driven Domain Wall Dynamics in Cylindrical Nanowires with Modulated Diameter

A. De Riz^{1*}, J.-C. Toussaint², Ch. Thirion², O. Fruchart¹, D. Gusakova¹

¹ Univ. Grenoble Alpes, CNRS, CEA, Grenoble INP, INAC-SPINTEC, Grenoble, France

² Univ. Grenoble Alpes, CNRS, Institut NEEL, Grenoble, France

*arnaud.deriz@cea.fr

Ordered arrays of cylindrical nanowires fabricated by template-assisted electroplating techniques are promising for the development of a three-dimensional memory. In such memory, the information would be carried by magnetic domains separated by domain walls (DWs) which are driven by spin-polarized current pulses via a spin-transfer effect. The control of the DWs position could be obtained by creating localized diameter modulations which act as pinning sites. In order to optimize the DWs propagation through the modulations, it is essential to understand the influence of the geometry on the magnetization vector field behavior. Numerical modeling is a powerful tool for this task. Here we consider a transverse DW inside a cylindrical nanowire presenting a smooth modulation in diameter [1]. We performed micromagnetic simulations using our finite elements based software FeeLLGood which solves the Landau-Lifshitz-Gilbert equation augmented with current-driven effects [2]. We develop a simple analytical model which allows us to calculate the domain wall position and thus to extract a scaling law for the domain wall pinning conditions as a function of geometrical parameters.

[1] J. A. Fernandez-Roldan, A. De Riz, B. Trapp, et al. (2018), submitted.

[2] M. Sturma, J.-C. Toussaint, D. Gusakova, J. Appl. Phys. **117**, 243901 (2015).

Signatures of van Hove singularity probed by the supercurrent in a graphene – hBN superlattice

D. I. Indolese^a, R. Delagrangé^{a*}, P. Makk^{a,b}, J. Wallbank^c, K. Watanabe^d, T. Taniguchi^d and C. Schönenberger^a

- a. Department of Physics, University of Basel, Klingelbergstrasse 82, CH-4056 Basel, Switzerland
 - b. Department of Physics, Budapest University of Technology and Economics and Nanoelectronics 'Momentum' Research Group of the Hungarian Academy of Sciences, Budafoki ut 8, 1111 Budapest, Hungary
 - c. National Graphene Institute, University of Manchester, Manchester, M13 9PL, United Kingdom
 - d. National Institute for Material Science, 1-1 Namiki, Tsukuba 305-0044, Japan
- * raphaelle.delagrangé@gmail.com

If a graphene layer is placed on top of hexagonal boron nitride such that their crystallographic axes are almost aligned, a Moiré superlattice forms. The resulting periodic potential modifies deeply the graphene band-structure, manifesting by the appearance of new Dirac peaks together with van Hove singularities at energies low enough to be reached with standard electrostatic gating. In this work, we investigate the Josephson effect in such a superlattice and find signature of its specific band-structure on the supercurrent and its distribution across the junction.

The sample is a Josephson junction in the long and diffusive regime, such that the product of the critical current I_c and of the normal state resistance R_n is expected to depend on the Thouless energy and thus on the density of states (DOS). In this regard, we find that our measurements are consistent with the DOS expected in such a system.

By measuring the interference pattern of the critical current as a function of the perpendicular magnetic field, we show as well that the current distribution depends on the gate voltage, exhibiting edge current at the van Hove singularity. This demonstrates that, while the current is suppressed in the bulk due to the strong reduction of the Fermi velocity associated to the divergence of the DOS, it is not the case in the edges. This result brings an additional light on previous studies reporting edge current for vanishing density of states at the charge neutrality point.

[1] Zhu et al. Edge currents shunt the insulating bulk in gapped graphene. Nat. Commun. **8**, 14552 (2017)

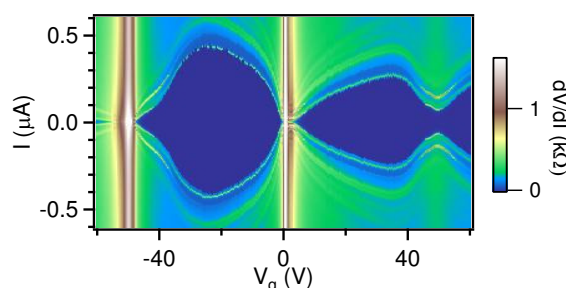


Figure 1: Differential resistance as a function of bias current I and gate voltage V_g , at zero magnetic field. The dark blue region corresponds to the superconducting state, its boundaries thus yields the critical current I_c .

COOPERATIVITY OF COMPLEXATION OF CHITOSAN OLIGOSACCHARIDES WITH SMALL INTERFERING RNA FOR GENE DELIVERY APPLICATIONS

Tim DELAS,^{a*} Olivier SANDRE,^a Christophe SCHATZ,^a Maxime MOCK-JOUBERT,^b Stéphane TROMBOTTO,^b Thierry DELAIR,^b Agnes CREPET,^b François DOLE^c

- a. Laboratoire de Chimie des Polymères Organiques (LCPO), Université de Bordeaux, CNRS, Bordeaux INP, UMR 5629, 33600 Pessac, France
- b. Laboratoire Ingénierie des Matériaux Polymères (IMP), CNRS UMR 5223, Université Claude Bernard Lyon 1, Univ Lyon, 69622 Villeurbanne, France
- c. Centre de Recherche Paul Pascal (CRPP), CNRS UPR 8641, Université de Bordeaux, 33600 Pessac, France

* Tim.Delas@enscbp.fr, <http://www.lcpo.fr/>

Keywords: small interfering RNA, chitosan, oligosaccharides, self-assembly, gene delivery

Abstract: Chitosan is a polycationic biopolymer used to protect and deliver small interfering RNA (siRNA) for biological applications. Chitosan prevents degradation and facilitates RNA entry into the target cells. However, the interaction between the polymer chains and the siRNA at the molecular level is poorly described since ill-defined chitosans of relatively high molecular weight are usually used to form complexes with siRNA. Here we used well-defined oligosaccharides of chitosan varying in degree of polymerization (DP) from DP=5 to DP=50 to study the role of the chitosan chain length on the thermodynamics of the complexation and the morphology of the complexes. The complexation was studied by Dynamic Light Scattering (DLS), fluorescence spectroscopy with the RiboGreen dye and Isothermal Titration Calorimetry (ITC) under various pH conditions. It was found that the chitosan chain length is a critical factor in the efficiency of the complexation. Longer chitosan chains have shown better complexation yield at various nitrogen to phosphate (N/P) ratios, illustrating the cooperative effect of the DP in complexing chitosan with siRNA. The global study provides a set of results of interest for the future design of siRNA delivery systems that must provide improved stability in the bloodstream, effective cell internalization and ease of dissociation in the cytoplasm.

[1] Alameh, M.; Lavertu, M.; Tran-Khanh, N.; Chang, C.-Y.; Lesage, F.; Bail, M.; Darras, V.; Chevrier, A.; Buschmann, M. D. *Biomacromolecules* 2018, 19 (1), 112–131.

[2] Bohr, A.; Tsapis, N.; Andreana, I.; Chamarat, A.; Foged, C.; Delomenie, C.; Noiray, M.; El Brahm, N.; Majoral, J.-P.; Mignani, S.; Fattal, E. *Biomacromolecules* 2017, 18 (8), 2379–2388.

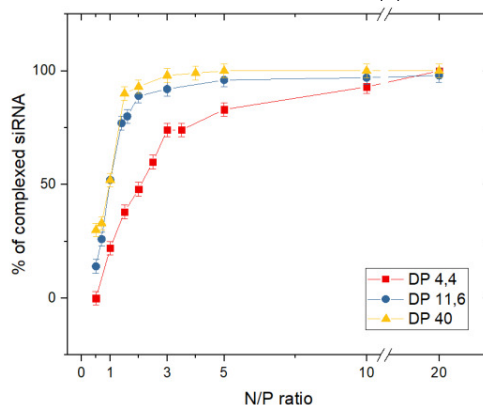


Figure 1 : Efficiency of the siRNA complexation at various N/P ratios with oligochitosans varying in DP as determined by fluorescence spectroscopy with the Ribogreen dye.

Levitated microdiamonds for optomechanics

Tom DELORD^a, Paul HUILLERY^a, Louis NICOLAS^a, et Gabriel HÉTET^{a*}

a. Laboratoire Pierre Aigrain, Ecole normale supérieure, PSL Research University, CNRS, Université Pierre et Marie Curie, Sorbonne Universités, Université Paris Diderot, Sorbonne Paris-Cité, 24 rue Lhomond, 75231 Paris Cedex 05, France.

* gabriel.hetet@lpa.ens.fr

The center of mass of levitating particles have shown record high quality factors under vacuum, stemming mostly from the absence of clamping losses. This makes levitating optomechanics a promising field to observe a macroscopic oscillator close to its quantum ground state. Inspired by ideas for mechanical control of oscillating cantilevers using magnetic field sensitive probes [1], trapped macroscopic objects coupled to single spins via magnetic field gradients are envisioned [2].

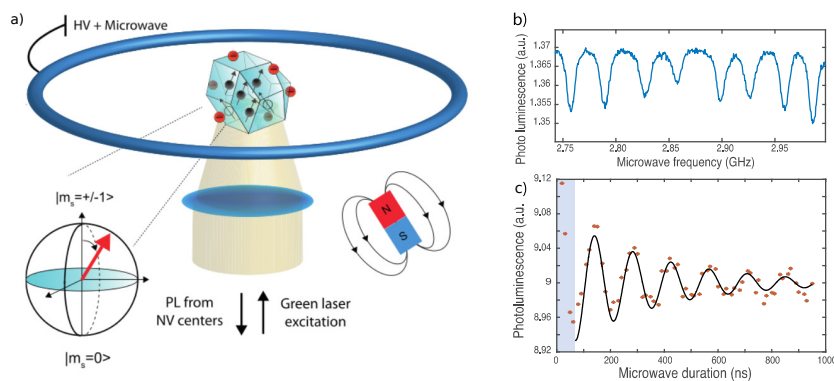


Figure 1: a) Set-up used for micro-diamond levitation. b) Electron Spin Resonance spectrum, c) Rabi oscillation from levitating micro-diamonds.

Here we levitate nano and microdiamonds in a Paul trap and study the spin of NV centers within these levitating diamonds. Contrary to the ubiquitous optical tweezers, levitation offered by Paul traps allows us to considerably reduce the large heating of the diamond when the pressure is lowered. Monitoring the NV spin enables us to demonstrate small heating under vacuum [3] and to show angular stability of the particle in the Paul trap. Moreover coherent manipulation of the spin ensembles is used to probe their coherence time and show negligible decoherence induced by the trap [4]. Finally, we theoretically show how one can use an NV spin to manipulate the angular degrees of freedom of a levitating diamond instead of its center of mass [5].

- [1] P. Rabl, et al. *Phys. Rev. B* 79, 041302 (2009)
- [2] Z. Yin, et al. *Science China Physics, Mechanics and Astronomy* 58, 1 (2015).
- [3] Delord, T., et al. *Applied Physics Letters* (2017), 111(1), 013101.
- [4] Delord, T., et al., arXiv (2018) arXiv:1801.07798.
- [5] Delord, T., et al. , *Phys. Rev. A* 96.6 (2017): 063810.

Topological geo-physical waves

Pierre Delplace^{a*}, Brad Marston,^b Antoine Venaille^a

a. Univ Lyon, Ens de Lyon, Univ Claude Bernard, CNRS, Laboratoire de Physique AF-69342 Lyon, France

b. Department of Physics, Box 1843, Brown University, Providence, RI 02912-1843 USA

* pierre.delplace@ens-lyon.fr

Several atmospheric and oceanic waves are known to be trapped around the Earth's equator. Strikingly enough, two of them (the so-called Kelvin and Yanai waves) can only propagate eastward. This remarkable uni-directional behavior looks similar to those of chiral boundary states in Chern insulators. Beyond this analogy, it can be shown that the solutions of the continuous shallow water model, commonly used in geo-physics to describe ocean and atmospheric dynamics over large distances, indeed carry a topological property that is quantified by a first Chern number, in agreement with the existence of two unidirectional modes [1].

[1] P. Delplace, B. Marston and A. Venaille, *Science* **358**, 1075 (2017)

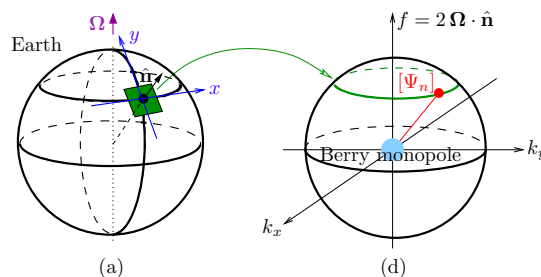


Figure 1: The dynamics of the fluid is described by the shallow water model in the tangent plane of earth. For each latitude, the waves that are solutions of this model can be parametrized on a sphere in (k_x, k_y, f) space, where f encodes the Coriolis force. The family of solutions, when f varies and changes sign, covers this sphere, but cannot be continuous and single-valued. This reflects a topological property of these waves that is quantified by the first Chern number.

In-situ biasing of semiconducting NWs in transmission electron microscopy: doping quantification and contact formation

M. den Hertog^{a,b*}, R. McLeod^{a,c,d}, F. Donatini^{a,b}, J. Pernot^{a,b,e}, E. Monroy^{a,c}, K. El Hajraoui^{a,b}, C. Zeiner^f, A. Lugstein^f, E. Robin^{a,c}, M. Lopez Haro^g, S. Kodjikian^{a,b}, F. Brunbauer^f, C. Sartet^h, V. Sallet^h and J.L. Rouviere^{a,c}

- a. Université Grenoble Alpes, Grenoble
- b. Institut Neel, CNRS, 25 rue des Martyrs, F-38042 Grenoble, France
- c. INAC, CEA-Grenoble, 17 avenue des Martyrs, F-38054 Grenoble, France
- d. Fondation Nanosciences, Grenoble, France
- e. Institut Universitaire de France, 103 boulevard Saint-Michel, F-75005 Paris, France
- f. Institute for solid state electronics, Vienna, Autriche
- g. Inorganic chemistry department, University of Cadiz, Cadiz, SPAIN
- h. Groupe d'étude de la Matière Condensée (GEMAC), CNRS Université de Versailles St Quentin, Université Paris-Saclay, F-78035 Versailles Cedex, France

* martien.den-hertog@neel.cnrs.fr

Semiconducting nanowires (NWs) are widely studied because the properties that stem from their three-dimensional, nanoscale nature open new opportunities for device design. Yet, to allow successful device integration, the quality of the NW/metal contacts and the control of carrier concentration are of paramount importance. We describe different kinds of semiconducting NW devices fabricated on electron transparent Si₃N₄ membranes, and we show how in-situ electrical transmission electron microscopy (TEM) can contribute to the understanding of NW doping, surface charges and contact formation.

First, we demonstrate that state-of-the-art off-axis electron holography in combination with electrical in-situ biasing can be used to detect active dopants and surface charges quantitatively in a single ZnO NW. We have acquired series of holograms on a reverse biased Schottky contact on a ZnO NW and analyzed the depletion width in the NW as a function of the reverse bias. Comparison of the experimental data with 3D simulations indicates an n-type doping level of $1 \times 10^{18} \text{ cm}^{-3}$ and a negative surface charge around $-2.5 \times 10^{12} \text{ cm}^{-2}$. The surface charge results in a surface depletion to a depth of 36 nm, providing excellent agreement between the simulated thickness of the undepleted core and the active thickness observed in the experimental data. On the other hand, we also present an original approach to create an atomically abrupt contact with low electrical resistance on NWs of group IV (silicon and germanium) using a thermally-induced propagation reaction of Al and Cu in the extremities of a Ge NW. To understand and control the metal diffusion into the NW that creates a metallic phase, detailed characterization at atomic length scales is necessary to understand how the metal atoms diffuse and incorporate into the formed phase at the reaction front and how these parameters relate to the electrical properties of the same interface. We show in-situ phase propagation of a metal-semiconductor phase of Cu and Al in Ge NWs in the TEM while measuring the current through the device, and analyze the metal diffusion process using structural and chemical characterization.

Synthesis and characterization of FeSe nanoparticles obtained by high-energy ball milling

A. Djekoun^{a*}, A. Chebli^a, N. Boudinar^a, M. Benabdeslem^b, B. Bouzabata^a

- a. *Laboratoire de Magnétisme et de Spectroscopie des Solides Université Badji Mokhtar Faculté des Sciences B. P: 12 (23000) ANNABA-Algérie.*
- b. *Laboratoire de Recherche d'Etudes des Surfaces et Interfaces de la Matière Solide (LESIMS), Département de Physique, Faculté des Sciences, Université d'Annaba, 23200 Sidi Amar, Algérie.*

abdel_djekoun@yahoo.fr « A.Djekoun »

Recently enough attention was given to iron selenide because of the unusual structure and electronic properties of transition metal chalcogenides. Iron selenide system presents two homogeneous and stable phases, α -FeSe and FeSe₂ [1,2], and a variety of structures. Fe-Se compound attracts more and more attention due to its wide application in optical electronic, photovoltaic, magnetic devices and solar cell. Several methods have been attempted to prepare the iron selenide: molecular beam epitaxy, ball milling, selenisation of evaporated iron thin films, and selenisation of amorphous iron oxide thin films predeposited by spray pyrolysis. In all these methods, enormous amount of energy is required for materials formation and is time consuming. In addition, when there is a large difference in the melting points of constituents iron (1535°C) and selenium (217°C), it becomes difficult to obtain FeSe compound with desired stoichiometry by these techniques.

The mechanical alloying (MA) method has been considered the most powerful tool for nanostructured materials, and it provides numerous advantages, because of its simplicity, relatively inexpensive equipment, and the possibility of producing large quantities, that can be scaled up to several tons.

Morphological, structural and thermal changes during milling were analyzed by scanning electron microscopy (SEM) coupled with EDAX microanalysis, X-ray diffraction (XRD) and differential scanning calorimetry (DSC). With milling time up to 6 h, combined XRD patterns and DSC show α -Fe and also some amorphous selenium. For the samples milled between 10 and 20 h, the orthorhombic FeSe₂ and β -FeSe hexagonal nanometric phases are formed and the volume fraction of the α -Fe phase decreases. For 33 and 52 h of milling, the α -Fe phase is completely gone and the emergence of new phase, also in nanometric scale, a typical of Fe₇Se₈ phase.

[1] B.X. Yuan, X.Q. Hou, Y.L. Han, W.L. Luan and S.T. Tu, *New J Chem.* **36**, 2101 (2012).

[2] B. Ouertani, J. Ouertfelli, M. Saadoun, B. Bessais, H. Ezzaouia and J.C. Bernède, *Sol. Energy Mater. Sol. Cells.* **87**, 501 (2005)

Ferroelectric leverages for solid state cooling

Brahim Dkhil*

Laboratoire Structures, Propriétés et Modélisation des Solides, CNRS-UMR8580,
CentraleSupélec, Université Paris-Saclay, 91190 Gif-sur-Yvette, France

*on behalf of the many authors

* brahim.dkhil@centralesupelec.fr

The search for alternative solid-state refrigeration materials to hazardous gases in conventional and cryogenic cooling devices is a very active field of condensed matter [1,2]. The use of phase transitions is a powerful tool to achieve giant caloric effects in ferroic materials in which magnetization, polarization, strain and/or volume can be strongly tuned under a moderate external stimulus. Here, we explored various aspects of ferroelectrics to reveal their potentialities as solid state coolers such as the ferroelectric phase transitions, the multiphase points composition, the stress-sensitivity through elasto- and baro-caloric responses, the inverse electrocaloric effect evidenced for instance in antiferroelectrics, the asymmetric effect arising from non-ergodic states, the use of dual-stimuli by taking advantage of multicaloric effects combining stress and electric field in ferroelectrics or magnetic and electric fields in multiferroics, as well as the use of defects [3-12].

- [1] X. Moya, S. Kar-Narayan, N. D. Mathur, *Nat. Mater.* **13**, 439 (2014)
- [2] T. Correia and Q. Zhang (Eds.). *Electrocaloric Materials*, Springer: Berlin, 2014
- [3] Y. Liu, J.F. Scott, B. Dkhil, *APL Materials* **4**, 064109 (2016)
- [4] Y. Liu, B. Dkhil, E. Defay, *ACS Energy Lett.* **1**, 521 (2016)
- [5] Y. Liu, L. C. Phillips, M. Bibes, A. Barthélémy, B. Dkhil, *Nat. Comm.* **7**, 11614 (2016)
- [6] Y. Liu, J.F. Scott, B. Dkhil, *Appl. Phys. Reviews* **3**, 031102 (2016)
- [7] Y. Liu, G. Zhang, Q. Li, L. Bellaiche, J.F. Scott, B. Dkhil, Q. Wang, *Phys. Rev. B* **94**, 214113 (2016)
- [8] R Faye, H Strozyk, B Dkhil, E Defay, *J. Phys. D: Appl. Phys.* **50**, 464002 (2017)
- [9] M Sanlialp, Z Luo, VV Shvartsman, X Wei, Y Liu, B Dkhil, DC Lupascu, *Appl. Phys. Lett.* **111**, 173903 (2017)
- [10] X Wang, J Wu, B Dkhil, B Xu, X Wang, G Dong, G Yang, X Lou, *Appl. Phys. Lett.* **110**, 063904 (2017)
- [11] T. Li et al., to be published
- [12] J. Li et al., to be published

B.D. acknowledge Fonds National de la Recherche (FNR) du Luxembourg through the InterMobility project 16/1159210 "MULTICALOR"

Photostriction in ferroelectric materials

M. Lejman^a, C. Paillard^{b,c}, G. Vaudel^a, N. Chigarev^d, S. Raetz^d, S. Matzen^e, P. Lecoeur^e, I. C. Infante^b, V. Juvé^a, V. E. Gusev^d, L. Bellaïche^c, B. Dkhil^b, P. Ruello^{a*}

a. Institut des Molécules et Matériaux du Mans, UMR CNRS 6283, Le Mans Université, 72085 Le Mans, France

b. Laboratoire Structures, Propriétés et Modélisation des Solides, CentraleSupélec, UMR CNRS 8580, Université Paris-Saclay, 91190 Gif-sur-Yvette, France,

c. Physics Department, University of Arkansas, Fayetteville, USA.

d. Laboratoire d'Acoustique de l'Université du Maine, UMR CNRS 6613, Université du Maine, 72085 Le Mans, France

e. Centre des Nanosciences et Nanotechnologies CNRS, Université Paris Saclay, France.

*pascal.ruello@univ-lemans.fr

Ferroelectrics are intrinsically multifunctional materials with a particular efficiency in electro-mechanical coupling which plays a central role in many devices in telecommunications and sensors technologies (motion-position control, electro-optic and acousto-optic devices). Controlling their acoustic response with ultrashort light pulses would pave the way of non-contact GHz-THz technologies. Among interests, we show in this communication how it is possible to manipulate the lattice dynamic (photostriction, photoinduced-strain) with light [1-4]. Different electron-phonon coupling mechanisms are involved during the light-matter interaction (inverse-piezoelectric effect, deformation potential) which permit to induce either expansion or contraction of the lattice at the picosecond-nanosecond time scale offering exciting perspective for advanced mechatronics. These light-matter interaction processes will be further discussed thanks to recent optical pump-probe experiments [5] combined with optical pump – time-resolved X-ray diffraction [6].

[1] Schick, D. et al., Phys. Rev. Lett. 110, 095502 (2013).

[2] Lejman M., Vaudel G., Infante, I. C., Gemeiner P., Gusev V., Dkhil B., Ruello P., Nature Comm. 5, 4301 (2014).

[3] H. J. Lee et al, Scientific Reports, 6, 38724 (2016)

[4] Lejman M., Vaudel G., Infante I-C., Chaban I., Pezeril T., Edely M., Nataf G., Guennou M., Kreisel J., Gusev V. E., Dkhil B., Ruello P., Nature Comm. 7, 12345 (2016).

[5] Lejman et al, in preparation

[6] Matzen et al, in preparation.

Etude de la cavitation dans des membranes mésoporeuses d'alumine et de silicium

Victor Doebele^{a*}, Hermann Böttcher^a, Fabien Souris^a, Panayotis Spathis^a, Laurent Cagnon^a, Annie Grosman^b, Isabelle Trimaille^b, Etienne Rolley^c et Pierre-Etienne Wolf^a

a. Institut Néel, CNRS/UGA, UPR2940, Grenoble

b. INSP, CNRS/UPMC, UMR 7588, Paris

c. LPS-ENS, CNRS/Univ. Paris Diderot/UPMC, UMR 8550, Paris

* victor.doebele@neel.cnrs.fr

Dans le cadre du projet CAVCONF [1], nous avons synthétisé par voie électrochimique des pores en forme de bouteille d'encre dans des membranes mésoporeuses d'alumine et de silicium. Chaque pore est constitué d'une cavité reliée au réservoir de vapeur par une constriction suffisamment étroite pour rester remplie jusqu'à caviter dans la cavité. Contrairement aux expériences antérieures reportées par Casanova [2], nous avons pu mettre en évidence l'évaporation par cavitation pour de l'hexane. Pour les membranes d'alumine (pores d'environ 40 nm de diamètre), nous trouvons que la cavitation se produit à une pression compatible avec la théorie classique de nucléation. De façon inattendue et pour l'instant inexplicée, les membranes de silicium, qui comportent des cavités de plus faible diamètre, et distribuées en taille (entre 10 et 50 nm), donnent une pression de cavitation supérieure. Nous présenterons également nos premiers résultats obtenus en utilisant comme fluide l'azote et l'hélium.

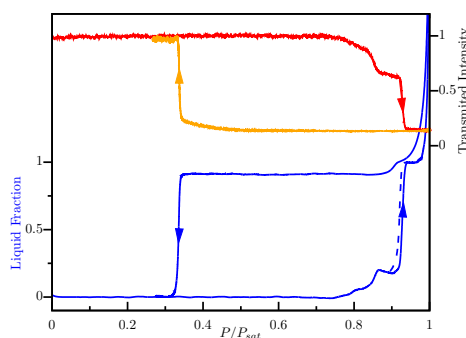


Figure 1: Mise en évidence de la cavitation dans des membranes d'alumine et de silicium poreux.

[1] P. Spathis et al, cette conférence

[2] F. Casanova, C. E. Chiang, C.-P. Li, and I. K. Schuller. Direct observation of cooperative effects in capillary condensation: The hysteretic origin, APL 91, 243103, (2007)

Ce travail est soutenu par l'ANR dans le cadre du projet CAVCONF*.

Les membranes d'alumine poreuse, un système modèle pour la condensation et l'évaporation en milieu confiné

Victor Doebele^{a*}, Hermann Böttcher^a, Fabien Souris^a, Panayotis Spathis^a, Laurent Cagnon^a, Annie Grosman^b, Isabelle Trimaille, Etienne Rolley^c et Pierre-Etienne Wolf^a

a. Institut Néel, CNRS/UGA, UPR2940, Grenoble

b. INSP, CNRS/UPMC, UMR 7588, Paris

c. LPS-ENS, CNRS/Univ. Paris Diderot/UPMC, UMR 8550, Paris

* victor.doebele@neel.cnrs.fr

L'évaporation et la condensation d'un fluide dans les milieux mésoporeux sont affectées par le confinement à l'échelle nanométrique. Cependant, les études expérimentales ont surtout été effectuées dans des milieux pour lesquels le désordre et le couplage entre pores jouent également un rôle. Pour distinguer spécifiquement les effets de confinement, nous étudions des membranes d'alumine poreuse. Obtenues par synthèse électrochimique, elles sont un système poreux versatile, présentant des pores indépendants avec une faible dispersion en diamètre. Etant transparentes, elles permettent également un suivi optique des processus de remplissage et de vidange.

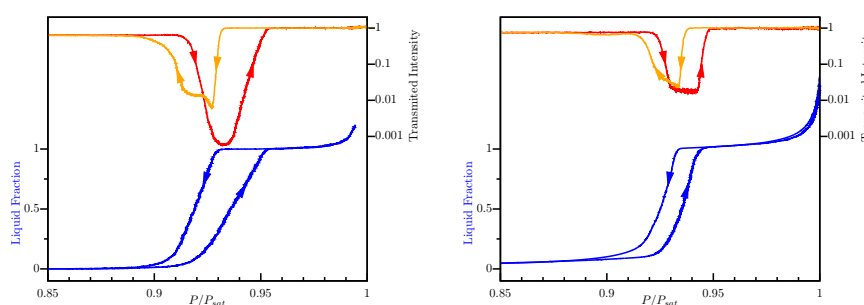


Figure 1: Isothermes de condensation et d'évaporation de l'hexane dans deux membranes d'alumine : a) pores ouverts des deux côtés ; (b) pores ouverts d'un seul côté. Les figures représentent la fraction condensée et la transmission optique en fonction de la pression.

Afin d'étudier les effets d'activation thermique et le rôle des interactions fluide-paroi, nous réalisons des mesures d'isothermes à l'hexane, l'azote et l'hélium. Nous observons que les phases de condensation et d'évaporation se produisent sur une plage étalée de pressions, contrairement à ce qui serait attendu pour des pores de diamètre identique. La forte diffusion de la lumière, et son hystérésis entre condensation et évaporation à même fraction condensée, indiquent de plus que les pores sont corrugués. Notre système expérimental offre ainsi l'opportunité d'étudier finement l'effet des corrugations sur les processus de condensation et d'évaporation, et de comparer les résultats à différents modèles.

Ce travail est soutenu par l'ANR dans le cadre du projet CAVCONF.

Drying of a water-filled channel within an artificial leaf

Benjamin Dollet^{a*}, Jean-François Louf^{a,b}, Mathieu Alonzo^a, Florie Mesple^a, Kaare H. Jensen^b et Philippe Marmottant^a

- a. Laboratoire Interdisciplinaire de Physique, UMR 5588 CNRS and Université Grenoble Alpes, 140 rue de la Physique, 38402 Saint-Martin-d'Hères, France
- b. Department of Physics, Technical University of Denmark, Fysikvej, Building 309, 2800 Kgs. Lyngby, Denmark

* benjamin.dollet@univ-grenoble-alpes.fr

The transport of sap in the vascular network of leaves is driven by evaporation at the surface of leaves, and it has been shown [1] that a relevant analogous physical system is a network of liquid-filled channels in a permeable polymer. As such, microfluidic systems made of PDMS are particularly suited. In our study, to understand how a leaf is susceptible to dry out if its supply of sap is stopped, we investigate the drying of water-filled channels, looking at air invasion in such channels.

We create a series of isolated channels of different widths and heights in thin layers of PDMS of different thicknesses, using standard microfluidic techniques. All channels are open at one end and closed at the other hand. They are initially filled with water, then placed under a dry atmosphere. They progressively dry as a meniscus separating the still liquid-filled part and the newly dried part advances in the channel (Fig. 1). We record the motion of the meniscus with a camera, thereby measuring the rate of evaporation as a function of time. This rate decreases as the channel progressively dries, but does not vanish at the moment where liquid water disappears in the channel. We rationalize our measurements by a model combining two contributions: (i) direct diffusion of water to the atmosphere through the PDMS layer; (ii) diffusion between newly dried parts containing humid air and the dry atmosphere. In particular, we derive an asymptotic analytical prediction for the evaporation rate due to this latter process, using the fact that diffusivity of water is much lower in PDMS than in air. The data and the model are found to be in good agreement, thereby providing a physical description for the drying-up of leaves. Preliminary results in more complex networks will also be presented.

[1] X. Noblin, L. Mahadevan, I. A. Coomaswamy, D. A. Weitz, N. M. Holbrook, M. A. Zwieniecki, Optimal vein density in artificial and real leaves, *Proc. Natl. Acad. Sci.* **105**, 9140-9144 (2008).

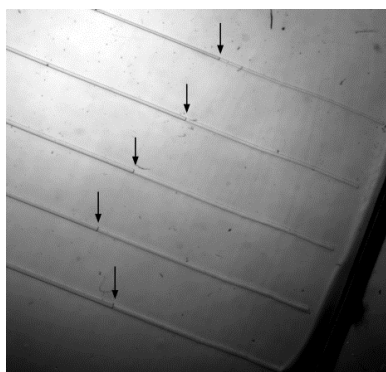


Figure 1 : Drying channels (from top to bottom, width 75, 100, 125, 150 and 175 μm) Arrows depict the menisci.

Preparing capsules from water-in-water emulsions, towards synthetic cells

Jean-Paul Douliez^{a*}, Adeline Perro^b, Thomas Beneyton^c, Valérie Ravaine^b, Jean-Paul Chapel^c, Jean-Christophe Baret^c, et Laure Béven^a

- a. UMR 1332, biologie et pathologie du fruit, INRA, Univ. Bordeaux, centre de Bordeaux, 33883 Villenave d'Ornon, France
- b. Institut des Sciences Moléculaires, Université Bordeaux, CNRS-UMR 5255, 351 Cours de la Libération, 33405 Talence, France
- c. CNRS, Univ. Bordeaux, CRPP, 115 Av. A. Schweitzer, 33600 Pessac, France

* jean-paul.douliez@inra.fr

We report the bulk preparation of hollow capsules having a gelatin shell. Hot aqueous dispersions (>40 °C) of gelatin/polyethyleneglycol (PEG) form aggregated gelled droplets upon cooling. However, addition of alginate (<0.1%) yields to non-aggregated PEG-in-gelatin-in-PEG double emulsion droplets possessing a multinuclear core. Upon resting the double emulsion above the melting temperature of gelatin, the inner PEG-in-gelatin droplets coalesced resulting in the formation of yolk (PEG)-shell (gelatin) mononuclear capsules dispersed in the PEG continuous phase. These capsules, which we called gelatinosomes, are shown to encapsulate payloads even when further dispersed in water, suggesting possible applications in microencapsulation, drug delivery and synthetic biology.

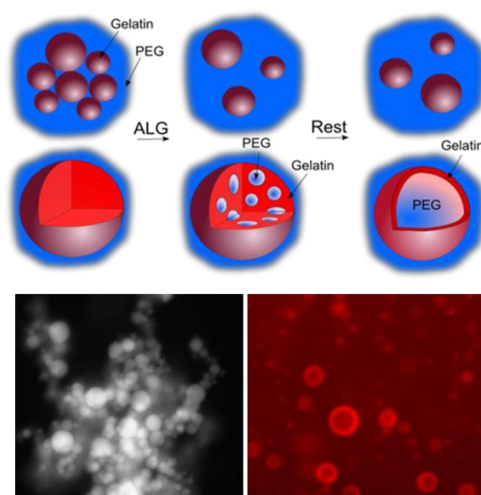


Figure 1: Up) Schematic representation showing how hollow capsules called ‘gelatinosomes’ are prepared. Bottom) Epifluorescence images of aggregated gelatin beads (left) and ‘gelatinosomes’ (labelled with Pyronin, right).

Thermal resistance measurements between a glass bead and a plane from large distance to contact

Joris Doumouro^{a*}, Elodie Perros^a, Alix Dodu^a, Dominique Leprat^b, Valentina Krachmalnicoff^a, Wilfrid Poirier^b, Rémi Carminati^a, and Yannick De Wilde^{a,1}

a. ESPCI Paris, PSL Research University, CNRS, Institut Langevin, 1 rue Jussieu, Paris, France

b. LNE-Laboratoire national de métrologie et d'essais, 78197 Trappes, France

* joris.doumouro@espci.fr

Thermal insulation materials such as glass wool are characterized in industrial laboratories at macroscopic scale but the urge to perform energy savings pushes industrials and researchers to gain knowledge about the heat transfer at the microscopic scale. In such materials the heat flow is guided through a complex network of fibers and contacts. There is a need for a better understanding of the resistance of contact between two fibers.

The physic of contact is complex. It involves solid-solid transfer and solid-liquid transfer through the water meniscus[1]. Some measurements of the resistance of contact between an heated silica bead on a SThM tip and a substrate have already been reported. They were made under vacuum conditions, where the solid-liquid interaction is negligible[2,3]. But it does not represent the *in situ* ambient conditions which are encountered in thermal insulation materials.

In this paper, we propose a SThM based method to measure the resistance of contact between a 20 μm glass bead and a glass surface under ambient conditions. This bead/surface situation is a first step to the fiber/fiber contact. First, a SThM tip is glued to a bead. Then the bead is heated by Joule Effect at a well-known distance from the surface. The latter is progressively reduced in a controlled manner thanks to the SThM, until the bead enters in contact with the glass surface while the temperature on top of the bead is monitored. In this situation, every heat paths are easily identifiable as an equivalent circuit of thermal resistors. An analytical approach combined with simulations is proposed to model the experimental temperature curve and to model and estimate the thermal resistance of contact.

- [1] A. Assy, S. Lefèvre, P.-O. Chapuis, and S. Gomès. Analysis of heat transfer in the water meniscus at the tip-sample contact in scanning thermal microscopy, *J. Phys. D : Appl. Phys.*, **47**: 442001, (2014)
- [2] A. Narayanaswamy, S. Shen, and G. Chen. Near-field radiative heat transfer between a sphere and a substrate, *Phys. Rev. B* **78**, 115303 (2008)
- [3] E. Rousseau, A. Siria, G. Jourdan, S. Volz, F. Comin, J. Chevrier, and J.-J. Greffet. Radiative heat transfer at nanoscale. *Nature photonics* **3**, 5514-517 (2009)

¹This research was supported by LABEX WIFI (Laboratory of Excellence within the French Program Investments for the Future) under references ANR-10-LABX-24 and ANR-10-IDEX-0001-02 PSL*, and Agence Nationale de la Recherche (ANR), Project CarISOVERRE, ANR-16-CE09-0012.

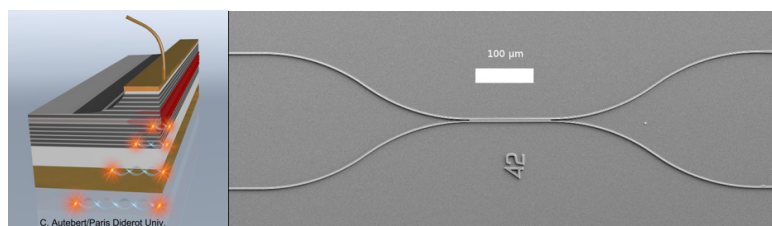
AlGaAs photonic devices for quantum information

S. Ducci *

Laboratoire Matériaux et Phénomènes Quantiques, Université Paris Diderot, Sorbonne Paris Cité, CNRS-UMR 7162, 75205 Paris Cedex 13, France

* sara.ducci@univ-paris-diderot.fr

Nonclassical states of light are key components in quantum information science; in this domain, the maturity of semiconductor technology offers a huge potential in terms of ultra-compact devices including the generation, manipulation and detection of many quantum bits [1]. Among the different resources under development, on-chip entangled photon sources play a central role for applications spanning quantum communications, computing and metrology. In this talk I will present our last achievements on AlGaAs photonic devices emitting non-classical states of light at room temperature via spontaneous parametric down conversion; the choice of this platform combines the advantages of a mature fabrication technology, photon pair emission in the C-telecom band, a direct band-gap and a high electro-optic effect. The characterization of the quantum states emitted by such devices demonstrates their ability to produce highly indistinguishable and entangled photons [2]. Different device designs can be adopted depending on the target application: geometries producing copropagating photon pairs are particularly interesting to generate broadband strongly anticorrelated frequency states which can be used for instance in multiusers quantum key distribution protocols [3]. Moreover, the cavity effect due to modal reflectivity at the waveguide's facets allow engineering the joint spectrum of the emitted biphoton state to get comb-like spectral correlations, leading high dimensional frequency entangled state (or qudits). Geometries generating counterpropagating photon pairs with a transverse pump configuration allow engineering and control a large variety of frequency states: separable states are produced to monolithically integrate heralded single photon sources and beam splitters [4], while original quantum states featuring non-Gaussian entanglement are obtained through amplitude and phase engineering of the pump beam.



The compliance of these sources with electrical pumping, together with the possibility to fabricate versatile and massively parallel circuits make the AlGaAs platform a promising candidate for real-world quantum information technologies.

[1] A. Orioux et al. 'Semiconductors devices for entangled photons generation: a review', Rep. Prog. Phys. 80 076001 (2017).

[2] C. Autebert et al 'Integrated AlGaAs source of highly indistinguishable and energy-time entangled photons', Optica 3, 143 (2016).

[3] C Autebert et al. 'Multi-user quantum key distribution with entangled photons from an AlGaAs chip', Quantum Sci. Technol. 1, 01LT02 (2016).

[4] J. Belhassen et al. 'On-chip III-V monolithic integration of heralded single photon sources and beamsplitters', Appl. Phys. Lett. 112, 071105 (2018).

GaN/InAlN multiple quantum well tubes

Christophe Durand^a, Jean François Carlin^b, Catherine Bougerol^c, Bruno Gayral^a, Jean-Paul Barnes^d, Joël Eymery^a, Raphaël Butté^b, Nicolas Grandjean^b

- a. Univ. Grenoble Alpes, INAC, CEA, 38000 Grenoble, France
- b. Institut de Physique de la matière condensée, Ecole Polytechnique Fédérale de Lausanne (EPFL), CH-1015 Lausanne, Suisse
- c. Univ. Grenoble Alpes, Institut Néel, CNRS, 38000 Grenoble, France
- d. Univ. Grenoble Alpes, LETI, Minatec Campus, CEA, 38000 Grenoble, France

Nanotubes are nowadays well-known nanostructures, but exhibit no or modest light emission. Indeed, the surface states and defects favor the non-radiative recombination that quench light emission. To overcome this problem, we have developed a new type of nanotubes with walls only composed of multiple quantum wells (MQWs), acting as the active region for light emission. The quantum wells composed of multiple nanometer-sized layers are well known for their remarkable light emission properties due to quantum confinement effects and are daily used in LEDs or lasers.

To successfully produce such MQW-tubes, GaN wires with core-shell GaN/InAlN MQW heterostructure grown by metal-organic vapor-phase epitaxy are simply annealed under H₂/NH₃ gas mixture [1]. This selective annealing only etches the inner GaN wire leading to tubes composed of MQWs. We demonstrated by ToF-SIMS measurements that the tube walls were actually composed of the GaN/InAlN heterostructure proving that the annealing did not degrade the quantum wells. Such smart MQW-tubes exhibit excellent light emission in the UV range (around 330 nm) until room temperature. The simplicity of the method to fabricate thin nitride tubes with embedded MQWs opens routes for the development of novel tube-based devices ranging from emitters to chemical and biological sensors.

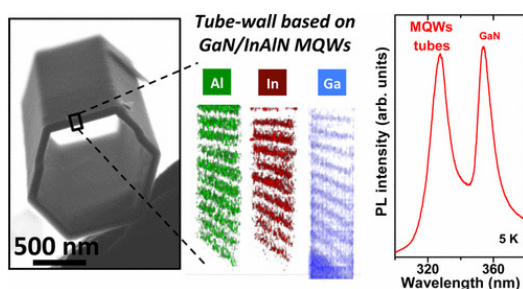


Figure 1: Nitride tubes with GaN/InAlN wells chemical signature in the tube wall observed by ToF-SIMS and optical features with UV emission by PL at 5K.

[1] C. Durand, JF. Carlin, C. Bougerol, B. Gayral, D. Salomon, JP. Barnes, J. Eymery, R. Butté, N. Grandjean, NanoLetters (2017), *Nano Lett.* **2017**, 17, 3347-3355.

Berry's phase atomic interferometers in graphene

C. Dutreix^{a*}, H. Gonzàles-Herrero^b, M. I. Katsnelson^c, I. Brihuega^{b,d}, C. Chapelier^e,
and V. Renard^{e*}

- a. Université de Bordeaux and CNRS, LOMA, UMR 5798, F-33400 Talence, France
- b. Universidad Autónoma de Madrid, DCMP & IFIMAC, E-28049 Madrid, Spain
- c. Radboud Universiteit, IMM, Nijmegen, The Netherlands
- d. Universidad Autónoma de Madrid, Instituto Nicolás Cabrera, E-28049 Madrid, Spain
- e. Université Grenoble Alpes/CEA, INAC-PHELIQS, F-38000 Grenoble, France

* clement.dutreix@u-bordeaux.fr; vincent.renard@cea.fr

Topological defects in waves is a concept introduced by Nye and Berry to explain the dislocations observed in some radio-echos sounding the ice sheet of Antartica [1]. It relies generically on the phase singularities of a complex scalar field. Here we shall discuss it in the context of scanning tunnelling microscopy (STM) images of the electronic interferences around H adatoms chemisorbed on graphene (cf. Fig. 1 (a)). If intravalley scattering is known to induce $2q_F$ -wave-vector Friedel oscillations in the electronic density [2,3], we shall see that intervalley scattering is the source of extra oscillations that do not relate to the Fermi wave vector q_F . When selecting a specific intervalley-scattering wave vector, these oscillations reveal a couple of edge dislocations in the interference pattern (cf. Fig. 1 (b)). We shall show that such topological defects appear as a real-space manifestation of the Berry's phase π that characterises the phase singularities of the wave functions at the Dirac points in momentum space. This demonstrates the ability of STM to image the geometrical phases of wave functions through static interferences; thus suggesting a new approach to probe the nodal band structures and topological gapped phases of condensed matter.

- [1] J. F. Nye and M. V. Berry, Proc. R. Soc. Lond. A **336**, 165 (1974)
- [2] J. Friedel, Phil. Mag. **43**, 153 (1952)
- [3] I. Brihuega et al., Phys. Rev. Lett. **101**, 206802 (2008)

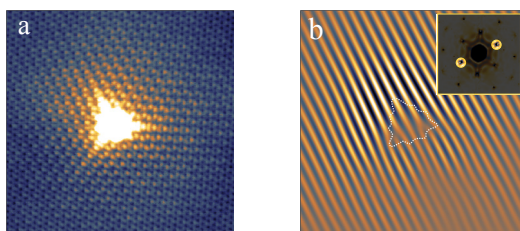


Figure 1: (a) STM image of a H adatom chemisorbed on graphene. (b) Filtered image of (a) showing edge dislocations in the scattering interferences of electronic standing waves.

Thermal Conductance of a Single-Electron Transistor

B. Dutta^{a*}, J. T. Peltonen^b, D. S. Antonenko^c, M. Meschke^b, M. A. Skvortsov^c, B. Kubala^d, J. König^e, C. B. Winkelmann^a, H. Courtois^a, J. P. Pekola^b

- a. Institut Néel, Univ. Grenoble Alpes, CNRS, Grenoble, France
- b. Aalto University School of Science, Helsinki, Finland
- c. Skolkovo Institute of Science and Technology, L. D. Landau Institute for Theoretical Physics, and Moscow Institute of Physics and Technology, Russia
- d. Institute for Complex Quantum Systems and IQST, University of Ulm, Germany
- e. Theoretische Physik and CENIDE, Universität Duisburg-Essen, Germany

* bivas.dutta@neel.cnrs.fr

Heat flow at mesoscopic scale is a fundamentally important issue, in particular, if it can be converted into energy by thermoelectric effect. While the understanding of charge transport in mesoscopic system has reached a great level of maturity, heat transport lagging far behind. According to the celebrated Wiedemann-Franz law, the charge conductance is proportional to the thermal conductance. In nanoscale devices, this law is predicted to be violated in the presence of strong electron-electron interaction^[1].

We have carried out a combined measurement of heat and charge transport through a single-electron transistor (SET) (Figure 1, (a, b)). A thermal gradient across the SET is created by cooling (heating) the source using a (pair of) NIS junction, while the bulky drain is at bath temperature. The electronic temperature of the source is measured simultaneously. A periodic modulation of the source temperature (Figure 1, (c)) as a function of gate voltage is observed, giving an evidence of heat flow through the SET. The device thus acts as a heat switch actuated by the voltage applied on the gate. The Lorentz ratio L/L_0 (L_0 being the Lorentz number) is calculated by comparing the charge and heat transport data (Figure 1, (d)). While the Wiedemann-Franz law predicts a unity value for the Lorentz ratio, a value up to 4 is observed^[2]. These observations agree well with theoretical calculations^[1].

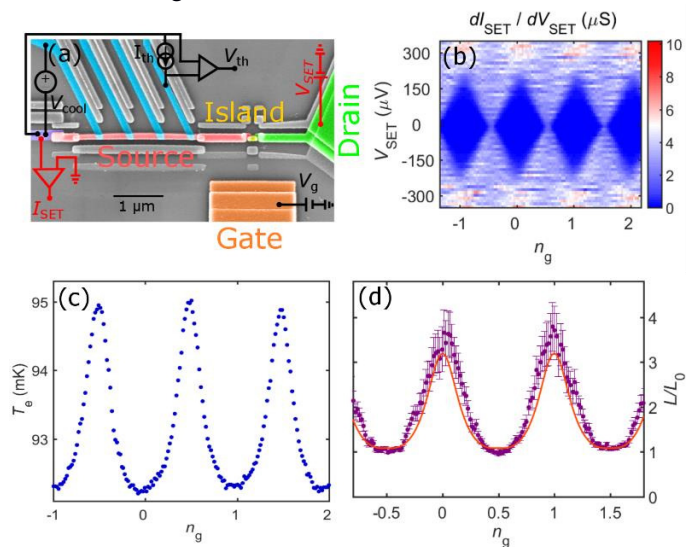


Figure 1: (a) SEM image of the device with different elements shown in color; (b) Coulomb diamonds in the charge conductance map of the SET; (c) temperature modulation of the source (when it is colder than drain) by the applied gate voltage; (d) Lorentz ratio as a function of the gate, with the theoretical curve shown as solid line.

While the Wiedemann-Franz law predicts a unity value for the Lorentz ratio, a value up to 4 is observed^[2]. These observations agree well with theoretical calculations^[1].

[1] B. Kubala, J. König, J. P. Pekola, *Violation of Wiedemann-Franz Law in a Single-Electron Transistor*, Phys. Rev. Lett. **100**, 066801 (2008).

[2] B. Dutta, J. T. Peltonen, D. S. Antonenko, M. Meschke, M. A. Skvortsov, B. Kubala, J. König, C. B. Winkelmann, H. Courtois, J. P. Pekola, *Thermal Conductance of a Single-Electron Transistor*, Phys. Rev. Lett. **119**, 077701 (2017).

Etude de la structure et de la durabilité chimique pour des bioverres à base de phosphate dans le système : $P_2O_5-CaO-Na_2O-TiO_2$

Y. Er-rouissi^{a*}, S. Aqdim^{a,b}, F. Hmimid^c, N. Bourhim^c

- a. Laboratoire Génie des Matériaux Environnement et Valorisation, département de chimie Université Hassan II Ain chock, Faculté des Sciences Casablanca Maroc
- b. Laboratoire Chimie Minérale, Département de Chimie Université Hassan II Ain chock, Faculté des Sciences Casablanca Maroc
- c. Laboratoire santé environnement Département de biologie Université Hassan II Ain chock, Faculté des Sciences Casablanca Maroc

* bioverres à base de phosphate, durabilité chimique, structure

Des vitrocéramiques de composition $P_2O_5-CaO-Na_2O-TiO_2$ ont été préparés par fusion direct du mélange $(NH_4)H_2PO_4$, $CaCO_3$, Na_2CO_3 et TiO_2 avec des proportions convenables. Tous les échantillons vitreux préparés sont transparents avec une coloration violette pâle qui devienne plus en plus foncé avec l'addition de TiO_2 . Les résultats expérimentaux obtenus montrent que la variation de la vitesse de dissolution en fonction du temps pour la série des verres : $P_2O_5-CaO-Na_2O-TiO_2$ indique une nette augmentation de la durabilité chimique lorsqu'on augmente la teneur de TiO_2 au détriment de Na_2O puis suivi d'une diminution lorsque la teneur de TiO_2 dépasse 2 mol %. Le diagramme ternaire nous permet de localiser nos échantillons entre les domaines métaphosphates et pyrophosphates. La mesure de la densité montre que le rayon ionique de l'atome d'oxygène reste presque constant pour l'ensemble des échantillons. En outre, l'analyse par diffraction de rayons X des verres recuits à $650^\circ C$ pendant 48h, indique l'apparition d'un mélange de phases métaphosphates et pyrophosphates. Ces dernières deviennent majoritaires lorsque la teneur en TiO_2 augmente dans le réseau vitreux. L'analyse par la spectroscopie infrarouge confirme les résultats obtenus par R-X et montre que les verres obtenus sont constitués de groupements pyrophosphate et des chaînes et / ou des anneaux de métaphosphates. D'autre part, lorsque la teneur de TiO_2 dépasse 2 mol %, ensemble, les spectres infrarouges et les spectres DRX indiquent l'apparition des nouvelles phases orthophosphate majoritaires au détriment des phases méta et pyrophosphates.

[1] Chabbou, Z., & Aqdim, S. (2014). Chemical Durability and Structural Proprieties of the Vitreous Part of the System $xCaO-(40-x) ZnO-15Na_2O-45P_2O_5$. *Advances in Materials Physics and Chemistry*, 4(10), 179.

Toward automatic design of co-transcriptional RNA switches

Joël G. ESPEL^a, Bianca M. MLADEK^b, Johannes GEISELMANN^a, Alexandre DAWID^{a*}

a. Univ. Grenoble Alpes, CNRS, LIPhy, 38000 Grenoble, France

b. Max F. Perutz Laboratories, Vienna, Austria

* alexandre.dawid@univ-grenoble-alpes.fr

Functional RNA molecules generally need to fold into a precise structure to achieve their function. However, the folding of RNA is intrinsically a hierarchical and dynamical process that occurs co-transcriptionally.

We are addressing the question of how the sequences of RNA molecules encode their folding, including the co-transcriptional folding path which guides the RNA folding process. To this aim, we use a learn-by-designing approach applied to a model system: transcription-regulating RNA switches, which regulate transcription by a terminator/anti-terminator switch mechanism.

We are developing automatic design algorithms and experimental approaches in order to systematically explore and evaluate general principles of RNA switches design and of sequence-encoding of co-transcriptional RNA folding.

We will present recent experimental results on the regulatory function of computationally designed RNA switches.

New turns of a single electron surfing on a sound wave: towards coherent manipulation of a flying qubit

Hermann Edlbauer^{a,*}, Shintaro Takada^{a,b}, Arne Ludwig^c, Andreas D. Wieck^c,
Tristan Meunier^a and Christopher Bäuerle^a

- a. Univ. Grenoble Alpes, CNRS, Grenoble INP, Institut Néel, 38000, Grenoble, France
- b. National Institute of Advanced Industrial Science and Technology (AIST), National Metrology Institute of Japan (NMIJ), Tsukuba, Ibaraki, 305-8563, Japan
- c. Lehrstuhl für Angewandte Festkörperphysik, Ruhr-Universität Bochum, 44780, Bochum, Germany

* e-mail: hermann.edlbauer@neel.cnrs.fr

Surface acoustic waves (SAWs) offer a promising platform for quantum computing applications in solid-state devices. Earlier experiments employed SAWs to transport a single electron between spatially separated quantum dots with high efficiency [1,2]. And recently, also long-range transfer of spin information has been achieved [3]. One appealing idea for scaling up qubit architectures is to use SAWs as conveyor of quantum information between nodes of an on-chip quantum network. Compared to photonic quantum computing approaches, SAW-driven electron transport additionally brings the possibility to perform quantum operations on the fly by exploiting Coulomb interaction. Here we present the next step towards that direction. First, we send a single electron over a distance of 22 μm with extremely high efficiency above 99 %. Using picosecond pulse triggering, we show the ability of synchronizing transport of single electrons in parallel paths. Coupling two quantum channels by a tunnel barrier, we realize a tunable beam splitter: As we change the energy detuning in the coupling region, we partition the electron on-demand into two paths. Gradually lowering the tunnel-barrier we additionally observe oscillations of the probability that the electron ends up in the upper or the lower detector quantum dot. Our results pave the way for the implementation of flying qubit architectures with single electrons.

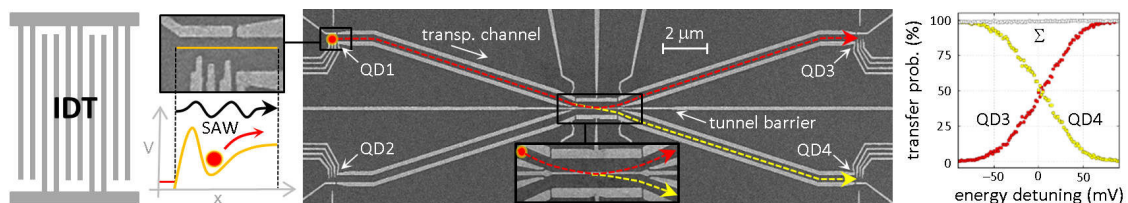


Figure 1: Schematic showing the experimental setup. An interdigitated transducer (IDT) sends a SAW to the nanostructure defined by electrostatic surface gates deposited on a GaAs heterostructure. An electron loaded at a source quantum dot (QD1 or QD2) is sent by the SAW through the tunnel-coupled region and ends up at one of the detector quantum dots (QD3 or QD4). The right panel shows the transfer probability as the energy detuning of the tunnel coupled channels is changed.

- [1] Hermelin et al., *Nature* **477**, 435–438 (2011)
- [2] McNeil et al., *Nature* **477**, 439–442 (2011)
- [3] Bertrand et al., *Nature Nanotech.* **11**, 672–676 (2016)

Catalytic DNA reactions on nanogels

Mathieu Coudert^a, Valérie Ravaine^b, et Juan Elezgaray^{a*}

- a. CBMN, UMR 5248, CNRS, Allée Saint Hilaire, bâtiment B14, 33600 Pessac
- b. ISM, UMR 5255, CNRS, 33400 Talence

* j.elezgaray@cbrmn.u-bordeaux.fr

DNA nanotechnology [1-3] has shown that the self-assembly properties of nucleic acids open many possibilities to design molecular devices, including motors and logic circuits. This paper focuses on DNA molecular circuits, constituted by sets of partially or fully hybridized DNA strands, interacting through strand displacement reactions. Several theoretical and experimental works [4] have shown the possibility to cascade strand displacement reactions in order to perform DNA-based computations. One of the difficulties of these systems is the fact that interactions time constants are diffusion limited. This translates, for usual concentrations in the nanomolar range, to time scales of several hours.

Tethering DNA circuits to structured platforms, such as DNA origamis, is a possible solution to this issue [5]. It has been shown that constraining the distances between different strands to a few nanometers decreases the time responses by two orders of magnitude (as compared to bulk reactions). The drawback of this approach is the difficulty to scale-up this type of platforms.

Here, we consider an alternative solution, by tethering DNA strands to a nanogel. We describe an original way to synthesize polyacrylamide nanogels that also bind DNA strands. We show that simple catalytic reactions take place on these floppy structures.

[1] Zhang, D.Y.; Winfree, E. Control of DNA Strand Displacement Kinetics Using Toehold Exchange. *J. Am. Chem. Soc.* (2009) 131, 17303-17314.

[2] Zhang, D. Y.; Turberfield, A. J.; Yurke, B.; Winfree, E. Engineering Entropy-Driven Reactions and Networks Catalyzed by DNA. *Science* (2007) 318, 1121-1125.

[3] Yin, P.; Choi, H.M.; Calvert, C.R.; Pierce, N.A. Programming Biomolecular Self-Assembly Pathways. *Nature* (2008) 451, 318-322.

[4] Qian, L.; Winfree, E. Scaling Up Digital Circuit Computation with DNA Strand Displacement Cascades. *Science* (2011) 332, 1196-1201.

[5] Mendoza, O.; Houladi, S.; Aimé, J.P. and Elezgaray, J., Signal replication in a DNA nanostructure, *J. Chem. Phys.* (2017) 146, 025102.

A Generalized Convex Hull Construction for Materials Discovery

A. Anelli,^a E. A. Engel^{a*}, C. J. Pickard,^{b,c} and Michele Ceriotti^a

- a. Laboratory of Computational Science and Modeling, IMX, École Polytechnique Fédérale de Lausanne, 1015 Lausanne, Switzerland
- b. Department of Materials Science and Metallurgy, 27 Charles Babbage Road, Cambridge CB3 0FS, UK
- c. Advanced Institute for Materials Research, Tohoku University, 2-1-1 Katahira, Aoba, Sendai 980-8577, Japan

* edgar.engel@epfl.ch

Searching for novel materials involves identifying potential candidates and selecting those that have desirable properties and facile synthesis. The identification of synthesizable compounds is a needle-in-a-haystack problem, best exemplified by the case of high-throughput computational structure searches. The typical size of the databases compiled in such searches generally prohibits bulk determination of accurate structural properties and viable synthetic pathways for all locally-stable structures generated. This renders the identification of synthesizable compounds and the relevant experimentally-realizable constraints a crucial step towards experimental realization of novel materials.

Conventionally, the screening is based on a convex hull constructions, which identify structures that (in the absence of kinetic effects) can be stabilized by manipulating a particular thermodynamic constraint (such as pressure or composition) chosen on the basis of experimental evidence or intuition. This is neither agnostic, nor capable of identifying structures stabilized by more complex sets of constraints. We therefore introduce a generalized convex hull (GCH) framework based on an abstract representation of structural similarity. The GCH is constructed on data-driven coordinates, such that the GCH represents the full structural diversity of the candidate compounds in an unbiased way. Moreover, we rigorously account for the inevitable uncertainty in input structures data, which renders the GCH probabilistic in nature. Not only is the resultant framework robust with respect to errors in the input data, it also facilitates automatic removal of redundant structures. It moreover provides a measure of the probability that a given structure is experimentally-realizable. Compared to the input (free) energies this represents a superior measure of stability, which is computed at negligible computational cost and can for instance also be used to assist experimental crystal structure determination. The GCH framework efficiently identifies candidates with high probabilities of being synthesizable and suggests the relevant experimentally-realizable constraints, thereby providing a much needed starting point for the determination of viable synthetic pathways. We demonstrate that our framework allows us to single out structures that can be stabilized by general thermodynamic constraints, ranging from pressure to the substitution of portions of organic compounds.

Measuring thermodynamic properties of nucleic acid nanostructures

Andre Estévez-Torres^{a*}

a. Sorbonne Université and CNRS, Laboratoire Jean Perrin, Paris, France

* andre.estevez-torres@upmc.fr

Nucleic acid nanostructures can be engineered for different purposes. Two examples are the manufacture of nanoobjects with precise geometry, as in DNA origami, or the design of RNA strands that regulate gene expression, known as riboregulators. While these two constructions increasingly find applications, few experimental methods exist for assessing the way they fold and function. In the first part of my talk I will describe a method for observing and controlling the folding pathway of 2D origami at the nanoscale using AFM [1]. In the second part, I will present how in vitro transcription-translation can be used to characterize the thermodynamics and the functional performance of translational riboregulators [2].

[1] J. Lee Tin Wah et al. ACS nano., 2016, <http://dx.doi.org/10.1021/acsnano.5b05972>

[2] A. Senoussi et al. ACS Synth Biol., 2018, <http://dx.doi.org/10.1021/acssynbio.7b00387>

Scattering of surface waves on an analogue black hole

Léo-Paul Euvé^{a*}, Scott Robertson^b, Nicolas James^c,
Alessandro Fabbri^{d,b} and Germain Rousseaux^a

- a. Institut Pprime, CNRS, Université de Poitiers, ISAE-ENSMA,
11 Boulevard Marie et Pierre Curie, 86962 Futuroscope
- b. Laboratoire de Physique Théorique, CNRS, Univ. Paris-Sud,
Université Paris-Saclay, 91405 Orsay
- c. Laboratoire de Mathématiques et Applications, CNRS, Université de Poitiers,
11 Boulevard Marie et Pierre Curie, 86962 Futuroscope
- d. Centro Fermi - Museo Storico della Fisica e Centro Studi e Ricerche Enrico Fermi,
Piazza del Viminale 1, 00184 Roma, Italy

* leo.paul.euve@univ-poitiers.fr

Recent years have witnessed an explosion of interest in Analogue Gravity in a great variety of physical systems. One of the goals of this field is to experimentally confirm Stephen Hawking's prediction that black holes emit thermal radiation.

With this objective in mind, we have embarked on the study of a hydrodynamical black hole horizon, created by a current rendered inhomogeneous thanks to the presence of an obstacle on the bottom of a hydraulic channel. In contrast to previous studies, the flow is here transcritical. In other words, we can distinguish two separate regions, in the first of which (the *subcritical* region) the flow speed is inferior to the speed of long-wavelength waves, while in the second (the *supercritical* region) it is superior to this speed. Moreover, the flow is accelerating, i.e. it is directed from the subcritical to the supercritical region. The flow is thus analogous to the curved spacetime in the vicinity of the horizon of an astrophysical black hole.

We show that an incident co-current wave, coming from the subcritical (exterior) region, is partially converted into a reflected wave propagating against the current, and partly into a negative-energy wave propagating with the current in the supercritical (interior) region. This gives a total of three outgoing waves, rather than two in the absence of transcriticality. The measured scattering coefficients are in good agreement with the predictions of the non-dispersive theory, where the kinematical description in terms of an effective spacetime metric is exact. An important feature of this process is that the scattering takes place in two stages a bit away from the horizon, and does not exhibit the thermality of the Hawking effect. Finally, we show the emergence of characteristic peaks in the two-point correlation function of free surface deformations, again indicating the presence of a horizon.

Flexible capacitive piezoelectric sensor with ultra-long vertical GaN wires

A. El Kacimi^a, E. Pauliac-Vaujour^a, J. Eymery^{b*}

a. Univ. Grenoble Alpes, CEA, LETI, MINATEC Campus, F-38054 Grenoble, France

b. Univ. Grenoble Alpes, CEA, INAC-MEM-NRS, 38000 Grenoble, France

* joel.eymery@cea.fr

GaN piezoelectric wire-based flexible devices can provide original solution for mechanical sensing applications thanks to their self-powered characteristic, robustness and long life-time. To investigate this track, we developed specific materials, i.e. the growth of ultra-long N-polar GaN wires by self-catalyst Metal Organic Vapor Phase Epitaxy on sapphire substrate with silane addition [1,2]. These 1D materials exhibit hexagonal cross-section (diameter < 2 μm), slight conical shape (conicity < 2 deg.) and length varying from 10 to 700 micrometers.

The aim of this communication will be to report a simple and scalable fabrication process of flexible capacitive piezoelectric sensors using vertically aligned GaN wires as well as to highlight their physical principles of operation [2]. Growth & structural studies will be reported first, enlightening the specificities of the MOVPE process.

The as-grown N-polar GaN wires are embedded into a polydimethylsiloxane (PDMS) matrix by spin-coating and directly peeled off from the sapphire substrate before metallic electrode contacting. This geometry provides an efficient control of the wire orientation and an additive contribution of the individual piezoelectric signals. The device output voltage and efficiency are studied by finite element calculations for compression mechanical loading as a function of the wire geometrical growth parameters (length and density). We demonstrate that the voltage output level and sensitivity increase as a function of the wire length and that a conical shape is not mandatory for potential generation as it was the case for horizontally assembled devices [4]. The optimal design to improve the overall device response is also optimized in terms of wire positioning inside PDMS, wire density, and total device thickness. Following the results of these calculations, we have fabricated experimental devices exhibiting outputs of several volts with a very good reliability under cyclic mechanical excitation [2].

As a conclusion, we will discuss the physical phenomena that have to be further studied in this type of materials, i.e. pyroelectricity, doping effects and technological issues.

[1] J. Eymery *et al.*, *Comptes Rendus Phys.* **14**, 221 (2013).

[2] A. El Kacimi *et al.*, *ACS Applied Materials & Interfaces* **10**, 4794 (2018).

[3] R. Koester *et al.*, *Nanotechnology* **21**, 015602 (2010).

[4] S. Salomon *et al.*, *Nanotechnology* **25**, 375502 (2014).

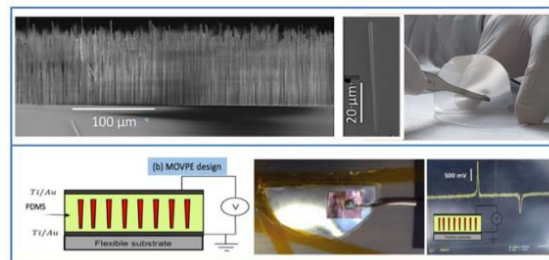


Fig. 1. (Top) Example of 100 μm long wire growth assembly & single wire, and peeling of PDMS containing wires. (Bottom) Design of the capacitive device & example with electrical results.

Revisiting Inversion Domain Boundaries in MOVPE GaN wires

J. Eymery^{a,*}, F. Lançon^a, L. Genovese^a, and D. Salomon^b

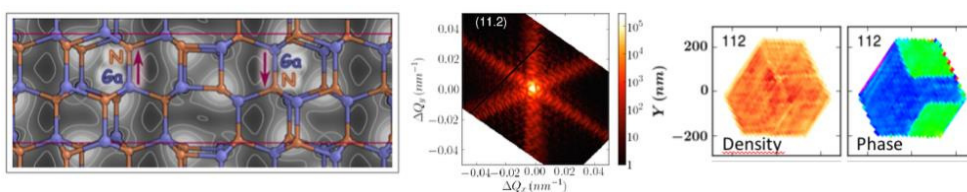
a. Univ. Grenoble Alpes, CEA, INAC-MEM, 38000 Grenoble Cedex, France

b. European Synchrotron Radiation Facility, 71 rue des Martyrs, 38000 Grenoble

* joel.eymery@cea.fr

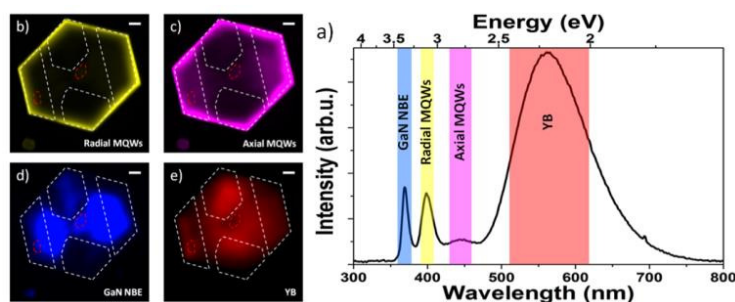
One-dimensional nitride heterostructures demonstrated novel optical and electronic properties making use of quantum confinement effects and strain engineering. The emergence of disruptive functionalities is strongly related to the growth and technology controls [1-5], but also to the development of advanced characterization techniques having high spatial resolution. Focused X-ray beams provide innovative solutions to analyse quantitatively the morphology, defects, strain and composition of these materials. We will present recent breakthroughs obtained at the European synchrotron radiation facility on nitride wires grown by Metal Organic Vapour Phase Epitaxy and their core-shell heterostructures.

The structure of single defects such as Inversion Domain Boundaries



(IDB) inside n-doped GaN wires has been determined from *X-ray coherent diffraction imaging* [6] with an unprecedented accuracy. The complex 3D IDB configuration inside a single wire is measured without any slicing in contrast to electron microscopy and the lattice displacements along/across the wire length is deduced from the analysis of the Bragg peak intensity by *phase retrieval* methods with pm resolution. We will show that the measured atomic configuration corresponds to a refinement of the usual IDB* model that is in full agreement with new electronic structure *ab initio* calculations [7].

The IDB* separates opposite polarities of GaN crystals that may impact the wire growth and the photoluminescence properties of GaN/InGaN Multiple Quantum Well (MQW) core-shell heterostructure deposited on m-plane sidewalls [2-5]. This system is first studied by scanning and transmission electron microscopy and then by *X-ray excited optical luminescence* and *X-ray Fluorescence* with multimodal hard X-ray nanoprobe [8]. It is shown that the optical luminescence of the near band edge of the GaN core is directly related to differential Si incorporation in N- and Ga-polar parts of thick wires, and that core-shell and top axial MQW luminescence can be analysed.



[1] R. Koester et al., Nano Lett. **11**, 4839 (2011).

[2] S. Salomon et al., Nanotechnology **25**, 375502-8 (2014).

[3] N. Guan et al., ACS Photonics **3**, 597 (2016).

[4] H. Zhang et al., ACS Applied Materials & Interfaces **8**, 26198 (2016).

[5] A. Messanvi et al., ACS Applied Materials & Interfaces **7**, 21898 (2015).

[6] S. Labat et al., ACS Nano **9**, 9210 (2015).

[7] F. Lançon, L. Genovese and J. Eymery, to be submitted.

[8] D. Salomon et al., Nano Lett. **17**, 946 (2017).

French contribution to the ESS instrumentation

Xavier FABREGES^{a*}

a. Laboratoire Léon Brillouin, CEA, CNRS, Université Paris-Saclay, CEA Saclay 91191 Gif-sur-Yvette France

* xavier.fabreges@cea.fr

The European Spallation Source (ESS [1]) is the next generation neutron source based on a linear protons accelerator. Currently in construction in Lund (Sweden), the source will be opened to external users in 2023. The initial instrument suite will be composed of 15 instruments covering most of the European scientific community needs in neutron scattering. Most of these instruments are built by European partners through an in-kind contribution.

In this context, France is involved in the construction of 6 instruments:

- 1) 3 diffractometers: MAGiC, DREAM and NMX
- 2) 2 spectrometers: CSPEC and BIFROST
- 3) 1 SANS: SKADI

An additional work package, covering the ESS needs for state of the art sample environment in low temperature, magnetic fields and high pressure is also under advanced discussions.

After a short introduction on the facility and its specificities, an overview of the French contribution will be presented with an emphasis on the new instrumental and scientific opportunities that will emerge from the source's high brilliance.

[1] <https://europeanspallationsource.se/science-instruments>

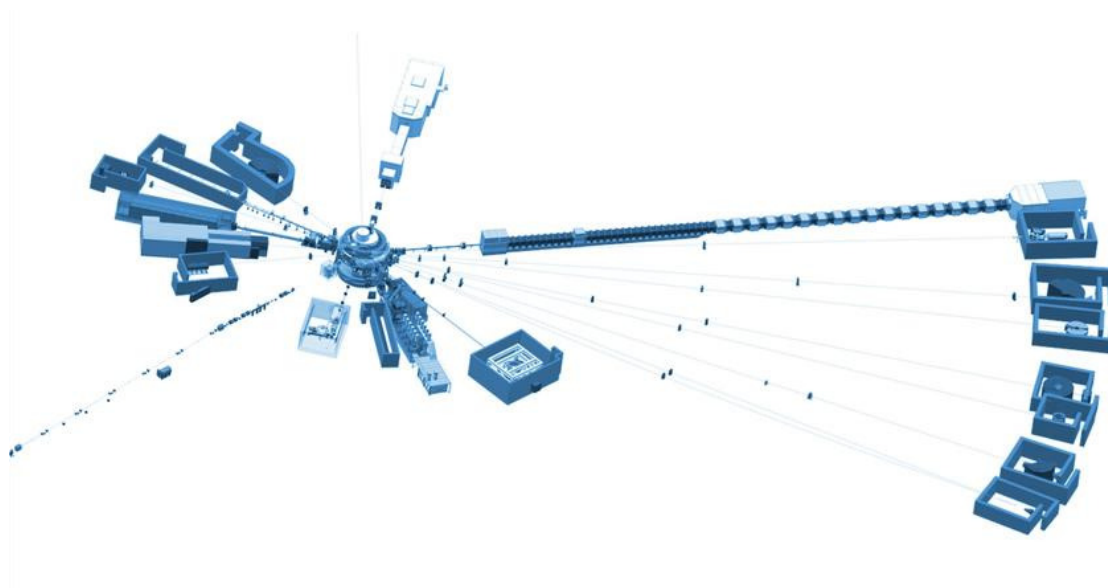


Figure 1: Artist's view of the ESS initial instrument suite at the horizon 2030. Instrument in which France is involved are colored in red.

Spin dynamics of the longitudinal spin density wave phase in the quasi-1D Ising-like antiferromagnet $\text{BaCo}_2\text{V}_2\text{O}_8$

Quentin Faure^{a,c*}, Shintaro Takayoshi^b, Sylvain Petit^d, Virginie Simonet^c, Louis Pierre Regnault^a, Jonathan White^e, Martin Månsson^f, Christian Rüegg^e, Pascal Lejay^c, Benjamin Canals^c, Thomas Lorenz^h, Shunsuke C. Furuyaⁱ, Thierry Giamarchi^b et Beatrice Grenier^a

- a. Université Grenoble Alpes, INAC/MEM/MDN-CEA, Grenoble, France.
- b. DPMC-MaNEP, University of Geneva, Geneva, Switzerland.
- c. Institut Néel CNRS, Grenoble, France.
- d. Laboratoire Léon Brillouin, CEA, CNRS, Université Paris-Saclay, Gif-sur-Yvette, France.
- e. Paul Scherrer Institut, Villigen, Switzerland.
- f. KTH Royal Institute of Technology, Stockholm, Sweden.
- g. Materials Physics, KTH Royal Institute of Technology, Stockholm, Sweden
- h. II. Physikalisches Institut, Universität zu Köln, Köln, Germany
- i. Condensed Matter Theory Laboratory, RIKEN, Wako, Saitama, Japan

* quentin.faure@neel.cnrs.fr

$\text{BaCo}_2\text{V}_2\text{O}_8$ is a realization of a spin-1/2 Ising-like quasi-one dimensional (1D) antiferromagnet with remarkable static and dynamical behaviors [1]. In zero-field, the excitations of the Néel phase consist in confined two spinon excitations stabilized by weak interchain interactions. They form two interlaced long-lived Zeeman ladders with respective transverse and longitudinal character regarding the direction of the magnetic moments (along the chain caxis) [2]. We have explored the influence of an external magnetic field on this spin dynamics by inelastic neutron scattering. A contrasting behavior is observed for a transverse and longitudinal magnetic field (i.e. perpendicular and parallel to the direction of the moments respectively). The former case has revealed a very interesting physics as a topological quantum phase transition occurs between two types of solitonic topological objects [3].

The present talk is devoted to our results obtained under the application of a longitudinal field in $\text{BaCo}_2\text{V}_2\text{O}_8$. We show that the Néel phase excitations keep their transverse or longitudinal character, simply showing a Zeeman splitting up to $\mu_0 H_c \approx 3.9$ T at which the Néel ordering turns into a longitudinal spin density wave (LSDW) [2,4]. This phase has raised a strong interest as it is a unique example of the Tomonaga-Luttinger liquid (TLL) physics experimentally accessible under moderate magnetic field [2,4,5]. The TLL longitudinal fluctuations expected in the purely 1D system [6], lacking long-range order, are transformed in a LSDW stabilized in $\text{BaCo}_2\text{V}_2\text{O}_8$ through the anisotropy and the weak interchain couplings. The dispersion spectrum in this exotic phase and the magnetic field dependence of the excitations have been investigated by neutron scattering on TASP (PSI) and through numerical calculations.

[1] B. Grenier, et al, PRL, **114**, 017201 (2015) ; *ibid.*, PRL, 115, 119902 (2015).

[2] E. Canévet, et al, PRB, **87**, 054408 (2013).

[3] Q. Faure, et al, Nature Physics (Published the 7th May 2018)

[4] S. Kimura, et al, PRL, **101**, 207201 (2008).

[5] S. Kimura, et al, PRL, **100**, 057202 (2008).

[6] T. Giamarchi, Quantum Physics in One Dimension (2003).

Understanding the effect of interfacial hydrodynamics on thermo-osmosis using molecular dynamics

Li Fu^{a*}, Samy Merabia,^a and Laurent Joly^a

a. Institut lumière matière, Université Claude Bernard - Lyon 1, Villeurbanne, France

* li.fu@univ-lyon1.fr

The fundamental influence of thermal gradients on the flux has received scanty attention until only the past decades. Thermophoretic phenomena were firstly studied for numerous applications such as optothermal DNA trap [1] or disease-related protein aggregates [2]. On the other hand, thermo-osmosis at solid-liquid interfaces is the least studied among the osmotic phenomena. It is usually interpreted as a thermal gradient-induced Marangoni flow, but the molecular level understanding is still lacking. Using molecular dynamics simulations, we measured the thermo-osmosis coefficient by both mechanocaloric and thermo-osmosis routes, against different solid-liquid interfacial energies. We show the critical role of interfacial hydrodynamics, which can reverse the direction of the flow, and strongly amplify it. Notably, we predicted giant thermos-osmotic flows at the water-graphene interface [3]. Following this prediction, we explored the practical implementation of waste heat harvesting with carbon-based membranes, focusing on model membranes of carbon nanotubes (CNT) [4]. Notably, we predicted giant thermos-osmotic flows at the water-graphene interface. Following this prediction, we explored the practical implementation of waste heat harvesting with carbon-based membranes, focusing on model membranes of carbon nanotubes (CNT) [2]. We show that, despite viscous entrance effects and a thermal short-circuit mechanism, CNT membranes can generate very fast thermo-osmotic flows, which can be used to desalinate seawater.

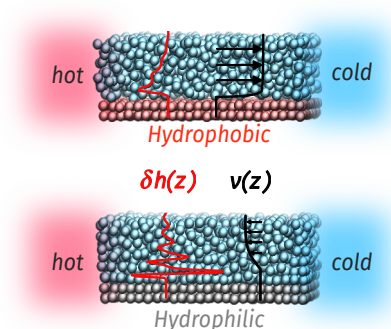


Figure 1: Illustration of the role of surface wettability on thermo-osmotic flows

- [1] S. Duhr and D. Braun, Phys. Rev. Lett. (2006).
- [2] M. Wolff, J. J. Mittag, T. W. Herling, E. De Genst, C. M. Dobson, T. P. J. Knowles, D. Braun, and A. K. Buell, Scientific Reports 6, 22829 (2016).
- [3] L. Fu, S. Merabia, and L. Joly, Phys Rev Lett 119, 606 (2017).
- [4] L. Fu, S. Merabia, and L. Joly, J. Phys. Chem. Lett 9, 2086 (2018)

Tunnel junctions in nitride heterostructures for optoelectronic applications

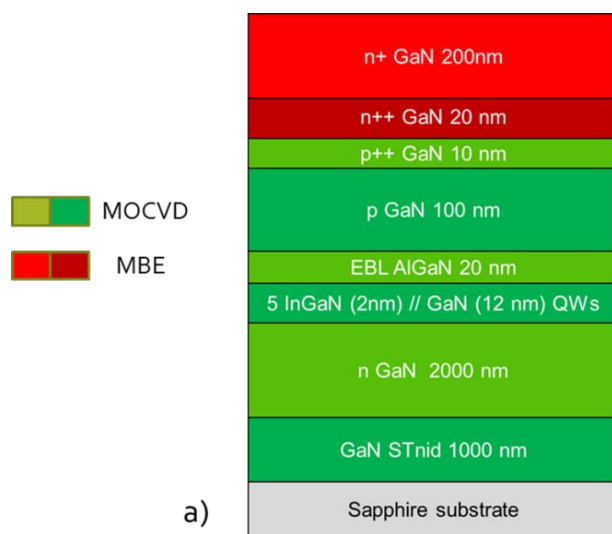
V. Fan Arcara^{1,2*}, B. Damilano¹, G. Feuillet², J. Brault¹, A. Courville¹, P. de Mierry¹,
S. Vézian¹, S. Chenot¹, J-Y. Duboz¹

¹: Université Côte d'Azur, CNRS, CRHEA, Rue B. Gregory, 06560 Valbonne, France

²: Université Grenoble Alpes, CEA, LETI, 17 Avenue des Martyrs, 38000 Grenoble, France

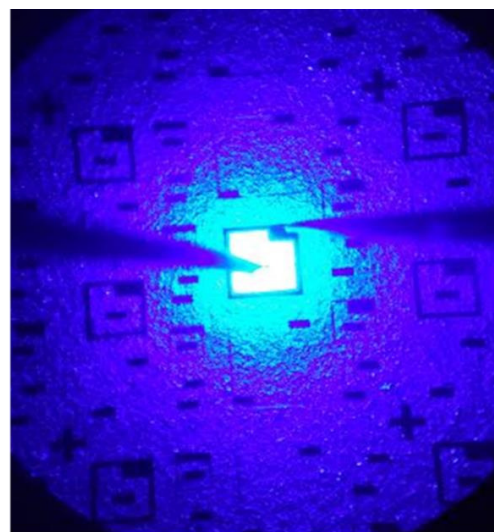
* Corresponding author: vfa@crhea.cnrs.fr

The efficiency of nitride-based UV LEDs suffers from an efficiency droop caused by the high acceptor activation energy in wide band gap semiconductors and poor light extraction efficiency. However, their efficiency can be improved by inserting a tunnel junction (TJ) on top of the structure, generating holes out of equilibrium and replacing the p-(Al)GaN contact layer by an n-contact layer, which is known to be less resistive. In the literature, the best GaN tunnel junctions are obtained using molecular beam epitaxy (MBE). However, all the LED industry is based on metal-organic chemical vapor deposition (MOCVD) and therefore understanding and improving the tunnel junctions grown by MOCVD would be of great interest. In this work we report the growth of different structures containing distinct GaN tunnel junctions – one grown by MBE, one by MOCVD and one hybrid combining MBE and MOCVD. The latter two TJs were grown on top of blue LED structures in order to evaluate their properties on visible LEDs before switching to UV-emitting devices. The samples were clean-room-processed using standard photolithography and reactive ion etching steps to fabricate LEDs. We measured the electrical and optical characteristics of these LEDs at room temperature under CW conditions. The MBE and the hybrid structures emitted light homogeneously throughout the surface – however, the emission in the all-MOCVD TJ LEDs was concentrated around the top n-contact. As expected, the hybrid TJ exhibited a lower voltage drop in comparison to the other structures. Inserting a 4-nm thick (Ga,In)N layer at the core of the tunnel junction grown by MOCVD will improve the LED electrical characteristics, reducing the gap between MBE and MOCVD tunnel junctions in the hybrid TJ. Ultimately, in order to reach UV-emissions, structures containing AlGaN TJs on top of AlGaN UV LEDs will be developed. This work is partially funded by GANEX (ANR-11-LABX-0014) and the CEA Grenoble.



a)

a) Growth stack of the hybrid TJ LED



b)

b) Hybrid TJ LED working under 20mA

Optics and magneto-optics of excitons in monolayers of transition metal dichalcogenides encapsulated in hBN

Maciej R. Molas^{a,b}, Artur O. Slobodeniuk^a, Karol Nogajewski^a, Miroslav Bartos^a, Kenji Watanabe^c, Takashi Taniguchi^c, Clement Faugeras^{a,*}, Marek Potemski^a

a. Laboratoire National des Champs Magnétiques Intenses, CNRS-UGA-UPS-INSA-EMFL, 25, avenue des Martyrs, 38042 Grenoble, France

b. Institute of Experimental Physics, Faculty of Physics, University of Warsaw, ul. Pasteura 5, 02-093 Warszawa, Poland

c. National Institute for Materials Science, 1-1 Namiki, Tsukuba 305-0044, Japan

* clement.faugeras@lncmi.cnrs.fr '

Semiconducting transition metal dichalcogenides MX_2 where $M = Mo$ or W and $X = S, Se$ or Te , are layered semiconductors that can be thinned down to the monolayer, showing an indirect to direct band gap transition for monolayers. Excitons in these purely 2D systems have a large binding energy of few hundreds of meV, a non-hydrogenic excitonic energy ladder and interband transitions are governed by chiral optical selection rules, allowing for the initialization of a valley population by a circularly polarized optical exciton.

Excitons excited states can be used to determine the type of electrostatic potential between the electron and the hole. This is done by determining the energy ladder of excited states. High quality van der Waals heterostructures allow for the direct observation both in the emission spectrum and in the reflectance spectrum of excited states of excitons in a monolayer of WSe_2 encapsulated in hBN. Using optical spectroscopy with and without high magnetic fields, we determine the energy sequence of these excited states, their diamagnetic shifts, and highlight the very particular case of WSe_2/hBN heterostructures, in which 2D excitons are not what they seem to be.

Magnetoresistance of semi-metals : the case of bismuth and antimony

Benoît Fauqué^{1,2}

¹*JEIP, USR 3573 CNRS, Collège de France, PSL Research University,
11, place Marcelin Berthelot, 75231 Paris Cedex 05, France.*

²*ESPCI ParisTech, PSL Research University; CNRS; Sorbonne Universités,
UPMC Univ. Paris 6; LPEM, 10 rue Vauquelin, F-75231 Paris Cedex 5, France*

Magnetoresistance is the change in the electrical resistance of a material in the presence of a magnetic field. As early as 1928, Kapitza discovered that the electric resistivity of bismuth increases by many orders of magnitude upon the application of a large magnetic field. More recently large unsaturated magnetoresistance has been reported in numerous semi-metals. Many of them have a topologically non-trivial band dispersion, such as Weyl nodes or lines. Both the amplitude of magnetoresistance and its field dependence have been put under scrutiny and are explored and discussed by experimentalists and theorists. Here, I will discuss the case of the two elemental semi-metals bismuth and antimony. I will show that antimony displays the largest high-field magnetoresistance among all known semi-metals which can be captured by a modified semi-classical theory.

[1] P. Kapitza, The study of the specific resistance of bismuth crystals and its change in strong magnetic fields and some allied problems, Proc. R. Soc. A, 119, 358 (1928) [2] B.Fauqué et al., <http://lanl.arxiv.org/abs/1803.00931>

Statistique des fluctuations de grande échelle en turbulence

Stéphan Fauve^{a*}

a. Laboratoire de physique statistique de l'Ecole normale supérieure 24 rue Lhomond 75005 Paris

* fauve@lps.ens.fr

Dans de nombreux écoulements turbulents, les fluctuations des échelles spatiales plus grandes que celle à laquelle l'écoulement est forcé, sont en equipartition. Après avoir montré cette propriété sur des exemples d'écoulement turbulent et de turbulence d'ondes, nous considérons les transitions entre différents régimes turbulents dans un écoulement forcé périodiquement dans l'espace à petite échelle. Nous observons que ces transitions sont caractérisées par différentes lois de probabilité pour le champ de vitesse de grande échelle. Nous montrons que ces régimes turbulents peuvent être reproduits en intégrant l'équation d'Euler tronquée au nombre d'onde de forçage de l'écoulement, et que les lois de probabilité correspondantes peuvent être prédites à partir de l'ensemble micro-canonique. Nous discutons finalement l'analogie avec les transitions de phase à l'équilibre thermodynamique.

- [1] V. Dallas, S. Fauve and A. Alexakis, Statistical equilibria of large scales in dissipative hydrodynamic turbulence, *Phys. Rev. Lett.* **115**, 204501 (2015)
- [2] G. Michel, J. Herault, F. Pétrélis and S. Fauve, Bifurcations of a large scale circulation in a quasi-bidimensional turbulent flow, *Europhysics Letters* **115**, 64004 (2016)
- [3] V. Shukla, S. Fauve and M. Brachet, Statistical theory of reversals in two-dimensional confined turbulent flows, *Phys. Rev. E* **94**, 061101 (2016)
- [4] G. Michel, F. Pétrélis and S. Fauve, Observation of thermal equilibrium in capillary wave turbulence, *Phys. Rev. Letters* **118**, 144502 (2017)

Lattice dynamics of low dimensional systems using neural networks potentials

Mauro Fava¹, Anton Bochkarev¹, Stefano Mossa², Ambroise Van
Roekeghem¹, and Natalio Mingo¹

¹CEA, LITEN, 17 Rue des Martyrs, 38054 Grenoble, France

²Univ. Grenoble Alpes, CEA, CNRS, INAC-SYMMES, 38000
Grenoble, France

Keywords: machine learning, materials science

Rotational and translational symmetries impose a quadratic behavior for the out-of-plane or out-of-line acoustic phonons in 2D or 1D materials. While inaccuracies in the numerical models led to a controversy about their reliability into representing the long wavelength limit, recent *Ab Initio* results[1] show without any doubt these quadratic modes.

We investigate them in low dimensional systems by using a Neural Network based potential, which we trained for many materials, starting from DFT datasets but also from already computed force constants.

References

- [1] Jesús Carrete, Wu Li, Lucas Lindsay, David A. Broido, Luis J. Gallego, and Natalio Mingo. Physically founded phonon dispersions of few-layer materials and the case of borophene. *Materials Research Letters*, 4(4):204–211, 2016.

Using microwave radiation to detect local topology or to induce topological properties in three-terminal Josephson junctions

Denis Feinberg^{a*}, Lucila Peralta Gavensky^b, Gonzalo Usaj^b, Carlos Balseiro^b

a. Institut Néel, CNRS and Université Grenoble Alpes, Grenoble, France

b. Instituto Balseiro, Centro Atomico Bariloche and CONICET, Bariloche, Argentina

* denis.feinberg@neel.cnrs.fr

We propose an experimental protocol to locally detect the Berry curvature of a three-terminal Josephson junction with a quantum dot by performing an ac nonlocal conductance measurement. We compare the results of an infinite-gap approximation and of the full Keldysh calculation including the continuum of quasiparticles. The comparison is favourable due to the concentration of the Berry phase in the low-energy regions. We also propose to induce topological phases with nonzero Chern numbers by irradiating a three-terminal junction, breaking time-reversal symmetry with a suitably polarised microwave field.

Pumping topological Josephson currents with microwaves

Denis Feinberg^{a*}, Benjamin Venitucci^a, Régis Mélin^a, Benoît Douçot^b

a. Institut Néel, CNRS and Université Grenoble Alpes, Grenoble, France

b. LPTHE, Université Paris VI and CNRS, Paris, France

* denis.feinberg@neel.cnrs.fr

Irradiating a Josephson junction with microwaves can operate not only on the amplitude but also on the phase of the Josephson current. This requires breaking time inversion symmetry, which is achieved by introducing a phase lapse between the microwave components acting on the two sides of the junction. General symmetry arguments and the solution of a specific single level quantum dot model show that this induces chirality in the Cooper pair dynamics, due to the topology of the Andreev bound state wavefunction. Another essential condition is to break electron-hole symmetry within the junction. A shift of the current-phase relation is obtained, which is controllable in sign and amplitude with the microwave phase and an electrostatic gate, thus producing a "chiral" Josephson transistor. The dot model is solved in the infinite gap limit by Floquet theory and in the general case with Keldysh nonequilibrium Green's functions. The chiral current is nonadiabatic: it is extremal and changes sign close to resonant chiral transitions between the Andreev bound states.

[1] B. Venitucci, D. Feinberg, R. Mélin and B. Douçot, ArXiv 1708.03262

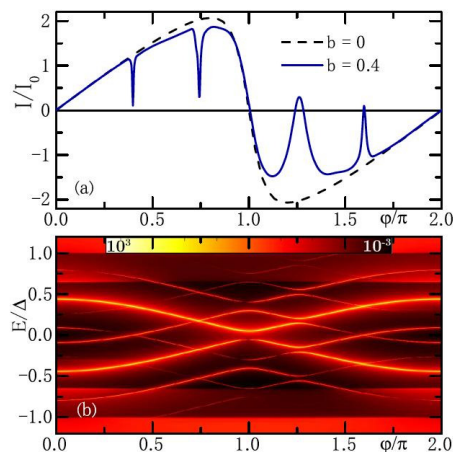


Figure : (Top) Current-phase characteristic of a junction irradiated with two dephased microwave fields. (Bottom) Density of states of the Andreev bound state spectrum. The asymmetry of the resonances and of the corresponding anticrossings reflect the chirality introduced by the microwave in the Floquet wavefunctions.

Direct observation of metal nanoparticles (NPs) electrodeposition on carbon nanotubes (CNTs) and glassy carbon supports by *situ* and *operando* TEM microscopy

L. Sacco^a, M. Ezzedine^a, C-S. Cojocaru^a, I. Florea^{a*}

^aLPICM, CNRS, Ecole Polytechnique, Université Paris-Saclay, 91128, Palaiseau

* lenuta-ileana.florea@polytechnique.edu

Metal Nanoparticles (NPs) are of great interest due to their exceptional catalytic, reactive and magnetic properties. Several applications, ranging from gas sensors, photodetectors, photovoltaic devices, and energy storage and conversion devices [1], are developed using as building block hybrid nanomaterials like decorated carbon nanotubes (CNT) or glassy carbon (GC). However, their device performances are strongly related with distribution, density, well-defined size, composition and morphology [2]. Particularly, electrodeposition process results a powerful method to form NP due to their key benefices, such as: low-cost of implementation, ambient operating conditions and the capability to control the properties of deposited materials such as size and density by adjusting the parameters involved in the deposition process. The real time survey of the evolution of nanosystems under certain electrochemical conditions (*operando*) enables to elucidate the NPs nucleation, formation and deposition depending on the electrodeposition parameters. The present work is mainly devoted to carry out in situ liquid TEM and STEM observations through a closed electrochemical cell, in order to distinguish the nucleation/formation NPs stages using different ionic salts. Firstly, cycle voltammetry (CV) technique was applied to identify the reduction peaks for the formation of different metal NPs (Fe, Ni, Co and Cu). Subsequently, pulsed chronoamperometry (CA) was adopted to decorate CNT and GC supports, recording the evolution of the whole process: from the nucleation up to the NP growth. Figure 1 shows a decorated CNT with Ni NPs and their corresponding electrodeposition current and cumulative charge during the decoration process. The presented approach enables studying the influence of the main electrochemical parameters, such as, applied potential, flow rate, pulse duration on the NP formation, distribution, density and composition. In conclusion, the present study introduce the route to get a better understanding of the CNT and GC decoration process in order towards the precisely tailor of hybrid materials for the next generation of nanotechnological devices.

[1] S. Carnot, *Réflexions sur la puissance motrice du feu et sur les machines propres à développer cette puissance* (Bachelier, Paris, 1824)

[1] A. Gohier et al., High-rate capability silicon decorated vertically aligned carbon nanotubes for li-ion batteries, *Adv. Mater.* **24**, 2592 (2012).

[2] R.M. Penner et al. A Nose for Hydrogen Gas: Fast, Sensitive H₂ Sensors Using Electrodeposited Nanomaterials, *Acc. Chem. Res.* **50**, 1902 (2017).

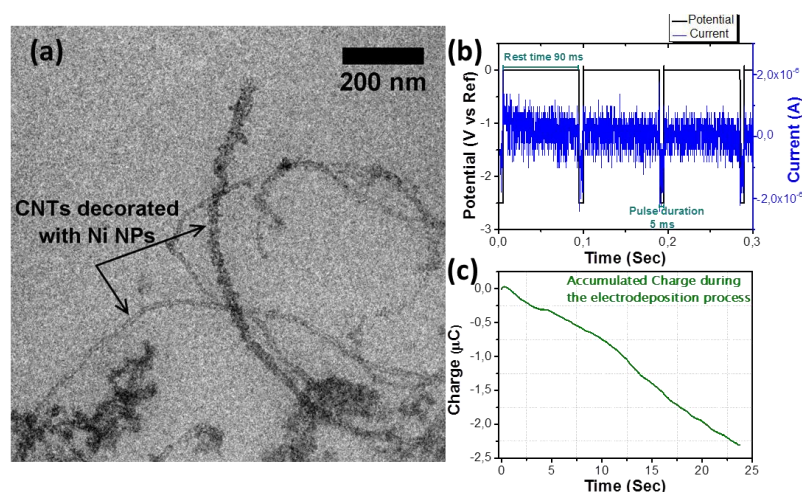


Figure 1: (a) Carbon nanotubes decorated with Ni NPs. (b) The associated applied potential during the electrodeposition process. (c) The corresponding accumulated charge.

Observing The Topological Invariant of Bloch Bands Using Quantum Walks in Superconducting Circuits

E. Flurin¹, V.V. Ramasesh¹, N. Yao², I. Siddiqi¹

¹*Quantum Nanoelectronics Laboratory, UC Berkeley*

²*Department of Physics, UC Berkeley*

The direct measurement of topological invariants in both engineered and naturally occurring quantum materials is a key step in classifying quantum phases of matter. Here we motivate a toolbox based on time-dependent quantum walks as a method to digitally simulate single-particle topological band structures. Using a superconducting qubit dispersively coupled to a microwave cavity, we implement two classes of split-step quantum walks and directly measure the topological invariant (winding number) associated with each. The measurement relies upon interference between two components of a cavity Schrödinger cat state and highlights a novel refocusing technique which allows for the direct implementation of a digital version of Bloch oscillations. Our scheme can readily be extended to higher dimensions, whereby quantum walk-based simulations can probe topological phases ranging from the quantum spin Hall effect to the Hopf insulator.

All-optical mapping of the position of single quantum dots embedded in a nanowire antenna

Romain FONS^{a*}, Andreas D. OSTERKRYGER^b, Petr STEPANOV^a, Eric GAUTIER^c, Joël BLEUSE^a, Jean-Michel GERARD^a, Niels GREGERSEN^b et Julien CLAUDON^a

a. : Univ. Grenoble Alpes, CEA, INAC, PHELIQS, joint group 'Nanophysique et semiconducteurs', F-38000, Grenoble, France

b. : DTU Fotonik, Department of Photonics Engineering, Technical University of Denmark, Ørstedes Plads Building 343, DK-2800 Kongens Lyngby, Denmark

c. Univ. Grenoble Alpes, CEA-CNRS, INAC, SPINTEC, F-38000, Grenoble, France

* : romain.fons@cea.fr

In the last years, nanowire antennas embedding isolated quantum dots (QDs) have appeared as a powerful platform for solid-state quantum optics. They have enabled the realization of bright sources of quantum light [1,2]. Such devices can be obtained by etching a planar semiconductor structure which contains a single sheet of self-assembled QDs. This top-down fabrication strategy leads to a random position of the QDs in the waveguide section. The QD position influences the device performance (optical brightness and likely QD spectral coherence).

In this context, mapping precisely the QD position inside the photonic structure is highly desirable. However, conventional optical imaging is here not applicable, because the antenna supports only one, or few optical guided modes. In this work, we introduce an all-optical mapping technique based on Fourier-space microscopy, and determine the position of individual QDs with an accuracy better than 10 nm [3].

The technique exploits two guided modes which feature very different transverse spatial profiles: (i) the fundamental guided mode with a Gaussian profile and (ii) the second-order guided mode with a ring profile. The fraction of spontaneous emission funneled into each mode strongly depends on the QD position. Consequently, the far-field emission pattern contains information on the radial and azimuthal position of the QD in the waveguide section. We have developed a Fourier microscopy setup which allows mapping the far-field emission of individual QDs, isolated by spectral filtering [4]. We investigate the far-field emission of distinct QDs embedded in the same structure. We obtain very different far-field maps, which highlights the large sensitivity of this quantity to the QD position. The results are in excellent agreement with numerical simulations based on the device geometry. Comparison with the experimental data yields the QD position with an accuracy on the order of 10 nm. As a first application, we also correlate the QD position with their measured photoluminescence lifetime. Our results open interesting perspectives for the fine characterization and optimization of single-QD nanowire devices.

[1] J. Claudon, et al., *Nature Photon.*, **2010**, 4, 174.

[2] M. Munsch et al., *Phys. Rev. Lett.*, **2013**, 110, 177402.

[3] R. Fons, et al., in preparation.

[4] P. Stepanov, et al., *Appl. Phys. Lett.*, **2015**, 107, 141106.

Fluctuations in a NESS: is there a universal behavior ?

Alex Fontana^{a,*}, Richard Pedurand^{a,b} et Ludovic Bellon^a

a. Univ Lyon, ENS de Lyon, UCBL, CNRS, Laboratoire de Physique, F-69342 Lyon, France

b. Laboratoire des Matériaux Avancés, CNRS/IN2P3, F-69622 Villeurbanne, France

* alex.fontana@ens-lyon.fr

The fluctuation-Dissipation Theorem is a cardinal tool of Statistical Physics. This relation yields to the Equipartition Principle, thanks to which we can link the fluctuations of an observable with the temperature of the system. All of this is nevertheless granted at *equilibrium*. Our purpose is to test what happens out of this safe region.

In our experiment, shown in Fig. 1, we study a system in a Non equilibrium Steady State (NESS): a silicon micro-cantilever subject to a heat flux due to a laser heating. We measure the thermal noise driven deflexion and torsion and quantify the amplitude of the fluctuations with an effective temperature T^{eff} , extending the equipartition principle:

$$\frac{1}{2}k_B T^{\text{eff}} = \frac{1}{2}k \langle x^2 \rangle$$

with k_B Boltzman's constant, k the stiffness and $\langle x^2 \rangle$ the mean square deformation. Out of equilibrium, an excess of fluctuations is usually expected, as found out for example by Conti et al. in a similar system¹ (Fig. 1). Following Geitner et al.² we find on the contrary a strong *deficit* of thermal noise of the cantilever with respect to the average temperature T^{avg} of the system ! Further experiments and theoretical progress are thus necessary to clarify these contracticting behaviors.

[1] L. Conti, et al. , J. Stat. Mech. P12003 (2013).

[2] M. Geitner, et al. Physical Review E **95**, 032138 (2017).

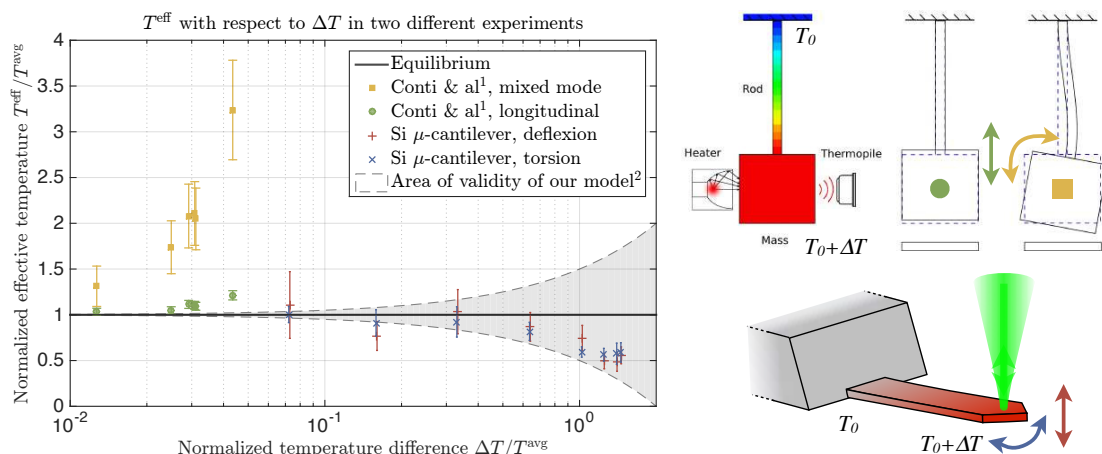


Figure 1: (Left) Effective temperature T^{eff} of a system under a heat flow as a function of the difference of temperature ΔT at its extremities. All temperatures are normalized to the average temperature T^{avg} . (Upper right) Conti's setup¹. (Lower right) Our experiment².

Elastic and plastic transformations of vitreous silica under pressure

Marie Foret^{a*}

a. L2C, University of Montpellier, CNRS, Montpellier, France

* Marie.Foret@umontpellier.fr

The talk focuses on the thermodynamic properties of vitreous silica submitted to high pressures in a diamond anvil cell as obtained directly from Brillouin Light Scattering experiments or indirectly from standard relations. The analysis reveals non-negligible differences between static and dynamic compressibilities which are mostly related to the existence of thermally activated relaxational processes. Estimate of the residual densifications after complete cycles of compression/decompression is discussed.

Coherent Revival of Ramsey Oscillations in the Fluxonium Qubit Coupled to a bath of Harmonic Oscillators

Farshad Foroughi^{a*}, Mattia Mantovani,^b Remy Dassonneville^a, Luca Planat^a, Javier Puertas^a, Sebastien Leger^a, Etienne Dumur^c, Yuriy Krupko^a, Wolfgang Belzig^b, Cecile Naud^a, Olivier Buisson^a, Nicolas Roch^a, Frank Hekking^a, Gianluca Rastelli^b, and Wiebke Guichard^a

- a. Univ. Grenoble Alpes, CNRS, Grenoble INP, Institut Néel, Grenoble, France.
- b. Fachbereich Physik, Universität Konstanz, Konstanz, D-78457, Germany.
- c. The institute for Molecular Engineering, University of Chicago, Chicago, IL, United States.

* farshad.foroughi@neel.cnrs.fr

We studied different fluxonium qubits in 2D and 3D cavity-structures and reached the state of the art for coherence and relaxation times. We observed a systematic increase of the relaxation time both in 3D and 2D at the optimal point of the qubit, when quasi-particle tunneling is strongly reduced. We aim to realize a 2D fluxoniums coupled to few on-chip lumped element resonators. We use a fast flux line to control the coupling between the fluxonium qubit and the resonators. We have studied theoretically the emerging spin-boson Hamiltonian for this particular circuit with the perspective of measuring revival effects in the coherent oscillations of the qubit. We started to implement measurements, revealing the effect on the qubit dynamics of a dissipative bath formed by a discrete set of harmonic oscillators.

Control of bi-dimensional localized biochemical structures through fluctuations and non-linearities

A. Kerjuan,^b C. Albiges-Rizo^b, and O. Destaing^b, B. Fourcade^{a*}

a. LIPhy, Université Grenoble-Alpes, CNRS.

b. Albert Bonniot Institute, Inserm, CNRS, Université Grenoble-Alpes.

*Bertrand.Fourcade@univ-grenoble-alpes.fr

Diffusion and reaction can work in consonance to produce stable stationary structures. In this work we focus on static and dynamic localized structures where essential non-linearities result from feedback mechanisms. Using stochastic simulations to model receptors diffusing on membrane and interacting with actin-ligand complexes, we study how self-sustained structure emerge in cooperative cell-adhesive phenomena. Our model underlines the role of receptor mobility and recruitment as a pivotal mechanism for self-organization. We describe a whole set of bifurcations between different families of transient, static and dynamic localized structures as a function of key parameters such as the the excitability of the adhesive complex medium. Finally, we illustrate this modelling approach in the framework of optogenetic experiments where we assume that the excitability of medium can be tuned via the light activation of a key kinase protein (Src) diffusing from the cytosol to the adhesive sites via a direct or a membrane indirect recruitment.

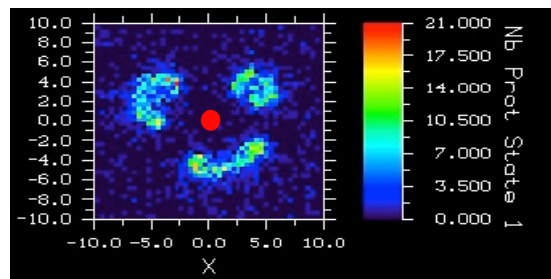


Figure 1: Example of excited adhesive structures given by a density plot for the number of receptor molecules per unit surface. This example corresponds to a dynamic solution of incomplete expanding rings following a local excitation (red circle centered at the origin).

Le problème ontologique de l'esprit et du cerveau face aux neurosciences

Éric Fourneret*

Philosophe, Philosophie, Pratiques et Langage (PPL EA 3699), Braintech (Inserm 1205),
Université Grenoble Alpes.

* efourneret@free.fr

Grâce à l'investigation savante du cerveau humain, une cartographie de plus en plus sophistiquée de ses mécanismes de fonctionnement se met en place, ce qui constitue un progrès considérable pour la médecine, en particulier pour compenser des déficiences de certaines capacités cognitives (par exemple, la perte de la parole). Mais en rendant visibles des processus cérébraux, les neurosciences et les neurotechnologies conduisent aussi à effacer progressivement la distinction entre l'esprit et le cerveau. En effet, en établissant des cartes cérébrales des processus mentaux, comme la parole intérieure, les neurosciences réalimentent un vieux débat philosophique que l'on peut faire remonter au moins jusqu'à Descartes : les états mentaux et les états physiques d'une personne sont-ils deux substances différentes ? Ou pour le dire autrement : l'esprit est-il autre chose que le cerveau ?

Sur cette question s'opposent, de façon radicale, deux courants de pensées : le premier soutient la dualité entre l'esprit et le cerveau : l'un et l'autre sont des réalités différentes, ou bien dans leur nature (*dualisme des substances*), ou bien dans leurs propriétés (*dualisme des propriétés*), ou bien dans notre façon de les décrire (*dualisme des prédicats*). Si le dualisme était vrai, alors les nouveaux dispositifs artificiels, permettant d'explorer le cerveau, ne risqueraient pas de dévoiler l'expérience intime d'une conscience individuelle humaine, tel les pensées intérieures (privauté mentale). L'accès à ce type d'activités mentales resterait le privilège de la personne et ne serait pas accessible par un explorateur extérieur, tel un neuroscientifique.

Néanmoins, le dualisme est contestable. Il l'est philosophiquement, mais il l'est aussi parce que les neurosciences tendent à renvoyer de plus en plus les fonctions dites « supérieures » à des processus cérébraux : l'esprit serait le cerveau ; le cerveau serait l'esprit. Ce courant de pensée s'appelle le physicalisme et s'oppose en cela au dualisme : les états mentaux sont des états physiques et d'ailleurs leur compréhension inspire le développement de réseaux de neurones artificiels. Mais si le dualisme tombe ainsi progressivement à l'abandon face aux avancées des neurosciences, le physicalisme a ses limites, invitant à rechercher des positions intellectuelles et scientifiques moins radicales, sans pour autant revenir à une forme de spiritualisme. Entre l'esprit et le cerveau, est-ce une question de dualité, d'identité ou, de façon plus complexe, un peu des deux ?

The 16-fold way in the Kitaev model

Jean-Noël Fuchs^{a,b*} et Julien Vidal^a

- a. Laboratoire de Physique Théorique de la Matière Condensée, CNRS UMR 7600, Sorbonne Université, 4 Place Jussieu, 75252 Paris
 - b. Laboratoire de Physique des Solides, CNRS UMR 8502, Université Paris-Sud, 91405 Orsay
- *fuchs@lptmc.jussieu.fr

We revisit the Kitaev compass model on the honeycomb lattice. This model maps on non-interacting real (Majorana) fermions in the presence of a Z_2 gauge potential consisting in the presence or absence of π -fluxes in each hexagonal plaquette of the lattice. Depending on the Chern number of the corresponding fermion groundstate, the gapped excitations are anyons of different types. Here, we show that the predicted 16 different types of anyons are possible in this simple model by playing with different vortex patterns.

Ductile-to-fragile transition in compressed amorphous silicon nanopillars by numerical simulations

C. Fusco^{a*}, P.-L. Jay^b, A. Tanguy^c, and T. Albaret^b

- a. INSA Lyon, MATEIS CNRS UMR5510, 69621 Villeurbanne, France
- b. Institut Lumière Matière, Université Lyon 1 CNRS UMR5306, 69622 Villeurbanne, France
- c. INSA Lyon, LAMCOS CNRS UMR5259, 69621 Villeurbanne, France

* claudio.fusco@insa-lyon.fr

Nanopillars are emerging nanostructures that have attracted much attention in the last years for their applications in different fields, such as nanoelectronics and nanobiotechnology. Therefore their mechanical properties are very important and need to be understood. Previous studies have already reported a brittle to ductile transition as a function of the nanopillar's diameter, but contradictory results have been found for different systems: a ductile behavior has been observed when decreasing the size of crystalline silicon nanopillars [1] and metallic glass nanowires [2] while an opposite trend has been reported for crystalline silicon nanowires with an amorphous shell [3]. Here we address the mechanical behavior of amorphous silicon nanopillars by Molecular Dynamics simulations in the quasi-static limit. We show that the mechanical properties of the a-Si nanopillars strongly increase by increasing the nanopillar's diameter. We also observe that the internal pressure of the sample decreases with the nanopillar's diameter following a power law with an exponent depending on the aspect ratio of the nanopillar. In order to get a deeper understanding of the mechanical behavior we perform a microscopic analysis of the plastic rearrangements occurring in the nanopillar. This analysis suggests that the plastic rearrangements are initiated near the surface of the nanopillar in the elastic regime, and then propagate in the bulk at larger strains. Furthermore this behavior can be ascribed to the propensity of plastic rearrangements to localize near structural defects at the surface for small strains, and then to move closer to defects in the bulk at large strains. This work opens the door to the possibility of playing in a controlled manner with the microstructure to control the initiation and propagation of plasticity.

[1] F. Ostlund and K. Rzepiejewska-Malyska, K. Leifer, L.M. Hale, Y. Tang, R. Ballarini, W.W. Gerberich, and J. Michler, Nanostructure Fracturing: Brittle-to-Ductile Transition in Uniaxial Compression of Silicon Pillars at Room Temperature, *Adv. Funct. Mater.* **19**, 2439 (2009).

[2] Q. Zhang, Q.-K. Li, and M. Li, Internal stress and its effect on mechanical strength of metallic glass nanowires, *Acta Materialia* **91**, 174 (2015).

[3] J. Guérolé, J. Godet, and S. Brochard, Plasticity in crystalline-amorphous core-shell silicon nanowires controlled by native interface defects, *Phys. Rev. B* **87**, 045201 (2013).

Clogging of microswimmers at a constriction. An analogy with crowd motion.

Andre Foertsch^{a*}, Walter Zimmermann^a, Salima Rafai^b et Philippe Peyla^b

a. Theoretische Physik I, Universität Bayreuth, 95440 Bayreuth, Germany

b. LIPHY, University Grenoble Alpes, 38402 Saint Martin d'Hères, France

* andre.foertsch@uni-bayreuth.de

We use the Lattice Boltzmann Method to simulate a suspension of force-dipols to model phototactic microswimmers confined between two walls (Hele-Shaw geometry) which migrate to a constriction (attracted by light). By analogy with crowd motion and panic behaviors, we analyze the clogging by calculating the time between two successive egresses τ . The cumulative probability $p(t > \tau)$ behaves as a decreasing power law as a function of τ . This behavior is very universal and it is shared by granular particles as well as pedestrians or colloid flows through a constriction [1].

Following the idea that an obstacle - placed in front of an exit - can facilitate the evacuation of pedestrians (and also the flow of grains through a silo's bottleneck), we study the effect of an obstacle in front of the constriction for microswimmers.

[1] Iker Zuriguel *et al*, Scientific Reports 4 : 7324 (2014)

Amorphous to crystalline transition in Phase Change Materials (GeTe) studied by coupled techniques

Gallard Manon^{a,b*}, R. Tholapi^b, M. Amara^b, C. Mocuta^a, M. Putero^b, S. Escoubas^b, C. Guichet^b, M.-I. Richard^c, P. Noé^d, C. Sabbione^d, L. Fellouh^d, M. Bernard^d, R. Chahine^d, P. Kowalczyk^d, A. André^d, N. Bernier^d, A. Kolb^d, A. Brenac^e, R. Morel^e, F. Hippert^f et O. Thomas^b

- a. Synchrotron SOLEIL, l'Orme des Merisiers, Saint-Aubin, 91192 Gif-sur-Yvette, France
- b. Aix-Marseille Université, CNRS, IM2NP UMR 7334, Campus de St-Jérôme, 13397 Marseille, France
- c. ID01/ESRF, The European Synchrotron, 71 rue des Martyrs, 38043 Grenoble, France
- d. Université Grenoble Alpes, CEA-LETI, MINATEC campus, 17 rue des Martyrs, 38054 Grenoble, France
- e. CEA/INAC, 17 rue des Martyrs, 38054 Grenoble, France
- f. LNCMI, CNRS-UGA-UPS-INSA, 25 rue des Martyrs, 38042 Grenoble, France

* manon.gallard@synchrotron-soleil.fr

The objective of this work is to characterize the crystallization of Phase Change Materials (PCMs, namely GeTe) by using a combination of different experimental techniques. PCMs (Ge-Sb-Te alloys) are used for data storage devices like PCRAM (Phase-Change Random Access Memory). The memory mechanism is based on the quick and reversible transition from amorphous to crystalline state [1-3]. During the transition, the 8% increase in GeTe density [4] leads to stress and fatigue that create defects, potentially leading to the failure of the device. Model samples considered here consisted of 100 to 5 nm GeTe thin films, capped with 10 nm of TaN to prevent oxidation [5] and deposited on 100 μm thick Si(001) substrates. Samples were characterized using a unique set-up installed on DiffAbs beamline (Synchrotron SOLEIL) allowing, during *in situ* annealing of the sample, the combination of X-ray Diffraction (XRD), X-ray Reflectivity (XRR) and optical curvature measurements (MOS, Multi-beam Optical Sensor). These coupled measurements give complementary information such as the evolution of microstructure, densification, stress and strain for different GeTe film thickness (1D confinement). Lattice parameter (XRD), film thickness (XRR) and average stress (MOS) evolutions are extracted and will be shown. The behavior of GeTe films during annealing and the crystallization mechanism (isothermals) will be detailed and discussed as well.

This work is funded by ANR within ANR SESAME ANR-15-CE24-0021 project

- [1] Phase Change Materials, edited by S. Raoux and M. Wuttig (Springer, Boston, MA, USA, 2009)
- [2] S. Raoux, W. Welnic, and D. Ielmini, Chem. Rev., 2010, 110(1), pp 240-267.
- [3] G. W. Burr, M. J. Breitwisch, M. Franceschini, D. Garetto, K. Gopalakrishnan, B. Jackson, B. Kurdi, C. Lam, L. A. Lastras, A. Padilla, B. Rajendran, S. Raoux, and R. S. Shenoy, J. Vacuum Sci. Technol. B: Microelectron. Nanometer Struct. 28, 223 (2010).
- [4] P. Noé and F. Hippert, in Phase Chang. Mem. (Springer, Cham, 2018), pp. 125-179
- [5] P. Noé, C. Sabbione, N. Bernier, N. Castellani, F. Fillot, and F. Hippert, Acta Mater. 110, 142 (2016)

Direct measurement of ferroelectric remanent polarisation with an atomic force microscope

Simon Martin,^a, Nicolas Baboux^b, David Albertini^b, Brice Gautier^{b*}

- a. Commissariat à l'énergie atomique (CEA-LETI) de Grenoble, Laboratoire de Caractérisation et Test Electriques, 17 rue des martyrs, 38054 GRENOBLE Cedex.
- b. Institut des Nanotechnologies de Lyon (INL), Institut National des Sciences Appliquées de Lyon (INSA), Université de Lyon, UMR-CNRS 5270, 7 Avenue Capelle 69621 VILLEURBANNE Cedex

* brice.gautier@insa-lyon.fr >>

Measuring the electrical properties of ferroelectrics at the nanoscale is a crucial step in the development of electronic devices based on such materials. Since more than two decades, Piezoresponse Force Microscopy (PFM), based on Atomic Force Microscopy (AFM) has been used to assess ferroelectricity at the nanoscale by means of direct domains writing with the AFM tip and obtention of local hysteresis loops.

Yet, PFM has also proved to suffer from severe artefacts in certain cases e.g. when the concentration of oxygen vacancies is high in the layer under study, or when electrostatic contributions are unavoidable. In these cases, relatively stable PFM images and hysteresis loops can be obtained on obviously non ferroelectric samples [1]. These artefacts prevent PFM from being able to assess ferroelectricity in the most critical cases. This is why alternative methods must be developed.

This communication presents a method called nano-PUND [2] which aims at measuring remanent ferroelectric polarisation at the nanoscale with an atomic force microscope. It is based on current measurement and detection of the polarisation switching displacement current. This is an adaptation at the nanoscale of the PUND method used on several hundreds of micrometers large electrodes [3]. Classical PUND method can not be used at the nanoscale due to the lack of signal to noise ratio inherent to the relative amplitudes of the expected current contributions. This is why the capacitive dielectric displacement current and (when applicable) the leakage current must be removed. We show that polarisation switching current can, under certain assumptions, be extracted from the noise thanks to a real-time correction procedure.

Examples of nano-PUND measurements will be shown. In particular, with PbZrTiO_3 samples, a 4.2 fC remanent polarisation charge has been measured [2]. Non ferroelectric (dielectric) samples, which lead to misleading PFM images, are also tested and allow to define the noise level of the nano-PUND method, which shows that it may be more reliable than PFM in certain cases.

[1] A. S. Borowiak et al. J. Appl. Phys. 105(1), 012906 (2014)

[2] S. Martin et al. Rev. Sci. Instr. 88, 023901 (2017)

[3] J.F. Scott et al., J. Appl. Phys, 64(2):787-792 (1988)

Water in hydrophobic micropores : dynamical behavior

Valentin Gérard^a, Loïc Michel^a, Elisabeth Charlaix^a et Cyril Picard^{a*}

a. Univ. Grenoble Alpes, CNRS, LIPhy, 38000 Grenoble, France

* cyril.picard@univ-grenoble-alpes.fr

The study of interactions between porous materials and gases or liquids confined in them can be achieved by different methods. Numerical studies by means of molecular dynamics simulations and neutron scattering provide, for example, microscopic information about either the structure of the confined fluid or that of the porous matrix. This couple of methods may thus fit in the *bottom up* description of matter. The present talk will describe an experimental and somewhat more *top-down* approach to the study of the behavior of liquids confined in micro-mesoporous matrices in the case where the liquid does not wet the porous surface. Such an interface is said to be *lyophobic*, or hydrophobic in the particular case of water and aqueous solutions.

The experimental studies of lyophobic nanoporous materials coupled with liquids under hydrostatic pressure has provided the scientific community with several facts regarding this kind of systems. Thus, it is now established that the pressure at which water enters the porous volume is given by the Laplace-Washburn law of capillarity for mesoporous materials with pore diameters of size down to a few nanometers with a negligible impact of the intrusion velocity [1]. For smaller pores, Michelin-Jamois experimentally shown that this behavior breaks, in particular when considering electrolyte aqueous solutions. For most saline solutions combined with ZIF-8 microporous matrix, the intrusion pressure of liquid is observed to follow the same trend as with pure water but with an offset pressure found to obey the Van't Hoff osmotic pressure law [2]. Moreover we have recently shown with this system that the intrusion time scale has a significant impact on the intrusion and extrusion pressure: in this case, pressures should not be understood solely under the assumption of equilibrium thermodynamics. In particular when decreasing temperature close to 0°C an unusual pressure-volume characteristic is observed in dynamical regime, with a non monotonic decrease of pressure during the extrusion process.

[1] L. Guillemot, T. Biben, A. Galarneau, *et al.* Activated drying in hydrophobic nanopores and the line tension of water, Proc. Natl. Acad. Sci. **109**, 19557 (2012),

[2] M. Michelin-Jamois, C. Picard, G. Vigier *et al.*, Giant osmotic pressure in the forced wetting of hydrophobic nanopores, Phys. Rev. Lett. **115**, 036101 (2015).

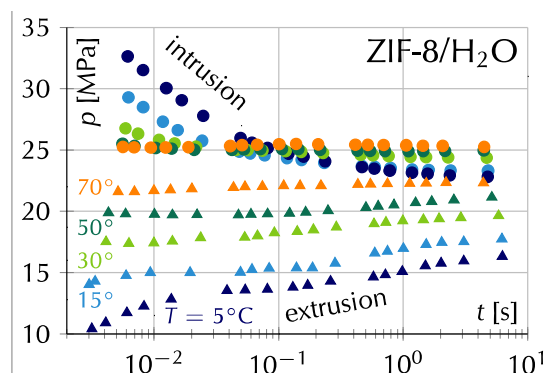


Figure 1 : Evolution of intrusion/extrusion pressures over the time at which pressure is applied for the ZIF-8/water lyophobic system at various temperatures.

Non-monotonous temperature dependence of spin-charge conversion at NiFe/X interfaces

O. Gladii,^{a*} L. Frangou,^a P. Noël,^a G. Forestier,^a R. L. Seeger,^a S. Auffret,^a S. Gambarelli,^b L. Vila,^a and V. Baltz^a

a. SPINTEC, Univ. Grenoble Alpes / CNRS / INAC-CEA / GINP, F-38000 Grenoble, France
b. SYMMES, Univ. Grenoble Alpes / INAC-CEA, F-38000 Grenoble, France

* olga.gladii@cea.fr

The spin-charge conversion has attracted considerable attention, facilitating advances in fundamental physics and closely related applications in the field of spintronics. The conversion arises from the spin-orbit interaction, which couples the spin and the orbital angular momentum of an electron. Several microscopic mechanisms such as the spin Hall effect [1], the Rashba-Edelstein effect [2] and their respective reciprocal counterparts can be responsible for such a conversion. The prevailing mechanism can sometimes be unclear. Recent results demonstrating 'self-induced' charge current generation in a 'single' NiFe ferromagnetic film at resonance added to this ongoing debate by putting into question the origin of the spin- to charge-current conversion [3]. In this work, we conducted temperature dependent experiments of spin-charge conversion in NiFe-based stacks where only the NiFe environment was varied, aiming at unravelling the mechanisms involved. In practice, out-of-equilibrium magnetization dynamics of the NiFe layer was driven by ferromagnetic resonance, which generated the spin-current. The subsequent spin-charge conversion was characterized via transverse dc voltage measurement. In some typical /SiO₂/NiFe/Cu/IrMn/ stacks, a first contribution to the transverse voltage is ascribed to the inverse spin Hall effect taking place in the IrMn antiferromagnet, consistent with the expected IrMn-thickness-dependence at room temperature [4,5]. An additional non-monotonous temperature dependence of transverse dc voltage, for which the position of the maximum remains independent on the NiFe and IrMn thicknesses overshadowed the effects expected from spin fluctuations while crossing the Néel temperature of the antiferromagnet [5,6]. It may also be ascribed to the spin-charge conversion at the oxide/NiFe interface. To get more insight about this, a further systematic study was conducted, where NiFe was encapsulated by several oxides. We will present how the various temperature dependence can be consistently ascribed to the oxide/NiFe interfaces into consideration.

[1] A. Soumyanarayanan et al, Emergent phenomena induced by spin-orbit coupling at surfaces and interfaces, *Nature* **539**, 509 (2016)

[2] J. Sinova et al, Spin Hall effect, *Rev. Mod. Phys.* **87**, 1213 (2015)

[3] A. Tsukahara et al, Self-induced inverse spin Hall effect in permalloy at room temperature, *Phys. Rev. B* **89**, 235317 (2014)

[4] W.M. Zhang et al, Spin Hall effects in antiferromagnets, *Phys. Rev. Lett.* **113**, 196602 (2014)

[5] V. Baltz et al, Antiferromagnetic spintronics, *Rev. Mod. Phys.* **90**, 015005 (2018)

[6] L. Frangou et al, Enhanced spin pumping efficiency in antiferromagnetic IrMn thin films around the magnetic phase transition," *Phys. Rev. Lett.* **116**, 077203 (2016)

Towards two-dimensional molecular crystals

A.C. Gómez Herrero^{1*}, M. Feron ², N. Bendiab¹, V. Reita¹, J. Coraux¹, F. Chérioux²

¹CNRS, Institute NEEL, F-38042 Grenoble, France

²CNRS, Univ. Bourgogne Franche-Comté, Institut FEMTO-ST, F25030 Besançon, France

*ana-cristina.gomez-herrero@neel.cnrs.fr

Novel classical and quantum phases have been discovered in inorganic crystals in the past years. The emergence of topological insulators (TIs) [1,2], which are materials characterized by the presence of conducting states in their edges and an insulating behavior in their bulk, is a striking illustration with potential applications in the fields of spintronics, micro-electronics and thermoelectricity.

The long-term goal of this work is to detect collective electronic states hosted in a crystalline organic material, in the form of a two dimensional molecular crystal. Polymerization of molecular units can yield low-cost crystalline materials with the additional advantage of properties engineering thanks to molecular unit design. Some covalently-bond polymers are in fact expected to host delocalised electronic states, possibly conducting or semiconducting throughout the whole material or its edges. In fact, the addition of metallic centers in such networks is besides predicted to bring significant spin-orbit coupling to the material, producing under the right circumstances a splitting, at Fermi level, of electronic bands that otherwise would be degenerate — this is the essence of bulk semiconducting properties evolving to dissipationless conductive states at the edges of the material.

A novel 2D polymerization method in solution has recently been discovered by some of us, which yields soluble organometallic 2D polymers [3]. The polymers growth takes places at the interface formed between two liquid phases, one organic and the other aqueous, each of them hosting specifically one of the two polymer precursors. After interfacial reaction of the precursors, the polymer is transferred to a substrate (highly oriented pyrolytic graphite or a thin silica layer on a Si substrate) by the Langmuir-Schäefer method, in the form of an ultra-thin layer. In this contribution we will present the physical-chemistry and physics characterization of this polymer based on optical microscopy, Raman spectroscopy and scanning electron microscopy.

[1] C L Kane, E J Mele. Quantum spin Hall effect in graphene. Phys. Rev. Lett. vol.95, p. 226801 (2005)

[2] M König, S Wiedmann, C Brune, A Roth, H Buhmann, L W Molenkamp, X-L Qi, S-C Zhang. Quantum spin Hall insulator state in HgTe quantum wells. Science vol.318, p.766 (2007)

[3] J. Coraux, W. Hourani, V. L. Meller, S. Lamare, D. A. Kamaruddin, L. Magaud, N. Bendiab, M. Den Hertog, O. Leynaud, F. Palmino, R. Salut, and F. Chérioux. Soluble Two-Dimensional Covalent Organometallic Polymers by (Arene)Ruthenium-Sulfur Chemistry. Chem. Eur. J. 23, 10969 – 10973 (2017)

Growth of Bi_2Se_3 on Ge (111): from 2D transport evidence to room temperature spin-to-charge conversion

T. Guillet¹, C. Zucchetti², F. Bottegoni², C. Beigné¹, C. Vergnaud¹, M.-T. Dau¹, A. Marty¹ and M. Jamet¹

¹SPINTEC, Univ. Grenoble Alpes/CEA/CNRS, F38000 Grenoble, France

²LNESS-Dipartimento di Fisica, Politecnico di Milano, 20133 Milano, Italy

E-mail: Thomas.guillet@cea.fr

Topological insulators (TI) have gained much interest in the field of spintronics for the generation and the detection of pure spin currents. Indeed, three-dimensional TI are predicted to host exotic properties like topologically protected surface states (TSS), which show Dirac-like band dispersion and strong spin-momentum locking [1]. Although the transport in TIs grown on insulator has been widely studied, TI films grown on semiconducting substrate are still challenging because of the parallel conduction canal.

In this work, we report the growth of single crystalline Bi_2Se_3 thin film on slightly p-doped Ge (111) by molecular beam epitaxy. Germanium is an optically active material with a relatively long spin diffusion length ($l_{sf} \approx 10 \mu\text{m}$) and it is compatible with the current Si technology platform. We carried out low temperature and high field magnetotransport measurements on micro-fabricated Hall bars, our results highlight a 2D transport in TSS through the weak-antilocalisation (WAL) signature (Fig. 1a). We propose an innovative method to probe the spin-to-charge conversion of Tis by taking advantages of Ge optical properties. We designed microdevices (Fig. 1b) where pure spin currents with in-plane spin polarization are generated by optical spin orientation by scanning a laser beam at the edge of Pt bar [2,3]. Spin currents are then detected in a non-local geometry by the inverse Rashba-Edelstein effect in a Bi_2Se_3 bar at room temperature. These results open a new way of investigating the spin properties of topological insulators.

[1] M. Z. Hasan and C. L. Kane, Rev. Mod. Phys. **82**, 3045 (2010)

[2] C. Zucchetti and *al*, Phys. Rev. B **96**, 014403 (2017)

[3] F. Bottegoni and *al*, Nature Materials volume **13**, pages 790–795 (2014)

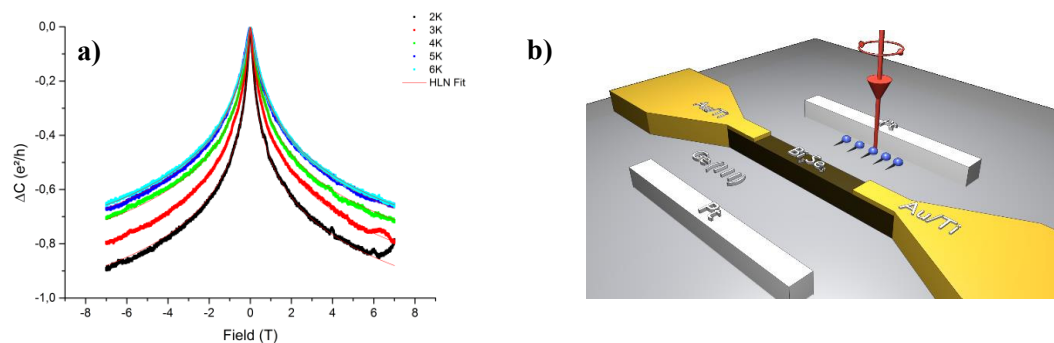


Fig 1. a) 4-probe longitudinal magnetoconductance of 10 QL Bi_2Se_3 film showing WAL effect (out-of-plane geometry). b) Scheme of the microdevice used for optical spin orientation.

Development of the Doping of ZnO Nanowires Using Metal (III) Elements in Aqueous Solution

P. Gaffuri^{a,b}, E. Appert^a, C. Verrier^{a,c}, O. Chaix-Pluchery^a, L. Rapenne^a, E. Sarigiannidou^a, Q. Rafhay^c, A. Kaminski-Cachopo^c, A. Ibanez^b, M. Salaün^b, and V. Consonni^a

a. Univ. Grenoble Alpes, CNRS, Grenoble INP, LMGP, F-38000 Grenoble, France.

b. Univ. Grenoble Alpes, CNRS, Institut Néel, F-38000 Grenoble, France.

c. Univ. Grenoble Alpes, CNRS, Grenoble INP, IMEP-LAHC, F-38000 Grenoble, France.

* pierre.gaffuri@grenoble-inp.fr

ZnO nanowires (NWs) have recently been used for a wide variety of devices, including gas sensors, piezoelectric nanogenerators, UV photodetectors, solar cells and UV LED. For those applications, extrinsic doping should be controlled thoroughly. Intrinsically n-type ZnO can intentionally be n-doped, for example by incorporating metal (III) elements. The doping of ZnO NWs has however been mainly performed by vapour phase deposition techniques and is still a major issue by solution deposition techniques. In the present work, ZnO NWs are doped with different dopants including Aluminium and Gallium by using the low-cost, low-temperature, and easily implemented chemical bath deposition technique. Metal nitrate is basically added in various concentrations to the standard precursors [1] in deionized water. This addition completely modifies both morphology and crystal structure of ZnO NWs, as shown by electron microscopy [2]. The formation mechanisms are thoroughly investigated and supported by thermodynamic simulations yielding theoretical solubility plots and speciation diagrams. Their dependence on the pH of the solution through the addition of ammonia is further studied thoroughly [3]. The incorporation of metal dopants is eventually investigated by energy dispersive x-ray spectroscopy using scanning transmission electron microscopy. Furthermore, temperature-dependent Raman spectroscopy shows the occurrence of characteristic additional modes, revealing the thermally activated doping of ZnO NWs from an annealing temperature of 200 °C [2]. These findings show a simple, thorough way to control the doping of ZnO NWs, which opens the way for their more efficient integration into nanoscale devices.

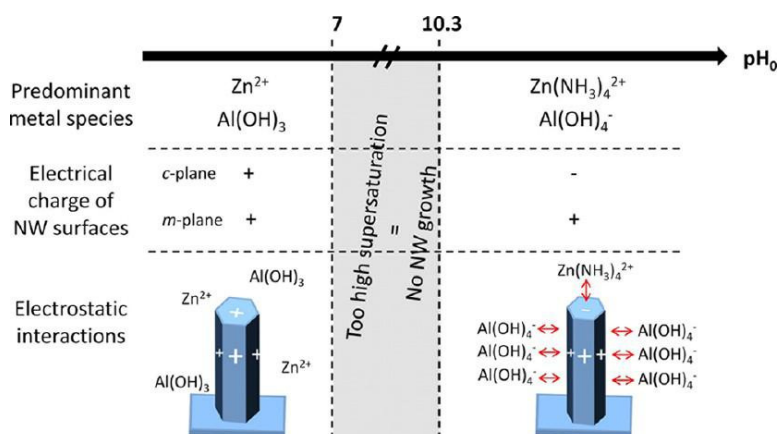


Figure 1. Schematic diagram showing the effects of the pH₀ of the solution on the formation mechanisms of ZnO NWs, mainly through the nature of the predominant Zn(II) and Al(III) species as well as the surface electrical charge of the polar c-plane and nonpolar m-plane. [3]

[1] R. Parize et al., The Journal of Physical Chemistry C 120, 5242 (2016)

[2] C. Verrier et al., The Journal of Physical Chemistry C 121, 3573 (2017)

[3] C. Verrier et al., Inorganic Chemistry 56, 3573 (2017)

New generation of lanthanides-free phosphors for white LEDs lighting prepared by the polymeric precursor method

P. Gaffuri^{1,2}, M. Salaün^{1*}, I. Gautier-Luneau¹,
E. Appert², V. Consonni², A. Ibanez¹

¹ Univ. Grenoble Alpes, CNRS, Institut Néel, F-38000 Grenoble, France.

² Univ. Grenoble Alpes, CNRS, Grenoble INP, LMGP, F-38000 Grenoble, France.

* mathieu.salaun@neel.cnrs.fr

Solid-state lighting (SSL) using light emitting diodes (LEDs) is recognized as a major disruptive technology expected to dominate the public lighting market in the near future. The main advantages of SSL sources are the energy saving (50 % compared to typical lighting devices), their potential stability to produce long lifetime devices, and the possibility they offer to develop smart lighting devices. At Néel Institute, we develop [1,2] a new type of phosphors based on metal aluminum borate powders without any lanthanide as doping. These innovating phosphors can produce broad emission bands extended in the whole visible range from emitting centers (structural defects) trapped in stable glassy grains of a few microns in diameters. Thus, from only one phosphor excited with a near-UV LED chip (UV (365- 390 nm), we can generate intense warm white light: internal quantum yields around 80-90% and very high color rendering indexes (CRI = 92-94) have been obtained. A low-cost near-UV LED is further developed at LMGP, based on the heterojunction of an array of n-type ZnO nanowires on p-type GaN. Eventually, the coupling of the two components as a **new generation of eco-efficient white LEDs** will be optimized and integrated in one Solid State Device.

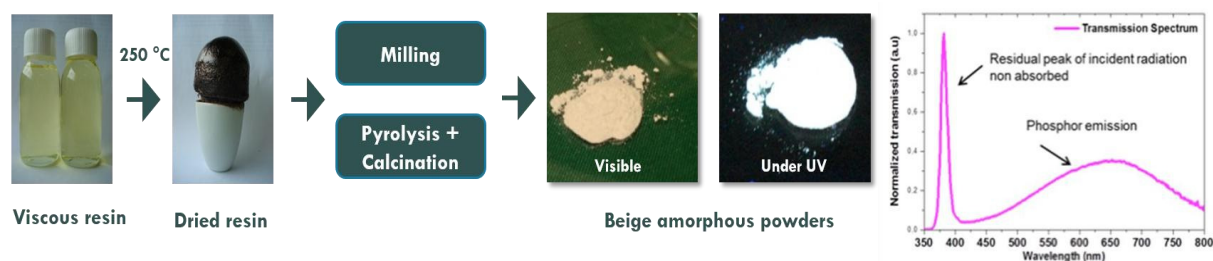


Figure 1. The step process: resin, after drying at 250°C, pyrolysed black powder and luminescent powder after a final calcination. Broad PL emission of the phosphor from 450 to 800 nm and residual near UV incident radiation of the LED chip (365 nm).

The main objective of this study is to optimize the chemical compositions, synthesis procedures, and thermal treatment conditions for these micrometric powders to enhance their luminescence properties. This is favoured by the great versatility of wet chemistry process, such as polymeric precursor methods. Complementary spectroscopic studies (EPR, NMR, FTIR, PL) and structural methods (X-ray Diffraction, Pair Distribution Functions (PDF), NMR, coupled with thermal analyses (DSC, DTA) - Thermogravimetry (TG) - Mass Spectrometry (MS)) are used to specify the chemical nature and structural environment of emitting centers.

- [1] V.F. Guimarães, L.J.Q. Maia, I. Gautier-Luneau, C. Bouchard, A.C. Hernandez, F. Thomas, A. Ferrier, B. Viana, A. Ibanez, *J. Mater. Chem. C*, 3, 5795 (2015).
- [2] V.F. Guimaraes, M. Salaün, P. Burner, L.J.Q. Maia, A. Ferrier, B. Viana, I. Gautier-luneau, A. Ibanez, *Solid State Sci.* 65, 6 (2017).

Application of wetting concepts to confined crystal growth and dissolution

Luca Gagliardi^a and Olivier Pierre-Louis^b

CNRS, ILM Institut Lumière Matière, Université Claude Bernard Lyon 1 Campus LyonTech-La Doua Batiment Brillouin, 10 rue Ada Byron F-69622 Villeurbanne, France

a. luca.gagliardi@univ-lyon1.fr b. olivier.pierre-louis@univ-lyon1.fr

Crystal growth or dissolution in confinement is characterized by a thin liquid solution film separating the crystal surface from the confining substrate allowing transport of solid units.

We describe the non-equilibrium dynamics within the contact region using a continuum thin film equation. Our model contains many instances typical of nanoscale wetting such as surface tension, hydrodynamics, capillary forces and disjoining pressure (crystal interface-substrate interaction). In addition physical ingredients specific to crystal growth such as attachment-detachment kinetics, bulk diffusion and the presence of an external load are considered to obtain self-consistently in the lubrication limit an evolution equation for the crystal interface.

Based on this model, we study dissolution under a macroscopic load and growth under an applied supersaturation [1]. During dissolution the functional form of the disjoining pressure appears to strongly influence the dynamics. A divergent repulsion leads to a flat contact and to a dissolution rate which increases indefinitely with the applied load. In contrast, a finite repulsion such as that induced by electrostatic interactions, implies a sharp pointy contact shape, and a dissolution rate independent from the applied load. In confined growth we show the generic formation of a single cavity in the contact region, which ultimately leads to the formation of a rim [2]. The results are supported by experiments on NaClO_3 . This transition appears to be supercritical or subcritical, depending on the functional form of the disjoining pressure and can be hindered by viscosity effects [3]. Finally the model allows to address the problem of the stress generated by a crystal growing in a pore under the effect of a supersaturated environment (crystallization force). We show that we are able to extend our understanding beyond the well known equilibrium thermodynamic description.

- [1] L. Gagliardi and Olivier Pierre-Louis. Thin film modeling of crystal dissolution and growth in confinement. *Physical Review E*, 97(1):012802, jan 2018
- [2] Felix Kohler, Luca Gagliardi, Olivier Pierre-Louis, and Dag Kristian Dysthe. Cavity formation in confined growing crystals. *Submitted, arXiv:1802.00310*, feb 2018.
- [3] L. Gagliardi and Olivier Pierre-Louis. Crystal growth in nano-confinement: Subcritical cavity formation and viscosity effects. *Submitted, arXiv:1803.06269*, mar 2018

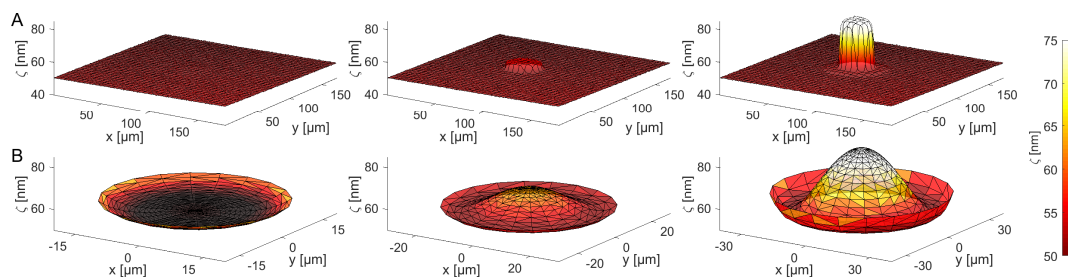


Figure 1: Cavity formation on the confined surface of a NaClO_3 crystal. **A.** Experimental data. **B.** Simulation results in an axisymmetric contact.

Ionosphere: A key plasma layer in planetary atmospheres

Marina Galand^{a*}

a. Department of Physics, Imperial College London, London, SW7 2AZ, UK.

* m.galand@imperial.ac.uk << Marina Galand >>

All planets and moons, which hold an atmosphere, have it partially ionised under solar illumination and bombardment of energetic particles from the space environment. This forms a conducting layer of plasma, the so-called “ionosphere”. It plays a crucial role in terms of space weather at Earth, atmospheric heating at the giant planets, and astrobiology at Titan, the largest moon of Saturn, to cite a few examples. It is also present in the coma, an envelope of gas which develops around a comet when the dusty, icy nucleus is close enough to the Sun to have its surface sublimating. There the ionosphere plays a critical role in the interaction of comets with the interplanetary medium among others.

Over the past decades I have developed comprehensive kinetic and fluid models in order to describe how solar and particle sources deposit their energy in planetary atmospheres and how an ionosphere is formed. This modelling work has been carried out in close interaction with instrument teams from space missions, such as Cassini probing the atmospheres of Saturn and Titan, and Rosetta scrutinising the coma of comet 67P/Churyumov-Gerasimenko. For instance, I have developed original analyses by organising multi-instrument data sets with a physics-based model in order to enhance the science return from space observations.

I propose to first focus on the energy deposition of solar ionising radiation, which extends from soft X-rays to Extreme Ultra-Violet (EUV). I will underline how this solar radiation ionises the upper atmosphere of Titan and initiates a complex, organic factory all the way to its surface. Secondly, I will contrast planetary ionospheres surrounding massive bodies with cometary ionospheres which escape the low-gravity field of the parent nucleus. Thirdly, I will highlight the relevance of auroral emissions, which have not only been fascinating human beings at Earth for centuries, but have also been playing a critical role in space weather. Auroral emissions have been observed throughout the Solar System and have revealed ionospheric species and plasma interactions. Finally, I will conclude by drawing special attention to the relevance of cross-body comparative analysis in order to gain deeper insight into ionospheres encountered in the Solar System and beyond.

Impact of electron-phonon scattering on optical and electrical properties of bulk semiconductor materials

Benoit Galvani^a, benoit.galvani@im2np.fr, Amaury Delamarre^{b,c}, Daniel Suchet^{b,d}, Marc Bescond^e, Fabienne Michelini^a, Michel Lannoo^a, Masakazu Sugiyama^{b,c}, Jean-François Guillemoles^{b,f}, Nicolas Cavassilas^{a,b}

- a. Aix-Marseille Université, CNRS, Université de Toulon, IM2NP UMR 7334, Marseille, France
- b. NextPV, LIA, CNRS-RCAST/U. Tokyo-U. Bordeaux, Tokyo 153-8904, Japan
- c. RCAST, The University of Tokyo, Tokyo 153-8904, Japan
- d. LPICM UMR 7647, Palaiseau, France
- e. LIMMS, CNRS-IIS, UMI 2820, University of Tokyo, 153-8505, Tokyo, Japan
- f. IPVF, Palaiseau, France

We present a numerical study of the impact of electron-phonon scattering (EPS) on the electronic density of states (DOS) of bulk semiconductor materials (GaAs and CH₃NH₃PbI₃). In order to calculate the DOS in a perturbed system, we use a model based on Green functions formalism [1]. We achieved to determine the DOS decreasing behavior in the bandgap. This behavior depends on the strength of the EPS (Fig. 1.a), but also depends on the phonon energy. Electron-phonon interactions have a straightforward impact on material optical properties. Indeed, the presence of electronic states within the bandgap allows absorption and emission of photons with an energy lower than this material bandgap. As shown in Fig. 1.b, the emission spectrum can be widely disturbed by this interactions. For purposes of photovoltaic systems, in both GaAs and perovskite materials, we report a decrease in the absorption/emission ratio when the EPS strength increases, and therefore a efficiency reduction [2]. This degradation is all the more important as the carrier mobility is low.

[1] N.Cavassilas, F.Michelini, M.Bescond, « Modeling of Nanoscale Solar Cells : The Green's Function Formalism », *J.Renewable Sustainable Energy* 6, 011203 (2014)

[2] L.C.Hirst and N.J.Ekins-Daukes, *Progress in Photovoltaics. Research and Applications* 19,286 (2011)

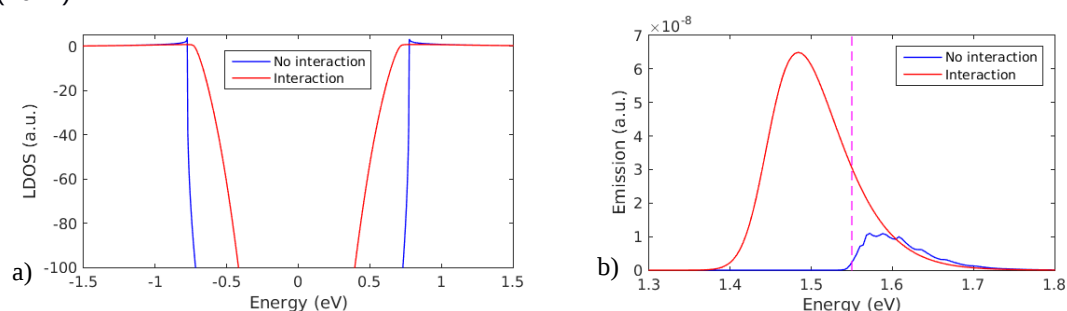


Figure 1 : a) Logarithm of the electronic density of states in CH₃NH₃PbI₃ with and without electron-phonon scattering. b) Emission spectrum of CH₃NH₃PbI₃ with and without interaction.

Gate-tunable quantum phase transition of the ground state of a magnetic impurity coupled to a superconductor

A. Garcia-Corral^{a*}, D. M. T van Zanten^a, S. Florens^a, D. M. Basko^b,
K. J. Franke^c, H. Courtois^a and C. B. Winkelmann^a

- a. Université Grenoble Alpes, CNRS, Institut Néel, 25 avenue des Martyrs, 38042 Grenoble, France
- b. Laboratoire de Physique et Modélisation des Milieux Condensés, Université Grenoble Alpes, CNRS, 25 avenue des Martyrs, 38042 Grenoble, France
- c. Institut für Experimentalphysik, Freie Universität Berlin, Arnimallee 14, 14195 Berlin, Germany

* alvaro.garcia-corral@neel.cnrs.fr

A quantum dot coupled to a superconducting surface may act as a tunable magnetic impurity, controlled by an external gate potential. The competition of magnetism and superconductivity can give rise to sub-gap excitations at the superconductor surface (Yu-Shiba-Rusinov bound states) [1]. Further, if the tunnel coupling to one of the leads is strong enough, quantum correlation effects can lead to a Kondo resonance, corresponding to a magnetic moment screened by the conduction electrons. By tuning the gate, we modulate the Kondo temperature T_K in the normal state, and consequently the energy of the sub-gap bound states $E_{B\pm}$. When the bound state energy goes to zero, a quantum phase transition of the system between a screened and unscreened local spin state occurs. Our results demonstrate the universality of this transition taking place at $\Delta/T_K \approx 2.5$, confirming previous theoretical predictions [2].

[1] B. W. Heinrich, J. I. Pascual and K. J. Franke, Single magnetic adsorbates on s-wave superconductors, arXiv:1705.03672v2 (2017)

[2] M.-S. Choi et al, Kondo effect and Josephson current through a quantum dot between two superconductors, Phys. Rev. B **70**, 020502(R) (2004)

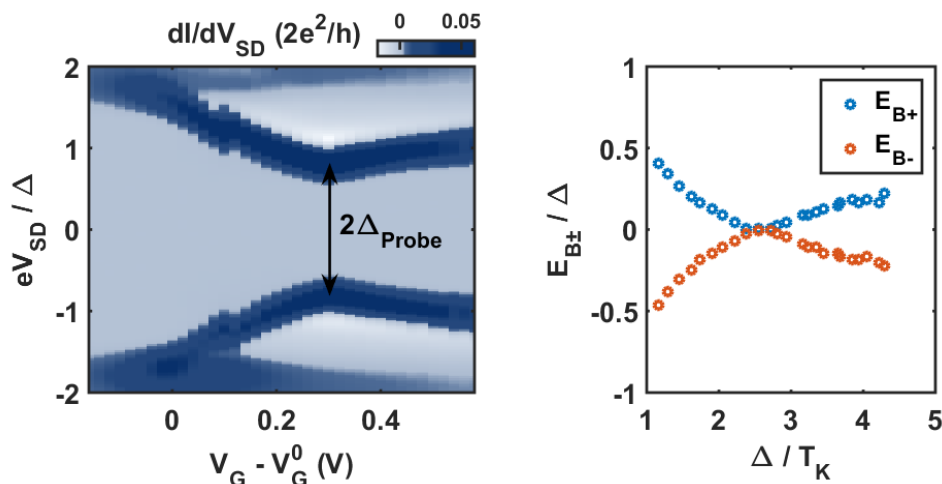


Figure 1: (a) Differential conductance mapping of the sub-gap states versus gate voltage. The system formed by a superconducting lead strongly coupled to the quantum dot is probed spectroscopically by a second, weaker coupled lead, also superconducting. (b) Extracted bounded states energy displaying the phase transition for $\Delta/T_K \approx 2.5$.

Atomic-scale magnetometry with a mobile molecular quantum sensor

Léo Garnier^{a,*}, Benjamin Verlhac,^a Nicolas Bachelier,^a Maider Ormaza,^a Paula Abufager,^b Nicolás Lorente,^{c,d} Markus Ternes^e, Marie-Laure Bocquet,^f et Laurent Limot^a

- a. Université de Strasbourg, CNRS, IPCMS, UMR 7504, F-67000 Strasbourg, France
- b. Instituto de Física de Rosario-CONICET-Universidad Nacional de Rosario, Rosario, Argentina
- c. Donostia International Physics Center (DIPC), 20018 Donostia-San Sebastián, Spain
- d. Centro de Física de Materiales (CFM), 20018 Donostia-San Sebastián, Spain
- e. Max Planck Institute for Solid State Research, Heisenbergstrasse 1, 70569 Stuttgart, Germany
- f. PASTEUR, Département de Chimie, Ecole Normale Supérieure, PSL Research University, Sorbonne Universités, UPMC Univ. Paris 06, CNRS, 75005 Paris, France

* leo.garnier@ipcms.unistra.fr, << Léo Garnier >>

Recent advances in scanning probe techniques rely on the chemical passivation of the probe-tip termination with single molecules weakly connected to the metallic apex. Valuable information, otherwise unaccessible with a metallic tip, can then be gathered, notably offering to image the skeletal structure and bonding of single molecules. The undeniable success of this approach opens the tantalizing prospect of introducing spin sensitivity through the probe-tip termination with a magnetic molecule. Here, we use a tip decorated by a single nickelocene molecule [1,2] and exploit it as a spin-sensitive mobile sensor. Nickelocene behaves as a two-level spin system where the uniaxial magnetic anisotropy (noted D) separates the magnetic ground state $|S = 1, M = 0\rangle$ from the excited state $|S = 1, M = \pm 1\rangle$. This nickelocene-terminated tip, or Nc-tip, offers the unique possibility of producing electrically-driven spin excitations on the tip apex. We show that when the Nc-tip is within 150 pm from a magnetic object, its spin excited spectrum is modified by the presence of an exchange interaction. Magnetic information may be probed with lateral and vertical atomic-scale resolution. Virtually all systems may be addressed with this detection scheme, including ferromagnetic surfaces, as we exemplify for a single Fe atom on Cu(100) and for surface atoms within a cobalt island grown on Cu(111).

- [1] M. Ormaza *et al.*, Nat. Commun. **8**, 1974 (2017)
- [2] M. Ormaza *et al.*, Nano Lett. **17**, 1877 (2017)

Bonding mechanism of Phase Change Materials : the role a non-harmonic deformation potential.

Jean-Pierre Gaspard^{a,b,*}

a. Institut Laue-Langevin - 71 avenue des Martyrs CS 20156, F-38042 Grenoble, France

b. University of Liège, Physics Department, SPIN, B-4000 Sart-Tilman, Belgium

* jp.gaspard@uliege.be

Phase Change materials (PCM) are promising materials as non-volatile memories and are the subject of an intense field of research [1]. These materials switch between an amorphous semiconducting phase and a metallic crystalline phase with an optical and/or an electrical contrast that allows storing the binary information. The switching mechanism is still controversial and many models have been suggested (umbrella flipping, resonance bonding,...). The amorphous semiconducting phase shows a local (pseudo)-symmetry breaking (Peierls distortion) while the metallic phase is less distorted than the amorphous structure.

PCM are alloys of covalent elements of groups IV, V and VI, most of them are Te-based.

We study the energetics of the covalent alloys as a function of their number of electrons, repulsive potential and ionicity. Expanding the effective potential as a function of the order parameter η of the distortion, $V(\eta) = a\eta^2 + b\eta^4$, we show that the condition for having a PCM is $\alpha \approx 0$ i. e. the potential has a vanishing harmonic contribution in the η parameter [2]. This defines a domain in the parameters and chemical compositions where good candidates for PCM are expected.

In addition, the condition $\alpha \approx 0$ is related to some specific signature of the neutron scattering structure factor $S(q)$ [3].

[1] Wuttig, M. and Yamada, N. *Nature materials*, 6(11), 824 (2007)

[2] Gaspard, J-P., *C. R. Physique*, 17, 389 (2016)

[3] Steimer, C. *et al.* *Advanced Materials*, 20(23), 4535-4540 (2008)

Negative thermal expansion (NTE) of Tellurium-based liquids.

J.-P. Gaspard^{a,b*}, J.-Y. Raty^a, F. Hippert^c and G. Cuello^b

- a. University of Liège, Physics department, SPIN, B-4000 Sart-Tilman, Belgium
 b. Institut Laue-Langevin, 71 avenue des Martyrs CS 20156, F-38042 Grenoble, France
 c. LNCMI-CNRS, 25, rue des Martyrs, B.P. 166, F-38042 Grenoble Cedex 9, France

* jp.gaspard@uliege.be

Most materials expands when heating with few exceptions among which the Tellurium-based liquids. Group VI elements have a low coordination number Z in the crystal ($Z=2$ for Te and Se) because of a spontaneous symmetry breaking mechanism (Peierls distortion leading to the octet rule) related to their number of p electrons [1]. We have shown that this symmetry breaking may still be present in the liquid at least at the lowest temperatures. When the liquid is heated, its volume shrinks in some temperature domain and simultaneously the coordination number increases. This is the case of $\text{Se}_x\text{Te}_{1-x}$ alloys. A combined analysis by diffuse neutron scattering on D4c (Fig. 1) and inelastic neutron scattering on IN6 at ILL have shown both an increase of the coordination numbers and a symmetrization of the first neighbours shell around atoms when the temperature rises. INS shows a clear change of the vibrational density of state along the NTE consisting in a red-shift of the highest frequencies with temperature. We conjecture that this behaviour should be common to all covalent systems. In addition, this shed some light on the mechanism of Phase Change materials.

- [1] Gaspard, J. P., Pellegatti, A., Marinelli, F., and Bichara, C. *Phil. Mag. B*, 77(3), 727-744 (1998)
 [2] Otjacques C., Gaspard J.-P., Raty J.-Y., Bichara C., Coulet M.-V., Schober H. and Johnson M., *Phys. Rev. Lett.* 103, 245901 (2009)

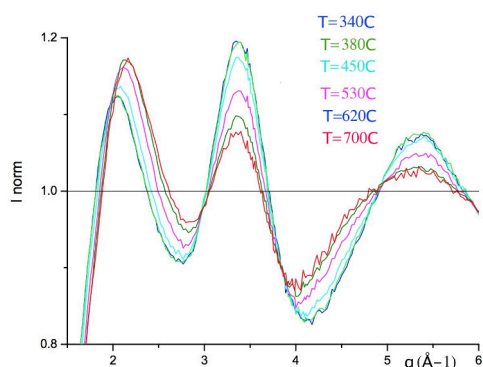


Figure 1: Structure factor of liquid $\text{Se}_{30}\text{Te}_{70}$ at different temperatures.

Magnetic properties of FeRh nanostructures

C. Gatel^{a*}, B. Warot-Fonrose^a, M. Liu^{a,b}, P. Benzo^a, H. Tang^a, M. Castiella^a, N. Tarrat^a, M. Respaud^c, J. Morillo^a and M. J. Casanove^a

^a CEMES, CNRS UPR 8011 and Université de Toulouse - Toulouse, France

^b Research Center of Laser Fusion, CAEP- Mianyang 621900, China

^c LPCNO, Université de Toulouse, INSA, UPS, CNRS - Toulouse, France

*gatel@cemes.fr

The control of a magnetic state by thermal or electrical activation is essential for the development of new magnetic devices, for instance in heat or electrically-assisted magnetic recording or room-temperature memory resistor [1-3]. FeRh is expected for such applications: it presents an unusual magnetic transition from a low temperature antiferromagnetic state to a high temperature ferromagnetic state close to 370K accompanied by a 1% volume expansion [4-5]. The transition is obtained for a narrow composition range $0.48 < x < 0.56$ in the B2-ordered α' crystal phase of $\text{Fe}_{1-x}\text{Rh}_x$.

While the FM-AFM transition is sharp in the bulk alloy, the persistence of a FM component at low temperature in FeRh thin films raised important questions about the effect of size reduction, interfaces and surface termination on their magnetic properties. In addition, the mechanisms involved in the transition are still under debate as they were mainly studied with surface investigation techniques without visualization of the magnetic reorganization in volume. We have combined advanced TEM investigations and first-principle calculations on FeRh nanoparticles and thin films for a deeper understanding of the properties of this alloy.

Using aberration-corrected (scanning) transmission electron microscopy, magnetometry experiments and theoretical calculations, we will show that the surface configuration can stabilize a low temperature ferromagnetic (FM) state in FeRh nanoparticles in the 6–10 nm range [7] synthesized by magnetron sputtering. In addition, *in situ* electron holography performed on epitaxial FeRh thin film in a cross-sectional view demonstrates the effects of discontinuities and defects on the magnetic transition at the nanometer scale [8]. An unexpected transition mechanism with first the appearance of a periodic spacing of nucleated ferromagnetic domains followed by a spatial extension during transition monitoring has been evidenced.

[1] J.-U. Thiele *et al.*, Appl. Phys. Lett. **82**, 2859 (2003)

[2] R.O. Cherifi *et al.*, Nat. Mater. **13**, 345 (2014)

[3] X. Marti *et al.*, Nat. Mater. **13**, 367 (2014)

[4] M. Fallot, M. Ann. Phys. **10**, 291–332 (1938)

[5] M. R. Ibarra *et al.*, Phys. Rev. B **50**, 4196–4199 (1994)

[6] M. Liu *et al.* EPL **116**, 27006 (2016)

[7] C. Gatel *et al.*, Nature Communications **8**, 15703 (2017)

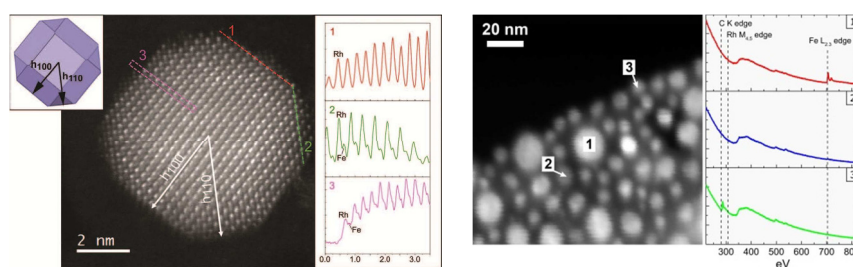


Figure 1: (left) HAADF-STEM image of a NP observed along the [001] direction of B2-FeRh. (right) EELS analyses of particles deposited by co-sputtering of Fe ad Rh targets).

From the "Ouzo effect" to Nanocapsules

Fabienne GAUFFRE^{a*}, Soizic CHEVANCE^a, Flavien SCIORTINO^a, Clément GOUBAULT^a, Myrtil KAHN^b and Marie-Bérengère TROADEC^c

- a. Univ Rennes, CNRS, ISCR (Institut des Sciences Chimiques de Rennes)-UMR6226, F-35000 Rennes
 - b. Laboratoire de Chimie de Coordination UPR8241, CNRS, 205 rte de Narbonne, Toulouse Cedex 04
 - c. Univ Rennes, CNRS, IGDR (Institut des Sciences Chimiques de Rennes)-UMR6226, F-35000 Rennes
 - d.
- * fabienne.gauffre@univ-rennes1.fr

Abstract: We report on a new method to generate hollow capsules with a hybrid shell made of nanoparticles and polymers, which were coined "hybridosomes". (Fig 1)[1]. The process is based on the formation of droplets in macroscopically miscible mixtures of organic solvent and water containing an hydrophobic solute, the so-called "ouzo effect". Our hypothesis is that nanoparticles stabilize such submicronic droplets by adsorbing at the liquid/liquid interface, similarly to Pickering emulsions. After addition of a crosslinking polymer and removal of the solvent core, hollow capsules of diameter ~100 nm are obtained. Nanocapsules were prepared from Quantum Dots, gold nanoparticles, superparamagnetic iron oxide nanoparticles and mixtures of different types of particles. The mechanical properties of the capsules were investigated using at the single hybridosome level via AFM nanoindentation as well as at the ensemble level using an osmotic pressure technique [2]. The entrapment of a fluorescent dye was also demonstrated. Thus, nanocapsules with dual properties (e.g. magnetic and fluorescent) are easily obtained. Interestingly, the magnetic/fluorescent nanocapsules enable Magnetic Resonance Imaging contrast enhancement of tumors *in vivo* and fluorescence imaging [1,2].

[1] F. Sciortino; G. Casterou; PA Eliat; MB Troadec; C; Gaillard; S. Chevance; M. L Kahn; F. Gauffre, Simple Engineering of Polymer-Nanoparticle Hybrid Nanocapsules ChemNanoMat 10.1002/cnma.201600155 (2016)

[2] F. Sciortino, M. Thivolle, M. Kahn, C. Gaillard, S. Chevance, F. Gauffre, Structure and Elasticity of Composite Nanoparticle/Polymer Nanoshells (hybridosome®), Soft Matter, DOI: 10.1039/C7SM00705A (2017)

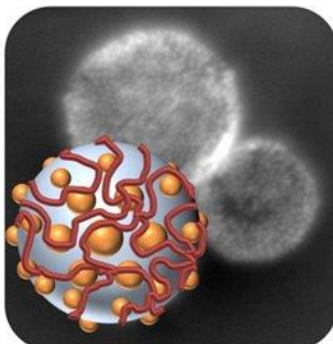


Figure 1 : Schematic representation of hybridosomes made from QD and poly(acrylic acid) and SEM image

Statistiques de courbure d'une fibre flexible dans un écoulement turbulent

Amélie Gay^{a*}, Benjamin Favier,^a et Gautier Verhille^a

a. Aix-Marseille Univ., CNRS, Centrale Marseille, IRPHE, Marseille, France

* amelie.gay@irphe.univ-mrs.fr

Dans une des premières études fondamentales d'une fibre flexible dans un écoulement turbulent, il a été suggéré que la fibre se comportait comme un polymère dans un solvant idéal soumis à l'agitation thermique [1]. Plus récemment, nous avons montré l'importance du rôle des corrélations spatiales et temporelles de l'écoulement sur les déformations moyennes de la fibre [2]. En effet, la transition flexible/rigide d'une fibre est gouvernée par le rapport entre la longueur de la fibre L et une longueur caractéristique l_e . Dans le cadre des polymères, cette longueur caractéristique appelée longueur de persistance est déterminée par un bilan d'énergie alors qu'en turbulence, elle est définie à partir d'un bilan de puissance [1]. De plus, les corrélations spatiales et temporelles de la turbulence sont aussi responsables d'une diminution de la courbure moyenne des fibres suffisamment longue par rapport à la longueur élastique [2].

Dans cette nouvelle étude, nous nous intéressons aux statistiques de courbure de fibres dans un écoulement turbulent, homogène et isotrope. Les données issues d'une simulation numérique indiquent que les corrélations modifient non seulement la moyenne de la courbure le long de la fibre mais aussi la forme des fonctions de distribution de probabilités de courbure. Les résultats obtenus sont comparés à un modèle de Langevin ce qui permet de comprendre l'évolution de la forme des distribution de courbure.

- [1] C. Brouzet, G. Verhille et P. Le Gal, Flexible fiber in a turbulent flow : A macroscopic polymer, *Phys.Rev. Lett.*, **112(7)**, 074501 (2014).
- [2] A. Gay, B. Favier et G. Verhille, Characterisation of flexible fibre deformations in turbulence, *Europhys. Lett.* (submitted).

High-resolution mapping of bifurcations in nonlinear biochemical circuits

Genot Anthony^{*a},

- a. LIMMS/CNRS-Institute of Industrial Science, The University of Tokyo, 4-6-3, Meguro, Tokyo, Japan
*genot@iis.u-tokyo.ac.jp

DNA has emerged in the past decades as a versatile and powerful polymer to build and program at the nanoscale. A rich library of devices has been built with DNA: origamis [1], biochemical neural networks [2], or reconfigurable plasmonic structures [3]. This DNA nanotechnology paves the route to societal applications such as smart therapeutics, autonomous chemical assembly lines or point-of-care diagnosis.

In LIMMS (CNRS/University of Tokyo), we recently developed a DNA-based toolbox to implement complex chemical dynamics, such as bistability or oscillations, with DNA and 3 enzymes [4]. But those nonlinear systems are extremely sensitive to their design parameters (concentrations of enzymes, DNA, temperature), which complicates design and characterisation. To tackle the resulting combinatorial explosion, we designed a droplet-based microfluidic platform to prepare tens of thousands of droplets with various combinations of parameters, allowing us to scan the parameter space efficiently [5].

Compared to conventional biochemical tools, the platform increased experimental throughput by 2 orders of magnitudes (from 100 to 10,000 data points/day) and reduced volumes by 5 orders of magnitudes (from 10 μ L to 100 pL per data point).

We used this unprecedented resolution to finely study the dynamics of a bistable switch and a DNA oscillator, revealing new insights about the biochemical mechanisms at play. Homing in on their bifurcations reveals the emergence of universal dynamics as well as stochastic behaviours – which may inform the study of biochemical systems *in vivo*.

[1] Rothmund, Nature 440.7082 (2006): 297-302.

[2] Qian et al., Nature 475.7356 (2011): 368-372.

[3] Kuzyk, Anton, et al., Nature materials 13.9 (2014): 862-866.

[4] Padirac et al., P.N.A.S. 109.47 (2012): E3212-E3220.

[5] Genot, A. J., et al., Nature Chemistry (2016).

X-ray Raman scattering as a novel probe to discriminate carbon-based compounds in ancient, art and fossil materials

Rafaella Georgiou^{a,b*}, Pierre Gueriau^a, Jean-Pascal Rueff^{b,c}, Uwe Bergmann^d, Nathan Daly^e, and Loïc Bertrand^{a,b}

- a. IPANEMA, CNRS, Ministère de la Culture, UVSQ, Université Paris-Saclay, BP 48 Saint-Aubin, 91192 Gif-sur-Yvette, France
- b. Synchrotron SOLEIL, BP 48 Saint-Aubin, 91192 Gif-sur-Yvette, France
- c. Sorbonne Universités, UPMC Université Paris 06, CNRS, UMR 7614, Laboratoire de Chimie Physique-Matière et Rayonnement, F-75005 Paris, France
- d. Stanford PULSE Institute, SLAC National Accelerator Laboratory, Menlo Park, California 94025, United States
- e. Getty Conservation Institute, 1200 Getty Center Drive, Los Angeles, CA 90049, United States

* rafaella.georgiou@synchrotron-soleil.fr

Deciphering the chemical nature of carbon-based compounds in ancient materials although challenging is an essential source of information in many archaeological and paleontological studies [1,2]. Carbon is ubiquitous and occurs in a diversity of chemical forms. However, difficulties in the characterization and identification of organic carbon compounds are common both due to specificities of the material (e.g., alteration during time, fine scale association with inorganic phases, turbostraticity) and to experimental constraints (high absorbance across the electromagnetic spectrum). X-ray Raman scattering (XRS) recently proved very promising to probe carbon speciation in complex heterogeneous solid ancient samples [3]. In this hard X-ray inelastic scattering technique, a small fraction of the X-ray energy is transferred to the electrons by inelastic scattering, allowing to collect speciation signal for light elements in a nondestructive manner, in air, with bulk sensitivity, to provide information not compromised by surface contamination, thus overcoming important constraints in the characterization of ancient materials [3].

The potential of XRS will be demonstrated through the analysis of carbon-based artists' pigments, which are until today poorly understood due to their complex chemistry [4]. We determined the carbon speciation of a consistent set of modern and historical samples used in the arts. As an example, the sensitivity of XRS is high enough to distinguish carbon black pigments obtained by the burning or pyrolysis of gas or oil from fine charcoal. We also collected XRS-based carbon K-edge XANES on fossil samples that allow discussing their fossilization. By providing information on the degree of aromaticity, the signatures of oxidized COO groups, the presence of carbon bound with heteroatoms and turbostraticity, XRS appears as a novel powerful and convenient probe to discriminate carbon-based compounds in complex, heterogeneous samples, and could be further applied to a wide range of ancient and historic materials.

[1] R. P. Evershed, *Archaeometry* 50.6 (2008): 895-924.

[2] D. Marguerie, Dominique, and J-Y. Hunot., *Journal of archaeological science* 34.9 (2007): 1417-1433.

[3] P. Gueriau, J-P. Rueff, S. Bernard, J.A. Kaddissy, S Goler, C. J. Sahle, D. Sokaras, R. A. Wogelius, P. L. Manning, U. Bergmann, L. Bertrand, *Analytical chemistry*, 89(20) (2017): 10819-10826.

[4] J. Winter, and E. W. FitzHugh, *Artists' pigments*, 4 (2007): 1-37.

Simulation of large scale open quantum systems for superconducting architectures

Serge Florens^{a*} et Nicolas Gheeraert^a

a. Institut Néel, CNRS/UGA, Grenoble, France

* serge.florens@neel.cnrs.fr

The increasing complexity of scalable quantum circuits, such as Josephson-based superconducting devices, asks for new theoretical ideas in order to simulate open many-body system under possibly non-equilibrium driving conditions. We present a simple yet powerful approach to this problem that relies on the superposition principle of trajectories in the phase space of the circuit elements [1]. This idea allows us to tackle reliably problems where brute force methods would require the exploration of an exponentially large Hilbert space. We illustrate this methodology by studying the challenging problem of particle production in the situation where photons scatter from a two-level system along a waveguide. We discover surprisingly that counter-rotating processes dominate the inelastic response due to the phase space associated to multiple photon creation [2].

[1] Nicolas Gheeraert, Xin H. H. Zhang, Soumya Bera, Nicolas Roch, Harold U. Baranger, and Serge Florens, "Particle Production in Ultra-Strong Coupling Waveguide QED ", preprint arXiv:1802.01665

[2] Nicolas Gheeraert, Soumya Bera, and Serge Florens, "Spontaneous emission of Schrödinger cats in a waveguide at ultrastrong coupling", New J. Phys. **19**, 023036 (2017)

PEN-DNA circuits: from particles programming to biosensing

Guillaume Gines^{a*}, André Estevez-Torres^b, Jean-Christophe Galas^b, Roberta Menezes^c, Kaori Nara^a, Valérie Taly^c, Anton S. Zadorin^d, Yannick Rondelez^a

- a. Laboratoire Gulliver, UMR-7083 ESPCI Paris/CNRS, 10 rue Vauquelin, 75005 Paris
- b. Laboratoire Jean Perrin, CNRS, UMR-8237 UPMC/CNRS, 4 place Jussieu, 75005 Paris
- c. UMR-S1147 Université Paris Descartes/INSERM, 45 rue des Saint-Pères, 75270 Paris
- d. Laboratoire de Biochimie, UMR-8231 ESPCI Paris/CNRS, 10 rue Vauquelin, 75005 Paris

* guillaume.gines@espci.fr

Molecular programming is a thriving discipline that deals with the design of artificial biomolecular circuits to perform information-processing tasks. These synthetic circuits can perform computations, store information, display dynamical behaviors, self-assemble into large supra-structures or act as biosensors. The predictable Watson and Crick base-pairing confers to DNA a unique programmability enabling the rational design of molecular circuits.

A few years ago, it has been developed a simple and versatile molecular programming language, named PEN-DNA toolbox (Polymerase Exonuclease Nickase-Dynamic Network Assembly) [1-2]. The topology of the networks is defined by a set of short synthetic DNA strands (templates) used as substrates by an enzymatic machinery to produce and degrade DNA strands. All of these reactions govern the dynamics and control the behavior of the system.

Here, we review the recent applications of these DNA circuits: we showed that we can trigger collective behaviors within microparticles populations encoded with DNA circuits [3]; these chemical reaction networks can be used to trigger the self-assembly of nano/microparticles; more recently, we conceived specific molecular programs dedicated to the ultrasensitive detection of biomolecules (manuscript under preparation).

- [1] K. Montagne, R. Plasson, Y. Sakai, T. Fujii, and Y. Rondelez, "Programming an in vitro DNA oscillator using a molecular networking strategy," *Mol. Syst. Biol.*, vol. 7, p. 466, Feb. 2011.
- [2] A. Baccouche, K. Montagne, A. Padirac, T. Fujii, and Y. Rondelez, "Dynamic DNA-toolbox reaction circuits: A walkthrough," *Methods*, vol. 67, no. 2, pp. 234–249, May 2014.
- [3] G. Gines, A. S. Zadorin, J.-C. Galas, T. Fujii, A. Estevez-Torres, and Y. Rondelez, "Microscopic agents programmed by DNA circuits," *Nat. Nanotechnol.*, vol. 12, no. 4, pp. 351–359, May 2017.

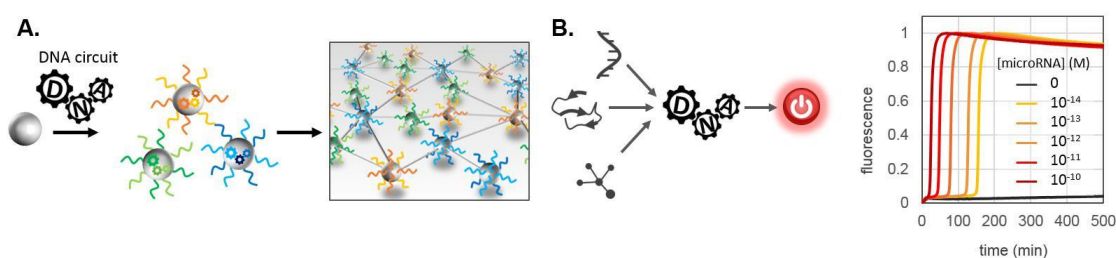


Figure: A. Microparticles programmed with DNA circuits exhibit collective behaviors. B. Specific molecular programs have been developed for the ultrasensitive detection of nucleic acids, protein or other analytes.

Wave dynamics and superfluidity of light in a hot atomic vapor

Quentin Glorieux^{a*}, Quentin Fontaine^a, Tom Bienaimé^a et Alberto Bramati^a

a. Laboratoire Kastler Brossel, Sorbonne Université, CNRS, ENS-Université PSL, Collège de France

* quentin.glorieux@lkb.ens.fr

A laser field propagating through a hot atomic vapor leads to a third-order nonlinear Kerr susceptibility. In the paraxial approximation the evolution of the transverse electric field is described by a 2D Gross-Pitaevskii equation. As such, this system is a promising platform to study phenomena related to Bose-Einstein condensation and superfluidity of light.

In this talk, we will report on the measurement of the dispersion relation of small amplitude density waves propagating on top of a photon fluid. We find a dispersion relation of Bogoliubov type: linear at small wave vector as expected in the superfluid regime and "particle-like" (quadratic) at larger wave vectors. In the superfluid regime, we characterize the dependence of the sound velocity with intensity (photon density) and compare our results with theoretical predictions.

When the perturbation on top of the photon fluid becomes large, it can propagate faster than the local speed of sound. This leads to the generation of dispersive shock waves. We will discuss and analyse the peculiar dynamics of these waves and confront our observations to analytical and numerical models.

Finally, we will discuss the potential application of this fluid of light to measure correlations that are analogous to spontaneous Hawking radiation.

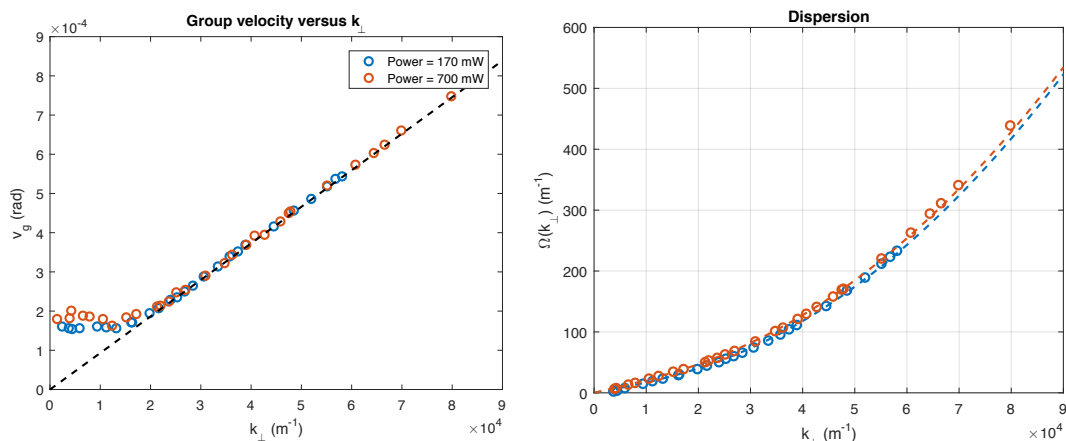


Figure : Left : group velocity as function of wavevector. Right : dispersion relation reconstructed from the group velocity measurement. Dashed lines are the best fit to the Bogoliubov dispersion relation.

STEM-EELS investigation of strain, oxygen octahedra rotation and charge distributions in perovskite oxide thin films

A. Gloter^{a*}, X. Li^a, G. Tieri^{a,b}, L. Bocher^a, V. Garcia^c, S. Fusil^c, A. Barthélémy^c, M. Bibes^c, J. Fowlie^b, D. Li^b, M. Gibert^b, S. Catalano^b, S. Gariglio^b, J.M. Triscone^b, O. Stéphan^a

- a. Laboratoire de Physique des Solides, CNRS UMR 8502, Université Paris-Sud, 91405 Orsay, France.
 - b. DQMP, Université de Genève, 24 Quai E.-Ansermet, 1211 Geneva, Switzerland.
 - c. Unité Mixte de Physique, CNRS, Thales, Univ. Paris-Sud, Université Paris-Saclay, Palaiseau, France.
- * alexandre.gloter@u-psud.fr

We will report recent scanning transmission electron microscopy (STEM) and electron energy loss spectroscopy (EELS) studies on perovskite oxide heterostructures, and at their interfaces. We will see how key parameters such as lattice, charge and orbital distribution can be investigated with a sub-nanometer spatial resolution. In a first example, we will present the case of LaAlO₃/SrTiO₃ interfaces [1] and discuss the strains, charges and orbital splitting at the vicinity of these interfaces for layers and bi-layers.

A second example concerns (La,Sr)MnO₃/SrTiO₃ bilayers (figure 1) and multilayers. A strong reconstruction of the oxygen octahedra rotation was observed for multilayers with small numbers of unit cells (<5 uc) [2]. We will discuss these structural reconstruction with respect to the magnetism of these films.

We will finally discuss new perspectives opened by the NION-CHROMATEM microscope (LPS@Orsay) for such oxides hetero-structures. Early 2018, an EELS energy resolution of 5 meV has been demonstrated, and angstrom resolved STEM images were obtained at room and at LN₂ temperature. We will discuss how such spectral-spatial unique combination could, for instance, give new insights for nickelate thin films studies and the understanding of their MIT properties.

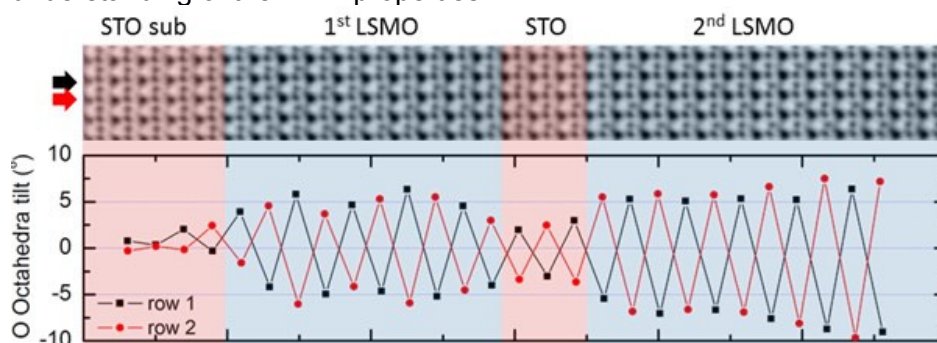


Figure 1 : STEM image in the annular bright field mode enabling a direct visualization of the oxygen columns and thus a possible quantification of the octahedra tilt in real space.

[1] D. Li, S. Gariglio, C. Cancellieri, A. Fête, D. Stornaiuolo and J.-M. Triscone, Fabricating superconducting interfaces between artificially grown LaAlO₃ and SrTiO₃ thin films, *APL Materials* **2**, 012102 (2014).

[2] X. Li, I. Lindfors-Vrejoiu, M. Ziese, A. Gloter, A. & P.A. van Aken, Impact of interfacial coupling of oxygen octahedra on ferromagnetic order in La_{0.7}Sr_{0.3}MnO₃/SrTiO₃ heterostructures. *Scientific Reports* **7**, 40068 (2017).

Single Large Nuclear Spin Coherent Manipulation

C. Godfrin^{a,b,*}, F. Balestro,^a W.Wernsdorfer^{a,c}

- a. Univ. Grenoble Alpes, CNRS, Grenoble INP, Institut Néel, 38000 Grenoble, France.
- b. Institut Quantique, Univ. de Sherbrooke, J1K 2R1 Sherbrooke, Canada.
- c. Institute of Nanotechnology, Karlsruhe Institute of Technology, 76344 Eggenstein-Leopoldshafen, Germany.

* Clement.Godfrin@usherbrooke.ca

Advances in experimental techniques offer physicists the opportunity to implement simple systems worth of the “gedanken-experiments” imagined by the founders of quantum theory. During the presentation, I propose to study one of these toy model systems, namely a single $3/2$ nuclear spin.

The presentation will start by investigating the read-out process and the coherent manipulation of the 4 nuclear spin states using a single molecular magnet transistor [1,2]. These preliminary results demonstrate that we have a fully controlled 4-level quantum system, a qudit, on which we recently implemented a quantum algorithm.

With their state space of large dimension, qudits open fascinating experimental prospects. Protocols based on a generalization of the Ramsey interferometry to a multi-level system enable to measure, among others, the accumulation of geometric phases and of quantum gate phase [3].

As an outlook, I will display how, using a larger single nuclear spin, we could apply quantum error correction protocol [4], to obtain a self-corrected qubit.

- 1 Thiele S. et al. Science 344, 1135 (2014)
- 2 Godfrin C. et al. Phys. Rev. Lett. 119, 187702 (2017)
- 3 Godfrin C. et al. submitted
- 4 Pirandola S. et al. Phys. Rev. A 77, 032309 (2008)

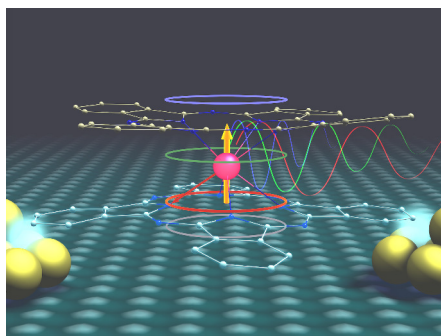


Figure 1: Artistic view of the TbPc₂ molecular spin transistor

Fermions de Dirac dans des semiconducteurs bi-dimensionnels

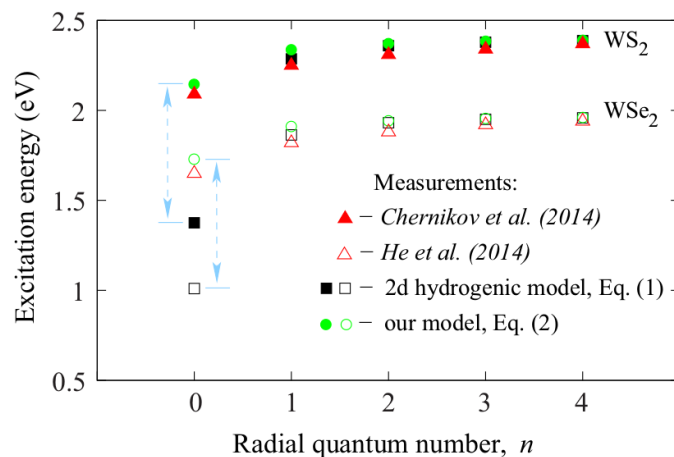
Mark O. Goerbig^{a*}

a. Laboratoire de Physique des Solides, CNRS UMR 8502, Bât. 510, Université Paris Sud, Université Paris Saclay, F-91405 Orsay cedex

* goerbig@lps.u-psud.fr

Dans la suite du graphène, une pléthore de matériaux bi-dimensionnels (2D) est désormais étudiée de manière intense, comme par exemple les dichalcogénures de matériaux de transitions (TMDC), le phosphore noir et le nitrure de bore, ainsi que divers empilement de ces matériaux. D'un point de vue théorique, ces matériaux partagent souvent avec le graphène le caractère « relativiste » de leurs électrons même si ces fermions de Dirac sont généralement massifs alors qu'ils sont sans masse dans le graphène. Je passerai en revue la différence entre les fermions de Schrödinger et de Dirac et leur pertinence dans la description des propriétés électroniques des semi-conducteurs 2D, notamment en présence d'un champ magnétique [1]. Cette différence se manifeste également dans les propriétés excitoniques, mises en évidence par exemple dans les TMDC, où le spectre excitonique ne peut être compris dans le cadre du modèle hydrogénique 2D. En effet, ce modèle et ses variantes prenant en compte des modifications du potentiel d'interaction entre l'électron et le trou constituant l'exciton ne prennent pas en compte le couplage entre les bandes de valence et de conduction. Ce couplage est à l'origine d'aspects topologiques intrigants, comme la courbure de Berry qui donne lieu à une correction de la vitesse des porteurs de charge ou encore un magnétisme orbital inhabituel. Plus spécifiquement, je montrerai comment ce couplage entre bandes fournit d'autres termes d'énergie et modifie, par conséquent, le spectre excitonique [2,3]. Celui-ci reflète ainsi un exemple de coexistence entre corrélations électroniques, qui sont à la base de la formation des excitons, et topologie sous forme de courbure de Berry due au couplage entre bandes.

Figure 1 : Spectres excitoniques dans WS₂ et WSe₂, comparaison entre mesures expérimentales (triangles) [4,5] et modèles théoriques. Le modèle hydrogénique sous-estime l'énergie excitonique pour de petites valeurs du nombre quantique radial, où des corrections dues à la courbure de Berry sont importantes. Reprise de [2].



- [1] M. O. Goerbig, G. Montambaux et F. Piéchon, EPL **105**, 57007 (2014).
 [2] M. Trushin, M. O. Goerbig et W. Belzig, Phys. Rev. B **94**, 041301(R) (2016).
 [3] M. Trushin, M. O. Goerbig et W. Belzig, Phys. Rev. Lett. **120**, 187401 (2018).
 [4] A. Chernikov *et al.*, Phys. Rev. Lett. **113**, 076802 (2014).
 [5] K. He *et al.*, Phys. Rev. Lett. **113**, 026803 (2014).

Diffusion and phase separation in silicate melts: physics problems inspired by glass industry

Emmanuelle Guillard^{a*}

a. Surface of Glass and Interfaces, Joint Unit CNRS/Saint-Gobain, Aubervilliers, France
* emmanuelle.guillard@saint-gobain.com

Silicate glass is among the oldest man-made materials, and was already fabricated in ancient Egypt. Glass is still used today for a variety of technological applications, from energy-efficient buildings to display cover glass or solar photovoltaic panels, requiring a good understanding of its properties. In the liquid state, silicate melts are liquids of high viscosity, due to the strongly polymerized silica network, interrupted in places by network modifiers cations such as sodium or calcium. This specific network structure is associated to several distinct timescales and results in intriguing transport phenomena, such as uphill molecular diffusion, or a large viscosity ratio between immiscible phases.

In this talk, I will discuss several transport phenomena such as coupled diffusion between species and phase separation in silicate melts. Such basic physics problems are studied at the joint unit CNRS/Saint-Gobain Surface of glass and Interfaces, and are inspired by questions from the glass melting and transformation industry. Chemical diffusion controls the dissolution of glass raw materials in industrial installations, but also the corrosion of furnace refractories. It is also involved in interdiffusion phenomena between glass substrate and thin films. I will discuss the coupled exchanges between the different species of silicate melts, which we studied both in bulk glasses and in thin films.

For the study of phase separation we have used in situ 3D imaging thanks to synchrotron micro- and nanotomography at the ESRF. Coarsening of a bicontinuous microstructure is controlled by hydrodynamic transport, with a dynamic asymmetry induced by the strong viscosity ratio between phases. Topology changes such as fragmentation or coalescence are characterized thanks to in situ imaging. In the case of phase-separated silicate thin films, specific coarsening mechanisms are observed, leading to nanotextured surfaces.

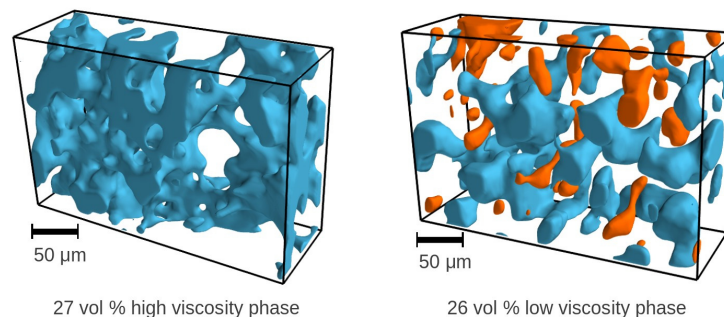


Figure 1: Microstructure of minority phase in phase-separated glasses, observed by in situ microtomography. Note the different morphology when the minority phase is the more viscous or fluid one. Different coarsening mechanisms are at play for the two phases.

The role of Ehrlich-Schwöbel barrier in the elongation mechanism of catalyst-free GaN nanowires grown by molecular beam epitaxy

Marion Gruart^{a,b,*}, Gwénoél Jacopin^c and Bruno Daudin^{a,b}

a. Université Grenoble Alpes, 38000 Grenoble, France.

b. CEA, INAC-PHELIQS "Nanophysics and semiconductors" group, F-38000 Grenoble, France.

c. Institut Néel, Université Grenoble Alpes, CNRS, Grenoble INP, 38000 Grenoble, France.

* marion.gruart@cea.fr

III-nitride-based light emitting diodes are now firmly established as the current solution for solid state lightning and related applications, despite the lack of adapted substrate leading to a high defect density in the epitaxial layers. Regarding nanowire-like structures grown by plasma-assisted molecular beam epitaxy (PA-MBE), typically 100 nm diameter, advantage is taken from the eased elastic strain relaxation resulting from the large aspect ratio of such objects. This allows a large mismatch accommodation in axial heterostructures and leads to quasi-defect free crystals.

In this study, we report on GaN PA-MBE regrowth on selective area-grown Ga-polar GaN columns with different pitches and sizes, ranging in diameter from nanowires to micro-columns. It is shown that the metal/nitrogen ratio, the growth temperature and the GaN columns geometry are interrelated parameters affecting the nanowire morphology. Then, the MBE grown section morphology can range from pyramids exhibiting semi-polar facets to nanoparasol-like structures with flat top and widening rate depending on the combination of aforementioned parameters.

Furthermore, the growth kinetics mechanism of GaN catalyst-free nanowires has been investigated by using the different morphologies previously described. For various diameter values of the upper flat surface, observation of either smooth or rough surface of the overgrown GaN section provides clues on the nucleation mechanism and Ga diffusion length, which is governed by both growth temperature and Ga/N flux ratio (Figure 1). In particular, edge nucleation on nanowire top is observed under N-rich conditions. This is assigned to an accumulation of gallium near the edges due to the potential energy barrier for moving to another crystallographic plane, similar to the case of "inverted wedding cake" previously described in ZnO nanowires [1].

[1] X. Yin et al, Inverted Wedding Cake Growth Operated by the Ehrlich–Schwoebel Barrier in Two-Dimensional Nanocrystal Evolution, *Angewandte Chemie International Edition* **55** 2217-2221 (2016)

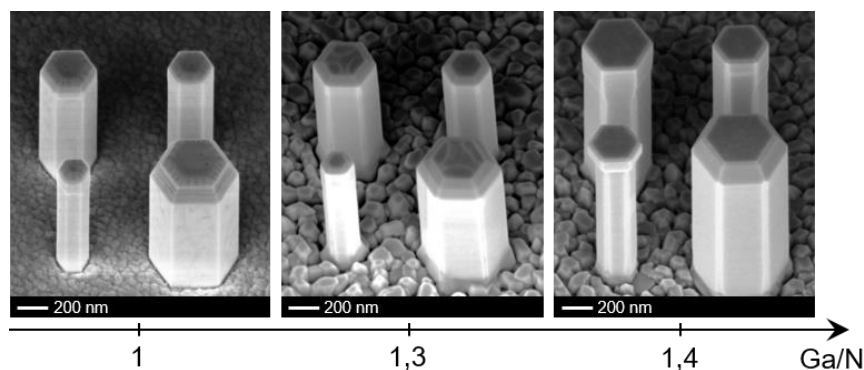


Figure 1 : Bird eye view SEM images of GaN wires after a GaN overgrowth with a variation of gallium/nitrogen ratio leading to a variation of gallium diffusion length, nuclei density and top surface roughness.

Deposition and selective switching of a cationic Fe(III) compound on Au(111) and Cu₂N

Manuel Gruber^{a*}, Torben Jasper-Tönnies^a, Sujoy Karan^{a,b}, Hanna Jacob^c, Felix Tuczek^c and Richard Berndt^a

- a. Institute of Experimental and Applied Physics, Christian-Albrechts-University Kiel, Germany
- b. Institute of Experimental and Applied Physics, University of Regensburg, Germany
- c. Institute of Inorganic Chemistry, Christian-Albrechts-University Kiel, Germany

* gruber@physik.uni-kiel.de

Spin-crossover (SCO) complexes contain a transition metal ion that can be switched between a low-spin and a high-spin state by external stimuli. Investigations of single SCO molecules is challenging as the interaction with the substrate often leads to fragmentation or loss of functionality. So far, the focus was on Fe(II) based molecules, while SCO complexes with different metal ions (different oxidation states) would be desirable.

Using scanning tunneling microscopy, we evidence the first successful deposition of a cationic Fe(III) SCO complex, [Fe(pap)₂]⁺ (pap = N-2-pyridylmethylidene-2-hydroxyphenylaminato), on Au(111) and Cu₂N/Cu(100). The deposited Fe(III) SCO compound is controllably switched between three different states, each of them exhibiting a characteristic tunneling conductance. The conductance is therefore employed to readily read the state of the molecules [1,2].

[1] Jasper-Toennies et al., J. Phys. Chem. Lett. **8**, 1569 (2017)

[2] Jasper-Toennies et al., Nano Lett. **17**, 6613 (2017)

Optimization of a ReaxFF potential for molecular dynamics simulations on MoTe₂ phase patterning process

Guehenneux Thomas^{a*}, Krueger Peter^a

a. Chiba University, 1-33, Yayoicho, Inage Ward, Chiba-shi, Chiba, 263-8522

* E-mail : thomasg@chiba-u.jp

Transition metal dichalcogenides (TMD) such as molybdenum disulfide (MoS₂) and molybdenum ditelluride (MoTe₂) are novel two-dimensional materials that are promising for future electronic devices because of the possibility of band gap tuning [1]. In 2015, a laser-induced phase patterning in MoTe₂ from 2H semi-conductor phase to 1T' semi-metallic phase has been experimentally demonstrated [2]. Thereby the Schottky contact between semi-conducting channel and metallic electrodes in 2D transistors can be avoided. This patterning is possible due to the small energy difference (0.03 eV) and low energy barrier (0.88 eV) between 2H and 1T'. In addition, previous first-principles calculations showed that the creation of tellurium vacancy highly promotes phase transition to 1T' from a kinetic point of view. In order to understand this phase patterning, it is necessary to find out optimum conditions for the semi-conductor to the semi-metallic phase transition.

In order to study this phase patterning process by Molecular Dynamics calculations, we have optimized a Reactive force-field (ReaxFF) potential for MoTe₂ with focus on the accurate description of the energetics of the 2H-1T' phase transition. A training-set composed of first-principles calculations of over 100 molecular or crystal structures composed of molybdenum, tellurium and hydrogen has been built. Periodic structures were calculated using VASP (Vienna ab initio simulation package) and in the generalized gradient approximation as parametrized by Perdew–Burke–Ernzerhof (GGA-PBE). Non-periodic systems were calculated using ORCA4 program [3]. Then, GARFField (Genetic Algorithm based Reactive Force Field optimizer) [4] program is used to optimize a ReaxFF potential against the training-set.

[1] M. Matsunaga et al., ACS Nano, 10, 9730–9737 (2016).

[2] S. Cho et al., Science, 349, 625–628 (2015).

[3] F. Neese, The ORCA program system, Wiley Interdiscip. Rev.: Comput. Mol. Sci., 2, 73–78 (2012).

[4] A. Jaramillo-Botero et al., J. Chem. Theory Comput., 10, 1426-1439 (2014).

Analysis of heat conduction in confined structures by means of scanning thermal microscopy

E. Guen^{a*}, D. Renahy^b, A. El Sachat^c, R. Rajkumar^d, Y. Zhang^d, P. Vincent^b, P. S. Dobson^d, F. Alzina^c, C. M. Sotomayor-Torres^c, A. Ayari^b, J. M. R. Weaver^d, P-O. Chapuis^a and S. Gomés^a

- a. Univ Lyon, CNRS, INSA-Lyon, UCBL1, CETHIL UMR5008, F-69621, Villeurbanne, France
 b. Univ Lyon, CNRS, UCBL1, ILM UMR 5306, F-69622, Villeurbanne, France
 c. Catalan Institute of Nanoscience and nanotechnology (ICN2), CSIC and BIST, Campus UAB, Bellaterra, 08193 Barcelona, Spain
 d. Univ Glasgow, School of Engineering, Glasgow, Scotland, United Kingdom

* eloise.guen@insa-lyon.fr

Scanning thermal microscopy (SThM) allows the thermal characterization of materials with a submicrometric spatial resolution [1]. Determining reliable thermal data from the experiments is challenging because the probe-sample heat exchange strongly depends on parameters such as the size, geometry and surface states of probe and sample [2-3]. To analyze thermal dissipation in confined systems, we first studied deposited thin films with a thickness ranging from few nanometers to one micrometer. Polystyrene films on silicon (Si) and quartz substrates, and silicon dioxide films on Si substrates were analyzed by means of SThM probes with various sizes. For a low thermal conductivity film on a high thermal conductivity substrate, results show an apparent thermal conductivity decrease as a function of the film thickness (see Fig.1), which persists up to few hundreds nanometers. They also demonstrate that the SThM technique is sensitive to films few nanometers thin and to oxidation. In a second step, 2D lateral confinement is addressed and the heat transferred from a heated probe to silicon cylinders of varying diameters and spaced with different distances was also measured (see Fig.2) under different environments, in particular within a SThM embedded in a scanning electron microscope. The diameters and distances of the cylinders were chosen to be higher than, of the same order of or lower than the mean free path of phonons in Si (~300 nm at room temperature). Results are discussed as a function of the ratios between the characteristic dimensions of the probe, sample geometry and mean free paths.

[1] S. Gomes et al., PSSA 212, 3 (2015), [2] Y. Ge et al., Nanotech. 27, 32 (2016), [3] F. Menges et al., RSI 87, 7 (2016)

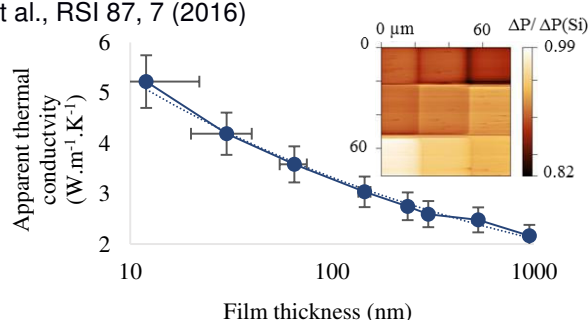


Figure 1: Apparent thermal conductivity as a function of SiO₂ film thickness. The insert provides the relative power dissipated in the sample for each SiO₂ thickness.

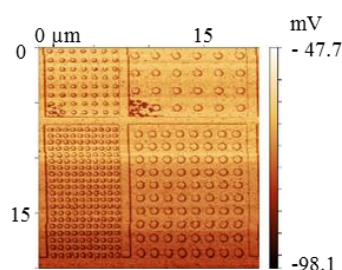


Figure 2: Thermal image (SThM probe voltage) of cylinders (diameters 300 and 600 nm) etched in silicon obtained in vacuum.

Acknowledgements: The research leading to these results has received funding from the EU FP7 Programme under grant agreement n°604668 and the French National Research Agency under the project: «Advanced Tools for Thermal Measurements in Scanning Electron Microscope»- LABEX iMUST.

Using Superconductivity to probe the hinge states of nanowires of Bismuth, a Higher Order Topological Insulator

Anil Murani¹, Bastien Dassonneville¹, Alik Kasumov^{1,2}, Shamashis Sengupta¹, Yu.A. Kasumov², V.T.Volkov², I.I. Khodos², F. Brisset³, Raphaëlle Delagrangé¹, Alexei Chepelianskii¹, Richard Deblock¹, Meydi Ferrier¹, Hélène Bouchiat¹, and Sophie Guéron^{1,*}

¹ *Laboratoire de Physique des Solides, CNRS, Univ. Paris-Sud, Université Paris Saclay, 91405 Orsay Cedex, France.*

² *Institute of Microelectronics Technology and High Purity Materials, Chernogolovka, Moscow Region, Russia.*

³ *Institut de Chimie Moléculaire et des Matériaux d'Orsay Bâtiments 410/420/430, Univ. Paris-Sud 11, 91405 Orsay cedex - France*

*Sophie.gueron@u-psud.fr

Bismuth has very recently been shown to belong to the family of Higher Order Topological Insulators [1], i.e. materials with insulating bulk and surfaces, but with metallic 1D “hinges” at the junction of its surfaces. In this talk I will show how our experiments on monocrystalline bismuth nanowires confirm this prediction [1]. Specifically, by using superconducting contacts we have detected hinge states (via interference patterns of the critical current in a magnetic field), revealed their ballistic and chiral character (via the measurement of the supercurrent-versus-phase relation [2]), and probed their topological protection (via high frequency measurements [3]).

[1] Schindler et al, arXiv:1802.02585

[2] Murani et al., Nature Comm. DOI: 10.1038/ncomms15941 (2017).

[3] Murani et al., Phys.Rev. B **96**, 165415 (2017) ; Murani et al., in preparation (2018).

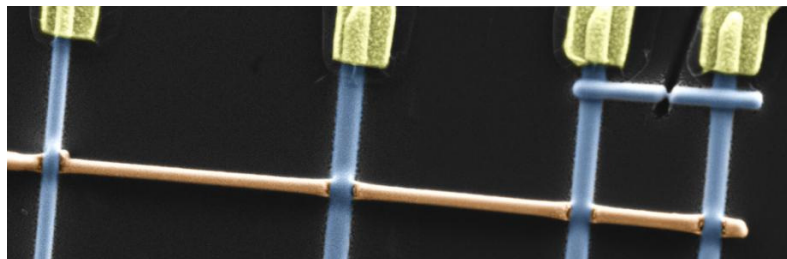


Figure 1 : Bismuth nanowire (in brown) connected to superconducting electrodes (in blue), including an asymmetric SQUID configuration enabling the supercurrent-versus-phase relation measurement.

Effect of loop size on the binding direct or reverse staples

Clothilde Coilhac,^a Jérôme Richard,^a Olivier Bourgeois^a and Hervé Guillou^{a*}

a. Institut Néel, UGA et CNRS, Grenoble, France

* herve.guillou@neel.cnrs.fr << corresponding author >>

DNA origami are nanostructures, self assembled from a large single stranded DNA molecule of biological origin, the scaffold and smaller synthetic strands, the staples. The set of staple is designed to fold the scaffold into a specific shape upon hybridization, consequently forming crossovers, holliday junctions and loops. Various type of structures have been designed, from the seminal 2D smiley to 3D, gigadalton-scale, gears like structure. The design algorithm consists in maximizing the binding of complementary bases while respecting the continuity of the scaffold. It is thus exclusively based on the geometry, i.e. the thermodynamics, which guarantees that the programmed shape minimizes the free energy of the systems. If the programmed shape do actually self-assemble within the laboratory time scale is not guaranted by the design algorithm and the question of the optimization of the design is still open. We assume that some elementary topologies that are formed during the assembly may be more stable and thus may nucleate the assembly of the whole structure. To test this hypothesis we designed single staple origami pictured in the figure1. In these elementary structures the two DNA strands may hybridize to form a loop. We measured by calorimetry the thermodynamic properties of these two simple systems and observed that the effect of the loop size are strikingly different in the two configurations. This indicates that one topology may be favorable to nucleate the assembly of the whole nanostructure. We will discuss what these results may involve for the optimization of the design of DNA origami.

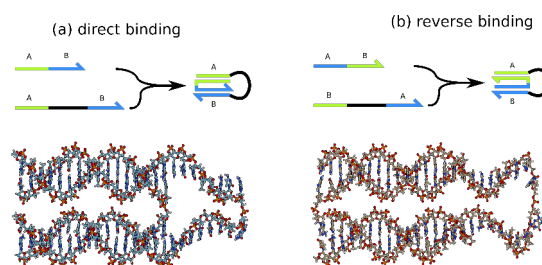


Figure 1: Elementary origami used in this study. (a) the complementary sequences of the staple and the scaffold are in the same order (direct binding), (b) the complementary sequences of the staple and the scaffold are in a reverse order (reverse binding). The all-atom pictures below are drawings of possible configurations and do not reflect the actual organization

Ballistic Electron Emission Microscopy (BEEM): a local and quantitative probe to study the quality of Au/hexadecanethiols/GaAs(001) heterostructures by imaging buried interfaces and drawing local energy band alignments

Sophie Guézo^{a*}, Alexandray Junay^a, Pascal Turban^a, Bruno Lépine^a, Gabriel Delhaye^a, Sylvain Tricot^a, Soraya Ababou-Girard^a et Francine Solal^a

a. Institut de Physique de Rennes, Département Matériaux-Nanosciences, UMR 6251, Université de Rennes 1, CNRS, 263 avenue du Général Leclerc, 35042 Rennes cedex, France

* sophie.guezo@univ-rennes1.fr

In molecular electronics, metallic top-contact deposition on organic molecular monolayer(OML)/semiconductor hybrid heterostructures is still a critical issue, leading to metal penetration through the molecules and monolayer's damage. Here, we report on the potentialities of BEEM (technique derived from the Scanning Tunneling Microscopy one) to quantitatively characterize the local transport properties at the nanometer scale and the degree of this penetration through the organic monolayer on Au-hexadecanethiols-GaAs(001) heterostructures. At RT, BEEM imaging mode provides mapping of the local hot-electron transmission and demonstrates pronounced inhomogeneities at buried interfaces. Using local transport measurements in spectroscopy mode, local barrier heights and the BEEM current attenuation are measured in each area and compared with the well-known Au/GaAs(001) Schottky contact [1,2]. In order to minimize the degree of gold penetration and obtain homogeneous heterojunctions, an alternative top-contact deposition method is used, based on Buffer-Layer Assisted Growth (BLAG) [3]. BEEM results obtained on such heterostructures are discussed and compared with macroscopic measurements [4]. In this framework, BEEM further appears as a highly powerful and complementary tool to commonly used spatially averaged diffusive transport experiments, essential for understanding such hybrid heterostructures of major interest for molecular electronics. The extension of this work to the case of OML/ferromagnets spinterfaces is in progress.

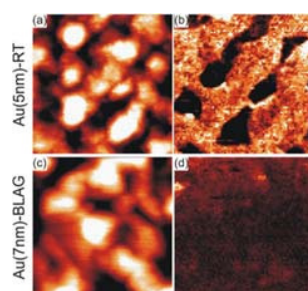


Figure 1 : 50x50nm² STM images of Au surfaces deposited on hexadecanethiols/GaAs(001) (a) at room temperature and (c) by BLAG method. (b) and (d) Corresponding BEEM images of buried interfaces.

[1] S. Guézo, P. Turban, *et al.*, *Physical Review B*, **81**, 085319 (2010).

[2] A. Junay, S. Guézo, *et al.*, *Journal of Applied Physics*, **118**, 085310 (2015).

[3] M. M. Maitani, D. L. Allara, *et al.*, *Applied Physics Letters*, **96**, 173109-3 (2010).

[4] A. Junay, S. Guézo, *et al.*, *The Journal of Physical Chemistry C*, **120**, 24056-24062 (2016)

Defect-influenced dynamics of Dzyaloshinskii domain walls under perpendicular and planar magnetic fields

Pierre Géhanne^{a*}, V. Jeudy^a, S. Rohart^a, A. Hrabec^a and A. Thiaville^a

a. Laboratoire de Physique des Solides, Univ. Paris-Sud, Université Paris Saclay, CNRS UMR 8502, 91405 Orsay

* pierre.gehanne@u-psud.fr

When dealing with the physics of spin current or domain wall manipulation at the interface between a ferromagnetic material and a metal with strong spin-orbit coupling, one has to take into account the presence of the interfacial Dzyaloshinskii-Moriya interaction (DMI). This antisymmetric exchange interaction appears in multilayer materials when the inversion symmetry is broken and can in some cases be comparable to the anisotropy energies, giving rise to new magnetization configurations such as skyrmions or chiral domain walls.

We study the dynamics of domain walls in Au/Co/Pt stacks, where the Cobalt thickness is around 1 nm. These stacks display perpendicular magnetic anisotropy as well as a strong interfacial DMI. It has been shown that the DMI changes the angle of the internal magnetization of the domain wall, from an achiral Bloch configuration to a chiral Néel configuration [1]. The energy and internal angle of such “Dzyaloshinskii domain walls” can be tuned by applying a strong static magnetic field in the plane of the sample [2], but the effects of chirality on the dynamics of domain walls are still to be understood.

Using a MOKE microscope built on purpose, we performed measurements of the velocity of the domain walls when subjected to out-of-plane magnetic field pulses over large ranges of amplitude and duration. The velocity/field curves display the creep, depinning and flow regime of motion [3]. Moreover, the velocity is found to vary by an order of magnitude with the in-plane field. Analyzing the universal behavior of the creep regime [4], we access to the material-dependent depinning parameters, and study their variation under the influence of DMI and in-plane field.

- [1] A. Thiaville *et al.*, Dynamics of Dzyaloshinskii domain walls in ultrathin magnetic films, *EPL*, **100**, 57002 (2012)
- [2] J. P. Pellegren *et al.*, Dispersive Stiffness of Dzyaloshinskii Domain Walls, *Phys. Rev. Lett.* **119**, 027203 (2017)
- [3] P. J. Metaxas *et al.*, Creep and flow regimes of magnetic domain-wall motion in ultrathin Pt/Co/Pt films with perpendicular anisotropy, *Phys. Rev. Lett.* **99**, 217208 (2007).
- [4] R. Díaz Pardo *et al.*, Universal depinning transition of domain walls in ultrathin ferromagnets, *Phys. Rev. B.*, **95**, 184434 (2017)

Elaboration and characterization of Ge_{1-x}Sn_x nanowires by chemical vapor deposition via vapor-liquid-solid mechanism

T. Haffner^{a*}, F. Bassani^a, P. Gentile^b, A. Gassenq^b, N. Pauc^b, E. Martinez^c, S. David^a, T. Baron^a, E. Robin^d, B. Salem^{a*}

^a Univ. Grenoble Alpes, CNRS, LTM, 38000 Grenoble, France

^b Univ. Grenoble Alpes, CEA, INAC-Pheliqs, 38000 Grenoble, France

^c Univ. Grenoble Alpes, CEA, LETI-DTSI, 38000 Grenoble, France

^d Univ. Grenoble Alpes, CEA, INAC-MEM, 38000 Grenoble, France

* Corresponding authors: thibault.haffner@cea.fr / bassem.salem@cea.fr

During the last few years, group IV semiconductors with direct bandgap, such as GeSn, have attracted a lot of interest for microelectronic and optoelectronic devices. Theoretical studies have shown that this alloy has a low band gap energy, high carrier mobility and direct bandgap for a tin concentration higher than 8% [1]. However, the low solid solubility, which is below 1%, of tin in germanium and the large lattice mismatch between Sn and Ge (~14%), are real challenges to be overcome in order to produce a high-crystalline quality GeSn alloy. Recently several research groups have shown the capability to elaborate 2D GeSn layers on Si substrates using chemical vapor deposition (CVD) and molecular beam epitaxy (MBE) [2]. These latter methods provide a good control for Sn incorporation and the possibility of developing heterostructures with sharp interfaces. However, due to the large lattice mismatch between GeSn and the silicon substrate (> 4.2 %), the elaboration of 2D films leads to a large number of misfit dislocations at the GeSn/Si interface for thick GeSn layers [3]. Different solutions to avoid these defects have been developed like the “GeSn on insulator” [4], or the growth of nanowires using the bottom-up approach via the vapor-liquid-solid (VLS) mechanism during the CVD process. Unfortunately, Sn incorporation in the nanowires is much more difficult to achieve with this technique, thus explaining the small amount of studies about GeSn nanowires (NWs) grown by CVD-VLS process.

In this context, we will report on the growth and Sn incorporation of GeSn NWs synthesized by CVD-VLS using Au as catalyst. Germane (GeH₄) and tin tetrachloride (SnCl₄) were used as gas precursors with an additional HCl gas in order to improve the morphology of the NWs. The influence of the growth temperature and P_{SnCl₄}/P_{GeH₄} ratio on the growth rate and Sn incorporation in GeSn NWs will be presented. We show that GeSn NWs exhibit a core-shell structure with a thin Sn rich shell (up to 10 at.%).

[1] D. Stange, et al., ACS Photonics 2, 1539 (2015).

[2] N. von den Driesch, et al., Chem. Mater. 27, 4693 (2015).

[3] H.S. Maczko, et al., Sci. Rep. 6, 34082 (2016).

[4] D. Lei, et al., Appl. Phys. Lett. 109, 22106 (2016).

L'analyse *in situ* en cosmétique

Philippe Hallégot^{a*}

a. L'Oréal R&I, 1 avenue Eugène Schueller, 93601 Aulnay-sous-Bois, France

* phallegot@rd.loreal.com

L'analyse *in situ*, et plus particulièrement la microanalyse, joue un rôle prépondérant dans l'innovation en cosmétique.

Les techniques microanalytiques permettent en effet une meilleure connaissance du cheveu, de la peau, du cil et de l'ongle, sains ou abîmés, et conduisent au développement de produits cosmétiques adaptés.

Ces mêmes techniques appliquées aux substrats, après un traitement cosmétique, en illustrent son action. Ces actions peuvent être d'ordre morphologique, et les microscopies électroniques à balayage et à transmission trouvent ici leur place, ou bien d'ordre mécanique et requièrent l'adjonction de platines de traction ou l'utilisation de l'AFM.

Mais les techniques de microanalyses jouent également un rôle majeur dans la validation de la structure des produits cosmétiques. Il faut souligner que l'eau étant garante de l'intégrité des produits et des substrats, les techniques environnementales et cryogéniques sont largement employées en recherche cosmétique.

Enfin, il est également important d'être en mesure de mettre en lumière le mode d'action d'un produit par son suivi jusqu'à son site d'action au moyen des techniques SIMS, EDS, Raman par exemple.

La performance des produits cosmétiques trouve souvent son origine dans des modifications ultrastructurales des substrats concernés et des architectures mises en place à l'échelle microscopique [1].

[1] P. Hallegot, G. Hussler, V. Jeanne-Rose; F. Leroy, P. Pineau, and H. Samain, Discovery of a sol-gel reinforcing the strength of hair structure: mechanisms of action and macroscopic effects on the hair, *J Sol-Gel Sci Technol* **79**:359–364 (2016)

Multiscale thermal characterization of different systems types

Georges Hamaoui^{*}, Nicolas Horny, and Mihai Chirtoc

GRESPI, Multiscale Thermophysics Lab.
Université de Reims Champagne-Ardenne URCA,
Moulin de la Housse BP 1039, Reims 51687, France

*Georges.hamaoui@univ-reims.fr

This decade witnessed a big advancement in technologies within each field of study (physics, chemistry, engineering, electronics...). The race of finding better component is at its peak. Researchers are focusing on making better materials or couple of materials with enhanced thermal/electrical properties for nano- and micro- electronic devices. These investigations aim to reduce heat losses in these device types and transform it to electricity for a better usage in thermoelectricity [1]. The materials in question can be a simple micrometer layer or a complicated nanometric layers or even membranes. Proper experimental techniques are then necessary to study the thermal properties of these new materials. In this study a characterization of thermal properties for different type of materials is made using a contactless method based on the measuring of emitted infrared (IR) radiations. These methods use Max Planck's principle to measure the IR radiations emitted from a material after being heated. Two types of photothermal radiometry (PTR) setups are present in the GRESPI lab [2]–[4]. One uses a frequency domain modulation up to 10 MHz and one uses a hybrid frequency/spatial domain modulation with $\sim 10\ \mu\text{m}$ resolution and up to 10 MHz. By using these methods, it is possible to extract independent parameters like the thermal diffusivity and thermal effusivity of thin films, and the thermal boundary resistance R_{th} [4]–[6]. These two setups are used jointly to characterize different type of material's combinations like:

- Phase changes materials,
- Metal/semiconductor or metal silicide/semiconductor couples,
- Organic materials,
- Irradiated graphite.

The results will help for a better understanding of thermal transport in these materials, and encourages novel ways to use them in diverse applications in different field of research.

- [1] J. Schaumann et al., "Improving the zT value of thermoelectrics by nanostructuring: tuning the nanoparticle morphology of Sb₂Te₃ by using ionic liquids," *Dalt. Trans.*, vol. 46, no. 3, pp. 656–668, 2017.
- [2] N. Horny, M. Chirtoc, A. Fleming, G. Hamaoui, and H. Ban, "Kapitza thermal resistance studied by high-frequency photothermal radiometry," *Appl. Phys. Lett.*, vol. 109, no. 3, 2016.
- [3] J. Pelzl, P. Kijamnajsuk, M. Chirtoc, N. Horny, and C. Eisenmenger-Sittner, "Correlation Between Thermal Interface Conductance and Mechanical Adhesion Strength in Cu-Coated Glassy Carbon," *Int. J. Thermophys.*, vol. 36, no. 9, pp. 2475–2485, Apr. 2015.
- [4] E. T. Swartz and R. O. Pohl, "Thermal boundary resistance," *Rev. Mod. Phys.*, vol. 61, no. 3, pp. 605–668, Jul-1989.
- [5] P. L. Kapitza, "Heat transfer and superfluidity of helium II," *Phys. Rev.*, vol. 60, no. 4, pp. 354–355, 1941.
- [6] G. L. Pollack, "Kapitza Resistance," *Rev. Mod. Phys.*, vol. 41, no. 1, pp. 48–81, Jan. 1969.

Préparation et caractérisation de semi-conducteurs ternaires

Cu_2SnSe_3

Khalida Hamdani^{a*}, M. Chaouche^a, M. Benabdeslem^a, L. Bechiri^a, N. Benslim^a, A. Amara^a, X. Portier^b, M. Bououdina^c, A. Otmani^d

- LESIMS, Département de Physique, Faculté des Sciences, Université Badji Mokhtar – Annaba, BP. 12, 23200 Sidi Amar (Algérie)
- CIMAP, Centre de recherche sur les ions, les matériaux et la photonique, CEA, UMR 6252 CNRS, ENSICAEN, UCBN, 6 Boulevard du Maréchal Juin, 14050 Caen cedex (France)
- Nanotechnology Centre, University of Bahrain, PO Box 32038, Kingdom of Bahrain, Department of Physics, College of Science, University of Bahrain, PO Box 32038, Kingdom of Bahrain.
- LRPCSI, faculté des Sciences Université de Skikda, BP26 route El-Hadaek (21000) Skikda, Algeria

*hamdani.khalida@yahoo.com « khalida hamdani »

Des poudres nanocristallines de Cu_2SnSe_3 ont été élaborées par mécanosynthèse à l'aide d'un broyeur planétaire à haute énergie de type (Pulverisette P7). Pour le processus de formation des composés des périodes de broyage de 60, 90 et 180 mn ont été retenues. Les propriétés physiques ont été étudiées au moyen de techniques variées.

Dans la partie expérimentale, En utilisant les techniques de Diffraction des rayons X (DRX), Microscopie Electronique à Balayage (MEB), analyse des rayons X par Dispersion d'Énergie (EDX). L'analyse par la diffraction RX a révélé la présence des raies essentielles de la phase cubique et a permis de déterminer le paramètre de la maille ainsi que la taille des particules. Cette structure a été confirmé par microscopie électronique en transmission pour la poudre broyée, le paramètre cristallin déterminé à partir du diagramme de diffraction est de 5,69Å Les micrographies MEB des poudres des deux séries montrent que leurs particules se présentent sous forme d'agglomérats. La spectroscopie en énergie dispersive (EDX) a montré que la composition finale des échantillons est proche de la stœchiométrie. Les mesures optiques ont montré que les valeurs du gap obtenues variées entre 0,86 à 0,94 eV avec un grand coefficient d'absorption plus de 10^4 cm^{-1} .

Mots clés : Cu_2SnSe_3 – Mécanosynthèse - Diffraction des rayons X

Radiative cooling by tailoring surfaces with microstructures

Armande Hervé^{a*}, Jérémie Drevillon^a, Younès Ezzahri^a and Karl Joulain^a

a. Institut Pprime, CNRS, Université de Poitiers, ISAE-ENSMA, F-86962 Futuroscope Chasseneuil, France

* armande.herve@univ-poitiers.fr

Lots of structures, such as multi-layer or photonic structures, have been proposed for applications of radiative cooling : total reflection in the solar spectrum and total emission in the atmospheric transparency window (8-13 μ m). In this study, we optimize a structure combining a multi-layer and a grating. It is the first time that simple gratings are used for radiative cooling applications.

We use optimized BN, SiC and SiO₂ gratings, which have emissivity peaks in the transparency window. We place under these gratings a metal/dielectric multi-layer structure to obtain a near perfect reflectivity in the solar spectrum and to enhance the emissivity in the transparency window. This design, combining grating and multi-layer, allows engineering adaptive thermal emission to radiative cooling requirements. Multi-layer structures create resonant radiative modes that help a heated structure to radiate thermal energy in the far-field. Gratings diffract non radiative modes like surface waves, such as surface phonon-polaritons. Thus, a structure combining a multi-layer and a grating allows to couple and radiate both radiative and non-radiative modes. It constitutes an advantage compared to other structures.

We used the Rigorous Coupled Wave Analysis (RCWA) method coupled to a particle swarm optimization (PSO) algorithm to optimize our structure. The optimized structures produce a good radiative cooling power density up to 80 W.m⁻² at night and a mean daytime radiative cooling power density of 55 W.m⁻², with local atmospheric and solar conditions in Poitiers.

2D gratings of our theoretical structure and experimental prototypes are also considered in order to converge to practical applications.

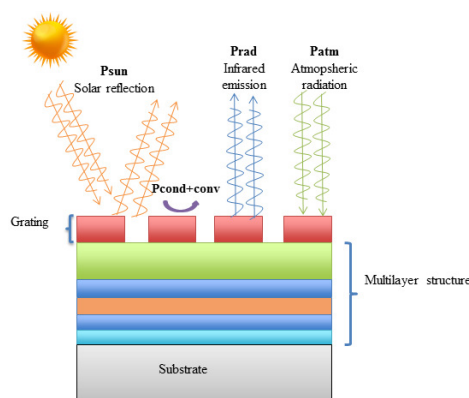


Figure 1 : Schematics of a radiative cooler composed of a multi-layer structure and a grating overhead with the radiative and non-radiative processes taking place

Graphene solution-gated field-effect transistor arrays for *in vivo* neural recording

Clement Hebert

Advanced Electronic Materials And Devices Group,
Institut Català de Nanociència i Nanotecnologia, Barcelona, Spain

clement.hebert@icn2.cat

After two decades of investigation and exploitation, the current electrical neural interface technologies are about to reach their limit both for fundamental neural investigation and for clinical applications. Important refinements are still needed to reach low invasiveness, long term efficacy as well as large number of recording/stimulating sites. Thanks to its biocompatibility, low dimensionality, mechanical flexibility and electronic properties, graphene offers new perspectives to address those issues. In this talk, I will present our recent development of graphene solution-gated field-effect transistor arrays for *in vivo* recording. The probes were implanted at the surface and inside the sensory cortex of rats in order to record the activity of the neural network under light and sound stimulation during acute experiments. Similarly, the implants were used for electroretinography. Recently, we also recorded cortical spreading depression, a type of low frequency signal (below 0.1Hz) that cannot be properly analysed using microelectrode technology.

Kohn anomaly of optical zone boundary phonons in uniaxial strained graphene: role of the electronic band structure

Sonia Haddad^{*} et Lassaad Mandhour

Laboratoire de Physique de la Matière Condensée, Département de Physique, Faculté des Sciences de Tunis, Université Tunis El Manar, Campus Universitaire 1060 Tunis, Tunisia

* soniahaddad09@gmail.com

One of the unique properties of graphene is its extremely high mechanical strength. Several studies have shown that the mechanical failure of graphene sheet under a tensile strain is due to the enhancement of the Kohn anomaly of the zone boundary transverse optical phonon modes [1,2]. In this work, we derive an analytical expression of the Kohn anomaly parameter α_K of these phonons in graphene deformed by a uniaxial strain along the armchair direction. We show that, the tilt of Dirac cones, induced by the strain, contributes to the enhancement of the Kohn anomaly under a tensile deformation and gives rise to a dominant contribution of the so-called outer intervalley mediated phonon processes. Moreover, the Kohn anomaly is found to be anisotropic with respect to the phonon wave vectors around the K point. This anisotropy may be at the origin of the light polarization dependence of the Raman 2D band of the strained graphene. Our results uncover, not only, the role of the Kohn anomaly in the anisotropic mechanical failure of the graphene sheet, under strains applied along the armchair and zigzag directions, but shed also light on the doping induced strengthening of strained graphene [1].

[1] C. Si, W. Duan, Z. Liu, and F. Liu, Phys. Rev. Lett. **109**, 226802 (2012).

[2] M. E. Cifuentes-Quintal, O. de la Peña-Seaman, R. Heid, R. de Coss, and K.-P. Bohnen, Phys. Rev. B **94**, 085401 (2016).

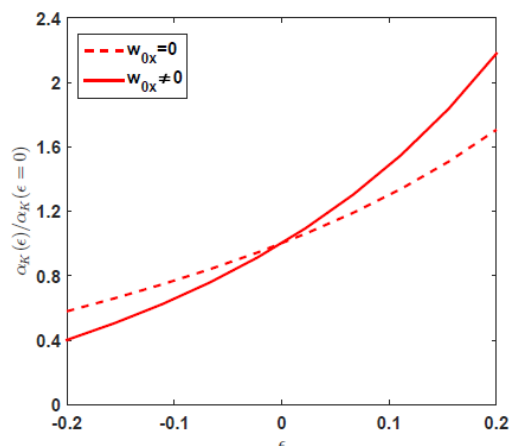


Figure 1 : KA slope as a function of strain. The data are normalized with respect to the value for the unstrained graphene. The solid line corresponds to the deformed Dirac cones including anisotropy and tilt effects while the dashed one is calculated for the untilted cones.

Thin liquid films for gas separation

Céline Hadji^{a*}, Benoît Coasne^a, Hugues Bodiguel^b, Benjamin Dollet^a, Elise Lorenceau^a

a. LIPhy, Université Grenoble Alpes and CNRS, Grenoble, France

b. LRP UMR5520, Université Grenoble Alpes and CNRS, Grenoble, France

*celine.hadji@univ-grenoble-alpes.fr

Gas and nanoparticle filtration is generally performed via complex and expensive porous membranes facing clogging issues; breaking these current technological limitations relies on decreasing the costs and simplifying the existing protocols. A good alternative lies in specific liquid materials such as thin liquid films [1]. The permeability of soap films to gas depends on their thickness, the gas solubility in the liquid, and the surfactant monolayers' structure and mutual interactions. Understanding the properties of such systems remains challenging due to their inherent complexity. We want to understand and predict the phenomenon of gas permeation through a soap film, and how the film properties (thickness, surfactant nature and concentration) affect its performances as a gas filter. We study the evolution of a system of two gas compartments (air + non soluble C_6F_{14} | air) in a glass syringe, separated by a soap film made of a 3g/L TTAB solution. Only the soluble gas (here, air) permeates through the membrane to balance both air concentrations (like osmosis phenomena in liquids).

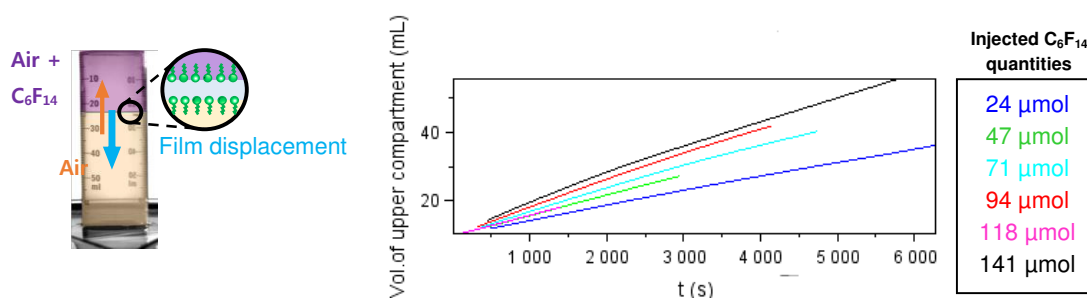


Figure 1: Time evolution of the volume of the compartment containing C_6F_{14} .

We develop a physical model to describe the evolution of the air + C_6F_{14} compartment and extract the film permeability k ($\text{cm}\cdot\text{s}^{-1}$), and establish a link between the film permeability and other properties of the system like the partial pressure of C_6F_{14} and adsorption phenomena.

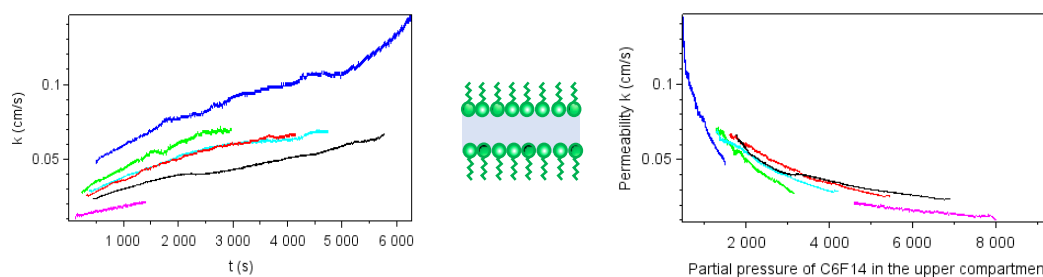


Figure 2: Evolution of the film permeability vs. time and the partial pressure of C_6F_{14} in the upper compartment. The observed increase of permeability with time is presumably linked to C_6F_{14} dilution along time, which limits its adsorption on TTAB film [2] (adsorption supposedly decreases with the partial pressure of C_6F_{14}).

[1] H. M. Princen and S. G. Mason, "The permeability of soap films to gases," *J. Colloid Sci.*, vol. 20, no. 4, pp. 353–375, 1965.

Anatomy of perpendicular magnetic anisotropy in conventional and non-conventional magnetic tunnel junctions

Ali Hallal^{a,b,c*} and M. Chshiev^{a,b,c}

- a. Univ. Grenoble Alpes, INAC-SPINTEC, F-38000 Grenoble, France.
- b. CNRS, SPINTEC, F-38000 Grenoble, France.
- c. CEA, INAC-SPINTEC, F-38000 Grenoble, France.

* ali.hallal@cea.fr

Magnetic tunnel junctions (MTJs) with perpendicular magnetic anisotropy (PMA) have been attracting a lot of interest due to their potential application in realizing the next generation of spintronic devices including nonvolatile memories and logic chips with high thermal stability. In particular, Metal/oxide interfaces with low spin-orbit coupling (SOC), such as Fe/MgO and Co/AlO_x, provide a convenient way to get simultaneously a large PMA required for memory retention together with weak Gilbert damping necessary for low switching current.

Using first-principle calculations, we study the microscopic origin of PMA at Fe/MgO interfaces through evaluation of layer resolved contribution as function of interfacial conditions [1]. Onsite projected analysis shows that the anisotropy energy is not localized at the interface but it rather propagates into the bulk showing an attenuating oscillatory behavior which depends on orbital character of contributing states and interfacial conditions. Then, we propose to further increase the PMA in Fe/MgO interfaces by doping the bulk of the storage layer by magnetic impurities of chromium (Cr) and/or vanadium (V). While the impurity near the interface has a drastic effect in decreasing the perpendicular magnetic anisotropy (PMA), its position within the bulk allows maintaining high interfacial PMA while reducing the bulk magnetization and correlatively the easy-plane demagnetizing energy [2]. At the same time, the interfacial spin polarization is not affected by the magnetic layer bulk doping by Cr or V impurities and even enhanced in most situations thus favoring an increase of tunnel magnetoresistance (TMR) amplitude. Finally, we present the enhancement of PMA of Co films by graphene coating. Our calculations show that graphene can dramatically boost the surface anisotropy of Co films up to twice the value of its pristine counterpart and can extend the out-of-plane effective anisotropy up to unprecedented thickness of 2.5 nm [3]. These findings point toward a possible engineering of magnetic anisotropy in conventional and non-conventional MTJs, which stands as a hallmark for future spintronic information processing technologies in a view of the long-standing challenge to promote large PMA in small size spintronic devices with weak SOC.

[1] A. Hallal, H. X. Yang, B. Dieny and M. Chshiev, Anatomy of perpendicular magnetic anisotropy in Fe/MgO magnetic tunnel junctions: First-principles insight, *Phys. Rev. B* **88**, 184423 (2013).

[2] A. Hallal, B. Dieny and M. Chshiev, Impurity-induced enhancement of perpendicular magnetic anisotropy in Fe/MgO tunnel junctions, *Phys. Rev. B* **90**, 064422 (2014).

[3] H. X. Yang, A. D. Vu, A. Hallal, N. Rougemaille, J. Coraux, G. Chen, A. K. Schmid and M. Chshiev, Anatomy and Giant Enhancement of the Perpendicular Magnetic Anisotropy of Cobalt-Graphene Heterostructures, *Nano. Lett.* **16**, 145 (2016).

High-throughput computational search for new opto-electronic materials

Geoffroy Hautier^a

a. Université catholique de Louvain, Belgium

Essential materials properties can now be assessed through ab initio methods. When coupled with the exponential rise in computational power, this predictive power provides an opportunity for large-scale computational searches for new materials. We can now screen thousands of materials by their computed properties even before the experiments. This computational paradigm allows experimentalists to focus on the most promising candidates, and enable researchers to efficiently and rapidly explore new chemical spaces.

In this talk, I will present the challenges as well as opportunities in materials discovery in high-throughput ab initio computing using examples where opto-electronic properties are of great importance (e.g., transparent conducting oxides). In addition to allowing the ability to navigate through a large volume of materials data to identify promising compounds, high-throughput computing also offers unprecedented data mining opportunities to detect new relationships between chemistry, structures, and properties. I will illustrate examples of these relationships through our recent work in crystal structure descriptors and automatic local environment identification, which merge traditional solid-state chemistry and materials science concepts through modern informatics.

The impact of high-throughput computing is multiplied when the generated data is shared with free and easy access. I will finish my talk by presenting the Materials Project (<http://www.materialproject.org>), a collaborative project which precisely targets such a data dissemination.

Complex Berry phase instability in PT-symmetric coupled waveguides

Rosie Hayward and Fabio Biancalana

School of Engineering and Physical Sciences, Heriot-Watt University, EH14 4AS Edinburgh, UK

We show that the analogue of the geometric phase for non-Hermitian coupled waveguides with PT -symmetry and at least one periodically varying parameter can be purely imaginary, and will consequently result in the manifestation of an instability in the system [1]. The instability peaks seen in the spectrum of the system's eigenstates after evolution along the waveguides can be directly mapped to the spectrum of the derivative of the geometric function. The instabilities are magnified as the exceptional point of the system is approached, and non-adiabatic effects begin to appear. As the system cannot evolve adiabatically in the vicinity of the exceptional point, PT-symmetry will be observed breaking earlier than theoretically predicted. This work can be extended to any two-level Hamiltonian system with multiple periodically varying parameters, with potential applications in optical and condensed matter physics. It is possible to study the instability which arises in such a system when the surface of constant energy in the system's parameter space forms a hyperboloid, which acts as an exact analogue of a hyperbolic magnetic monopole [2].

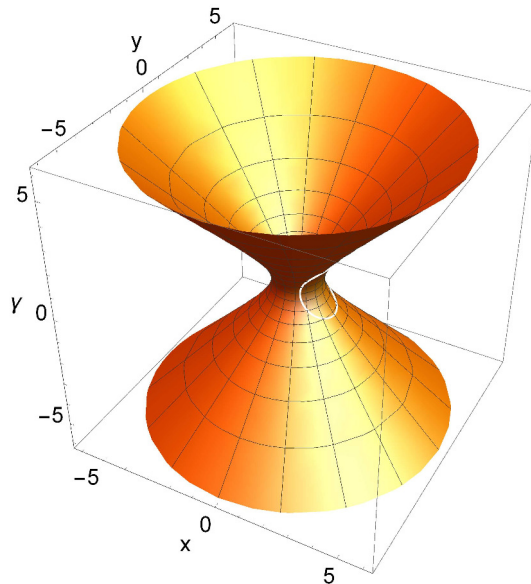


FIG. 1: Hyperbolic magnetic monopole formed in parameter space for a two-level system with periodically varying parameters. An example path taken by the parameters, which can be used to calculate the geometric phase, is shown on the monopole's surface.

[1] R. Hayward and F. Biancalana, <https://arxiv.org/pdf/1804.11117.pdf> (2018).

[2] A. I. Nesterov and F. Aceves de la Cruz, *J. Phys. A: Math. Theor.* **41**, 485304 (2008).

Towards DNA-Templated Molecular Electronic Devices

Seham Helmi, Jonathan Bath, Arzhang Ardavan & Andrew J. Turberfield*

Clarendon Laboratory, Department of Physics, University of Oxford, Oxford, UK

* andrew.turberfield@physics.ox.ac.uk

The ultimate miniaturization of active electronic components requires the construction of electronic devices from single molecules [1]. Molecular electronics would provide advantages in device architecture, power consumption and functionality. However, building a single-molecule device is challenging as it requires absolute control over the fabrication process including the integration of heterogeneous components, unrelated to materials currently used in semiconductor fabrication, and their positioning with near-atomic precision.

Here we present a new method for the templated conjugation of marginally water-soluble organic molecules to DNA-adapters, with the aim to provide close control over the position and orientation of the molecule within self-assembled single-molecule electronic devices. This method provides a way to conjugate different DNA sequences to the same molecule without the need to provide orthogonal chemistries on the target molecule. It also allows purification of the intended product and screening for the correctly assembled device. It thus provides a promising new tool for the programmable fabrication of molecular electronics.

[1] Aviram A, Ratner MA 1974. *Chem. Phys. Lett.* **29**, 277

Electrolyte transport through single-walled carbon nanotubes

François HENN^{a,*}, Khadija YAZDA^{a,b}, Saïd TAHIR^a, Thierry MICHEL^a, Bastien LOUBET^c, Manoel MANGHI^c, Jeremy BENTIN^d, Fabien PICAUD^d, John PALMERI^a, Vincent JOURDAIN^a

- a. Equipe Nanomatériaux, Laboratoire Charles Coulomb, UMR 5221 CNRS, Univ. Montpellier, Montpellier, France
- b. Nanoscience for energy technology and sustainability, ETH, Zürich, Switzerland;
- c. Laboratoire de physique théorique (IRSAMC), UMR 5152 CNRS, Université Toulouse 3 Paul Sabatier, Toulouse, France
- d. Laboratoire de Nanomédecine Imagerie et Thérapeutique (NIT), EA4662, Université de Bourgogne Franche-Comté, UFR ST & CHU Médecine, France

* francois.henn@umontpellier.fr

The strong interest for nanofluidics stems from the unique transport phenomena that appear as fluids are confined in nanoscale geometries where surface effects become of central importance. Among the different nanochannels studied so far, single-walled carbon nanotubes (SWCNTs) have gained special attention due to their perfect tubular structure, their high aspect-ratio and their smooth walls in addition to other remarkable mechanical, electronic and optical properties. However, creating and studying SWCNT-based nanofluidic systems free of damage, plugs or leaks remain extremely challenging [1]. We will present ionic current measurements through microfluidic devices containing one or several SWCNTs with diameters between 1.2 to 2 nm showing a linear or, unexpectedly, a voltage-activated, i.e. a non-linear, I-V dependence [2,3]. Transition from an activated to a linear behaviour and stochastic fluctuations between different current levels were notably observed. For linear devices, the high conductance confirmed with different chloride salts indicates that the nanotube/water interface exhibits both a high surface charge density and flow slippage, in agreement with previous reports. In addition, the sublinear dependence of the conductance on the salt concentration points toward a charge-regulation mechanism. Theoretical modelling and computer simulations show that the voltage-activated behaviour can be accounted for by local energy barriers along or at the ends of the nanotube. Raman spectroscopy reveals strain fluctuations along the tubes induced by the polymer matrix but displays insufficient information about doping or variations of doping to account for the apparent surface charge density and energy barriers revealed by ion transport measurements. Finally, experimental evidence points toward chemical moieties at the nanotube mouths as being responsible for the voltage-activated transport of ions through SWCNTs within this diameter range.

- 1) "Fabrication of Microfluidic Devices for the study of Ion transport through Single-Walled Carbon Nanotubes", Yazda et al, MRS Advances, 1(28), 2085-2090, (2016)
- 2) "Evidence of selective cation transport through sub-2 nm single-walled carbon nanotubes", Yazda et al, MRS Advances, 1(28), 2079-2084, (2016)
- 3) "Voltage-activated transport of ions through single-walled carbon nanotubes", Yazda et al, Nanoscale 9, 11976, (2017)

Self-assembly and strain engineering of bimetallic nanowires: tuning magnetic nanoalloy properties via vertical epitaxy

M. Hennes,^{a*} X. Weng,^a A. Coati,^b A. Vlad,^b Y. Garreau,^{b,c} M. Sauvage-Simkin,^b
E. Fonda,^b D. Demaille,^a Y. Zheng,^a and F. Vidal^a

- a. Sorbonne Université, CNRS-UMR 7588, Institut des NanoSciences de Paris, INSP, F-75005 Paris, France
- b. Synchrotron Soleil, L'Orme des Merisiers Saint-Aubin BP 48, 91192 Gif-sur-Yvette Cedex, France
- c. Université Paris Diderot, Sorbonne Paris Cité, MPQ, UMR 7162 CNRS, Bâtiment Condorcet, Case courrier 7021, 75205 Paris Cedex 13, France

* hennes@insp.jussieu.fr

Strain is a key parameter affecting the physical properties of nanosized objects. In addition to size and composition, it represents another degree of freedom which allows for functionality tuning of nanoalloys. During the last decade, vertically assembled nanocomposites, *i.e.* hybrid columnar structures with strong interfacial coupling, have emerged as a novel platform for strain engineering approaches. But while oxide-oxide systems have been studied extensively [1,2], the full potential of multicomponent metallic structures vertically epitaxied in oxide matrices has not been explored in detail yet [3].

With this background, we present results on hybrid Co-based metal-oxide systems obtained *via* sequential pulsed laser deposition. Using high-resolution transmission electron microscopy, X-ray diffraction and X-ray absorption spectroscopy, we demonstrate that our synthesis approach allows to grow ultrathin nanoalloy wires, vertically epitaxied in various oxide matrices like SrTiO₃ or CeO₂. Depending on the nanoalloy, these wires can be perfectly mixed (*e.g.* CoNi), or display interesting segregation patterns (*e.g.* CoAu). By complementing these results with detailed magnetometry measurements, we demonstrate how $\langle \epsilon_{zz} \rangle$, the average axial strain in the wires resulting from nanoalloy-matrix interactions, impacts the effective magnetic anisotropy of the composites. We eventually show that $\langle \epsilon_{zz} \rangle$ can be tuned by changing the nanoalloy size, composition or the oxide matrix type, thereby paving the way for full strain engineering of these hybrid nanoalloy-based systems.

- [1] J. Huang, J. MacManus-Driscoll and H. Wang, *Journal of Materials Research* **32** (2017) 4054-4066
- [2] A. Chen, J.-M. Hu, P. Lu, T. Yang, W. Zhang, L. Li, T. Ahmed, E. Enriquez, M. Weigand, Q. Su, H. Wang, J.-X. Zhu, J. L. MacManus-Driscoll, L.-Q. Chen, D. Yarotski and Q. Jia, *Science Advances* **2** (2016) e1600245
- [3] F. J. Bonilla, A. Novikova, F. Vidal, Y. Zheng, E. Fonda, D. Demaille, V. Schuler, A. Coati, A. Vlad, Y. Garreau, M. Sauvage Simkin, Y. Dumont, S. Hidki, and V. Etgens, *ACS Nano* **7** (2013) 4022-4029

Thermodynamics of metabolic energy conversion under muscle load

Ch. Goupil,^a, E. Herbert^{a*}, H. Ouerdane^b et Y. D'Angelo^{a,c}

- a. Laboratoire Interdisciplinaire des Energies de Demain (LIED), CNRS UMR 8236, Université Paris Diderot, 5 Rue Thomas Mann, 75013 Paris, France
- b. Center for Energy Systems, Skolkovo Institute of Science and Technology, 3 Nobel Street, Skolkovo, Moscow Region 143026, Russia
- c. Laboratoire Mathématiques & Interactions J. A. Dieudonné, Université Côte d'Azur, UNS, CNRS UMR 7351, Parc Valrose, 06108 Nice, France

* eric.herbert@univ-paris-diderot.fr

The complexity of the metabolic processes at the heart of energy conversion in living organisms is a great obstacle to the development of tractable thermodynamic models of metabolism, which would be based on the definition of a small set of physical parameters. In this talk, we construct such a thermodynamic model and show how it can apply in biomechanics by considering the case of muscle load. We assume that living organisms are dynamical systems experiencing a feedback loop, in the sense that they can be considered as thermodynamic systems subjected to mixed (coupled potentials and fluxes) boundary conditions. These feedback effects give rise to homeostatic mechanisms keeping key physiological parameters such as, e.g., body temperature and osmotic pressure, within specific and narrow ranges. The complex nature of such a kind of systems may be dealt with at the cost of raising the abstract analysis to a higher level, but with the advantage of offering a compact approach that relies on a few generic parameters only. To this purpose, we consider a conversion zone as an equivalent thermodynamic working fluid under mixed boundary conditions. The energy conversion process becomes a combination of “one-to-many” (entropy generating) and “many-to-one” (work producing) processes. We introduce and derive the generalized thermoelastic coefficients of the working fluid equivalent, as well as the metabolic transport coefficients from which we define the metabolic figure of merit. Intrinsic muscle friction dissipates the converted energy during muscle mechanical activity, but the chemical-mechanical coupling also causes a dissipative mechanism, which we call the feedback resistance. We discuss the impact of the feedback resistance on the metabolic energy conversion under muscle load. Finally, our approach allows to give a thermodynamic ground to Hill's widely used muscular operational response theory.

- [1] Y. Apertet, H. Ouerdane, C. Goupil, and Ph. Lecoœur, *Phys. Rev. E* **90**, 012113 (2014).
- [2] A. V. Hill, *Proc. Royal Soc. B*, **126**, 612 (1938).

Structural relaxation related to resistance drift in amorphous GeTe thin films

F. Hippert^{a*}, J.-Y. Raty^{b,c}, F. d'Acapito^d, P. Montéléon^c, C. Sabbione^c,
N. Castellani^c, P. Kowalczyk^c, N. Bernier^c and P. Noé^c

- a. LNCMI (CNRS, Université Grenoble Alpes, UPS, INSA), Grenoble, France.
- b. Physics of Solids Interfaces and Nanostructures, Université de Liège, Belgium.
- c. Université Grenoble Alpes, CEA-LETI, Grenoble, France.
- d. CNR-IOM-OGG c/o ESRF, Grenoble, France.

*Francoise.Hippert@lncmi.cnrs.fr

Chalcogenide phase-change materials (PCM) such as Ge₂Sb₂Te₅ or GeTe alloys can be quickly and reversibly switched between an amorphous and a polycrystalline phase with very different optical and electrical properties [1]. This outstanding combination of properties led to their use first in optical and recently in resistive non-volatile memories. Resistive PCM memories are a promising candidate in order to replace the FLASH memories at technology nodes under 28 nm and to fill the gap between DRAM and NAND [2]. In a PCM memory, the amorphous or crystalline state of a small confined volume of the PCM is selected by application of a programming current pulse. One major issue in the development of PCM memories is to understand and reduce the resistance drift (resistance increase with time, i.e. with ageing) of the amorphous phase, especially for the development of multi-level cell storage technology. The origin of the resistance drift in chalcogenide phase-change glasses has been widely debated but no consensus emerged up to now on the nature of the structural relaxation occurring during ageing. *Ab initio* simulations of the amorphous GeTe phase [3] have suggested that the number of homopolar Ge-Ge bonds decreases with ageing. The Ge-Ge bonds are inherent to the presence of tetrahedrally bonded Ge atoms. The fully relaxed amorphous structure would be a Peierls-distorted structure consisting of 3-fold (distorted octahedral environment) Ge and Te atoms with only Ge-Te bonds. This ideal structure reminds that of the GeTe crystal structure but with much larger local Peierls distortions. In contrast with these predictions we observed from the analysis of Extended X-Ray Absorption Fine Structure (EXAFS) at the Ge K-edge [4] and Fourier-transform infrared (FTIR) spectroscopy that the number of Ge-Ge bonds increases upon ageing in amorphous GeTe thin films deposited by sputtering. One possible explanation of these results could be a clustering of the Ge atoms in amorphous GeTe upon ageing. Such a segregation is indeed found in Transmission Electron Microscope images of an aged film and confirmed by the excellent agreement found between the total structure factor measured by X-ray scattering and calculated by new *ab initio* simulations that include Ge segregation [5].

[1] S. Raoux and M. Wuttig, *Phase Change Materials: Science and Applications* (Springer Science & Business Media, New York, USA, 2009).

[2] A. Redaelli, *Phase Change Memory, Device Physics, Reliability and Applications* (Springer International Publishing AG, 2018).

[3] J.Y. Raty *et al*, Aging mechanisms in amorphous phase-change materials, *Nature. Com.* **6**, 7467 (2015); S. Gabardi, S. Caravati, G. C. Sosso, J. Behler and M. Bernasconi, Microscopic origin of resistance drift in the amorphous state of the phase-change compound GeTe, *Phys. Rev. B* **92**, 054201 (2015).

[4] P. Noé *et al*, Structural change with the resistance drift phenomenon in amorphous GeTe phase change materials thin films, *J. Phys. D: Appl. Phys.* **49**, 035305 (2016).

[5] P. Noé *et al*, to be published.

Printed organic photodetectors

Lionel HIRSCH

a. Univ. Bordeaux, IMS, CNRS, UMR 5218, Bordeaux INP, ENSCBP, F-33405 Talence, France

* lionel.hirsch@ims-bordeaux.fr

Printed organic photodetectors (OPDs) can transform plastic, paper or glass into smart surfaces. This innovative technology is now growing exponentially due to the strong demand in human-machine interfaces [1, 2]. To date, only niche markets are targeted since organic sensors. But as their performances start to compete their inorganic counterparts, their use will spread over the market.

Our work establishes the rules to achieve a *state-of-the-art* organic photodetector by printing techniques [3]. We demonstrate that it is possible to engineer a highly efficient organic sensor approaching the performances of Si-based photodiodes in terms of dark current, responsivity and detectivity by using low-cost printing technology. As a result, we simplified the device architecture as much as possible to make the whole process compatible with large-area printed technologies and industrial constraints. In a second part, we also report long operational lifetimes of organic photodetectors (OPDs) and the failure mechanisms investigation [4]. The combination of the thermally stimulated current (TSC) and the I-V characteristics versus temperature (I-V-T) techniques along with the extensive use of the drift-diffusion simulations all reveal that the observed degradation is the consequence of the generation of shallow traps (0.2 eV, $N_T = 10^{16} \text{ cm}^{-3}$) that significantly reduce the charge carrier mobility. In contrast, deep traps (0.7 eV, $N_T = 7 \times 10^{15} \text{ cm}^{-3}$) are found to be present on freshly prepared samples and their concentration remains unchanged after ageing.

References

- [1] Rim, Y. S., Bae, S.-H., Chen, H., De Marco, N. and Yang, Y. *Adv. Mater.* 28, 4415–4440 (2016).
- [2] Armin, A., Jansen-van Vuuren, R. D., Kopidakis, N., Burn, P. L. and Meredith, P. *Nat. Commun.* 6, 6343 (2015).
- [3] Kielar, M., Dhez, O., Pecastaings, G., Curutchet, A. and Hirsch, L., *Scientific Reports* 6, 3920; (2016).
- [4] Kielar, M., Daanoun M., François-Martin O., Flament B., Dhez O., Pandey A. K., Chambon S., Clerc R. and Hirsch L., *Adv. Electron. Mater.* 1700526 (2018).

Emergent Electrochemistry in Spin Ice: Debye–Hückel Theory and Beyond

P. C. W. Holdsworth^{a*}, V. Kaiser^{a,b}, J. Bloxom^c, L. Bovo^c, S.T. Bramwell^c, R. Moessner^b

- a. Université de Lyon, ENS de Lyon, Université Claude Bernard, CNRS, Laboratoire de Physique, F-69342 Lyon, France.
- b. Max-Planck-Institut für Physik komplexer Systeme, 01187 Dresden, Germany.
- c. London Centre for Nanotechnology and Department of Physics and Astronomy, University College London, London WC1H 0AH, United Kingdom

* peter.holdsworth@ens-lyon.fr << corresponding author >>

The low-temperature picture of dipolar spin ice in terms of the Coulomb fluid of its fractionalised magnetic monopole excitations has allowed analytic and conceptual progress far beyond its original microscopic spin description. Here we develop its thermodynamic treatment as a ‘magnetolyte’, a fluid of singly and doubly charged monopoles, an analogue of the electrochemical system $2\text{H}_2\text{O} = \text{H}_3\text{O}^+ + \text{OH}^- = \text{H}_4\text{O}^{2+} + \text{O}^{2-}$, but with perfect symmetry between oppositely charged ions. For this lattice magnetolyte, we present an analysis based on Debye–Hückel theory, which is accurate at all temperatures and incorporates ‘Dirac strings’ imposed by the microscopic ice rule constraints at the level of Pauling’s approximation. Our results are in close agreement with the specific heat from numerical simulations as well as new experimental measurements with an improved lattice correction, which we present here, on the spin ice materials $\text{Ho}_2\text{Ti}_2\text{O}_7$ and $\text{Dy}_2\text{Ti}_2\text{O}_7$. Our study of the magnetolyte shows how electrochemistry can emerge in non-electrical systems. We also provide new experimental tests of Debye–Hückel theory and its extensions. The application of our results also yields insights into the electrochemical behaviour of water ice and liquid water, which are closely related to the spin ice magnetolyte.

- [1] Vojtech Kaiser, Jonathan Bloxom, Laura Bovo, Steven T. Bramwell, Peter C.W. Holdsworth, Roderich Moessner “Emergent Electrochemistry in Spin Ice: Debye-Huckel Theory and Beyond”, arXiv:1803.04668.

Figure 1: To add a figure, save it as figure1.eps (as figure1.pdf for pdflatex), and remove the % before `\includegraphics` in the .tex file. Please make the image file as small as possible, while keeping reasonable resolution on screen (max 0.1MB).

Silicon for Beauty and Structure

Roland Horisberger^{a*}

a. Paul Scherrer Institute, CH-5232 Villigen, Switzerland

* roland.horisberger@psi.ch

The early development of highly segmented and very precise silicon particle detectors happened historically in field of high energy physics in the early 1980's. At the time this was very much driven by the needs in particle physics experiments to detect and identify pico-second long lived particles, containing beauty and charm quarks. The presentation will give a brief historical overview of this development and the driving requirements that defined its developments. Over the years the new detector technology has gone through an enormous growth and improvement in capability and complexity. This was on one hand through the growing demands on the performance of the particle tracking systems at the newest accelerators like the LHC proton-proton collider at CERN and at the same time due to the technological progress in microelectronics, symbolized by Moore's Law. The potential of using this new and precise detector technology in other domains of physics was realized early on. By now, the use of highly segmented silicon strip and pixel detectors has made a phenomenal impact in the field of photon science at synchrotron facilities and free electron X-ray laser machines. They allow now to resolve in an almost unprecedented way the structural and functional information on complex solid state systems and biological molecules. The talk recalls how in the case of the PILATUS, MYTHEN and EIGER pixel system the silicon detector revolution in photon science has happened. Furthermore it will attempt to give an outlook on how the next generation detectors might evolve, given the requirements from future photon science experiments.

Development of a high brightness ultrafast Transmission Electron Microscope based on a laser-driven cold field emission source

F. Houdellier^{1*}, G-M. Caruso¹, S. Weber¹ and A. Arbouet^{1*}
¹ CEMES-CNRS, 29 Rue Jeanne Marvig, 31055 Toulouse, FRANCE-EU
* florent.houdellier@cemes.fr and arnaud.arbouet@cemes.fr

The potential of scientific instruments for materials science is largely conditioned by the properties of the particle source on which they rely. For instance, in Transmission Electron Microscopy (TEM), it is the superior brightness of cold field emission (CFE) sources that enables the acquisition of electron holograms, from which modifications of the phase of the electron wave function can be retrieved and traced back to the electrostatic, magnetic or strain fields of the sample, or that allowed the amount of coherent probe current to be maximized for optimum high resolution STEM imaging and spectroscopy. The first Ultrafast Transmission Electron Microscopes (UTEM) provided a unique insight into the physics of nano-objects with both sub-picosecond temporal resolution and nanometer scale spatial resolution but could not be used for ultrafast electron holography because of the poor brightness of their electron source [1,2].

We report on the development of an ultrafast cold field electron source and its use for Ultrafast Transmission Electron Microscopy [4,5]. We follow a different approach compared to the recently developed ultrafast laser-driven Schottky electron source in which electron emission is confined to the apex of a tip by the use of the additional suppressor electrode available on usual Schottky type module and by chemical selectivity using a zirconia wetting layer on the [100] oriented front facet of the tungsten (W) tip [3].

In the present work, we have modified a cold field emission source to integrate laser optics in the immediate vicinity of the [310] oriented W nanotip to minimize the size of the laser focal spot on the tip apex, minimize the size of the emission region and therefore maximize the brightness of the source [4]. Most problems related to the integration of optical components in the ultra-high vacuum and high voltage area close to the FE tip have been solved, by paying particular attention to the global electron optics performance of the 200kV based CFE gun (mainly spherical and chromatic aberrations). We will describe the architecture of this ultrafast CFEG, report on numerical simulations of the electron beam properties and electric field in the electron gun. The performance of the electron source as a function of laser parameters, extraction voltage, gun lens strength, as well as the properties of the electron probe (brightness, angular current density, stability) will be addressed [5]. Finally, the potential of this high-brightness ultrafast CFEG-TEM for conventional imaging, diffraction in parallel and convergent beam, high resolution imaging, electron energy loss spectroscopy and off-axis holography using 150keV ultrashort electron pulses will be illustrated.

- [1] Zewail, A. H., *Science*, 2010, 328, 187-193
- [2] Zewail, A. H., USPTO n°US7,154,091 of December 26. 2006
- [3] A.Feist *et al*/Ultramicroscopy. 176, 63-73, (2017)
- [4] G.M. Caruso *et al*/Appl. Phys. Lett. 111, 023101, (2017)
- [5] F.Houdellier *et al*/Ultramicroscopy. 186, 128-138, (2018)

Memory-driven run and tumble deterministic dynamics

Maxime Hubert^{a*}, Stéphane Perrard^{b,c,d}, Matthieu Labousse^{b,e}, Nicolas Vandewalle^a et Yves Couder^b

- a. GRASP, UR CESAM, Institute of Physics, Université de Liège, Liège, Belgium, EU
- b. Matière et Systèmes Complexes, CNRS UMR 7057, Université Paris Diderot, Sorbonne Paris Cité, 75013 Paris, France, UE
- c. LadHyX, CNRS UMR 7646, École Polytechnique, 91128, Palaiseau, France, EU
- d. Laboratoire FAST, CNRS UMR 7608, Univ. Paris-Sud, CNRS, Université Paris-Saclay, 91405 Orsay, France, EU
- e. Gulliver, CNRS UMR 7083, ESPCI Paris and PSL University, 75005 Paris France, UE

* maxime.hubert@uliege.be

Walking droplets show unique properties thanks to their peculiar feature: the wave path-memory [1]. The original experiment involves an oil millimetric droplet bouncing periodically on a vertically shaken liquid surface [2]. The successive impacts of the droplet create standing waves, keeping track of its previous positions and propelling it along the surface. Thanks to the Faraday instability, the wave time of persistence can be remotely controlled. One has a unique physical system: a particle evolving in synergy with its self-generated wavefield which acts as a memory of tunable duration.

We focus here on the regime of extremely long persistence time from a numerical point of view, which exhibits a macroscopic diffusive behavior as seen in Fig.1. The diffusive dynamics is composed of two successive phases: straight line motion interspersed with chaotic exploration of small areas. This behavior mimics dynamics encountered in biology in the case of foraging animals [3] or for the run and tumble motion of bacteria [4]. We show that the overall dynamics is driven by a Shil'nikov-type chaos in the velocity space. We also discuss the diffusive dynamics of the walker, where the memory duration tunes its superdiffusive behavior. This is the first evidence of controlled and tunable diffusive motion of a single particle ruled by deterministic dynamics and driven by memory effects.

- [1] Eddi, A., Sultan, E., Moukhtar, J., Fort, E., Rossi, M. & Couder, Y. Information stored in Faraday waves: the origin of a path memory, *J. Fluid Mech.* **674**, 433-463 (2011).
- [2] Couder, Y., Protière, S., Fort, E. & Boudaoud, A. Walking and orbiting droplets, *Nature* **437**, 208 (2005).
- [3] Viswanathan, G. M., Afanasyev, V., Buldyrev, S. V., Murphy, E. J., Prince, P. A. & Stanley, H. E. Lévy flight search patterns of wandering albatrosses, *Nature* **381**, 413-415 (1996).
- [4] Tailleur, J. & Cates, M. E., Statistical Mechanics of Interacting Run-and-Tumble Bacteria, *Phys. Rev. Lett.* **100**, 218103 (2008).

Transient string formation in colloid monolayers at bubble interfaces under ultrafast deformation

Axel Huerre*, Marco De Corato, Valeria Garbin

Department of Chemical Engineering, Imperial College London, London SW7 2AZ, United Kingdom

*axel.huerre@gmail.com

Droplets and bubbles stabilized by a monolayer of microparticles are exploited in encapsulation and catalysis. Particle-stabilized bubbles are the building blocks of lightweight materials based on foams, and are central in enhanced oil recovery. Despite their importance in applications, our fundamental understanding of the behaviour of particle-laden interfaces under dynamic deformation remains limited. While shear rheology has been the focus of recent research [1-2], the effect of compression remains largely unexplored.

To impart controlled, dynamic compression of a particle-laden interface, we subject particle-coated bubbles to ultrasonic driving. This method enables us to achieve compression-expansion of the monolayer in the frequency range 10-100 kHz [3, 4]. The bubbles (60-400 μm), stabilized by a monolayer of microparticles (1-5 μm), are monitored with high-speed video microscopy to resolve the evolution of the monolayer, and extract single-particle trajectories. We then characterize the dynamics of the 2D microstructure through order parameters, interparticle distance and pair correlation function. We find that the periodic oscillation of the interface drives a qualitatively different evolution of the monolayer compared to what is commonly observed under shear deformation. Specifically, we observe self-assembly of the particles into a network of strings (Figure 1b).

We ascribe the emergence of strings to transient interparticle interactions occurring during dynamic deformation. A simple force balance on a sphere attached to the interface by capillary forces, and undergoing oscillations normal to the interface, reveals the importance of the particle's inertia for a micron-sized colloid on the ultrafast timescale of our experiments. The motion of the particle normal to the interface causes a deformation of the interface leading to transient capillary interactions between the particles (Figure 1a). Particle-based simulations show that the emergence of strings can be explained by the coupling of this transient deformation with the equilibrium deformation initially present due to nanoscale undulations of the contact line.

This work [5] provides the first demonstration of unique dynamical phenomena upon extreme deformation of complex fluid interfaces, and lays the foundations for studies of high-frequency rheology of particle-laden interfaces.

- [1] I. Buttinoni, Z. A. Zell, T. M. Squires and L. Isa, 2015, *Soft Matter*, **11**, 8313.
- [2] N. C. Keim and P. E. Arratia, 2015, *Soft Matter*, **11**, 1539.
- [3] V. Poulichet and V. Garbin, 2015, *Proceedings of the National Academy of Sciences*, **112**, 5932.
- [4] V. Poulichet, A. Huerre and V. Garbin, 2017, *Soft Matter*, **13**, 125.
- [5] A. Huerre, M. De Corato and V. Garbin, 2018, *ArXiv:1802.09318*.

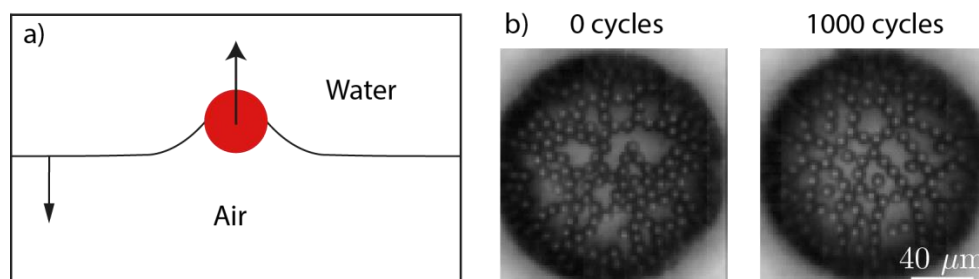


Figure 1 a) Schematics of the colloidal particle attached at the interface. Under oscillations, the particle deforms the interface. b) This deformation leads to complex capillary interactions between particles, favouring the appearance of an ordered structure composed of strings.

Emergence of the spontaneous and stimulation-induced neural activity on the brain connectome

Etienne Hugues^{a*}, et Olivier David^a

a. INSERM U1216, Grenoble Institut des Neurosciences, Grenoble, France.

* etienne.hugues@univ-grenoble-alpes.fr

Motivated by the discovery of a complex spatial structure in resting state BOLD fMRI functional connectivity (FC) and the availability through the use of diffusion MRI of the human connectome –linking local neural networks through white matter fibers, a lot of theoretical work has been devoted in the last decade to the understanding of the underlying mechanisms behind such spatial organization. A plausible dynamical scenario is that the neural dynamics at each local node of the brain but also at the global network level, fluctuates around a fixed point under the effect of local noise [1,2]. More recently, the spontaneous state of the brain has also been found to exhibit scale-free neural avalanches. The preceding theoretical scenario is found to be unable to reproduce such behaviour. Moreover, when trying to reproduce the well established propagation of neural activity on the brain network in response to an external stimulation, this scenario fails to reproduce it, the response decaying strongly while propagating on the network [1], even when trying to correct for such decay [2].

In this work, we address these problems by proposing a new biologically plausible dynamical scenario. At the single node level, we propose that the neural network dynamics also exhibits a fatigue mechanism, like neuronal adaptation. Such a mechanism is found to locally lead to a possible bistability in the dynamics, with a low and a high activity state. While the relative couplings between nodes are given by the connectome, the tuning of their absolute value through a global coupling allows to explore the emerging global dynamics. For an intermediate level of this coupling, and under the effect of noise, scale-free avalanches are found, consisting of series of local low to high activity state switch events. For a sufficiently strong stimulation, a specific propagation of neural activity occurs on the network, as classically observed experimentally, accompanied by a reduction of neuronal firing variability -across trials- as widely observed in electrophysiological experiments [3]. Moreover, for this level of global coupling, BOLD FC is found to fit best the empirical FC, and better than in the case where the model exhibits the preceding fluctuation scenario, that is for model parameters for which local state switches are made impossible. In conclusion, placing the model dynamics in a regime of scale-free avalanches allows to reproduce the diverse signatures of spontaneous and stimulation-induced neural activity on the brain connectome.

[1] G. Deco, A. Ponce-Alvarez, P. Hagmann, G.L. Romani, D. Mantini, and M. Corbetta, How local excitation-inhibition ratio impacts the whole brain dynamics, *J. Neurosci.* **34**, 7886 (2014)

[2] M.R. Joglekar, J.F. Mejias, G.R. Yang, and X.-J. Wang, Inter-areal balanced amplification enhances signal propagation in a large-scale circuit model of the primate cortex, *bioRxiv*, doi: <http://dx.doi.org/10.1101/186007> (2017)

[3] M.M. Churchland et al., Stimulus onset quenches neural variability: a widespread cortical phenomenon, *Nature Neurosci.* **13**, 369 (2010)

Hawking Radiation and Quantum Fluctuations in BEC

Mathieu Isoard^{a*}, Nicolas Pavloff,^a

a. LPTMS, CNRS, Univ. Paris-Sud, Université Paris-Saclay, 91405 Orsay, France

* isoard.mathieu@gmail.com >>

We study the density-density correlation function $g_2(x, x')$ near the acoustic horizon in a quasi uni-dimensional transonic flow realized in a Bose-Einstein condensate. The aim is to accurately describe for the first time the detailed structure of g_2 near the horizon in a realistic configuration. For this purpose one needs to take the specifics of the flow into account and to include evanescent modes in the theoretical description of the elementary excitations. This should make it possible to perform a detailed comparison with the recent experimental findings of Steinhauer [1].

- [1] J. Steinhauer, Observation of quantum Hawking radiation and its entanglement in an analogue black hole, Nature Physics volume 12, pages 959–965 (2016)

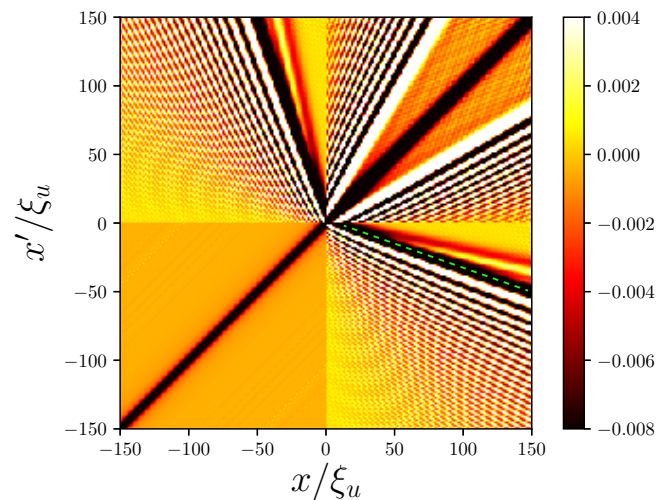


Figure 1: Density-density correlation function $\xi_u n_u g_2(x/\xi_u, x'/\xi_d)$. The variables ξ_u and n_u are the healing length and the asymptotic density in the subsonic region (outside the black hole). The green dashed line corresponds to a signature of the analogue of the Hawking signal.

Effet de l'anisotropie cristalline sur l'homogénéisation des microstructures en solidification eutectique

Maxime IGNACIO^{a*}, Mathis Plapp^a

a. Laboratoire de Physique de la Matière Condensée, École Polytechnique

* maxime.ignacio@gmail.com

Comprendre la micro-structuration lors d'expériences de solidification d'alliage eutectique est essentiel pour les applications technologiques, mais aussi d'un point de vue fondamental. En effet, ces systèmes sont un très bel exemple de système dynamique dissipatif où l'on observe la formation spontanée de motifs (auto-organisation).

Jusqu'à présent, les effets de l'anisotropie cristalline sur la sélection des motifs, et plus largement sur leurs évolutions, restent mal compris. Dans des conditions de solidification proche du point eutectique, la phase solide croît sous forme d'un réseau de lamelles. Durant la solidification, il existe des processus de type diffusif qui tendent à homogénéiser l'espacement lamellaire, soit par élimination de lamelles, soit par uniformisation. Les récentes observations expérimentales de solidification directionnelle de couches minces du groupe de S. Akamatsu (INSP Paris) [1] montrent que l'anisotropie peut modifier, en encore bloquer l'homogénéisation des espacements lamellaires. Analytiquement, nous avons obtenu une équation d'évolution du front de solidification prenant en compte l'anisotropie (équation de diffusion de la phase). Nos prédictions analytiques montrent que l'anisotropie modifie non seulement le seuil de stabilité pour lequel il n'existe pas d'élimination de lamelles, mais aussi le coefficient de diffusion gouvernant l'évolution lamellaire. Ces prédictions sont comparées à des simulations de type champs de phases (mésoscopique) nous permettant d'obtenir l'évolution lamellaire.

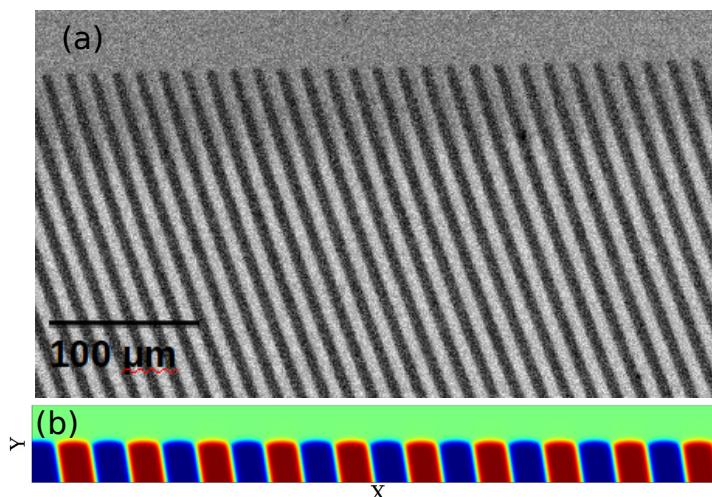


Figure 1 : (a) Image expérimentale de croissance directionnelle d'un alliage CBr₄-C₂Cl₆. (b) Simulation champs de phases d'un alliage symétrique en présence d'anisotropie.

[1] S. Akamatsu, S. Bottin-Rousseau, M. Serefolgu, G. Faivre, « *A theory of thin lamellar eutectic growth with anisotropic interphase boundaries* », Acta Materialia 60, 3199 (2012)

Magnetic field free spin torque induced oscillations in magnetic tunnel junction with perpendicular polarizer and planar free layer

V. Iurchuk^{a*}, N. Lamard^a, J. Langer^b, J. Wrona^b, I. L. Prejbeanu^a, L. Vila^a,
R. Sousa^a and U. Ebels^a

a. Univ. Grenoble Alpes, CEA, CNRS, INAC, SPINTEC, F-38000 Grenoble, France

b. Singulus Technologies AG, 63796 Kahl am Main, Germany

* vadym.iurchuk@cea.fr

Spin torque nano-oscillators (STNOs) are non-linear auto-oscillating systems known to produce steady state magnetization precession in the microwave range, which occur when current-induced spin-transfer torque (STT) balances the intrinsic Gilbert damping of a magnetic layer. STNOs based on magnetic tunnel junctions (MTJ) are considered as attractive alternative to the conventional voltage controlled oscillators due to its nanoscale size, large frequency tunability, and simple integration with conventional CMOS technology. To improve the microwave performances recent studies concentrate on STNOs where either polarizer or free layer has strong interfacial perpendicular anisotropy which may lead to enhanced output power and eventual zero-field operation [1,2].

Here we report on the observation of the room-temperature zero-magnetic-field STT-induced microwave generation in the MTJ with perpendicular polarizer and planar free layer (Figure 1(a)). Above the critical current $I_C \sim -0.6$ mA, the excitations are steady state auto-oscillations with frequencies up to 3 GHz and emitted power up to 7 nW. The frequency of the signal strongly depends on the driving current above the critical value exhibiting the pronounced “redshifting” behavior, with the value of the frequency-current tuning ratio $df/dI \sim 5.7$ GHz/mA (Figure 1(b)), several times larger than reported up to now [3]. This opens a possibility of current-induced wide-range frequency modulation in such devices.

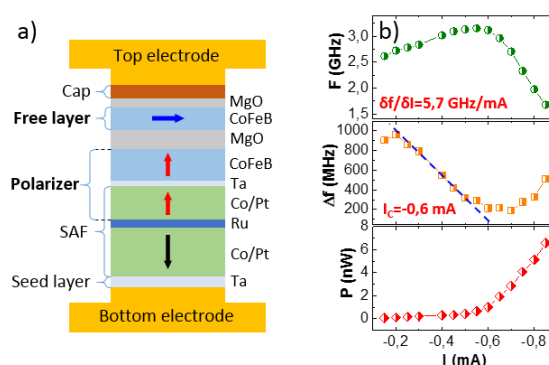


Figure 1 : (a) Schematics of the MTJ stack. Arrows denote the magnetization orientations at zero field. (b) Center frequency, FWHM linewidth and peak power of the generated signal at zero magnetic field

- [1] D. Houssameddine, et al, Spin-torque oscillator using a perpendicular polarizer and a planar free layer *Nat. Mater.* **6** 447–53 (2007)
- [2] H. Kubota, et al, Spin-Torque Oscillator Based on Magnetic Tunnel Junction with a Perpendicularly Magnetized Free Layer and In-Plane Magnetized Polarizer *Appl. Phys. Express* **6** 103003 (2013)
- [3] B. Fang, et al, Zero-field spin transfer oscillators based on magnetic tunnel junction having perpendicular polarizer and planar free layer *AIP Adv.* **6** 125305 (2016)

Visualization of out of equilibrium superconductivity

T. Jalabert^{1*}, F. Lévy-Bertrand², C. Chapelier¹

1. Université Grenoble Alpes, CEA, INAC-PHELIQS, 38000 Grenoble, France
2. ²Université Grenoble Alpes, CNRS, Institut Néel, 38000 Grenoble, France

* thomas.jalabert@cea.fr

Strongly disordered superconductors (MoSi, WSi, TiN, NbN,...) have recently gained a lot of interest for the engineering community, in particular for photon detection, in radioastronomy (KIDs) and telecommunications (SNSPDs). Up to now, only transport measurements over macroscopic samples in the gigahertz range have been performed, and reveal some electromagnetic anomalies preventing optimal detection.

Besides, Scanning Tunneling Microscopy (STM) is the ideal tool to map the electronic properties on a nanometer scale in order to characterize the spatial inhomogeneities in disordered superconductors. Thus, we etched nanowires in order to perform simultaneously transport measurements and scanning tunneling spectroscopy on a superconducting single mesoscopic device, and we succeed in our experimental setup to locate and probe a single superconducting nanowire driven out-of-equilibrium.

A second kind of imaging can be performed with a STM, that we named *scanning critical current microscopy*. In this technique the pair breaking efficiency of the injection of quasiparticle at different energies by the STM tip is deduced by monitoring the critical current of the superconducting nanowire as a function of the tip position. Furthermore, when exposed to a magnetic field, vortices, which carry quantized flux, develop in superconducting films. Their cores bear a singularity of the superconducting order parameter and therefore behave as quasiparticles traps. These vortices can be imaged with an STM by polarizing the tunneling junction near the superconducting gap edge energy.

Up to now, we demonstrated the influence of the tunneling current on the superconducting critical current of our nanowires, we characterized bare films of disordered superconductors and developed an etching technique for the nanowires but we only performed measurement on conventional superconductors.

The possible correlation of the scanning critical current current microscopy with the spatial inhomogeneities in the gap amplitude, sub-gap states or vortices will be analyzed. The results will be used to understand better the position dependence of the photon detection efficiency, the role of inhomogeneity in the behavior of superconducting detectors and the competition between the trapping of quasiparticles inside the vortex and the recombination process into Cooper pairs.

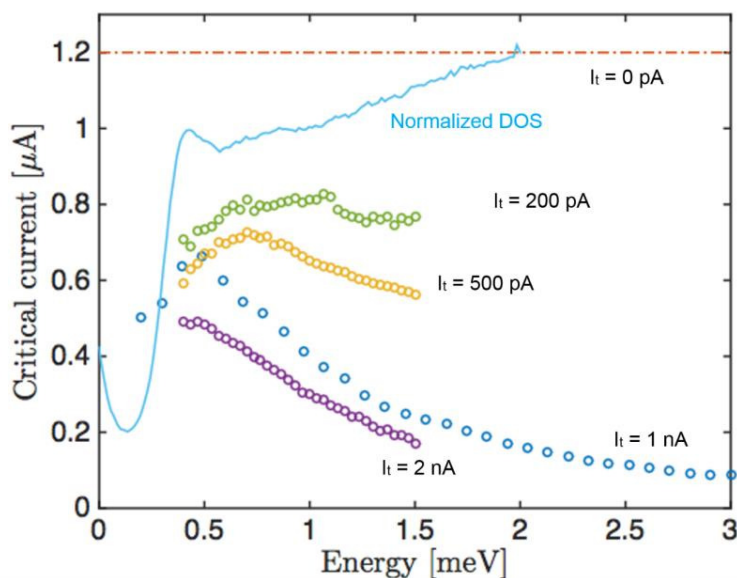


Figure 1 : The energy of the quasiparticles injected by the STM tip, as well as their injection rate affects the superconducting critical current and is believed to be related to the Cooper pairs recombination time.

Piezoresponse force microscopy on semiconductor III-Nitride bulk, thin film and single nanowires

Lucas Jaloustre^{1,2,3}, Simon Le-Denmat^{1,2}, Franck Dahlem³ and Rudeesun Songmuang^{1,2}

¹Université Grenoble Alpes, F-38000, Grenoble, France

²CNRS, Institut Néel, Nanophysique et Semiconducteurs group, F-38000, Grenoble, France

³Laboratoire de Tribologie et Dynamique des Systemes, UMR CNRS 5513, Ecole Centrale de Lyon, 36 avenue Guy de Collongue - 69134 Ecully Cedex France

Coupling between piezoelectric and semiconducting properties of piezoelectric semiconductor nanowires such as wurtzite ZnO or GaN has been proposed as a promising feature that can integrate a small mechanical movement to function electronic/photonic nano-devices [1]. These nano-objects have also been used for generating electrical energy from mechanical energy from tiny vibrations in our environments [2]. For fundamental studies and applications, it is crucial to access the electromechanical properties of these nanowires. Scanning probe microscopy (SPM) is considered as one of the most powerful tools; besides challenging, that are able to locally probe these properties in nanostructures.

Here, we applied piezoresponse force microscopy (PFM) to explore a reversed piezoelectric effect, in III-Nitride nanowires. It is known that the PFM signal can be strongly influenced by various parameters such as an electrostatic effect induced by a surface potential or surface charges, a non-uniform electric field caused by a nanoscale SPM tip's diameter, a contribution of lateral piezoelectric displacement of the material to a vertical movement of the SPM tip. Our intensive works done on different reference samples; i.e. Periodically Poled Lithium Niobate, Langasite, GaN bulks and GaN thin films, show that those mentioned factors significantly hinder quantitative PFM measurements in both amplitude and phase which directly correspond to the piezoelectric coefficient and the material polarity, respectively. The electrostatic contribution from the surface potential is probed by Kelvin probe force microscopy (KPFM). Its effect is minimized by applying a direct voltage on the substrate during the PFM measurements, by using high spring constant cantilever, or by depositing metallic electrodes on the sample surface. Those electrodes also improve the uniformity of the applied electric field but at the price of a reduced lateral resolution. We show that the vertical and lateral piezoelectric displacement can be observed separately by properly setting the sample configuration.

The studies on these reference samples were used as a general guideline for the PFM measurement of single nanowires i.e. GaN nanowires and GaN/AlN nanowire heterostructures. The vertical and lateral movements detected by the SPM tip are visible when a modulated AC voltage is applied on the nanowires. To be better spatially resolved, the measurements are further performed at the mechanical resonant frequency of the SPM cantilever to enhance the PFM signal. The origin of those detected PFM signals will be discussed.

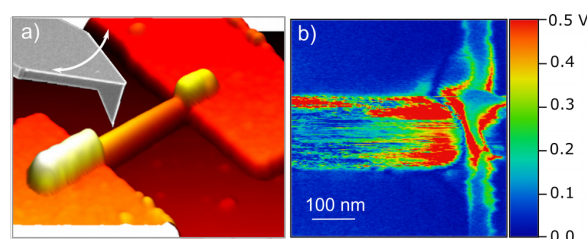


Figure 1 (a) Schematic representation of the PFM measurement on single contacted nanowire. White arrow shows the lateral movement direction of the AFM cantilever during the application of AC voltage. (b) Lateral PFM amplitude showing the mechanical movement along the nanowire axis.

[1] Z. L. Wang, Towards self-powered nanosystems: From nanogenerators to nanopiezotronics, *Adv. Funct. Mater.* **18**, 3553–3567 (2008)

[2] Z. L. Wang, J. Song, Piezoelectric nanogenerators based on zinc oxide nanowire arrays, *Science*. **312**, 242–246 (2006)

Out-of-equilibrium Mott insulators to metal transitions: from fundamental issues to applications in non-volatile memories and in artificial intelligence

Etienne Janod ^{a*}, Benoit Corraze ^a, Julien Tranchant ^a, Marie-Paule Besland ^a,
Coline Adda ^a, Danylo Babich ^a, Madec Querré ^{a,b}, Pablo Stoliar ^{a,c}, Marcelo
Rozenberg ^d, D. Lorcy ^e et Laurent Cario ^a

- a. Institut des Matériaux Jean Rouxel, Univ. de Nantes – CNRS, Nantes, France
- b. now at STMicroelectronics, Crolles, France
- c. now at National Institute of Advanced Science and Technology (AIST), Tsukuba, Japan
- d. Laboratoire de Physique des Solides, CNRS – Univ. Paris Saclay, Orsay, France
- e. Institut des Sciences Chimiques de Rennes, Univ. Rennes 1 – CNRS, Rennes, France

* etienne.janod@cnsr-imn.fr

The study of strongly correlated materials in nonequilibrium conditions has developed into one of the most exciting branches of condensed matter physics. These systems have already fascinating properties at equilibrium, such as high temperature superconductivity. Driving them out of equilibrium might yield even richer physics, of which only a small fraction has been discovered so far. Mott insulators correspond to the archetype of correlated systems. The famous Mott insulator to metal transitions (IMT), driven at equilibrium by on-site electron repulsion or electronic doping, has sparked a huge interest over the last fifty years. Interestingly, recent developments have unveiled the possibility to trigger out-of-equilibrium IMT in Mott insulators, by applying either ultra-short laser pulses [1] or electric fields [2]. The transition driven by electric field turned out to be a universal feature of canonical Mott insulators [3,4,5]. In these compounds, an abrupt drop of electrical resistance occurs above a threshold electric field E_{th} typically in the 1-10 kV/cm range. This Electric Mott Transition (EMT), volatile for fields slightly above E_{th} , becomes non-volatile at larger electric fields. These EMT allows envisioning applications in the emerging field of Mottronics (domain aiming at using Mott insulators properties in microelectronics) such as non-volatile Mott memories [6]. Moreover, it was recently demonstrated that the volatile Electric Mott transition can be used to implement the three basic functions Leaky, Integrate and Fire expected for artificial neurons [7], paving the way of their use in Hardware Neural Networks. In parallel, significant progresses have been recently achieved in the understanding of the nature of the phases associated with the non-volatile states and of the microscopic mechanisms driving the EMT's. These recent advances, as well as the remaining opened theoretical issues, will be presented and discussed.

-
- [1] H. Yamakawa *et al.*, Mott transition by an impulsive dielectric breakdown, *Nature Mater.* **16**, 110 (2017)
 - [2] E. Janod *et al.*, Resistive Switching in Mott Insulators and Correlated Systems, *Adv. Func. Mater.* **25**, 6287 (2015).
 - [3] L. Cario *et al.*, Electric-Field-Induced Resistive Switching in a Family of Mott Insulators: Towards a New Class of RRAM Memories, *Adv. Mater.* **22**, 5193 (2010).
 - [4] P. Stoliar *et al.*, Resistive Switching Induced by Electric Pulses in a Single-Component Molecular Mott Insulator, *J. Phys. Chem. C* **119**, 2983 (2015).
 - [5] P. Stoliar *et al.*, Universal Electric-Field-Driven Resistive Transition in Narrow-Gap Mott Insulators, *Adv. Mater.* **25**, 3222 (2013).
 - [6] M. Querré *et al.*, Non-volatile resistive switching in the Mott insulator $(V_{1-x}Cr_x)_2O_3$, *Physica B* **536**, 327 (2018)
 - [7] P. Stoliar *et al.*, A Leaky-Integrate-and-Fire Neuron Analog Realized with a Mott Insulator, *Adv. Funct. Mater.* **27**, 1604740 (2017)

Reentrance behaviour in the vicinity of classical spin liquids.

L.D.C. Jaubert^{a*}, O. Benton^b, K. Essafi^c, R. Pohle^d,
M. Udagawa^e, J. Oitmaa^f, R. Singh^g, N. Shannon^d

- a. CNRS, Université de Bordeaux, LOMA, UMR 5798, 33400 Talence, France
- b. RIKEN Center for Emergent Matter Science (CEMS), Wako, Saitama, 351-0198, Japan
- c. Sorbonne Universités, LPTMC, 4 Place Jussieu, 75252 Paris Cedex 05, France
- d. Okinawa Institute of Science and Technology, Onna-son, Okinawa 904-0495, Japan
- e. Department Physics, Gakushuin University, Mejiro, Toshima-ku, Tokyo 171-8588, Japan
- f. School of Physics, The University of New South Wales, Sydney 2052, Australia
- g. Department of Physics, University of California, Davis, California 95616, USA

* ludovic.jaubert@u-bordeaux.fr

Quantum critical points famously separate different phases at zero temperature via a continuous phase transition. Their effects are being felt over a broad temperature range, whose quantum critical fluctuations often support neighbouring exotic magnetic phases. In this poster, we will explore its classical analogue when one of the two neighbouring phases is a spin liquid. The enhancement of symmetry at this zero-temperature boundary would naively suggest a “more disordered” phase than the neighbouring spin liquid. However, this enhanced ground-state manifold may actually allow for critical fluctuations (soft modes) to concentrate on regions of the phase space that are otherwise inaccessible at low temperature. Order by disorder then plays its role, and the magnetic order of this high-symmetry point spreads like a fan at finite temperature. This fan gives rise to a reentrant behaviour above the spin liquid, and is continuously connected to more traditional order on the other side of the phase diagram. When order by disorder is not possible, then an extension of the idea of reentrance is possible for the competition between disordered spin liquids at finite temperature. To illustrate the different facets of this physics, several models will be discussed in two and three dimensions.

Collective excitability in a mesoscopic neuronal model of epileptic activity

Maciej Jedynek^{a,b,c,d,*}, Antonio J. Pons^a and Jordi Garcia-Ojalvo^b

- a. Departament de Física, Universitat Politècnica de Catalunya (UPC), Terrassa, Spain
- b. Department of Experimental and Health Sciences, Universitat Pompeu Fabra (UPF), Parc de Recerca Biomèdica de Barcelona, Barcelona, Spain
- c. INSERM U1216, Grenoble Institut des Neurosciences, Grenoble, France.
- d. Université Grenoble Alpes, Grenoble, France.

* maciej.jedynak@protonmail.com

At the mesoscopic scale, the brain can be understood as a collection of interacting neuronal oscillators, but the extent to which its sustained activity is due to coupling among brain areas is still unclear. Here we address this issue in a simplified situation by examining the effect of coupling between two cortical columns described via Jansen-Rit neural mass models. Our results show that coupling between the two neuronal populations gives rise to stochastic initiations of sustained collective activity, which can be interpreted as epileptic events. For large enough coupling strengths, termination of these events results mainly from the emergence of synchronization between the columns, and thus it is controlled by coupling instead of noise. Stochastic triggering and noise-independent durations are characteristic of excitable dynamics, and thus we interpret our results in terms of collective excitability.

[1] Jedynek, M., Pons, A. J., & Garcia-Ojalvo, J. (2018). Collective excitability in a mesoscopic neuronal model of epileptic activity. *Physical Review E*, 97(1), 012204.

Effect of the environment on the elastic properties of CeO₂ nanocubes studied by *in situ* ETEM nanocompression

L. Joly-Pottuz^{a*}, T. Epicier^a, M. Cobian^b, T. Albaret^c, D. Stauffer^d, K. Masenelli-Varlot^a

- a. Univ Lyon, INSA-Lyon, MATEIS UMR5510, Bât. Blaise Pascal, 7 Avenue J. Capelle, 69621 Villeurbanne Cedex, France
 - b. Univ Lyon, ECL Ecully, LTDS UMR5513, 36 Avenue de Collongue, 69134 Ecully, France
 - c. Univ Lyon, UCB Lyon 1, ILM, CNRS UMR 5306, 69621 Villeurbanne, France
 - d. Bruker Nano surfaces, Hysitron Inc, 9625 W 76th St., Minneapolis, MN 55344, USA
- * lucile.joly-pottuz@insa-lyon.fr

Characterization of nanomaterials or materials at the nanoscale has drastically been improved during the last decades. A challenge lies in the *in situ* microstructural characterization of such materials as it can give access to valuable information regarding the microstructural changes induced by their use in working conditions (for instance during compaction process in the case of ceramic nanoparticles). The availability of dedicated TEM (Transmission Electron Microscopy) holders equipped with nano-indenters, e.g. hard tips, is of very high interest to test *in situ* the mechanical properties of nanometer-sized objects [1]. In the case of plastic deformation of crystalline nano-objects, Molecular Dynamics simulations have shown that dislocation nucleate at the surface [2, 3]. Therefore, it might be interesting to investigate such mechanical aspects with experiments in a controlled environment (i.e. under gas pressure) which reproduces the real one.

A Hysitron PI 95 Picoindenter has recently been installed on a Cs-corrected FEI Titan ETEM (Environmental TEM) microscope. It opens the possibility of performing *in situ* compression under gas pressure, with high resolution imaging capabilities. We will present a comprehensive study on CeO_x nanocubes. Nanocubes are compressed either under vacuum or under air pressure, with different irradiation doses to obtain various compositions ($1.5 < x < 2$). In order to minimize data dispersion due to mechanical accommodation for instance, we focus on the elastic regime. This way, it is possible to compare the elastic moduli deduced from a Digital Image Correlation based analysis on the same nanocube but with different oxygen contents. To better understand the reduction/oxidation process and its effect on the mechanical properties, we present DFT+U simulations on bulk systems with various compositions. The stability of each crystallographic phase is in agreement with the literature [4] and with experimental observations. Significant changes in the calculated elastic moduli are obtained and compared with experimental results.

[1] Q. Yu, *et al.* MRS Bulletin 40, 62-70 (2015); [2] S. Lee, *et al.* Nat. Commun. 5:3033 (2014); [3] I. Issa *et al.* Acta Mater. 86, 295-304 (2015); [4] J.L.F. Da Silva, Phys. Rev. B 76 (2007), p. 193108.

Acknowledgements: LABEX iMUST (ANR-10-LABX-0064) of Université de Lyon, within the program "Investissements d'Avenir" (ANR-11-IDEX-0007) operated by the ANR, CLYM (www.clym.fr) for the access to the microscope and A.K.P. Mann, Z. Wu and S.H. Overbury (ORNL, USA) for having provided the samples.

Non-equilibrium transport in multi-terminal topological superconductor systems

T. Jonckheere^{a*}, J. Rech^a, A. Zazunov^b, R. Egger^b, T. Martin^a

- a. Centre de Physique Théorique, CNRS, Aix-Marseille Univ., Campus de Luminy, case 907, 13009 Marseille
- b. Institut für Theoretische Physik, Heinrich Heine Universität, D-40225 Düsseldorf, Germany

* thibaut.jonckheere@cpt.univ-mrs.fr

A topological superconductor (TS) nanowire has unique properties, including a Majorana bound states at each of its ends. These Majorana bound states have a strong impact on the transport properties. While most studies of the transport have been devoted to the transport between two TS or between a TS and a normal metal electrode, considering a 3-terminal system allows to explore more subtle properties of the Majorana bound states. These 3-terminals systems have the potential to uncover new physics, and to give access to new ways to characterize unambiguously the presence of Majorana bound states in experiments.

I will first present results on a topological superconductor beam splitter,[1] where a central TS nanowire is connected to two normal leads which are set at arbitrary voltages. Using a Hamiltonian formalism, we compute the mean current and the current-current correlations. We observe that the sign of the current-current correlations is opposite to the case of a standard BCS superconductor beam splitter, and we show that this is a direct consequence of the electron-hole symmetric nature of the majorana bound state.

Then I will show results for a 3-terminal system made of 3 TS nanowires.[2] There the behavior is richer and more complex. The mean current shows features typical of multiple Andreev reflection (MAR) processes, while the current-current correlations can reach huge values. I will explain how this surprising behaviour is due to a combination of MAR processes and fluctuations created by direct coupling between the Majorana bound states.

[1] T. Jonckheere, J. Rech, A. Zazunov, R. Egger and T. Martin Phys. Rev. B **95**, 054514 (2017)

[2] T. Jonckheere, J. Rech, A. Zazunov, R. Egger and T. Martin, *in preparation*

La dispersion du rayonnement X: cristaux et réseaux

Philippe JONNARD^{a*}

- a. Sorbonne Université, Faculté des Sciences et Ingénierie, CNRS UMR 7614, Laboratoire de Chimie Physique – Matière et Rayonnement, 4 place Jussieu, F-75252 Paris cedex 05, France

* philippe.jonnard@upmc.fr

Il est possible de connaître l'état physico-chimique d'un atome en examinant son spectre d'émission X. Pour cela une bonne résolution spectrale est nécessaire. En conséquence le rayonnement polychromatique émis par l'échantillon doit être analysé en spectroscopie à dispersion de longueur d'onde (ou WDS, wavelength dispersive spectrometry). Les spectromètres WDS comportent un élément dispersant le rayonnement X, cristal, pseudo-cristal ou réseau, et un détecteur.

Afin de faire de la spectroscopie WDS, nous présentons les moyens de disperser le rayonnement électromagnétique dans le domaine XUV (énergie supérieure à 30 eV). Nous aborderons tout d'abord la diffraction de Bragg, utilisée classiquement en microanalyse X quantitative pour disperser le rayonnement X (énergie supérieure à 150 eV). La diffraction par une lame cristalline permet d'analyser le rayonnement X d'énergie supérieure à 500 eV. Pour disperser de rayonnement plus mou, il n'existe pas de cristaux ayant de distance réticulaire adaptée. Il faut alors utilisé des pseudo-cristaux, qui sont en fait des multicouches périodiques. Leur période nanométrique permet d'accéder à la gamme des rayons X mous (150 – 500 eV). Cependant, leur résolution spectrale est limitée. Nous montrerons rapidement que cette limitation peut être contournée en gravant ces multicouches. Dans un second temps, nous aborderons la diffraction des réseaux, utilisée pour disperser le rayonnement dans une large gamme spectrale, 30 – 1000 eV. Nous exposerons la loi des réseaux et les montages classiques basés sur ce principe. Nous terminerons en présentant deux schémas de spectromètres, basés sur les réseaux à pas variable et sur les lentilles de Fresnel, permettant de travailler en champ plan, c'est-à-dire d'obtenir le spectre avec un détecteur linéaire sans réaliser de balayage angulaire.

La diffraction de Kossel combinée à l'émission X induite par protons pour l'étude de multicouches nanométriques

Philippe JONNARD^{a*}, Meiyi Wu^a, Karine Le Guen^a, Ian Vickridge^b, Didier Schmaus^b, Emrick Briand^b, Philippe Walter^c, Qiushi Huang^d, Zhanshan Wang^d

- Sorbonne Université, Faculté des Sciences et Ingénierie, CNRS UMR 7614, Laboratoire de Chimie Physique – Matière et Rayonnement, 4 place Jussieu, 75252 Paris cedex 05
- Sorbonne Université, Faculté des Sciences et Ingénierie, CNRS UMR 7588, Institut des NanoSciences de Paris, 4 place Jussieu, 75252 Paris cedex 05
- Sorbonne Université, Faculté des Sciences et Ingénierie, CNRS UMR 8220, Laboratoire d'Archéologie Moléculaire et Structurale, 4 place Jussieu, 75252 Paris cedex 05
- Key Laboratory of Advanced Micro-Structured Materials, Institute of Precision Optical Engineering, School of Physics Science and Engineering, Tongji University, Shanghai 200092, China

* philippe.jonnard@upmc.fr

Les multicouches constituées d'un empilement périodique de couches nanométriques sont largement utilisées pour disperser le rayonnement X. Cependant, afin de présenter une bonne réflectivité, et donc une bonne efficacité, il est nécessaire qu'il existe un fort contraste entre les indices optiques des différentes couches. Toute interdiffusion aux interfaces va diminuer ce contraste et limiter les performances de la multicouche. C'est pourquoi il est important de comprendre les phénomènes prenant place aux interfaces de ces structures.

Dans ce but, nous développons une méthodologie pour analyser les films minces à l'échelle nanométrique en combinant la diffraction de Kossel avec l'émission de rayons X induite par des ions (PIXE). Cette technique s'apparente à la méthode des ondes stationnaires. Nous rapportons la diffraction de Kossel, générée par l'irradiation avec un faisceau de protons de 2 MeV, de multicouches d'épaisseur nanométrique à base de Pd/Y. Ces multicouches sont préparées soit avec l'ajout d'azote dans le gaz de pulvérisation, soit avec l'ajout de barrières de diffusion, de fines couches de B₄C, aux interfaces. Ces stratégies de dépôt visent à limiter la diffusion entre les couches de palladium et d'yttrium.

L'intensité de l'émission caractéristique Pd L α est mesurée en fonction de son angle de détection. Une oscillation d'intensité est observée lorsque l'angle de détection varie autour de l'angle de Bragg, défini par l'énergie de l'émission et la période de la multicouche. En effet, dans les conditions de Bragg, une onde stationnaire ayant la période de la multicouche se développe et se décale perpendiculairement aux couches quand l'angle change. La variation de l'angle de détection entraîne un décalage des ventres et nœuds du champ électrique émis dans la multicouche et permet donc de sonder différents endroits de l'empilement. Grâce à l'emploi d'une caméra CCD permettant à tout angle d'une plage angulaire donnée la sélection de l'énergie des rayons X, l'ensemble de la configuration expérimentale est fixe et aucun balayage angulaire n'est requis.

En comparant les formes des courbes de Kossel, nous sommes en mesure de déduire que la multicouche Pd/Y nitrurée a beaucoup moins de mélange aux interfaces que la multicouche non-nitrurée. Les résultats montrent qu'il est possible de distinguer par la forme des courbes de Kossel des échantillons déposés avec des couches barrière B₄C situées à des interfaces différentes ou ayant des épaisseurs différentes. Cela démontre que la diffraction de Kossel est sensible à la structure de l'empilement.

Ionic liquids: the prepeak paradox

Patrick Judeinstein^{a*}, Manuel Maréchal^b, Laurence Noirez^a, Benoit Coasne^c

- a. LLB, UMR12 (CNRS-CEA), CEA Saclay, 91191 Gif sur Yvette, France
- b. SyMMES, UMR 5819 (Univ. Grenoble Alpes-CNRS-CEA), 38000 Grenoble, France
- c. LiPhy, UMR 5588 (CNRS & Univ. Grenoble Alpes), 38402 Saint Martin d'Hères Cedex

*patrick.judeinstein@cea.fr

Room-temperature ionic liquids are pure salts which are liquid at room temperature. Their chemical structure is a subtle combination of two antagonist counterparts, a polar and an apolar domains which are chemically linked together. This intimate assembly leads to nanoscale segregation, which have:

i) a dynamical signature: cation dynamics present a multi modal scale-dependant behavior, with a localized motion within the IL nanometric domains at shorter time scale and a genuine long-range translational motion for longer times.¹

ii) a structural signature: a strong scattering called pre-peak is often observed at small scattering vector (below 0.5 \AA^{-1}) corresponding to correlation lengths larger than the size of the ions ($1 - 3 \text{ nm}$).²

However, the physical origin of the prepeak is still not explicit: it is related to the segregation between polar and apolar unfriendly domains but only slight change of the molecular structure may wipe off this specific feature.

In this talk, we propose a robust approach to describe $S(Q)$ scattering curves and propose a clearer image of IL nanostructuration: wide-angle neutron scattering (WANS) on selectively deuterated IL samples allows to contrast the different counterparts of these complex liquids. A detailed analysis of these findings will be proposed from a molecular dynamic approach.

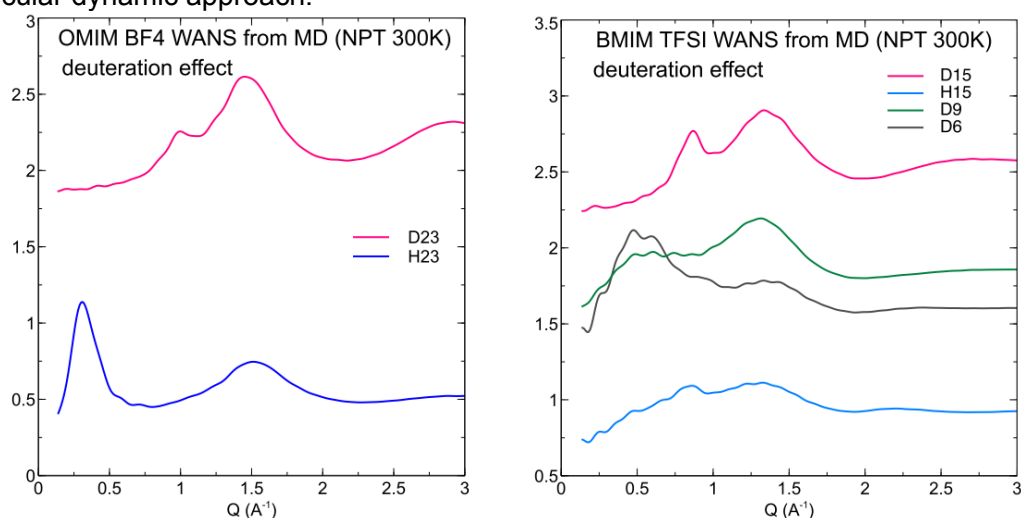


Figure 1: Effects of deuteration sites on neutron structure factor $S(Q)$ profiles as obtained from Molecular Dynamic approach for two different ionic liquids: i) OMIMBF₄ (left) ; H23 all hydrogen, D23 all deuterium ; ii) BMIMTFSI (right); H15 all hydrogen, D15 all deuterium, D6 imidazolium deuterated, D9 alkyl chain deuterated.

[1] F. Ferdeghini, Q. Berrod, J.-M. Zanotti, P. Judeinstein, et al., *Nanoscale*, **9**, 1901 (2017)

[2] A. Martinelli, M. Maréchal, Å. Östlund, J. Cambedouzou, *Phys. Chem. Chem. Phys.*, **15** 5510 (2013)

Manipulation of magnetic skyrmions in ultrathin Pt/Co/MgO nanostructures

R. Juge^a, S-G Je^a, D. de Souza Chaves^b, S. Pizzini^b, L. D. Buda-Prejbeanu^a, L. Aballe^c, M. Foerster^c, A. Locatelli^d, T. O. Mendes^d, F. Maccherozzi^e, S. S.Dhesi^e, S. Auffret^a, G. Gaudin^a, J. Vogel^b and O. Boulle^{a,*}

[a] SPINTEC, CEA-INAC, CNRS, Université Grenoble Alpes, Grenoble INP, Grenoble, France.

[b] Institut Néel, CNRS, Université Grenoble Alpes, Grenoble, France.

[c] ALBA Synchrotron Light Facility, Cerdanyola Del Vallès, Barcelona, Spain.

[d] Elettra Sincrotrone, Trieste, Italy.

[e] Diamond Light Source, Chilton, Didcot, UK.

*Corresponding author: olivier.boulle@cea.fr

Magnetic skyrmions are nanoscale whirling spin configurations. Their small size, topological protection and the fact that they can be manipulated by small in-plane current densities have opened a new paradigm to manipulate the magnetisation at the nanoscale. This has led to proposal for novel memory and logic devices in which the magnetic skyrmions are the information carriers [1]. The recent observation of room-temperature magnetic skyrmions [2,3] and their current-induced manipulation [4,5] in ultrathin sputtered magnetic nanotracks have lifted an important bottleneck toward the practical realisation of such devices.

Here we report on the manipulation of isolated room-temperature magnetic skyrmions in sputtered single-layered Pt/Co/MgO nanostructures using external magnetic field [6] and in-plane current pulses. Using X-ray Magnetic Circular Dichroism - Photo-Emission Electron Microscopy (XMCD-PEEM), we observed a fast current-induced motion of small skyrmions ($\sim 150\text{nm}$) in μm -wide tracks. In Fig.1.(a-c), we present a series of images showing a magnetic skyrmion after two consecutive 11 ns current pulses with opposite polarities and with an amplitude of $6 \times 10^{11} \text{ A/m}^2$. The skyrmion is dragged back and forth with a motion characteristic of a left-handed Néel skyrmion: it moves against the electron flow with a component of the velocity transverse to it, an effect referred to as the Skyrmion Hall Effect. Mean velocities up to 100 m/s were observed for a current density of about $6.75 \times 10^{11} \text{ A/m}^2$ (Fig 1.(d)).

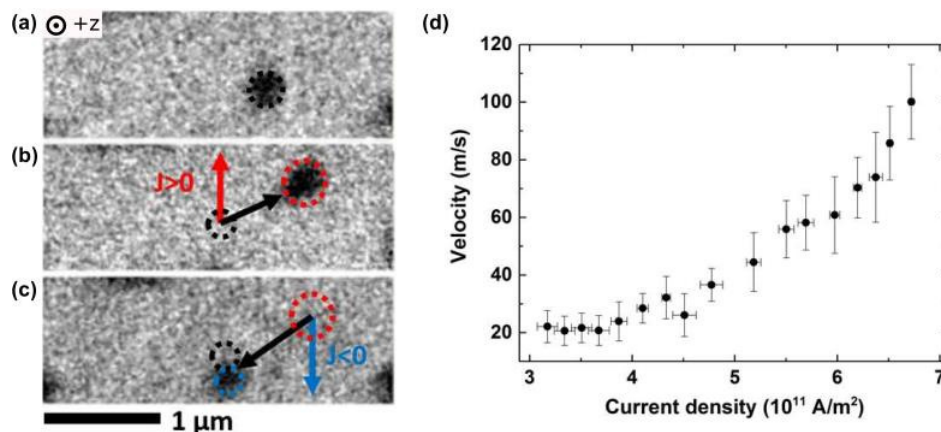


Figure 1 : (a-c) XMCD-PEEM images of a magnetic skyrmion (a) before, (b) after a positive 11 ns in-plane current pulse and (c) after a negative one with $|J|=6 \times 10^{11} \text{ A/m}^2$. The applied field is $\mu_0 H_z = -4\text{mT}$. (d) Average skyrmions velocity measured in $3 \mu\text{m}$ -wide tracks as a function of the current density.

- [1] Fert *et al.*, Nat Nano 8 (3), 152 (2013)
- [2] Moreau-Luchaire *et al.*, Nat Nano, 11 (5), 444 (2016)
- [3] Boulle *et al.*, Nat Nano 11 (5), 449 (2016)
- [4] Jiang *et al.*, Science 349 (6245), 283 (2016)
- [5] Woo *et al.*, Nat Mat 15 (5), 501 (2016)
- [6] Juge *et al.*, JMMM 455, 3-8 (2018)

Effects of micro-confinement on diphasic systems.

Marie-Caroline Jullien^{a,*}, Julien Marchalot^a, Vincent Miralles^a, Axel Huerre^a, Benjamin Reichert^a, Olivier Theodoly^b and Isabelle Cantat,^c

a. UMR Gulliver 7083, ESPCI Paris, PSL Research University

b. IPR UMR 6251, Université de Rennes 1

c. LAI UMR 7333, Aix Marseille University

* << marie-caroline.jullien@espci.fr >>

The emergence of microfluidics has led to a significant increase in the study of multiphase fluid flows at micrometric scales, both for dense (foams, emulsions) and diluted systems. Although multiphase flows have been studied for many decades, a simple question arises: are there other mechanisms involved at these scales (e.g. by the presence of interfaces) that modify the behavior of the studied systems? This question is crucial as droplet microfluidic systems are becoming more complex and their development requires an understanding of the peculiarities of flows at these scales. This presentation does not intend to present the results of a specific experiment, but rather to show through two experimental configurations, that there are a number of situations where microfluidics provide new experimental and theoretical advances to better understand the dynamics of micro-confined two-phase flows.

In a first step, we will present the main results obtained in the case of dense systems, namely a two-dimensional soap foam. Because of the small confinement, the pressures involved are large, preventing the development of liquid films between adjacent bubbles. This property has the advantage of reducing the theoretical aging time of microscale dry foams and making them model systems for flow studies. More precisely, we will show that the monodispersity of foams obtained in these systems, coupled with the absence of films, make them model systems for studying interfacial rheology. In a second step, we addressed the crucial question in microfluidics, to determine the velocity of a droplet in a Hele-Shaw cavity when it is carried by an external fluid of set velocity. Predicting the speed of the droplets requires identifying beforehand the mechanisms of dissipation in the droplet, in the menisci and in the lubrication film. Our approach was therefore initially to analyze the topography of the lubrication film by adapting an interferometric instrumentation (RICM). In particular, we show that the intermolecular forces, the disjoining pressure, intervening on the nanometric scale directly influence the dynamics of the droplets. Microfluidics even makes it possible to establish isotherms of disjoining pressure. The analysis of the topography of the lubrication film makes it possible to go back to the local properties of the interface (interfacial velocity, surface tension).

- [1] V. Miralles, E. Rio, I. Cantat and M.-C. Jullien, Investigating the role of a poorly soluble surfactant in a thermally driven 2D microfoam, *Soft Matter* **12**, 7056-7062 (2016)
- [2] A. Huerre, O. Theodoly, A. Leshanky, M.-P. Valignat, I. Cantat, and M.-C. Jullien, *Phys. Rev. Lett.*, **115**, 064501 (2015).
- [3] B. Reichert *et al.*, JFM submitted.

Abrupt change in thermoelectric transport due to a quantum dot's bound state

Etienne Jussiau^{a*}, Robert S. Whitney^a

a. Université Grenoble-Alpes, CNRS, LPMMC, 38000 Grenoble, France

* etienne.jussiau@lpmmc.cnrs.fr

We study a quantum thermoelectric made up of a single-level quantum dot coupled to two leads that can be described by the exactly solvable Fano-Anderson Hamiltonian [1]. We consider the case of a power-law spectral density with a band edge [2]. In this configuration, one may distinguish two regimes depending on the strength of the coupling between the dot and the reservoirs: If the coupling parameter is higher than a critical value, a bound state outside of the continuum and thus with infinite lifetime appears. We analyze the influence of the latter on the steady state of the system and show that the reduced dynamics of the dot explicitly depends on the existence of the bound state. We show that there is an abrupt change in the thermoelectric transport properties at the critical point. Typically, the thermoelectric efficiency grows as the coupling approaches its critical value, but then drops sharply at the critical point.

- [1] U. Fano, Effects of configuration interaction on intensities and phase shifts, Phys. Rev. 124(6), 1866 (1961)
 [2] G. Engelhardt, G. Schaller and T. Brandes, Bosonic Josephson effect in the Fano-Anderson model, Phys. Rev. A 94, 013608 (2016)

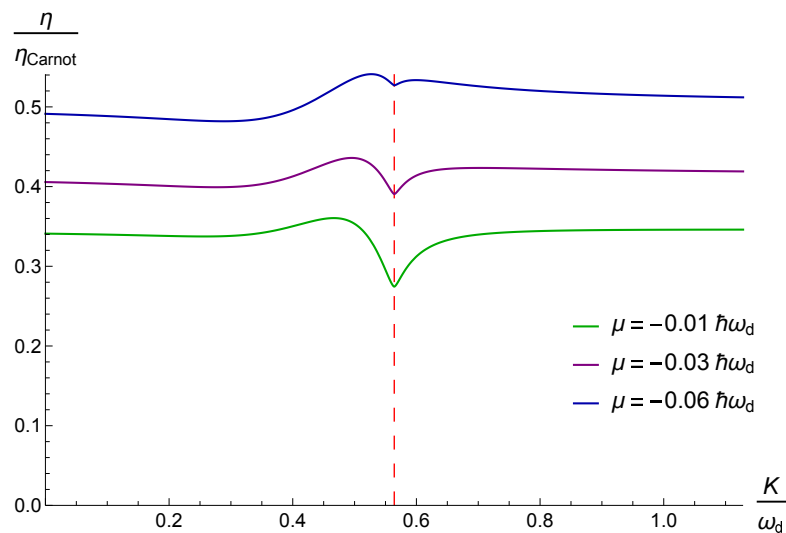


Figure 1: Efficiency of the thermoelectric as a function of the coupling between the quantum dot and the leads for various chemical potentials. The red dashed line represents the critical value of the coupling parameter. One can clearly see that the efficiency grows and then sharply drops approaching this point.

Study of the influence of crystal structure on ion migration energy from high throughput bond valence calculations

Nebil A. Katcho^{a*}, J. Rodríguez Carvajal^a, J. Carrete^b, N. Mingo^c, J. Carrasco^d

- Institut Laue-Langevin, 71 Avenue des Martyrs, CS 20156, 38042 Grenoble Cedex 9, France
- Institute of Materials Chemistry, TU Wien, A-1060 Vienna, Austria
- CEA-LITEN, 17 Avenue des Martyrs, 38000 Grenoble, France
- CIC Energigune, Albert Einstein 48, 01510 Vitoria-Gasteiz, Spain

* katcho@ill.fr

Progress in energy-related technologies demands new and improved materials with high ionic conductivities. Na- and Li-based compounds have high priority in this regard due to their importance for batteries. Recent developments in bond valence (BV) theory have made it possible a fast determination of ion diffusion energy barriers and ion diffusion paths [1,2]. An immediate application of these advances is the identification of potential high ionic conductors from the screening of large crystal structure databases. In this communication, we present a high-throughput exploration of the chemical space for such compounds. We show that there are significantly fewer Na-based conductors with low migration energies, as their favorable properties hinge on exceptional combinations of properties. To perform this analysis, we introduce a methodology based on bond-valence theory, graph percolation and a combined geometric and topological analysis of each structure. Specifically, we combine short-range descriptors based on a Voronoi construction, with a search for the global bottleneck in the ion transport path based on a hard-sphere model. A machine-learning analysis reveals that the ion migration energy depends mainly on the bottleneck, the coordination number of the cation and the volume fraction of the mobile species. We have implemented this workflow in the open-source Crystallographic Fortran Modules Library (CrysFML) [3].

[1] S. Adams and R. P. Rao, *Struct. Bond.* 158, 129-160 (2014)

[2] I. D. Brown, *Chem. Rev.* 109, 6858-6919 (2009)

[3] <https://forge.epn-campus.eu/projects/crysfml>

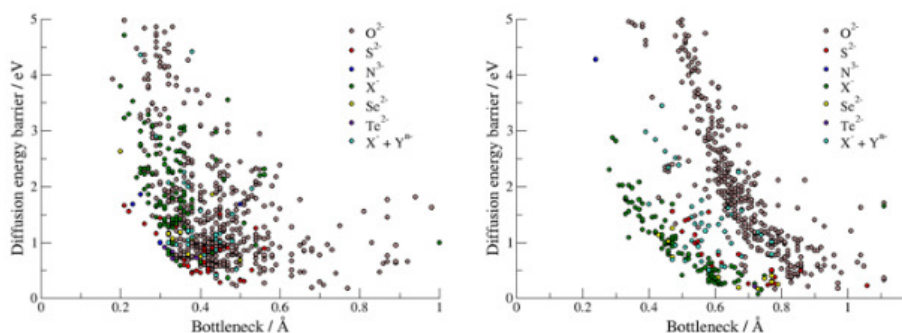


Figure 1 : High-throughput screening results for Li (left) and Na (right) compounds of the ICSD.

Green/Yellow/Red Emission From *m*-plane Core-shell InGaN/GaN Nanowires

A. Kapoor^{a*}, N. Guan^b, L. Mancini^b, C. Bougerol^{a, d}, F. H. Julien^b, J.P. Barnes^e, M. Tchernycheva^b, C. Durand¹ and J. Eymery^c

- a.* Univ. Grenoble Alpes, CEA, INAC-PHELIQS, 38000 Grenoble, France
b. Center of Nanoscience and Nanotechnologies (C2N), UMR 9001 CNRS, Paris, France
c. Univ. Grenoble Alpes, CEA, INAC-MEM, 38000 Grenoble, France
d. Univ. Grenoble Alpes, CNRS, Institut Néel, 38000 Grenoble, France
e. Univ. Grenoble Alpes, CEA, LETI, DTSI, SCMC, F-38000 Grenoble, France.

*Author contact: akanksha.kapoor@cea.fr

The realization of efficient LEDs using core-shell *m*-plane InGaN/GaN nanowires has been mainly demonstrated for the blue emission [1,2]. Green and other longer wavelength emissions still remain a challenge for this core-shell geometry due to a lower In incorporation on the *m*-plane with respect to the *c*-plane [3]. This work demonstrates a multi-color emission from self-assembled wires with InGaN multi-quantum wells (MQWs), which are used to demonstrate flexible LEDs. Self-assembled catalyst-free GaN microwires have been grown by metalorganic vapor phase epitaxy (MOVPE) with silane addition on sapphire in situ capped with SiN_x mask. This was followed by the growth of seven InGaN/GaN QWs and completed with the growth of a p-GaN shell [1,4]. The electrical and optical characterization of the flexible LED device was performed using micro electroluminescence (μ EL); and photoluminescence (PL) and cathodoluminescence (at 4K) respectively.

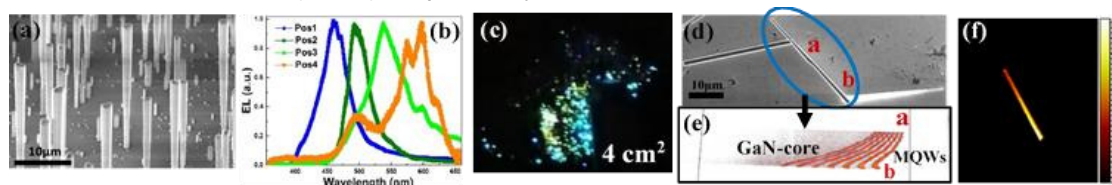


Figure 1 : (a) SEM image of virgin NWs; (b) EL spectra at four different positions; (b) Emission observed during EL measurement; (d) SEM image of NWs dispersed on Si; (e) 3D mapping of In using TOF-SIMS; (f) Color profile of secondary In⁺ counts on single NW.

Fig. 1 (a) shows the SEM image of as-grown nanowires. The EL measured at injection current of 60 mA in Fig. 1(b) revealed different wavelength emission at 460 nm, 500 nm, 540 nm and 600 nm. Different color emission can be seen from the flexible LED device in Fig. 1(c) captured during current injection. Further investigations using ToF-SIMS analysis on single nanowires were also performed to quantify the indium incorporation in the InGaN/GaN core-shell structure [4]. The 'ab' section of an identified single nanowire as seen in the SEM image of Fig. 1(d) was analyzed by ToF-SIMS and the 3D profile of In present in this section can be seen in Fig. 1(e). The secondary ion count for In⁺ in Fig. 1(f) shows a gradient of In-content along the length of the nanowire. These results indicate high and inhomogeneous In incorporation in the side-walls thus resulting in the variation in wavelength emission of the core-shell nanowires. This work highlights the possibility to obtain multi-color emission from blue to red from core-shell *m*-plane InGaN/GaN MQWs in GaN nanowire-based LEDs that opens the route for monolithic white flexible LED without phosphors.

- [1] R. Koester et al. *Nano Lett.*, vol. **11**, 4839 (2011)
 [2] N. Guan et al. *ACS Photonics.*, **3**, 597–603 (2016)
 [3] Y. J. Hong et al. *Adv. Mater.*, **23**, 3284–3288 (2011)
 [4] X. Dai et al. *Nano Lett.*, **15**, 6958 (2015)

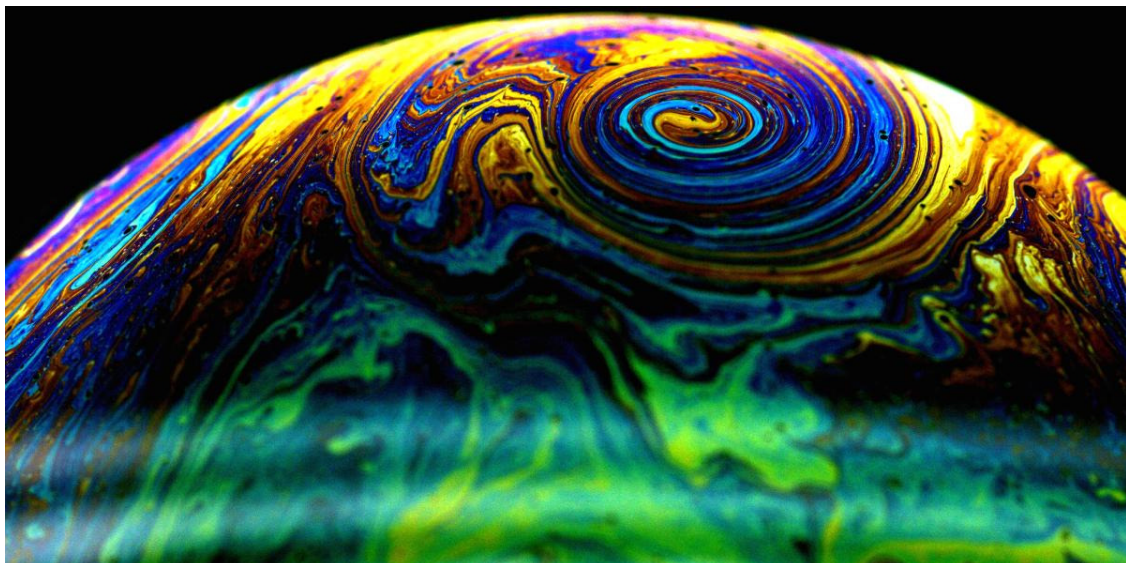
Hydrodynamics experiments using soap films and soap bubbles

Hamid Kellay

Université de Bordeaux et Institut Universitaire de France
Laboratoire Ondes et Matière d'Aquitaine, UMR 5798 CNRS/U.Bx, 351 cours de
la Libération, 33405 Talence

* hamid.kellay@u-bordeaux.fr

I will describe experiments using soap films and soap bubbles to illustrate the interest of these common objects to some fluid mechanics problems. The flow in the very thin layer of these films is basically two dimensional and this property brings fundamental differences with fluid flows in three dimensions as well as experimental simplification. I will use three examples for this talk : the interaction between a flow and different structures in fast flowing soap films, the measurement of viscous drag in turbulent soap film channels, and thermal convection in soap bubbles. In all these cases, the two dimensional nature of the flow allows to capture some of the key features of the underlying dynamics such as a symmetry breaking mechanism leading to locomotion of passive objects in the first case, the role of the structure of the turbulence on the scaling of the viscous drag in the second case, and the appearance of large scale vortices in the last case.



A vortex in a soap bubble.

Design and development of 3D arrays of coupled Quantum Dots in SOI CMOS technology

Y.J. Kim^{a,d*}, B. Bertrand^{a,d}, L. Hutin^{a,d}, S. De Franceschi^{b,d}, T. Meunier^{c,d}, M. Vinet^{a,d}

a. CEA, LETI, Minatec Campus, F-38054 Grenoble, France, * Yoonji.KIM@cea.fr

b. CEA, INAC-PHELIQS, F-38054 Grenoble, France

c. Institut Néel, F-38042 Grenoble, France ,

d. University Grenoble Alpes, F-38000 Grenoble, France

Silicon-based spin qubits are an extremely attractive option for large-scale quantum computing owing to their relatively long spin coherence time, as well as their potential for leveraging the technological maturity of the IC manufacturing industry towards mass fabrication. Thus, the development of various structures and array of Quantum Dots (QDs) have been studied, and scaling the number of qubits is necessary for the next challenge [1-3]. In order to demonstrate a full-scale universal quantum computer, error correction code should be developed, and it can be realized in 2D arrays of QDs [4]. Thus, recent proposals of 2D arrays are offered, using crossbar addressing of the QDs and the tunnel junctions in order to reduce the number of I/Os [5,6]. However, the proper balance between tunability, integration density, cross-talk and variability management is still being evaluated.

Here we suggest an array with a 3D elementary cell as shown in Fig. 1(a). Fig. 1(b) shows the structure of 3D elementary cell composed of five dots, which are one measurement (M), four data (D), and one sensing (S) dots in two layers. In the top layer, M dots are coupled to the D dots in 2D array to implement a quantum error correction. The localization and coupling of electrons can be controlled with tuning tunnel junction between M and D dots by applying voltage to the plug Gates above dots (Fig. 1(c)). Moreover, S dots are coupled to the M dots by a silicon pillar, which can be controlled with line/column addressing by wrapping Gates (Gate-All-Around geometry). Thus the S dots can be used either to load electrons into the QDs in the top layer, or to sense spin-related charge events occurring in the top dots (Fig. 1(d)). Then our current work aims at paving the way for the realization of the full structure by validating the dimensions and feasibility of the main technological modules (patterning, epitaxial growth, bonding, etc.)

[1] D.M. Zajac et al., Resonantly driven CNOT gate for electron spins, *Science*, **359**, 439-442 (2018)

[2] R. Maurand et al., A CMOS silicon spin qubit, *Nat. Commun.*, **7**, 13575 (2016)

[3] T.F. Watson et al., A programmable two-qubit quantum processor in silicon, *Nature*, **555**, 633-637 (2018)

[4] A.G. Fowler, Surface codes: Towards practical large-scale quantum computation, *Phys. Rev. A*, **86**, 032324 (2012)

[5] M. Veldhorst et al., Silicon CMOS architecture for a spin-based quantum computer, *Nat. Commun.*, **8**:1766 (2017)

[6] R. Li et al., A Crossbar Network for Silicon Quantum Dot Qubits, arXiv:1711.03807 (2017)

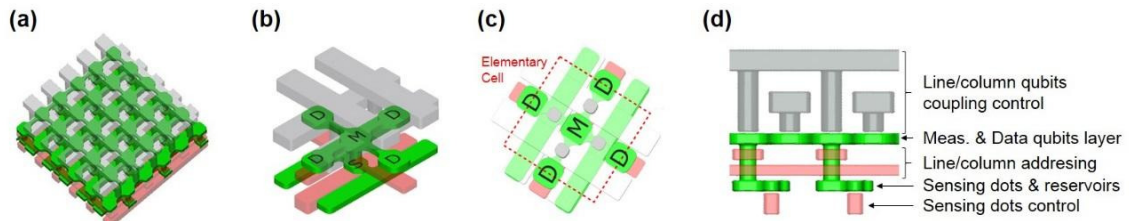


Fig. 1(a) The full structure of an array with 3D elementary cell, **(b)** the structure of 3D elementary cell, **(c)** top view and **(d)** cross-section of 3D elementary cell.

Flower - like azimuthal instability of axisymmetrically - fed surface flows

G. Koleski^{a*}, T. Bickel^a, J - C. Loudet^b and B. Pouligny^b

a. Laboratoire Ondes et Matière d'Aquitaine (LOMA), Talence, France.

b. Centre de Recherche Paul Pascal (CRPP), Pessac, France.

* goce.koleski@u-bordeaux.fr

We are interested in the propulsion mechanism of micrometer - sized swimmers within self - induced Marangoni flows in the low Reynolds number regime. The flows of interest are due to temperature or concentration inhomogeneities. The project is based on the observation that *initially axisymmetric flows on a water - air interface are azimuthally unstable*. In this presentation, this fact is illustrated by two experiments.

- Our first experiment (I) involves a micrometric carbon bead which is trapped at the water/air interface and heated up with a laser beam [1]. This hot spherical particle generates a temperature gradient that drives a thermocapillary flow. Most strikingly, the flow exhibits structures that range from slightly polar, to dipolar and even multipolar at sufficiently high laser powers.
- In our second experiment (II) we simply inject water through a narrow vertical tube located below the WA interface. The gap between the injector and the interface ($\sim 1\text{mm}$) is kept constant by means of a feedback loop. The fluid contains a small amount of sodium dodecyl sulfate (SDS, cmc/100), a well - known surfactant. Gradients in the surface concentration of SDS play a role analogous to that of temperature gradients in (I) as being the source of Marangoni flows. Similarly to what occurs in (I) we observe a symmetry - breaking of the primary axisymmetric flow in the form of complex dipolar and even multipolar patterns.

Dipolar flows (Fig.1 below), emerging as pairs of contra - rotating vortices, are thought to be the mechanism by which hot spherical particles move at large velocities (~ 100 particle diameter/s) on the WA interface. Such flows stem from the destabilization of initially toroidal flows [2] that display similar shapes in both experiments (I) and (II). We currently focus our efforts on understanding how the instability sets in.

[1] A. Girot, N. Danné, A. Würger, T. Bickel, F. Ren, J - C. Loudet, and B. Pouligny. 'Motion of Optically Heated Spheres at the Water - Air Interface.' *Langmuir* **32**, 2687-2697 (2016).

[2] V. Shtern and F. Hussain. 'Azimuthal instability of divergent flows.' *J. Fluid Mech.* **252**, 518 (1993).

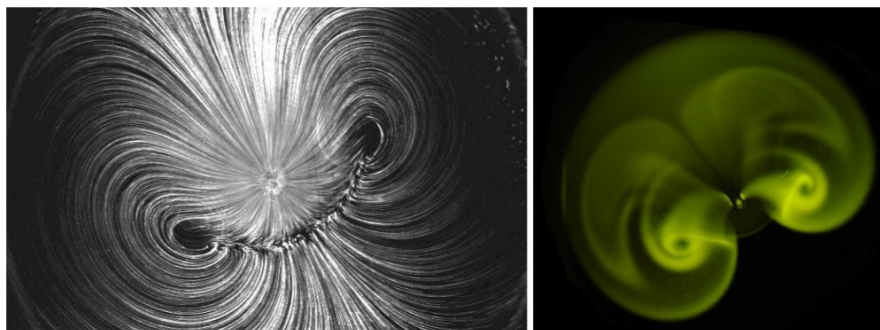


Figure 1: Example of a dipolar flow seen from above the WA interface in experiment (II). (a): Streamlines (left). (b): Structure unveiled by a droplet of fluorescent dye sent through the injector (right).

Ground state selection and dynamical crossover in the quantum pyrochlore magnet $\text{Yb}_2\text{Ti}_2\text{O}_7$

E. Kermarrec^{a*}, R. K. Sharma^{a*}, C. Decorse^b, S. Petit^c, R. Khasanov^d, Z. Guguchia^d, C. Ritter^e, J. Gaudet^f and B. D. Gaulin^f

- a. Laboratoire de Physique des Solides, Univ. Paris Sud, Bât. 510, Orsay
- b. Institut de Chimie Moléculaire et des Matériaux d'Orsay, Univ. Paris Sud, Bât. 410, Orsay
- c. Laboratoire Léon Brillouin, CEA Saclay
- d. Laboratory for muon spectroscopy, Paul Scherrer Institut, Villigen
- e. Institut Laue-Langevin, Grenoble
- f. Department of Physics and Astronomy, McMaster University, Hamilton

* edwin.kermarrec@u-psud.fr, ramender.sharma@u-psud.fr

The pyrochlore magnet $\text{Yb}_2\text{Ti}_2\text{O}_7$ is a promising quantum spin ice candidate as it possesses both an effective $S = 1/2$ spin, thanks to the well isolated crystal field Kramers doublet ground-state appropriate to Yb^{3+} , and strong quantum fluctuations brought by anisotropic exchange interactions and an XY g-tensor [1]. However, the magnetic properties of $\text{Yb}_2\text{Ti}_2\text{O}_7$ at low temperature have eluded a global understanding, notably because of the presence of extra Yb^{3+} on the B (non-magnetic) pyrochlore site, that clearly impact on its physical properties [2]. By combining neutron diffraction and muon spin relaxation (μSR) techniques, we establish the pressure-temperature phase diagram of $\text{Yb}_2\text{Ti}_2\text{O}_7$ and further evidence a magnetic transition from a disordered, non magnetically ordered, ground state at ambient pressure to a splayed ferromagnetic ground state under hydrostatic pressure [3]. We use applied pressure to counterbalance the effect of negative chemical pressure induced by $\text{Yb}^{3+}/\text{Ti}^{4+}$ anti-site occupation. Furthermore, we have recently achieved controlled isovalent substitutions of Zr on the Ti site that allowed us to apply chemical pressure in the series $\text{Yb}_2(\text{Ti}_{1-x}\text{Zr}_x)_2\text{O}_7$, and explore in more details the quantum crossover regime between the fluctuating and the ferromagnetic regions of the phase diagram at low temperatures.

[1] K. A. Ross, L. Savary, B. D. Gaulin and L. Balents, *Phys. Rev. X* 1, 021002 (2011)

[2] K. E. Arpino, B. A. Trump, A. O. Scheie, T. M. McQueen, *et al.*, *Phys. Rev. B* 95, 094407 (2017)

[3] E. Kermarrec, J. Gaudet, K. Fritsch, R. Khasanov *et al.*, *Nat. Commun.* 8, 14810 (2017)

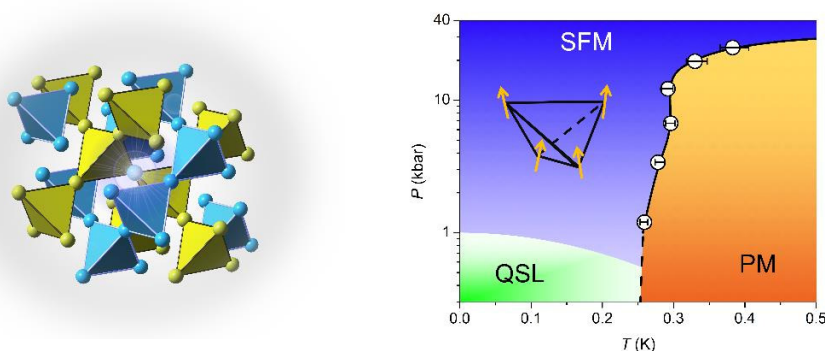


Figure 1 : (Left) Non magnetic (Ti, yellow) and magnetic (Yb, blue) pyrochlore lattices in $\text{Yb}_2\text{Ti}_2\text{O}_7$. Excess Yb^{3+} ion can occupy a Ti^{4+} site and create a local defect. (Right) Pressure-temperature phase diagram of $\text{Yb}_2\text{Ti}_2\text{O}_7$ established by μSR (black circles) highlighting the existence of a non magnetically ordered region (QSL), a splayed ferromagnetic region (SFM) and a collective paramagnetic (PM) region. Line is a guide to the eye.

Implementing a “quantum hammer”: towards the excitation of nanomechanical motion using a single quantum dot

J. Kettler^{a*}, N. Vaish^a, P.-L. de Assis^b, J. Claudon^c, J.-M. Gérard^c, A. Auffèves^a, M. Richard^a, and J.-Ph. Poizat^a

- a. Univ. Grenoble Alpes, CNRS, Institut NEEL, Grenoble, France
 b. Gleb Wataghin Institute of Physics, University of Campinas - UNICAMP, Campinas, São Paulo, Brazil
 c. Univ. Grenoble Alpes, CEA, INAC-PHELIQS, Grenoble, France

* jan.kettler@neel.cnrs.fr

Hybrid nanomechanical systems feature a coupling between a two-level system and a nanomechanical oscillator. Decreasing the size of such systems can lead to extremely sensitive sensor whose position read-out can benefit from the hybrid coupling. Alternatively, these systems can also lead to nano-engines powered by a single two-level system.

Our approach relies on a hybrid nanomechanical system consisting of an InAs quantum dot (QD) embedded in a vibrating GaAs photonic nanowire (see fig. 1). Both system components are in reciprocal interaction via strain: When vibrating, the nanowire experiences deformations yielding to strain changes at the QD location. These strain changes result in frequency shifts of the excitonic resonance, whose detection can therefore be used for monitoring the wire motion in an extremely sensitive manner [1,2]. Conversely, each photon emitted by the QD comes along with a strain back-action which can drive the wire motion [3].

In this contribution, we will present our latest results towards setting the wire in motion via such a “quantum hammer”. Each hammer hit is given by the absorption-emission cycle of a single resonantly excited QD [3,4].

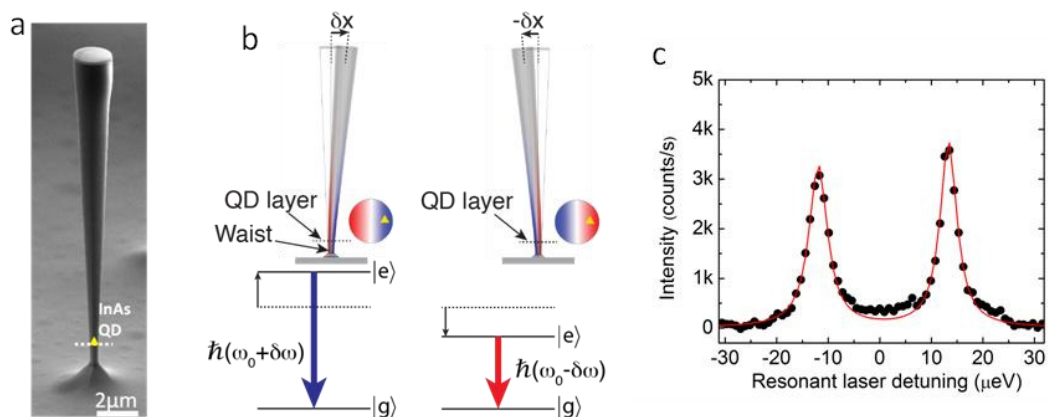


Fig. 1. Scanning electronic microscope image of the photonic wire. **b.** The strain field (color scale) induced by the wire oscillation shifts the quantum dot energy. **c.** Resonant excitation of the photoluminescence of a single QD.

- [1] I. Yeo, et al, [Nat. nanotech.](#) **9**, 106 (2014)
 [2] M. Munsch, et al, [Nat. Comm.](#) **8**, 76 (2017)
 [3] A. Auffèves and M. Richard, [Phys. Rev. A](#) **90**, 023818 (2014)
 [4] H.A. Nguyen et al, [arXiv:1705.04056](#), to appear in Phys. Rev. B (Rapid Comm)

Effet de la fonctionnalisation sélective sur l'ouverture du gap dans la bicouche du graphène

Jouda Jemaa Khabthani^{a*}, Ahmed Missaoui^b, Didier Mayou^c et Guy Trambly de Laissardière

- a. Laboratoire de Physique de la Matière Condensée, Faculté des Sciences de Tunis, Université Tunis El Manar, 2092 Tunis, Tunisie
- b. Laboratoire de Spectroscopie Moléculaire et Applications, Faculté des Sciences de Tunis, Université Tunis El Manar, 2092 Tunis, Tunisie
- c. Univ. Grenoble Alpes, Inst Neel, F-38042 Grenoble, France
- d. Laboratoire de Physique théorique et modélisation, CNRS et Université de Cergy-Pontoise, 95302 Cergy-Pontoise, France

* jemaajouda@gmail.com

Le graphène et ses dérivés permettent la conception de nouveaux matériaux et ouvrent la voie à de nouveaux dispositifs électroniques performants. Dans ce travail, on se propose d'étudier les propriétés électroniques de la bicouche AB de graphène fonctionnalisée par des adsorbats via une modélisation numérique [1-3]. Nos résultats montrent qu'en réalisant une distribution sélective d'adsorbats, on peut varier le gap ainsi que la conductivité électrique qui pour des énergies très proches du gap présente un comportement anormal.

La fonctionnalisation par des adsorbats (atomes ou molécules) représente un des moyens parmi d'autres qui permettent de contrôler les propriétés électroniques du graphène, ainsi que de la majorité des matériaux bidimensionnels. Dans la bicouche bernal de graphène, les sites cristallographiques dans une couche ne sont pas équivalents par le fait qu'ils n'ont pas le même nombre de coordination. La fonctionnalisation sélective de l'un des deux sites est alors possible. Dans ce travail, nous présentons une étude théorique de la structure électronique ainsi que du transport électronique en utilisant deux modèles : un premier qui ne tient compte que des premiers voisins et un deuxième qui est plus réaliste puisqu'il permet d'aller au delà des premiers voisins.

Notre étude montre que pour certaines fonctionnalisations, un gap de mobilité variable se forme et peut atteindre 0,5 eV autour de l'énergie de Dirac. Ceci est réalisé pour une concentration d'adsorbats plus grande que 0,01. De plus, aux énergies autour du gap, la conductivité présente un comportement inattendu et augmente fortement lorsque la concentration c augmente. Nous avons montré que ce comportement résulte directement de la symétrie particulière de la structure atomique de la bicouche du graphène [4].

Ces résultats sont d'une grande importance pour des expériences futures et des investigations théoriques des divers phénomènes originaux relatifs au transport électroniques impliqués dans une bicouche de graphène bernal.

[1] G. Trambly de Laissardière et al, Phys.Rev. B **86**, 125413 (2012)

[2] G. Trambly de Laissardière et al, Phys. Rev. B **93**, 235135 (2016)

[3] G. Trambly de Laissardière et al C. R. Physique **15**, 70 (2014)

[4] A. Missaoui, J. J. Khabthani, N. Jaidane, D. Mayou and G. T. De Laissardière, Eur. Phys. J. B (2017) **90** 75

CdSe/ZnSe nanowire quantum dots for efficient single-photons sources

T. Cremel^{1,2}, M. Jeannin^{1,3}, S. Gosain^{1,2}, E. Bellet-Amalric^{1,2}, L. Cagnon^{1,3}, N. Gregersen⁴, R. André^{1,3}, C. Bougerol^{1,3}, J. Cibert^{1,3}, G. Nogues^{1,3} and K. Kheng^{1,2*}

1. Univ. Grenoble Alpes, F-38000 Grenoble, France
2. CEA, INAC-SP2M, F-38000 Grenoble, France
3. CNRS, Institut Néel, F-38000 Grenoble, France
4. DTU Fotonik, Technical University of Denmark, DK-2800 Kongens Lyngby, Denmark

* kkheng@cea.fr

The single-photons source is a key element in the framework of quantum communication where single-photons act as flying qubits for the information exchanges. Such a source can be obtained using semiconductor quantum dots (QDs), as demonstrated in various material system, but their operation is mostly restricted to cryogenic temperatures. CdSe QD inserted in ZnSe nanowire (NW), namely a NW-QD, offers the possibility to emit single-photons up to room temperature [1] opening the prospect for a realistic application in quantum information technologies. However, the emission efficiency strongly decreases at high temperature. To make such a system an efficient single-photons source, we investigate the growth of core-shell type NW heterostructures in order to enhance the emission quantum yield and the coupling of these nano-emitters to photonic structures for an efficient light extraction and collection.

In this contribution, we present our work on the growth and optical studies of vertically oriented CdSe/ZnSe NW-QDs by molecular beam epitaxy. The NW-QDs are grown on a ZnSe(111)B buffer layer with a ZnMgSe passivating shell to increase the (otherwise weak) QD luminescence. The NWs diameter is typically 10 nm and single QDs shows clearly exciton, biexciton and charged exciton transitions.

Single-photons can be extracted more efficiently along the NW axis if the NW-QD is embedded in a photonic wire [2], providing directivity of the photon emission. We show that such a photonic wire can be obtained with a thick conformal dielectric coating of Al₂O₃ using Atomic Layer Deposition (ALD) [3] (fig. 1). Optical studies of single NW-QDs show that a 4-fold increase of the collected photoluminescence intensity is obtained with an oxide shell of 110 nm thick. This improvement is due to an increase of the QD emission rate (as confirmed by decay time measurements) and a redirection of the emitted light [4] as shown by numerical simulations.

We will discuss the parameters to be mastered in this NW system in order to obtain a workable single-photon source.

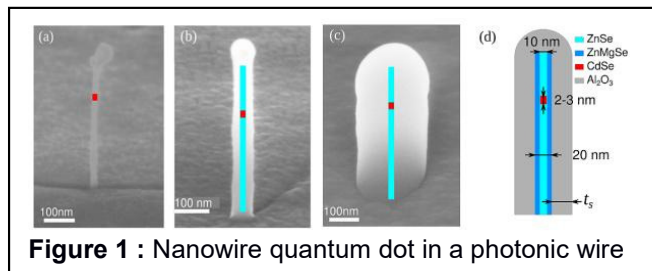


Figure 1 : Nanowire quantum dot in a photonic wire

- [1] S. Bounouar, M. Elouneq-Jamroz, M. den Hertog, C. Marchutt, E. Bellet-Amalric, R. André, C. Bougerol, Y. Genuist, J.-P. Poizat, S. Tatarenko, and K. Kheng, *Nano Lett.* **12**, 2977 (2012).
- [2] J. Claudon et al., *Nat. Photonics* **4**, 174 (2010).
- [3] M. Jeannin, T. Cremel, T. Häyrynen, N. Gregersen, E. Bellet-Amalric, G. Nogues, and K. Kheng, *Phys. Rev. Applied* **8**, 054022 (2017)

Effect of milling on the microstructural and magnetic properties of Fe₂O₃/(Al, Si) nanocrystalline powders

A. Kihal^{a*}, B. Bouzabata^a, D. Fruchart^b

- a. Laboratoire de Magnétisme et Spectroscopie des Solides (LM2S), Université Badji Mokhtar-Annaba, BP-12, 23000 Annaba, Algérie
- b. Institut Néel, CNRS, 25 Rue des Martyrs, BP-166, 38042 Grenoble-Cedex 9, France.

* amel.kihal@gmail.com

Due to their special chemical and physical properties which can be modified by varying the particle size and metal volume fraction, a great interest was given to nanocomposite materials consisting of metal particles with nanometer dimension embedded in a nonmagnetic medium. α -Fe₂O₃ (Al / Si) nanocomposites were prepared by high energy ball milling. The structural and microstructural variations of the milled powders were followed by X-ray diffraction. The change of the magnetic behavior with the milling time has been studied by magnetic measurements.

The Rietveld refinement of the X-ray diffraction spectra revealed the formation of α -Fe nanoparticles dispersed in an amorphous matrix. The reaction induced between α -Fe₂O₃ and Al occurs rapidly after 1 hour of milling with the presence of Fe particles in an Al₂O₃ matrix. In the α -Fe₂O₃/Si powder mixture, there is a gradual transformation of the crystalline SiO₂ phase into amorphous induced by the mechanical process at higher milling times. After 15 hours of milling, the final products are mainly composed of alpha iron (53% by weight), amorphous SiO₂ (43% by weight) with crystallite sizes of 28 and 3 nm respectively.

The observed variations of the saturation magnetization and the coercive field are related to the reduction of the size of iron nanoparticles, the high rates of defects and the formation of the amorphous matrix. They also depend on the amount of Fe nanoparticles dispersed in the amorphous matrix.

Structure Determination of a new Molecular White-Light Source

B. D. Klee^{a*}, E. Dornsiepen^a, J. R. : Stelhorn^{a,b}, B. Paulus^a, S. Hosokawa^{a,b}, S. Dehnen^a, W.-C. Pilgrim^a

- a. Department of Chemistry, Philipps-University, Hans-Meerwein Str. 4, 35032 Marburg, Germany
 b. Department of Physics, Kumamoto University, Kumamoto 860-8555, Japan

* benjamin.klee@staff.uni-marburg.de

The molecular structure of the white light generating amorphous material $[(\text{PhSn})_4\text{S}_6]$ is investigated using X-ray scattering coupled with a rigid molecular Reverse-Monte-Carlo (RMC) modeling approach. Experimental proof for an adamantane-like molecule structure is found (see fig. 1). The intermediate-range structure is analysed, indicating a strong preference for distinct cluster orientations. It is shown that rigid molecular RMC simulations are feasible for structure analysis without using potential-related features. [1-3]

[1] N. W. Rosemann, J. P. Eußner, E. Dornsiepen, S. Chatterjee, S. Dehnen, Organotetrel Chalcogenide Clusters: Between Strong Second-Harmonic and White-Light Continuum Generation, *Journal of the American Chemical Society* **138**(50), 16224-16227 (2016).

[2] N. W. Rosemann, J.P. Eußner, A. Beyer, S. W. Koch, K. Volz, S. Dehnen, S. Chatterjee, A highly efficient directional molecular white-light emitter driven by a continuous-wave laser diode, *Science* **352**(6291), 1301-1304 (2016).

[3] B. D. Klee, E. Dornsiepen, J. R. Stelhorn, B. Paulus, S. Hosokawa, S. Dehnen, W.-C. Pilgrim, Structure Determination of a new Molecular White-Light Source, submitted to *Physica Status Solidi B* in February 2018.

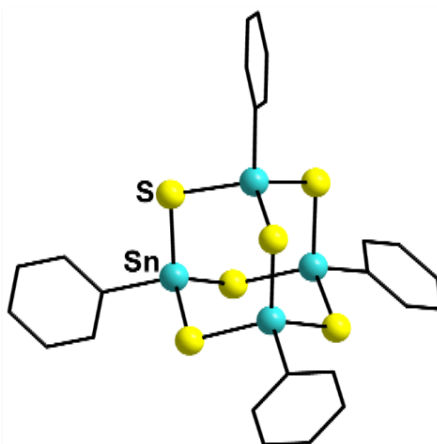


Figure 1 : Molecular Structure of $[(\text{PhSn})_4\text{S}_6]$.

Importance of nonlocal electron correlation in the BaNiS₂ semimetal from quantum oscillations studies

Yannick Klein^{a*}, Michele Casula^a, David Santos-Cottin^b, Alain Audouard^c, David Vignolles^c, Gwendal Fève^d, Vincent Freulon^d, Bernard Plaçais^d, Marine Verseils^a, Hancheng Yang^a, Lorenzo Paulatto^a, and Andrea Gauzzi^a

a. IMPMC, Sorbonne Université, CNRS, IRD, MNHN, 4 place Jussieu 75005 Paris

b. LPEM - ESPCI Paris, PSL Research University; CNRS; 10 rue Vauquelin, 75005 Paris

c. LNCMI (UPR 3228 CNRS, INSA, UGA, UPS), 143 avenue de Rangueil, 31400 Toulouse

d. LPA, Ecole Normale Supérieure-PSL Research University, CNRS, Sorbonne Université, Université Paris Diderot-Sorbonne Paris Cité, 24 rue Lhomond, 75005 Paris

* yannick.klein@sorbonne-universite.fr

Quasi 2D BaNiS₂ exhibits an anomalously large spin-orbit Rashba coupling, even in the absence of heavy (electronically active) element ($Z_{Ni} = 28$) [1]. The magnitude of the splitting, which is due to the presence of a staggered electric field at the Ni site in a pyramidal environment, is comparable to the highest measured values [2]. This makes BaNiS₂ a candidate for applications involving the transport of spins rather than charges.

By a combined study of Shubnikov de Haas and de Haas van Alphen effects on high-quality single crystals, the Fermi surface of BaNiS₂ is investigated. Ab initio electronic structure calculations, in the DFT framework, show that the inclusion of screened exchange, through a HSE hybrid functional with 7% of exact exchange, is necessary to account for the experimental Fermi pockets. The importance of non-local screened-exchange interactions in BaNiS₂, and, more generally, in 3d compensated semimetals, is underlined [3].

[1] D. Santos-Cottin et al., Nature Commun. **7**, 11258 (2016)

[2] H.M. Benia et al., Phys. Rev. B **94**, 121407(R) (2016)

[3] Y. Klein et al., Phys. Rev. B **97**, 075140 (2018)

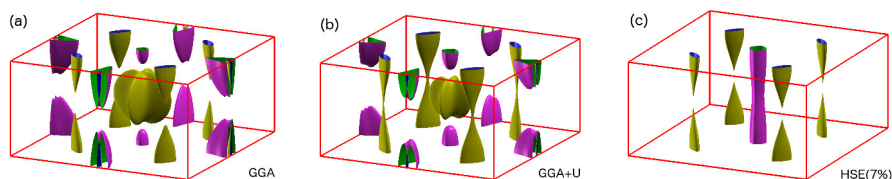


Figure 1: Fermi surfaces of BaNiS₂ from ab initio calculations with GGA (a), GGA + U (= 3 eV) (b), and modified HSE with 7% of exact exchange (c).

Non-equilibrium Glass Transitions and the Non-monotonic Behavior in Crowded Active Colloids

Natsuda Klongvessa^a, Félix Ginot^{a,b}, Christophe Ybert^a, Mathieu Leocmach,^a and Cécile Cottin-Bizonne^{a,*}

- a. Institut Lumière Matière, CNRS UMR5306, Université Claude Bernard Lyon 1, Université de Lyon, 69100 Villeurbanne Cedex, France
- b. Laboratoire de Synthèse et Fonctionnalisation des Céramiques, CNRS UMR3080 , 84306 Cavaillon cedex, France

* cecile.cottin-bizonne@univ-lyon1.fr << corresponding author >>

Active matter, where an energy injection occurs at an elementary level and is converted to self-propulsion, opens new questions for out-of-equilibrium physics. Here, we study experimentally active matter in a crowded condition, where glass transition meets collective motion. Our system is a monolayer of micron-size gold-platinum Janus particles in water. Upon addition of hydrogen peroxide, the colloids become self-propelled due to the different chemical gradient on both sides. Besides, the amount of activity can be controlled by the concentration of hydrogen peroxide. From this setup, we are able to investigate its behavior at various density regimes and levels of activity. In the dense regime, we notice a non-monotonic behavior as the activity level rises up. Starting from a passive glassy system, introducing a very low activity drastically decreases the mobility. As the activity is further increased, we observe the opposite trend: the system becomes more fluid as expected in the first place. We correlate this non-monotonic trend with the density-dependence of effective diffusion in order to find out how the glass transition is affected by non-equilibrium active forces.

- [1] F. Ginot, I. Theurkauff, D. Levis, C. Ybert, L. Bocquet, L. Berthier and C. Cottin-Bizonne, Nonequilibrium Equation of State in Suspensions of Active Colloids, *Phys. Rev. X* **5**, 011004 (2015)
- [2] L. Berthier, E. Flenner and G. Szamel, How active forces influence nonequilibrium glass transitions, *New Journal of Physics* **19**, 125006 (2017)

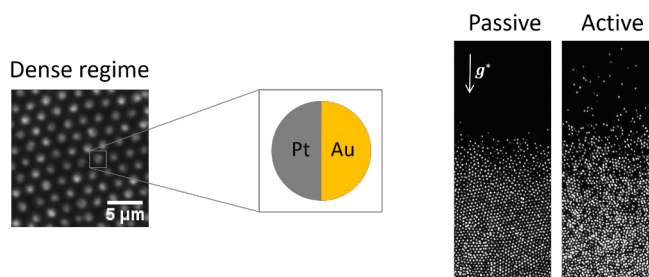


Figure 1: (left) A monolayer dense regime of the colloids. (right) Profile of the sedimentation comparing between the passive and the active cases. The colloids are confined by the effective gravity $g^* \ll g$.

Spontaneous emission in optical analogue gravity systems

Friedrich Koenig^{a*} and Maxime Jacquet^{a,b}

- a. School of Physics and Astronomy, SUPA, University of St. Andrews, North Haugh, St. Andrews, KY16 9SS, United Kingdom
- b. Vienna Center for Quantum Science and Technology, Faculty of Physics, University of Vienna, Boltzmannngasse 5, Vienna, A-1090, Austria

* fewk@st-andrews.ac.uk'

Quantum fluctuations in curved space-time cause the emission of particles. Under certain conditions, event horizons can create one-way doors, as in the case of black holes. Here we investigate and demonstrate the role of event horizons for the production of entangled pairs in a dispersive analogue system. We find that horizons lead to an order of magnitude increase in the pair production, strong and purified quantum correlations, and a characteristic shape of the photon emission spectrum.

We consider a moving refractive index perturbation in an optical medium, which exhibits optical event horizons. Based on the field theory in curved space-time we formulate an analytical method to calculate the scattering matrix that completely describes mode coupling leading to the emission of photon pairs in various configurations. We quantify the emission by the emission spectrum and the spectrally resolved photon number correlations, as they would be observed in the laboratory. Moreover, we apply our method in a case study, in which we consider a moving refractive index step in bulk fused silica. We calculate the emission flux in the moving frame as well as in the laboratory frame. The flux from horizons is particularly enhanced and carries a signature spectral shape. In both frames, we observe significant spectral quantum correlations between modes of opposite norm, evidence of their vacuum origin. If the modes form horizons, the correlation with the partner photon mode increases and approaches unity. These methods and findings pave the way to the observation of particles from the event horizon in optical systems. Furthermore, they will be relevant in a number of other optical and non-optical systems exhibiting horizons.

Screened potential constraint in a Reverse Monte Carlo (RMC) modeling

M. KOTBI¹, M. HABCHI², S. M. MESLI⁴

1 Laboratoire de Physique Théorique (LPT), Université de Tlemcen (Algérie)

To explore a certain number of structural features of an aqueous electrolyte LiCl-6H₂O type, a Reverse Monte Carlo (RMC) modeling is applied [1, 2]. This is based essentially on neutron scattering data [3, 4] consisting of four partial distribution functions issue from the technique of the isotopic substitution. Instead of introducing the interaction potential as in the classical methods (MD, MC), one computes a parameter χ^2 representing the difference between the calculated structure function and that are of the experiment within standard deviation.

One examines the system at glassy (120K) and liquid (300K) state compared to pure water at room temperature. The chlorine and lithium ions charged -1 and +1, respectively, the water molecule is represented by a flexible model [8] charged as -0.8476 for the oxygen and +0.4238 for each hydrogen atom [7, 8]. The results one obtains could include some artifacts [5, 6]. To remedy for this, we could make a propose choice of screened potential model.

In conclusion, we could suggest that the choice of the interaction model as a function of atomic or molecular properties forming the system could bring a meaningful improvement to the results. An improvement in the coordination of this function is noticed. RMC is generally limited to explore structural property of a system with or without interaction model. Introducing potential as constraint in RMC simulation suggests a useful test of an interaction potential model for classical methods as Monte Carlo (MC) and Molecular Dynamic (MD) with which one can compute thermodynamic

-
1. R.L. Mc Greevy, M.A. Howe, J.D. Wicks, RMCA Version 3, A General Purpose Reverse Monte Carlo Code, October 1993.
 2. R.L. Mc Greevy and Pusztai, Mol. Simul. 1 (1988) 359.
 3. J.F. Jal, K. Soper, P. Carmona, J. Dupuy, J. Phys. Cond. Matter (3) (1991) 551.
 4. B. Prével, J.F. Jal, J. Dupuy Philon, A.K. Soper, J. Chem. Phys. 103 (1995) 1886.
 5. M. Kotbi, Hong Xu, M. Habchi, Z. Dembahri, Phy. Lett. A 315 (2003) 463.
 6. H. Xu, M. Kotbi, Chem. Phys. Lett., 248 (1996) 89.
 7. M.-C. Bellissent-Funel and G.W. Neilson, series C: Math. and Phys. Sciences Vol.205, ISBN 90-277-253469.
 8. P.A. Bopp, I. Okada, H. Ohtaki and K. Heinsinger, 1985, Z. Naturforsch, 40a, 116.

Structure de bandes d'une monocouche de silicatène sur Ru(0001)

G. Kremer^{a*}, S. Lisi^{b,c}, M. Sicot^a

- a. Université de Lorraine, CNRS, IJL, F-54000 Nancy, France
- b. CNRS Néel Institut, Grenoble 38000, France
- c. Université Grenoble-Alpes, Grenoble 38000, France

*geoffroy.kremer@univ-lorraine.fr

Les matériaux bidimensionnels (2D) possèdent des propriétés physiques radicalement différentes de celles du volume. Ils sont aujourd'hui largement étudiés en physique des surfaces, notamment les films ultra-minces de silice bidimensionnelle (silicatène) à la surface de métaux monocristallins [1,2]. Une telle réduction de dimensionnalité pourrait induire l'émergence de transitions de phases structurales réversibles, idéales en vue d'applications technologiques. C'est pourquoi la croissance de silicatène à la surface de substrats métalliques a été activement étudiée. Néanmoins, ses propriétés électroniques restent mal connues, en particulier sa structure de bandes.

Notre travail porte sur l'étude d'une monocouche de silicatène cristallin épitaxié sur Ru(0001) [1].

La structure atomique a été étudiée par XPS, LEED et STM. Ces données mettent en évidence une reconstruction de surface (2x2) ordonnée en nid d'abeilles et des liaisons chimiques caractéristiques du silicatène [1-5]. La structure de bandes, étudiée par ARPES, laisse apparaître des états dispersifs ayant une périodicité double par rapport à ceux du substrat, en accord avec nos calculs théoriques. Nous démontrerons l'apport de cette étude dans la compréhension des propriétés structurales et électroniques du système, en particulier concernant les interactions de la monocouche de silicatène avec son substrat de Ru(0001).

[1] G. Kremer et al, in preparation

[2] S. Shaikhutdinov et al, *Advanced Materials* 25, (2012), 49

[3] S. Shaikhutdinov et al, *Physical Review Letters* 95, (2005), 076103

[4] S. Mathur et al, *Physical Review B* 92, (2015), 161410(R)

[5] B. Yang et al, *Physical Chemistry Chemical Physics* 14, (2012), 11344

LASER RUBAN A POLARITONS : DU GUIDE D'ONDE EN ZNO AU LASER A TEMPERATURE AMBIANTE

G. Kreyder^{a,*}, F. Réveret^a, P. Disseix^a, F. Médard^a, M. Mihailovic^a,
D. Solnyshkov^a, G. Malpuech^a, A. Moreau^a, J. Leymarie^a, E. Cambril^b,
S. Bouchoule^b, M. Leroux^c, C. Deparis^c, J. Zuniga-Perez^c

- a. Université Clermont Auvergne, CNRS, SIGMA Clermont, Institut Pascal, 63000 Clermont-Ferrand, France
- b. Centre de Nanosciences et de Nanotechnologies, CNRS, Université Paris Sud, Université Paris-Saclay, C2N-Marcoussis, 91460 Marcoussis, France
- c. Université Côte d'Azur, CNRS, CRHEA, Rue Bernard Gregory, 06560 Valbonne, France

* E-mail : Geoffrey.KREYDER@uca.fr

Les exciton-polaritons (polaritons) résultent du couplage fort entre un mode photonique et une transition excitonique. Ils se comportent comme des quasi-particules bosoniques ce qui a permis d'apporter la preuve de leur condensation de Bose-Einstein, de démontrer la superfluidité du condensat polaritonique et d'étudier divers types de défauts topologiques. Le laser à polaritons, contrairement à un laser « classique », ne nécessite aucune inversion de population : la relaxation des polaritons est stimulée par l'occupation de l'état final et leur recombinaison produit une émission cohérente de lumière. Ce mécanisme permet d'envisager une diode laser présentant un faible seuil. Celui-ci correspond à la puissance d'excitation nécessaire pour obtenir la condensation des polaritons.

La physique des polaritons a largement été étudiée dans les microcavités planaires pour des semi-conducteurs à large bande interdite tels que le nitrure de gallium (GaN) ou l'oxyde de zinc (ZnO), notamment l'effet laser à polaritons sous excitation optique à température ambiante. Récemment une géométrie unidimensionnelle est apparue comme intéressante, vu qu'elle permet de longues distances de propagation (100 μm) par l'intermédiaire de modes guidés et qu'elle pourrait ouvrir la voie à des composants polaritoniques pour l'informatique optique.

Nous étudions deux guides d'onde à base de $\text{ZnO-Zn}_x\text{Mg}_{1-x}\text{O}$, élaborés par épitaxie par jets moléculaires (MBE) sur des substrats de ZnO plan-m. L'épaisseur de la couche active des structures étudiées est soit de 50 nm (échantillon 1) ou de 130 nm (échantillon 2). L'échantillon 1 est recouvert par une couche de SiO_2 sur laquelle sont gravés des réseaux, perpendiculaires à l'axe c de ZnO, dont la périodicité permet d'extraire les modes polaritoniques guidés. L'échantillon 2, comme l'échantillon 1, est traversé par une série de fissures qui assurent le confinement dans le plan (résonateurs) en même temps que l'extraction de la lumière. Dans un premier temps, les propriétés linéaires des polaritons sont étudiées par des expériences de micro photoluminescence en champ lointain (imagerie de Fourier) : la relation de dispersion est obtenue à partir du réseau de l'échantillon 1. Des simulations numériques basées sur la résolution des équations de Maxwell et la continuité du champ électromagnétique dans les différentes couches donnent une estimation du couplage de Rabi. Dans un deuxième temps, l'effet laser est étudié pour les deux échantillons de 5 K à température ambiante sous injection optique. La combinaison de ces expériences montre sans ambiguïté la nature polaritonique du mode laser jusqu'à 300 K.

Projet supporté par l'ANR (PLUG-AND-BOSE ANR-16-CE24-0021) et le réseau RENATECH.

First-Principles Investigation of Functionalized Metal-Organic-Frameworks for Energy Efficient CO₂ Capture

Aseem Rajan Kshirsagar and Roberta Poloni

Univ. Grenoble Alpes, CNRS, Grenoble INP, SIMAP, 38000 Grenoble, France

* aseem-rajan.kshirsagar@grenoble-inp.fr

Efficient technologies for CO₂ capture and its sequestration (CCS) can be vital in mitigation of the problem of climate change arising due to increasing CO₂ emissions¹. Metal organic frameworks (MOFs) are crystalline solids with high porosity and affinity for CO₂³. We explore Photo-responsive MOFs (Ph-MOFs) with photo-isomerizing azo functionalization for the application in CCS. Compared to existing amine scrubbing method of CO₂ separation, reversible CCS using Ph-MOFs shall require smaller energy costs. Pioneering experimental work by Park et.al². demonstrated reversible CCS in case of PCN123 Ph-MOF. Our recent work unraveled the mechanism of steric blocking (*cis*)-unblocking(*trans*) of the metal nodes of PCN123 with light stimuli resulting in variable adsorption of CO₂. To increase the difference in amount of CO₂ adsorbed, the maximum yields of the *cis* and *trans* configurations of the azo group have to be achieved. The yields of isomers depend strongly on photo-chemical properties of azo group, e.g. electronic excitation energies and the energy profile along isomerization pathway. These photo-chemical properties are sensitive to chemical environment around azo group and structural changes induced by embedding. Using advanced computational methods, e.g. DFT, TD-DFT and GW-BSE, we are studying these photo-chemical properties to tune the chemical and structural composition of Ph-MOFs for more efficient carbon capture.

- [1] Pacala, S.; Socolow, R. Science 2004, 305, 968-972.
 [2] Park, J.; Yuan, D.; et. al. Journal of the American Chemical Society 2011, 134.
 [3] Poloni, R.; Smit B.; Neaton J. B. The Journal of Physical Chemistry A 2012, 112.

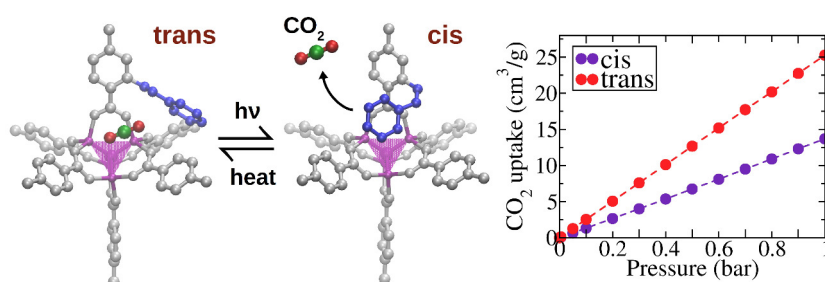


Figure 1: Left: reversible photo-isomerization of functional group (blue) in PCN-123 MOF causing blocking-unblocking of metal node (violet), right: calculated adsorption isotherm showing reversible change in CO₂ uptake.

NEMS for probing individual tunneling two level systems (TLS)

Sumit Kumar^{a*}, Xin Zhou^b, Eddy Collin^a, and Andrew Fefferman^a

- a. Institut Néel/CNRS & UGA
b. CNRS UMR 8520 - IEMN, Univ.Lille

* sumit.kumar@neel.cnrs.fr

The low temperature dissipation in nanomechanical resonators is dominated by low energy excitations, i.e., intrinsic defects in glassy materials that are modeled as TLSs (tunneling two level systems). Here we present NEMS for studying individual TLSs. Using top-down nanofabrication techniques, we made $4\ \mu\text{m}$ long, $300\ \text{nm}$ wide and $100\ \text{nm}$ thick high-stress SiN doubly-clamped beam resonators with $30\ \text{nm}$ of aluminum on top [Figure 1]. We will first characterize the mechanical properties of the devices using the magnetomotive technique. Then the devices, with fundamental frequency around $70\ \text{MHz}$, will be cooled to $1\ \text{mK}$, so that they are in their quantum ground state. The motion of the beams will be detected by capacitively coupling the NEMS to a superconducting microwave cavity, allowing us to probe the dynamics of individual TLSs inside the glass beam.

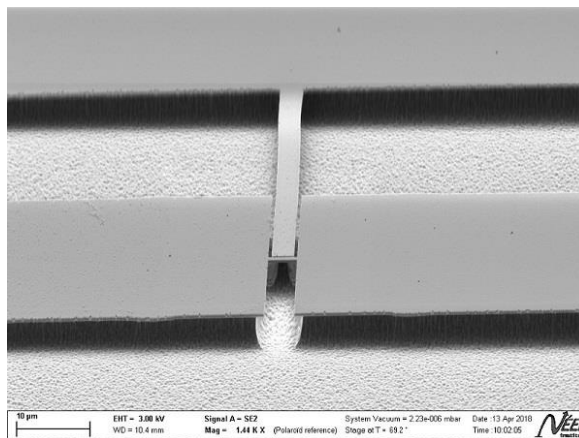


Figure 1 : $4\ \mu\text{m}$ long, $300\ \text{nm}$ wide and $100\ \text{nm}$ thick SiN mechanical resonator with side pads for electrical contacts and a gate. The pads, gate and the beam are exposed using e-beam lithography on a chip with $100\ \text{nm}$ pre-stressed SiN on Si. After removal of the exposed resist, Al is deposited using e-beam evaporation. Then the remaining resist is lifted off (along with the Al on top) using N-methyl-2-pyrrolidone at $80^\circ\ \text{C}$. The remaining Al masks part of the SiN layer during subsequent reactive ion etching, which structures the device. The beam is finally released using XeF_2 gas, which isotropically etches the Si beneath the SiN layer.

Excitations élémentaires dans les gaz de fermions superfluides

Hadrien Kurkjian et Alice Sinatra^{1,2,*}

¹TQC, Université Antwerpen, Universiteitsplein 1, B-2610 Antwerpen, Belgium

²Laboratoire Kastler Brossel, ENS-PSL, 24 rue Lhomond, 75231 Paris Cedex 05, France

Les gaz de fermions appariés sous leur température de superfluidité possède un riche spectre d'excitation : branche bosonique d'ondes sonores, excitations fermioniques liées à la rupture des paires et modes collectifs de Higgs. Nous étudions les couplages entre ces excitations élémentaires, mécanismes essentiels qui permettent à l'énergie de circuler entre les modes et donc déterminent les propriétés dissipatives du gaz, telles que sa viscosité, l'amortissement de ses oscillations, sa perte de cohérence temporelle ou son temps de thermalisation. Nous montrons notamment qu'en choisissant bien la force des interactions entre les particules, les gaz de fermions peuvent présenter une branche bosonique subsonique pour laquelle les couplages dominants mettent en jeu 4 quasiparticules, phonons ou excitations fermioniques. Cette physique nouvelle pourrait être observée en laboratoire avec les techniques actuelles, en suivant la décroissance temporelle d'une excitation du profil de densité du gaz. [1–3]

Paired Fermi gases under their superfluid temperature have a rich excitation spectrum : a bosonic sound branch, pair-breaking fermionic excitations and collective Higgs modes. We study the couplings between these elementary excitations, essential mechanisms that allow energy to flow between modes and therefore determine the dissipative properties of the gas, such as its viscosity, the damping of its oscillations, its loss of temporal coherence or its thermalization time. We show in particular that by tuning the strength of the interactions between the particles, Fermi gases can exhibit a subsonic bosonic branch for which the dominant couplings involve 4 quasiparticles, phonons or fermionic excitations. This new physics could be observed in the laboratory using state-of-the-art techniques by following the temporal decay of an excitation of the density profile of the gas. [1–3]

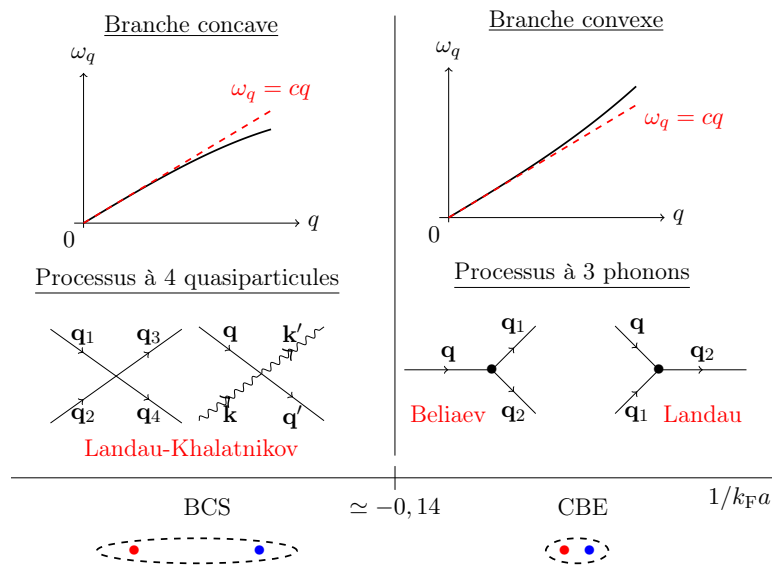


FIGURE 1. Amortissement des phonons dans le raccordement BEC-BCS

- [1] Hadrien KURKJIAN, Yvan CASTIN et Alice SINATRA : Landau-Khalatnikov phonon damping in strongly interacting Fermi gases. *EPL (Europhysics Letters)*, 116(4):40002, 2016.
- [2] Yvan CASTIN, Alice SINATRA et Hadrien KURKJIAN : Landau Phonon-Roton Theory Revisited for Superfluid ⁴He and Fermi Gases. *Phys. Rev. Lett.*, 119:260402, décembre 2017.
- [3] Hadrien KURKJIAN et Jacques TEMPERE : Absorption and emission of a collective excitation by a fermionic quasiparticle in a Fermi superfluid. *New Journal of Physics*, 19(11):113045, 2017.

* hadrien.kurkjian@uantwerpen.be

Theoretical prediction and experimental evidences of 2D monolayered transition metal oxide films family

Dmitry G. Kvashnin^{a,c*}, Konstantin V. Larionov^b, Leonid A. Chernozatonskii^c and Pavel B. Sorokin^{a,b,c}

- a. *National University of Science and Technology MISiS, Moscow, Russian Federation*
- b. *Technological Institute for Superhard and Novel Carbon Materials, Moscow, Russian Federation*
- c. *Emanuel Institute of Biochemical Physics RAS, Moscow, Russian Federation*

* dgkvashni@phystech.edu

2D and quasi-2D materials have attracted attention since the discovery of graphene, which can maintain its structure due to strong covalent bonding within a layer, whereas the weak van der Waals forces acting between the layers allow its isolation. Like graphene hexagonal boron nitride (h-BN) and quasi-2D sheets of transition metal dichalcogenides have been found so far, and reported to exhibit unique and attractive properties. These materials have their bulk counterparts with layered structures.

In contrast to the above reports, non-layered materials with wurtzite and cubic crystal structures were theoretically predicted to form 2D layers, and this possibility is important as it significantly widens the range of potential 2D materials. Recently, graphene-like 2D zinc oxide clusters and 2D iron clusters with a square lattice have been observed by aberration-corrected transmission electron microscopy. In both cases, the 2D layers were in the small pores in graphene, and their edges can be stabilized by bonding with carbon, whereas such geometry limits the size and properties of 2D materials.

Here we report the structure and properties of a novel family of 2D material, transition metal oxides (TMO), studied by theoretical methods which data perfectly supported by available experimental results. In particular, observed atomic structure of 2D CuO sheets agrees very well with our predictions.

Density functional theory allowed to elucidate the nature of the stability of observed metal nanofilms. It was defined a critical role of the oxygen impurity atoms in the formation of stable 2D CuO cluster with unexpected orthogonal crystal lattice. It was found that the structure and stability of 2D CuO clusters strongly depends on the concentration and relative arrangement of oxygen impurities. Number of oxygen configurations was analyzed and the stable configuration was found corresponded well with experimental data.

We predict that 2D TMO sheets have unusual electronic and magnetic properties depending on the composition. We study of stability of such films and its stabilization in the graphene 2D matrix. We combine crystal growth theory and atomistic computations for the prediction of the energy favorable structure of 2D TMO/graphene composite.

Results of this investigations were published in *Nanoscale* journal and submitted to *The Journal of Physical Chemistry Letters*.

Authors acknowledge the financial support of the RSF according to the research project № 17-72-20223. D.G.K. also acknowledges grant RFBR № 18-32-00682.

IN SITU NANO-INDENTATION OF SINGLE Au NANO CRYSTALS IN COMBINATION WITH BRAGG COHERENT DIFFRACTION IMAGING

F. Lauraux^{a*}, T.W. Cornelius^a, S. Labat^a, E. Rabkin^b, O. Thomas^a

a. Aix-Marseille Université de Toulon, CNRS, IM2NP UMR 7334, 13397 Marseille France

b. Technion Israel Institute of Technology, Technion City, Haifa 3200003, Israel

* florian.lauraux@im2np.fr

The mechanical properties of micro and nanostructures have been demonstrated to vary significantly from their bulk counterparts. However, despite numerous studies, plasticity at the nanoscale is not fully understood yet. In situ experiments are perfectly suited for the fundamental understanding of the onset of dislocation nucleation. In particular, Bragg Coherent X-ray diffraction imaging (BCDI), which is non-invasive and does not need complicated sample preparation, is perfectly adapted for in-situ nano-mechanical studies thanks to its high sensitivity to strain and defects. Previous BCDI on indented Au crystals demonstrated the capability to image a single prismatic loop induced by nano-indentation and trapped inside the crystal [1].

Here, Au crystals grown on sapphire substrates by dewetting magnetron sputtered Au thin films with a thickness of 45 nm at 900 °C for 24h, were indented using the scanning force microscope SFINX [2] and the elastic and plastic deformation was imaged by in-situ BCDI of the Au 111 Bragg peak at the ID01 beamline at ESRF. Since any movements of diffractometer motors may induce vibrations that eventually lead to damaging the nano-crystal under load, ordinary rocking scans are not suitable for recording 3D reciprocal space maps in-situ. Thanks to the achromacity of the KB mirrors, we scanned instead the energy of the incident X-ray beam, thus probing the intensity distribution in reciprocal space. Such E-BCDI was performed at different loading steps, hence imaging the evolution of strain and defects.

3D coherent diffraction patterns obtained during nano-indentation by scanning the energy of the incident X-ray beam as well as the phase are presented in Fig 1. With increasing applied mechanical load, the central part of the diffraction peak splits which translates in the appearance of defects separating the crystal in two domains (Fig. 1(b)). We further evidenced changes in the strain field with the increase of the applied load (Fig. 1(c-f)) which probably shows the deformation around the indent. After unloading the peak splitting and the corresponding defects as well as the variation in the strain field disappear. The high resolution 3D reconstructions of individual Au nano-crystals obtained by E-BCDI during nano-indentation thus give access to their morphology, the strain field, and dislocations therein as a function of the applied mechanical load.

To the best of our knowledge, this is the first time that E-BCDI has been successfully employed during in-situ experiments providing direct insight into the plasticity at the nanoscale and, in particular, the onset of defect nucleation.

[1] M.Dupraz, 3D imaging of a dislocation loop at the onset of plasticity in an indented nanocrystal, *Nano Lett.* 17 (2017)

[2] Z. Ren; Scanning force microscope for in situ nanofocused X-ray diffraction studies, *J. Synchrotron Radiat.* 21 (2014)

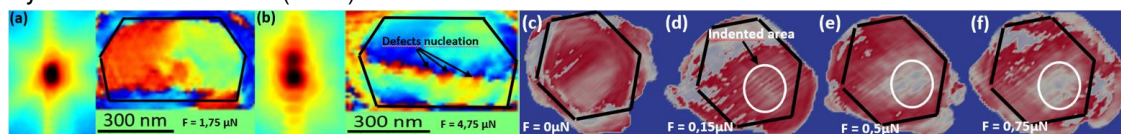


Figure 1 : a,b) Qz-Qy integrated images of the core of 3D diffraction patterns for two different mechanical loads and Z-y cut of reconstructions of the phase for the corresponding mechanical loads. c,d,e,f) X-y cut of reconstructions of the strain field for different mechanical loads.

Tuning the Properties of Confined Water in Standard and Hybrid Nanotubes: an Infrared Spectroscopic Study

Yuanyuan Liao^a, Pierre Picot^a, Jean-Blaise Brubach^b, Pascale Roy^b, Antoine Thill^a and Sophie Le Caër^{a*}

- a. LIONS, NIMBE, UMR 3685, CEA, CNRS, Université Paris-Saclay, CEA Saclay Bât. 546, F-91191 Gif-sur-Yvette Cedex, France
- b. Synchrotron SOLEIL AILES Beamline, L'Orme des Merisier, Saint-Aubin, BP 48, F-91192, Gif-sur-Yvette Cedex, France

* sophie.le-caer@cea.fr

Imogolite is a natural nanotubular aluminum silicate clay mineral, originally found in volcanic soils. Its well-defined, yet tunable structure makes it a good candidate for the study of water confined in a one-dimensional structure. Water confined in imogolite self-sustaining thin films was studied by means of infrared spectroscopy [1]. Two types of synthetic imogolites were investigated: a pristine imogolite (IMO-OH) with a hydrophilic inner surface fully covered with Si-OH groups and a hybrid imogolite (IMO-CH₃) with a hydrophobic inner surface fully covered with Si-CH₃ groups. Both imogolites have the same outer surface, covered with Al-OH groups. The infrared spectra were recorded in the 20 - 4000 cm⁻¹ spectral range as a function of the relative humidity. In particular, a detailed analysis of the O-H stretching band provides information on the H-bonding of confined water molecules inside and outside the IMO-OH tubes. The analysis of the various infrared signatures reveals the scenario for water filling as a function of relative humidity for the two systems. The adsorption in the IMO-OH tubes starts at the lowest relative humidity (< 10%). The inner surface of the tubes is first covered with water molecules, followed by the filling-up of the central part of the tubes, leading to very strong H-bonds and a structured spectrum. In contrast, the H-bonds of water adsorbed at the outer surfaces of these tubes are weaker. A different scenario is evidenced for water inside IMO-CH₃: very weakly H-bonded water molecules are present, a situation similar to what has been observed in carbon nanotubes. The present work shows that water confinement in imogolites is governed by the hydrophilicity of the inner walls. Indeed, at similar partial pressure, water can be less or more H-bonded depending on its interactions with the nanotube wall [2].

[1] Y-Y. Liao, P. Picot, J.-B. Brubach, P. Roy, S. Le Caër and A. Thill, Self-supporting thin films of imogolite and inogolite-like nanotubes for infrared spectroscopy, *Appl. Clay. Sci.* (2017), <https://doi.org/10.1016/j.clay.2017.1006.1005>

[2] Y-Y. Liao, P. Picot, M. Lainé, J.-B. Brubach, P. Roy, A. Thill and S. Le Caër, Tuning the Properties of Confined Water in Standard and Hybrid Nanotubes: an Infrared Spectroscopic Study, *Nano Research*, in press.

Size tunable Si/SiGe nanowire heterostructures

Luong M.A.^a, Robin E.^a, Den Hertog M.I.^{b*}, Pauc N.^c, Gentile P.^c, Baron T.^d,
Salem B.^d, Sistani M.^e, Lugstein A.^e

- a. Univ. Grenoble Alpes, CEA, INAC, MEM, F-38000 Grenoble, France
- b. Institut NEEL CNRS/UGA UPR2940, 25 avenue des Martyrs, 38042 Grenoble, France
- c. Univ. Grenoble Alpes, CEA, INAC, PHELIQS/SINAPS, F-38000 Grenoble, France
- d. Univ. Grenoble Alpes, CNRS, LTM, 38054 Grenoble, France
- e. Institute of Solid State Electronics, Technische Universität Wien, Floragasse 7, 1040 Vienna, Austria

* «martien.den-hertog@neel.cnrs.fr»

This paper reports the fabrication of Si/SiGe/Si quantum dot (QD) heterostructures, sandwiched between monocrystalline aluminium contacts using a thermally activated solid-state reaction between aluminium contacts on a SiGe NW. Such heterostructures can have promising applications in opto-electrical devices operating in the infrared, both in detection or emission, as well as for the fabrication of spin qubits. The contacts on the NW were defined by electron beam lithography using an electron transparent silicon nitride membrane as substrate, allowing in-situ TEM combined with characterization by high resolution scanning TEM as well as energy dispersive X-ray spectroscopy.

Using electrical in-situ TEM, we monitor the propagation of a crystalline Al phase inside the NW, and observe the spontaneous formation of an epitaxial and monocrystalline Al-Si-SiGe-Si-Al heterostructure. The advancement of the Al metal inside the NW pushes the Si atoms forward, creating a very silicon rich section between the Al metal and the original SiGe NW. First experiments indicate that the reaction stops when a segment of pure Si is created. The size of the created Si barriers appears to be depending on several parameters including the initial NW diameter, as well as the composition of the original SiGe alloy NW. In this paper we present a quantitative EDX study of the fabricated heterostructures.

Careful study of this interesting phenomenon may allow reproducible and self-limited fabrication of such heterostructures using a simple heating procedure. Moreover, the feature size of the created heterostructure does not depend on the spatial resolution of a lithography technique.

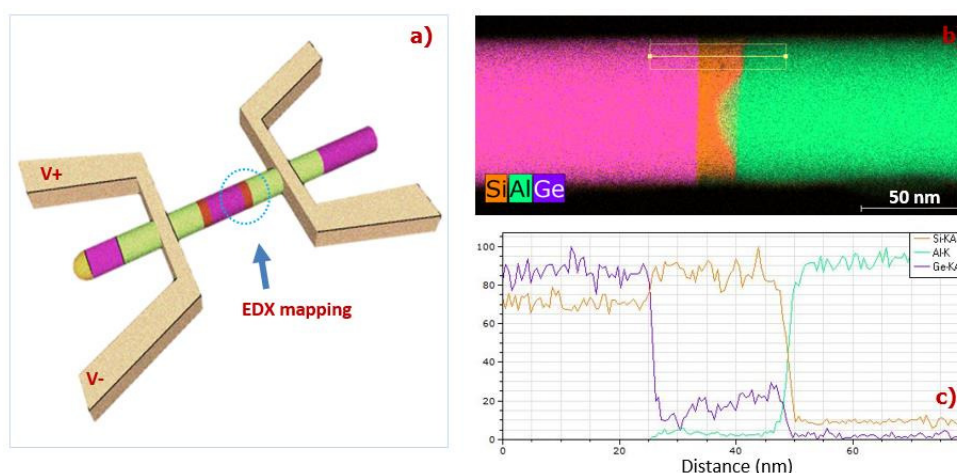


Figure 1 : (a) Schematic illustration of the Si/SiGe/Si NW heterostructure formation after Aluminium propagation in the SiGe NW by Joule heating technique. The blue circle indicates the position of EDX analysis. (b) EDX mapping of elements at the interface shows the presence of Si, Ge and Al. (c) The linescan crossing the interface demonstrates the Si "pile up" effect at the Al reaction interface.

Quasi-ballistic transport of spin-helical Dirac fermions in 3D topological insulator quantum wires

V. Labracherie^a, L. Veyrat^b, J. Dufouleur^a, S. Hampel^a, R. Giraud^{a,c*}

- a. Leibniz Institute for Solid State and Materials Research, IFW Dresden, D-01069 Dresden, Germany
 - b. Univ. Grenoble Alpes, CNRS, Grenoble INP, Institut Néel, 38000 Grenoble, France
 - c. Univ. Grenoble Alpes, CNRS, CEA, Grenoble INP, INAC-Spintec, 38000 Grenoble, France
- * romain.giraud@cea.fr

Despite strong disorder, the transport of surface Dirac fermions remains quasi-ballistic in narrow (quantum) nanostructures of a 3D topological insulator, as evidenced with Bi₂Se₃ or Bi₂Te₃ nanowires [1,2]. We demonstrate that such a unique behavior for a mesoscopic conductor results from the spin helicity of all quasi-1D surface modes, rather than from the topological nature of a single perfectly-transmitted mode. The weak coupling of spin-helical modes can be revealed by the non-universal behavior of conductance fluctuations [3], and the spin and energy-dependence of transmissions is well captured by both analytical and numerical models. It is further discussed that, under appropriate conditions, such 3D topological insulator quantum wires could be used not only for ballistic spin transport but also as spin filters.

- [1] J. Dufouleur *et al.*, Phys. Rev. Lett. **110**, 186806 (2013)
- [2] L.A. Jauregui *et al.*, Nat. Nano. **11**, 345 (2016)
- [3] J. Dufouleur *et al.*, Sci. Rep. **7**, 45276 (2017)

Spin injection into fonctionnalized multiwall carbon nanotubes

Philippe Lafarge^{a*}, Roméo Bonnet^a, Maria Luisa Della Rocca^a, Pascal Martin^b,
Jean-Christophe Lacroix^b, et Clément Barraud^a

- a. Matériaux et Phénomènes Quantiques, université Paris Diderot, Sorbonne Paris Cité, UMR 7162, CNRS, 75205 Paris cedex 13, France
- b. Laboratoire ITODYS, université Paris Diderot, Sorbonne Paris Cité, UMR 7086, CNRS, 75205 Paris cedex 13, France

* philippe.lafarge@univ-paris-diderot.fr

Due to their weak spin-orbit coupling and hyperfine interaction carbon based nanomaterials such as carbon nanotubes and graphene are promising materials for spin transport [1,2]. However, the contact resistance remains a key issue for an efficient spin injection at the interface between ferromagnetic metals and this kind of materials. Here, we show that using multiwall carbon nanotubes covalently fonctionnalized by diquonium molecules one can consistently control and increase the resistance to ferromagnetic electrodes. We will also present magnetoresistance measurements performed on the functionalized nanotubes and describe how it is influenced by the superlattice effects present in these systems.

[1] P. Seneor et al., Spintronics with graphene, MRS Bull. **37**, 1245 (2012)

[2] L. Hueso et al, Transformation of spin information into large electrical signals using carbon nanotubes, Nature **445**, 410 (2007)

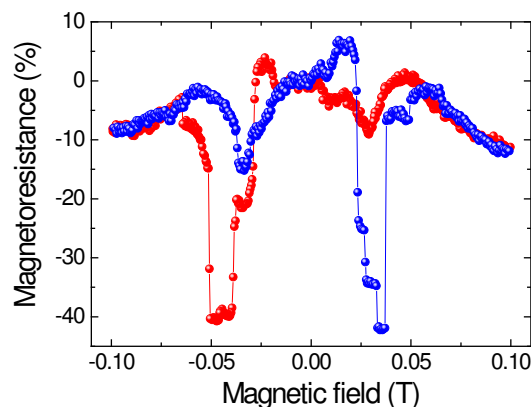


Figure 1 : Magnetoresistance of a multiwall functionalized carbon nanotube contacted with Ni electrodes measured at T = 1.5 K.

Rise and fall of frustration in Han Purple $\text{BaCuSi}_2\text{O}_6$

Nicolas Laflorencie^{a*}, Frédéric Mila,^b

a. Laboratoire de Physique Théorique, Université de Toulouse, CNRS, UPS, France

b. Institute of Physics, Ecole Polytechnique Fédérale de Lausanne (EPFL), Switzerland

* nicolas.laflorencie@irsamc.ups-tlse.fr << corresponding author >>

The ancient chinese pigment "Han purple", also known as $\text{BaCuSi}_2\text{O}_6$, has stimulated a lot of debates during the past decade [1,2,3,4,5]. The very peculiar properties of the Bose-Einstein condensation transition observed upon applying a strong magnetic field [2] have been thought to be a prototypical example of an exotic dimensional reduction mechanism induced by a *perfectly frustrated* 3D coupling between bilayers. However, the perfect frustration scenario was questioned in a recent theoretical work [6]. Here we aim at giving a comprehensive overview of this material. Building on NMR [4] and neutron scattering data [7] we theoretically address the current status of this compound through two different quantum spin models, with and without frustration.

- [1] M. Jaime *et al.*, Phys. Rev. Lett. **93**, 087203 (2004).
- [2] S. E. Sebastian *et al.*, Nature **441**, 617 (2006).
- [3] C. Rüegg *et al.*, Phys. Rev. Lett. **98**, 017202 (2007).
- [4] S. Krämer *et al.*, Phys. Rev. B **76**, 100406(R) (2007) ; **87**, 180405(R) (2013).
- [5] N. Laflorencie and F. Mila, Phys. Rev. Lett. **102**, 060602 (2009); **107**, 037203 (2011).
- [6] V. Mazurenko *et al.*, Phys. Rev. Lett. **112**, 107202 (2014).
- [7] S. Allenspach *et al.*, in preparation.

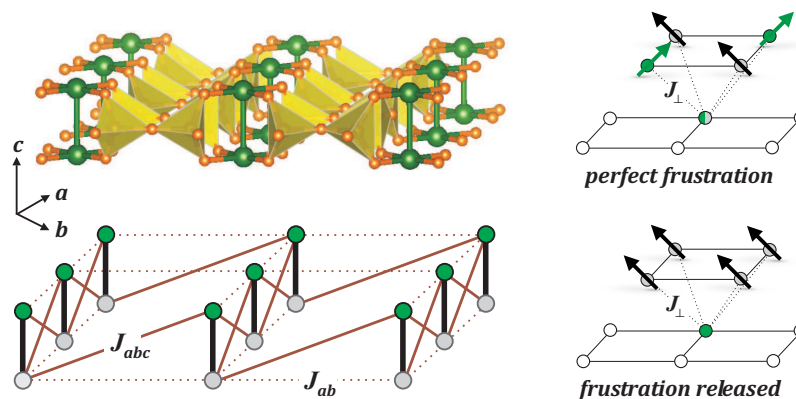


Figure 1: Two competing scenarios for the 3D coupling between bilayers units of $\text{BaCuSi}_2\text{O}_6$

Disorder-Induced Bose-Einstein Condensate in the Quantum Magnet DTNX at High Magnetic Fields

Nicolas Laflorencie^{a*}, Maxime Dupont^a, Sylvain Capponi^a, Anna Orlova^b, Rémi Blinder^b, Edwin Kermarrec^b, Hadrien Mayaffre^b, Claude Berthier^b, Armando Paduan-Filho^c, Mladen Horvatić^b

- a. Laboratoire de Physique Théorique, Université de Toulouse, CNRS, UPS, France
 b. Laboratoire National des Champs Magnétiques Intenses, CNRS, EMFL, UGA, UPS, and INSA, Grenoble, France
 c. Instituto de Física, Universidade de São Paulo, Brazil

* nicolas.laflorencie@irsamc.ups-tlse.fr << corresponding author >>

The high magnetic field regime of the disordered (Br-doped) quasi-one-dimensional $S=1$ antiferromagnetic material DTNX, $\text{Ni}(\text{Cl}_{1-x}\text{Br}_x)_2\cdot 4\text{SC}(\text{NH}_2)$, was believed to provide the first experimental realization of the elusive *Bose-Glass* phase in a quantum magnet [1]. However, the recent experimental and theoretical works [2-5] revealed a much richer scenario where *impurity-induced* localized bosonic degrees of freedom (building blocks for the putative Bose-Glass) form a new kind of Bose-Einstein condensate at low temperature: the BEC^* phase (Fig. 1). This is a purely many-body effect where interactions and disorder cooperate to restore a phase coherence via an "order-by-disorder" mechanism [6].

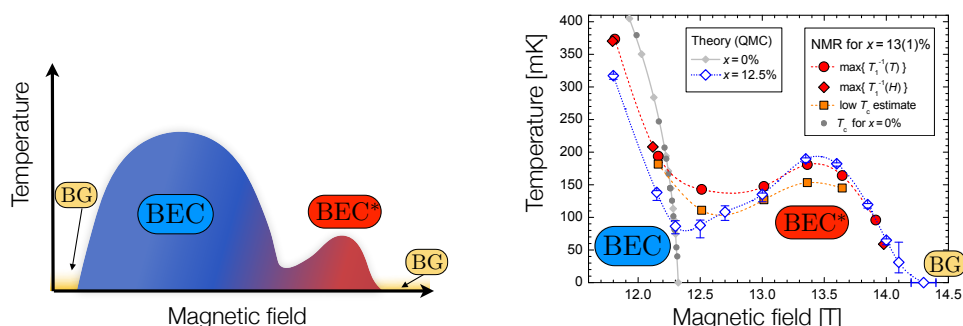


Figure 1: Left: Sketch of the global phase diagram of DTNX, where colors denote the BEC (blue) and BEC^* (red) phases, and the Bose-glass (BG, yellow) regime. Right: Focus on the higher field regime. The critical temperature determined from quantum Monte Carlo simulations for $x = 12.5\%$ doping (blue open diamonds) is compared to T_c estimates from $1/T_1$ NMR data in an $x = 13 \pm 1\%$ doped sample. Adapted from [5].

- [1] R. Yu *et al.*, Nature **489**, 379 (2012).
 [2] A. Orlova *et al.*, Phys. Rev. Lett. **118**, 067203 (2017).
 [3] M. Dupont, S. Capponi and N. Laflorencie, Phys. Rev. Lett. **118**, 067204 (2017).
 [4] M. Dupont *et al.*, Phys. Rev. B **96**, 024442 (2017).
 [5] A. Orlova *et al.*, preprint, arXiv:1801.01445.
 [6] J. Villain *et al.*, J. Phys. France **41**, 1263 (1980).

Particle removal efficiency correlation with the droplet impact pressure of high velocity spray

A. Lallart^{a,b,c*}, E. Lorenceau^b, P. Garnier^a, A. Cartellier^c et E. Charlaix^b

- a. STMicroelectronics Crolles2, 850 rue Jean Monnet 38921 Crolles, France
- b. Univ. Grenoble Alpes, CNRS, LIPhy, 38000 Grenoble, France
- c. Univ. Grenoble Alpes, Grenoble INP, LEGI, 38000 Grenoble, France

* adeline.lallart@st.com

In order to keep a high yield during integrated circuits production, a continuous improvement has been carried out in the particles cleaning area. Moreover, as typical dimension of microelectronic circuit is getting smaller and smaller, tinier and tinier particles have to be removed. Integrated circuit industry is thus seeking for robust solutions to clean nanoparticles, keeping finest transistors features integrity, and extremely low material consumption [1]. Indeed, to remove a particle from a surface, an external stress large enough to break the link between the particle and the surface must be applied. This has been successfully performed for several years using the pressure developed during the impact of micronic high speed droplets of the cleaning sprays.

Even though the adhesion of particles and droplet impact on solid surfaces have been studied and documented for years, there is no clear physical understanding on the spray process cleaning mechanism. Indeed, measurements from literature using micronic transducer [2], report dynamical impact pressures in the order of ρV^2 where ρ is the liquid density and V the impact velocity, which are too low to detach the particles.

In order to improve and understand the removal efficiency of high velocity sprays, we perform a comprehensive study by artificially contaminating the surfaces with calibrated nanoparticles ranging from 40 nm up to 200 nm. By using a laser diffractometer able to individually count these nanoparticles, we quantify the efficiency of the spray action over the different parameters of the process, focusing especially on the influence of τ_{aging} , the contamination time, and on t_s , the time during which the spray is applied.

Two regimes of particle removal have been highlighted. A first regime of low adhesion, observed for long t_s and short τ_{aging} , exhibits a saturated removal efficiency: the number of removed particles N_p is equal to N_i the number of particle initially present on the surface, while in the second regime obtained for long τ_{aging} and short t_s , the adhesion is strong and the efficiency limited. To explain those observations and quantify the removal efficiency, we propose a new model based on the following features. First, to describe the evolution of the adhesion force over time, we rely on the classical moisture induced aging model initially proposed for granular matter [3] which predicts a logarithmic temporal evolution of the adhesion force. Then to explain the influence of the spray time, we rely on numerical simulations [4], [5] and asymptotic expansions [6] of the pressure field below a droplet impacting a solid surface, which diverges at short time. This allow us to collapse all our data points and predicts that in the high adhesion regime, the removal efficiency is proportional to $\frac{t_s}{(\ln \tau_{aging})^2}$.

We therefore believe that our results are the first experimental validation of the predicted short time self-similar regime of drop impact. This is due to the nanoscale nature of the particular defects we use, that allows us to probe the divergency of the pressure field at a nanometer scale.

Analogue of cosmological particle creation in electromagnetic wave-guides

Sascha Lang^{a*} and Ralf Schützhold^b

- a. Fakultät für Physik, Universität Duisburg-Essen, Lotharstrasse 1, 47057 Duisburg, Germany
- b. Helmholtz-Zentrum Dresden-Rossendorf, 01328 Dresden, Germany
- c. Institut für Theoretische Physik, Technische Universität Dresden, 01062 Dresden, Germany

* sascha.lang@uni-due.de

Quantum field theory in curved space-time predicts a mechanism of pair-wise particle creation to occur in expanding universes. A similar effect is expected to arise in systems which have fixed spatial dimensions but a time-dependent speed of light.

In this talk, we consider a one-dimensional array of coupled harmonic oscillators that can be implemented with a row of *LC*-circuits. By suddenly changing the coupling constant for all pairs of neighbouring oscillators, the effective speed of light c_{eff} inside the wave-guide can be manipulated.

Quantum mechanical calculations of the two-point correlation function for the canonical variables reveal that a step-wise change in the velocity c_{eff} instantaneously produces pairs of particles that move in opposite directions.

Investigation of the formation mechanisms of ZnO nanowires on Au thin films by chemical bath deposition

Clément Lausecker^{a,b,c*}, Bassem Salem^b, Xavier Baillin^c, Hervé Roussel^a, Eirini Sarigiannidou^a, Franck Bassani^b, Estelle Appert^a, Sebastien Labau^b, and Vincent Consonni^a

a. Univ. Grenoble Alpes, CNRS, Grenoble INP, LMGP, 38000 Grenoble, France

b. Univ. Grenoble Alpes, CNRS, LTM, 38000 Grenoble, France

c. Univ. Grenoble Alpes, CEA, LETI, 38000 Grenoble, France

* clement.lausecker@grenoble-inp.fr

Chemical bath deposition (CBD) is an efficient technique to form dense arrays of ZnO nanowires at low cost and low temperature (< 100 °C). In order to achieve the desired dimension and morphology of ZnO nanowires, a pre-deposited seed layer is required to favor the heterogeneous nucleation process. While polycrystalline ZnO seed layers are extensively used, alternative metallic seed layers are needed for specific applications like piezoelectric generators. Au thin films is a potential candidate to be used as direct metallic contact in these devices and promising results have already been obtained [1]. Nevertheless, the morphological control of the ZnO nanowire array is still limited as the understanding of their nucleation and growth mechanisms on Au thin films has not been addressed yet.

In this context, several silicon wafers with varying Au thicknesses in the range of 5 to 100 nm are prepared, on which ZnO nanowires are grown by CBD under identical standard conditions using zinc nitrate and hexamethylenetetramine in aqueous solution [2]. The evaporated Au seed layers show a polycrystalline structure with a strong texture along the <111> direction, which is favorable for the nucleation and growth of ZnO nanowires. The structural properties of ZnO nanowires and its relationship with the morphology of the Au seed layers are investigated by scanning electron microscopy, atomic force microscopy, x-ray diffraction, and x-ray pole figures. Furthermore, a thorough study of the properties of the grain/nanowire interfacial region is carried out by transmission electron microscopy, allowing us to establish a complete nucleation and growth diagram. Electron beam lithography is eventually used to implement selective area growth on top of the Au seed layers, as a prerequisite for their efficient integration into piezoelectric nanogenerators.

[1] S. Xu et al, J. Mater. Res., **23**, 2072-2077 (2008)

[2] R. Parize et al., J. Phys. Chem. C, **120**, 5242-5250 (2016)

Quantum Noise in a Quantum Dot in the Kondo regime

M. Lavagna^{a*}, S. Sahoo^{a,b}, T.Q. Duong^c, R. Zamoum^d, and A. Crépieux^c

- a. Université Grenoble Alpes, CEA, INAC, PHELIQS, F-38000 Grenoble, France
- b. Physics Department and Research Center OPTIMAS, University of Kaiserslautern, 67663 Kaiserslautern, Germany
- c. Aix Marseille Université, Université de Toulon, CNRS, CPT UMR 7332, 13288 Marseille, France
- d. Faculté des sciences et des sciences appliquées, Université de Bouira, rue Drissi Yahia, Bouira 10000, Algeria

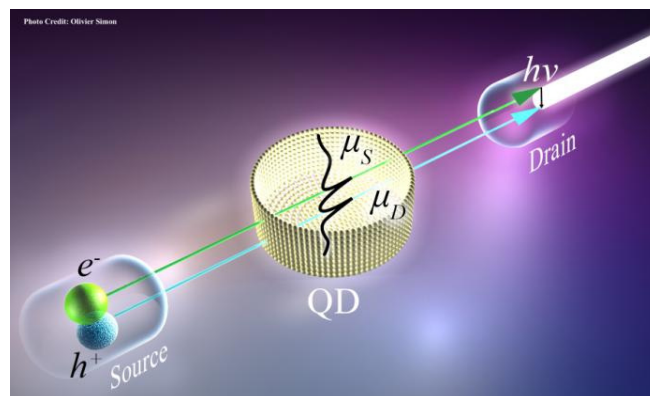
* mireille.lavagna@cea.fr

The fluctuations of electrical current provide information on the dynamics of electrons in quantum devices. Understanding the nature of these fluctuations in a quantum dot is thus a crucial step insofar as this system is the elementary brick of quantum circuits. In this context, we develop a theory for calculating the noise at finite-frequency in a quantum dot connected to two reservoirs in the presence of interactions and for any symmetry of the couplings to the reservoirs [1,2]. This theory is developed in the non-equilibrium Keldysh Green function technique. We establish an analytical expression for the noise in terms of the various transmission amplitudes between the reservoirs and of some effective transmission coefficient which we define. The obtained expression can be seen as the analog of the Meir-Wingreen formula for the current in the sense that it includes inelastic scattering contributions. We give a physical interpretation of the result on the basis of the transmission of an electron-hole pair to the concerned reservoir where it emits an energy after recombination. The interactions are then treated by solving the self-consistent equations of motion for the Green functions. We find that the noise derivative is zero until the voltage reaches a threshold value set by the measuring frequency, beyond which a Kondo peak appears when the system is in the Kondo regime. Our findings are in very good agreement with recent measurements in carbon nanotube quantum dots [3].

[1] A. Crépieux, S. Sahoo, T.Q. Duong, R. Zamoum, and M. Lavagna, Phys. Rev. Lett. **120** (2018)

[2] R. Zamoum, M. Lavagna, and A. Crépieux, Phys. Rev. B **93**, 235449 (2016)

[3] R. Delagrance, J. Basset, H. Bouchiat, and R. Deblock, Phys. Rev. B **97**, 041412(R) (2018)



Zinc oxide based heterostructures for terahertz quantum cascade lasers

N. Le Biavan^{a*}, M. Hugues^a, M. Montes Bajo^b, J. Tamayo-Arriola^b, A. Jollivet^c, B. Hinkov^d, B. Meng^e, D. Lefebvre^a, Y. Cordier^a, B. Vinter^a, F.-H. Julien^c, A. Hierro^b, G. Strasser^d, J. Faist^e, J.-M. Chauveau^a

- a. Université Côte d'Azur, CNRS, CRHEA, 06560 Valbonne, France
- b. ISOM and Ing. Electrónica, Universidad Politécnica de Madrid, Avda. Complutense 30, 28040 Madrid
- c. Centre de Nanosciences et de Nanotechnologies, CNRS, University Paris-Sud, University Paris-Saclay, C2N-Orsay, 91405 Orsay Cedex, France
- d. Center for Micro- and Nanostructures, Vienna University of Technology, Floragasse 7, 1040 Vienna, Austria
- e. Institute of Quantum Electronics, ETH Zurich, August-Piccard-Hof 1, Zurich 8093, Switzerland

* nlb@crhea.cnrs.fr

While mid-infrared Quantum Cascade Lasers (QCL) are widely spread and even commercialized, the operating temperature of QCL in the terahertz range is still limited under 200K. This effect comes from the low LO-phonon energy of materials which are commonly used for this purpose – as GaAs for instance (LO-phonon energy: 36 meV). To overcome this issue, material systems with high LO-phonon energy have been proposed: GaN and ZnO (respectively, 90 meV and 72 meV). The advantage of ZnO compared to GaN is the availability of non-polar native substrates. On one side, non-polar orientations make easier the QCL design because there is no electric field to take into account. On the other side, native substrates improve drastically the crystal quality, which is necessary for electrical injection.

In this study state-of-the-art ZnO/(Zn,Mg)O multi-quantum wells (MQWs) were grown on m-plane ZnO substrates by molecular beam epitaxy. They exhibit a surface roughness under 0.5 nm and thicknesses were determined with a precision of one monolayer. The residual doping is as low as 10^{15} cm^{-3} . The high quality of our MQWs has led to the observation of ISBT at room temperature by absorption experiment in the infrared domain. The dependence of the transition energy with the quantum well thickness perfectly matches the calculations [1,2]. Photoluminescence on coupled quantum wells reveals that tunnel effect is possible through the observation of exciton transfer across the barrier. Thus the two physical effects on which the QCL is based are present in our samples. This study paves the way for the realization of ZnO QCLs.

This work was funded by EU commission under the H2020 FET-OPEN program; project “ZOTERAC” FET-OPEN 6655107.

[1] N. Le Biavan, M. Hugues, M. Montes Bajo, J. Tamayo-Arriola, A. Jollivet, D. Lefebvre, Y. Cordier, B. Vinter, F.-H. Julien, A. Hierro, and J.-M. Chauveau, *Appl. Phys. Lett.* **111**, 231903 (2017)

[2] M. Montes Bajo, J. Tamayo-Arriola, A. Jollivet, M. Tchernycheva, F.-H. Julien, R. Peretti, J. Faist, M. Hugues, J.-M. Chauveau, and A. Hierro, *Proc SPIE* **10105**, 101050O (2017)

FDSOI cryogenic electronics for quantum computing

L. Le Guevel^{a*}, G. Billiot^a, H. Bohuslavskiy^a, S. Barraud^a, L. Hutin^a, M. Vinet^a,
S. De Franceschi^b, M. Sanquer^b, X. Jehl^b, L. Jansen^b, and G. Pillonnet^a

a. Univ. Grenoble Alpes, CEA, LETI, Minatec Campus, F-38000 Grenoble, France

b. Univ. Grenoble Alpes, CEA, INAC, PHELIQS, F-38000 Grenoble, France

* loick.leguevel@cea.fr

Cryogenic electronics has challenging applications for low noise circuits such as detectors in spacecraft missions, high energy physics, or metrology but appears to be mandatory in future quantum computing experiments to avoid the heat load from room temperature due to the increasing number of cables needed to control many qubits operating at hundreds of mK. A typical architecture[1] of a solid-state quantum computer consists of multiple layers with different functionalities at different operating temperatures. Most of the electronics is placed at the 4 K stage to benefit of the larger dissipation budget (1 W). For the case of silicon qubits, the typical operation temperature is below 100 mK. Even though higher temperatures of around 1 K may as well be possible, the development of control and read-out electronics operating at 1 K or below seems desirable.

Most technologies used at liquid nitrogen temperature such as BiCMOS or CMOS suffer from substrate carrier freeze-out at liquid helium temperatures that deteriorates the functioning of transistors. The newly developed Fully Depleted Silicon On Insulator (FDSOI) technology based on an extremely thin MOSFET channel-structure has promising applications at low temperatures with less sensitivity to cryogenic freeze-out effects, lower dissipation, and faster operation with the potential of forming a monolithic system with FDSOI qubits.

Using the cryogenic characterization done at CEA-INAC[2] of MOSFETs based on 28-nm FDSOI technology, we designed building blocks of electrical circuits (multiplexers, transimpedance amplifiers, ring oscillators, ...) for operation at low temperatures. Examples of circuit design will be shown together with electrical tests at liquid helium temperature.

[1] E. Charbon et al., Cryo-CMOS for quantum computing, in *Electron Devices Meeting*, 2016, p. 13-5

[2] H. Bohuslavskiy et al., 28nm FDSOI Technology: Cryogenic Control Electronics for Quantum Computing, in *Silicon Nanoelectronics Workshop*, 2017, p. 143-144

CNT field emission sources for X-ray imaging

P. Legagneux

Thales Research & Technology, Palaiseau, France
pierre.legagneux @thalesgroup.com

Carbon nanotube (CNT) based X-ray source technology has been investigated for imaging applications because of CNT cathode attractive characteristics including high current emission and fast switching.

The field emission properties of vertically aligned multiwalled CNTs will be presented. This will include the emission characterization of individual CNTs and arrays of CNTs. Both the current density and the long term stability will be shown.

For the switching functionality, we propose two different approaches based on the optical control of a CNT cathode. The first one is an array of CNTs, each CNT being associated with a p-i-n photodiode. The functions of photon-electron conversion and electron emission are thus separated. This photocathode combines the very good field emission properties of carbon nanotubes and the excellent efficiency provided by semiconductor photodiodes. The second one relies on an array of CNTs, each CNT being associated with a coplanar electrode. In this case, the whole cathode emission is controlled with a common photoswitch.

The performances of X-ray tubes based on these switchable CNT field emission sources will then be presented.

Probing the influence of many-body fluctuations on Cooper pair tunneling using circuit QED

S. Léger^{a*}, J. Puertas Martínez^a, L. Planat^a, R. Dassonneville^a, K. Bharadwaj^a, F. Foroughi^a, O. Buisson^a, C. Naud^a, W. Guichard^a, S. Florens^a, I. Snyman^b and N. Roch^a

a. Univ. Grenoble Alpes, CNRS, Grenoble INP, Institut Néel, 38000 Grenoble, France

b. Mandelstam Institute for Theoretical Physics, School of Physics, University of the Witwatersrand, Johannesburg, South Africa

* sebastien.leger@neel.cnrs.fr

Because of the value of the hyperfine constant ($\alpha \sim 1/137$) observing many body effects in light-matter interaction is challenging. Reaching this unexplored regime is now possible using the tools of circuit Quantum ElectroDynamics (cQED) [1]. Indeed, in such circuits one can build capacitances, inductances and Josephson junctions in order to design harmonic oscillators (which will simulate the light) and quantum bits (which will simulate the matter). Then light-matter interaction can be made both very strong and tunable by engineering properly the different parts of our circuit.

In this work we investigate the interactions between the plasma modes sustained by arrays of more than 2000 SQUIDs (the light) and a small Josephson junction (the matter). Moreover, the characteristic impedance of the SQUIDs array can be tuned in situ by applying a magnetic field. Having such a knob is extremely powerful since this impedance sets the amplitude of the voltage fluctuations associated to these plasma modes. Since light-matter interaction is huge in our circuit, these fluctuations can directly affect the Cooper pair tunneling across the small Josephson junction, as predicted 40 years ago [2]. Thus we can investigate this phenomenon in great detail and more specifically the competition between quantum and thermal fluctuations. It is easy to reduce the tunneling across a Josephson junction (or equivalently its critical current) using thermal fluctuation, it is much more difficult to do so with only quantum fluctuations, and even more difficult to discriminate what is coming from the thermal and quantum fluctuations. Nonetheless, by engineering the shape of the impedance of the SQUIDs array as a function of the frequency and by using a self-consistent theory we are pretty confident in the fact that we are able to renormalize the critical current of our small junction up to half of its bare value only because of the many-body quantum fluctuations produced by the plasma modes.

[1] J. Puertas Martínez, S.Léger, N. Gheereart, R. Dassonneville, N. Planat, F. Foroughi, Y. Krupko, O. Buisson, C. Naud, W. Guichard, S. Florens, S. Snyman, and N. Roch, "Probing a transmon qubit via the ultrastrong coupling to a josephson waveguide," arXiv preprint arXiv:1802.00633 (2018).

[2] A. O. Caldeira and A. J. Leggett, "Influence of Dissipation on Quantum Tunneling in Macroscopic Systems", Physical Review Letters 46, 211 (1981).

Ferroelectric and magnetic properties of hybrid multiferroic layers

LEMAITRE Matthieu^{a*}, PIRAUX Luc^a, JONAS, Alain M^a, et NYSTEN Bernard^a

a. Institute of Condensed Matter and Nanosciences, Université catholique de Louvain, Place Croix du Sud 1, B-1348 Louvain-la-Neuve, Belgium

* Email of corresponding author : matthieu.lemaitre@uclouvain.be

Multiferroic nanostructured materials combine ferroelectric and ferromagnetic properties, leading to magnetoelectricity, which is of interest of multiple channel data storage and sensor applications.

In this context, we are studying nanostructured arrays in which the ferromagnetic and ferroelectric elements are repeated over a regular bidimensional lattice (see Figure 1), in the aim of maximizing the magnetoelectric coupling by proper design of the topology. Here, we present the fabrication of multiferroic layers containing NiCo or CoFe magnetic binary alloys and a ferroelectric polymer phase (PVDF-TrFE). The process requires the combination of a series of techniques - spin coating, nanoimprint lithography and electrodeposition. This process provides access to complementary nanostructured patterns of 0-2 and 2-0 bidimensional connectivity.

In this communication, we will focus on the optimization of the nanoimprint and electrodeposition processes, which are crucial to have a final hybrid layer of well defined geometry. The connectivity and topography of the layers are studied by atomic force microscopy (AFM) and scanning electron microscopy (SEM). Furthermore, we will discuss first results by piezoresponse force microscopy (PFM) and alternating gradient magnetometry (AGM), performed to investigate the coupling between electrical and magnetic phases.

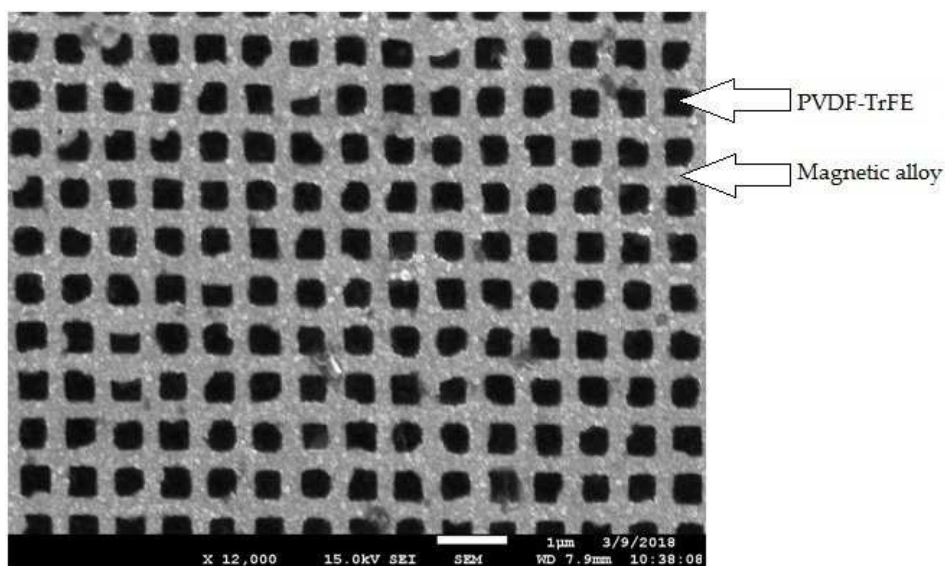


Figure 1 : SEM image of CoFe grid around TrFE squares

Role of nonlocal Coulomb correlations in pure and electron-doped Sr_2IrO_4

Benjamin Lenz^{a*}, Cyril Martins,^b and Silke Biermann^{a,c}

- a. Centre de Physique Théorique, Ecole Polytechnique, CNRS UMR 7644, Université Paris-Saclay, 91128 Palaiseau, France
- b. Laboratoire de Chimie et Physique Quantiques, UMR 5626, Université Paul Sabatier, 118 route de Narbonne, 31400 Toulouse, France
- c. Collège de France, 11 place Marcelin Berthelot, 75005 Paris, France

* benjamin.lenz@polytechnique.edu

The quasi-2D spin-orbit system Sr_2IrO_4 has raised tremendous interest recently, due to intriguing similarities to the high- T_c superconducting copper oxides. We study the evolution of the electronic structure of this material using a combination of ab initio density functional theory and many-body techniques. The effects of spin-orbit coupling, distortions of the oxygen octahedra and Hubbard interactions are included on a first-principles level. We calculate the momentum-resolved spectral function and compare to recent angle-resolved photoemission data, finding good agreement with experiment. Furthermore, we study the evolution of the electronic structure of Sr_2IrO_4 upon electron-doping. We show that short-range antiferromagnetic fluctuations are crucial to account for the electronic properties of the material even in the high-temperature paramagnetic phase. The emerging exotic metallic state exhibits pseudo-gap spectral features in good agreement with experiments on La-doped Sr_2IrO_4 , for which we propose a surprisingly simple theoretical mechanism.

- [1] C. Martins, B. Lenz, L. Perfetti, V. Brouet, F. Bertran, and S. Biermann, Nonlocal Coulomb correlations in pure and electron-doped Sr_2IrO_4 : Spectral functions, Fermi surface, and pseudo-gap-like spectral weight distributions from oriented cluster dynamical mean-field theory, *Phys. Rev. Materials* **2**, 032001 (2018)

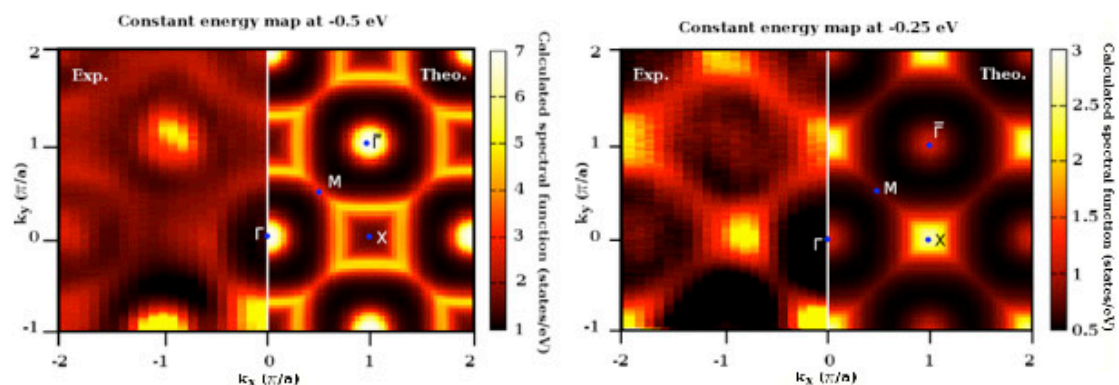


Figure 1: Constant energy maps of the spectral density at -0.5eV (left) and -0.25eV of undoped Sr_2IrO_4 . Experimental and theoretical spectral densities show good agreement.

Classical analogue of the Unruh effect

Ulf Leonhardt^{a*}, Itay Griniasty^a, Sander Wildeman^b, Emmanuel Fort^b, and Mathias Fink^b

a. Weizmann Institute of Science, Rehovot 761001, Israel

b. Institut Langevin, ESPCI, CNRS, PSL Research University, 1 rue Jussieu, 75005 Paris, France

* ulf.leonhardt@weizmann.ac.il

In the Unruh effect [1] an accelerated observer perceives the quantum vacuum as thermal radiation. This has been one of the most significant results of theoretical physics of the second half of the 20th century, but it has never been observed yet. We discovered that the Unruh effect has a deep root in the classical physics of waves. Although noise like the vacuum noise is random in space, it is organized in space-time, because it is carried by waves. This organization of wave noise creates the Unruh effect. Following this idea we performed a simple experiment with water waves where we see the first indications of a Planck spectrum in the correlation energy [2]. We have thus observed an Unruh effect for the first time.

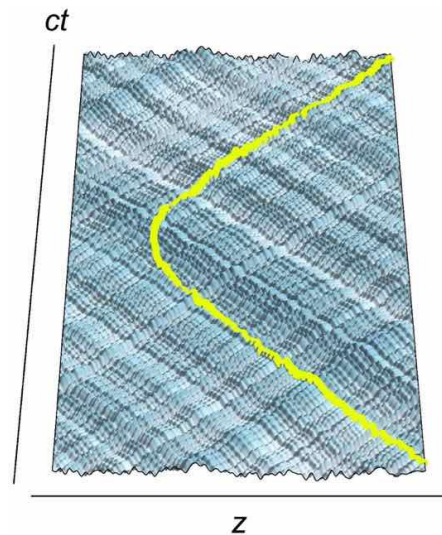


Figure 1: Principal idea. A container is filled with water subject to noise creating ripples on the water surface. Spatial noise is organized in space time. Correlations are observed along the trajectory of an accelerated observer.

- [1] W. G. Unruh, Notes on black-hole evaporation, *Phys. Rev. D* **14**, 870 (1976).
 [2] U. Leonhardt, I. Griniasty, S. Wildeman, E. Fort and M. Fink, Classical analogue of the Unruh effect, arXiv:1709.02200 (2017).

Origine de la polarisation et couplage magnéto-électrique dans la famille de composés multiferroïques RMn_2O_5

Marie-Bernadette Lepetit^{*a,b}

a. Institut Néel, UPR2940 CNRS/UGA, 25 av. des Martyrs, 38042 Grenoble, France

b. Institut Laue Langevin, 71 av. des Martyrs, 38042 Grenoble, France

* Marie-Bernadette.Lepetit @ neel.cnrs.fr

Les composés multiferroïques sont des matériaux multifonctionnels qui ont la propriété de coupler plusieurs ordres de nature différente. C'est ainsi le cas de matériaux magnéto-électriques qui couplent la polarisation avec l'ordre magnétique. Dans de tels systèmes, lorsque le couplage est linéaire et de forte amplitude, il est possible de renverser la polarisation électrique en appliquant un champ magnétique et de modifier l'ordre magnétique par l'application d'un champ électrique.

La famille RMn_2O_5 présente dans certains composés ce type de couplage fort [1], ou bien des polarisations de grande amplitude [2], et dans d'autres systèmes un couplage nul [3]. Dans ce travail nous présenterons la manière dont la frustration magnétique est à l'origine de la polarisation observée [3-5] et de son amplitude selon la nature des terres rares.

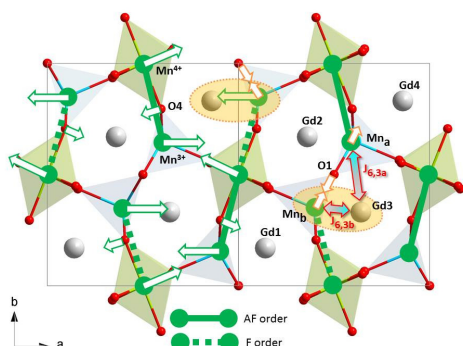


Figure 1: Atomic displacement releasing the magnetic frustration and responsible for the polarisation.

- [1] N. Hur, S. Park, P. A. Sharma, J. S. Ahn, S. Guha and S-W. Cheong, Nature 429, 392 (2004)
- [2] B.Kh. Khannanov, E.I. Golovenchits and V.A. Sanina, Journal of Physics: Conference Series 572, 012046 (2014)
- [3] G. Yahia, F. Damay, S. Chattopadhyay, V. Balédent, W. Peng, E. Elkaim, M. Whitaker, M. Greenblatt, M.-B. Lepetit et P. Foury-Leylekian, Phys. Rev. B 95, 184112 (2017)
- [4] Ghassen Yahia, Françoise Damay, Sumantha Chattopadhyay, Victor Balédent, Wey Peng, S.W Kim, M. Greenblatt, Marie-Bernadette Lepetit, Pascale Foury-Leylekian, Phys. Rev. B 97, 085128 (2018)
- [5] Sumantha Chattopadhyay, Sylvain Petit, Eric Ressouche, Stéphane Raymond, V. Balédent, Ghassen Yahia, Wey Peng, Julien Robert, Marie-Bernadette Lepetit, M. Greenblatt and Pascale Foury-Leylekian, Scientific Reports 7, 14506 (2017)

Contrôle de l'ordre orbital dans des super-réseaux de manganite

Marie-Bernadette Lepetit^{*a,b}

- a. Institut Néel, UPR2940 CNRS/UGA, 25 av. des Martyrs, 38042 Grenoble Cedex 9, France
- b. Institut Laue Langevin, 71 av. des Martyrs, 38042 Grenoble Cedex 9, France

* Marie-Bernadette.Lepetit @ neel.cnrs.fr

Le contrôle des propriétés des matériaux par les interfaces, lorsque ceux-ci sont déposés dans des super-réseaux est l'un des sujets qui ont été très étudiés ces dernières années. Dans ce cadre là les oxydes de métaux de transition de structure perovskites présentent de nombreux atouts à la fois du point de vue de la qualité de l'épitaxie et de la possibilité qu'offrent ces matériaux de moduler leurs propriétés. En effet, les oxydes de métaux de transition sont des systèmes fortement corrélés dans lesquels de nombreux degrés de liberté sont en compétition. Il en résulte des diagrammes de phases très riches et une compétition entre différents états fondamentaux que l'on peut ainsi choisir par des contraintes extérieures comme les interactions aux interfaces.

Dans ce travail [1] nous présenterons une étude théorique de la possibilité de contrôle de l'ordre orbital dans des super-réseaux de manganites par l'intermédiaire de l'interface avec la couche d'intercalation. Nous montrerons ainsi comment le choix du matériau pour cette dernière permet de favoriser l'occupation de l'orbitale $d_{x^2-y^2}$ ou d_{z^2} au niveau de Fermi de la manganite. Alors que l'occupation préférentielle de l'orbitale d_{z^2} favorise une elongation des couches à l'interface et de faibles couplages magnétiques dans le plan, l'occupation préférentielle de l'orbitale $d_{x^2-y^2}$ favorise une contraction des couches à l'interface, de forts couplages magnétiques dans le plan, et par conséquent une température de Curie élevée [2,3].

- [1] Ayşegül Begüm Koçak, Julien Varignon, Sébastien Lemal Philippe Ghosez et Marie-Bernadette Lepetit, Phys. Rev. B **96**, 125155 (2017), "Control of the orbital ordering in manganite superlattices and impact on properties"
- [2] Aymeric Sadoc, Bernard Mercey, Charles Simon, Dominique Grebille, Wilfrid Prellier et Marie-Bernadette Lepetit, Phys. Rev. Letters **104**, 046804 (2010), "Large increase of the Curie temperature by orbital ordering control"
- [3] Marie-Bernadette Lepetit, Bernard Mercey et Charles Simon, Phys. Rev. Letters **108**, 087202 (2012), "Understanding interface effects in perovskites thin films."

Reissner-Nordström Black Hole in Bose-Einstein Condensates of Light

Lei Liao^{a,c}, Erik C. I. van der Wurff,^{a,c} Dries Van Oosten,^{b,c} Henk Stoof^{a,c,*}

- a. Institute for Theoretical Physics, Utrecht University, Princetonplein 5, 3584 CC Utrecht, The Netherlands
- b. Debye Institute for Nanomaterials Science, Utrecht University, Princetonplein 5, 3584 CC, The Netherlands
- c. Center for Extreme Matter and Emergent Phenomena, Utrecht University, Princetonplein 5, 3584 CC, The Netherlands

* h.t.c.stoof@uu.nl

By fabricating suitable devices, it is possible to create a sink for light in the center of a microcavity. This sink results in the creation of a so-called radial vortex, which is in fact a two-dimensional Reissner-Nordström black-hole analogue. We theoretically investigate the analogue Hawking radiation and the associated greybody factor of this Reissner-Nordström black-hole in a Bose-Einstein condensate (BEC) of photons. Finally, we determine the density-density and velocity-velocity correlation functions of this Hawking radiation, which can be measured by observing the spatial correlations in the fluctuations in the light emitted by the cavity.

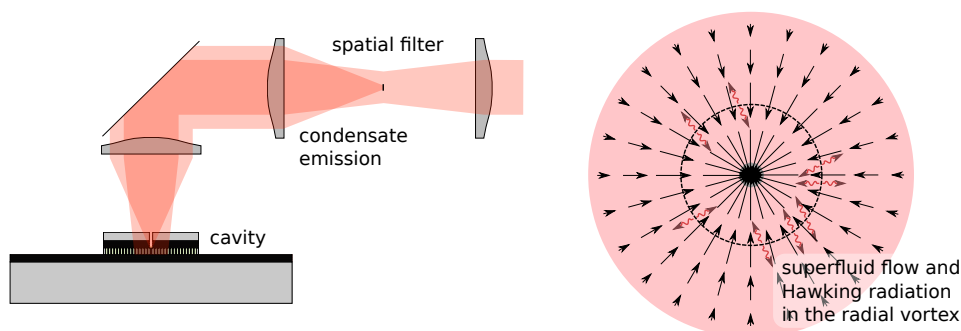


Figure 1: Schematic illustrating the black-hole experiment. We fabricate a cavity with a small hole in the top mirror in the center of the cavity. Light from the condensate leaks out from this hole, which induces a flow in the photon condensate towards the hole and results in a so-called sonic horizon.

Using external synchronization of spin torque oscillators for data transmission via phase shift keying

A. Litvinenko^{a*}, C. Murapaka^a, P. Sethi^a, A. Jenkins^b, L. Vila^a, V. Cros^c, P. Bortolotti^d, R. Ferreira^b and U. Ebels^a

- a. Univ. Grenoble Alpes, CEA, CNRS, INAC, SPINTEC, F-38000 Grenoble, France
- b. International Iberian Nanotechnology Laboratory (INL), Braga, Portugal
- c. Unité Mixte de Physique CNRS, Thales, Univ. Paris-Sud, Université Paris-Saclay, Paris, France
- d. THALES TRT, Palaiseau, France

* artem.litvinenko@cea.fr

Spin torque oscillators (STO) are promising for wireless communication schemes due to their nano-scale size and their frequency tunability over a decade frequency range via either a dc current or an applied field. However, one of the main issues is their relatively large linewidth and high phase noise figure which can limit the data transmission rate of STO based system in frequency and amplitude shift keying schemes [1,2]. One possibility to reduce the STO phase noise is to couple several oscillators or to injection lock the STO to an external rf current or field source [3, 4]. Such synchronization opens the possibility of implementing the third concept of data transmission which is phase shift keying (PSK) as will be demonstrated here. A specific feature of the synchronization phenomenon is that the phase of the locked oscillator is shifted with respect to the source [5]. This phase shift $\Delta\psi$ is determined by the detuning which is the frequency difference of the free running oscillator and the rf source. For STOs, due to their non-isochronous properties the frequency of the free running state and thus the detuning can be easily changed through the DC current or DC field. In this presentation we exploit the phenomenon of synchronization to implement signal modulation via phase shift keying for magnetic tunnel junction based vortex STOs whose free running parameters are $f=300\text{MHz}$, $\Delta f=100\text{kHz}$ and $P=1\mu\text{W}$. A phase noise reduction of -50dBc/Hz at 10kHz offset frequency was obtained in the synchronized state at f and $f/2$. The frequency detuning is induced by an additional low frequency modulation current source. Maximum phase difference between $\Delta\psi$ shifts close to $\Delta\phi = \pi/2$ and π were achieved for the synchronization at $2f$ and $f/2$ respectively. We obtained 4Mb/s PSK data transmission rate for the synchronization at $2f$ which is of the order of the amplitude relaxation frequency. We also demonstrate advanced PSK techniques such as quadrature phase shift keying QPSK and discuss the use of a field line for synchronization and modulation. This concept can be applied also for uniform devices oscillating at higher frequencies and consequently at higher data rates [2]. This gives prospect for novel, robust wireless communication schemes based on STOs, at high signal to noise ratio.

The work has been supported in part by the FP7 program ICT MOSAIC 317950. Financial support is acknowledged from the French space agency CNES for CM and PS, and from ERC MagiCal 669204 for AL and UE.

- [1] H. S. Choi et al., Sci. Rep. **4**, 5486 (2014).
- [2] A. Ruiz-Calaforra et al, Applied Physics Letters **111**, 082401 (2017).
- [3] M. Tortarolo et al., Scientific Reports **8**, 1728 (2018),
- [4] R. Lebrun et al. Phys. Rev. Lett. **115**, 017201 (2015)
- [5] A. Pikovsky, M. Rosenblum, and J. Kurths, Synchronization : a universal concept in nonlinear sciences. Cambridge University Press, Cambridge, 2001

La dynamique des fluctuations critiques observée par la spectrométrie de speckles en rayons X (XPCS)

Frédéric Livet^{a*}, Guillaume Beutier^a, Mathieu Fèvre^b, Mark Sutton^c et Fadi Abouhilou^d

- a. SIMAP, CNRS-Université de Grenoble
- b. ONERA, Chatillon-Sous-Bagneux
- c. McGill, Montreal, Canada
- d. UTHM, Alger, Algérie

* frederic.livet@simap.grenoble-inp.fr << corresponding author >>

Le système étudié (AuAgZn₂) a une transition de mise en ordre de type Heussler et il se comporte dynamiquement de manière équivalente aux systèmes de type A [1], dits "à paramètre d'ordre non conservé". Au voisinage du point critique ($T_c \simeq 336.0^\circ\text{C}$), la dynamique des fluctuations locales du paramètre d'ordre par échange d'atomes entre sites voisins s'apparente à celle des "spin flips" sur les sites atomiques dans le modèle d'Ising.

Les fluctuations au voisinage du point critique sont observées par diffusion au voisinage de la position de Bragg de surstructure (i.e. la raie 1/2 1/2 1/2 de la maille cubique de la structure haute température). En contrôlant la température à 2-3mK près, on observe des fluctuations jusqu'à l'échelle de 1000Å. Ce système vérifie bien les comportements statiques de Ising, on observe la divergence des fluctuations critiques en $q=0$. Si on pose: $\theta = |T - T_c|/T_c$, on vérifie que $S(0) \propto \theta^{-\gamma}$ et que l'extension des fluctuations: ξ diverge en $t^{-\nu}$, avec $\gamma = 1.241$ et $\nu = 0.631$.

Dans les conditions de diffraction cohérente, la diffusion critique a une structure en "speckles" (tavelures) fugitive et dans une expérience "in situ" suffisamment rapide, ces speckles qui représentent une "photographie" des fluctuations évoluant avec le temps se moyennent très rapidement. Dans une expérience dynamique on observe leur temps caractéristique $\tau(q, \theta)$. Ce temps varie avec q et $\theta = |T - T_c|/T_c$ et on observe l'invariance d'échelle dynamique: $\tau(q, \theta) \propto \theta^{-z\nu}$ ($q \ll \xi$) et $\tau \propto q^{-z}$, où z est l'exposant dynamique, de l'ordre de 2. C'est un moyen unique d'observation du ralentissement critique dans les systèmes de "type Ising".

Pour cela, il faut calculer la fonction de corrélation temporelle pour chaque pixel du détecteur et étudier ses variations temporelles en fonction de q et θ . La figure [absente: pas de place!] montre un certain nombre de ces résultats, représentés avec une échelle logarithmique en temps. Une interprétation est d'écrire le temps de corrélation τ estimé à partir de fits des courbes semblables à la figure sous la forme: $\tau(q, T) = \tau_0(T)/(1 + (q/q_0)^2)$. Nos résultats sont compatibles avec $z=2$, mais avec une très mauvaise précision. Cette précision sera fortement améliorée avec la nouvelle configuration de l'ESRF.

[1] .C. Hohenberg, B.I. Halperin, Rev. Mod. Phys. 49, 435 (1977)

Room Temperature Valley Polarization and Coherence in Transition Metal Dichalcogenide-Graphene van der Waals Heterostructures

Etienne Lorchat^a, Stefano Azzini^b, Thibault Chervy^b, Takashi Taniguchi^c, Kenji Watanabe^c, Thomas W. Ebbesen^b, Cyriaque Genet^b, Stéphane Berciaud^{a*}

- a. Université de Strasbourg, CNRS, IPCMS, UMR 7504, F-67000 Strasbourg, France
- b. ISIS & icFRC, Université de Strasbourg and CNRS, UMR 7006, F-67000 Strasbourg, France
- c. National Institute for Materials Science, Tsukuba, Ibaraki 305-0044, Japan

* stephane.berciaud@ipcms.unistra.fr

Van der Waals heterostructures made of graphene and transition metal dichalcogenides (TMD) are an emerging platform for opto-electronic, -spintronic and -valleytronic devices that could benefit from (i) strong light-matter interactions and spin-valley locking in TMDs and (ii) exceptional electron and spin transport in graphene. The operation of such devices requires significant valley polarization and valley coherence, ideally up to room temperature. Here, using a comprehensive Mueller polarimetry analysis, we report *artifact-free* room temperature degrees of valley polarization up to 40 % and, remarkably, of valley coherence up to 20 % in monolayer tungsten disulfide (WS₂)/graphene heterostructures. Valley contrasts have been particularly elusive in molybdenum diselenide (MoSe₂), even at cryogenic temperatures. Upon interfacing monolayer MoSe₂ with graphene, the room temperature degrees of valley polarization and coherence are as high as 14 % and 20 %, respectively. Our results are discussed in light of recent reports of highly efficient interlayer coupling and exciton transfer in TMD/graphene heterostructures and hold promise for room temperature chiral light-matter interactions and coherent opto-valleytronic devices.

- [1] E.Lorchat, S.Azzini, T.Chervy *et al.*, Room Temperature Valley Polarization and Coherence in Transition Metal Dichalcogenide-Graphene van der Waals Heterostructures arXiv:1804.06725

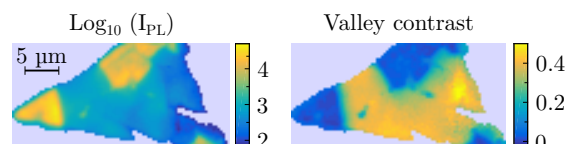


Figure 1: (a) Photoluminescence intensity Map and (b) degree of valley polarization of a Boron nitride (BN)-capped WS₂/Graphene heterostructure optically excited at 633 nm (1.96 eV)

Monitoring the Verwey transition in Magnetite by Time Resolved X-Ray diffraction

A. von Reppert^{a*}, J. Pudell^a, A. Koc^b, F. Zamponi^a, S. Geprägs^c, F. Fetta^d, L. Ortega^e, M. Reinhardt^a, M. Bargheer^{a,b} and J.E. Lorenzo^{d**}

- a. Institut für Physik, U. Potsdam, Karl-Liebknecht-Str. 24-25, 14476 Potsdam, Germany
- b. Helmholtz-Zentrum Berlin BESSY II, Albert-Einstein Str. 15, 12489 Berlin, Germany
- c. Walther-Meißner-Institut, Bayerische Akademie d. Wissenschaften, 85748 Garching, Germany
- d. Institut Néel, CNRS & Univ. Grenoble Alpes, 38042 Grenoble, France
- e. Laboratoire de Physique des Solides, CNRS, Université Paris-Saclay, 91405 Orsay, France

* reppert@uni-potsdam.de

** emilio.lorenzo@neel.cnrs.fr

Ultrafast X-Ray diffraction (UXRD) can provide direct insights into the structural response in magnetic, crystalline materials, which are driven out of equilibrium by femtosecond laser pulses[1,2]. We exemplify how the combination of a Laser based Plasma-X-ray source setup (≈ 250 fs time resolution) and the microsecond delays that are accessible at a synchrotron facilities yield a versatile scheme to fully characterize a laser induced phase transition cycle.

Here we study a 300 nm thin Magnetite (Fe_3O_4) film that is driven across the Verwey transition ($T_V = 123$ K) by fs-laser excitation. Our hard X-Ray diffraction experiments complement recent time resolved investigations of this prototypical metal to insulator transition, which have reported subpicosecond timescales for the phase transition of the electron system by monitoring the optical reflectivity changes [5] and the charge and orbital order [3,4] peaks via resonant x-ray diffraction [6]. We observe the previously reported [7] formation of differently oriented few μm -size monoclinic twin domains as a pronounced broadening in structural Bragg peaks of the cubic high temperature phase. Thus we are able to follow the laser induced structural domain transformation by monitoring the Bragg peak width and find that the dynamics are limited by strain propagation across film thickness that occurs with $v_{\text{sound}} = 6.75$ nm/ps. We additionally observe that the timescale of the monoclinic domain recovery, dictated by thermal transport, depends crucially on the proximity of T_{start} to T_V and obtain the evolution of the structural domains.

- [1] von Reppert et al., Structural dynamics **3**, 053302 (2016).
- [2] Koc et al., arXiv 1701.05918 (2017).
- [3] Nazarenko et al., Phys. Rev. Lett, 97.5, 056403 (2006).
- [4] Senn. et al., Nature, 481.7380 (2012).
- [5] F. Randi et al. Phys. Rev. B 93, 054305 (2016).
- [6] De Jong & Kukrieka et al. Nature Materials 12.10, 882-886 (2013).
- [7] T. Kasama et al. Earth and Planetary Science Letters 297, 10 (2010).

Self-heating in nanostructures: a quantum mechanical view

Mathieu Luisier^{a*}, Reto Rhyner^b, and Aron Szabo^a

a. Integrated Systems Laboratory, ETH Zurich, 8092 Zurich, Switzerland

b. Synopsys Switzerland LLC, Thurgauerstrasse 40, 8059 Zurich, Switzerland

* mluisier@iis.ee.ethz.ch

Over the years, driven by Moore's scaling law, the active dimensions of electronic devices have been pushed down towards their ultimate limit. This especially concerns Silicon-based logic switches, for which the supply voltage has not been reduced as fast as their size. As a consequence, the amount of power dissipated per area has kept increasing from one generation of transistors to the other, reaching nowadays alarming values [1]. To stop this trend, it is important to first understand what physical mechanisms govern power and heat dissipation in nanostructures, how much self-heating occurs at the nanoscale, and how this effect could be potentially circumvented by adopting novel device geometries or by replacing Si with another material.

Technology computer aided design (TCAD) can help address these issues, provided that advanced simulation tools based on suitable physical models exist. When the device dimensions do not exceed a few nanometers anymore, quantum mechanical phenomena, e.g. energy quantization, confinement, or tunneling, start to play a fundamental role. To produce accurate results or predict the performance of not-yet-fabricated components, they must be properly accounted for, not only to describe electron transport, but also the propagation of heat through a given medium. Here, a modeling approach that fulfills these requirements will be presented. It relies on coupled electron and phonon transport at the quantum mechanical level. The material properties are expressed either in an empirical (tight-binding for electrons, valence-force-field for phonons) or in a fully *ab-initio* (density-functional theory) basis. Exemplary results of electro-thermal transport simulations are shown in Fig. 1 for a Si nanowire transistor. The case of self-heating in 2-D materials, in particular MoS₂, will also be discussed.

[1] E. Pop, S. Sinha, and K. E. Goodson, Heat Generation and Transport in Nanometer-Scale Transistors, Proc. IEEE **94**, 1587 (2006).

[2] R. Rhyner and M. Luisier, Atomistic modeling of coupled electron-phonon transport in nanowire transistors, Phys. Rev. B **89**, 235311 (2014).

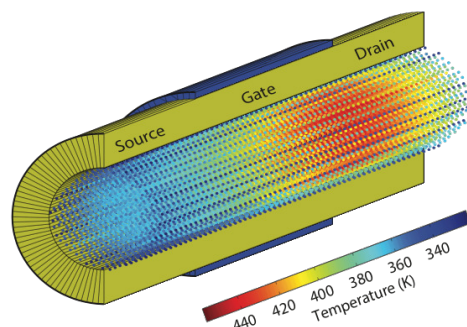


Figure 1: Atomically-resolved temperature distribution inside a Si gate-all-around nanowire transistor with a diameter $d=3$ nm. A significant temperature increase close to the drain side of the device can be observed.

Reversed electro-dialysis energy harvesting from polyelectrolytes and hydrogels functionalized conical nanopores

TianjiMa^a, EmmanuelBalanzat^b, Jean-MarcJanot^a, Sébastien Balme^a

- a. Institut Européen des Membranes, UMR5635 UM ENSM CNRS, Place Eugène Bataillon, 34095 Montpellier cedex 5, France
- b. Centre de recherche sur les Ions, les Matériaux et la Photonique, UMR6252 CEA-CNRS-ENSICAEN, 6 Boulevard du Maréchal Juin, 14050 Caen Cedex 4, France

* tianji.ma@umontpellier.fr

Water is used as an energy resource since hundreds years. Besides of hydroelectric process, the difference of salinity is also the source of power using two methods: pressure-retarded osmosis and reversed electro-dialysis which were close to commercialization nowadays¹. However they suffer from low yield. For reversed electro-dialysis, the membrane permselectivity is a crucial limiting factor². To improve that, we design two kinds of ion selective membranes based on PET conical membranes functionalized by polyelectrolytes and hydrogels. For anion-selective membranes, polyethylenimine and a hydrogel³ containing (3-acrylamidopropyl)trimethylammonium chloride, acrylamide, bis were considered. For cation-selective membranes, poly-L-lysine/polyacrylic acid and hydrogel containing 3-sulfopropyl acrylate (potassium salt), 2-hydroxy-4-(2-hydroxyethoxy)-2-methylpropiophenone, acrylamide, bis were considered. First, we have studied the ionic transport and the selectivity on single nanopore. Rectification factor and osmotic current were recorded by current-voltage measurements. Second, the single nanopores were scaled-up to low-density multipore membranes and the power measurements were performed. Finally a stacked multi-pair membrane systems were tested to evaluate the real power density as its commercial form.

[1] B. E. Logan, M. Elimelech, Membrane-based processes for sustainable power generation using water, *Nature* 488, 313–319 (2012)

[2] S. Balme, T. Ma, E. Balanzat, J. Janot, Large osmotic energy harvesting from functionalized conical nanopore suitable for membrane applications, *J. Membr. Sci.* 544, 18–24 (2017)

[3] T. B. H. Schroeder, A. Guha, A. Lamoureux, G. VanRenterghem, D. Sept, M. Shtein, J. Yang, M. Mayer, An electric-eel-inspired soft power source from stacked hydrogels, *Nature* 552, 214–218 (2017)

Spin Caloritronics In Germanene Nanoribbons

Danial Majidi^{a,b*}, Tabassom Arjmand^c, Hamid Rahimpour Soleimani^c, Rahim Faez^d

- a. Univ. Grenoble Alpes, CNRS, Grenoble INP, Institut Néel, 38000 Grenoble, France.
- b. Department of Electrical, Biomedical and Mechatronics Engineering, Qazvin Branch, Islamic Azad University, Qazvin, Iran.
- c. Computational Nanophysics Laboratory (CNL), Department of Physics, University of Guilan, P.O.Box 41335-1914, Rasht, Iran.
- d. Department of Electrical Engineering, Sharif University of Technology, Azadi Ave., Tehran, Iran.

* danial.majidi@neel.cnrs.fr

Spin seebeck effect (SSE), the central topic in spin caloritronics, provide an exciting research direction for future low power consumption technology [1,2]. To this end, we construct a spin caloritronics device which is composed of ferromagnetic double-single-hydrogen-terminated zigzag germanene nanoribbon (ZGeNRs). We report our calculation based on this asymmetric $sp^2 - sp^3$ edges, using first-principles calculations combined with a non-equilibrium Green's function method. In our previous work, we have shown that ZGeNRs are a promising candidate due to spin splitting bandstructure in spin caloritronic applications [3]. Here, we demonstrate a spin-Seebeck diode behavior in asymmetrically passivated ZGeNRs, displaying a spin up and spin down current, can be generated by temperature difference, rather than by bias voltage, furthermore, total spin current driven by a negative temperature gradient, but not by a positive one, which is originates from the asymmetrical thermal-driven conducting electrons and holes in transmission spectra.

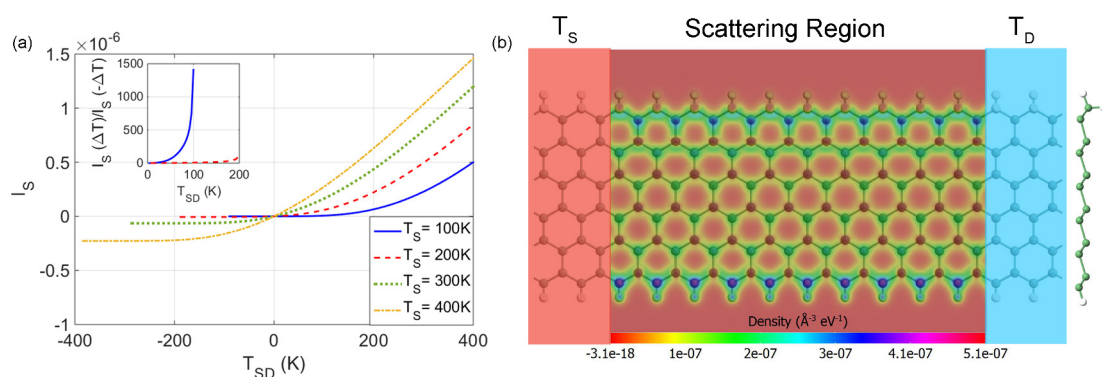


Figure 1: (a) Total spin current $I_s = I_{up} - I_{down}$ as a function of T_{SD} , $T_{SD} = T_S - T_D$. (b) Local density of states along the transport direction.

- [1] Wolf, S. A., et al. Spintronics: a spin-based electronics vision for the future. Science 294.5546 (2001): 1488-1495.

Thermoelectricity of a Kondo-correlated Quantum Dot Junction

B. Dutta^{a*}, D. Majidi^a, A. Garcia-Corral^a, J. T. Peltonen^b, J. P. Pekola^b, C. B. Winkelmann^a, H. Courtois^a.

a. Univ. Grenoble Alpes, CNRS, Grenoble INP, Institut Néel, 38000 Grenoble, France.

b. Low Temperature Laboratory, Department of Applied Physics, Aalto University School of Science, P.O. Box 13500, 00076 Aalto, Finland.

* bivas.dutta@neel.cnrs.fr

Quantum dots are an attractive model system for basic studies and applications in thermoelectricity, owing to their tunable electronic transmission and electron-hole asymmetry [1]. Further, as electronic devices' dimensions shrink towards the nano-scale, quantum effects associated to electron interactions [2] and correlation [3] gain increasing importance. Here, we report on measurements of the thermopower of a single quantum dot junction, at very low temperatures and in a regime where Kondo-correlations, due the spin degeneracy of the odd charge states q_{QD} of the quantum dot, dominate the electron transport processes. While in the absence of Kondo correlations, thermoelectric signals are generically periodic in q_{QD} with period e , we observe here a $2e$ -periodic thermoelectric response, in good agreement with theoretical predictions for a Kondo-correlated quantum dot junction [4].

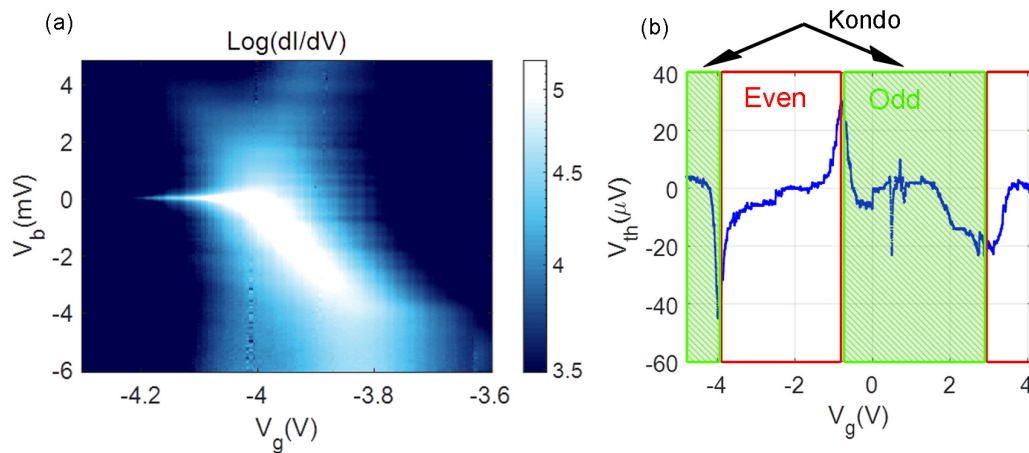


Figure 1: (a) Differential conductance map near a charge degeneracy point at $V_g = -4V$. Kondo correlation manifest as a zero-bias peak at $V_g < -4V$. (b) Thermovoltage across different charge states as a function of gate voltage, showing a $2e$ -periodic pattern.

[1] Y. Dubi, M. Di Ventra, Colloquium: Heat flow and thermoelectricity in atomic and molecular junctions, Reviews of Modern Physics 83 (1) (2011) 131.

Liquid crystalline structures and elasticity in a cubic chiral helimagnet – a neutron scattering study

N. Martin^{a*}, M. Deutsch^b, G. Chaboussant^a, F. Damay^a, C. Franz^c, P. Bonville^d,
L.N. Fomicheva^e, A.V. Tsvyashchenko^{e,f}, U.K. Rößler^g and I. Mirebeau^a

- a. Laboratoire Léon Brillouin, CEA-Saclay, 91191 Gif-sur-Yvette, France
- b. Université de Lorraine, Laboratoire CRM2, 54506 Vandœuvre-lès-Nancy, France
- c. Heinz Maier-Leibnitz (MLZ), 85748 Garching bei München, Germany
- d. Service de Physique de l'État Condensé, CEA-Saclay, 91191 Gif-sur-Yvette, France
- e. Vereshchagin Institute for High Pressure Physics, 142190 Troitsk, Moscow, Russia
- f. Skobeltsyn Institute of Nuclear Physics, Vorob'evy Gory 1/2, 119991 Moscow, Russia
- g. IFW Dresden, PO Box 270116, 01171 Dresden, Germany

* nicolas.martin@cea.fr

Condensed matter provides convenient ways to observe and manipulate a large variety of complex long-range orders. Currently, a strong focus is put on the study of chiral magnets (ChM) belonging to the B20 family, such as MnSi, FeGe, MnGe, *etc.* These compounds indeed display a plethora of multiply modulated phases, including the topologically non-trivial skyrmion (SK) lattice stabilized under an applied magnetic field.

In a recent elastic neutron scattering study of the $\text{Mn}_{1-x}(\text{Co,Rh})_x\text{Ge}$ solid solutions, we have discovered that, upon chemical substitution, a ChM can undergo a transition from a helimagnetic to a weakly ferromagnetic ground state through a mixed-phase, within which topological defects proliferate even in zero field [1] (see Figure). The formal equivalence between the latter and the "twist-grain boundary" (TGB) phase already evidenced in certain chiral liquid crystals (ChLC) [2] underscores the deep connections between the two classes of systems.

In turn, this implies that ChMs might inherit the rich phenomenology of ChLCs. In the frame of this unifying gesture, we have recently checked the prediction of Radzihovsky and Lubensky that the helimagnetic ground state should support phason-like Goldstone modes [3]. To that end, we have used a cutting-edge quasi-elastic scattering method, the so-called MIEZE spectroscopy (see *e.g.* [4] and references therein), to study the temperature-dependence of the helimagnetic order lifetime in pure MnGe. We found that the latter is finite in a large temperature interval below the macroscopic ordering temperature. This suggests that thermally activated walls are moving across the ordered domains, in agreement with the above theoretical expectations.

[1] N. Martin *et al.*, Phys. Rev. B **96**, 020413(R) (2017)

[2] L. Navailles *et al.*, Phys. Rev. Lett. **71**, 545 (1993)

[3] L. Radzihovsky and T.C. Lubensky, Phys. Rev. E **83**, 051701 (2011)

[4] N. Martin, Nucl. Instr. and Meth. in Phys. Res. A **882** (2018) 11-16

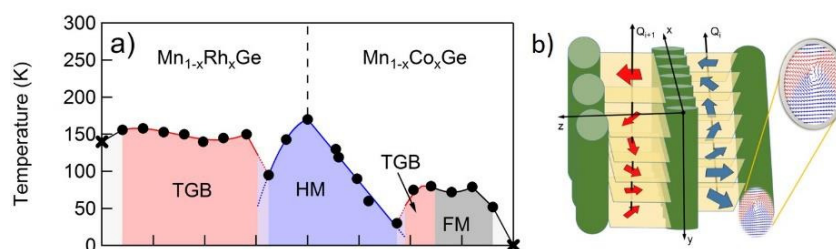


Figure: a) Magnetic phase diagram of the $\text{Mn}_{1-x}(\text{Co,Rh})_x\text{Ge}$ series. b) Proposed magnetic TGB phase, where screw dislocation lines separate elongated helimagnetic domains.

How to push one's way through a dense crowd

T. Metivet^{a*}, L. Pastorello^b and P. Peyla^b

a. Institut de Recherche Mathématique Avancée, Univ. Strasbourg, 67000 Strasbourg

b. Lab. Interdisciplinaire de Physique, Univ. Grenoble Alpes / CNRS, 38000 Grenoble

* metivet@math.unistra.fr

Understanding the collective behaviour of pedestrians in confined geometries is a key challenge to meet high security expectations in mass events. Such events in particular raise the issue of providing assistance to someone in the middle of a dense crowd, or to escape such a crowd.

In this work [1], we propose a simple mechanical – social force [2] – model to simulate the dynamics of a dense crowd of individuals with different behaviours. On the one hand, we study the case of a moving person trying to escape a static crowd with individuals attached to their “favourite” position. We analyze the effects of the strategy of the moving person and the rigidity of the crowd, and show that some rheological law can be extracted to describe the moving person velocity dependence on the crowd density. On the other hand, we consider the case of person – a star – moving in a crowd of individuals converging towards it. We investigate the moving person limit velocity and show that motion can become impossible even for relatively low crowd densities.

[1] Metivet, T., Pastorello, L. and Peyla, P., 2018. How to push one's way through a dense crowd. EPL, to be published

[2] Helbing, D., Farkas, I. and Vicsek, T., 2000. Simulating dynamical features of escape panic. Nature, 407(6803), p.487.

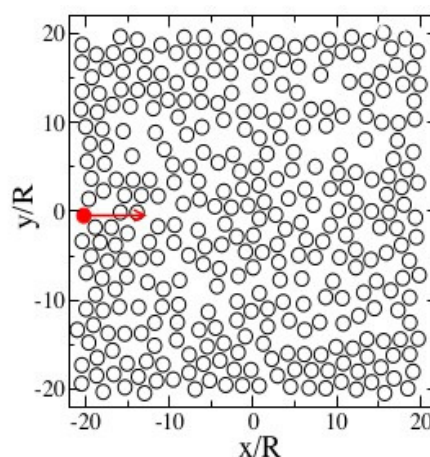


Figure 1: Snapshot of a person moving through a crowd.

Functional characterisation of membrane proteins stably incorporated in tethered lipid bilayers

M. Maccarini,^{*,1} L. Gayet,¹ J-P Alcaraz,¹ L. Liguori,¹ E. B. Watkins,³ J-L Lenormand,¹ D. K. Martin¹

¹ *Laboratoire TIMC-IMAG, Université Grenoble Alpes, France;* ³ *Los Alamos National Laboratory, USA*

* *marco.maccarini@univ-grenoble-alpes.fr*

Systems composed of membrane proteins (MP) embedded in lipid bilayers have relevant potential application in biomedical science. They have the potentiality of becoming the core of novel biomimetic implantable devices with a wide range of applications, such as the monitoring of chemical messengers and biological markers inside the body for improved prognosis, energy scavenging devices to produce energy directly within the body of a patient or animal, or new drug delivery systems. We investigated the functional incorporation of different proteins into tethered lipid bilayer membranes (tBLMs). tBLM consists of a planar lipid bilayer supported by an array of tethered lipids anchored to a molecularly smooth substrate [1]. tBLMs are more stable due to the chemical attachment to the substrate necessary condition for the design of practical devices.

We will present a nanostructural and functional characterisation of two important MPs performed by a combination of techniques including Neutron Reflectometry and Electrical Impedance Spectroscopy [2]. *OprF*, the main porin of the *P. Aeruginosa* bacterium outer membrane, is thought to have an important role in the antibiotic resistance of the bacterium that is responsible for 10% of all hospital-acquired infections. *OprF* is a very novel target for new drugs that will kill bacteria resistant to standard antibiotics. In our laboratories a cell-free method to synthesis the protein has been developed to provide controlled studies of the structure and function of *OprF* [3]. The *NhaA* protein is a pH-dependent sodium-proton antiporter found in prokaryotes that was used by our laboratory to develop a prototype of energy device that transforms a gradient of salt to an electrical potential [4]

These studies showed that MPs purified using optimised protocols and then incorporated into tethered lipid bilayers yield controllable (and measurable at the nanoscale) biomimetic systems constructed in vitro. These systems provides the means to identify ways to control membrane proteins, and hence to foster the development of novel biomimetic devices.

[1] M. Maccarini, B. Stidder, J-P. Alcaraz, E. B. Watkins, B. A. Cornell, D. K. Martin 'Nanostructure determination of lipid bilayers tethered to gold substrates' *Eur. Phys. J. E* (2016) 39: 123

[2] M. Maccarini, L. Gayet, B. Stidder, J-P. Alcaraz, E. Watkins, L. Liguori, J-L. Lenormann, D. Martin 'Functional nanostructure of the *Pseudomonas aeruginosa* porin *OprF* incorporated into a tethered lipid bilayer membrane' *Langmuir* (2017) 33(38), 9988

[3] L. Liguori, B. Marques, A. Villegas-Mendez, R. Rothe, J-L. Lenormand 'Liposomes-mediated delivery of proapoptotic therapeutic membrane proteins' *Journal of Controlled Release* (2008), 126: 217-227

[4] Cinquin P, Martin DK (2007). "Biomimetic artificial membrane device" PCT/EP2008/058253, WO/2009/003936

Rare earth environment modification by Electron and femtosecond laser irradiation in metaphosphate and polyphosphate glasses

Mohamed Mahfoudhi^{a*}, Matthieu Lancry^b, Nadège Ollier^a

- a. Laboratoire des Solides Irradiés (LSI), CNRS UMR 7642, CEA-DRF-IRAMIS, Ecole polytechnique, 91128 Palaiseau cedex, France
- b. Institut de Chimie Moléculaire et des Matériaux d'Orsay (ICMMO), Université Paris-Sud, 11, UMR 8182, Rue du doyen Georges Poitou, 91405 Orsay cedex – France

* Mohamed.mahfoudhi@polytechnique.edu

The rare earth (RE) doped phosphate glasses are attractive materials in optics, nuclear industry and data storage due to their low transition temperature and a high capacity to dissolve rare earth ions compared to silicate glasses. In this work, we are interested in understanding the mechanisms leading to the structural modifications of Zn polyphosphate and metaphosphate glasses under various kinds of irradiations in order to study and control the RE doping ions environment and the resulting luminescence properties [1,2]. Electrons of 700 KeV and 2.5 MeV (SIRIUS Accelerator, LSI) were used as well as femtosecond laser pulses (1030 nm, 250fs, 0,1-5μJ/pulse, 0,6 NA focusing) at low repetition rate (10 KHz) and high repetition rate (500 KHz) leading to heat accumulation in the last case.

The glasses compositions deal with mixing different alkaline and alkali-earth ions (Na, Li, K and Mg) and different polymerization degree of phosphate glasses. After both 2.5 MeV and 700 keV electron irradiations, the Raman spectra traduce a significant depolymerization of the polyphosphate vitreous network from 10⁸ Gy dose opposite to metaphosphate glasses that remain more stable. The modification of the glass network seems not to strongly affect the local environment of Eu³⁺ as demonstrated by the significant increase of the asymmetry ratio (As) of Eu³⁺ ions in irradiated metaphosphate glasses compared to polyphosphate glasses. Under 700 keV irradiation, the Eu³⁺ As variation can be noticed in a larger volume than the penetration depth of the electrons. Moreover, the variation depends on the alkaline ion type showing a role of alkaline migration on the Eu³⁺ environment modification. Furthermore, the shift of the ⁵D₀→⁷F₀ transition associated with a broadening indicates a modification of the Eu³⁺ crystal field and larger site distribution of Eu³⁺ ions in polyphosphate glasses. We also reveal that the reduction of Eu³⁺ into Eu²⁺ is more efficient under 700 keV irradiation by a factor four to seven compared to 2.5 MeV. On the other hand, there is only a slight change of the polyphosphate glass structure under femtosecond laser waveguide writing conditions compared to electron irradiation. The Eu environment remains quite stable in the written lines by fs laser whatever the repetition rate.

[1] Fletcher, L. B., Witcher, J. J., Troy, N., Reis, S. T., Brow, R. K., Vazquez, R. M., ... & Krol, D. M. (2011). Femtosecond laser writing of waveguides in zinc phosphate glasses. *Optical Materials Express*, 1(5), 845-855.

[2] De Bonfils, J., Panczer, G., de Ligny, D., Peugeot, S., & Champagnon, B. (2007). Behaviour of simplified nuclear waste glasses under gold ions implantation: A microluminescence study. *Journal of nuclear materials*, 362(2-3), 480-484.

Transition metal delafossites: from 2D metallicity to multiferroism

Antoine MAIGNAN^{a*}, Ramzy DAOU^a, Raymond FRESARD^a, Sylvie HEBERT^a
and Christine MARTIN^a

a. *Laboratoire de Cristallographie et Sciences des Matériaux, Normandie Univ, ENSICAEN, UNICAEN, CNRS, CRISMAT- 6 Bd du Maréchal Juin -14050 Caen cedex- France*

* antoine.maignan@ensicaen.fr

Delafossite oxides of AMO_2 formula are exhibiting a very broad range of physical properties related to their layered structure. The latter can be viewed as “natural” heterostructures made of alternating triangular A^+ and $(MO_2)^-$ layers. On the one hand, in the case of $A=Cu^+$ and $M^{3+}=3d$ magnetic cation, multiferroic properties connected to complex antiferromagnetic structures, as in $CuCrCO_2$ [1], are observed, whereas, on the other hand, as for $A=Pd^+$ and $B=Co^{3+}$ (d^6 , LS, $S=0$), a very 2D metallic behaviour is evidenced with strong anisotropies of both resistivity and thermal conductivity (Fig.1). In the presentation, some examples will be chosen to illustrate the richness of the physical properties for these 2D materials [2].

[1] M. Poienar et al, Phys. Rev. B **79**, 014412 (2009).

[2] R. Daou et al, Science and Technology of Advanced Materials, **18:1**, 919-938 (2017).

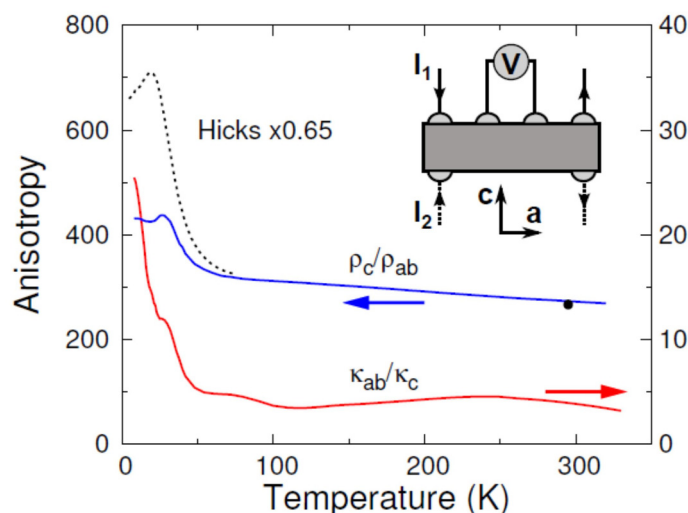


Fig.1: Anisotropic transport in $PdCoO_2$ crystals.

Superradiant Scattering: From Theory to Experiment

Calum Maitland^{a*,b}, Angus Prain,^{a,b} Fabio Biancalana^a and Daniele Faccio^b

a. Institute for Photonics and Quantum Sciences, Heriot-Watt University, Edinburgh EH14 4AS, UK

b. School of Physics & Astronomy, University of Glasgow, Glasgow G12 8QQ, UK

* << cm350@hw.ac.uk >>

Superradiance is a scattering effect whereby signals reflected from a rotating black hole are amplified, extracting rotational energy and angular momentum in the process [1]. An analogue gravity experiment demonstrating this effect for gravity waves on a draining water vortex was successfully reported last year [2]. Efforts to replicate these findings in photon superfluids [3] are ongoing. Typically, superradiance is defined by a reflection coefficient greater than unity for solutions to the background wave equation. Performing a clean measurement of the reflection coefficient is challenging in current optical experimental settings, where only short timescales for wave propagation are accessible. A more viable measure in this case is the conserved Noether current, defining superradiance from an analogue black hole by a growth in the integrated current outside the event horizon during a partial scattering process. We numerically simulate this scattering to predict possible experimental signatures.

- [1] R. Penrose, Gravitational Collapse: the Role of General Relativity, Riv. Nuovo Cim., **1**, 252 (1969)
- [2] T. Torres *et. al.*, Rotational superradiant scattering in a vortex flow, Nature Physics **13**, 833 (2017)
- [3] D. Vocke *et. al.*, Rotating black hole geometries in a two-dimensional photon superfluid, arXiv:1709.04293 (submitted to Optica, March 2018)

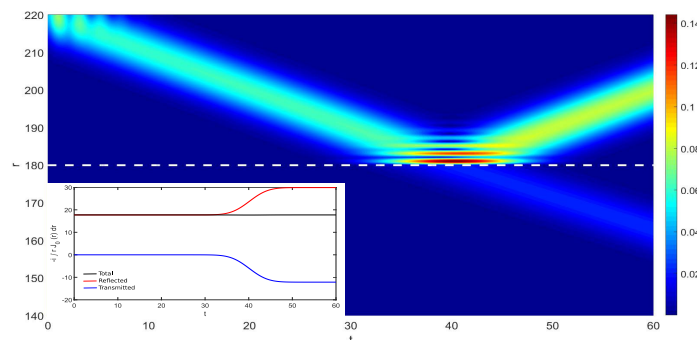


Figure 1: Wavepacket scattering from a solid rotational flow (edge shown by dashed white line). Colour scale shows wave modulus, r and t axes are radial distance and time respectively. Inset: integrals of current on either side of the white line.

Emission d'électrons par effet de champ et assistée par impulsions laser ultra-courtes à partir de nano-pointes de diamant

M.-H. Mammez^{a*}, M. Borz^a, I. Blum^a, G. Da Costa^a, F. Delaroche^a, J. Houard^a, S. Idlahcen^b, A. Haboucha^b, A. Hideur^b et A. Vella^a

- a. GPM, UMR CNRS 6634, Normandie Université, Université-INSA de Rouen, Avenue de l'Université BP 12, 76801 Saint-Etienne-du-Rouvray, France
 b. CORIA UMR 6614, CNRS-INSA-Université de Rouen, Normandie Université, Avenue de l'université, BP. 12, 76801 Saint Etienne du Rouvray, France
 * marie-helene.mammez@univ-rouen.fr

Le développement de sources d'électrons impulsionnelles est rendu possible grâce au couplage de l'émission de champ et de l'excitation électronique sous éclairage laser [1]. En l'absence d'éclairage, les électrons sont émis sous l'action d'un champ électrique très intense, d'où l'emploi de nano-pointes. L'application d'un éclairage laser permet l'excitation des électrons et leur émission à des champs plus faibles. L'équipe d'instrumentation du GPM développe un spectromètre pour l'étude de l'émission d'électrons par effet de champ assistée par impulsion laser ultra-courte [2]. Ce travail s'effectue en collaboration avec le département optique et laser du laboratoire CORIA pour le développement d'une source laser impulsionnelle (durée d'impulsion $t = 1$ ps) à fibre dopée Ytterbium émettant dans la gamme infrarouge ($\lambda = 1040$ nm). Le schéma de fonctionnement de l'instrument est présenté à la figure 1. L'instrument est résolu spatialement grâce à la combinaison de galettes de micro-canaux, d'un écran de phosphore et d'une caméra CCD rapide.

Nous présenterons les résultats obtenus à partir de nano-pointes de diamant [3,4] en particulier les caractéristiques d'émission (courbes courant-tension et spectre en énergie) sous différentes conditions d'éclairage laser (énergie par impulsion et taux de répétition).

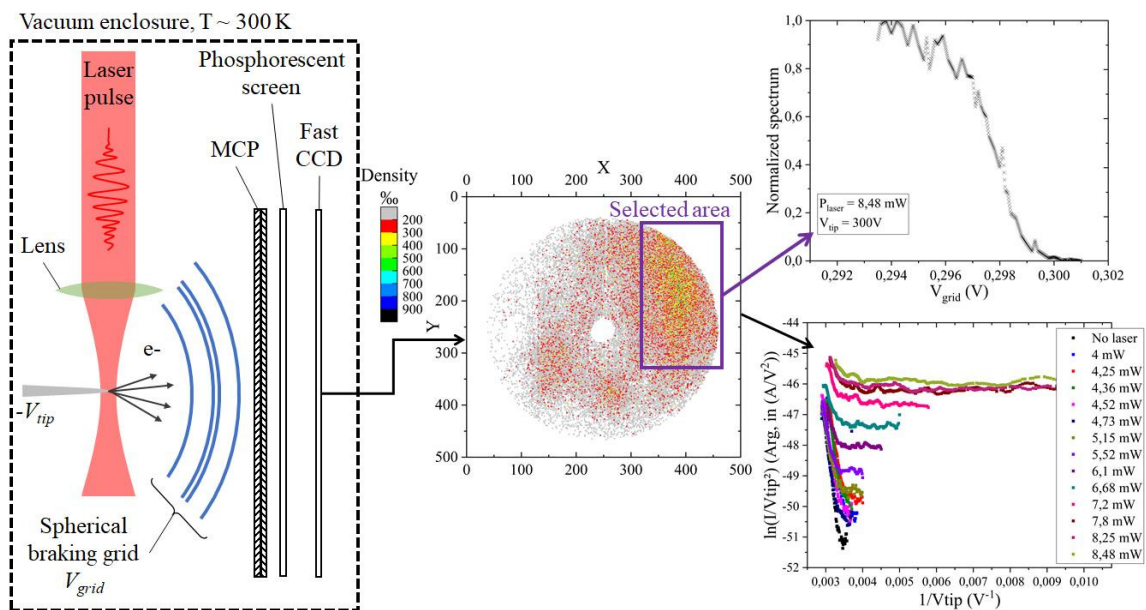


Figure 1 : Principe du spectromètre résolu spatialement. L'énergie des électrons émis est mesurée via le potentiel appliqué à la grille de freinage. Le courant est mesuré en comptant le nombre d'impacts sur l'écran de phosphore via la caméra CCD.

- [1] P. Hommelhoff et al., Field emission tip as a nanometer source of free electron femtosecond pulses, Phys. Rev. Lett., 96, 077401 (2006)
 [2] M. Borz et al., Field emission and field ion microscopy from single crystal diamond needle, 30th IVNC, 86-87 (2017)
 [3] V. I. Kleshch et al., Single crystal diamond needle as point electron source, Sci. Rep., srep35260 (2016)
 [4] V. Porshyn et al., Photoinduced effects in field electron emission from diamond needles, Appl. Phys. Lett., 110, 182101 (2017)

Theoretical insights of electrolyte transport in nanopores

Manoel Manghi^{a*}, John Palmeri,^b et B. Loubet^a

- a. Laboratoire de Physique Théorique, IRSAMC, Université de Toulouse, CNRS, UPS, Toulouse.
- b. Laboratoire Charles Coulomb, UMR 5221 CNRS-Université de Montpellier, Montpellier.

* manghi@irsamc.ups-tlse.fr

Fundamental understanding of ionic transport at the nanoscale is essential for developing biosensors based on nanopore technology and new generation high-performance nanofiltration membranes for separation and purification applications.

After a general introduction on the theoretical modeling of ionic transport in nanopores, we present a mesoscopic theoretical approach for the electrolyte conductivity inside nanopores. The model considers explicitly ion advection by electro-osmotic flow, possible flow slip at the pore surface (when the pore is hydrophobic) [1], dielectric exclusion of the ions [2], hard core repulsion between ions [3], and surface charge regulation [4]. Various regimes where the conductivity has a relatively simple analytical expression are identified.

The theory is then compared to experimental measurements of ionic transport through single putatively neutral hydrophobic nanopores and with a well controlled cylindrical geometry [1] and through single wall carbon nanotubes [5]. We focus on the dependence of the nanopore conductance with the reservoir ionic concentration, showing various behaviours depending on the experimental conditions.

- [1] S. Balme, F. Picaud, M. Manghi, J. Palmeri, M. Bechelany, S. Cabello-Aguilar, A. Abou-Chaaya, P. Miele, E. Balanzat, J.-M. Janot, Ionic transport through sub-10 nm diameter hydrophobic nanopores : experiment, theory and simulation, *Scientific Reports* **5**, (2015) 10135
- [2] S. Buyukdagli, M. Manghi, J. Palmeri, Ionic capillary evaporation in weakly charged nanopores, *Phys. Rev. Lett.* **105**, 158103 (2010)
- [3] B. Loubet, M. Manghi, J. Palmeri, A variational approach to the liquid-vapor phase transition for hardcore ions in the bulk and in nanopores, *J. Chem. Phys.* **145**, (2016) 044107
- [4] M. Manghi, J. Palmeri, K. Yazda, F. Henn, V. Jourdain, Role of charge regulation and flow slip on the ionic conductance of nanopores : an analytical approach, arXiv:1712.01055 (2017)
- [5] K. Yazda, S. Tahir, T. Michel, B. Loubet, M. Manghi, J. Bentin, F. Picaud, J. Palmeri, F. Henn, V. Jourdain, Voltage-activated transport of ions through single-walled carbon nanotubes, *Nanoscale*, **9**, (2017) 11976

Anisotropic spin separation in the Gd pyrochlore iridate

L. Mangin-Thro^{a*}, E. Lefrançois^{a,b}, E. Lhotel^b, J. Robert^b, S. Petit^c, P. Lejay^b, V. Cathelin^b, C. V. Colin^b, F. Damay^c, J. Ollivier^a, H. Fischer^a, L. C. Chapon^a, R. Ballou^b, V. Simonet^b

a. Institut Laue-Langevin, CS 20156, 38042 Grenoble, France

b. Institut Néel, CNRS & UGA, 38042 Grenoble, France

c. Laboratoire Léon Brillouin, CEA, CNRS, Univ. Paris-Saclay, 91191 Gif-sur-Yvette, France

* mangin-thro@ill.fr

The Ir-5d electrons in most iridate pyrochlores $R_2\text{Ir}_2\text{O}_7$ (R = Rare Earth) exhibit a spin-orbit driven metal-insulator transition accompanied by an ordering of the Ir sublattice in the so-called "all-in all-out" order: magnetic moments pointing towards or away from the centre of each corner-sharing tetrahedron, as shown in the figure. This induces a non-collinear magnetic field on the R moments through the R-Ir magnetic interactions. **This well-controlled staggered molecular field is a new parameter allowing to explore the rich physics of frustrated rare-earth pyrochlores** [1]. At low temperature, it favours new magnetic ground states in these systems due to its competition with the single-ion anisotropy of the rare-earth (with respect to the local $\langle 111 \rangle$ directions of the tetrahedron) and with the interactions between the rare-earth ions. In $\text{Ho}_2\text{Ir}_2\text{O}_7$, this staggered molecular field leads to the fragmentation of the magnetization [2,3].

At variance with the Ising Ho^{3+} moment, here we focus on the behaviour of the much more isotropic magnetic moment of the Gd^{3+} ion on the rare-earth site that we study through magnetometry and neutron scattering. We find a complex situation in $\text{Gd}_2\text{Ir}_2\text{O}_7$ where different components of the magnetic moment are decoupled. They contribute respectively to a high temperature all-in all-out order (easy-axis component of the magnetic moments) polarized by the Ir molecular field and to complex antiferromagnetic correlations between the easy-plane components that tend to order at much lower temperature. We succeeded in reproducing these exotic behaviours with a simple model comprising in particular the anisotropic dipolar interactions.

[1] E. Lefrançois *et al.* Phys. Rev. Lett **114**, 247202 (2015).

[2] E. Lefrançois *et al.* Nature Communications **8**, 209 (2017).

[3] Brooks-Bartlett *et al.* Phys. Rev. X **4**, 011007 (2014).

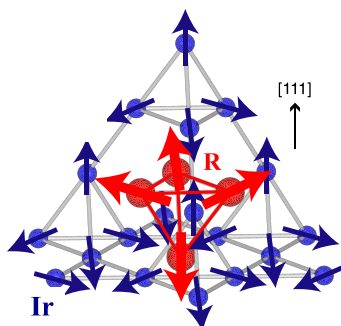


Figure 1: The two interpenetrating pyrochlore lattices with Ir^{4+} (blue) and the rare-earth R^{3+} (red). The Ir sublattice orders in the all-in all-out arrangement inducing the same magnetic order on the R sublattice.

Micromagnetic simulation of an isotropically coercive free layer for MTJ-based artificial synapses

M. Mansueto^{*}, L. D. Buda-Prejbeanu, I. L. Prejbeanu and B. Dieny

SPINTEC, CEA-INAC/ CNRS / Univ. Grenoble Alpes, France

* marco.mansueto@cea.fr

Bio-inspired technologies are very appealing today for many potential applications. In particular, brain-like network is representing an example of efficient and low power consumption computational tool for big data analysis tasks. In this context, the development of a proper hardware is essential and memristive devices, with their synapse-like behaviour, represents a key element for this purpose.

Our objective is to conceive a spintronic memristor, based on the angular variation of tunnel magneto-resistance in a nanopillar with the magnetic state controlled by spin transfer torque. One of the main challenge is represented by the realization of a special magnetic media able to stabilize the magnetization along various directions in the plane of the layer. Here we are simulating such a media by exploiting the anisotropy direction distribution arising in a polycrystalline FeCoB thin layer. The statistical distribution (randomly chosen) allows the stabilization of the magnetization along a finite number of angles (Figure a). The influence of some magnetic parameters (such as damping constant, anisotropic energy, etc.) has been studied in order to better understand the dominating physical phenomena in the system. The effect of Spin Transfer Torque has been also investigated through the insertion of the appropriate terms in the Landau Lifshitz Gilbert equation. Thanks to the micromagnetic code Micro3D, successful rotation of the magnetization between stable angles has been simulated with the application of voltage pulses (see Figure b). The monotonicity of the magnetization angle variation with both voltage amplitude and pulse length demonstrates the memristive character of the simulated device.

[1] N. Locatelli, V. Cros and J. Grollier, NATURE MATERIALS, VOL. 13, pp. 11-20, (2014)

[2] J. Grollier, D. Querlioz and M. D. Stiles, PROCEEDINGS OF THE IEEE, 104, 10, 2024 (2016)

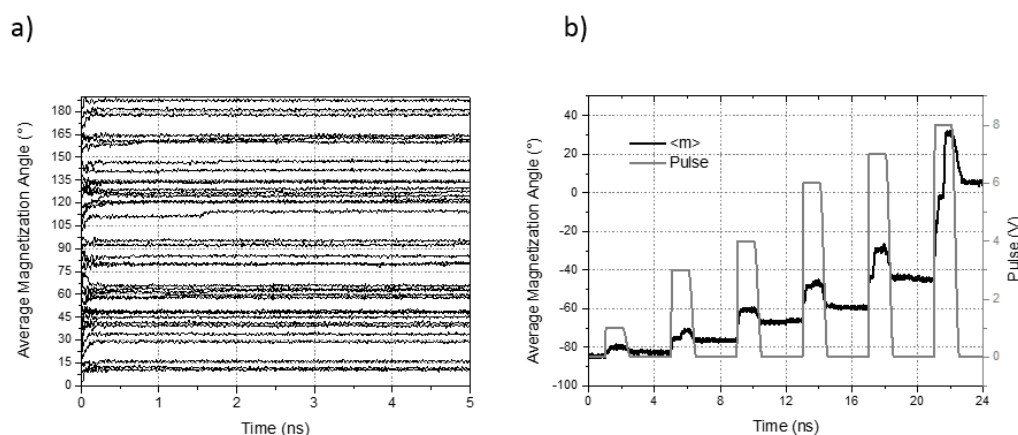


Figure : a) Stable magnetization angles found between 0° and 180°. b) Example of sequential magnetization rotation through the application of voltage pulses.

Periodically driven chains with particle-hole symmetry

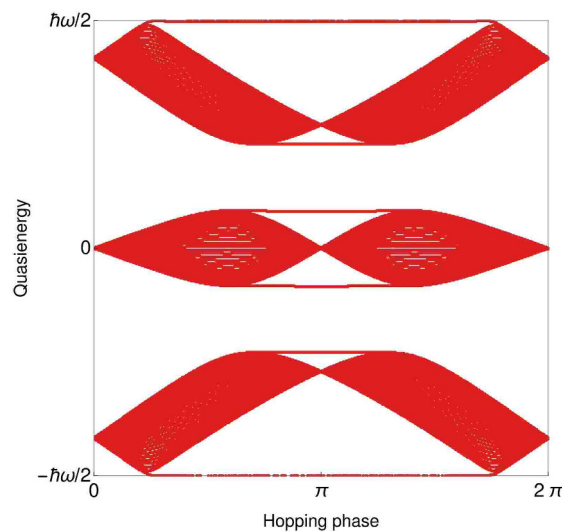
Marco Marciani^{a*}, Lavi K. Upreti,^a and Pierre Delplace^a

a. Univ Lyon, Ens de Lyon, Univ Claude Bernard, CNRS, Laboratoire de Physique, F-69342 Lyon, France

* marco.marciani@ens-lyon.fr

Periodically driven systems possess topological features that have no analog in static systems. In this talk, I will focus on driven chains with particle-hole symmetry. Here, non-trivial drives are responsible for the appearance of edge modes with quasi-energy pinned at half the driving frequency. We discover a novel and computable \mathbb{Z}_2 invariant associated to such states. Finally, I will discuss instances of optical and electronic systems where our theory might be tested.

- [1] R. Roy, F. Harper, Phys. Rev. B **96**, 155118 (2017).
- [2] L. Jiang, T. Kitagawa, J. Alicea, A. R. Akhmerov, D. Pekker, G. Refael, J. I. Cirac, E. Demler, M. D. Lukin, and P. Zoller Phys. Rev. Lett. **106**, 220402 (2011).



Computational study of spin crossover MOFs for carbon capture

A.L. Mariano^{a*} and R. Poloni ^a

a. Univ. Grenoble Alpes, CNRS, Grenoble INP, SIMaP, F-38000 Grenoble, France

* antonio-lorenzo.mariano@grenoble-inp.fr

Even today fossil fuels dominate the global energy production and the resulting increase of carbon dioxide emission is at the core of the greenhouse effect. To effectively prevent carbon dioxide from entering the atmosphere, metal-organic frameworks (MOFs) have been widely investigated as selective CO₂ adsorbents from flue gases [1]. We propose to computationally design a novel family of MOFs whose high affinity for CO₂ can be modified under external stimulus potentially leading to an efficient capture and release process. Recently, J.R Long et al. employed CO gas molecules to demonstrate the guest-induced cooperative spin transition mechanism in open-metal sites MOFs [2]. Our idea is rather to use temperature to trigger a spin crossover transition from low spin to high spin on the open-metal sites upon CO₂ uptake. Due to the occupation of antibonding molecular orbitals in the high spin state, a significant lowering of the CO₂ binding energy is expected [3]. Specifically, we study the well characterized Hofmann-like clathrate Fe(pz)Pt(CN)₄ (pz=pyrazine) and its porous extension Fe(bpac)[M(CN)₄] (bpac=bis(4-pyridyl)acetylene, M=Fe,Pt,Ni). In this proof-of-concept work, we employ density functional theory to demonstrate the novelty and implications of this strategy by computing the magnetization curve and the thermodynamics of adsorption of CO₂ before and after the transition.

[1] Zhou H.C., Long J.R. & Yaghi O.M. *Chem. Rev.* **112**, 673-674 (2012).

[2] Long J.R. et al. *Nature* **550**, 96 (2017).

[3] Poloni R., Lee K., Berger R.F., Smit B. Neaton J.B. *J. Phys. Chem. Lett.* **5**, 861-865 (2014).

Phase diagram of α -uranium: CYCLOPS contribution to the study of satellite reflections

J.C. Marmeggi^{a,b*}, P. Bastie^c, J. Bossy^a, A. Filhol^b, X. Tonon^b et B. Ouladdiaf^b

- a. UPR 2940 Institut Néel/Université Grenoble Alpes, BP 166, F-38042 Grenoble cedex 9
 b. Institut Laue-Langevin, CS 20156, F-38042 Grenoble cedex 9
 c. UMR 5588 LIPhy/Université Grenoble Alpes, BP 87, F-38042 St Martin d'Hères

* E-mail: marmeggi@ill.fr

α -uranium is the only pure chemical element exhibiting a CDW instability. The orthorhombic lattice undergoes an incommensurate phase transition $\mathbf{q}_{\text{cdw}} = \langle q_x, q_y, q_z \rangle$ at 43 K, and then successive q_x and q_y locking at 37 K and 22 K respectively [1]. This was observed by means of neutron diffraction: Laue diffractometer S42 [1] and 4-circle diffractometer D10 with a double-monochromator setup [2]. It is worth noting that low-frequency damped phonons (Kohn anomaly) soften exactly at the incommensurate CDW position: $\mathbf{q}_{\text{min}}(T = 43 \text{ K}) = [0.497(1), 0.13(1), 0.21(1)] = \mathbf{q}_{\text{cdw}}$ [3].

CYCLOPS [4] made it possible to measure large parts of the reciprocal space of α -uranium at 45, 39, 37, 24 K and 1.5 K and for two sample orientations [5]. Many satellites reflections were observed for each of the three known incommensurate phases and successfully indexed (cf. Fig. 1) with the software Esmeralda [6]. This opens up the door to the refinement of the corresponding low temperature structures of α -U since a foreseen new version of Esmeralda will allow to extract normalized structure factors for both the main and satellite reflection. We also demonstrated that temperatures below the superconducting transition ($T_{\text{sc}} \sim 0.48 \text{ K}$) can be reached on that instrument.

- [1] J.C. Marmeggi, A. Delapalme (1980) *Physica*, **102B**, 309-312.
 [2] J.C. Marmeggi, *et al.* (1990) *Phys. Rev. B* **42**, 9365-9376.
 [3] J.C. Marmeggi, *et al.* (2007) *J. of Physics: Conf. Series* **92**, 012173.
 [4] B. Ouladdiaf, *et al.* (2012) *J. Appl. Cryst.* **44**, 392-397.
 [5] J.C. Marmeggi, *et al.* (2017) ILL experimental report, TEST-2536.
 [6] L. Fuentes-Montero, and *al.* (2015) DOI: [10.13140/RG.2.1.4954.1202](https://doi.org/10.13140/RG.2.1.4954.1202)

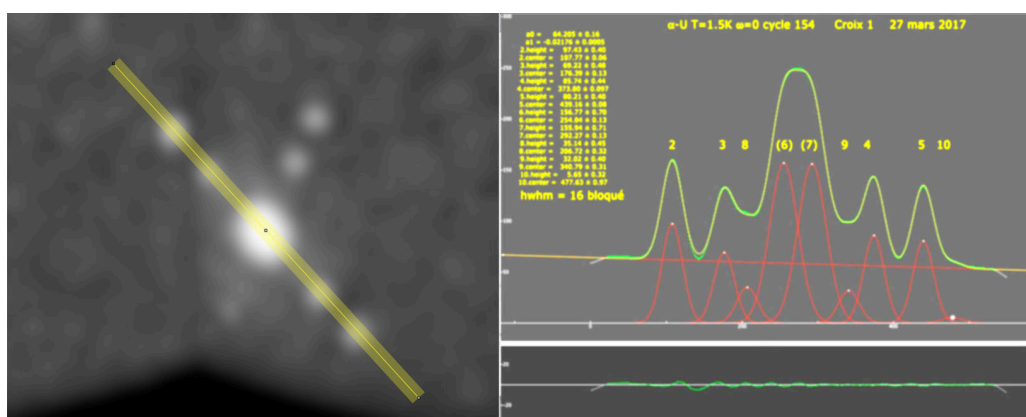


Figure 1: Left image: typical satellites in the α -U pattern at 1.5 K as observed with CYCLOPS; the main reflection is $(-2\ 0\ 4)$.

Right image: satellite intensity fit and indexing from data from the strip drawn on the pattern:
 2: $(112)^{++}$ 3: $(314)^{+++}$ 8: $(216)^{++}$ 9: $(318)^{-}$ 4: $(316)^{-}$ 5: $(114)^{-}$

Pulsation of cubic bubbles

Maxime Harazi^a, Philippe Marmottant^{a*}, Matthieu Rupin^a, Olivier Stephan^a

a. LIPhy, CNRS and Univ. Grenoble Alpes, 140 rue de la Physique, 38400 Saint Martin d'Hères

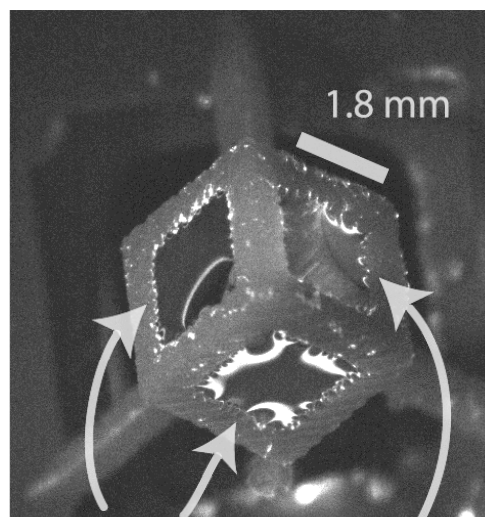
* philippe.marmottant@univ-grenoble-alpes.fr

Due to their great compressibility, bubbles are known to be excellent acoustic resonators and exhibit strong nonlinearities [1]. Furthermore, since the wavelength in the lowest frequency mode (Minnaert resonance) is way larger than the bubble size, they represent perfect candidates for building acoustic metamaterials [2]. One difficulty, though, is to create stable and precisely designed bubbly media.

We propose here to use 3D printing technique to overcome these two problems. We study experimentally the oscillations of a millimetric cubic cavity of air trapped in a 3D printed frame. In this configuration, the water-air interfaces are flat and attached to the printed frame, which increases the stability of the bubble. Furthermore, this new object does not behave as the usual spherical bubble, exhibiting for example a lower fundamental resonance frequency than the Minnaert frequency. Another interesting result is the possibility to shape the bubble frame in order to have different resonance frequencies for each side of the cube, giving the possibility to induce acoustic streaming in a specific chosen direction.

[1] Leighton, T. *The Acoustic Bubble*. (Academic Press, 1997).

[2] Leroy, V. et al. Design and characterization of bubble phononic crystals. *Appl. Phys. Lett.* 95, 171904 (2009).



Water/air interfaces

Figure : Example of a 3D printed cubic bubble with six openings, in water. Air gets trapped in the bubble by capillarity, leading to the creation of six water-air interfaces on the faces of the cube (only three of them being visible on the picture).

Revisiting the ferroelectric field effect in a SrRuO₃ electrode

Thomas Maroutian^{*}, Amina Aidoud, Sylvia Matzen, Guillaume Agnus, Pascal Aubert, et Philippe Lecoer

Centre de Nanosciences et de Nanotechnologies, CNRS UMR 9001, Univ Paris-Sud, Université Paris Saclay, C2N-Orsay, 91405 Orsay, France

* thomas.maroutian@u-psud.fr

The ferroelectric field effect can modulate the electrode resistance in capacitor geometry, depending on the ferroelectric polarization direction. Either charge accumulation or charge depletion is obtained, leading to an increase or a decrease of the electrode resistance, respectively. This effect is expected to be vanishingly small upon increasing the electrode thickness, being tied to the screening length at the ferroelectric/electrode interface. In this picture, we report on the resistance variation of a SrRuO₃ (SRO) film in the 1-10 nm thickness range, with either BaTiO₃ or PbTiO₃ as ferroelectric layer. All perovskite oxides were grown by pulsed laser deposition on SrTiO₃ substrates [1]. The devices were fabricated combining optical lithography, reactive ion etching of the oxide layers and lift-off process for the Pt top electrodes. The resistance variation of the SRO electrode was systematically measured upon switching the ferroelectric polarization, ranging from 0.4% (10 nm-thick SRO) to 25% (1 nm-thick SRO). The thickness and polarization dependences are discussed in terms of the charge screening and the ionic distortions at the ferroelectric/electrode interface.

[1] A. Aidoud *et al.*, Tuning the growth and strain relaxation of ferroelectric BaTiO₃ thin films on SrRuO₃ electrode: Influence on electrical properties, *Eur. Phys. J. Appl. Phys.* **80**, 30303 (2017)

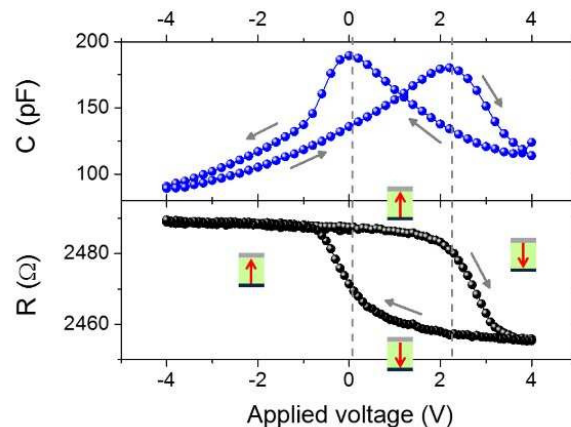


Figure 1 : Capacitance of a BaTiO₃ ferroelectric layer (top) and SrRuO₃ electrode resistance (bottom) as a function of applied bias on the capacitor. The hysteretic behavior (gray arrows) is tied to the reversal of the polarization in the ferroelectric layer (red arrows), as depicted in the figure.

Spin-to-charge interconversion in ferromagnetic/nonmagnetic nanostructures using direct and inverse spin Hall effects

V. T. Pham^a, P. Noël^a, G. Zahnd^a, A. Marty^{a*}, C. Bouard^a, W. Savero-Torres^a,
L. Vila^a and J.-P. Attané^a

a. SPINTEC, Univ. Grenoble Alpes / CEA / CNRS, F-38000 Grenoble, France

* alain.marty@cea.fr

Pure spin currents correspond to the case of spin up and spin down electrons in equal number, flowing in opposite directions so that there is a transfer of angular momentum without overall charge current flow. Spin-orbit (SO) interactions can be used to achieve the conversion between charge currents and pure spin currents: the direct (charge to spin) or inverse (spin to charge) conversions can occur by spin Hall effect (SHE) in the bulk of metals [1], semiconductors [2] and superconductors, by Rashba effect in 2D electron gas [3], or in topological insulators [4]. The angular momentum carried by pure spin currents can be used to excite or to switch the magnetization [5] by means of spin-orbit torque. The promising use of SO interactions in spintronics has given birth to an expanding field of research, the spinorbitronics [6].

The precise evaluation of the conversion efficiency becomes a crucial issue, the need for straightforward ways to observe this conversion has emerged as one of the main challenges in spintronics. Here [7], we propose a simple device, akin to the ferromagnetic/nonmagnetic bilayers used in most spin-orbit torques experiments, and consisting of a SHE wire connected to two transverse ferromagnetic electrodes (figure 1). We show that this system allows probing electrically the direct and inverse conversion in a SHE system, and measuring both the spin Hall angle and the spin diffusion length. By applying this method to several SHE metals (Pt, Pd, Au, Ta, and W), we show that it represents a promising tool for the metrology of spin-orbit materials.

- [1] Hirsch, J. E. Phys. Rev. Lett. 83, 1834 (1999)
 [2] Dyakonov M. I., *et al.*, V. I. Phys. Lett. A 35, 459 (1971)
 [3] Rojas-Sánchez J. C., *et al.*, Nature Comm. 4, 2944 (2013)
 [4] Küfner S., *et al.*, Phys. Rev. B 90, 125312 (2014)
 [5] Miron I. M., *et al.*, Nature 476, 189 (2011)
 [6] Sinova J., *et al.*, Rev. Mod. Phys. 87, 1213 (2015)
 [7] V. T. Pham, *et al.*, Nano Lett. 16,6755 (2016)

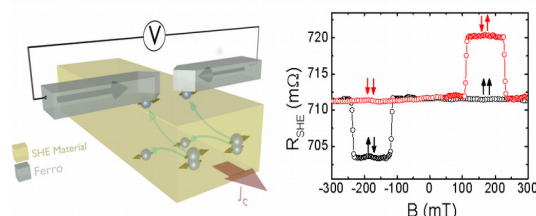


Figure 1 : left : scheme of the conversion device. A charge current J_c flows along SHE wire and generates a spin accumulation, which is detected by the ferromagnetic electrodes giving rise a voltage difference in the antiparallel configuration. Right : the corresponding SHE signal in the conversion device of CoFe/Pt.

Structural and electronic interactions in van der Waals heterostructure MoSe₂/few-layer graphene

M. T. Dau^a, M. Gay^b, D. Di Felice^c, C. Vergnaud^a, A. Marty^{a*}, C. Beigné^a, G. Renaud^d, O. Renault^b, P. Mallet^e, T. Le Quang^e, J-Y. Veuillen^e, L. Huder^f, V. Renard^f, C. Chapelier^f, G. Zamborlini^g, M. Jugovac^g, V. Feyer^g, Y. J. Dappe^c, P. Pochet^d and M. Jamet^a

- a. INAC-SPINTEC, CEA/CNRS, Université Grenoble Alpes, F-38000 Grenoble, France
- b. CEA, LETI, Minatec campus, Université Grenoble Alpes, F-38054 Grenoble, France
- c. SPEC, CEA, CNRS, Univ. Paris Saclay, CEA Saclay, 91191 Gif-sur-Yvette Cedex, France
- d. INAC-MEM, CEA, Université Grenoble Alpes, F-38000 Grenoble, France
- e. Institut Néel, CNRS, Université Grenoble Alpes, F-38000 Grenoble, France
- f. INAC-PHELIQS, CEA, Université Grenoble Alpes, F-38000 Grenoble, France
- g. Peter Grünberg Institute, Forschungszentrum Jülich GmbH, D-52425, Jülich, Germany

* alain.marty@cea.fr

In the route to novel functionalities of two-dimensional (2D) materials, three-dimensional entities conceptualized from 2D-lego pieces have drawn particular attention because of the dimensionality effect and exotic properties [1,2]. As 2D layers are held together by a van der Waals (vdW) force, fabrication of vertical heterostructures is a genuine approach offering a fertile platform to study fascinating vdW-driven properties: commensurate lattice coincidence, electronic structure and band structure line-up, spin-orbit coupling induced by proximity effect and by inversion symmetry breaking.

We will discuss on the synthesis and characterization of the van der Waals heterostructure : MoSe₂/few-layer-graphene by molecular beam epitaxy [3]. The fabrication consists in depositing MoSe₂ on graphitized graphene-SiC substrate, leading to a pure vdW interface which enables us to study properly the intrinsic properties. We employed surface-sensitive techniques in order to probe structural and electronic properties of the heterostructure ranging from atomic resolution (STM-STs) to microscopic scale (synchrotron diffraction, photoemission electron microscopy k-PEEM). At the atomic standpoint, the STM shows point defects and twin boundaries. This kind of defects is in general observed in MBE-2D layers due to Se vacancies and domain merging. STs measurement at selected point on MoSe₂ layer indicates a band gap of 2.1 eV separating the valence band maximum and conduction band minimum. Regarding the microscopic scale measurements, we found that the crystallographic directions of the MoSe₂ lattice align along the ones of graphene. The structural analysis by synchrotron diffraction is consistent with the constant energy map in k-space of the electronic band structures of MoSe₂-graphene probed by k-PEEM. We observe a clear evolution of the band structure of the heterostructure compared to the one of bare few-layer-graphene, which is a direct consequence of the interlayer coupling between the MoSe₂ layer and graphene. Indeed, we have evidenced a large bandgap opening in few-layer-graphene resulting from significant charge transfer between vdW layers.

[1] G. R. Bhimanapati, *et al.* ACS Nano, 9, 11509 (2015)

[2] Y. Lui, *et al.*, Nat. Rev. Mater. 1, 16042 (2016)

[3] M.-T. Dau, *et al.*, ACS Nano 12, 2319 (2018)

As-grown state of pinwheel artificial spin ice

M. Massouras^{a*}, F. Montaigne^a, D. Lacour^a et M. Hehn^a

a. Institut Jean Lamour, CNRS UMR 7198, Université de Lorraine, 54000 Nancy, France

*e-mail: maryam.massouras@univ-lorraine.fr

Artificial Spin Ice (ASI) systems made of two-dimensional arrays of nanomagnets in close interaction provide a playground to directly observe magnetic frustration^[1, 2]. By the use of shape anisotropy, mesoscopic Ising-like spins could be patterned with various spatial distributions. In this study, we examine the square lattice and modified such that each nanomagnet is tilted around its central point from 5° to 45° every 5° . Both extreme cases, square and 45° -tilted lattice have been studied^[1, 2], the latter is called “pinwheel ASI”. They are fabricated using electron beam lithography and liftoff to define 20nm-thick Permalloy nanomagnets with $400 \times 100 \text{ nm}^2$ lateral dimensions. Before any field history, we investigated the as-grown state just after lift-off. Magnetic Force Microscopy (MFM) configurations are shown in Fig. 1 (a) and (b). We find that the ground state (GS) of the regular square lattice is different from the pinwheel ASI: one corresponding to the ice-rule and the other a ferromagnetic state respectively. In this talk, we will give a comprehensive picture of the evolution of the GS and micromagnetic configuration as a function of angle.

- [1] Morgan, J. P., Stein, A., Langridge, S., & Marrows, C. H. (2011). Thermal ground-state ordering and elementary excitations in artificial magnetic square ice. *Nature Physics*, 7(1), 75.
 [2] Gliga, S., Hrkac, G., Donnelly, C., Büchi, J., Kleibert, A., Cui, J., et al. (2017). Emergent dynamic chirality in a thermally driven artificial spin ratchet. *Nature materials*, 16(11), 1106.

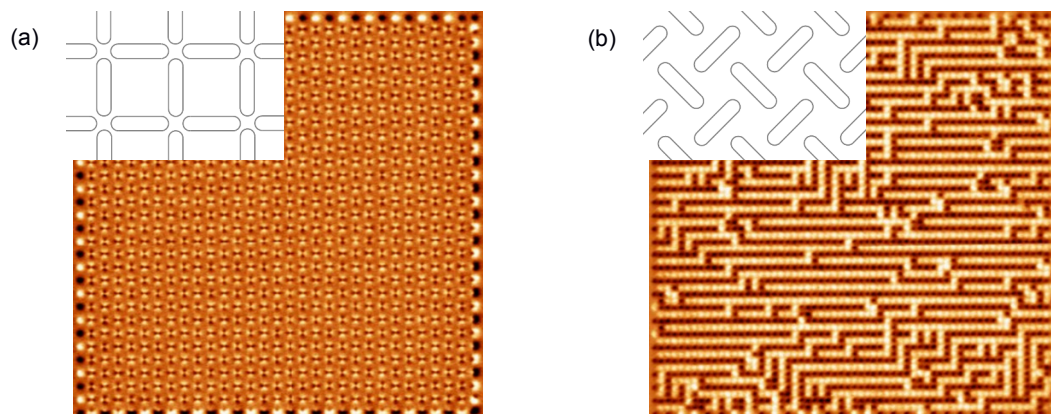


Figure 1: (a) MFM image of an as-grown square ice network exhibiting GS following the ice rule (b) MFM image of a 45° tilted network exhibiting ferromagnetic GS.

La microscopie électronique à balayage sous environnement gazeux. Principes – Limitations – Applications in Situ.

Christian Mathieu*

a. Université d'Artois, Faculté Jean Perrin rue Jean Souvraz 62307 Lens Cedex

* christian.mathieu@univ-artois.fr

Le microscope électronique à balayage conventionnel (MEB-C) est un instrument dédié à l'observation d'échantillons. L'échantillon, pour être observable, doit cependant répondre à une double contrainte. Il doit être conducteur pour éviter les phénomènes de charge entraînant des distorsions dans les images. La seconde contrainte qu'il doit supporter est le dégazage car l'observation dans un MEB-C requiert une pression dans la chambre de l'échantillon de l'ordre de 10^{-3} Pa. Pour des échantillons fragiles (échantillon biologique), le phénomène de dégazage entraîne une modification de l'échantillon et un intérêt limité de l'observation dans de telles conditions. Une solution qui permet de pallier à la double contrainte (non conductivité-dégazage) de nombreux échantillons est l'introduction d'un gaz à une pression relativement importante dans la chambre de l'échantillon comme dans la microscopie électronique à balayage sous environnement gazeux (MEB-EG). Cette dénomination permet de regrouper sous un même terme le MEB environnemental et le MEB à pression contrôlée. La présence du gaz a induit une conception différente de la colonne électronique et de la détection des signaux. Les différents aspects de l'instrument seront présentés. Les interactions entre le gaz et les différents signaux (électrons, photons X) seront discutées. Des exemples d'applications [1-4] dans différents domaines seront présentés afin de montrer l'intérêt en terme de manipulation in situ.

[1] F. Brisset, M. Repoux, J. Ruste, F. Grillon et F. Robaut, Microscopie électronique à balayage et microanalyses, EDP sciences, ISBN 878-27598-0082-7 (2008).

[2] D.J. Stokes, Principles and Practice of Variable Pressure/Environmental Scanning Electron Microscopy (VP-ESEM), John Wiley & Sons, Ltd., Chichester, UK (2008).

[3] R. Podor, J. Ravaux, H. P. Brau In Situ Experiments in the Scanning Microscope Chamber, Scanning Electron Microscopy, Viacheslav Kazmiruk (Ed.), ISBN: 978-953-51-0092-8, InTech, 31-54 (2012).

[4] L. Khouchaf, C Mathieu La microscopie électronique à balayage sous environnement gazeux (MEB-EG) du principe à l'étude optimisée des matériaux, Ellipses, ISBN : 9782340018068, Paris (2017).

Ultrafast photostriction in devices based on piezoelectric thin films

Sylvia Matzen^{a*}, Loïc Guillemot^a, Thomas Maroutian^a, Guillaume Agnus^a, Dafiné Ravelosona^a, Philippe Lecoeur^a, Sheena Patel^b, Oleg Shpyrko^b, Eric Fullerton^b, Haidan Wen^c, Anthony DiChiara^c, Roopali Kukreja^d

- a. Centre de Nanosciences et de Nanotechnologies, UMR CNRS 9001, Université Paris Saclay, 91405 Orsay, France
- b. University of California San Diego, USA
- c. Argonne National Laboratory, Argonne, USA
- d. University of California Davis, Davis, USA

* sylvia.matzen@u-psud.fr

Among ferroic materials, ferroelectric oxides are particularly promising due to their numerous functional properties and their potential coupling. Manipulating and integrating these functionalities in devices can pave the way for innovative oxide-based electronics. Photostriction, described as a combination of both photovoltaic and inverse piezoelectric effects, is a complex physical mechanism inducing non thermal strain under illumination. Recent studies in ferroelectric thin films have reported photo-induced strain in the picosecond time range [1-4], thus opening a new route for ultrafast strain engineering and optical actuation in devices. However, the polarization is usually in as-grown state, so its contribution on the photostrictive response is not well understood.

Ultrafast studies have been conducted on photo-induced strain in ferroelectric thin films based devices with an in-situ control of the polarization state. Our time-resolved x-ray diffraction studies performed at Advanced Photon Source (APS) revealed that both magnitude and sign of strain can be controlled by the polarization state, giving a better understanding of the ultrafast photostriction mechanism in ferroelectric devices.

- [1] D. Daranciang, et al. Ultrafast Photovoltaic Response in Ferroelectric Nanolayers. *Phys. Rev. Lett.* 108, 087601 (2012)
- [2] H. Wen, et al., Electronic Origin of Ultrafast Photoinduced Strain in BiFeO₃. *Phys. Rev. Lett.* 110, 037601 (2013)
- [3] D. Schick, et al. Localized Excited Charge Carriers Generate Ultrafast Inhomogeneous Strain in the Multiferroic BiFeO₃. *Phys. Rev. Lett.* 112, 097602 (2014)
- [4] Y. Li, et al. Giant optical enhancement of strain gradient in ferroelectric BiFeO₃ thin films and its physical origin. *Scientific Reports* 5, 16650 (2015).

Funding acknowledgments:

DIM Oxymore Grant (Ile-de-France)

Research at UCSD supported by NSF Award DMR-1411335.

In vitro biocompatibility evaluation of nanostructured polymers

Jean-Marie MAYAUDON^{a,b,*}, Anne QUESNEL-HELLMANN^a, Lionel ROUSSEAU^c,
Blaise YVERT^{a,b}, Gaëlle PIRET^{a,b}

- a. BrainTech Lab., INSERM U1205, 2280 rue de la piscine, 38400 Saint Martin d'Hères, France
- b. Université Grenoble Alpes, Grenoble, France
- c. ESYCOM, ESIEE-Paris, Cité Descartes, 2 Boulevard Blaise Pascal, 93160 Noisy-le-Grand

* jean-marie.mayaudon@inserm.fr

Implantable Multi-Electrode cortical arrays are key neuronal interfacing systems in neurophysiological and clinical research to better understand healthy and pathological brain dynamics. One of the major challenge is to propose a biocompatible device that remains stable over a long period of time and therefore that minimizes undesirable brain tissue reactions. Several studies indicate that surface structuration can promote neuron adhesion to the implant surface while it could limit glial cell proliferation (Piret et al. [1-4], Cesca et al. [5]). As the major part of the implant in direct contact with the surface of the neural tissue is the insulating material, a method to nanostructure the polymeric surface of the implant was needed. Using plasma etching procedures, it was possible to get reproducible nanostructure topologies of SU-8, polyimide and parylene polymers. The biocompatibility of these different nanostructured polymers was then studied on rat primary cortical cells cultures.

[1] Piret et al "Neurite outgrowth and synaptophysin expression of postnatal CNS neurons on GaP nanowire arrays in long-term retinal cell culture", *Biomaterials* 34(4), pp. 875-887(2013).

[2] Piret, G and Prinz, CN "Could the use of nanowire structures overcome Some of the current limitations of brain electrode implants?" *Nanomedicine*11 (7), 745-747(2016)

[3] Piret et al "Support of neuronal growth over glial growth and guidance of optic nerve axons by vertical nanowire arrays" *ACS applied materials & interfaces*7(34), 18944-18948(2015)

[4] Piret et al "3D-nanostructured boron-doped diamond for microelectrode array neural interfacing" *Biomaterials*53, 173-183(2015)

[5] Cesca et al "Fabrication of biocompatible free-standing nanopatterned films for primary neuronal cultures" *RSC Advances*, 4, 45696-45702(2014)

Gold-intercalated graphene on Re(0001)

Estelle Mazaleyrat^{a,b*}, Alexandre Artaud^{a,b}, Johann Coraux^b et Claude Chapelier^a

- a. Univ. Grenoble Alpes, CEA, INAC, PHELIQS, 38000 Grenoble, France
- b. Univ. Grenoble Alpes, CNRS, Grenoble INP, 38000 Grenoble, France

* estelle.mazaleyrat@neel.cnrs.fr

Graphene, a one-atom thick material made of carbon atoms, presents a weak intrinsic spin-orbit coupling. Inducing large spin-orbit coupling in graphene would allow to use graphene in active elements of spintronics, such as the Das-Datta spin field effect transistor.

We have investigated the local density of states of gold-intercalated graphene on Re(0001) by means of low-temperature scanning tunneling spectroscopy measurements. The intercalation of a sub-monolayer of gold atoms was monitored by reflection high energy electron diffraction. The lattice mismatch and the strong electronic coupling between graphene and rhenium result in a periodic undulation of graphene on top of rhenium. This long wavelength beating is called a moiré superlattice. As opposed to the moiré of graphene on rhenium, gold-intercalated regions show a shallow moiré of graphene on gold ascribed to the local decoupling of graphene from rhenium. The decoupling is confirmed by Raman spectroscopy measurements.

Spectroscopy measurements show broad resonances at large energies, attributed to a giant spin-orbit splitting (~ 100 meV) induced in intercalated graphene by gold atoms. The spin-orbit splitting is found to be moiré-sensitive: we find correlations between the energies at which we observe the resonances and the topography. At smaller energies, we find no spatial variation of the density of states: the superconducting character of rhenium extends to graphene via the proximity effect both in intercalated and in non-intercalated regions.

Adsorption-Induced Slip Inhibition for Polymer Melts on Ideal Substrates

J.D. McGraw*^{a,b,c}, M. Ilton^{d,c}, T. Salez^{e,b,f}, P.D. Fowler^c, M. Rivetti^g, M. Aly^a, M. Benzaquen^{b,h}, E. Raphaël^b, K. Dalnoki-Veress^{c,b}, O. Bäumchen^g

- a. Département de Physique, ENS/PSL, CNRS, 24 Rue Lhomond, 75005 Paris, France
- b. UMR CNRS Gulliver 7083, ESPCI Paris, PSL Research University, 75005 Paris, France
- c. Department of Physics & Astronomy, McMaster University, Hamilton, Ontario, Canada
- d. Polymer Science & Engineering Department, UMASS Amherst, USA
- e. Univ. Bordeaux, CNRS, LOMA, UMR 5798, F-33405 Talence, France
- f. Global Station for Soft Matter, Hokkaido University, Sapporo, Hokkaido, Japan
- g. Max Planck Institute (MPIDS), Am Faßberg 17, 37077 Göttingen, Germany
- h. Ladhyx, UMR CNRS 7646, Ecole Polytechnique, 91128 Palaiseau Cedex, France

* joshua.mcgraw@espci.fr

In the study of capillary-driven fluid dynamics [1], relatively simple departures from equilibrium offer the chance to quantitatively model the resulting relaxations. These dynamics in turn provide insight on both practical and fundamental aspects of thin-film and near-surface hydrodynamics. In this talk, we will describe two model experiments — dewetting and capillary levelling— allowing to elucidate polymeric slip in thin polymer films. Slip is a fundamental phenomenon in fluid dynamics that governs liquid transport at small scales. For polymeric liquids, de Gennes predicted [2] that the Navier boundary condition together with the theory of polymer dynamics imply extraordinarily large interfacial slip for entangled polymer melts on ideal surfaces. By comparing two different relatively simple departures from equilibrium, we show [3] that the slip length manifested in a capillary-driven flow experiment in fact depends sensitively on the experimental configuration. A levelling experiment [3, 4] and a dewetting experiment [5] may indeed present vastly different slip boundary conditions even when the probed materials are identical and the surfaces are atomically smooth.

[1] Oron et al., *Reviews of Modern Physics* (1997)

[2] de Gennes, *C.R. Acad. Sci. B* (1979)

[3] Ilton et al, *Nature Comm.* (2018)

[4] McGraw et al, *Physical Review Letters* (2012)

[5] Bäumchen et al, *Physical Review Letters* (2009)

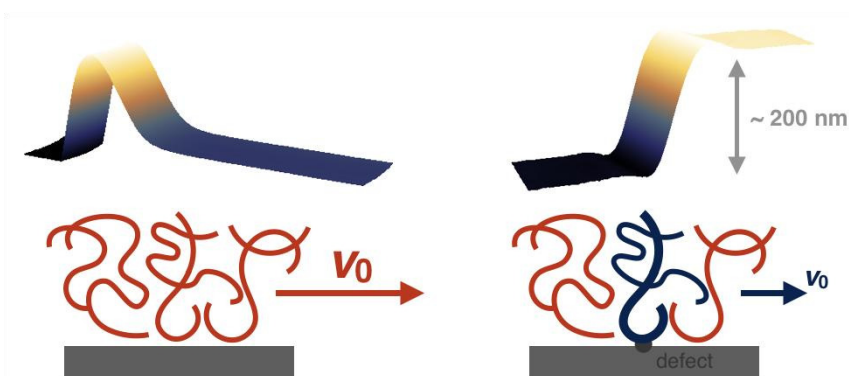


Figure 1 : Fluid velocity at the substrate can be largely impacted by the choice of capillary driving method, whether the latter is dewetting (left) or stepped-film levelling (right).

Correlations between heat transfer and friction in double wall carbon nanotubes

Akif Ramzan,^a and Samy Merabia^{a*}

a. Institute Light and Matter ILM, 6, rue Ada Byron, Université Lyon 1, 69622 Villeurbanne

* samy.merabia@univ-lyon1.fr

Low-dimensional Carbon nanotubes have exceptional potential to be used in nanoscale mechanical devices due in part to the ultralow friction they display, that make them ideal for many nanoscale thermoelectromechanical devices. Theoretical models have also been devised to understand the friction in telescopic double wall carbon nanotubes [1] (DWCNTs). However, no study to date has been carried out to study the correlations between friction and interfacial heat transfer across DWCNTs, although some work point toward that direction [2].

In this project we study such correlations in double-walled CNTs using molecular dynamics simulations. We employ techniques based on equilibrium Green-Kubo formalism and non-equilibrium molecular dynamics simulations to investigate the correlations. We systematically characterize the effects of CNT length, temperature and chirality on nanoscale friction and interfacial heat transfer.

This study potentially provides a theoretical foundation for thermo- mechanical devices that could measure ultra-low friction in CNTs by simply probing heat flux across surfaces, or vice versa.

[1] J. Servantie, and P. Gaspard, Phys. Rev. B 73, 125428 (2006)

[2] M. V. D. Prasad, and B. Bhattacharya, Nano Lett. 17, 2131 (2017)

Multimode nanomechanics in non-conservative force fields

Laure Mercier de Lépinay^a, Benjamin Pigeau^a, Benjamin Besga^a, Francesco Fogliano^a and Olivier Arcizet^{a*}

a. Institut Néel, CNRS and Université Grenoble Alpes, 25 rue des Martyrs F-38042 Grenoble, France

* olivier.arcizet@neel.cnrs.fr

Nanomechanical resonators display extreme sensitivities to external force fields. Consequently nearly-degenerate modes of multidimensional oscillators such as nanotubes, nanowires or optically trapped particles are strongly affected by transverse force fields components. These resonators are then particularly interesting as force probe since the multidimensionality of vector fields is a necessary condition for the existence of vorticity.

It has been shown that a rotational force field is applied on a singly-clamped SiC nanowire (NW) when it is positioned at the edge of the waist of a strongly focused laser beam[1]. Thanks to a novel vectorial force measurement technique based on the dual-channel optical detection of the NW vectorial displacement[4], we study the perturbation of its thermal and driven motion by the non-conservative force field.

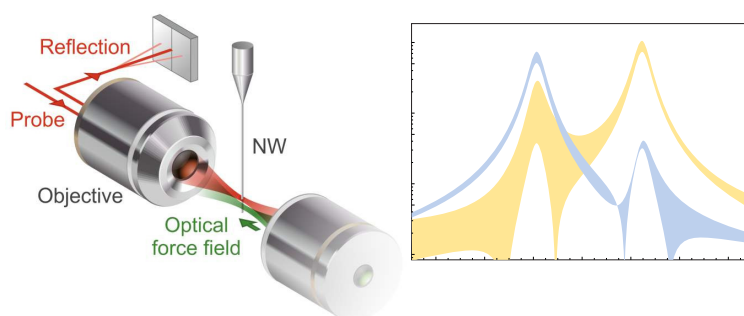


Figure 1: **a.** Experiment scheme. **b.** Experimental observation of the deviation to the FDR. **c.** Thermal noise distribution in space in a purely rotational force field.

In addition to the bifurcation and dynamic instability uncovered previously[1], this experiment reveals the existence of a large deviation to the standard fluctuation-dissipation relation[3]. This deviation can be interpreted as stemming from the shearing of the motion eigendirections, as can be seen from a derived new modified version of the fluctuation-dissipation relation valid in such force fields.

Furthermore, a large excess of total thermal noise is observed. Thanks to an experimental adjustment of our vectorial motion detection setup, we showed that the noise distribution is structured in space so that some directions of the oscillation plane actually show *reduced* thermal fluctuations[4]. A parallel can be drawn with the evolution of motion quadratures in parametric squeezing. The conclusions of this work can also be adapted to the description of non-reciprocal optomechanical systems.

- [1] A. Gloppe et al., Nature Nano. **9**, 920-926 (2014)
- [2] L. Mercier de Lépinay et al., Nature Nanotech. **12**, 156-162 (2016)
- [3] L. Mercier de Lépinay et al., Nature Commun. (accepted)
- [4] L. Mercier de Lépinay et al., (in preparation)

” Non-conventional magnetoelectric ferroics”

H.T.T. Nong^a, A. Gómez^b, A. N. Nguyen^a, Ch. Ben Osman^c, J. Solard^d, C. Ibrahim^a,
N. T. Lan^a, M. Simon Carillo^b and Silvana Mercone^{a*}

- a. Laboratoire de Sciences des Procédés et des Matériaux (LSPM-CNRS UPR-3407), Université Paris 13, 93430 Villetaneuse, France
- b. Instituto de Ciencia de Materiales de Barcelona (ICMAB-CSIC), Campus UAB, 08193 Bellaterra, España
- c. Laboratoire Matière Molle et Chimie, ESPCI, 75005 Paris, France
- d. Laboratoire de Physique des Lasers (LPL-CNRS UMR-7538), Université Paris 13, 93430 Villetaneuse, France

* silvana.mercone@univ-paris13.fr << corresponding author >>

Multiferroic materials, which possess at least two ferroic properties among ferroelectricity, ferromagnetism and ferroelasticity, are attractive systems due to the possible giant cross coupling between these three orders. In the case of multiferroic magnetoelectric (**ME**) composites, this cross coupling occurs between two ferroics subsystems (magnetic and electric one) and it can give rise to a large direct and/or converse magnetoelectric effect (DME, CME). Indeed, thanks to an efficient DME (CME), it becomes possible to control the dielectric polarization **P** (respectively the magnetization **M**) by a magnetic field **H** (electric field **E**). Thus $\Delta P = \alpha_H \Delta H$ ($\mu_0 \Delta M = \alpha_E \Delta E$) where $\alpha_{H/E}$ is the coupling coefficient. In the ME composites, showing physically separated magnetic and electric order phases, both DME and CME coupling can be mediated through (a) the strain, (b) the charge carrier and (c) the spin exchange. After a brief introduction of these possible couplings, we will focus on composite materials showing a strain-mediated CME effect. This latter is a product tensor property that results from the elastic coupling between the piezoelectric and magnetostrictive components, which are artificially coupled together in a single composite structure. Several connectivity between the two phases are possible, we report in Figure 1 two of the interfacial bonding we have been studying. The influence of the interface geometries as well as their hybrid nature shown in Figure 1, will be illustrated and discussed both upon the magnetic and the electric properties of the composite nanostructures.

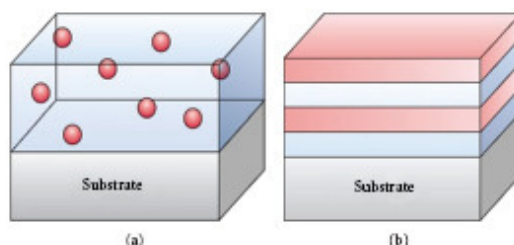


Figure 1: Schematic illustration of 2 common connectivity in ME composites: (a) 0-3 particulate composite and (b) 2-2 laminate one. In both these two nanostructures, the red volume corresponds to the ferromagnetic inorganic material while the light blue is the piezoelectric organic one.

Cooling a Macroscopic Mechanical Oscillator close to its Quantum Ground State

Rémi Metzdorff^{a*}, Leonhard Neuhaus^a, Salim Zerkani^a, Sheon Chua^a, Thibaut Jacqmin^a, Samuel Deléglise^a, Tristan Briant^a, Pierre-François Cohadon^a, Antoine Heidmann^a

a. Laboratoire Kastler Brossel, Sorbonne Université, CNRS, ENS-Université PSL, Collège de France

* remi.metzdorff@lkb.upmc.fr

We present our recent results about the optomechanical cooling of a 33 μg , 1 mm thick quartz micropillar with a compression-dilatation mode oscillating at 3.6 MHz with Q-factor above 10^6 . A mirror coated on top of the pillar allows to construct a high-finesse Fabry-Perot cavity to optically detect and control the oscillator motion. In recent experiments, we have reached mechanical quality factors as high as 70×10^6 and an optical finesse near 10^5 at temperatures below 10 K in a dilution cryostat.

With a low-power laser beam locked to the cavity resonance in cryogenic operation, we have observed Brownian motion corresponding to mode temperatures down to 110 mK. When driving the optomechanical cavity with a red-detuned laser beam of powers up to 25 μW , we have been able to cool the mechanical oscillator to a mean thermal occupation number of 20 phonons. This limit is due to light absorption by the micropillar that causes an increased thermal bath temperature. The injection of even higher powers to enable further cooling is prevented by the self-oscillation of low-frequency suspension modes. New schemes to implement feedback cooling are presented to lower the mean thermal occupation number of phonons.

While our optomechanical device now fulfills the requirements for ground state cooling in a cryogenic environment, this experiment is prevented by about 10 dB excess cavity phase noise due to coupling mirror motion. We are currently designing mirror substrates structured with a phononic crystal in order to decrease this excess noise and enable cooling of our system to the mechanical quantum ground state. In this regime, we plan to inject squeezed light into our optomechanical cavity to test schemes for measuring mechanical displacement with sensitivities below the standard quantum limit.

- [1] M. Aspelmeyer, T. J. Kippenberg, and F. Marquardt, "Cavity Optomechanics," *Rev. Mod. Phys.* 86, 1391 (2014).
- [2] The LIGO scientific collaboration, "Enhanced sensitivity of the LIGO gravitational wave detector by using squeezed states of light," *Nat. Photon.* 7, 613 (2013).
- [3] A. G. Kuhn, J. Teissier, L. Neuhaus, S. Zerkani, E. van Brackel, S. Deléglise, T. Briant, P.-F. Cohadon, A. Heidmann et al., "Free-space cavity optomechanics in a cryogenic environment," *Appl. Phys. Lett.*, 104, 44102 (2014).

Electron waiting times in hybrid junctions with topological superconductors

Shuo Mi^{a,b*}, Pablo Buset^a, and Christian Flindt^a

- a. Department of Applied Physics, Aalto University, 00076 Aalto, Finland
- b. Univ. Grenoble Alpes, CEA, INAC-Pheliqs, 38000 Grenoble, France

* shuo.mi@univ-grenoble-alpes.fr

We investigate the waiting time distributions (WTDs) of superconducting hybrid junctions, considering both conventional and topologically nontrivial superconductors hosting Majorana bound states at their edges. To this end, we employ a scattering matrix formalism that allows us to evaluate the waiting times between the transmissions and reflections of electrons or holes. Specifically, we analyze normal-metal–superconductor (NIS) junctions and NISIN junctions, where Cooper pairs are spatially split into different leads. The distribution of waiting times is sensitive to the simultaneous reflection of electrons and holes, which is enhanced by the zero-energy state in topological superconductors. For the NISIN junctions, the WTDs of trivial superconductors feature a sharp dependence on the applied voltage, while for topological ones they are mostly independent of it. This particular voltage dependence is again connected to the presence of topological edge states, showing that WTDs are a promising tool for identifying topological superconductivity [1].

[1] Shuo Mi, Pablo Buset, and Christian Flindt, [arXiv:1805.01704](https://arxiv.org/abs/1805.01704)

X-ray Laue Diffraction 3D Microscopy

Loïc Renversade^{a, c}, Odile Robach^{a, c}, Olivier Ulrich^{a, c}, Jean-Sébastien Micha^{b, c, *}

a. Univ. Grenoble Alpes, CEA, INAC-MEM, 38000 Grenoble, France

b. Univ. Grenoble Alpes, CNRS, CEA, INAC-SyMMES, 38000 Grenoble, France

c. CRG-IF BM32, ESRF, BP 220, 38043 Grenoble Cedex 9, France

* micha@esrf.fr

Laue microdiffraction is a powerful and widely-used technique for spatially-resolved characterization of crystalline microstructures [1]. Using a white micro-focused X-ray beam from a synchrotron source, it allows mapping orientation and elastic strain fields with a spatial resolution down to 100 nm and an angular resolution as good as 10^{-4} , which allows for detailed investigations of crystal-related phenomena, such as plastic deformation and damage.

The classical analysis of Laue patterns provides in practice surface information that integrates the intensity diffracted all along the penetration course of the incident beam. Therefore, the 3D Laue microdiffraction, or « Differential Aperture X-Ray Microscopy » [2], was proposed to resolve this dimension along the beam with a submicron resolution and get from “2D” to spatially 3D characterizations. To this end, an absorbing wire placed between the sample and the detector is used to scan the sample surface in micron steps and gradually mask portions of the scattered spots. Analyses of the intensity variations between successive images, combined with geometrical considerations, allow then to reconstruct the scattered intensity profiles as a function of depth below the sample surface.

Such a 3D imaging instrument is now available to the users of the CRG-IF BM32 beamline at ESRF (cf Figure). This was achieved in the last years, thanks to improvements of calibration and reconstruction algorithms, the development of a software package for complete data treatment and the recent commissioning of a faster camera. Here, we describe these advances and illustrate with a few examples the perspectives offered by this technique.

[1] Ulrich O., Biquard X., Bleuet P., Geaymond O., Gergaud P., Micha J.S., Robach O. and Rieutord F, Rev. Sci. Instr., **2011**, 82.

[2] B.C. Larson, W. Yang, G.E. Ice, J.D. Budai et J.Z. Tischler, Nature, **2002**, 415.

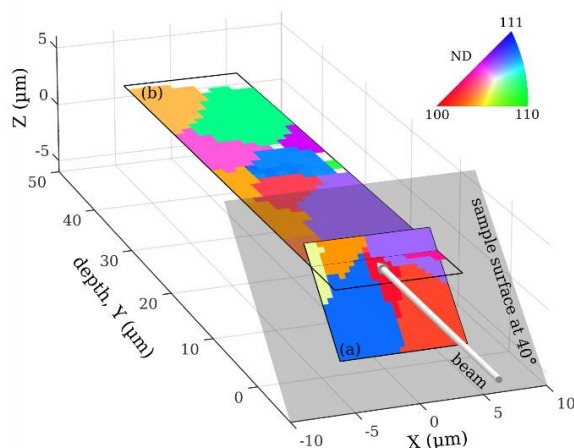


Figure: Polycrystalline thin film of yttria-stabilized zirconia: (a) μ Laue orientation map of sample surface tilted at 40° and (b) depth reconstruction by 3D- μ Laue. Inverse pole figure coloring.

Clustering-induced self-propulsion of isotropic catalytic particles

Akhil Varma^a, Thomas D. Montenegro-Johnson,^b & Sébastien Michelin^{a*}

a. LadHyX – Département de Mécanique, CNRS – Ecole Polytechnique, 91128 Palaiseau, France

b. School of Mathematics, University of Birmingham, Edgbaston, Birmingham B15 2TT, United Kingdom

* sebastien.michelin@ladhyx.polytechnique.fr

Catalytic particles exploit local gradients in solute concentration to self-propel at the micron scale. A fundamental requirement for their self-propulsion is to break the symmetry of the concentration around them: an isotropic active particle can not swim. Different routes have already been identified for breaking this symmetry. Some are based on the design of the system (e.g. chemical patterning [1], or geometric asymmetry [2]), while another is linked to the non-linear advective coupling of the solute and fluid dynamics [3]. Here, we demonstrate that a fourth route exist, which exploits interactions between individually-non-motile isotropic systems. Such uniform and isotropic particles can achieve self-propulsion by forming geometrically-anisotropic clusters with other particles under the influence of phoretic and hydrodynamic interactions.

Using full numerical simulations as well as theoretical modeling of the clustering process, we obtain the statistics of the propulsion properties for arbitrary initial arrangement of the particles. The robustness of these results to thermal noise is also analysed.

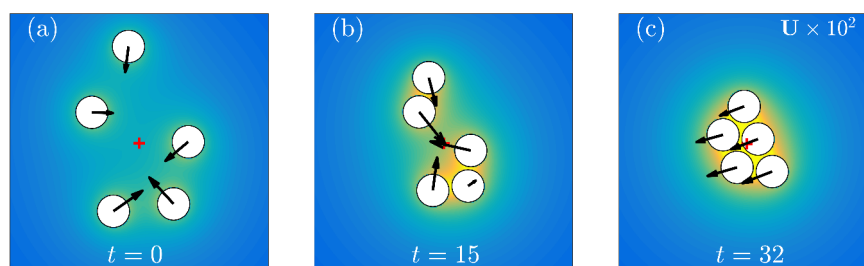


Figure 1: Clustering dynamics of five identical isotropic catalytic particles. Phoretic attraction of the particles resulting from the inhomogeneous concentration field (in color) leads to the formation of cluster (a,b), which can then self-propel due to its geometric asymmetry (c).

- [1] J. L. Moran & J. D. Posner, Phoretic self-propulsion, *Annu. Rev. Fluid Dyn.*, **49**, 511–540 (2017)
- [2] S. Michelin & E. Lauga, Autophoretic locomotion from geometric asymmetry, *Eur. Phys. J. E*, **38**, 7 (2015)
- [3] S. Michelin, E. Lauga & D. Bartolo, Spontaneous autophoretic motion of isotropic particles, *Phys. Fluids*, **25**, 061701 (2013)

Comprendre la structure de systèmes désordonnés avec des simulations moléculaires

Matthieu Micoulaut^{a*},

a. Paris Sorbonne Université, LPTMC, Boite 121, 4 place Jussieu 75252 Paris cedex 05 France

* mmi@lptmc.jussieu.fr

La diffusion de rayons X ou neutrons indique que les liquides et les verres se caractérisent par un certain ordre à courte distance mais sont désordonnés à longue distance, toute la difficulté étant d'accéder à des informations sur la structure allant au-delà des premiers voisins.

Dans cet exposé, nous montrerons comment les développements de simulations de dynamique moléculaire classiques ou quantiques permettent de produire des modèles structuraux réalistes validant non seulement les données expérimentales mais permettant aussi de donner une multitude d'informations supplémentaires à l'échelle atomiques telles que la structure à moyenne distance (anneaux), la géométrie locale, la dynamique et les propriétés vibrationnelles.

Nous illustrerons notre propos en donnant quelques résultats récents portant sur le chalcogénures tels que les systèmes binaires vitreux Ge-Se [1,2], As-Se [2] ou les liquides Ge-Sb-Te [3] ou Ge-Te [4].

[1] *Revealing the crucial role of molecular rigidity on the fragility evolution of glass-forming liquids*, C. Yildirim, J.-Y. Raty, M. Micoulaut, Nature Communications 7, 11086 (2016).

[2] *Compositional thresholds and anomalies in connection with stiffness transitions in network glasses*, M. Bauchy et al., Physical Review Letters 110, 165501 (2013)

[3] *Effect of tellurium concentration on the structural and vibrational properties of phase change Ge-Sb-Te liquids*, H. Flores-Ruiz et al., Physical Review B 92, 134205 (2015)

[4] *Effect of the composition on structure in liquid Ge_xTe_{100-x} : a combined density functional and neutron scattering study*, M. Micoulaut et al., Physical Review B 89, 174205 (2014)

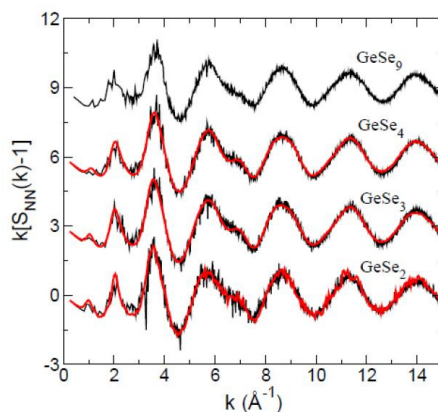


Figure 1 : Fonction interférence déduite de l'expérience (rouge), comparée aux simulations « Premiers principes » des amorphes Ge-Se en compositions variables. Phys. Rev. B **88**, 054203 (2013).

InAs Nanowires for Topological Quantum Computing

Cristina Mier González^a, Yann Genuist^a, Gilles Nogues^a, Moira Hocevar^{a*}

a. University Grenoble Alpes, CNRS-Institut Néel, 38000 Grenoble, France

* moira.hocevar@neel.cnrs.fr

One interesting and promising proposal for quantum computation relies on the so called topological protected quantum bits. Realizing such quantum bits depends on the ability to make materials that can host Majorana bound states. Signatures of such states were reported in 2012 in one-dimensional semiconductors with high spin-orbit coupling, coupled to a superconductor [1]. Since then, nanostructured hybrid materials based on superconductor/semiconductor interfaces have received increased attention. Yet, controlled formation of topological protected states can only be realized if the superconductor/semiconductor interface is of high quality. Creating those interfaces in an epitaxial fashion has many advantages, among them better transparency, controlled interface chemistry, higher current injection and lower disorder [2].

Despite a large plebiscite for Al in current hybrid nanowire devices, using higher critical field superconductors such as V or Nb would open more possibilities for Majorana experiments. Yet a special care in the orientation of the nanowires surface is required during the epitaxy of V and Nb, as the orientation of the material source with respect to the nanowire facets influences the quality of the epitaxial layer. We propose to grow nanowires on substrates of different crystal orientations, i.e (111) and (100), to control their growth orientation. Indeed, inclined wires allow smoother epitaxial superconducting shells [3].

We present preliminary results on the controlled growth (orientation and position) of InAs nanowires that will further be covered by epitaxial superconducting shells. The InAs nanowires were grown by Molecular Beam Epitaxy using the vapour liquid solid mechanism assisted by gold catalysts. The gold catalysts are either randomly distributed on the substrate by colloidal solution or patterned using electron beam lithography.

- [1] Mourik, V., et al. Signatures of Majorana fermions in hybrid superconductor-semiconductor nanowire devices. *Science*, 336(6084), 1003-1007 (2012).
- [2] Krogstrup, P. et al. Epitaxy of semiconductor–superconductor nanowires. *Nature Materials* 14, 400–406 (2015).
- [3] Gusken, N. A., et al. MBE growth of Al/InAs and Nb/InAs superconducting hybrid nanowire structures, *Nanoscale*, vol. 9, pp. 16735–16741 (2017).

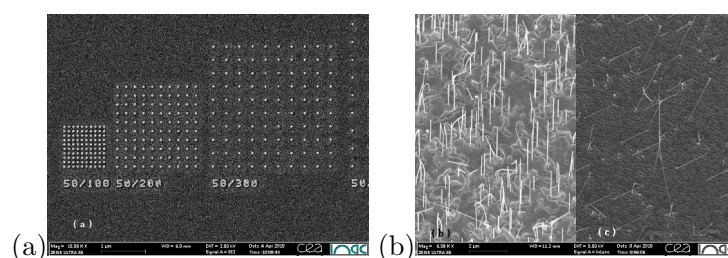


Figure 1: (a): SEM image of the lithographically designed gold pattern. (b): SEM image of InAs NWs grown on InAs (111) substrate (left) and on InAs (100) substrate (right).

Size and spin-state dependences of the lattice dynamics in spin crossover nanoparticles through NIS

Mirko Mikolasek^{a,*}, G. Félix^c, H. Peng^b, W. Nicolazzi^b, A. Chumakov^a, L. Salmon^b, G. Molnár^b and A. Bousseksou^b

- a. ESRF-The European Synchrotron, CS40220, 38043 Grenoble Cedex 9, France
- b. LCC-CNRS and Université de Toulouse (UPS, INP), 205 route de Narbonne, 31077 Toulouse, France
- c. ICG, Université Montpellier 2, place Eugène Bataillon, 34095 Montpellier, France

* mirko.mikolasek@esrf.fr

In recent years, investigation of nano-objects displaying spin transition has attracted many attention. Indeed, the phase stability and the transformation kinetics are in general highly size-dependent. In a large number of spin crossover (SCO) compounds, size effects lead to a loss of the hysteresis properties, a shift of the transition temperature or the occurrence of an incomplete transition. At the opposite, in other cases, the size effects are small and these compounds display a hysteresis at the extreme size reduction [1].

Since the bistability depends mainly on the strength of the elastic interactions, we have investigated the lattice dynamics of SCO nanoparticles and especially the acoustic phonon modes by elastic and inelastic (ESRF) Mössbauer spectroscopy in order to deduce vibrational and elastic constants for different particle sizes [2-4]. A stiffening of the particles was detected at the extreme size reduction limit (below ca. 10 nm). This presentation introduces the spin transition at the nanoscale and presents recent findings about the size-dependence of lattice dynamics in spin-crossover coordination networks and the consequences on the spin transition.

- [1] A. Bousseksou et al, Chem. Soc. Rev. 40, 3313 (2011); H. J. Shepherd Eur. J. Inorg. Chem. 653 (2013); M. Mikolasek et al, New. J. Chem. 38, 1834 (2014)
- [2] G. Félix et al., Phys. Rev. Lett. 110, 135 (2013)
- [3] G. Félix et al., Phys. Rev. B 91, 024422 (2015)
- [4] M. Mikolasek et al., Phys. Rev. B. 96, 035426, 2017

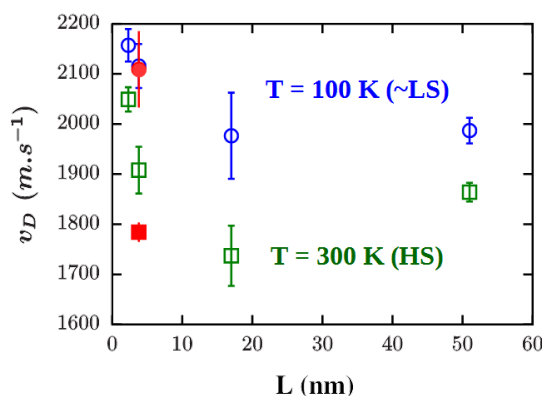


Figure 1: Debye sound velocity as a function of the particle size for the high spin (squares) and low spin (circles) states for AOT matrix (green and blue) and Chitosan matrix (filled red symbols).

Ab initio multiscale thermal transport simulations with almaBTE

Natalio Mingo^{a*}, Bjorn Vermeersch^a, J. Carrete^b, A. van Roekeghem^a, A. Katre^a,
T. Wang^e, G. Madsen^b, A. Nejim^c, C. Miccoli^d, V. Cinnera^d

- a. CEA-Grenoble, France
- b. TU Wien, Austria
- c. Silvaco Europe, UK
- d. ST microelectronics, Catania, Italy
- e. Ruhr University Bochum, Germany

* natalio.mingo@cea.fr

Understanding and tailoring thermal transport is an urgent issue for many cutting edge technologies where heat poses a bottleneck to further progress, such as power electronics, nanoelectronics, interconnects, thermoelectric energy conversion, phase change memories, turbine coatings, and many other disciplines. Predictive ab initio simulation of thermal transport in these systems, from the atomic to the device level, can help understand and solve the current heat challenges.

During the past three years we have built almaBTE, an open source code capable of solving the space and time dependent Boltzmann transport equation for phonons in nano and microstructured systems, fully from first principles[1]. I will illustrate almaBTE's use in several materials and devices of technological relevance, including the role of point defects in SiC [2] and GaN [3] thermal conduction, the thermal conductivity of InAs/GaAs [4] and SiGe superlattices[5], and the design of finFETs, as well as LED and HEMT substrates [6].

Work supported by the EC via H2020 project ALMA.

[1] J. Carrete *et al.*, "almaBTE : A solver of the space–time dependent Boltzmann transport equation for phonons in structured materials," *Comput. Phys. Commun.*, vol. 220, pp. 351–362, Nov. 2017.

[2] A. Katre, J. Carrete, B. Dongre, G. K. H. Madsen, and N. Mingo, "Exceptionally Strong Phonon Scattering by B Substitution in Cubic SiC," *Phys. Rev. Lett.*, vol. 119, no. 7, p. 75902, Aug. 2017.

[3] A. Katre, J. Carrete, T. Wang, G. K. H. Madsen, and N. Mingo, "Phonon transport unveils the prevalent point defects in GaN," *ArXiv171208124 Cond-Mat*, Dec. 2017.

[4] J. Carrete *et al.*, "Predictive Design and Experimental Realization of InAs/GaAs Superlattices with Tailored Thermal Conductivity," *J. Phys. Chem. C*, vol. 122, no. 7, pp. 4054–4062, Feb. 2018.

[5] P. Chen *et al.*, "Evolution of thermal, structural, and optical properties of SiGe superlattices upon thermal treatment," *Phys. Status Solidi A*, vol. 213, no. 3, pp. 533–540, Mar. 2016.

[6] B. Vermeersch *et al.*, to be published.

Spin textures induced by quenched disorder in a reentrant spin glass: vortices versus frustrated skyrmions

I. Mirebeau^{a*}, N. Martin^a, M. Deutsch^b, L. J. Bannenberg^c, C. Pappas^c,
G. Chaboussant^a, R. Cubitt^d, C. Decorse^e, A. O. Leonov^{f,9}

- a. Laboratoire Léon Brillouin, Univ. Paris-Saclay, CEA Saclay 91191 Gif-sur-Yvette, France
- b. Université de Lorraine, CNRS, CRM2, Nancy, France
- c. Faculty of Applied Science, Delft University of Technology, Delft, the Netherlands
- d. Institut Laue Langevin, BP156, F-38042 Grenoble France
- e. ICMMO, Université Paris-Sud, Univ. Paris-Saclay, F-91405 Orsay, France
- f. Chiral Research Center, Hiroshima University, Higashi-Hiroshima, 739-8526, Japan
- g. Department of Chemistry, Hiroshima University Kagamiyama, Higashi Hiroshima, Japan

* isabelle.mirebeau@cea.fr

Disorder plays a central role in the advent of the most spectacular quantum phenomena observed in condensed matter. Reentrant spin glasses (RSG's) are nice playground to study the influence of disorder on frustrated ferromagnets, and see how it affects topological defects. RSG's develop vortex-like textures under magnetic field [1,2], which we investigate in comparison with the frustrated skyrmions predicted by theory [3,4].

Our recent study of a $\text{Ni}_{1-x}\text{Mn}_x$ single crystal by small angle neutron clarifies their internal structure and shows that these textures are randomly distributed. Using two magnetic field geometries, we found that transverse spin components rotate over length scales of 3-15 nm, decreasing as field increases from 0 up to 8 T according to a scaling law [5].

Monte-Carlo simulations reveal that the internal structure of the vortices is strongly distorted and differs from that assumed for frustrated skyrmions. The pattern of topological charge density depends on the bond distribution. The vortices keep an anisotropic shape on a 3 dimensional lattice, recalling "croutons" in a "ferromagnetic soup". Their size and number can be tuned *independently* by the magnetic field and concentration x (or heat treatment), respectively. This opens an original route to understand and control the influence of quenched disorder in systems hosting non trivial spin textures.

[1] M. Hennion *et al.*, Europhys. Lett. **2**, 393, (1986); [2] S. Lequien *et al.*, Phys. Rev. B **35**, 7279, (1987); [3] T. Okubo *et al.*, Phys. Rev. Lett. **108**, 017206 (2006); [4] A. O. Leonov and M. Mostovoy, Nature Comm. **6**, 8725 (2015); [5] I. Mirebeau, N. Martin *et al.*, submitted (2018).

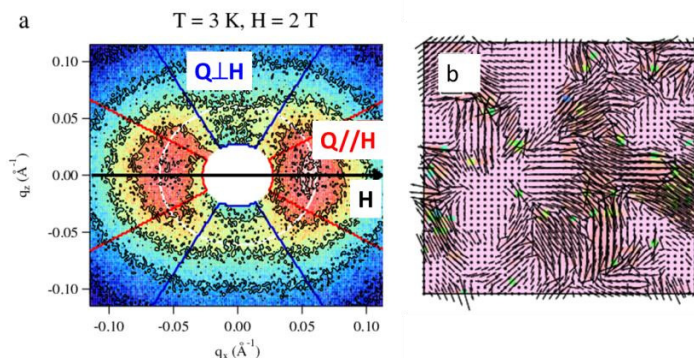


Figure 1 :

a) Scattering pattern of the vortex-like texture when the field H is perpendicular to the neutron beam.

b) Monte Carlo simulation of the quenched spin distribution.

Acoustical engineering for integrated optomechanical oscillators

Giuseppe Modica^a, Rui Zhu^a and R.Braive^{a,b}

- a. Centre de Nanosciences et de Nanotechnologies, CNRS, Univ. Paris-Sud, Université Paris-Saclay, C2N Marcoussis, 91460 Marcoussis, France
- b. Université Paris Diderot, Sorbonne Paris Cité, 75207 Paris Cedex 13, France

* giuseppe.modica@c2n.upsaclay.fr

A new generation of oscillators based on integrated optomechanical crystals could lead to high-spectral purity and low phase noise signals directly at the frequency of interest allowing an easy on-chip integration at μm scale (useful for potential on-board applications such as navigation and telecommunication systems, metrology or sensing). In the proposed system, the resonator part is made by a 2D photonic crystal membrane suspended over a silicon waveguide, sustaining optical modes around $1.55 \mu\text{m}$ and mechanical modes around a few GHz. The mechanical excitation and stabilization of such a system will be implemented thanks to Surface Acoustic Waves (SAWs) transducers allowing a full mechanical control of the oscillating structure. Moreover, implementation of phononic crystal waveguides will open a novel way to engineer the group velocity of the acoustical waves in order to achieve the desired delay for the stabilization of the oscillations. Simulation, fabrication and experimental work of resonant mechanical excitation in the GHz range will be discussed with particular emphasis on SAWs transducers and phononic crystal waveguides for acoustic delay engineering (Figure 1).

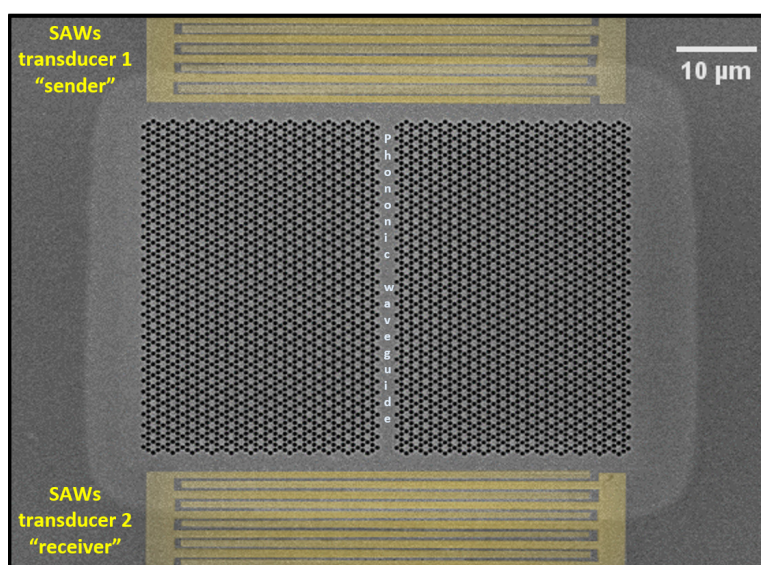


Figure 1: Suspended phononic waveguide, designed to have low group velocity, between two SAWs transducers for transmission measurements.

High pressure phase diagram of the Mott insulator GaV_4S_8

Julia Mokdad*, Georg Knebel, Christophe Marin, Daniel Braithwaite.

Univ. Grenoble Alpes and CEA, INAC-PHELIQS, F-38000 Grenoble, France

* julia.mokdad@cea.fr

The ternary chalcogenide Mott insulators with the deficient Spinel GaMo_4S_8 structure have recently sparked considerable interest owing to their proximity to a metal insulator transition that can be induced in various ways, for example by applying pressure or electric field[1]. They are also of interest for the different low temperature ground states that are present, like antiferromagnetic or ferromagnetic order, as well as more exotic states including a skyrmion lattice phase reported in GaV_4S_8 [2]. We report an experimental study using a.c. calorimetry in a diamond anvil cell to explore the effect of pressure on the low temperature phases of the system GaV_4S_8 .

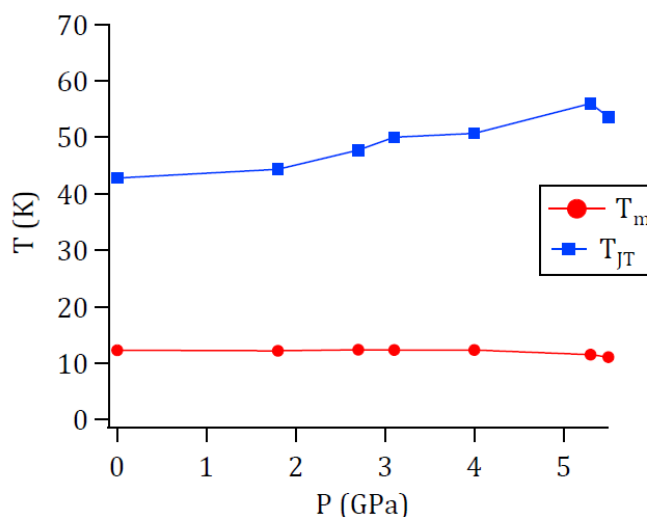


Figure 1: Pressure - temperature phase diagram of GaV_4S_8 . T_m is the ferromagnetic transition and T_{JT} the temperature of the Jahn-Teller transition from the high temperature cubic to the low temperature rhomboedric phase.

[1] C. Vaju, L. Cario, B. Corraze, E. Janod, V. Dubost, T. Cren, D. Roditchev, D. Braithwaite, and O. Chauvet, *Adv Mater* **20**, 2760 (2008).

[2] E. Ruff, S. Widmann, P. Lunkenheimer, V. Tsurkan, S. Bordacs, I. Kezsmarki, and A. Loidl, *Sci Adv* **1** (2015).

"Directional Solidification" in a Granular System

Pierre Molho

Univ. Grenoble Alpes, CNRS, Grenoble INP, Institut Néel, 38000 Grenoble, France

pierre.molho@neel.cnrs.fr

Granular matter, when shaken vertically in a box, is known to behave either like a solid or like a gas, depending on the acceleration imposed to the box. Varying this parameter leads to phase transitions [1].

A solid on a thermal gradient, its melting temperature being between the minimum and maximum temperatures, shows an interface between solid and liquid phases. Moving the solid toward lower temperature leads to "directional solidification", and interface instabilities depending on the motion speed [2].

We are studying the equivalent of "directional solidification" in a box containing a layer of steel beads, shaken vertically by a setup providing a gradient of acceleration along the box (fig. 1-a). The box is attached to a bar, one extremity of which is fixed, the other one being shaken via a loudspeaker. The gradient of acceleration along the box depends on the position of the box along the bar, and on the vibration amplitude and frequency imposed by the loudspeaker to the bar extremity, namely the "imposed acceleration", Γ_3 .

For a given value of amplitude and frequency, one observe a "solid phase" on the side of the box where the acceleration is low, a "gas" phase" where the acceleration is high, and an interface between the two phases (fig. 1-b). The interface position within the box depends on the imposed acceleration, and on the box position.

Applying a magnetic field, uniform on the scale of the box, parallel to the beads layer and perpendicular to the acceleration gradient, induces interactions between the beads, changing the interface energy, "solidifying" lines of beads otherwise in the gas phase.

Changing the magnetic field moves the interface, and allows evaluating the interface energy, relating the melting energy to the magnetic energy of interacting beads.

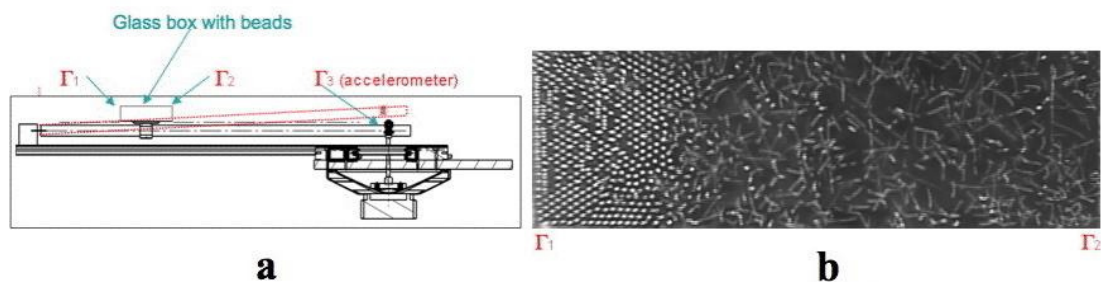


Figure 1: (a) Experimental setup to create an acceleration gradient. (b) Image of the box from above: "solid" phase (low acceleration), "gas" phase (higher acceleration), and interface between them.

[1] J. F. Olafsen and J. S. Urbach, "Clustering, Order, and Collapse in a Driven Granular Monolayer", *Phys. Rev. Lett.*, **Vol. 81**, 4369 (1998).

[2] D. J. Wollkind and L. A. Segel, "A Nonlinear Stability Analysis of the Freezing of a Dilute Binary Alloy", *Phil. Mag.* **268A**, 351-380 (1970).

Pulsing normal and collective counter-currents driven by the Hall voltage in a mesa junction of the sliding charge density wave under a quantized magnetic field

S. Brazovskii^{a*}, A.P. Orlov^b, A.A. Sinchenko^b, P. Monceau^c

^a LPTMS-CNRS, Université Paris-sud, Université Paris-Saclay, Orsay, France

^b Kotelnikov Institute of Radioengineering and Electronics of RAS, Moscow, Russia

^c Institut Neel, CNRS, Université Grenoble Alpes & LNCMI, Grenoble, France

* brazov@lptms.u-psud.fr

Remnant pockets of carriers left over after formation of a charge density wave (CDW) could be brought to a current-carrying state at quantized Landau Levels. The generated Hall voltage polarizes and puts to sliding the flexible CDW background. The screening from the CDW allows for a so strong redistribution of normal electrons density under the action of the Lorentz force alone, that an integer filling of the lowest Landau level might be reached at one edge at the expense of the full depletion at another edge of the Hall bar. With the Hall field exceeding the sliding threshold, the regime of exactly compensated collective and normal counter-currents develops in the open-circuit direction across the bar. The annihilation of the two currents proceeds via a regular sequence of phase slips which are the space-time vortices of the CDW phase around the enforced nodes of the CDW amplitude. The resulting spontaneous generation of coherent high \sim GHz frequency signals was detected by observations of multiple Shapiro steps. This picture results from experiments on micron-sized Hall bars in crystals of NbSe₃ prepared by means of focused ion beams [1]. The interpretation is confirmed and illustrated by a numerical solution of equations coupling normal and collective subsystems and the electrostatic potential [1,2].

[1] A.P. Orlov, A.A. Sinchenko, P.Monceau, S. Brazovskii and Yu.I. Latyshev.

NPJ Quantum Materials, **2**, 61 (2017).

[2] S. Brazovskii, Physica B, **460**, 236 (2015).

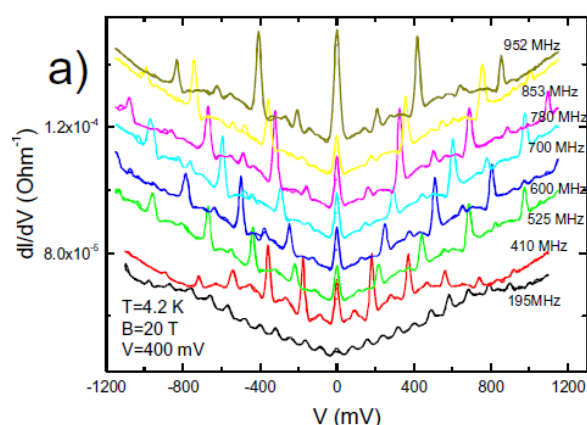


Figure 1 : Spontaneous generation of coherent high frequency periodic pulses measured here at the field 20T via Shapiro steps seen in the voltage dependence of the conductance.

Structural resolution of inorganic nanotubes with complex stoichiometry

Geoffrey Monet^{a,*}, Mohamed S. Amara^a, Stéphan Rouzière^a, Erwan Paineau^a
and Pascale Launois^a

a. Laboratoire de Physique des Solides, UMR CNRS 8502, Université Paris Sud, Université Paris Saclay, 91405 Orsay Cedex, France

* geoffrey.monet@u-psud.fr

Determination of the atomic structure of inorganic single-walled nanotubes with complex stoichiometry remains elusive due to the too many atomic coordinates to be fitted with respect to X-ray diffractograms inherently exhibiting rather broad features. Here we introduce a new approach which enables resolution of their structure [1]. It is based, first, on the use of helical symmetries allowing one to consider the smallest unit cell and then on semi-empirical energy minimization leading to a reduction of the number of structural parameters to be fitted.

We applied this method to recently synthesized methylated aluminosilicate and aluminogermanate imogolite nanotubes of nominal composition $(\text{OH})_3\text{Al}_2\text{O}_3\text{Si}(\text{Ge})\text{CH}_3$ [2]. Thanks to their chemical versatility, imogolite nanotubes (INT) are promising candidates for applications in molecular storage, recognition and separation [3]. Fit of wide-angle X-ray scattering (WAXS) diagrams of methylated INTs enabled us to determine their atomic structure. Unlike their (N,0) zigzag hydroxylated analog, methylated INTs roll up into a (N,N) armchair structure (Figure).

The transferability of the approach opens up for improved understanding of structure-property relationships of inorganic nanotubes, to the benefit of fundamental and applicative research in these systems.

The authors acknowledge Erik Elkaim from beamline CRISTAL (synchrotron SOLEIL), where WAXS diagrams were recorded.

[1] G. Monet et al., submitted (2018).

[2] I. Bottero et al., Synthesis and Characterization of Hybrid Organic/Inorganic Nanotubes of the Imogolite Type and Their Behaviour Towards Methane Adsorption, *Phys Chem Chem Phys* **13**, 744–750 (2011).

[3] D.-Y. Kang et al., Direct Synthesis of Single-Walled Aminoaluminosilicate Nanotubes with Enhanced Molecular Adsorption Selectivity, *Nat Commun* **5**, 3342 (2014).

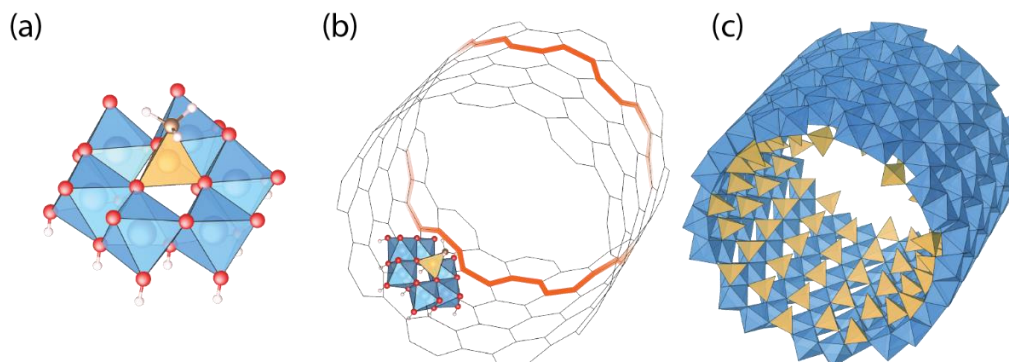


Figure: (a) An octahedral gibbsite-like layer (in blue) with isolated $(\text{Si}(\text{Ge})\text{O}_3)\text{CH}_3$ tetrahedron units (in yellow). (b) and (c) The methylated INT structure. Its armchair character is highlighted by the thick orange line in (b).

Energy conversion in a hybrid optomechanical system: Laser-like behavior and cooling

Juliette Monsel^{a*}, Cyril Elouard^b, Maxime Richard^a and Alexia Auffèves^a

a. Univ. Grenoble Alpes, CNRS, Grenoble INP, Institut Néel, 38000 Grenoble, France

b. Department of Physics and Astronomy and Center for Coherence and Quantum Optics, University of Rochester, Rochester, New York 14627, USA

* juliette.monsel@neel.cnrs.fr

A hybrid optomechanical system consists of a two-level system parametrically coupled to a nano-mechanical oscillator (Fig. 1a). Because of this coupling, the transition frequency ω of the two-level system depends on the position of the mechanical oscillator. The ultra-strong coupling regime $g_m \gtrsim \Omega$ is now experimentally reachable [1,2,3] which opens new perspectives, including energy conversion. g_m is the optomechanical coupling strength and Ω the mechanical frequency.

Here we propose to convert electromagnetic energy into mechanical energy by shining a detuned laser on the two-level system. As a result of the optomechanical coupling, the two-level system enters in and out of resonance with the laser. In the case of a blue detuning (Fig. 1b), at each resonance, the two-level system can absorb a high-energy photon and, later, spontaneously emit a photon with a lower energy. The energy difference is provided to the mechanical oscillator in the form of work. We demonstrate that, with this mechanism, a coherent phonon state can be built upon thermal noise and that the system exhibits a laser-like behavior. On the other hand, in the case of a red-detuning, the two-level system absorbs low-energy photons and emits higher-energy ones, resulting in a cooling down of the mechanical oscillator.

- [1] I. Yeo *et. al.*, Strain-Mediated Coupling in a Quantum Dot–mechanical Oscillator Hybrid System, *Nat. Nanotech.* **9**, 106–110 (2014)
- [2] O. Arcizet *et. al.*, A Single Nitrogen-Vacancy Defect Coupled to a Nanomechanical Oscillator, *Nat. Phys.* **7**, 879 (2011)
- [3] J.-M. Pirkkalainen *et. al.*, Hybrid Circuit Cavity Quantum Electrodynamics with a Micromechanical Resonator, *Nature* **494**, 211-215 (2013)

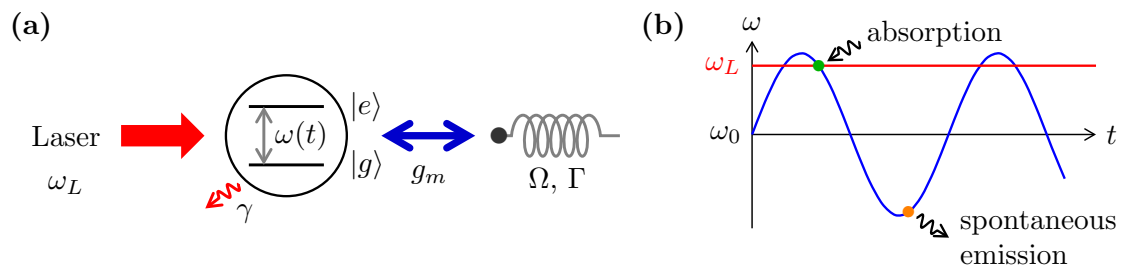


Figure 1: **(a)** Hybrid optomechanical system: a two-level system parametrically coupled to a mechanical oscillator. **(b)** Principle of the energy conversion: frequency of the transition of the mechanical oscillator as a function of time.

Development and Characterization of $\text{Ni}_x\text{Pt}_{1-x}$ Nanoalloy; Analysis of Carbon Solubility Effects in Catalysed Carbon Nanotubes Growth

Cora MOREIRA DA SILVA^{a*}, Frederic FOSSARD^a, Ileana FLOREA^b, Armelle GIRARD^{a,c}, Costel-Sorin COJOCARU^b, Vincent HUC^d et Annick LOISEAU^a

- a. LEM, Laboratoire d'Etude des Microstructures - ONERA, 92320 Châtillon, France
- b. LPICM, Laboratoire de Physique des Interfaces et des Couches Minces, École Polytechnique/CNRS, 91128 Palaiseau, France
- c. UVSQ, Université de Versailles Saint Quentin, 78000 Versailles, France
- d. ICMMO, Institut de Chimie Moléculaire et des Matériaux d'Orsay, CNRS, Université Paris-Saclay, 91405 Orsay, France

* cora.moreira_da_silva@onera.fr

Nowadays, Chemical Vapor Deposition (CVD) on catalytic nanoparticles (NPs) is the most studied and promising method for single wall carbon nanotubes (SWCNT) synthesis. However, this process suffers from a lack of control of tube diameter and chirality, which directly influence tube properties (conducting/semiconducting)[1]. This non-selectivity is due to an insufficient knowledge of the parameters controlling the growth mechanisms. One of the research path focuses on the catalytic NPs role, and notably its carbon solubility. In order to inspect deeper the role of this parameter, we have studied the influence of $\text{Ni}_x\text{Pt}_{1-x}$ NP on the SWNT growth. Nickel is indeed known to be an efficient catalyst for the CNTs growth thanks to its ability to solubilize carbon, unlike platinum [2]. We used the colloidal route to synthesize five compositions of $\text{Ni}_x\text{Pt}_{1-x}$ NPs (pure Ni, Ni_3Pt , NiPt , NiPt_3 and pure Pt) and obtain monodisperse alloyed NPs, with size and shape control and homogeneous compositions. Structure and chemical composition of the NPs are fully characterized before and after NTCs growth (Transmission Electron Microscopy, Energy-Dispersive X-ray spectroscopy, Electron diffraction). Further, we used the LPICM FENIX platform, which is able to reproduce CVD environment growth coupled with surface analysis techniques follow-up (XPS, AES, LEED ...), to detect any NPs chemical changes during CNTs growth. Finally, we performed *in-situ* CNTs growth in an FEI Titan ETEM to study the interplay between chemical composition of the catalytic NPs and SWNT growth mode.

[1] V. Jourdain and C. Bichara, Carbon **58**, 2-39 (2013)

[2] A. Castan, S. Forel, L. Catala, I. Florea, F. Fossard, F. Bouanis, A. Andrieux-Ledier, S. Mazerat, T. Mallah, V. Huc, A. Loiseau, C.S. Cojocaru, Carbon **123**, 583-592 (2017)

From collective stubbornness to collective oscillations in colloidal flocks: Response of active liquids to external fields

Alexandre Morin^{a*}, et Denis Bartolo^a

a. Univ Lyon, ENS de Lyon, Univ Claude Bernard Lyon 1, CNRS, Laboratoire de Physique, F-69342 Lyon, France

* alexandre.morin@ens-lyon.fr

We investigate the response of colloidal flocks to external fields. We first show that individual colloidal rollers align with external flows as would a classical spin with magnetic fields. Assembling polar active liquids from colloidal rollers, we experimentally demonstrate their hysteretic response: confined colloidal flocks can proceed against external flows. We theoretically explain this collective robustness, using an active hydrodynamic description, and show how orientational elasticity and confinement protect the direction of collective motion. Finally, we exploit the intrinsic bistability of confined active flows to devise self-sustained microfluidic oscillators.

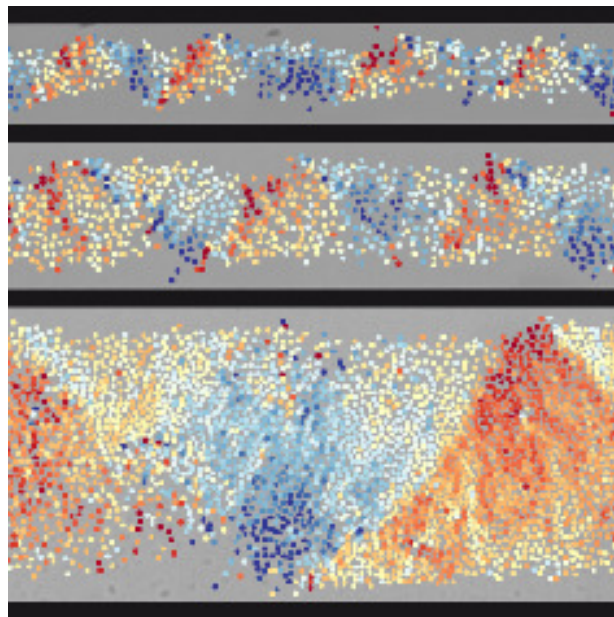


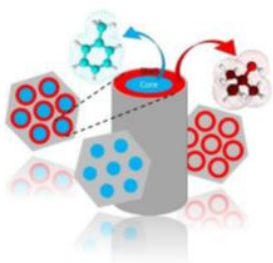
Figure 1 : The flows of confined colloidal flocks buckle to resist opposing external fields.

Core-shell ordered phase of binary solvents confined in mesopores

Denis Morineau^a, Ronan Lefort^a, Alain Moréac^a, Ramona Mhanna^{a,b}, Sujeet Dutta^a, Bernhard Frick^b, Christiane Alba-Simionesco^c, Laurence Noirez^c, Florence Porcher^c

- a. Institute of Physics of Rennes, CNRS-University of Rennes 1, France
- b. Institute Laue-Langevin, Grenoble, France
- c. Laboratoire Léon Brillouin, CEA-CNRS, Gif-Sur-Yvette, France

* denis.morineau@univ-rennes1.fr



The properties of liquids confined in nanometric cavities can be very different from their bulk counterparts, which raises exciting new questions for basic condensed matter physics and nanomaterials science. Among many confinement effects, we focused on the formation of new liquid structures of binary solvents confined in mesoporous materials.

We will report on a peculiar state observed for prototypical fully miscible solvents when they are confined within nanochannels [1,2]. It corresponds to a well-ordered concentric arrangement of two co-existing liquid regions with typical sizes that can be tuned as a function of the composition and the pore dimension [3].

The liquids forming the core and the shell of this nanostructure never crystallize down to cryogenic temperatures. They exhibit two distinct molecular dynamics, which leads to separate glass transitions [4]. This core-shell phenomenon is probably more general. We believe it is related to interfacial interactions that have been quantified by sorption experiments [5]: a situation which is awaited for a variety of other solvents in nanopores

[1] *Press release of the American Institute of Physics*, January 10th (2017): <https://publishing.aip.org/publishing/journal-highlights/zeroing-true-nature-fluids-within-nanocapillaries>

[2] [Micro-Phase Separation of Binary Liquids Confined in Cylindrical Pores](#) A. R. Abdel Hamid, R. Mhanna, R. Lefort, A. Ghoufi, C. Alba-Simionesco, B. Frick and D. Morineau, *J. Phys. Chem. C*, **120**, 9245 (2016).

[3] [More room for microphase separation: An extended study on binary liquids confined in SBA-15 cylindrical pores](#), R. Mhanna, A. R. Abdel Hamid, S. Dutta, R. Lefort, L. Noirez, B. Frick and D. Morineau, *J. Chem. Phys.*, **146** 024501 (2017).

[4] [Multiple Glass Transitions of Microphase Separated Binary Liquids Confined in MCM-41](#), A. R. Abdel Hamid, R. Mhanna, P. Catrou, Y. Bulteau, R. Lefort and D. Morineau, *J. Phys. Chem. C*, **120**, 11049 (2016).

[5] [Thermodynamics of binary gas adsorption in nanopores](#), S. Dutta, R. Lefort, D. Morineau, R. Mhanna, O. Merdrignac-Conanec, Arnaud Saint-Jalmes and T. Leclercq, *Phys. Chem. Chem. Phys.*, **18**, 24361 (2016).

Coherent displacement of individual electron spins in a two-dimensional array of tunnel coupled quantum dots

Pierre A. Mortemousque,^{a*} Hanno Flentje,^a Emmanuel Chanrion,^a
Arne Ludwig,^b Andreas D. Wieck,^b
Matias Urdampilleta,^a Christopher Bauerle,^a and Tristan Meunier^a

- a. Univ. Grenoble Alpes, CNRS, Grenoble INP, Institut Neel, 38000 Grenoble, France
- b. Lehrstuhl für Angewandte Festkörperphysik, Ruhr-Universität Bochum, Universitätsstraße 150, D-44780 Bochum, Germany

* pierre-andre.mortemousque@neel.cnrs.fr

Controlling nanocircuits at the single electron spin level in quantum dot arrays is at the heart of any scalable spin-based quantum information platform. The cumulated efforts to finely control individual electron spins in linear arrays of tunnel coupled quantum dots have permitted the recent coherent control of multi-electron spins and the realization of quantum simulators. However, the two-dimensional scaling of such control is a crucial requirement for simulating complex quantum matter and for efficient quantum information processing, and remains up to now a challenge.

Here we demonstrate such two-dimensional coherent control using individual electron spins in arrays up to 9 tunnel-coupled lateral quantum dots. The demonstrated charge control with one and two electrons loaded in the dot arrays permits to explore coherent spin control and displacement. To realize this, two electrons are prepared in the coherent singlet state, and separately displaced within the quantum dot arrays. We show that the electron spin coherence can be maintained over 5 micrometers and 80 ns, and that the motion of the electrons is not detrimental for their spin coherence properties. Actually, the fast control of the potential landscape induces moving quantum dots, in which the electron spins, through a motional narrowing process, are effectively decoupled from the substrate nuclear spins. This work demonstrates key quantum functionalities, crucial for using two-dimensional quantum dot arrays for quantum simulation and computation.

References:

H. Flentje, P.-A. Mortemousque, R. Thalineau, A. Ludwig, A. D. Wieck, C. Bäuerle, T. Meunier, *Coherent long-distance displacement of individual electron spins*, Nat. Comm. **8**, 501 (2017).

P.-A. Mortemousque, H. Flentje, E. Chanrion, A. Ludwig, A. D. Wieck, M. Urdampilleta, C. Bäuerle, T. Meunier, *Coherent displacement of individual electron spins in a two-dimensional array of tunnel-coupled quantum dots*, in preparation.

Simulating artificial graphene with superconducting resonators

Alexis Morvan^{a*}, Mathieu Féchant^a, Gianluca Aiello^a, Julien Gabelli^a, Jérôme Estève^a

a. Laboratoire de Physique des Solides, CNRS, Univ. Paris-Sud, Université Paris-Saclay, 91405 Orsay Cedex, France

* alexis.morvan@u-psud.fr

We present experimental studies of two artificial honeycomb lattices made of superconducting resonators. We image the spatial distributions of the modes using a low temperature laser scanning microscopy based on the variation of the microwave transmission of the lattice (Fig. 1.a and 1.b). This variation is induced by the absorbed laser power by a site of the lattice and is proportional to the weight of the probed mode on this site. In addition to mode labeling, mode imaging enables the reconstruction of the dispersion relation by Fourier transform. We were able with this technique to investigate edges-states modes of graphene (Fig. 1.b, bottom right image) and domains walls modes at the interface between two gapped graphene (see Fig 1.d).

We also have developed an *ab initio* method to calculate lattice spectrum by simulating a few resonators on electromagnetic software. This provides an effective tight-binding Hamiltonian that is in good agreement with experimental data (Fig. 1.c for the graphene).

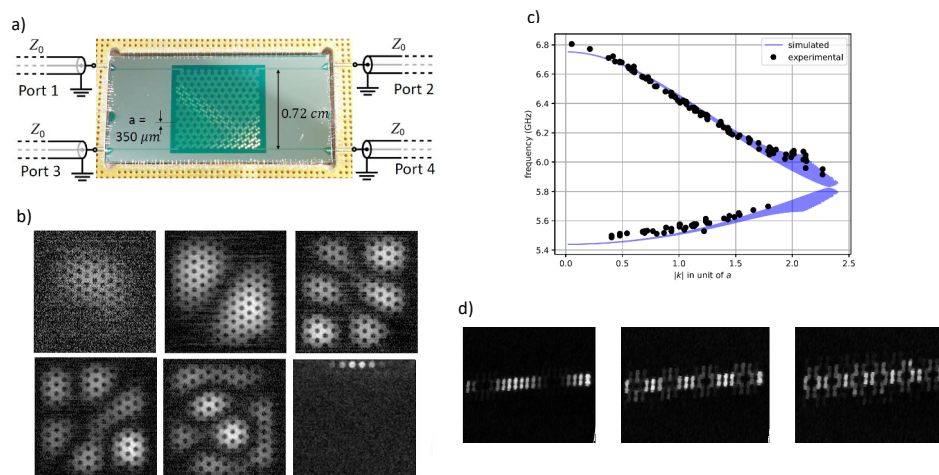


Figure 1. a) Image of the artificial graphene sample. b) Spatial distribution of a few modes. The one at the bottom right is one of the observed edge state. c) Comparison of experimental results and simulation for the dispersion relation of the lattice. d) Wall domains modes at the interface of two gapped graphene.

The fate on an ionic liquid confined at the nanoscale

Stefano Mossa^{a*}

a. Univ. Grenoble Alpes, CEA, CNRS, INAC-SYMMES, 38000 Grenoble, France

* stefano.mossa@cea.fr

Ionic liquids are mixtures of cations and anions which stay liquid at room conditions, a feature making them potentially ideal materials for energy storage and conversion technologies. Here they are often employed in contact with solid interfaces, or even constrained in pores whose size can be less than a nanometer. In such extreme environments the properties of matter are drastically modified compared to the bulk counterparts. In this context one can address a primary issue: Does the phase nature of an ionic liquid change when it is confined in pores of nanometric size? The simplicity of this question is misleading. Experiments which probe ionic liquids at the nanoscale, in fact, are extremely difficult and sometimes in mutual contradiction, failing so far to provide a generally accepted answer.

I have tackled this issue systematically by extensive Molecular Dynamics simulation of a model ionic liquid confined in a slit pore[1]. In this talk I will discuss how, by appropriately tuning size and temperature of the latter, I revealed unexplored phase modifications. For instance, following an increase of the confinement, I observed the formation of ionic liquid-crystal structures, which unexpectedly transform into plain stable liquid states and subsequently freeze in new crystal phases. I will also show how these changes reflect on the relative organization of the ions and on their dynamical state. I will finally build on the MD results to provide a consistent general picture of these systems, by also involving in the discussion disparate very recent inspiring work.

[1] Stefano Mossa, Re-entrant phase transitions and dynamics of a nanoconfined ionic liquid, pre-print arXiv:1803.08888

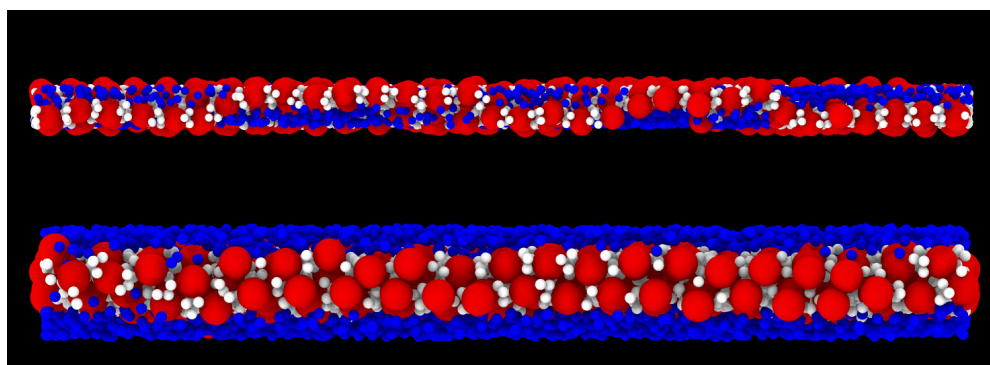


Figure 1: Side views of the considered ionic liquid system adsorbed in the pore in different conditions of confinement. Red beads identify the anions ($[PF_6]$), while white and blue correspond to polar and apolar parts of the cation ($[C_{10}mim]$), respectively.

Un ordre chimique subtil dans les nanoalliages

Alexis Front^{a*}, Christine Mottet^a, Guy Tréglia^a et Bernard Legrand^b

a. CINaM, CNRS / Aix-Marseille Université, Campus de Luminy, Marseille, France.

b. DEN-SRMP, CEA, Université Paris-Saclay, F91191 Gif-sur-Yvette, France.

* mottet@cinam.univ-mrs.fr << corresponding author >>

Les nanoalliages constituent un terrain de jeu attractif pour les théoriciens, comme pour les expérimentateurs, puisqu'ils présentent un grand nombre de degrés de liberté au niveau de leur structure, morphologie, et ordre chimique [1], auxquels s'ajoutent des questions thermodynamiques [2] et cinétiques liées à leur taille finie.

Nous présentons ici une étude comparée de deux systèmes à tendance à l'ordre (Co-Pt et Ag-Pt) dans lesquels la phase ordonnée à l'équiconcentration présente une alternance de plans purs dans deux directions différentes (voir figure): la direction (100) pour la phase $L1_0$ et la direction (111) pour la phase $L1_1$. Alors que les nanoalliages de Co-Pt ont donné lieu à de nombreuses études théoriques et expérimentales [3], ceux de Pt-Ag n'ont été élaborés et caractérisés que très récemment dans le cadre d'une thèse à Orléans [4] et la phase $L1_1$ a pu être observée dans les nanoparticules de quelques nm.

Les phases d'équilibre sur l'ensemble des compositions de nanoalliages de différentes tailles, structures et morphologies sont déterminées par des simulations Monte Carlo et un modèle énergétique semi-empirique. Une différence majeure entre les deux systèmes, outre les différents types de phases ordonnées $L1_1$ versus $L1_0$, est que Pt-Ag présente une forte tendance à la ségrégation de surface, absente dans Co-Pt.

- [1] R. Ferrando, Volume 10 of the series Frontiers of Nanoscience, Elsevier (2016)
- [2] F. Calvo, Phys. Chem. Chem. Phys. **17**, 27922 (2015)
- [3] P. Andréazza et al., Surf. Sci. Rep. **70**, 188 (2015)
- [4] J. Pirart, thèse en préparation.

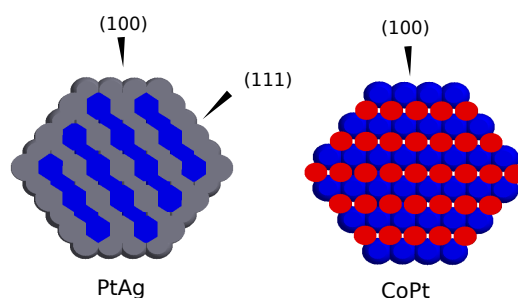


Figure 1: Représentation schématique des phases ordonnées $L1_1$ (Pt-Ag) et $L1_0$ (Co-Pt) avec une alternance de plans purs dans les directions (111) et (100) respectivement.

Molecular streaming and voltage gated response in Angström scale slits

T. Mouterde^a, A. Keerthi^{b,c}, A. R. Poggioli^a, S. A. Dar^{b,c}, A. Siria^a, A. K. Geim^{b,c},
R. Boya^{b,c}, L. Bocquet^{a,*}.

- a. Laboratoire de Physique Statistique – PSL, École Normale Supérieure, UMR 8550 du CNRS, 24 rue Lhomond, 75005 Paris, France
- b. School of Physics and Astronomy, University of Manchester, Manchester M13 9PL, United-Kingdom
- c. National Graphene Institute, University of Manchester, Manchester M13 9PL, United-Kingdom.

* corresponding authors: radha.boya@manchester.ac.uk, lyderic.bocquet@ens.fr

The field of nanofluidics has shown a great development over the past decade thanks to key instrumental advances, leading to a number of exotic transport behaviours for fluids and ions in extreme confinement [1-2]. Recently, van der Waals assembly of 2D materials allowed the fabrication of artificial angstrom scale channels that can be used for molecular confinement. This ultimate size reduction indeed revealed original behaviours for both mass [3] and ionic [4] transport. In this work, we report ionic molecular streaming induced by coupled pressure and voltage forcing. Under pressure and voltage forcing, we observe a new hydro-electric coupling leading to a gating-like response of the molecular streaming. This effect, observed with both boron-nitride and graphite slits, is found to be material dependent and related to the salt concentration in the channel. A potential difference of a fraction of a volt results in a mobility up to 100 times larger than the potassium mobility. This corresponds to an equivalent zeta potential three orders of magnitude higher than the gating voltage (higher than 100 V). Our results suggest that molecular scale confinement may lead to new flow control mechanisms.

1. Siria, A. *et al.* Giant osmotic energy conversion measured in a single transmembrane boron nitride nanotube. *Nature* **494**, 455–458 (2013).
3. Secchi, E. *et al.* Massive radius-dependent flow slippage in single carbon nanotubes. *Nature*, **537**, 210–213, (2016).
4. Radha, B. *et al.* Molecular transport through capillaries made with atomic-scale precision. *Nature*, **538**, 222–225, (2016).
5. Esfandiar, A. *et al.* Size effect In Ion transport through angstrom-scale slits. *Science*, **358**, 511–513 (2017).

How to deal with a reduced palette of elements: materials, methods and architectures.

Materials scientists face a challenge in designing new or improved materials and devices since some of the building blocks can no longer be freely used. These are the so called critical elements, which are elements which should be avoided or minimized in reason of their toxicity, limited availability, uneven spread, and economic impact.

The most conventional approach to reduce the utilization of critical elements or materials is by the design of alternative materials in which these elements are not present, or in a much lower amount. But it is also possible to make an impact on the amount of critical materials used by designing improved alternative deposition or fabrication methods and device architectures.

In my talk I will present an overview of the activities carried out at LMGP on new materials, methods and device architectures that are currently being developed and that can contribute to a lower use of critical materials. I will then focus on my past and current research on Cu based materials. Cu is an attractive element since it is abundant and non-toxic, and it has a high potential in optoelectronic devices. Several examples of deposition of Cu based oxides by atmospheric chemical approaches will be given and the application to optoelectronic devices with improved architectures will be illustrated.

Direct imaging of electrical fields using a scanning single electron transistor

Jorge P. Nacenta Mendivil^{a*}, Roman B. G. Kramer^a, et Laurent Lévy^a

a. Univ. Grenoble Alpes, CNRS, Grenoble INP, Institut Néel, 38000 Grenoble, France

* jorge.nacenta@neel.cnrs.fr

We have developed a scanning microscope which uses a single electron transistor (SET) as a local probe of surface charges and electric fields. It works at very low temperatures (50 mK) and high magnetic fields (18 T). The SET consists of a small metallic island connected to source and drain electrodes through two tunnel junctions. The current through the SET varies periodically with respect to the electrostatic potential of the island coming from the local electric field. In the low temperature regime ($T \ll 5$ K) small electric field variations lead to strong current changes which makes the device a highly sensitive charge detector. A side gate close to the island is used to tune the operating point of the transistor through conducting and blocked regions (Coulomb diamonds) as shown in figure 1(a). The SET is engineered close to a sharp corner of a silicon wafer in order to approach it to a few nanometer from the sample surface. When the SET scans above the surface, the island's electrical potential is governed by local electrical fields making it possible to map the sample's surface electrical properties.

Here we use the side gate in a feedback loop to keep the current constant during the scanning. Monitoring the side gate voltage enable us to map directly the local electric field. We demonstrate this new method on an interdigitated array of nanometer scale electrodes shown in figure 1(b). Figure 1(c) shows the electrical field of the electrodes measured in a distance of about $1 \mu\text{m}$ above the surface. Besides the precise mapping of electrical fields the SET can be used to measure the compressibility of electronic states making it a unique tool to investigate localized and delocalized states in quantum Hall systems e.g. in GaAs [1], graphene [2] and topological insulators.

-This project has been supported by the Nanoscience Foundation and LANEF, Grenoble.

[1] M. J. Yoo et al. Science **276** (1997) 579.

[2] B. E. Feldman, B. Krauss, J. H. Smet, A. Yacoby Science **337** (2012) 1196.

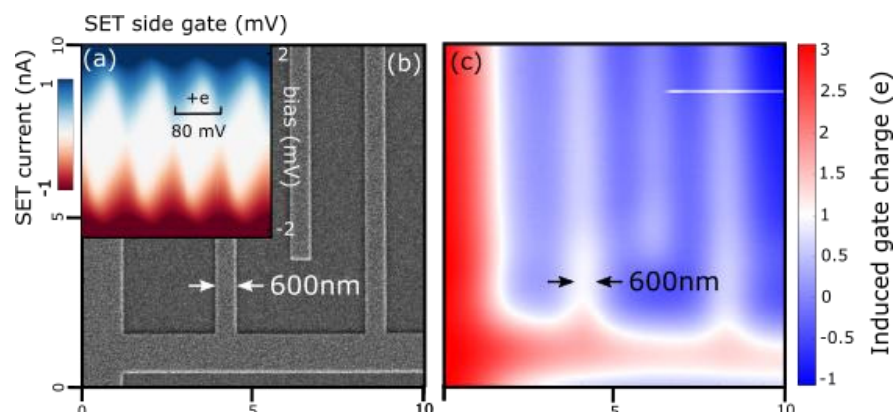


Figure 1 : (a) Coulomb diamonds of the SET measured at 50 mK (b) $10 \times 10 \mu\text{m}$ SEM image of the interdigitated array of 600nm large Al electrodes on a Si-SiO₂ substrate. (c) $10 \times 10 \mu\text{m}$ SET image of the same region showing the electrostatic potential.

Dense pedestrian crowds at bottlenecks: How do the pedestrians' behaviours kick in ?

Alexandre NICOLAS^{a*}

a. LPTMS, CNRS et Univ. Paris-Sud, Univ. Paris-Saclay, F-91405 Orsay, France
 * alexandre.nicolas@polytechnique.edu

Public facilities (railway stations, stadiums, etc.) should be designed so as to allow optimal pedestrian flows and quick evacuation in the event of an emergency. While these issues have traditionally been left to empirical approaches, agent-based models have emerged in the last two decades to describe pedestrian dynamics. One of the most widely used among these models, the social force model, considers pedestrians as self-propelled particles subjected to attractive and repulsive « social » interactions, thus making them amenable to a physical approach.

In this talk, I will first wonder if there exists a *fundamental* difference between the dynamics of a pedestrian and that of dry active particles. Leaving aside the complexity of pedestrian motion, we will see that the reaction time may play a key role in such a distinction.

Then, we will study the impact of the *behaviours* (which are specific to pedestrians) on the dynamics of a dense crowd in a particular situation : a bottleneck flow through a narrow door. To this end, we performed controlled experiments in which heterogeneous behaviours were prescribed to the participants [1]. It turns out that the main flow properties were controlled, not by the detail of the behaviours, but by the pedestrian density in front of the door, at least as long as crowd pressure was low. Paying closer attention to the microscopic flow dynamics, we noticed the existence of robust statistical patterns, such as the alternation between short and long time intervals between successive escapes. These statistical features can be rationalised by generic minimal models [2] and thus appear not to be specific to pedestrians.

[1] Nicolas, A., Bouzat, S., & Kuperman, M. N. (2017). Pedestrian flows through a narrow doorway: Effect of individual behaviours on the global flow and microscopic dynamics. *Transportation Research Part B: Methodological*, 99, 30-43.

[2] Nicolas, A., & Touloupas, I. (2018). Origin of the correlations between exit times in pedestrian flows through a bottleneck. *Journal of Statistical Mechanics: Theory and Experiment*, 2018(1), 013402.

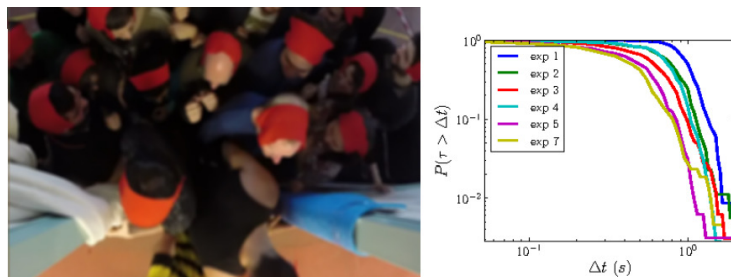


Figure 1 : (Left) Snapshot of an evacuation experiment through a narrow door. (Right) Survival functions of the time intervals Δt between successive pedestrian escapes for different behavioural prescriptions (to be described in the talk).

Observation and simulation of Si and Ge nanowires in the NanoMAX transmission electron microscope

E. Ngo*, W. Wang, M. Foldyna, P. Roca i Cabarrocas and J.-L. Maurice

Laboratoire de Physique des Interfaces et Couches Minces, CNRS, Ecole polytechnique, Université Paris-Saclay, 91128 Palaiseau, France

* eric.ngo@polytechnique.edu

The diamond-hexagonal phase (polytype 2H) does not appear in the phase diagrams of silicon or germanium. However, we have obtained silicon nanowires having that structure using the plasma assisted vapour-liquid-solid growth method [1]. In silicon, polytype 2H is predicted to have a direct band gap under stress [2] or in nanowires, where it is also tunable by varying their radius [3]. This could yield specific and interesting luminescence properties. Given these properties, such nanowires are potential candidates for use in new kinds of optoelectronic devices, like light emitting diodes or solar cells.

The goal of the present work is to understand how the 2H structure stabilises itself in Si and Ge during nanowire growth. For this, we perform atomic scale observations of the nanowire in a modified transmission electron microscope (TEM), called NanoMAX, designed for *in situ* growth thanks to radical and molecular beam epitaxy sources. Comparisons between experimental and ideal TEM images, obtained through numerical simulation of nanowires with JEMS software, are made (Figure 1). This enables precise identification of specific structures, allowing in particular to differentiate between multiple twinning and hexagonal stacking during *in situ* growth.

- [1] J. Tang, J.-L. Maurice, F. Fossard, I. Florea, W. Chen, E. V. Johnson, M. Foldyna, L. Yu and P. Roca i Cabarrocas, *Nanoscale*, 2017, 9, 8113-8118
- [2] C. Rödl, T. Sander, F. Bechstedt, J. Vidal, P. Olsson, S. Laribi and J.-F. Guillemoles, *Phys. Rev. B*, 2015, 92, 045207
- [3] M. Amato, T. Kazwmaraya, A. Zobelli, M. Palumno and R. Rurali, *Nano Lett.* 2016, 16, 5694-5700

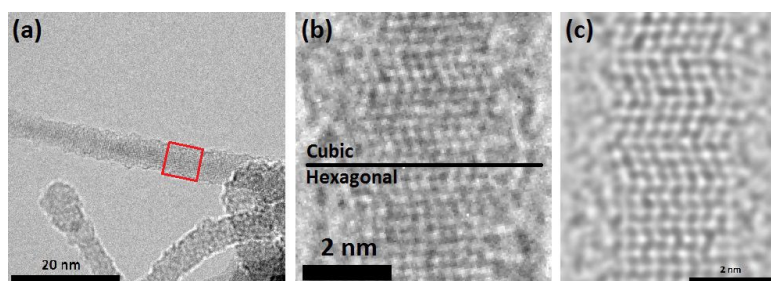


Figure 1: (a) TEM image of a silicon nanowire grown in a PECVD reactor using a Sn catalyst. (b) Zoom of the red area of (a), showing both a hexagonal and a twinned cubic phase in the nanowire. (c) Simulated TEM image of the nanowire shown in (a) and (b).

Impact of the amorphisation routes on physical properties of amorphous materials

F. Ngono^{1,2}, F. Affouard¹, J.F. Willart¹, G. J. Cuello², M. Jiménez-Ruiz²

¹ Université Lille Nord de France, Unité Matériaux et Transformations, UMR CNRS 8207, Av. Paul Langevin, F-59655 Villeneuve d'Ascq, France

² Institut Laue Langevin, 71 Av. des Martyrs, CS 20156, F-38042, Grenoble, France

f.ngono-mebenga@ed.univ-lille1.fr

So far, substances of pharmacy (active pharmaceutical ingredients and excipients) are most often prepared in the crystalline state (ordered) for obvious reasons of stability. Many pharmaceuticals, either by accident or design, may also exist in a total or partially amorphous state (disordered). This situation is encountered more and more frequently due to the increasing complexity of synthesized molecules. The amorphous state has a lower stability but a higher solubility than the corresponding crystalline forms. The formulation of active substances in the amorphous state, has thus motivated a strong interest in the last decade to increase the solubility of poorly soluble drugs^[1].

In this study, the amorphisation process and the amorphous state of lactulose (C₁₂H₂₂O₁₁), a disaccharide of pharmaceutical interest, have been investigated by combining a wide range of experimental and numerical techniques in order to probe structural, dynamical and thermodynamical physical properties. The amorphous compounds obtained by milling were compared to other amorphous forms designed by alternative amorphisation routes such as melt-quenching, freeze-drying, spray-drying^[2]. Recently, neutron diffraction with polarization analysis has been developed on D3 and successfully applied to mixtures of light and heavy water^[3]. For the first time, we were able to experimentally obtain the coherent structure factor of highly hydrogenated lactulose samples using D3 and D7 neutron diffractometers available at ILL. In addition, differences between the amorphous samples due to thermal degradations and chemical changes have been clarified aiming to unravel the true impact of the amorphisation mechanism itself. In this lecture, the observed structural differences between the amorphous samples will be presented.

This project has received funding from the Interreg 2 Seas programme 2014-2020 co-funded by the European Regional Development Fund under subsidy contract 2S01-059_IMODE.

REFERENCES

- 1 G. P. Johari and R. M. Shanker, *On the solubility advantage of a pharmaceutical's glassy state over the crystal state, and of its crystal polymorphs*, *Thermochimica Acta* 598, 16 (2014)
- 2 J. F. Willart and M. Descamps, *Solid State Amorphization of Pharmaceuticals*, *Molecular Pharmaceutics* 5, 905 (2008)
- 3 L. Temleitner et al., *Neutron diffraction of hydrogenous materials: Measuring incoherent and coherent intensities separately*, *Phys. Rev. B* (2015)

Semiconducting nanonets: Design and integration into functional devices for multiple sensing applications

Thuy Nguyen^{a,*}, Fanny Morisot^{a,b}, Maxime Legallais^{a,b}, Mireille Mouis^b, Valérie Stambouli^a, Bassem Salem^c, and Céline Ternon^{a,c}.

- a. Univ. Grenoble Alpes, CNRS, Grenoble INP, LMGP, F-38000 Grenoble, France
 b. Univ Grenoble Alpes, CNRS, Grenoble INP, IMEP-LaHC, F-38000 Grenoble, France
 c. Univ Grenoble Alpes, CNRS, LTM, F-38000 Grenoble, France

* thithuthuy.nguyen@grenoble-inp.fr

Randomly oriented semiconducting nanowire (NW) networks, also called nanonets (NN), are novel nanostructured materials which are electrically active, transparent, fault tolerant and readily functionalized [1]. We strongly believe that such highly versatile networks will offer a great potential for an easy connection from nanostructures to macroscale applications. Currently focused on silicon and zinc oxide nanonets, our research aims to develop chemical and biological sensors, notably to detect the acetone in the breath of diabetic patients (ZnO) and DNA markers in the blood of cancer ones (SiNN).

Several important achievements will be presented. Firstly, both SiNN and ZnO-NN are homogeneously and reproducibly assembled using simple, versatile, and low-cost technique. This makes possible to transfer these networks onto any desired substrate (transparent or opaque, flexible or rigid ...), therefore allows us to apply for several large-scale applications. Secondly, the passivation step, which strongly enhances the electrical conductivity of NN and stabilizes them in air for several years, will be reported. Finally, the most important breakthrough is the successful integration of these nanonets into highly performant field-effect transistors (FETs) via standard microelectronic technology [2]. This process is quite compatible with CMOS integration that motivates us to extend our research from lab-level to industrial fabrication. The devices obtained, as shown in figure 1, have good electrical characteristics, even when the channel length is much longer than NW one. To the best of our knowledge, it is the first time that such functional nanonet devices have been reached. Their primary electrical responses to acetone and DNA hybridization will be also discussed [3].

[1] Ternon C. *et al.*, Phys Status Solidi – Rapid Res Lett. 7(10) (2013), 919-923.

[2] Legallais M *et al.*, Solid-State Electronics, 143, (2018), 97-102.

[3] This work has received funding from the EU H2020 RIA project Nanonets2Sense under grant agreement n°688329.

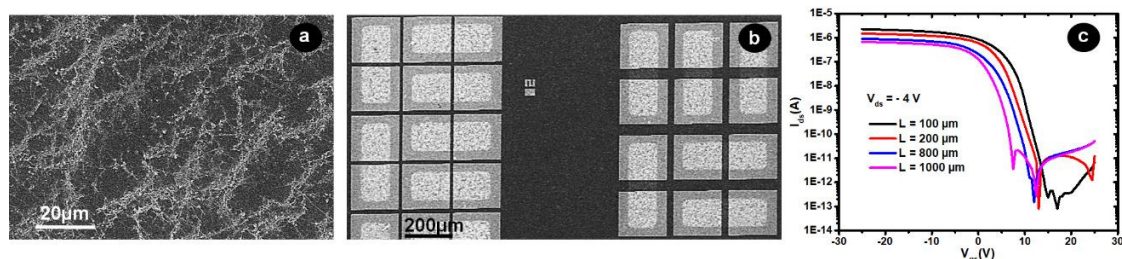


Figure 1 : (a) SEM image of assembled SiNN; (b) SEM image of SiNN-FET devices; (c) Transfer characteristics of NNFETs with channel length (L) from 100 μm to 1000 μm which clearly show the great conduction of NN through numerous NW/NW junctions (NW length = 7 μm).

La physique des plantes

Xavier Noblin^{a*}

a. Institut de Physique de Nice (INPHYNI), UMR 7010 UNS/UCA/CNRS.
Parc Valrose, 06108 Nice Cedex 2

* xavier.noblin@unice.fr

Les plantes ont développé depuis des millions d'années une multitude de stratégies pour générer des forces, du mouvement, transporter de l'eau ou des nutriments. Ces phénomènes font l'objets de nombreuses études actuelles dont la portée dépasse largement les aspects fondamentaux en biologie et biophysique. Les solutions originales trouvés par les plantes constituent autant de thématiques qui peuvent conduire à des avancées à la fois en physique fondamentale et dans la perspective d'innovations technologiques. Je décrirai tout d'abord dans cette exposé différentes avancées récentes de la communauté dans l'étude de problématiques liées aux mouvements rapides [1, 2] et aux phénomènes de transport [3, 4] chez les plantes. Je décrirai ensuite en particulier les travaux obtenus à l'Institut de Physique de Nice sur les phénomènes de pressions négatives et de dynamique de la cavitation, à la fois sur des systèmes naturels et synthétiques [5,6].

- [1] Jacques Dumais & Yoël Forterre, Vegetable Dynamicks. *Ann. Rev. of Fluid Mech.* 44 (2012).
[2] Y. Forterre, P. Marmottant, C. Quilliet and X. Noblin, *Europhysics News*, 47, p. 27–30 (2016).
[4] T. D. Wheeler & A. D. Stroock, The transpiration of water at negative pressures in a synthetic tree, *Nature* (2008).
[3] K. H. Jensen et al. Sap flow and sugar transport in plants, *Rev. Mod. Phys.* 88 (2016)
[5] X. Noblin et al., The fern sporangium: a unique catapult, *Science* (2012).
[6] C. Llorens et al. The fern cavitation catapult: mechanism and design principles, *J. Roy. Soc. Interface* (2016)

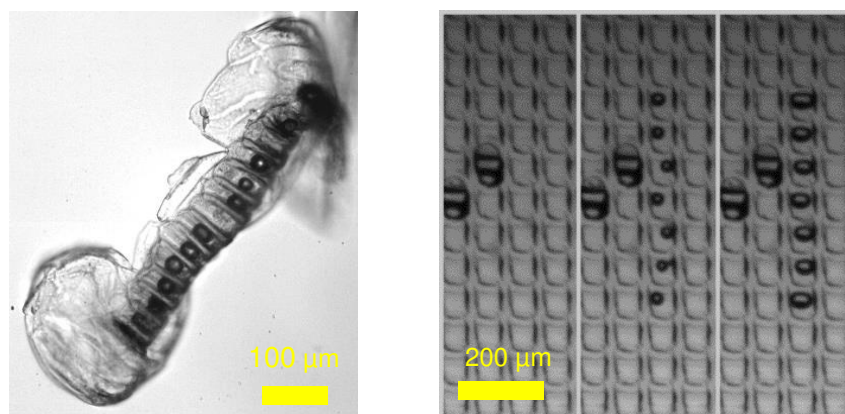


Figure 1 : Gauche : Sporangium de fougère lors de son mouvement rapide. On note les bulles de cavitation dans la plupart des cellules de l'anneau dont la nucléation en quelques microsecondes déclenche le catapultage. Droite : Bulles de cavitation dans un système synthétique mimétique en hydrogel.

Superfluid helium films on carbon nanotube

Adrien Noury ^{*† 1}, Jorge Vergara ¹, Pascal Morfin ², Bernard Plaçais ²,
Maria Carmen Gordillo ³, Jordi Boronat ⁴, Sébastien Balibar ⁵, Adrian
Bachtold ¹

¹ The Institute of Photonic Sciences (ICFO) – Mediterranean Technology Park Av. Carl Friedrich Gauss, 3 08860 Castelldefels (Barcelona), Spain, Espagne

² Laboratoire Pierre Aigrain (LPA) – École normale supérieure - Paris, Université Pierre et Marie Curie - Paris 6, Université Paris Diderot - Paris 7, Centre National de la Recherche Scientifique : UMR8551 – Département de Physique Ecole Normale Supérieure 24, rue Lhomond F-75231 Paris Cedex 05, France

³ Universidad Pablo de Olavide (UPO) – Departamento de Sistemas Físicos, Químicos y Naturales. Carretera de Utrera km1, 41013, Sevilla, Espagne

⁴ Universitat Politècnica de Catalunya [Barcelona] (UPC) – Universitat Politècnica de Catalunya C. Jordi Girona, 31. 08034 Barcelona, Espagne

⁵ Laboratoire Pierre Aigrain (LPA) – CNRS : UMR8551, Université Pierre et Marie Curie (UPMC) - Paris VI, Université Paris VII - Paris Diderot, École normale supérieure [ENS] - Paris – Département de Physique Ecole Normale Supérieure 24, rue Lhomond 75231 Paris Cedex 05, France

*Intervenant

†Auteur correspondant: adrien.noury@umontpellier.fr

Highly efficient spin-to-charge current conversion in strained HgTe surface states protected by a HgCdTe layer

P. Noel^a, C. Thomas^b, Y. Fu^a, L. Vila^a, B. Haas^c, P-H. Jouneau^c, S. Gambarelli^d, T. Meunier^e, P. Ballet^b, J.P. Attané^{a*}

- a. Univ. Grenoble Alpes, CEA, CNRS, Grenoble INP, INAC, SPINTEC, F-38000 Grenoble, France
- b. Univ. Grenoble Alpes, CEA, LETI, MINATEC campus, F38054 Grenoble, France
- c. CEA, INAC-MEM, 38054 Grenoble, France
- d. CEA, Institut Nanosciences et Cryogénie, SyMMES F-38000 Grenoble, France
- e. CNRS, Institut NEEL, 38042 Grenoble, France

* jean-philippe.attane@cea.fr

In order to generate spin current in spintronic devices it is needed to find an efficient way to transform charge current into spin current and make the opposite conversion to detect spin current. Classical spintronics generally uses magnetic materials for such conversions but they can be obtained by exploiting the spin-orbit coupling in materials containing heavy atoms. An efficient current conversion can be obtained through Spin Hall Effect in heavy metals such as Pt or Ta [1]. Yet a more efficient conversion can be obtained in two dimensional electron gas at surfaces and interfaces such as Rashba Interfaces [2] and newly discovered materials topological insulators.

Among topological insulators strained HgTe is a promising material for spintronic applications. Due to the band inversion in bulk HgTe, gap opening and Topological insulator properties can be induced by applying a tensile strain that can be achieved by growing HgTe on a substrate with a larger lattice constant, such as CdTe [3].

We studied the spin to charge current conversion in strained HgTe thin films by ferromagnetic resonance spin pumping [4]. The spin to charge current conversion rate, was measured to be one to two orders of magnitude larger than in Bi-based topological insulators [5]. Such high conversion rate can be related to the large value of the mobility [6] and mean free path of the surface states of strained HgTe and the lower bulk to surface conductivity ratio at room temperature.

[1] J. E. Hirsch, Physical Review Letters 83, 9 (1999)

[2] C. R. Ast, J. Henk, A. Ernst, L. Moreschini, M. Falub, D. Pacilé, P. Bruno, K. Kern, and M. Grioni, Phys. Rev. Lett. 98, 186807 (2007)

[3] L. Fu and C. L. Kane, Phys. Rev. B 76, 045302 (2007)

[4] P. Noel, C. Thomas, Y. Fu, L. Vila, B. Haas, P-H. Jouneau, S. Gambarelli, T. Meunier, P. Ballet, and J. P. Attané, Phys. Rev. Lett. 120, 167201 (2018)

[5] H. Wang, J. Kally, J.S. Lee, T. Liu, H. Chang, D.R. Hickey, K.A. Mkhoyan, M. Wu, A. Richardella, and N. Samarth Phys. Rev. Lett. 117, 076601 (2016)

[6] D. A. Kozlov, Z. D. Kvon, E. B. Olshanetsky, N. N. Mikhailov, S. A. Dvoretzky, and D. Weiss Phys. Rev. Lett. 112, 196801 (2014)

Les sources compactes, une nouvelle manière de produire des neutrons pour la diffusion neutronique.

Frédéric Ott

Laboratoire Léon Brillouin, CEA/CNRS, Université Paris-Saclay, CEA Saclay 91191 Gif sur Yvette

* Frederic.Ott@cea.fr

On observe actuellement à travers l'Europe un intérêt croissant autour du potentiel des sources de neutrons utilisant un accélérateur de basse énergie (10-50 MeV). Les progrès dans la technologie des accélérateurs qui permettent de produire des courants de particules de près de 100mA ainsi que les progrès dans la conception des modérateurs de neutrons permettent d'envisager la construction de sources dont les performances sont compétitives avec les réacteurs de recherche ou les sources à spallation de moyenne puissance. Le principe de conception de ces machines sera présenté ainsi que les différentes techniques qui permettent à ces sources d'être compétitives pour la diffusion neutronique.

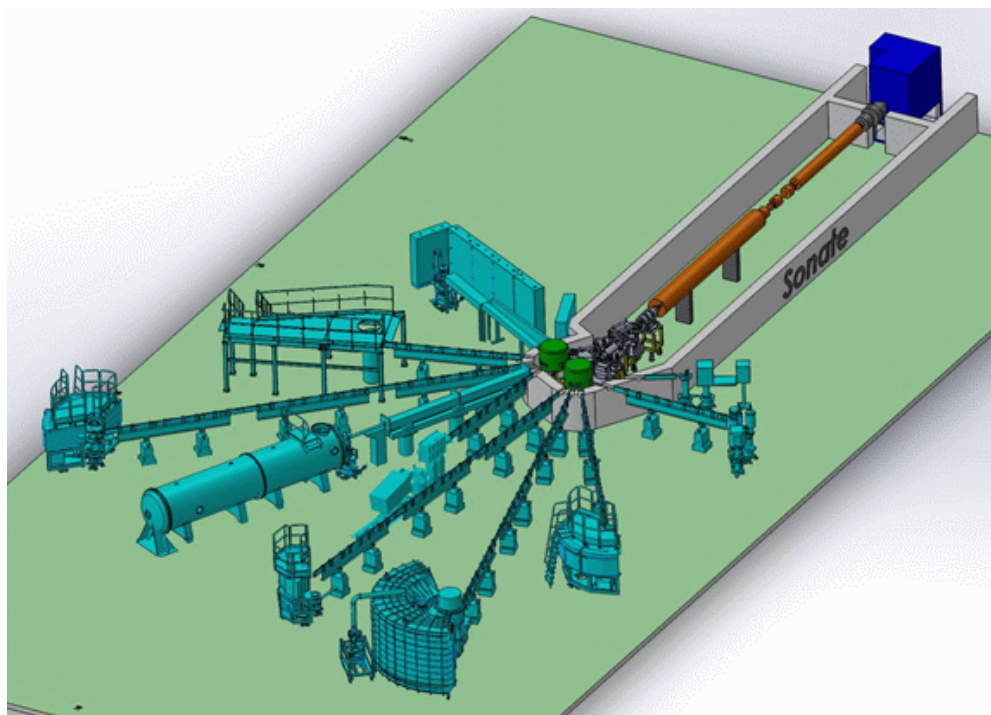


Figure 1 : Exemple de l'implantation possible d'une dizaine d'instruments de diffusion neutronique autour d'une source utilisant un accélérateur de protons de 20MeV.

Ising and Berezinskii-Kosterlitz-Thouless phase transitions of a two-leg boson ladder in flux

Edmond Orignac^{a*}, Roberta Citro,^b Mario Di Dio^c et Stefania De Palo^c

- a. Univ Lyon, Ens de Lyon, Univ Claude Bernard, CNRS, Laboratoire de Physique, F-69342 Lyon, France
- b. Dipartimento di Fisica "E.R. Caianiello", Università degli Studi di Salerno and Unità Spin-CNR, Via Giovanni Paolo II, 132, I-84084 Fisciano (Sa), Italy
- c. Dipartimento di Fisica Teorica, Università Trieste, Strada Costiera 11, I-34014 Trieste, Italy

* << Edmond.Orignac@ens-lyon.fr >>

Two chains of bosons coupled by interchain hopping present a transition under flux between a one dimensional analog of the Meissner state and a one dimensional analog of the Vortex state.¹ With only intrachain interactions between the bosons, the Meissner-Vortex phase transition belongs to the commensurate-incommensurate universality class.² As interchain interactions are added, an intermediate phase density wave (DW) phase appears between the Meissner and the Vortex phase. The M-DW transition belongs to the Ising universality class, and the DW-V transition to the Berezinskii-Kosterlitz-Thouless universality class. Inside the DW phase, incommensuration with the underlying lattice develops in some correlation functions at the disorder point. We present DMRG calculations of various observables that allow the characterizations of the different phases.^{3,4}

- [1] Atala, M Aidelsburger, M Lohse, M Barreiro, JT Paredes, B and Bloch, I Nature Physics **10** 588 (2014).
- [2] Kardar, M Physical Review B **33** 3125 (1986); Orignac, E and Giamarchi, T Physical Review B **64** 144515 (2001).
- [3] Orignac, E Citro, R Di Dio, M and De Palo, S Phys. Rev. B **96** 014518 (2017) and arXiv:1802.04997.

Interface coupling in graphene/ferroic hybrid structures

Zied Othmen^{a,b}, Kais Daoudi^b, Michel Boudard^c, Antonella Cavanna^d, Pascale Gemeiner^a, Meherzi Oueslati^b, Brahim Dkhil^a, Ali Madouri^d, Claire Mathieu^e

^a Laboratoire Structures, Propriétés et Modélisation des Solides, Centrale Supélec, CNRS-UMR 8580, Université Paris-Saclay, 92290 Châtenay-Malabry France

^b Unité Nanomatériaux et Photonique, Faculté des Sciences de Tunis, Université de Tunis El Manar, 2092, Tunis, Tunisie ^cUniv. Grenoble Alpes, CNRS, LMGP, F-38000 Grenoble, France

^dCNRS/C2N, Route de Nozay, F-91460 Marcoussis, France

^eSPEC, CEA, CNRS, Université Paris-Saclay, CEA Saclay, 91191 Gif sur Yvette cedex, France

* zied.othmen@centralesupelec.fr

Recently, hybrid structures made of graphene and ferroic oxides have received numerous attention for their potential applications in various fields including electronics, photonics and optoelectronics [1]. The physical properties of ferroic oxides arise from competition between spin, charge, orbital, polar and/or lattice degree of freedom [2]. Growing graphene (Gr) (zero bandgap semiconductor with high electron and hole mobility, unusual diamagnetism, ...) layer on top of such materials may thus give rise to a wide variety of proximity phenomena with interesting implications for fundamental science and device concepts. Here, we selected two representative ferroic oxides namely the cobaltite $\text{La}_{0.7}\text{Sr}_{0.3}\text{CoO}_3$ (LSCO) and the titanate BaTiO_3 (BTO) systems characterized by ferromagnetic and ferroelectric order parameter, respectively. We combined several techniques to investigate the consequences on the properties of both ferroic and graphene components in Gr/LSCO and Gr/BTO heterostructures. We show for instance using Raman spectroscopy that Jahn-Teller active Raman modes related to oxygen octahedral distortions are induced in the Gr/LSCO (20 nm) nanostructure which drastically differs to the situation of LSCO (20 nm) without graphene. This observation is attributed to a charge transfer from graphene to LSCO promoting the intermediate spin states of $\text{Co}^{3+/4+}$. The electronic and magnetic structures are also affected in Gr/LSCO structure [Z. Othmen et al., to be published]. Graphene properties are also changed as for instance in case of Gr/BTO heterostructure where the so-called 2D graphene Raman mode changes its behavior as a function of temperature concomitantly to ferroelectric phase transitions of BTO [Z. Othmen et al., to be published]. These results show how the ferroic properties can be affected/tuned by the graphene layer and conversely.

[1] Uang-Xin Ni et al., ACS Nano, 2012, 6 (5), pp 3935–3942

[2] A. Podlesnyak et al., Phys. Rev. Lett. 97, 247208 (2006)

Polymer physics in confined space at single molecule level: Experiments and scaling laws

Abdelghani Oukhaled^a

a. Laboratoire LAMBE, UMR 8587, Université de Cergy Pontoise 95000

* abdelghani.oukhaled@u-cergy.fr

Statics and dynamics of polymers in confined space were examined both theoretically and experimentally since more than 4 decades. In the first part of my talk I will briefly introduce the physics of polymers in confined spaces and then I will discuss the statics and dynamics of polymer chains in the situation where the polymers do not interact with the tube walls. In the second part I will examine the situation where the polymer chains interact with the tube walls and I will discuss the driving forces leading the partitioning of polymers into these pores. Relevant experimental results dealing with the statics and dynamics of chains (synthetic polymers, DNA, proteins, peptides) inside nanopores coupled to an electrical detection will be highlighted. In the third part I will summarize the research activity of the group which has been dealing with nanopores for years and I will introduce recent works of the group in particular using nanopore as a mass spectrometer for the size discrimination of polymers towards de novo protein sequencing.

Nanopore single-molecule analysis towards peptide and protein sequencing

Hadjer Ouldali^{a*}, Fabien Piguet^a, Juan Pelta^b, Abdelghani Oukhaled^{a*}

a. LAMBE UMR 8587, University of Cergy-Pontoise, 95300 Cergy-Pontoise, France

b. LAMBE UMR 8587, University of Evry-Val-d'Essonne, 91000 Evry, France

* hadjer.ouldali@u-cergy.fr ; abdelghani.oukhaled@u-cergy.fr

Nanopore-based protein sequencing is of crucial importance for the development of proteomics analysis applications in order to develop highly performant devices for tomorrow's medicine. Up to now, either wild-type biological nanopores or artificial nanopores did not provide a sufficient resolution to screen or to read peptides with a single amino acid resolution. In the first part of my talk, I will present our latest results showing the detection and discrimination of short peptides with a single amino acid resolution [1]. In the second part of my talk, I will discuss our strategy leading to provide the first sequence library of all the 20 different amino acids. Our work opens new perspectives towards biomarkers analysis, peptide sample purity analysis, and *de novo* protein sequencing.

[1] Piguet, F., Ouldali, H., Pastoriza-Gallego, M., Manivet, P., Pelta, J., & Oukhaled, A. (2018). Identification of single amino acid differences in uniformly charged homopolymeric peptides with aerolysin nanopore. *Nature Communications*, 9(1), 966.

Topological Insulator characteristics for $\text{Bi}_2\text{Te}_2\text{Se}$ and Sb doped $\text{Bi}_{2-x}\text{Sb}_x\text{Te}_2\text{Se}$ ($x = 0.05$ and 0.1)

Amit S. PAWBAKE^a, KanagaRaj MOORTHI^b, Sebastian C. PETER^b, Marie-Aude MEASSON^{a*}

a. Institute NEEL-CNRS Grenoble, 38042 **FRANCE**.

b. Jawaharlal Nehru Centre for Advanced Scientific Research, Bangalore, 560064 **INDIA**.

* marie-aude.measson@neel.cnrs.fr

The topological insulator is a unique state of matter that possesses a metallic surface state of massless particles known as Dirac fermions, which have coupled spin and momentum quantum numbers. Owing to the preservation of time-reversal symmetry, this coupling protects the wavefunctions against disorder [1]. Initially, most of research was focused either on alloys ($\text{Bi}_{1-x}\text{Sb}_x$) or binary chalcogenides (HgTe , Bi_2Se_3 , Sb_2Te_3 , Bi_2Te_3). Numerous chalcogenides have been proposed, theoretically, to be potential new platforms for topological quantum phenomena, where the inherent flexibility of crystallographic, electronic, and superconducting parameters provides a multidimensional basis for both scientific and technical exploration [2].

Ternary topological insulators, like $\text{Bi}_2\text{Te}_2\text{Se}$, attributed a considerable attention due to the simple structure with one Dirac cone crossing the band gap, which makes it attractive for experimental investigations. It has a well ordered structure comprising of Te-Bi-Se-Bi-Te quintuple layers. The stoichiometric $\text{Bi}_2\text{Te}_2\text{Se}$ is always a heavy doped n -type material showing metallic behavior. Higher bulk resistivities with the lowest possible bulk concentration can be obtained by applying the composition process. The most effective way is by introducing light metal doping. Partial substitution of Bi atoms with Sb may slightly modify the electronegativity of the cation site, as well as create chemical pressure. The Sb impurity influences the electronic band structure of the material, creating a defect states close to the top of the valence band. In consequence, doping increases the contribution of the surface conduction states typical for topological insulators, which is clearly indicates in figure 1. In additional Hall measurement data supports to the resistivity measurements.

[1] M. Z. Hasan, and C. L. Kane, Colloquium: topological insulators, *Rev. Mod. Phys.* **82**, 3045 (2010)

[2] H. Zhang, C. X. Liu, X. L. Qi, X. Dai, Z. Fang, and S. C. Zhang, Topological insulators in Bi_2Se_3 , Bi_2Te_3 and Sb_2Te_3 with a single Dirac cone on the surface. *Nat. Phys.* **5**, 438 (2009)

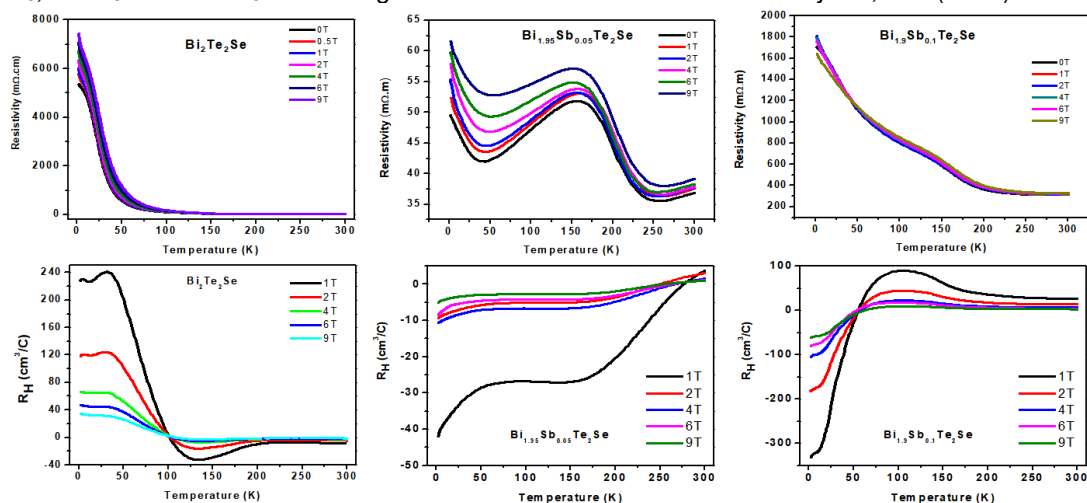


Figure 1 : Resistivity and Hall coefficients Vs Temperature for undoped and Sb doped $\text{Bi}_2\text{Te}_2\text{Se}$.

Nanopore-based Single-Molecule Size-Discrimination (Np-SMSD) of short homopeptides under different experimental conditions.

Fabien Piguet^{a*}, Hadjer Ouldali^a, Juan Pelta^b and Abdelghani Oukhaled^{a*}

a. LAMBE UMR 8587, University of Cergy-Pontoise, 95300 Pontoise, FRANCE

b. LAMBE UMR 8587, University of Evry-Val-d'Essonne, 91000 Evry, FRANCE

* fabien.piguet@u-cergy.fr, abdelghani.oukhaled@u-cergy.fr

Nanopores have been recently used to perform the single-monomer-resolution size-discrimination of synthetic polymers [1,2,3], of short oligonucleotides [4] and of short homopeptides [5]. The high resolution and high sensitivity of this technology have major applications, as demonstrated by already commercialized nanopore-based DNA sequencing devices. It also opens new perspectives towards early *in vitro* diagnostics and protein sequencing. Experimental conditions have been shown to have a crucial impact on Np-SMSD. For example, we demonstrated that high temperature enables the single-monomer-resolution size-discrimination of synthetic polymers of high molar mass, not possible at room temperature [3]. In this talk, following our recent results [5], I shall present the effect of voltage, temperature and electrolyte concentration on the single-amino-acid-resolution size-discrimination of short homopeptides using a biological nanopore.

- [1] Robertson, J. W. F. *et al.* Single-molecule mass spectrometry in solution using a solitary nanopore. *Proc. Natl. Acad. Sci. USA* **104**, 8207-8211 (2007)
- [2] Baaken, G. *et al.* High-resolution size-discrimination of single nonionic synthetic polymers with a highly charged biological nanopore. *ACS Nano* **9**, 6443-6449 (2015)
- [3] Piguet, F. *et al.* High temperature extends the range of size discrimination of nonionic polymers by a biological nanopore. *Sci. Rep.* **6**, 38675 (2016)
- [4] Cao, C. *et al.* Discrimination of oligonucleotides of different lengths with a wild-type aerolysin nanopore. *Nat. Nanotechnol.* **11**, 713-718 (2016)
- [5] Piguet, F. *et al.* Identification of single amino acid differences in uniformly charged homopolymeric peptides with aerolysin nanopore. *Nat. Commun.* **9**, 966 (2018)

Accelerating connectomics with X-ray holographic nanotomography

Alexandra Pacureanu^{a*}, Aaron Kuan^b, Jasper Maniates-Selvin^b, Yang Yang^a, Julio Caesar da Silva^a, Sylvain Bohic^{a,c}, Wei Allen Lee^b and Peter Cloetens^a

- a. European Synchrotron Radiation Facility, Grenoble, France
- b. Harvard Medical School, Boston, USA
- c. Université Grenoble Alpes, Grenoble, France

* joitapac@esrf.eu

Mapping the connections between neurons in tissue is a fundamental requirement in neurosciences and it remains out of reach due to the necessary spatial resolution and to the complexity of the circuitry spanning over extended areas. State of the art techniques are based on electron microscopy [1-2]. While these techniques enable 3D high resolution imaging, the covered volumes are very limited and they rely on tissue ultrathin slicing. Our aim is to accelerate the connectomics field by developing adequate X-ray holographic nanotomography. By joining forces of cutting edge X-ray focusing optics [3], together with highly brilliant sources and exceptional sensitivity of phase contrast in the hard X-ray regime [4], we can achieve sufficient spatial resolution for connectomics (Figure 1) while covering in hours volumes which require months of continuous seamless operation of EM based instruments [2].

- [1] Wei Allen Lee, Vincent Bonin, Michael Reed, Brett J Graham, Greg Hood, Katie Glattfelder, Clay R Reid. "Anatomy and function of an excitatory network in the visual cortex." **Nature**, 532, 7599, 370-374 (2016)
- [2] C Shan Xu, Kenneth J Hayworth, Zhiyuan Lu, Patricia Grob, Ahmed M Hassan, José G García-Cerdán, Krishna K Niyogi, Eva Nogales, Richard J Weinberg, Harald F Hess "Enhanced FIB-SEM systems for large-volume 3D imaging" **eLife** 6:e25916 (2017)
- [3] Julio Cesar da Silva, Alexandra Pacureanu, Yang Yang, Sylvain Bohic, Christian Morawe, Raymond Barrett, and Peter Cloetens, "Efficient concentration of high-energy x-rays for diffraction-limited imaging resolution," **Optica** 4, 492-495 (2017)
- [4] Anna Khimchenko, Christos Bikis, Alexandra Pacureanu, Simone E. Hieber, Peter Thalmann Hans Deyhle, Gabriel Schweighauser, Jürgen Hench, Stephan Frank, Magdalena Müller-Gerbl, Georg Schulz, Peter Cloetens, Bert Mueller. "Hard X-Ray Nanoholotomography: Large-Scale, Label-Free, 3D Neuroimaging beyond Optical Limit", **Advanced Science**, 2198-3844, doi:10.1002/adv.201700694 (2018)

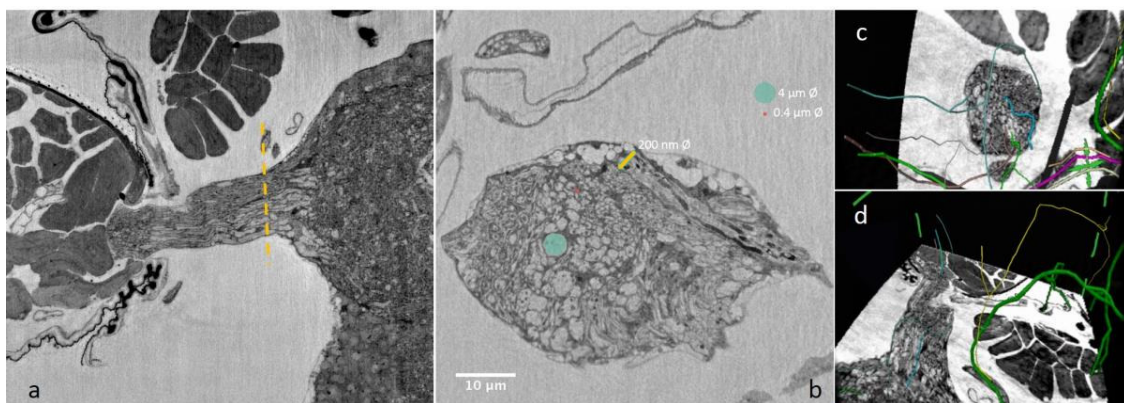


Figure 1: Resolving circuitry controlling locomotion in drosophila with X-ray holographic nanotomography. **a-b:** Regions of interest in reconstructed orthogonal slices (dotted line in panel **a** indicates position of slice illustrated in panel **b**) showing the connections between the ventral nerve cord, which makes most of the central nervous system, and the leg. **c-d:** snapshots illustrating segmentation of the axons using a virtual reality software.

Probing optical properties of TMDs at the nanoscale.

Luis Enrique Parra Lopez^a, Michael Chong^a, Etienne Lorchat^a,
Stéphane Berciaud^{a*}, et Guillaume Schull^{a*}

a. Université de Strasbourg, CNRS, IPCMS, UMR 7504, F-67000, Strasbourg, France.

* Stephane.berciaud@ipcms.unistra.fr ; Guillaume.schull@ipcms.unistra.fr

Semiconductor Transition metal dichalcogenides (TMDs) are a vast family of covalently bound layered compounds (with chemical formula MX_2 , $M = \text{Mo, W}$ and $X = \text{S, Se, Te}$) held together by van der Waals interactions, that display electronic, vibrational and optical properties that sensitively depend on the number of layers. For example, bulk TMDs have an indirect optical bandgap, and therefore, are bad light emitters, whereas in the monolayer limit, the same TMDs displays a direct optical bandgap, enhancing its light emission yield [mak10]. Therefore, TMD are perceived as an extremely promising material for two-dimensional optoelectronic applications (see [Mak16] for detailed review). Another remarkable particularity of the TMDs is linked to the presence of embedded defects which act as single-photon emitters/sources (SPE/SPS) as highlighted for WSe₂ monolayers in recent articles published in the May 2015 issue of Nature Nanotechnology [sri15, kop15, he15]. Those sources are essential for the realization of components exploiting the quantum nature of light, especially in the field of quantum cryptography and quantum information processing [lou05]. Here, micro-photoluminescence spectroscopy and cryogenic STM are used to characterize the electronic and optical properties of TMD samples. The aim of this work is to perform, with atomic-scale resolution, optical and time resolved spectroscopies of luminescent defects in the TMD layer that are expected to behave as single-photon sources.

[lou05] B. Lounis et al., Rep. Prog. Phys. 68, 1129 (2005).

[mak10] K-F.Mak et al., Phys. Rev. Lett. 105, 136805 (2010) .

[Mak16] K. F. Mak, J. Shan Nature Nanotech. 10, 216 (2016).

[sri15] A. Srivastava et al, Nature Nanotechnol. 10, 491 (2015).

[kop15] M. Koperskiet al., Nature Nanotechnol. 10, 503 (2015).

[he15] Y-M. He et al., Nature Nanotechnol. 10, 497 (2015).

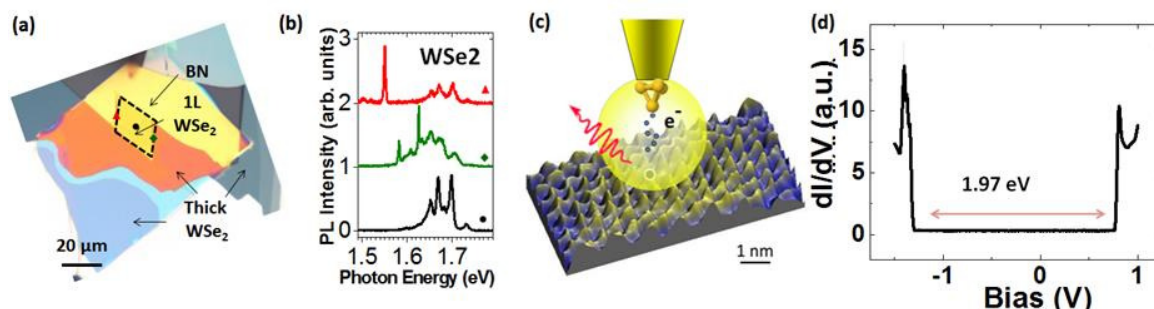


Figure 1 : (a) Example of a van der Waals heterostructure composed of a WSe₂ flake transferred on top of a ~100 nm thick BN terrace. A monolayer WSe₂ domain is highlighted with a dashed contour. (b) Spectra taken at different positions on the sample indicated by the colored symbols. (c) Scheme illustrating the principle of STM-induced luminescence. The atomically resolved STM image has been measured at IPCMS on a MoSe₂ monolayer. (d) Measured gap on MoSe₂ monolayer with the STM. The measured gap is larger than the expected bandgap, likely due to the large resistivity of the MoSe₂ channel at low temperature.

Thermal conductivity measurements and interfacial thermal resistance : a comparative study of extended 3 ω techniques

J. Paterson^{a,b*}, D. Singhal^{a,b}, D. Tainoff^{a,b}, J. Richard^{a,b} and O. Bourgeois^{a,b}

a. Institut Néel, CNRS, 38000 Grenoble, France

b. Univ. Grenoble Alpes, Grenoble, France

* jessy.paterson@neel.cnrs.fr

The study of nanoscale heat transport is of growing interest following the industry's trend of downsizing chip components. It is of great interest for both the industrial and scientific community to understand heat transfer at low dimensions in order to improve devices performances as well as understanding physical phenomena emerging from this downsizing. One important challenge to overcome is to accurately measure the thermal properties of low-dimensional materials. Indeed, creating both a heat source and a thermometer in size-constrained materials is challenging from a technological point of view, and the interpretation of experimental data is as well more complex when the size of the probed material becomes comparable to the heat source, thermometer or even to the heat carriers characteristic lengths.

The so-called 3 ω method is an electrical-based technique allowing the thermal conductivity measurement of substrates and thin films. A thin metallic layer deposited on top of the studied material acts simultaneously as a heat source and as a thermometer, resistance thermometry then allows to extract the underlying material thermal properties accurately.

The thermal conductivity measurement of very thin layers is challenging due to the presence of interfacial thermal resistances between the studied film and the neighboring materials. The contribution of these unknown thermal resistances to the total heat balance impedes a sensitive estimation of the thermal conductivity of the thin films. The constraints on the geometries and thermal properties of the system (transducer, stacking of thin films and substrate) often lead to use approximate models to facilitate data treatment, or to use comparative technique such as the so-called differential 3 ω in order to extract the thin film contribution from the total measured thermal resistance.

Here we will present experimental results comparing the thermal conductivity of SiN very thin films (30-120nm) extracted from the complete analytical solution given by Borca et al. and the thermal conductivity obtained from a differential setup (requiring two samples) [1]. The results obtained with two different techniques are in perfect agreement and allow an estimation of the interfacial resistance of the whole stacking being measured.

We also present interfacial thermal resistance measurements of a multilayer system composed of Ge/Al₂O₃/Pt as a function of temperature. The interfacial thermal resistance measurements are carried out on several stacking with varying thicknesses of the Al₂O₃ layer to isolate the effect of the interfacial thermal resistances. This allows as well the extraction of the Al₂O₃ thermal conductivity as a function of temperature with the two techniques (differential and analytical solution). Although each technique has its benefits and limitations, the present results show a great viability and reproducibility between the two methods.

[1] Borca-Tasciuc, T., Kumar, A. R., & Chen, G. (2001). Data reduction in 3 ω method for thin-film thermal conductivity determination. *Review of Scientific Instruments*, 72(4), 2139–2147. <https://doi.org/10.1063/1.1353189>

Observation in-situ dans un microscope électronique à transmission de la croissance par Epitaxie par Jets Moléculaires de nanostructures de semiconducteurs III-V

G. Patriarche^{a*}, J.-C. Harmand^a, F. Glas^a, L. Largeau^a, L. Travers^a, Y. Ollivier^a,
I. Florea^b, J.-L. Maurice^b et F. Panciera^a

- a. Centre de Nanosciences et de Nanotechnologies, CNRS, Univ. Paris-Sud, Univ. Paris-Saclay, C2N – Marcoussis, 91460 Marcoussis, France
- b. LPICM, Ecole polytechnique, CNRS, Univ. Paris-Saclay, 91128 Palaiseau, France

* gilles.patriarche@c2n.upsaclay.fr

Le projet Nanomax permet d'observer la croissance de nanostructures jusqu'à l'échelle atomique dans un microscope électronique en transmission. Il est prévu d'étudier en temps réel la croissance de nombreuses nanostructures : nanofils de semiconducteur III-V ou de silicium/germanium mais également des nanotubes de carbone. La croissance est réalisée in-situ dans un microscope électronique en transmission Titan ETEM équipé d'un correcteur d'aberration géométrique sur l'image. Nous avons mis au point pour ce microscope des microcellules à effusion pour éléments III et éléments V permettant de réaliser la croissance in-situ de nanofils de semiconducteur III-V (en particulier GaAs, InAs et GaSb). Les sources sont très collimatées afin d'éviter la contamination de la chambre du microscope, elles émettent sans perturber le fonctionnement du microscope. Nous montrons qu'il est possible d'étudier la croissance par EJM de nanofils de semiconducteur in-situ dans le microscope à une résolution atomique.

Les premières études nous ont permis de mettre en évidence l'influence de l'angle de contact du catalyseur sur la phase cristalline des nanofils. L'observation de la croissance à l'échelle atomique en temps réel permet d'accéder directement à la statistique de nucléation des marches et à leur vitesse de déplacement en fonction des conditions de croissance. En modifiant le rapport des flux III/V, on observe en direct le changement de volume du catalyseur et la modification de l'angle de mouillage de la goutte, qui entraîne un changement de la phase cristalline du nanofils (hexagonale vs cubique). Le projet Nanomax est développé dans le cadre de l'Equipex « TEMPOS ».

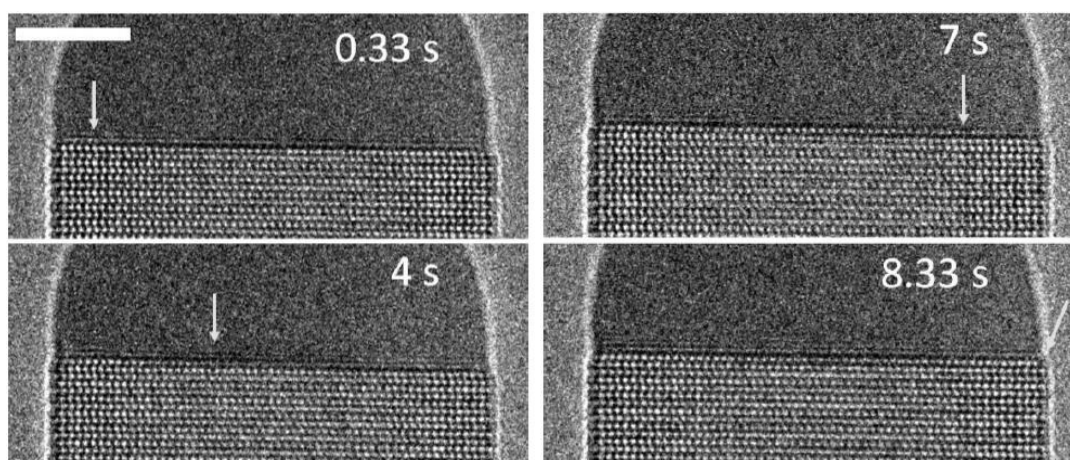


Figure 1 : Images extraites d'un film montrant la progression d'une marche atomique durant la croissance d'un nanofils de GaAs de structure wurtzite (barre d'échelle : 5nm).

Colloidosomes tailored by water-in-water emulsion

Adeline Perro^{a,*} Jean-Paul Douliez^b and Valérie Ravaine^a

- a. Institut des Sciences Moléculaires, Université Bordeaux, CNRS-UMR 5255, 351 Cours de la Libération, 33405 Talence, France.
- b. Biologie et pathologie du fruit, INRA, Univ. Bordeaux, UMR 1332, centre de Bordeaux, 33883 Villenave d'Ornon, France.

* adeline.perro@enscbp.fr

Water-in-water emulsions found their interest in the sequestration of fragile molecules as the internal and external phases are constituted of water. Typically, all aqueous phase separation occurs when two water soluble molecules are mixed together. This phenomenon also called coacervation has the ability to sequester spontaneously various entities from small molecules to complex cells. Nevertheless, the stability of such coacervates is not efficient and required the use of stabilizing agents such as colloids. We have exploited ampholyte polymer chains to create highly stable micrometric coacervates stabilized by colloidal particles. The main advantage of these complex assemblies results from their ability to sequester spontaneously fragile molecules such as DNA, proteins. This phenomenon was highlighted by introducing fluorescent molecules as illustrates in Figure 1A. Moreover, we have noticed the regular deposition of polymer microgels around the coacervate surface as presented in Figure 1B & 1C. These hybrid self-assembly, compatible with physiological media, found their application in drug delivery or sensors.

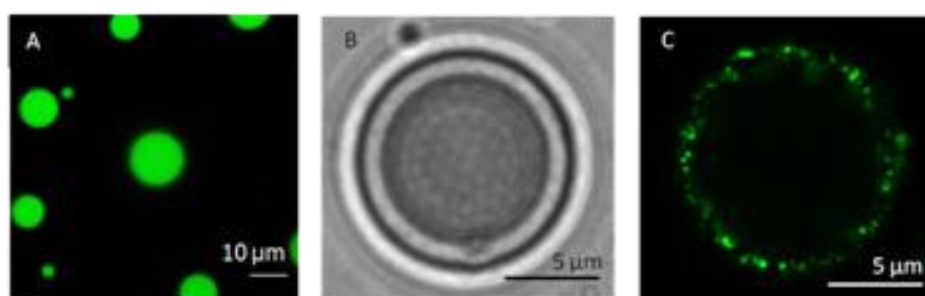


Figure 1 : A) Confocal image of coacervates containing fluorescent polymer chains. Microscopic pictures of the regular organization of fluorescent microgels B) Optical microscopy, C) Confocal image.

Noninvasive Relaxometry Evidence of Linear Pore Size Dependence of Water Diffusion in Nano-confinement

H. Chemmi ^a, D. Petit ^{a,b,*}, P. Levitz ^c, R. Denoyel ^d, A. Galarneau ^e, J.-P. Korb ^a

a. Physique de la Matière Condensée, Ecole Polytechnique, 91128 Palaiseau, France

b. Laboratoire Charles Coulomb, CNRS/Université de Montpellier, Montpellier, France

c. Physicochimie des Electrolytes et Nanosystèmes Interfaciaux, UPMC, Paris, France

d. MADIREL, Université Aix-Marseille, Centre de St Jérôme, Marseille, France

e. Institut Charles Gerhardt Montpellier, UMR 5253 CNRS-UM-ENSCM, Montpellier, France

* dominique.petit@umontpellier.fr

Abstract: We propose an original experimental method based on NMR at variable magnetic fields experiments (NMRD) and a theoretical analysis of the data that allows probing the spatial dependence of the diffusion coefficient of liquids specifically at proximity to pore surfaces. One of the key results found from these experiments is the linear relationship between average parallel diffusion coefficients and pore radii ¹. Another result is the robustness of the frequency scaling ^{1,2,3,4} of the master curve approach able to take into account the complexity of the water dynamics at pore surface for samples of different geometries. This approach has proven useful for evaluating the efficiency of the coupling between liquid layers within nanopore by extracting gradients of diffusion coefficients. The application of this method to water confined in synthesized calibrated nano-pores like MCM-41 for cylindrical geometry ⁵ and SEOS for spherical geometry ⁶ has been successful to deal with several dynamical processes on pore surface for different materials. This shows the ability of the proposed method to discriminate between the influence of the geometrical confinement on intra-pore dynamics and the chemistry of the interface induced by different synthesis of the materials. For instance, the frequency selectivity of NMRD profiles has been able to separate the different couplings coming from the spatial heterogeneities on the pore surfaces ^{1,2}. This frequency selectivity of NMRD has also allowed discriminating several steps of a complex dynamics process composed by both loops in water and surface diffusion during adsorption events ^{7,8,9}. Based on our experimental and theoretical results, we believe that the proposed noninvasive method allows exploring the interplay between molecular and continuous description of fluid dynamics relevant in physical and biological confinements.

[1] H. Chemmi, D. Petit, P. Levitz, R. Denoyel, A. Galarneau, J.-P. Korb, *J. Phys. Chem. Lett.* 7 (2016) 393–398.

[2] H. Chemmi, PhD thesis, Ecole Polytechnique, Fr., 2011 <pastel-00671390v1>.

[3] H. Chemmi, D. Petit, J.-P. Korb, R. Denoyel, P. Levitz, *Micro. and Meso. Mater.* 178 (2013) 104-107.

[4] H. Chemmi, D. Petit, V. Tarel, J.-P. Korb, R. Denoyel, R. Bouchet, P. Levitz, *Eur. Phys. J. Special Topics* 224 (2015) 1749.

[5] B. Coasne, A. Galarneau, F. Di Renzo, R. J. M. Pellenq, *Langmuir* 22 (2006) 11097.

[6] E. Bloch, T. Phan, D. Bertin, P. Llewellyn, V. Hornebecq, *Micro. and Meso. Mater.* 112 (2008) 612.

[7] P. Levitz, J.-P. Korb, D. Petit, *Eur. Phys. J. E* 12, 1 (2003) 29.

[8] P. Levitz, J.-P. Korb, *Europhys. Lett.* 70, 5 (2005) 684.

[9] J.-P. Korb, P.E. Levitz, *AIP Conf. Proc.* 1081 (2008) 55.

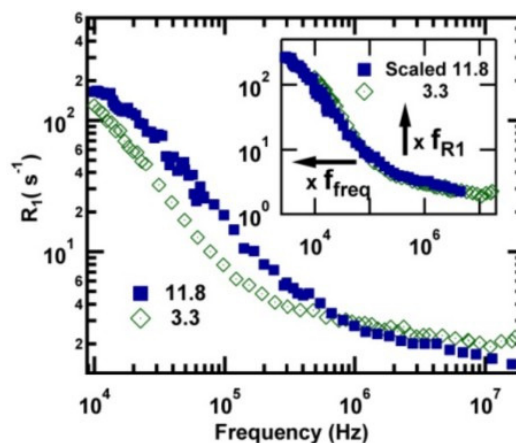


Figure 1 : ¹H NMRD profiles of MCM41 saturated samples with 3.3 nm (diamond) and 11.8 nm (square) pore diameters (main figure). In inset, the master curve obtained by scaling both relaxation rate and frequency by the factors $f_{R1} = 1.6$ and $f_{freq} = 3.3/11.8$, respectively is superposed to the MCM41 of 11.8 nm pore diameter.

Review of quantum effects in frustrated pyrochlore magnets

Sylvain Petit^{a*}

a. Laboratoire Léon Brillouin, CEA-CNRS-Université Paris-Saclay, CE-Saclay, F-91191 Gif sur Yvette

* sylvain.petit@cea.fr

La frustration magnétique, c'est à dire l'incapacité d'un système à satisfaire simultanément l'ensemble de ses interactions, fait l'objet de nombreuses recherches en physique de la matière condensée. Ce phénomène, qui peut être lié à la topologie du réseau cristallin ou aux compétitions entre interactions, constitue la source de nouveaux états exotiques de la matière, dont la description va au delà des modèles classiques. Les "glaces de spin" et leurs analogues quantiques, constituent un exemple emblématique de cette physique. La structure cristallographique de ces matériaux est basée sur un réseau de type "pyrochlore", formé d'un ensemble de tétraèdres connectés par leurs sommets, chaque nœud étant occupé par un ion de terre rare magnétique (Tb, Dy, Ho, Pr, etc.). Dans ces composés, les orbitales électroniques pertinentes ont une forme d'aiguille très fine, allongée en direction du centre de chaque tétraèdre. Le moment magnétique de chaque ion ne peut alors pointer que vers l'intérieur ou vers l'extérieur d'un tétraèdre, à l'instar des états ± 1 d'une variable Ising. L'état fondamental classique d'un tel système est très particulier car infiniment dégénéré. En effet, la seule prescription pour le construire est de suivre une règle locale qui stipule que chaque tétraèdre doit comporter deux spins "in" qui pointent vers l'intérieur et deux spins "out" qui pointent vers l'extérieur. Ces dernières années, les physiciens théoriciens ont proposé une vision nouvelle du problème, remarquant que la règle "two in-two out" est en fait analogue à la loi de conservation d'un flux magnétique fictif $\text{div}B = 0$ en électromagnétisme [1]. L'analogie est complète dès lors qu'on incorpore les fluctuations quantiques. En effet, les fluctuations du champ magnétique fictif B , créent en vertu de la loi de l'induction $\text{rot}E = -\partial B/\partial t$ un champ électrique "émergent" E . Selon les prédictions théoriques, une glace de spin quantique devrait comporter un spectre d'excitation particulier caractérisé par un mode analogue au photon de l'électromagnétisme.

A l'aide d'exemples tirés de la littérature, nous montrerons dans cet exposé qu'en dépit de nombreux travaux, les expériences réalisées jusqu'à aujourd'hui dans cette famille de composés n'ont pas encore permis de mettre en évidence cette dynamique particulière, à l'exception possible de $\text{Pr}_2\text{Hf}_2\text{O}_7$. Toutefois, l'influence des effets quantiques a très clairement été observée, mettant en lumière une très grande richesse de comportements. Nous discuterons en particulier le cas de $\text{Tb}_2\text{Ti}_2\text{O}_7$, l'influence des défauts dans $\text{Pr}_2\text{Zr}_2\text{O}_7$, la fragmentation magnétique dans $\text{Nd}_2\text{Zr}_2\text{O}_7$, ainsi que, au-delà de la physique propre aux spins Ising, l'ordre par le désordre dans $\text{Er}_2\text{Ti}_2\text{O}_7$ et la compétition d'interactions dans $\text{Yb}_2\text{Ti}_2\text{O}_7$.

[1] Quantum spin ice: a search for gapless quantum spin liquids in pyrochlore magnets, M.J.P. Gingras and P.A. McClarty, Rep Prog Phys **77** (2017) 056501.

Micromagnetic study of Skyrmion and Antiskyrmion stability

Jose Antonio Pena Garcia^{a*}, Lorenzo Camosi^a, Simone Moretti^{b,c} and Jan Vogel^a

a. Université Grenoble Alpes, CNRS, Institut Néel, F-38000 Grenoble, France

b. Universität Konstanz, Universitätsstrasse 10, 78464 Konstanz

c. Universidad de Salamanca, Plaza de los Caidos, 37001 Salamanca

* jose.pena-garcia@neel.cnrs.fr

Skyrmions (Sk) are chiral nanoscale topological magnetic solitons. Sk are stabilized by the Dzyaloshinskii-Moriya interaction (DMI) [1-2] or by dipolar interactions. Antiskyrmions (ASk) can be stabilized when an anisotropic DMI with opposite sign along perpendicular directions ($D_x = -D_y$) is present [3-4]. Sk and ASk show a different distribution of dipolar volume charges (Fig. 1). Therefore, when the dipolar interaction is comparable with the other energies, significant differences in energy and stability between Sk and ASk are predicted [5].

Micromagnetic simulations have been performed with a homemade modified version of Mumax3 open source software [6] containing the anisotropic DMI. The Sk and ASk stability has been studied by tuning the D_y/D_x ratio obtaining a D_x - D_y phase diagram. The phase diagram shows two different zones where Sk and ASk are stable. Moreover, a zone is found where a transition occurs between a Sk and an ASk when the D_y/D_x ratio is varied from positive to negative. The frontier where this transition takes place is studied as a function of the dipolar strength. Finally, a detailed study of the phase diagram allows us to determine under which conditions Sk and ASk are stable.

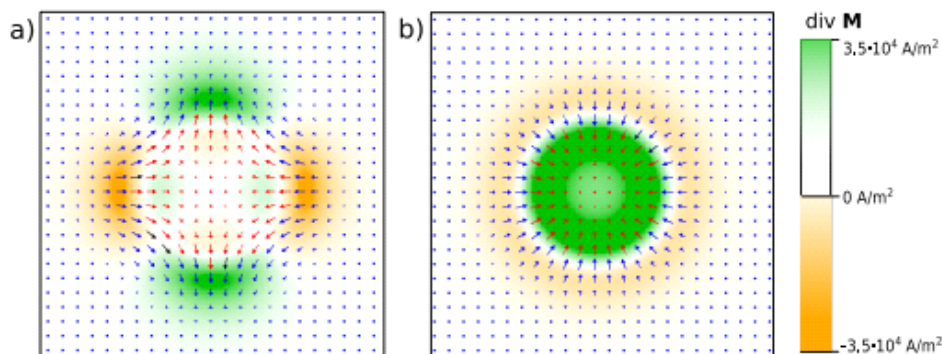


Figure 1 : Top view of a magnetic skyrmion **(a)** and an anti-skyrmion **(b)** in a nanodot with a lateral size of 115 nm. The colours represent the magnetic volume charges ($div \mathbf{M}$) as indicated in the scale bar. The arrows represent the out-of-plane magnetic components (red = up, blue = down). Taken from [5].

- [1] I. Dzyaloshinskii, *Sov. Phys. JETP* **5**, 1259 (1957).
- [2] T. Moriya, *Physical Review B* **120**, 91 (1960)
- [3] L. Camosi, et al, *Physical Review B*, **95**, 214422 (2017)
- [4] M. Hoffmann et al. *Nature Commun.* **8**,308 (2017).
- [5] L. Camosi et al, *Physical Review B*, **97**, 13 (2018).
- [6] A. Vansteenkiste et al., *AIP Advances* **4**,107133 (2014)

Chip Temperature Fields computed by Multi-Scale FEM Modelling and probed by Scanning Thermal Microscopy

A. Pic^{a,b,*}, R. Prieto^{a,c,d}, S. Gallois-Garreignot^a, J.-P. Colonna^c and P.-O. Chapuis^b

- a. STMicroelectronics, 850 Rue Jean Monnet, 38920 Crolles, France
- b. Univ. Lyon, CNRS, INSA-Lyon, Université Claude Bernard
- c. Univ. Grenoble Alpes, F-38000 Grenoble France CEA, LETI, MINATEC Campus, F-38054 Grenoble, France
- d. Univ. Grenoble Alpes, G2Elab, F-38000 Grenoble, France CNRS, G2Elab, F-38000 Grenoble, France

* axel.pic@st.com & axel.pic@insa-lyon.fr

Heat dissipation is one of the main challenges faced by microelectronics due to the increase of integration density. For applications involving the Silicon-On-Insulator (SOI) technology based on a very thin silicon layer and imagers with high sensitivity to temperature spatial variations, accurate thermal characterizations with reliable temperature measurements are needed to quantify thermal performances at the device and package levels [1-2]. In this work, a 3D Hybrid Bonding (HB) assembly designed to highlight the heat dissipation issues is studied by means Finite Element Modelling (FEM). Experimental investigations of the HB assembly by successive means of resistive thermometry and Scanning Thermal Microscopy (SThM) allow feeding the model with accurate parameters and determining the full temperature field.

The test device designed to investigate the thermal behavior of the HB assembly [3] is made of two chips bonded by means of HB and involves materials typically used in microelectronics such as silicon bulk, oxides, nitrides and copper for interconnections. Four metal levels are considered - two in the bottom chip and two in the top one -, which all lay on top of a silicon die and a printed circuit board: the device is therefore a simplified version of more advanced chips. In the bottom metal level an electrical resistance is used to generate heat by Joule dissipation. The power dissipated represents that which would be generated in the integrated circuit (IC) of a real device.

The temperature in the chip is determined by means of numerical FEM studies at two different scales: the one of the heater and that of the whole package. However, some key parameters linked to the heat sink and the dissipation to ambient are needed. Embedded electro-thermal sensors made of resistive serpentine ($12 \times 12 \mu\text{m}^2$) located in highest metal level of the chip [4] allow determining them. Once the full temperature field is computed, SThM, a surface mapping technique based on atomic force microscopy, is performed on the chip surface to validate the numerical results. Two probes are used successively: the Wollaston and Pd tips. It is important to mention that the SThM sensors need also to be simulated through FEM in order to get quantitative data from the measurements, as they modify the heat dissipation channels when set in contact with the HB assembly.

The results show an interesting match of the experimental SThM data and the computed ones. SThM is particularly useful when optical techniques cannot be used. The mid-term goal of the project is to develop a library of effective parameters for the FEM simulation tools and validate simulation methods for such issue. This will allow predictions of thermal behaviors of more complex electronic stacks with improved accuracy.

References

- [1] G. Garegnani et al, *Microelec. Rel.* 63, 90, 2016
- [2] D.L. Lin et al, *IEEE Trans. Elect. Dev.* 57, 2010
- [3] C. Sart et al, *Proceedings of ESTC6*, 2016
- [4] R. Prieto et al, *Proceedings of THERMINIC*, 2016
- [5] M. Nonnenmacher et al, *Appl. Phys. Lett.* 61, 168, 1992
- [6] A. Assy, PhD Thesis, INSA Lyon, 2015

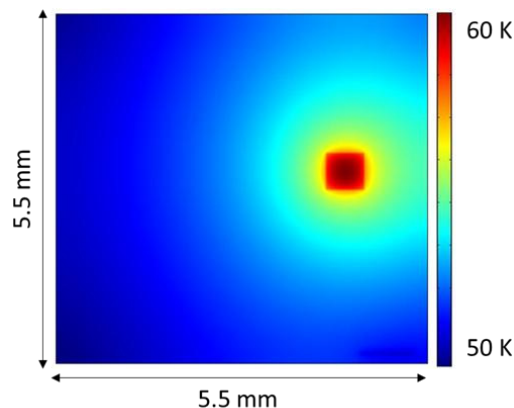


Figure: Temperature rise of the chip surface calculated by FEM

Raise and fall of a bright soliton in an optical lattice

Piero Naldesi^{a,*}, Juan Polo Gomez^a, Boris Malomed^{b,c}, Maxim Olshani^d, Anna Minguzzi^a et Luigi Amico^{e,f,g,h,i}

- a. Université Grenoble-Alpes, LPMMC, F-38000 Grenoble, France and CNRS, LPMMC, F-38000 Grenoble, France
- b. Department of Physical Electronics, School of Electrical Engineering, Faculty of Engineering, Tel Aviv University, P.O.B. 39040, Ramat Aviv, Tel Aviv, Israel
- c. Center for Light-Matter Interaction, Tel Aviv University, P.O.B. 39040, Ramat Aviv, Tel Aviv, Israel
- d. Department of Physics, University of Massachusetts Boston, Boston, MA 02125, USA
- e. Dipartimento di Fisica e Astronomia, Via S. Sofia 64, 95127 Catania, Italy
- f. Centre for Quantum Technologies, National University of Singapore, 3 Science Drive 2, Singapore 117543, Singapore
- g. MajuLab, CNRS-UNS-NUS-NTU International Joint Research Unit, UMI 3654, Singapore
- h. CNR-MATIS-IMM & INFN-Sezione di Catania, Via S. Sofia 64, 95127 Catania, Italy
- i. LANEF 'Chaire d'excellence', Université Grenoble-Alpes & CNRS, F-38000 Grenoble, France

* piero.naldesi@lpmmc.cnrs.fr << Piero Naldesi >>

We study an ultracold atomic gas with attractive interactions in an one-dimensional optical lattice. We find that its excitation spectrum displays a quantum soliton band, corresponding to N -particle bound states, and a continuum band of other, mostly extended, states. For a system of finite size, the two branches are degenerate in energy at small interactions, while a gap opens above a threshold value for the interaction strength. We find that the interplay between degenerate extended and bound states has important consequences in both static and dynamical properties of the system. In particular, the solitonic states result to be protected from spatial perturbations and random disorder. We discuss how such dynamics implies that our system effectively provides an example of quantum many-body system that, as function of the bosonic lattice filling, crosses over from integrable non-ergodic to non-integrable ergodic dynamics, through non-integrable non-ergodic regimes.

Shubnikov-de Haas oscillations in back-gated WSe₂ / h-BN heterostructures

Mathieu Pierre^{a*}, Banan Kerdi^a, Michel Goiran^a et Walter Escoffier^a

a. Laboratoire National des Champs Magnétiques Intenses (LNCMI), Université de Toulouse, INSA, UPS, UGA, CNRS UPR 3228, EMFL, Toulouse, France

* mathieu.pierre@lncmi.cnrs.fr

We investigated the electronic properties of few-layer WSe₂ devices with transport measurements under pulsed magnetic field up to 55 T. Few-layer flakes of WSe₂ were deposited on h-BN flakes, etched in a Hall bar configuration, and electrically contacted with Pt/Au electrodes. By applying a negative gate voltage to the substrate, we were able to study the hole conduction regime, despite non-ohmic contacts. While a weak magnetoresistance is observed, clear $1/B$ -periodic conductance oscillations appear above 20 T. The transverse Hall voltage was simultaneously measured. We extract information on the carrier concentration, their mobility and effective mass, as well as their degeneracy. At low carrier density, we observed Shubnikov-de Haas oscillations with odd filling factors, which is a consequence of a large Zeeman splitting at the Γ point in the valence band. Our fabrication process allows to obtain devices with sufficient mobility to reach the quantum transport regime. Work is under progress to improve the device mobility and the ohmicity of the contacts, and to fabricate monolayer devices.

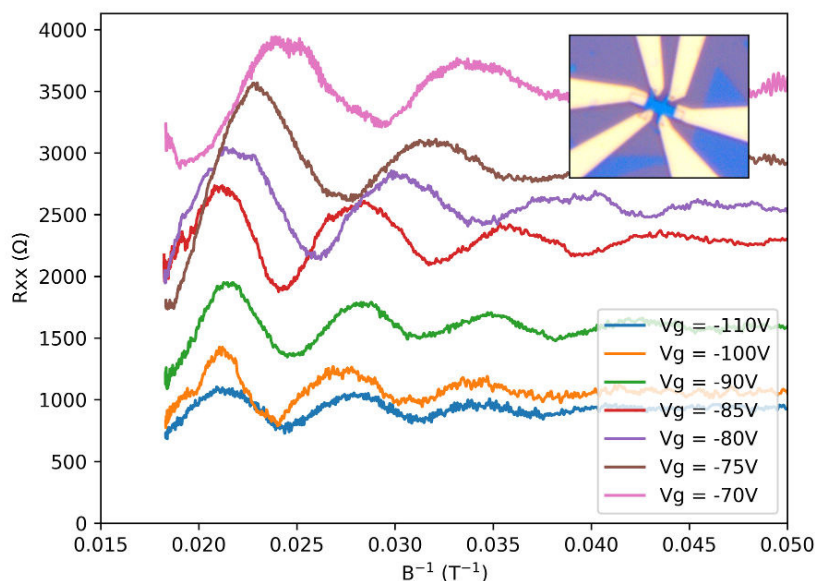


Figure 1: Longitudinal resistance of a WSe₂ Hall bar device, measured at 4.2 K and up to 55 T for several back-gate voltages. A small background has been subtracted. Shubnikov-de Haas oscillations are observed, with a gate-dependant period, ranging from 150 T at $V_g = -110$ V to 105 T at $V_g = -70$ V. Insert: optical microscope image of the 1.5 μm -wide WSe₂ Hall bar.

Magnetic short range order in Fe_{1-x}Cr_x alloys

Véronique Pierron-Bohnes^{a*}, Georges Parette^b, and Isabelle Mirebeau^b

- a. Université de Strasbourg, CNRS, UMR7540 Institut de Physique et Chimie des Matériaux de Strasbourg, 23 rue du Loess BP 43, 67034 Strasbourg Cedex 2 France
 b. Laboratoire Léon Brillouin, CEA-CNRS, Université Paris-Saclay, CEA-Saclay, F-91191 Gif-sur-Yvette, France

* vero@unistra.fr

FeCr alloys now encounter high interest due to their ability to eliminate irradiation damages spontaneously at high temperature. This property makes them crucial ingredients in future fusion and fission reactors, where materials suffer extensive damage from high energy neutrons irradiation. The unique stability of FeCr is likely related to an inversion of atomic short range order (SRO) at $x_c=0.11$ [1,2], and to a sign inversion of the heat of formation [3]. Below x_c , the Cr atoms repel each other, leading to ordering, whereas above x_c they tend to cluster. Such inversion is theoretically explained by the influence of band ferromagnetism on the atomic interactions, leading to a change of sign of the atomic pair potential with Cr content [4].

In FeCr alloys, chemical and magnetic local orders are strongly coupled. To investigate this coupling, we studied Fe_{1-x}Cr_x bcc solid solutions (for $0.03 < x < 0.15$) by neutron diffuse scattering, using both polarized and unpolarized neutrons. Polycrystalline alloys were annealed to ensure equilibrium SRO states [2]. At low Cr content, the Cr moment orients anti-parallel to the Fe moment, with a value of $-1.14(1) \mu_B$. The Cr moment perturbs the neighboring Fe moments, decreasing their magnitude for the near Fe neighbors and increasing it for farther Fe neighbors. At high Cr content, the Cr moment decreases, being strongly sensitive to the number of Cr neighbors.

These results extrapolate well with *ab initio* predictions performed in the dilute limit [5], for the amplitude and sign of the local moments and perturbations (Figure). At high Cr content, the decrease of the Cr moment is qualitatively explained by magnetic frustration effects [6]. New DFT calculations coupled with MC simulations are now in progress to evaluate the moments and perturbations for the actual SRO states. The whole study brings out the pivotal role of magnetism in iron defects, a key feature to control the design of steel materials for fusion energy [7].

[1] I. Mirebeau and G. Parette, Phys. Rev. B **82**, 104203 (2010). [2] I. Mirebeau *et al*, Phys. Rev. Lett. **53**, 687 (1984). [3] P. Olson *et al*, Phys. Rev. B **73**, 104416 (2006). [4] M. Hennion, J. Phys. F **13**, 2351 (1983). [5] B. Drittler *et al*, Phys. Rev. B **40**, 8203 (1989). [6] T. P. C. Klaver *et al*, Phys. Rev. B **74**, 094435 (2006). [7] I. Cook, Nature **5**, 1978 (2006).

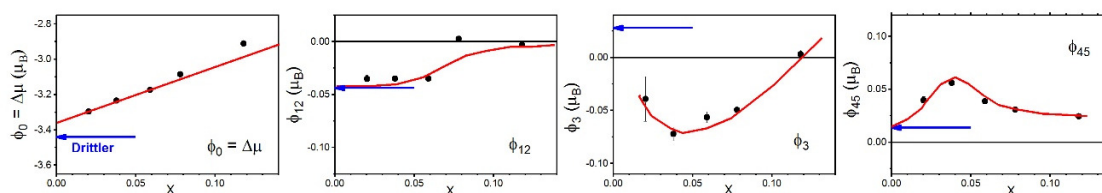


Figure 1: Moment difference ($\mu_{Cr}-\mu_{Fe}$) and magnetic perturbations of Fe moment due to the presence of a Cr atom in the nearest neighbor shells. Experimental results are compared to the predictions of [5] using LDA-DFT *ab initio* calculations in the single-impurity limit (blue arrow).

Disorder-order transition and segregation effect in PtAg nanoalloys

J. Pirart^{a*}, P. Andreazza^a, C. Andreazza^a, A. Lemoine^{a,b}, Y. Garreau^b,
A. Coati^b, R. Ferrando^c

- a. ICMN, CNRS, Univ. Orléans, 1b rue de la Férollerie, 45071 Orléans Cedex 2, France.
- b. Synchrotron Soleil, L'Orme de Merisiers, Saint Aubin, 91192 Gif-sur-Yvette, France.
- c. Università di Genova, via Dodecaneso 33, 16146 Genova, Italy.

* jerome.pirart@cnsr-orleans.fr

Pt-based alloys are especially known to be efficient catalysts and electrocatalysts for different reactions [1]. Most of studies try to combine the Pt to another metal in order to increase the stability of single-metal catalysts as well as to improve the catalytic selectivity and/or activity. In this prospect, PtAg alloyed nanoparticles (NPs) are particularly interesting for carbon monoxide oxidation: Pt sites can chemisorb CO and Ag sites activate O₂ [2]. Therefore, a quite uniform distribution of Pt and Ag surface sites is essential, the reaction efficiency being more efficient if Ag and Pt sites are close to each other.

At the macroscopic scale, PtAg alloy shows an interesting but complex phase diagram at low temperature [3] (under 800 °C). Indeed, an ordered alloy is formed within the miscibility gap which extends from 15 % to 97 % of Ag. This ordered alloy, which is a L₁ phase (alternative planes of Ag and Pt in the [111] direction of the fcc lattice), is formed only at the equicomposition of PtAg [4]. At the nanoscale, the size reduction and the segregation effect can modify the stability of the ordered alloy. Indeed, due to its low surface energy and its large atomic radius, the Ag has a high tendency to go to the surface of the nanoparticles in order to form a core/shell segregation depending on the Ag concentration [5], [6].

Our objective is to determine, through high resolution structural investigation technique combined with DFT calculations, the equilibrium phase for the PtAg alloy at different compositions. PtAg nanoalloys was prepared by atomic evaporation using two separate sources operating simultaneously under ultra-high vacuum (UHV) conditions. The obtained nanoparticles show an ordered L₁ core with a monolayer-thick Ag shell depending on the composition. These experimental results are in agreement with our DFT calculations.

- [1] C. Wang, N. M. Markovic, et V. R. Stamenkovic, « Advanced Platinum Alloy Electrocatalysts for the Oxygen Reduction Reaction », *ACS Catal.*, vol. 2, no 5, p. 891-898, mai 2012.
- [2] S. Y. Hwang, C. Zhang, E. Yurchekfrod, et Z. Peng, « Property of Pt–Ag Alloy Nanoparticle Catalysts in Carbon Monoxide Oxidation », *J. Phys. Chem. C*, vol. 118, no 49, p. 28739-28745, déc. 2014.
- [3] P. Durussel et P. Feschotte, « A revision of the binary system Ag–Pt », *J. Alloys Compd.*, vol. 239, no 2, p. 226–230, 1996.
- [4] G. L. Hart et al., « Revisiting the revised Ag-Pt phase diagram », *Acta Mater.*, vol. 124, p. 325–332, 2017.
- [5] K. Yun et al., « Monte Carlo simulations of the structure of Pt-based bimetallic nanoparticles », *Acta Mater.*, vol. 60, no 12, p. 4908-4916, juill. 2012.
- [6] F. Calvo, E. Cottancin, et M. Broyer, « Segregation, core alloying, and shape transitions in bimetallic nanoclusters: Monte Carlo simulations », *Phys. Rev. B*, vol. 77, no 12, mars 2008.

A band-gap engineered Travelling Wave Parametric Amplifier

L. Planat^{a*}, M. Proust^a, K. Bharadwaj^a, O. Buisson^a, R. Dassonneville^a, F. Foroughi^a,
W. Guichard^a, S. Léger, C. Naud^a, J. Puertas-Martinez^a, and N. Roch^a

a. Univ. Grenoble Alpes, CNRS, Grenoble INP, Institut Néel, 38000 Grenoble, France

* luca.planat@neel.cnrs.fr

Josephson Parametric Amplifiers (JPA) are key to research fields involving microwave signals in the quantum regime, such as superconducting quantum bits or nano electromechanical systems. Their elementary building block, the Josephson junction, is at the same time strongly non-linear and non-dissipative. Therefore they provide both large gain [1,2] and noise performances close to the quantum limit [3,4]. To obtain reasonable gain (typically 20 dB), the interaction time between the weak signal, the strong pump and the non-linear medium must be maximized. Up to now, this interaction time was increased by coupling the Josephson element to a resonant cavity, but at the expense of a reduced bandwidth. Despite continuous improvement[5,6,7], these resonant amplifiers still display a bandwidth below 1 GHz.

Increasing this interaction time is also possible using distributed non-linear media, similar to non-linear optical fibers, thus overriding the difficulties created by resonant cavities. Such devices are called Traveling Wave Parametric Amplifier (TWPA) and require arrays of at least one thousand Josephson junctions to obtain more than 10 dB gain over more than 1 GHz bandwidth. Fabricating such amplifiers is now technically possible [8]. However, these travelling-wave amplifiers raise new issues.

TWPA must be perfectly impedance matched with the rest of the setup, which is typically $50\ \Omega$, to transmit the amplified signal without spurious reflection. Josephson junctions are very inductive elements (450 pH/sq), thus junction arrays usually show characteristic impedance far above $50\ \Omega$. We will present the fabrication process we developed to match such arrays with the rest of the setup. However, fabricating a perfectly matched array is not enough and leads to 10 dB/12 dB maximum gain over a band of 1.5 GHz. In a second part we will show that an imperative condition to increase the maximum gain and the bandwidth of the TWPA is to phase match the strong pump and the weak signal, which is not trivial in a non-linear medium. We have chosen to engineer band-gap in the dispersion relation of the array to compensate the different phase velocities. We will show gain greater than 12 dB while having bandwidth larger than 3 GHz.

- [1] B. Yurke *et al.*, Applied Physics Letters 69, 3078 (1996).
- [2] M. J. Feldman *et al.*, Journal of Applied Physics 46, 4031 (1975)
- [3] M. A. Castellanos-Beltran *et al.*, Nature Physics 4, 928 (2008)
- [4] C. M. Caves, Physical Review D 26, 8 (1982)
- [5] T. Roy *et al.*, Applied Physics Letters 107, 262601 (2015)
- [6] X. Zhou *et al.* Physical Review D 89, 214517 (2014)
- [7] J. Y. Mutus *et al.* Applied Physics Letters 104, 263513 (2014).
- [8] C. Macklin *et al.* Science 350, 6258 (2015)

Formation and stability of physical gels: what we learn from Quasi-Elastic Neutron Scattering

Marie Plazanet^{a*}, Miguel A. Gonzalez^b, Isabelle Morfin^a and Sylvie Spagnoli^a.

a. Laboratoire Interdisciplinaire de Physique, CNRS and Université Grenoble-Alpes.

b. Institut Laue-Langevin, Grenoble

* marie.plazanet@univ-grenoble-alpes.fr

Physicals gels formed by low molecular weight organic gelators (LMMOG) are composed of a rigid network formed by the gelators, in which is trapped a large quantity of solvent. Gathering properties of both liquids and solids, they find applications as functionalized nanomaterials in diverse domains, although applications suffer several limitations, such as the unexpected collapse after some time or the difficulty to predict gelation ability of new molecules. The subtle interplay of the different forces exerted between the solvent and gelators enable the gels to reversibly assemble in a restricted temperature range in a complex structure that depends on the solvent. The interface between gelators and solvent is soft and ill-defined. Because of the intrinsic complexity, at the molecular level, of the structural organization and the dynamics, these materials are quantitatively studied with difficulty. In this context, we undertook the study of the microscopic dynamics in a model physical molecular gel, methyl-4,6-O-benzylidene- α -D-mannopyranoside (α -manno) [1] in water and toluene are probed by neutron scattering [2] and Transient Grating Spectroscopy [3]. The α -manno is an amphiphilic gelator that adopts different organizations in both solvents. We were able to distinguished, on a timescale from a few ps to few ns, several dynamical populations of solvent molecules in interaction with the rigid network formed by the gelators. We found that only few toluene molecules per gelator participate to the network which is formed by hydrogen bonding between the gelators' sugar moieties. In water, however, the interactions leading to the solid network assembly are weaker and each gelator forms a tens of hydrogen bonds with the surrounding water molecules, that are stable over few hundreds of ps only. Eventually, the gelator network dynamics can be distinguished just before the melting when its characteristic relaxation time enters the ns timescale. This study shows that quantitative information can be obtained about the behaviour of solvent confined in a molecular gel, also relevant to diffuse interfaces as often encountered in soft matter systems.

[1] Gronwald O., Shinkai S., Sugar-Integrated Gelators of Organic Solvents, Chem. Eur. J. 7, 4328-4334 (2001).

[2] Spagnoli S., Morfin I., Gonzalez M.A., Carcabal P., Plazanet M., Solvent contribution to the stability of a physical gel characterised by quasi-elastic neutron scattering, Langmuir 31, 2554-2560 (2015).

[3] Morfin I., Spagnoli S., Rambaud C., Longeville S., Plazanet M., Behaviour of a solvent trapped in a physical molecular gel, Phil. Mag., 809-815 (2016).

Excitons in hybrid perovskites via high magnetic field spectroscopy

Paulina Plochocka^a

^a. Laboratoire National des Champs Magnétiques Intenses, UPR 3228, CNRS-UGA-UPS-INSA, Grenoble and Toulouse, France.

* paulina.plochocka@lncmi.cnrs.fr

Solid-state perovskite-based solar cells have made a dramatic impact on emerging PV research with efficiencies of over 22% already achieved. Nevertheless, many of the basic electronic properties of the perovskites remain unexplored.

First, I will demonstrate that the absorption measurements performed in very high magnetic fields up to 150T gives a direct access to basic electronic properties such as exciton binding energy and effective mass of the carriers for Organic-Inorganic or fully inorganic Tri-halide Perovskites. I will show that for all the family of these materials, the binding energy of the exciton is smaller than or comparable with the thermal energy at 300K, explaining the excellent performance of the devices [1].

In the second part, I will focus on the exciton fine structure in single crystal MAPbBr₃. To the best of our knowledge, the fine structure splitting of the bright exciton triplet state has never been observed in a bulk semiconductor. Here we report on the observation a giant FSS of the bright 1s exciton states in a bulk high quality MAPbBr₃ single crystal. We have performed a detailed magneto-optical investigation to reveal the FSS as large as 200 μ eV. Such a large FSS in bulk material indicates a strong symmetry breaking in the orthorhombic crystal lattice and/or significant Rashba enhancement of the FSS. For our bulk single crystal quantum confinement can be excluded so our results give direct insight into the FSS related solely to the crystal structure of bulk MAPbBr₃. [2]

[1] Nature Physics 11, 582 (2015), Energy Environ. Sci. 9, 962 (2016), Energy Environ. Sci. 10, 1358 (2017), J. Phys. Chem. Lett 8, 1851 (2017), ACS Energy Letters 2, 1621 (2017)

[2] M. Baranowski et al submitted.

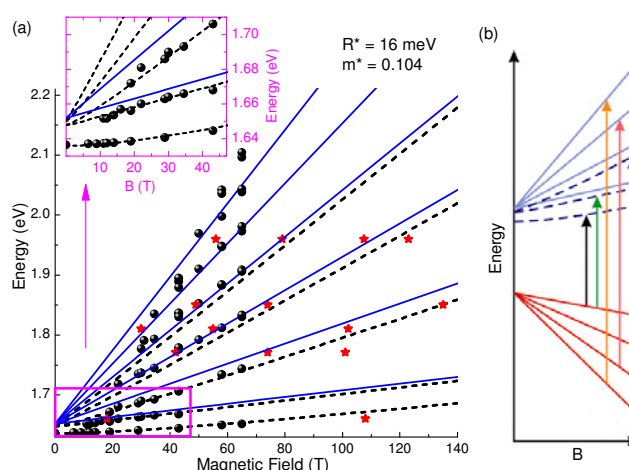


Figure 1 : (a) Full fan using data from long pulse fixed field spectra (black circles) and fixed energy fast field sweep data (red stars). Inset to (a) lower fields measured using fixed field spectra. (b) shows a schematic of the transitions between the free electron and hole levels (solid lines) and the excitonic transitions (dashed lines).

Damping of Josephson oscillations in strongly correlated one-dimensional atomic gases

J. Polo^{a*}, V. Ahufinger,^b F. W. J. Hekking^a, and A. Minguzzi^a

a. Univ. Grenoble Alpes, CNRS, LPMMC, F-38000 Grenoble, France

b. Departament de Física, Universitat Autònoma de Barcelona, E-08193 Bellaterra, Spain

* juan.polo@lpmmc.cnrs.fr

We study the Josephson oscillations of two strongly correlated one-dimensional bosonic clouds separated by a localized barrier. Using a quantum-Langevin approach and the exact Tonks-Girardeau solution in the impenetrable-boson limit, we determine the dynamical evolution of the particle-number imbalance, displaying an effective damping of the Josephson oscillations which depends on barrier height, interaction strength and temperature. We show that the damping originates from the quantum and thermal fluctuations intrinsically present in the strongly correlated gas. Thanks to the density-phase duality of the model, the same results apply to particle-current oscillations in a one-dimensional ring where a weak barrier couples different angular momentum states.

Electric-field induced doping of $\text{YBa}_2\text{Cu}_3\text{O}_7$

R. Poloni^{a*}, A. L. Mariano^a, and J. Garcia-Barriocanal^b

a. SIMaP Laboratory, CNRS, Univ. Grenoble Alpes, Grenoble

b. Characterization Facility, University of Minnesota, Minneapolis MN 55455

* roberta.poloni@grenoble-inp.fr

Electrostatic doping by means of electric double layer (EDL) techniques has recently been demonstrated to be an ideal tool to study the physics of high T_c cuprates. They enable controlled changes of carrier concentration [1,2] by making use of an ionic liquid as a gate dielectric. A high density of charge carriers (as high as 10^{14-15}cm^{-2}) is accumulated at the oxide interface to screen the strong electric field generated within the EDL. Large changes of the doping concentration allow exploring wide regions of the phase diagram and examining boundaries between superconducting and non superconducting phases. Aside from these electrostatic doping effects, recent studies of the EDL gating revealed that the electric field may also create vacancies in these oxides [3], which in turn may have a doping effect that could resemble that obtained from traditional chemistry methods.

We have recently addressed the doping mechanisms involved in EDL gating of a thin film of the high temperature superconductor $\text{YBa}_2\text{Cu}_3\text{O}_{7-d}$ (YBCO) by combining experiments and theory [4]. In order to explain our experimental results of in-situ x-ray absorption spectroscopy and electric transport measurements, we performed density functional theory simulations of the NEXAFS region for electrostatically doped YBCO and for oxygen doped $\text{YBa}_2\text{Cu}_3\text{O}_6$, using bulk calculations, in order to assist the interpretation of the data. Our computed spectra show that the measured NEXAFS is compatible with a progressive decrease of oxygen coordination of the Cu, suggesting changes in the oxygen content of the sample. We demonstrate that the reduced Cu-O coordination is specifically taking place at the CuO chains of the cuprate and not affecting the superconducting CuO planes [4]. Recently, we explicitly addressed the role of the electric field by computing the vacancy formation energy and the energy barrier for oxygen migration as a function of an applied field on a thin film of YBCO and discuss our results in the context of our previous experiments.

- 1 A. T. Bollinger et al., *Nature (London)* **472**, 458 (2011)
- 2 J. García-Barriocanal et al., *Phys. Rev. B* **87**, 024509 (2013)
- 3 J. Jeong et al., *PNAS* **112**, N4 1013 (2015)
- 4 A. Perez-Munoz et al., *PNAS* **114**, 215 (2017)

High temperature cuprate superconductors

Cyril Proust

Laboratoire National des Champs Magnétiques Intenses (CNRS, EMFL, INSA, UGA, UPS), Toulouse / Grenoble.

cyril.proust@lncmi.cnrs.fr

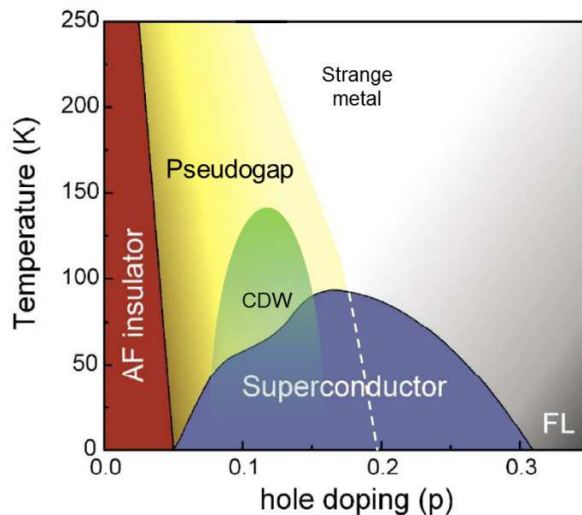


Figure 1: Generic temperature–doping phase diagram of high temperature superconductors. Various states are revealed: superconductivity, an antiferromagnetic Mott insulator at low doping, the pseudogap phase below a temperature T^* ending at a critical point p^* , a charge density wave (CDW) phase and a strange metal phase just above p^* . At high doping, a Fermi liquid (FL) behaviour is recovered.

After more than three decades, copper oxide superconductors continue to fascinate physicists. Not only the unique properties of superconductors—from loss-free transmission of electrical power, through levitated trains to the ultimate sensitivity in MRI—could all be accessed using liquid nitrogen but also there is a growing conviction that these materials host novel quantum phenomena. The core mysteries of the cuprates—the origin of electron pairing, the normal state pseudogap, the strange metal and the prominence of various forms of collective fluctuations such as charge density wave—arise from electron interactions that are most likely responsible for the exceptionally strong superconductivity. These are cornerstones of modern condensed matter physics that have acted as a catalyst for the development of experimental and theoretical tools.

Here, we aim to give a brief overview of the state of the art of high temperature superconductors [1]. We will then focus on the ground state properties of these materials, once superconductivity is removed by the application of a magnetic field [2-5].

[1] B. Keimer *et al.* From quantum matter to high-temperature superconductivity in copper oxides. *Nature* **518**, 179 (2015).

[2] N. Doiron-Leyraud *et al.* Quantum oscillations and the Fermi surface in an underdoped high- T_c superconductor. *Nature* **447**, 565 (2007).

[3] W. Wu *et al.* Magnetic-field-induced charge-stripe order in the high-temperature superconductor $\text{YBa}_2\text{Cu}_3\text{O}_y$. *Nature* **477**, 191 (2011).

[4] S. Badoux *et al.* Change of carrier density at the pseudogap critical point of a cuprate superconductor. *Nature* **531**, 210 (2016).

[5] S.E. Sebastian and C. Proust. Quantum oscillations in hole-doped cuprates. *Annu. Rev. Condens. Matter Phys.* **6**, 411 (2015).

Spin lattices of walking droplets

Giuseppe Pucci^{a,b*}, Pedro J. Sáenz^a, Alexis Goujon^a,
Jörn Dunkel^a, and John W. M. Bush^a

- a. Department of Mathematics, Massachusetts Institute of Technology, 77 Massachusetts Avenue, Cambridge, MA 02139, USA
- b. Institut de Physique de Rennes, UMR 6251 CNRS and Université Rennes 1, 35042 Rennes Cedex, France

* gpucci@mit.edu

Millimetric liquid droplets can walk while bouncing on the surface of a vibrating liquid bath [1, 2]. We present experiments that demonstrate the spontaneous emergence of collective behavior in spin lattices of these walking droplets [3]. Circular wells at the bottom of the fluid bath encourage individual droplets to walk in clockwise or counter-clockwise direction along circular trajectories centered at the lattice sites. A thin fluid layer between the wells enables wave-mediated interactions between neighboring walkers resulting in coherent rotation dynamics across the lattice. When the pair-coupling is sufficiently strong, interactions between neighboring droplets may induce local spin flips leading to anti-ferromagnetic order.

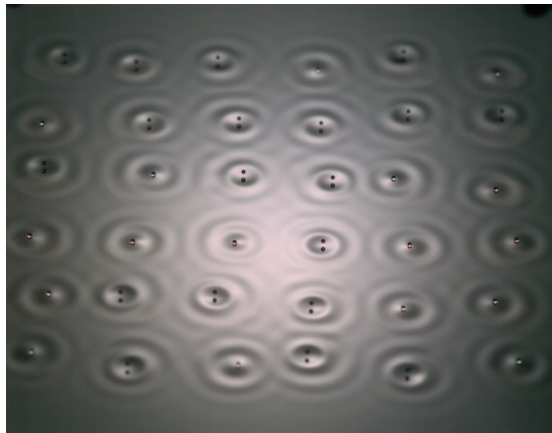


Figure 1: A 2D spin lattice of walking droplets.

This work was supported by the US National Science Foundation through grants CMMI-1333242, DMS-1614043 and CMMI-1727565. G. P. thanks the program CNRS Momentum for its support.

- [1] Y. Couder, S. Protière, E. Fort, and A. Boudaoud. Walking and orbiting droplets. *Nature*, 437:208 (2005).
- [2] J. W. M. Bush. Pilot-wave hydrodynamics. *Ann. Rev. Fluid Mech.*, 47:269–292 (2015).
- [3] P. J. Sáenz, G. Pucci, A. Goujon, T. Cristea-Platon, J. Dunkel, J. W. M. Bush. Spin lattices of walking droplets, to appear in *Phys. Rev. Fluids* (2018).

The Low Energy Frontier of Particle Physics or the Quest for Dark Matter with Experimental Tools of Condensed Matter Physics

Pierre Pognat^{a*}

a. LNCMI, CNRS/UGA, 38042 Grenoble, Cedex 9, France

* Pierre.Pognat@lncmi.cnrs.fr

Particle physics is not only confined to the high energy range. There are unexplored territories at ultra-low energies, *i.e.* sub-eV to eV, which are also very promising for the identification of the dark matter (DM) of our Universe. The emblematic particle of this physics is the axion, a pseudo-scalar particle predicted independently in 1978 by two Nobel Prize Laureates in Physics, S. Weinberg [1] and F. Wilczek [2], to solve the fundamental problem of the apparent non-violation of the CP symmetry by the strong interaction (QCD). This constitutes one of the remaining sand grains in the gear of the standard model of particle physics. Standard axion at the electroweak scale with a mass around 100 keV has been excluded after extensive experimental searches. This has led the scientific community to consider the case of "almost" invisible axion, *i.e.* with a mass and coupling to other particles extremely weak. If the axion mass is in the range 10^{-6} to 10^{-2} eV, this particle could also be responsible for the DM of our universe and constitutes one of the rare non-supersymmetric candidates. On the other hand, various ultra-light and weakly interacting scalar and pseudo-scalar particles are naturally present in string theory without the need of solving the strong CP problem. This new family of particles has coined the name of WISPs for Weakly Interacting Slim Particles in complement to the WIMPs standing for Weakly Interacting Massive Particles. P. Sikivie showed in 1983 [3] that the invisible axion as well as axion like particles (ALPs), a subfamily of WISPs, could be detected via a chiral anomaly that modifies Maxwell's equations. In this context, the OSQAR experiment at CERN aims to detect ALPs from the light shining through wall scheme and the interaction of 20 W CW laser beam with magnetic field lines produced by two spare LHC dipoles. It will be presented in detail together with the last results obtained, which are the most sensitive to date for this type of experiment [4]. More recently this experiment has been extended in the search of Chameleons [5], a special type of particle with a mass depending on the density of the surrounding medium and which could be responsible for the dark energy. Other types of WISP search experiments in operation worldwide will also be briefly described as well as future projects. One of them, a new haloscope will be housed in the modular hybrid magnet platform in construction at LNCMI-Grenoble to profit from the static magnetic fields produced, ranging from 43 T in 34 mm diameter down to 9 T in 800 mm diameter [6], and will probe the flow of DM of our galactic halo crossing the Earth [7]. This unique opportunity will also be presented as well as the technological challenges to overcome.

[1] S. Weinberg, Phys. Rev. Lett. 40, 223 (1978).

[2] F. Wilczek, Phys. Rev. Lett. 40, 279 (1978).

[3] P. Sikivie, Phys. Rev. Lett. 51, 1415 (1983); Phys. Rev. D 32 2988 (1985).

[4] R. Ballou, P. Pognat *et al.* (OSQAR collaboration), Phys. Rev. D 92, 092002 (2015)

[5] <https://cds.cern.ch/record/2001850/files/SPSC-P-331-ADD-1.pdf>

[6] P. Pognat *et al.*, IEEE Trans. Appl. Supercond. vol. 28, no. 3 (2018), 4300607.

[7] <https://bib-pubdb1.desy.de/record/395493/files/fulltext.pdf>

Theoretical approaches to cavitation in confined conditions

Fatima Ait-Hellal^a, Pierre-Etienne Wolf^b and Joël Puibasset^{a*}

- a. Interfaces, Confinement, Matériaux et Nanostructures, CNRS et Université d'Orléans, UMR 7374, Orléans
- b. Institut Néel, CNRS/UGA, UPR2940, Grenoble

* puibasset@cnrs-orleans.fr

Today, the common trend to deal with cavitation in confined systems is to rely on detailed numerical simulations. Due to their high computational cost, these simulations are however limited to simple geometries, such as a single pore ink-bottle shaped, and cannot be extended to more complex geometries, such as disordered porous glasses. One of the goals of the ANR CAVCONF is to go beyond this limitation.

In this contribution, we first present a simplified model of cavitation in confined geometries. This new model extends the Saam and Cole's model [1] of adsorption and desorption in a single cylindrical pore to the case of finite thermal activation. It thus describes activated nucleation for condensation, and cavitation for evaporation, generalizing in the latter case the Classical Nucleation Theory (CNT) by including the effect of the fluid interaction with the walls. In the CAVCONF project, we aim to compare the predictions issued from this model to experimental results for helium and nitrogen, so as to assert its validity for simple fluids in large enough cavities. This approach has however limitations, in particular with respect to the continuum (macroscopic) description of the fluid. This led us to develop at ICMN numerical simulations based on a realistic atomistic modelisation of the fluid, allowing to tackle issues like the influence on cavitation of the fluid structure near the solid, or the influence of the solid heterogeneity on cavitation. This approach is also well suited to study more complex fluids, in particular polar molecules such as water, or linear molecules such as alkanes. We will describe the first results of this approach.

- [1] W. F. Saam and M. W. Cole. Excitations and thermodynamics for liquid-helium films. *Phys. Rev. B*, 11, 1086–1105, (1975).

Ce travail est soutenu par l'ANR dans le cadre du projet CAVCONF.

Molecular simulation study of confined supercooled water

J. Puibasset^{a*}, J.-M. Zanotti^b, P. Judeinstein^b

- a. Interfaces, Confinement, Matériaux et Nanostructures, UMR7374, CNRS, Université d'Orléans, 1b rue de la Férollerie, 45071 Orléans cedex 02
- b. Laboratoire Léon Brillouin (CEA-CNRS), Université Paris-Saclay, 91191 Gif-sur-Yvette, France

* puibasset@cnrs-orleans.fr

L'eau présente de nombreuses propriétés originales, souvent en lien avec sa structure à l'échelle moléculaire, ou au-delà à travers le réseau de liaisons hydrogène. Comment évoluent ces propriétés lorsqu'on se place dans des conditions de frustration géométrique du réseau de liaisons hydrogène, par exemple en situation de confinement bidimensionnel ? Par ailleurs, en dessous de 0°C, l'eau liquide métastable présente aussi des propriétés très originales. Or, le confinement de l'eau permet souvent d'atteindre plus facilement cet état surfondu. Nous nous proposons donc d'étudier les propriétés thermodynamiques de l'eau métastable surfondue en situation de confinement au sein d'un matériau poreux hydrophile.

Les résultats expérimentaux obtenus pour de l'eau confinée dans de la silice nanoporeuse sous forme de films bidimensionnels montrent un comportement paradoxal de l'eau surfondue [1].

L'approche expérimentale sera complétée par une étude par simulation moléculaire. En effet, les dimensions mises en jeu permettent un traitement statistique par Monte Carlo ou Dynamique Moléculaire à l'aide de potentiels semi-empiriques. Différents modèles d'eau seront choisis afin d'évaluer la robustesse des résultats. Les calculs seront effectués pour des films d'eau de différentes épaisseurs adsorbés sur des surfaces plus ou moins hydrophiles de type silice, à des températures entre 150K et 270K. Le travail s'attachera à évaluer des propriétés structurales et thermodynamiques afin d'interpréter les résultats expérimentaux.

[1] J.-M. Zanotti, P. Judeinstein, S. Dalla-Bernardina, *et al.*, Competing coexisting phases in 2D water, *Sci. Reports*, 6, 25938 (2016)

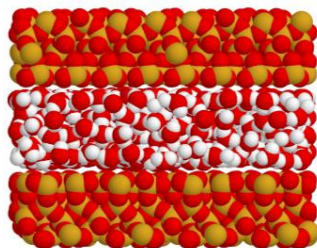


Figure 1 : eau confinée dans un nanopore de silice.

Molecular simulation study of silver nanoparticles on silica substrate

J. Puibasset^{a*}, C. Andreazza-Vignolle^a, P. Andreazza^a and C.Mottet^b

- a. Interfaces, Confinement, Matériaux et Nanostructures, UMR7374, CNRS, Université d'Orléans, 1b rue de la Férollerie, 45071 Orléans cedex 02
- b. Centre Interdisciplinaire de Nanoscience de Marseille (CINaM), UMR 7325 CNRS-AMU, Campus de Luminy, case 913, 13288 Marseille, Cedex 9, France

* puibasset@cnsr-orleans.fr

Properties of metallic nanoparticles differ from bulk. Moreover, experimental and simulation data show that the support used to produce these nanoparticles, despite weakly interacting like amorphous silica, may have a non-negligible effect, in particular on the morphology and structure of the nanoparticle [1]. We are thus interested in the prediction of the relative stability of the various structures a supported nanoparticle can adopt.

Considering the typical dimensions of the system (few nanometers), a molecular approach based on effective potentials will be considered. The metal-metal interaction is modeled by a tight-binding semi-empirical potential within the second moment approximation (TB-SMA), the interactions between atoms constituting silica are described by the mTTAM potential, and the metal-silica interaction is based on a Lennard Jones potential, with parameters adjusted on experimental and Density Functional Theory calculations. The support will be varied, in particular its surface nature and roughness.

[1] A. C. Ngandjong, C. Mottet, and J. Puibasset, J. Phys. Chem. C 120, 8323 (2016), J. Phys. Chem. C 121, 3615 (2017)

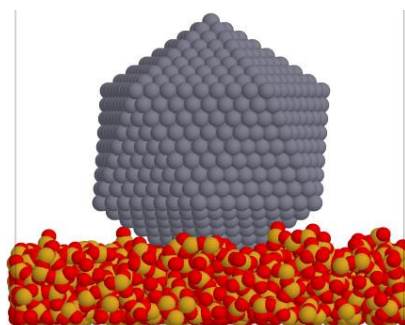


Figure 1 : Silver icosahedron on rough silica support.

Introduction to scattering with new x-ray sources

Sylvain Ravy*

Laboratoire de Physique des Solides, bât. 510, Univ. Paris-Sud, Université Paris-Saclay, CNRS,
91405 Orsay, France

* sylvain.ravy@u-psud.fr

The advent of new X-ray sources such as 3rd generation synchrotron, their upgraded offsprings, or X-ray Free Electron Lasers (XFEL), have considerably changed the way we use X-rays to study condensed matter. This talk aims at discussing pedagogically the conceptual leaps these sources have achieved, and how scattering experiments have evolved to take advantage of the coherent, temporal, or nanometric properties of modern X-ray beams.

LES NANOTUBES: UNE VOIE VERS L'OPTOÉLECTRONIQUE

B. Réa^{a*}, Y. Chen^a, G. Royal^b, S. Cobo^b, E. Flahaut^c, N. Bendiab^a, L. Marty^a

- a. Univ. Grenoble Alpes, CNRS, Grenoble INP, Institut Néel, 38000 Grenoble, France
- b. Univ. Grenoble Alpes, DCM UMR-5250, 38058 Grenoble, France
- c. CIRIMAT, UMR CNRS-UPS-INP, 31062 Toulouse, France

* brice.rea@neel.cnrs.fr

Les propriétés optiques des nanotubes offrent la possibilité de concevoir de nouveaux types de transistors, notamment avec des nanotubes suspendus. Il reste possible d'ajuster leur dopage à l'aide d'une grille électrostatique [1]. Nous nous sommes donc intéressés aux propriétés optoélectroniques afin de réaliser un effet de conversion photon/électron à l'aide de molécules photoactives. Une excitation lumineuse permet alors de modifier les propriétés électroniques des nanotubes [2] (Figure 1.a).

Pour pouvoir optimiser la réponse des nanotubes nous cherchons à obtenir des nanotubes individuels suspendus. Ainsi nous nous affranchissons des interactions avec le substrat accédant à leurs propriétés intrinsèques. Les nanotubes sont fabriqués par CVD et caractérisés par Raman et transport électronique.

Deux voies sont à l'étude, consistant à déposer des molécules à la surface par "π-stacking" ou à greffer des molécules de manière covalente (Figure 1.b). Nous testerons 2 types de molécules: des chromophores de type porphyrine et des switches optiques (ces molécules change de conformation avec la lumière) [3]. À terme, nous déterminerons quels sont les mécanismes en jeu, actifs et/ou efficaces. Ce qui nous conduira à des applications en nanoélectronique ou électronique moléculaire.

- [1] S. Liu, J. Zhang, and J. P. Nshimiyimana, Ultraclean individual suspended single-walled carbon nanotube field effect transistor, *Nanotechnology*, **29**, 175302 (2018).
- [2] Y. Chen et al., Light Control of Charge Transfer and Excitonic Transitions in a Carbon Nanotube/Porphyrin Hybrid, *Adv. Mater.*, **29**, 1605745 (2017).
- [3] D. Roldan et al., Charge transport in photoswitchable dimethyldihydropyrene-type single-molecule junctions. *J. Am. Chem. Soc.*, **135** (16), 5974 (2013)

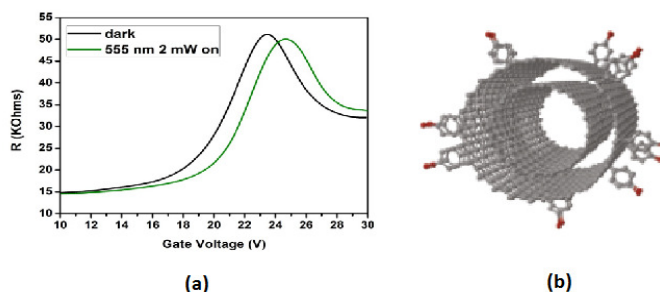


Figure 1 : (a) Modification de la caractéristique de transfert d'un transistor nanotube hybride (CNT/TPPZn) par excitation lumineuse à une longueur d'onde de 555nm (vert) par rapport à un état sans excitation (noir). (b) Reconstitution 3D d'un nanotube avec des molécules greffées de façon covalente à la surface.

Droplets-based millifluidic for the establishment of protein-polysaccharide phase diagrams

Chloé Amine, Joëlle Davy, Adeline Boire, Denis Renard*

UR1268 Biopolymères Interactions Assemblages, INRA, 44316 Nantes, France

* denis.renard@inra.fr

Texture, structure, taste as well as stability of food products are strongly related to its constituent's interactions. The understanding of these interactions is still a challenge in food-processing. Besides lipids or flavour, proteins and polysaccharides are widely used in food products. It is already well known that under specific conditions protein-polysaccharide mixture can lead to liquid-liquid phase separation, of segregative or associative type. To highlight the conditions of phase separation, a phase diagram is established. However, such a study, generally performed in bulk is time and raw material consuming. Therefore alternative strategies for rapid phase diagram determination using microfluidics recently emerged. Microfluidic enables a large reduction of engaged volume, a precise control over experimental conditions and mixed systems composition as well as an acceleration of reaction time. Nevertheless, these techniques were only described for segregative phase separated systems [1], [2]. In the present work we developed a droplets-based millifluidic device for rapid phase diagram building of associative phase separated system [3]. Binodal curve was determined by turbidity measurements within the droplets using image analysis. Cloud points, corresponding to the onset of phase separation, were defined as the composition corresponding to a 10% increase in turbidity compared to the original reference solution. The first part of the study was dedicated to the proof of concept using a colloidal suspension of titan dioxide. We evidenced proportionality between the turbidity measured in bulk using spectrophotometry and those determined within the droplet by image analysis. The second part of the study was devoted to establish the phase diagram of an associative phase separated system: β -lactoglobulin (BLG) / Gum Arabic (GA), first in bulk and then using the more innovative droplets-based millifluidic approach where the composition and total concentration were finely tuned by flow rates variation (Figure 1). Considering the high similarities obtained at both scales, we now plan to extend the method to several protein-polysaccharide mixtures.

[1] J. Leng, M. Joanicot and A. Ajdari. Microfluidic exploration of the phase diagram of a surfactant/water binary system. *Langmuir*, **23**, 15-17 (2007).

[2] D. Silva, A. Azevedo, P. Fernandes, V. Chu, J. Conde and M. Aires-Barros. Determination of aqueous two phase system binodal curves using a microfluidic device, *J.Chromatogr. A.*, **1370**, 115-120 (2014).

[3] C. Amine, A. Boire, J. Davy, M. Marquis and D. Renard, Droplets-based millifluidic for the rapid determination of biopolymers phase diagrams, *Food Hydrocolloids* **70**, 234 (2017)

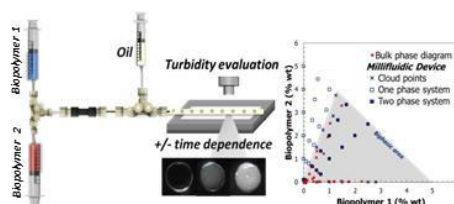


Figure 1. Droplets-based millifluidic device to rapidly map phase diagrams of biopolymers mixtures

Liquides de spins classiques et quantiques du réseau Rubis

Julien Robert^{a*} et Arnaud Ralko,^{a*}

a. Institut Néel, CNRS and Univ. Grenoble Alpes, 38042 Grenoble, France

* julien.robert@neel.cnrs.fr, arnaud.ralko@neel.cnrs.fr,

Nous nous intéressons dans la présente étude aux propriétés classiques et quantiques du modèle de Heisenberg sur réseau rubis (cf. Fig. 1). Le principal intérêt de ce système réside dans le fait que les trois types d'interactions J_1 , J_2 , et J_3 présentes permettent de le décrire, selon l'interaction dominante, de différentes manières : un réseau hexagonal de triangles, un réseau triangulaire d'hexagones, ou encore un réseau de chaînes entrelacées. De la compétition de ces trois régimes extrêmes résulte des diagrammes de phases classique et quantique très riches incluant tout un panel d'états allant de simples ordres magnétiques à des phases plus complexes n'étant caractérisées par aucun paramètre d'ordre local (liquides de spin), en passant par des phases partiellement ordonnées par le désordre. Nous montrons en particulier qu'à la limite classique ce diagramme de phase permet de voir sous un jour nouveau la phase magnétique présentant la plus grande dégénérescence ($J_1 = J_2 = J_3 > 0$), récemment caractérisée comme l'équivalent classique d'un liquide de spin quantique \mathbb{Z}_2 [1]. Ici, ses corrélations originales apparaissent comme un mélange des différents modes locaux des liquides de spin voisins. Lorsque les fluctuations quantiques sont prises en compte via une théorie de bosons de Schwinger, nous montrons que certaines phases classiques entraînent l'apparition de phases de singulets de spins gappées, e.g. une phase résonnante de plaquettes hexagonales ou encore des liquides de spins quantiques [2].

[1] J. Rehn, A. Sen, and R. Moessner, PRL **118**, 047201 (2017)

[2] J. Robert and A. Ralko, in preparation (2018)

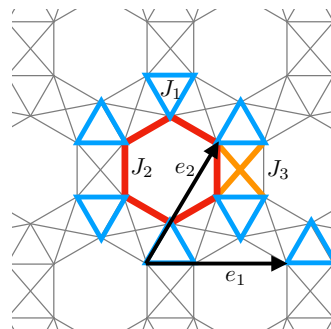


Figure 1: Représentation du réseau rubis constitué des trois interactions J_1 , J_2 , et J_3

Topological insulators and Rashba interfaces as efficient spin-charge current converters

J.-Carlos Rojas-Sánchez^{a*}, A. Fert^b, J.-L. Bello^a, D. Cespedes-Berrocal^{a,c}, C. Guillemard^{a,e}, S. Andrieu^a, O. Copie^a, M. Hehn^a, S. Petit-Watlot^a, A. Barthélémy^b, M. Bibes^b, J.M. George^b, H. Jaffres^b, E. Lesne^b, N. Reyren^b, D.-C. Vaz^b, L. Vila^d, J.P. Attané^d, Y. Fu^d, S. Gambardelli^d, M. Jamet^d, A. Marty^d, S. Oyarzun^d, Y. Ohtsubo^e, P. LeFèvre^e, F. Bertran^e, A. Taleb-Ibrahimi^e

- a. *Université de Lorraine*, CNRS, Institute Jean Lamour, F-54011 Nancy, France
- b. CNRS/Thales, F-91767 Palaiseau, France
- c. *Universidad Nacional de Ingeniería*, Lima, Peru
- d. Université de Grenoble Alpes, CEA, CNRS, INAC-SPINTEC, F-38000 Grenoble, France
- e. Synchrotron SOLEIL, Gif-sur-Yvette F-91192, France

* juan-carlos.rojas-sanchez@univ-lorraine.fr

New materials with large efficiency of spin-charge current interconversion are highly desirable to study new physical phenomena as well as for spintronics applications. The spin-orbit coupling (SOC) in the 2DEG states at Topological Insulator (TI) or Rashba Interfaces is predicted to be more efficient than their 3D counterparts for such interconversion. We have found the highest efficiency at room temperature using the topological insulator α -Sn [1]. The spin-to-charge current conversion in such 2D systems is called Inverse Edelstein Effect (IEE), also known as spin galvanic effect [2]. We will show results of spin-to-charge conversion by spin pumping experiments and their analysis in term of inverse Edelstein Length [1,3-5]. I will also show additional examples of conversion between spin-to-charge at the following Rashba interfaces: Ag/Bi(111) [3], Fe/Ge(111) [4] and LAO/STO(001) [5].

Experimental results based on ARPES and spin pumping indicate that direct contact of metallic ferromagnetic layer is detrimental for the surfaces states of topological insulators but we can keep the surfaces states of α -Sn using Ag spacer [1]. I will use the conversion parameter obtained at room temperature with α -Sn to demonstrate the very large advantage of the SOC effects in 2D interface states with respect to the Spin Hall Effect (SHE) of 3D metals and the resulting perspective for low power spintronic devices. I will focus especially in the prediction of giant spin Seebeck effect using insulator ferrimagnet $Y_3Fe_5O_{12}$ (YIG) in YIG/ α -Sn films structures.

[1] J.-C. Rojas-Sánchez. et al. *Phys. Rev. Lett.* **116**, 096602 (2016). ArXiv 1509.02973 (2015)

[2] S. D. Ganichev et al. *Nature* **417**, 153 (2002)

[3] J.-C. Rojas-Sánchez et al. *Nat. Comm* **4**, 2943 (2013)

[4] S. Oyarzun, J.-C. Rojas-Sánchez et al. *Nat. Comm.* **7**, 13857 (2016)

[5] E. Lesne, J.-C. Rojas-Sánchez et al. *Nat. Mat.* **15**, 1261 (2016)

Electronic and magnetic properties of CePt₂In₇

M. Raba^{a,b,c,*}, E. Ressouche^d, N. Qureshi^e, C. V. Colin^{b,c}, V. Nassif^{b,c},
S. Ota^f, Y. Hirose^g, R. Settai^g, D. Aoki^h, P. Rodière^{b,c} and I. Sheikin^a

- a. Laboratoire National des Champs Magnétiques Intenses (LNCMI-EMFL), CNRS, UGA, 38042 Grenoble, France
- b. Université Grenoble Alpes, Institut Néel, F-38000 Grenoble, France
- c. CNRS, Institut Néel, F-38000 Grenoble, France
- d. INAC, CEA and Univ. Grenoble Alpes, CEA Grenoble, F-38054 Grenoble, France
- e. Institut Laue Langevin, 71 rue des Martyrs, BP156, 38042 Grenoble Cedex 9, France
- f. Graduate School of Science and Technology, Niigata University, Niigata 950-2181, Japan
- g. Department of Physics, Niigata University, Niigata 950-2181, Japan
- h. IMR, Tohoku University, Ibaraki, Japan

* matthias.raba@lncmi.cnrs.fr

The appearance of unconventional superconductivity in the vicinity of a quantum critical point (QCP), a second order phase transition at zero temperature, is a common trend in Ce-based heavy fermion compounds. A more recent and still somewhat controversial issue is the effect of the Fermi surface (FS) dimensionality on this superconductivity. Indeed, reduced dimensionality of the FS leads to nesting-type magnetic instabilities and thus enhances the superconductivity. The exact knowledge of the FS topology of heavy fermion systems is, therefore, essential. In addition, this information allows distinguishing if the *f*-electrons are itinerant or localized, i.e. whether they contribute to the FS or not.

At ambient pressure and zero magnetic field, the heavy-fermion compound CePt₂In₇ exhibits an antiferromagnetic (AFM) phase below 5.5 K. The AFM order is suppressed at a pressure-induced (QCP) at $P_c = 3.2$ GPa [1], around which a superconducting dome emerges. A magnetic-field-induced QCP is also expected at $H_c \sim 55$ T [2]. The 4*f*-electrons of Ce are known to be fully localized at ambient pressure and moderate magnetic fields [3]. However, the question of whether the *f*-electrons are itinerant or localized above the QCPs is still open due to the lack of quantum oscillation studies either at high pressure or high magnetic field.

The AFM structure of this compound, as determined from a single-crystal neutron diffraction [4], suggests that its magnetic Brillouin zone is eight times smaller than the crystallographic one. That is why high enough magnetic fields are required to observe large FSs of CePt₂In₇ via magnetic breakdown.

Our recent results of quantum oscillations measured by torque technique in pulsed magnetic fields suggest that the FSs do not change up to 70 T, which is well above the field induced QCP. However, a drastic change of the effective masses occurs close to H_c . I will also present first quantum oscillation measurements under pressure, which will allow us to probe the FSs across P_c .

[1] V. A. Sidorov et al., Phys. Rev. B **88**, 020503(R) (2013)

[2] Y. Krupko et al., Phys. Rev. B **93**, 085121 (2016)

[3] K. Götze et al., Phys. Rev. B **96**, 075138 (2017)

[4] M. Raba et al., Phys. Rev. B **95**, 161102(R) (2017)

Reciprocity in diffusive spin-current circuits

Revaz Ramazashvili^{a*}, Yaroslav Bazaliy,^b

a. Laboratoire de Physique Théorique, Université de Toulouse, CNRS, UPS, France

b. University of South Carolina, Columbia SC 29208, USA

* revaz@irsamc.ups-tlse.fr

Similarly to their purely electric counterparts, spintronic circuits may be presented as networks of lumped elements. Due to interplay between spin and charge currents, each element is described by a matrix conductance $\mathcal{G}_{tt'}^{ab}$, where a and b denote spin and charge indices, while t and t' label the terminals. We establish reciprocity relations [1] between the entries of the conductance matrix of a multi-terminal linear diffusive device, comprising normal-metal and strong-ferromagnet elements:

$$\mathcal{G}_{tt'}^{ab} = \mathcal{G}_{t't}^{ba}.$$

In particular, reciprocity equates the spin transmissions through a two-terminal element in the opposite directions: $\mathcal{G}_{12}^{ab} = \mathcal{G}_{21}^{ba}$. When applied to “geometric spin ratchets”, reciprocity shows that certain effects, announced [2] for such devices, are, in fact, impossible.

- [1] Ya. B. Bazaliy and R. R. Ramazashvili, Reciprocity in diffusive spin-current circuits (to appear; unpublished at the moment of the abstract submission)
- [2] R. M. Abdullah, A. J. Vick, B. A. Murphy, and A. Hirohata, “Spin-current signal amplification by geometrical ratchet”, *J. Phys. D: Appl. Phys.* **47**, 482001 (2014); R. M. Abdullah, A. J. Vick, B. A. Murphy, and A. Hirohata, “Optimisation of geometrical ratchets for spin-current amplification”, *J. Appl. Phys.* **117**, 17C737 (2015).

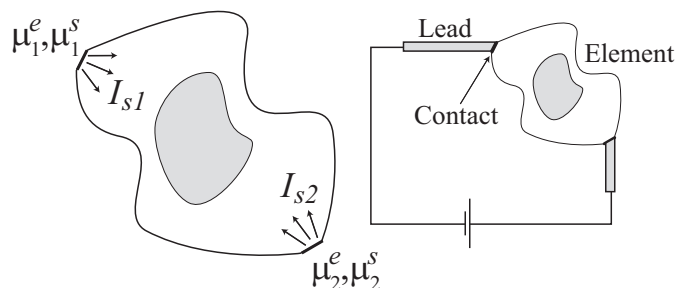


Figure 1: Left: a two-terminal element, an island with two contacts, where spin potentials $\mu_{1,2}^s$ and electric potentials $\mu_{1,2}^e$ are applied. White denotes a normal metal, gray denotes a ferromagnet. Right: the same connected to ferromagnetic leads (gray) in a spin circuit.

Diffusion inélastique des neutrons polarisés sur le spectromètre trois-axes à neutrons froids IN12

S. Raymond^{a*}, K. Schmalzl^b, W. Schmidt^b et T. Brückel^c

- a. Univ. Grenoble Alpes, CEA, INAC-MEM, 38000 Grenoble, France
- b. Forschungszentrum Jülich GmbH, Jülich Centre for Neutron Science at ILL, 38000 Grenoble, France
- c. Forschungszentrum Jülich GmbH, Jülich Centre for Neutron Science and Peter Grünberg Institut, 52425 Jülich, Germany

* raymond@ill.fr

La rénovation du spectromètre trois-axes à neutrons froids IN12 situé à l'Institut Laue Langevin, Grenoble a permis de rendre beaucoup plus régulière l'utilisation des neutrons polarisés [1]. Ceci est dû au fort flux de neutrons polarisés disponible et à la facilité de mise en place de la polarisation. Les éléments essentiels pour la polarisation sont sur IN12 : (a) un polariseur en transmission escamotable qui constitue une section de guide de neutrons, (b) une bobine de Helmholtz assurant un champ de guidage autour du monochromateur graphite à double focalisation (PG(002)) et (c) un analyseur d'Heusler à focalisation horizontale (Cu₂MnAl(111)). Les différentes configurations possibles concernent la polarisation longitudinale (avec bobine de Helmholtz et flipper de Mezei), la polarisation sphérique (avec CRYOPAD) et les expériences sous fort champ magnétique (vertical 12 T et horizontal 4 T). Ce dernier type d'expérience est largement facilité par la présence d'un flipper avant le monochromateur graphite qui de ce fait est peu sensible aux champs de fuite des bobines utilisées comme environnement échantillon.

Les thématiques en physique de la matière condensée couvrent les études fondamentales de magnétisme allant de la connaissance de base en lien avec des concepts théoriques innovants (systèmes de spins quantiques, supraconducteur non-conventionnels, frustration magnétique) aux études des mécanismes microscopiques en relation avec une propriété physique dans les matériaux magnétiques fonctionnels (composés magnétocaloriques, composés multiferroïques). Nous illustrons les possibilités d'expériences de diffusion inélastique de neutrons polarisés sur IN12 par des exemples d'études récentes sur la résonance de spin dans le supraconducteur CeCoIn₅ [2], la séparation des modes transverses et longitudinaux sous fort champ magnétique (12 T) dans le composé à chaîne de spin BaCo₂V₂O₈ [3] et la séparation entre les ondes de spin et les fluctuations de spin dans le composé à effet magnétocalorique inverse Mn₅Si₃ [4]

[1] K. Schmalzl, W. Schmidt, S. Raymond, H. Feilbach, C. Mounier, B. Vettard and T. Brückel, Nucl. Instrum. Methods A 819 (2016) 89.

[2] S. Raymond and G. Lapertot, Phys. Rev. Lett. 115 (2015) 037001.

[3] Q. Faure, S. Takayoshi, S. Petit, V. Simonet, S. Raymond, L.-P. Regnault, M. Boehm, J. S. White, M. Månsson, Ch. Rüegg, P. Lejay, B. Canals, T. Lorenz, S. C. Furuya, T. Giamarchi, B. Grenier, arXiv : 1706.05848

[4] N. Biniskos, K. Schmalzl, S. Raymond, S. Petit, P. Steffens, J. Persson and T. Brückel, arXiv:1802.07511.

SAMSON: Software for Adaptive Modeling and Simulation Of Nanosystems

Stephane Redon^{a+}

a. Univ. Grenoble Alpes, Inria, CNRS, Grenoble INP*, LJK, 38000 Grenoble, France

* Institute of Engineering Univ. Grenoble Alpes

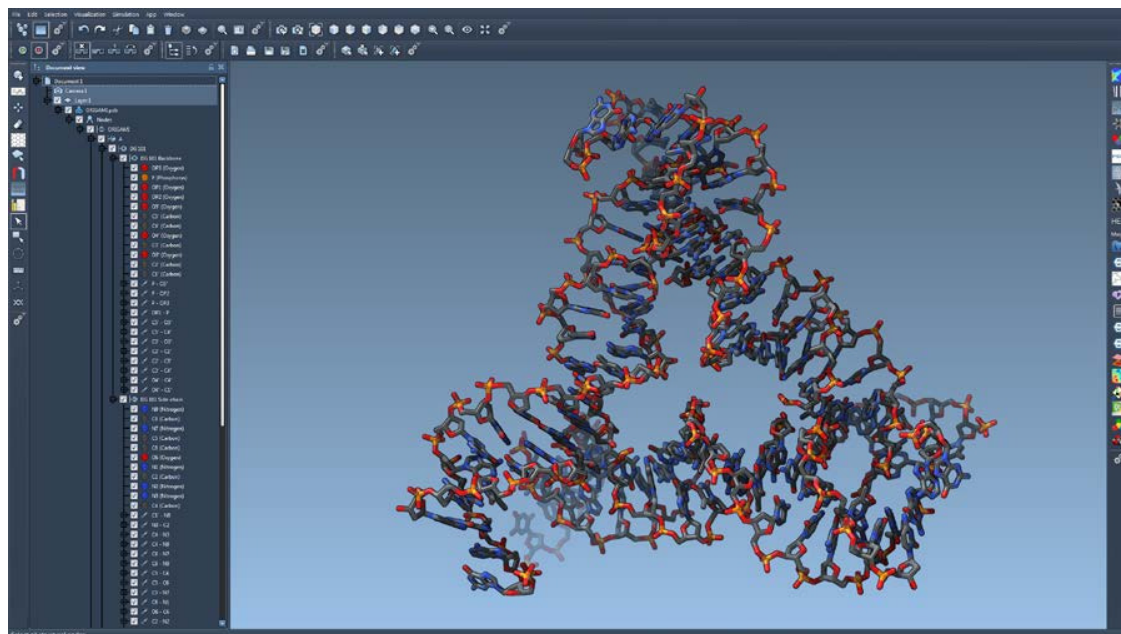
+ stephane.redon@inria.fr

SAMSON is a software platform for computational nanoscience that can be downloaded from SAMSON Connect at <https://www.samson-connect.net>.

SAMSON integrates modeling and simulation to aid in the analysis and design of molecular systems. For example, as-rigid-as-possible algorithms make it easy to produce large-scale deformations of DNA strands and protein structures. Force fields and minimization algorithms help users produce realistic models, and interactive simulations help users precisely control the shapes they want to produce. Furthermore, adaptive simulation algorithms make it easy to focus calculations on the most relevant part to increase performance [1-6].

Most important, a Software Development Kit allows developers to extend SAMSON's functionality by developing SAMSON Elements (modules for SAMSON), including e.g. new interaction models, editors, apps, wrappers or interfaces to existing software, connectors to web services, etc. SAMSON Connect is open for developers and users to share SAMSON Elements.

We will present SAMSON and its general design principles, as well as specific applications to structural biology and materials science.



- [1] S. Artemova and S. Redon, Physical Review Letters, 109:19, 2012
- [2] M. Bosson et al, Journal of Computational Physics, 231:6, 2012
- [3] M. Bosson et al, Journal of Computational Chemistry, 34:6, 2013
- [4] K. K. Singh and S. Redon, Modelling and Simulation in Materials Science and Engineering, 2017
- [5] S. Edoth and S. Redon, Journal of Computational Chemistry, 2018
- [6] K. K. Singh and S. Redon, Journal of Computational Chemistry, 39:8, 2018

Experimental study of a soliton gas

I.Redor^{a*}, H.Michallet^a, E.Barthelemy^a and N.Mordant^a

a. LEGI, CNRS, Grenoble-INP, Univ. Grenoble Alpes, France

* ivan.redor@univ-grenoble-alpes.fr

We study experimentally water surface gravity wave propagation in shallow water in a 36m long unidirectional glass-wall flume equipped with a piston-type wave-maker. The water depth is constant ($h = 12\text{cm}$) and the far end of the flume is a vertical wall where the waves can reflect. We measure with 7 cameras the water surface elevation along 14 meters with accuracy better than 1 mm at 20 frames per second.

We first compare our measurements to theoretical results in the simple cases of pair interactions between solitons.

Forcing continuously with a sinusoidal stroke at relatively low frequency (typically 0.6 Hz), the monochromatic wave generated at the wave-maker rapidly disintegrates into trains of solitons. The solitons reflect at each end of the flume, losing about half their amplitude through a flume length travelling distance. After multiple reflections of the first train, a soliton turbulence regime is reached (figure 1), in the sense that the wave energy is equally distributed along single straight lines in the wave number / frequency plane.

A similar regime has been observed in the ocean by Costa et al in 1. It can be viewed as a dense soliton gas theoretically described by the fully integrable Kaup-Boussinesq system of equation 2.

We discuss the applicability of such a theoretical framework relatively to experimental dissipation.

A set of experiments has been conducted for different stroke frequencies, amplitudes and water depths. We show that the soliton gas regime is obtained in a certain range of the Ursell number.

[1] Costa et al, PRL 113, 108501 (2014)

[2] Dabbs et al, Physical review, E 67, 016306(2003)

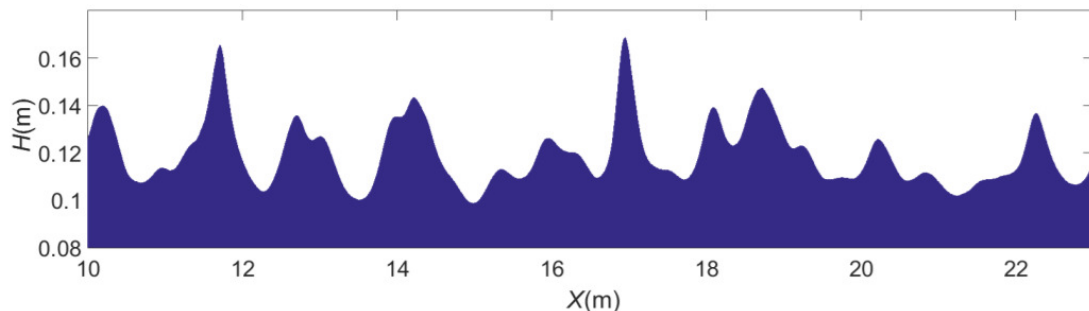


Figure 1: Surface elevation with distance from the wave maker in the soliton turbulence regime

Unexpected order-disorder phase transition in diacetylene alcohol Langmuir monolayer

S. Spagnoli¹, C. Allain², M-C Fauré³, M. Goldmann^{3,4}, M. Schott³, T.Rego³

¹ LIPhy, 140 avenue de la physique, BP87, 38402 Saint Martin d'Hères France.

² PPSM, 61 avenue du president Wilson 94235 Cachan France

³ INSP, Sorbonne Université, 4 place Jussieu 75252 Paris Cedex 05 France

⁴ Synchrotron SOLEIL L'Orme des Merisiers Saint-Aubin-BP48 91192 Gif/Yvette Cedex France

E-Mail address: rego@insp.upmc.pt

13-nOH ($\text{CH}_3(\text{CH}_2)_{12}\text{-C}\equiv\text{C-C}\equiv\text{C-(CH}_2)_{n-1}\text{-CH}_2\text{OH}$) with $n = 4, 6, 8$ are newly synthesized diacetylenic (DA) alcohols. These molecules present the advantage in forming a stable monolayer at the air/water interface with respect to DA acids (such as PCDA), which stable structure at the air/water interface arrangement is multilayered (trilayer). With the objective of characterizing the structure of 13-nOH Langmuir monolayers at the air/water interface, GIXD measurements (SIRIUS beamline – SOLEIL) were done at various temperatures from 12°C up to 18 °C.

We have highlighted for the three studied n values of 13-nOH monolayer an unexpected phase transition from a rectangular ordered structure to a disordered phase when the surface pressure increases. This transition is reversible and its surface pressure π_t decreases when the value of n increases. For instance, at $T = 12^\circ\text{C}$, we obtained $\pi_t = 22 \text{ mN/m}$, 15 mN/m and 10 mN/m for $n = 4, 6$ and 8 respectively. In the ordered phase (LC), the 13-4OH chain are tilted and the unit cell area is 0.26 nm^2 . The measured phase diagram for 13-4OH is presented figure 1. In the case of 13-6OH and 13-8OH, in-situ UV-vis absorption measurement shows that some polymerization occurs under X-ray irradiation leading to an evolution of the structure during the GIXD experiment.

The DA block ($\text{C}\equiv\text{C-C}\equiv\text{C}$) is formed by 4 rigid carbon meaning that 6 carbons are aligned. The observed unusual transition may then be due to a mismatch between the stable conformations of the DA and the one of the flexible parts of the chain. The unique difference, between the three molecules, is the length of the alkyl part between the DA group and the OH head. Fatty acids and fatty alcohols exhibit the same generic phase diagram indicating that small polar heads have no major impact on the structure. However, to the best of our knowledge, such a transition has not been observed in DA-acid, so we assume that the hydrophilic part must play an unneglectable role in the self-assembly of these DA alcohols.

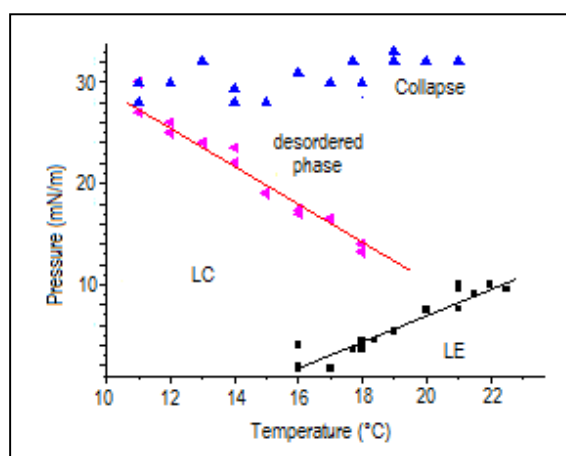


Figure 1: 13-4OH phase diagram

The Casimir interaction in a one-dimensional Bose gas

Reichert Benjamin^{a*}, Aleksandra Petković,^a Zoran Ristivojević^a

a. Laboratoire de Physique Théorique, Université de Toulouse, CNRS, UPS, 31062 Toulouse, France

* reichert@irsamc.ups-tlse.fr

When two impurities are immersed in a one-dimensional Bose gas, they impose constraints to density and phase fluctuations of the Bose gas. This modifies the ground state energy of the system, leading to a Casimir interaction between the two impurities. In prior publications, a short-range attraction that exponentially decays beyond the healing length ξ of the system was found, while at large distances ℓ between impurities, the effective interaction scales as $1/\ell^3$. The descriptions of the system used to find these behaviors were either not taking into account quantum corrections for the former, or described excitations using a linear dispersion relation, valid only at low energy, for the latter. In our work [1], we develop a consistent microscopic theory which overcomes these shortcomings. We are able to treat simultaneously the nonlinear spectrum of excitations and the quantum fluctuations. We obtain an analytical expression for the Casimir interaction, valid at all distances, resolving the discrepancies in the literature.

[1] B. Reichert, A. Petković, Z. Ristivojević, *manuscript under preparation*

Polarisation et anisotropie magnétique aux interfaces entre des métaux magnétiques et des couches moléculaires

K. Bairagi^a, A. Bellec^a, V. Repain^{a*}, C. Chacon^a, Y. Girard^a, S. Rousset^a, A. Smogunov^b, et C. Barreteau^b

a. Matériaux et Phénomènes Quantiques, Université Paris Diderot

b. Service de Physique de l'Etat Condensée, CEA Saclay

* vincent.repain@univ-paris-diderot.fr

La compréhension du couplage entre une couche moléculaire et une électrode magnétique est un élément central de l'électronique de spin moléculaire. Nous avons abordé cette question par des expériences sous ultra-vide de microscopie à effet tunnel polarisée en spin et d'effet Kerr magnéto-optique. Nous avons ainsi pu montrer que la polarisation en spin d'une molécule en contact avec un substrat magnétique était fortement dépendante de sa géométrie d'adsorption et de la symétrie du substrat [1]. Nous avons également mis en évidence l'influence importante d'une couche moléculaire sur l'anisotropie magnétique interfaciale, résultat a priori peu intuitif du fait du faible couplage spin-orbite des matériaux organiques [2].

Nous avons plus particulièrement travaillé sur les molécules de C₆₀, relativement simples à simuler de par leur haute symétrie. L'adsorption de ces molécules sur des substrats de cobalt et de chrome modifie ainsi leurs propriétés ainsi que celles du substrat.

Nous avons dans un premier temps réalisé des expériences de microscopie à effet tunnel polarisé en spin sur des molécules individuelles déposées sur une surface de chrome et de cobalt. Sur le chrome, nous avons mesuré une forte polarisation de spin du C₆₀ en géométrie d'adsorption pentagonale alors qu'en géométrie hexagonale et aussi sur le cobalt, le C₆₀ ne montre pas de polarisation évidente dans les spectres tunnel. Des comparaisons avec des calculs ab initio permettent de mieux comprendre l'influence du substrat et des géométries d'adsorption sur les propriétés observées [1].

Nous avons également étudié la modification du magnétisme du cobalt par magnéto-optique in situ lorsqu'une couche de molécules (C₆₀, alkanethiols ou Alq₃) est déposée sur des films ultraminesces Co/Au(111) et Co/Pt(111) [2,3]. Étonnamment, la couche moléculaire peut induire une transition de réorientation de l'aimantation, favorisant l'aimantation hors plan. Des mesures quantitatives d'anisotropie montrent que l'importance de cet effet dépend fortement des détails de l'interface. Ainsi, par comparaison avec des calculs ab initio, nous avons pu montrer que la géométrie d'adsorption ainsi que la structure cristalline du substrat influent sur cette anisotropie d'interface.

[1] D. Li et al., Phys. Rev. B 93, 085425 (2016)

[2] K. Bairagi et al., Phys. Rev. Lett. 114, 247203 (2015)

[3] P. Campiglio et al., New J. Phys. 17, 063022 (2015)

Diffusion centrale anormale de rayons X en incidence rasante pour l'étude de matériaux fonctionnels

Christine Revenant

Univ. Grenoble Alpes, CEA, INAC-MEM, 38000 Grenoble, France

christine.revenant@cea.fr

La diffusion centrale de rayons X en incidence rasante, en anglais Grazing Incidence Small Angle X-ray Scattering (GISAXS) est une technique puissante pour l'étude de la morphologie de deux phases en présence à l'échelle nanométrique. Lorsque plus de phases existent à la surface ou sous la surface d'un matériau, le GISAXS anormal (AGISAXS) s'avère être une excellente technique pour étudier la morphologie des différentes phases en présence. La variation de l'énergie des rayons X près d'un seuil d'absorption d'un élément considéré permet d'isoler la contribution de cet élément. Les expériences GISAXS sont réalisées à plusieurs énergies près d'un seuil d'absorption sur une ligne synchrotron. Cette technique permet la séparation de la diffusion d'un type de nanoparticules de celle provenant d'autres types de nanoparticules, de pores, de rugosité de surface ou de défauts. Les potentialités de cette technique seront présentées dans le cadre de nanoparticules à base de Ga_2O_3 .

- [1] C. Revenant, M. Benwadih, M. Maret, Self-organized nanoclusters in solution-processed mesoporous In-Ga-Zn-O thin films, *Chem. Commun.* **51** (7), 1218 (2015).
 [2] C. Revenant, M. Benwadih, Morphology of sol-gel porous In-Ga-Zn-O thin films as a function of annealing temperatures, *Thin Solid Films* **616**, 643 (2016).
 [3] C. Revenant, Anomalous grazing-incidence small-angle X-ray scattering of Ga_2O_3 -based nanoparticles, *J. Appl. Cryst.* **51**, 436 (2018).

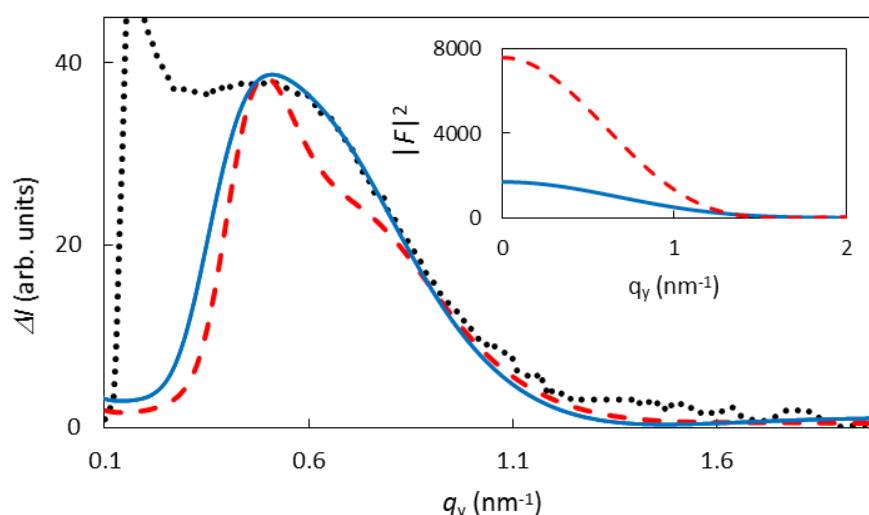


Figure 1 : Intensité AGISAXS obtenue par la méthode différentielle de films minces de InGaZnO avant le seuil K du Ga (10367 eV) avec un angle d'incidence de 0.3 degrés : expérience (pointillé noir), simulation pour des pores décorés par Ga_2O_3 (ligne bleue) et pour des particules de Ga_2O_3 (pointillé rouge). Coupe horizontale à $q_z = 0.50 \text{ nm}^{-1}$ (correspondant à α_c). Encadré : module au carré du facteur de forme $|F(q)|^2$ calculé pour des pores décorés par Ga_2O_3 (ligne bleue) et pour des particules de Ga_2O_3 (pointillé rouge).

Twistable electronics with dynamically rotatable heterostructures

Rebeca Ribeiro-Palau^{*,1,2}, Changjian Zhang^{2,3}, Kenji Watanabe,⁴
Takashi Taniguchi,⁴ James Hone,² and Cory R. Dean¹

¹Department of Physics, Columbia University, New York, NY, USA

²Department of Mechanical Engineering, Columbia University, New York, NY, USA

³Department of Electrical Engineering, Columbia University, New York, NY, USA

⁴National Institute for Materials Science, 1-1 Namiki, Tsukuba, Japan

*rebeca.ribeiro@c2n.upsaclay.fr

In situ band structure manipulation of 2D materials offers unique opportunities toward understanding of multiple physical phenomena and the design of novel opto-electronic devices. A simple, yet effective, way to modify the band structure of these materials is by controlling the relative orientation between the layers in van der Waals heterostructures. The clearest example of this effect is graphene on hexagonal boron nitride (BN), in which the layer orientation determines the wavelength of the Moiré superlattice, which in turn modifies the native band structure of graphene opening an energy gap and generating minigaps at higher energies. However, current techniques are limited to fabrication of samples with fixed interlayer angles. Studies of angular dependence are therefore limited to static properties, and require multiple samples, which imposes experimental challenges and introduces uncertainty due to sample-to-sample variations. Here we present optical, mechanical and electronic characterization of BN/graphene/BN heterostructures where the angle between layers is changed continuously with a control of 0.2 degrees. In room-temperature experiments, we confirm the layer alignment by measurement of the angle- dependent broadening of the Raman 2D peak, consistent with previous results. As the layers approach alignment, friction between the BN and graphene increases and electronic transport measurements show satellite resistance peaks growing and moving toward the main peaks at charge neutrality. The energy gaps for the main and satellite peaks, as determined from low-temperature measurements, show remarkably different angular dependence. Combining these three measurements in the same device demonstrates the new capability to precisely tune in situ optical, mechanical and electronic properties of a van der Waals heterostructure. Our new experimental technique opens the possibility to study the angle- dependent properties of van der Waals heterostructures and in situ band structure engineering of 2D materials.

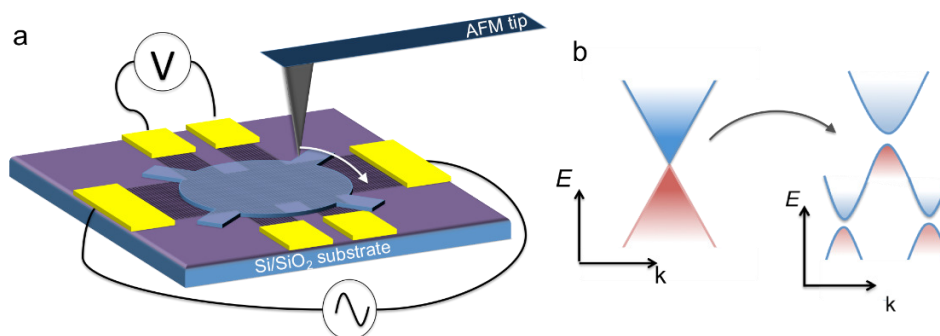


Figure 1 : (a) technique description, an AFM tip is used to rotate the upper most layer of the heterostructure and therefore change the crystallographic orientation between the two layers. (b) Representation of the modification in the electronic band structure of graphene when it is aligned to h-BN.

Physics of heat transfer with a nonequilibrium quantum fluid of polaritons

Maxime Richard^{a,*}, Petr Stepanov^a, Sebastian Klemmt^{a,b},
Thorsten Klein^c, Anna Minguzzi^d

- a. CNRS, Université Grenoble Alpes - Institut Néel, 38000 Grenoble, France
- b. Technische Physik, Universität Würzburg, Am Hubland, D-97074 Würzburg, Germany.
- c. University of Bremen, P.O. Box 330440, 28334 Bremen, Germany
- d. CNRS, Université Grenoble Alpes - LPMMC, 38000 Grenoble, France

* maxime.richard@neel.cnrs.fr

(ENGLISH BELOW) Exciton-polaritons in semiconductor microcavities have been nowadays well established as a new class of quantum fluids, with defining phenomena such as Bose-Einstein condensation and Superfluidity [1]. Unlike ultra-cold atoms or liquid Helium, this unique class of fluid is characterized by the fact that the particles lifetime is too short to reach thermal equilibrium, and thus are not constrained by it.

This feature opens up unconventional mechanisms of heat exchange between the fluid and its solid-state environment (thermal phonons). In this talk, I will present an experimental work showing that a polariton fluid can be pumped in a “cold” state, in which it absorbs heat from the warmer phonon bath and releases it into the (much colder) electromagnetic vacuum. The irreversibility of this mechanism is a direct consequence of the fluid nonequilibriumness [2].

In the latter regime, the heat flux was negligible as compared to the particle loss rate. We thus examined experimentally the strong heating regime, in which heat, drive and losses contribute equally in establishing the fluid steady-state. We characterized how the normal to condensed phase transition is affected by the amount of absorbed heat, and how heat is “stored” in the condensate degrees of freedom, in a way that is not fixed by an equilibrium distribution [3].

[1] I. Carusotto and C. Ciuti, Quantum fluids of light, *Rev. Mod. Phys.* **85**, 299 (2013).

[2] S. Klemmt *et al.* Exciton-Polariton Gas as a Nonequilibrium Coolant, *Phys. Rev. Lett.* **114**, 186403 (2015).

[3] S. Klemmt *et al.* Thermal Decoherence of a Nonequilibrium Polariton Fluid, *Phys. Rev. Lett.* **120**, 035301(2018).

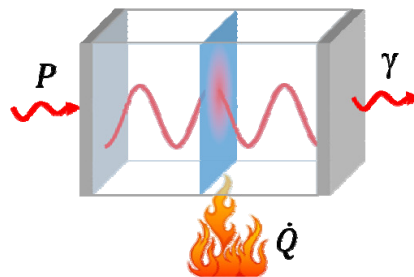


Figure 1: Sketch illustrating the specific nonequilibrium situation of polariton fluids. P is the polariton excitation rate achieved by an external optical source, γ is the loss rate, and \dot{Q} is the heating rate of polaritons.

Sieving mechanism within chemically tuned 2D nanochannels for membrane desalination

Lucie Ries^{a*}, Philippe Miele^{a,b}, et Damien Voiry^a

- a. Institut Européen des Membranes, IEM, UMR 5635, Université Montpellier, ENSCM, CNRS, 34095 Montpellier Cedex5, France
 b. Institut Universitaire de France (IUF), MESRI, 1 rue Descartes, 75231 Paris cedex 05, France

* Correspondence to: lucie.ries@umontpellier.fr

Membrane separation technology plays an important role in various fields including water treatment, chemicals and gas separation in many industrial processes, and food processing. There has been a renewed focus on 2D material for membrane application since their atomic thickness and confined interlayer spacing could theoretically lead to enhanced separation performance¹. Indeed, multilayer assembly of single nanosheets creates 2D capillaries that can efficiently sieve chemical species depending on their size. Selectivity- and size controlled diffusion of these nanochannels can be modified to tune the transport mechanism within the structure.

In fact, graphene-based membranes are promising candidates as nanolamellar structures for molecular sieving but their instability in aqueous media alters their sieving performance². Exfoliated nanosheets of transition metal dichalcogenides (TMDs) constitute attractive platforms as nanolaminate membranes. Recent works carried out on nanolaminate membrane made of molybdenum disulfide (MoS_2)³ have demonstrated improved stability⁴. In addition, chemical modifications of the surface of the nanosheets *via* functionalization⁵ have opened new avenues for tuning the membrane properties in both fields of molecular³ and gas sieving. Yet the influence of functionalization of nanolaminate membranes on the sieving performance remains unclear. In order to assess the role of the surface chemistry of the nanosheets on the membrane performance, we developed strategies to covalently functionalize MoS_2 nanosheets⁵. Here we will present our recent investigations on the performance of lamellar membranes based on chemically functionalized MoS_2 nanosheets towards water desalination and micropollutant decontamination. Our results open novel directions for fine tuning the sieving behavior of membranes based on 2D materials.

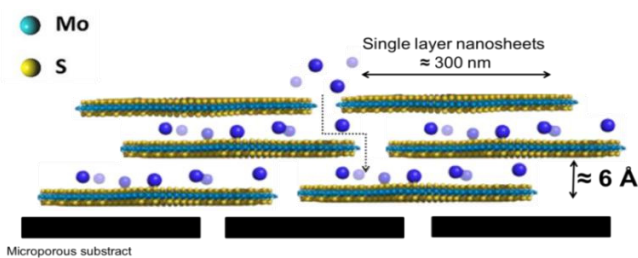


Figure 1. Schematic representation of the diffusion mechanism along continuous 2D capillaries formed within MoS_2 -based nanolaminate membranes [Lr]

[1] W. Kim, S. Nair, Chem. Eng. Sci., 2013, 104, pp 908-924

[2] C. N.Yeh J. X. Huang, Nat. Chem., 2015

[3] M. Deng, H.G. Park, Nano Lett., 2017, 17 (4), pp 2342-2348

[4] L. Sun, X. Peng, ACS Nano, 2014, 8 (6), pp 6304-6311

[5] D. Voiry, M. Chhowalla, Nature Chemistry, 2015, 7, pp 45-49

Examples of phenomena in cell physics : cell motility, cell division, epithelial elongation

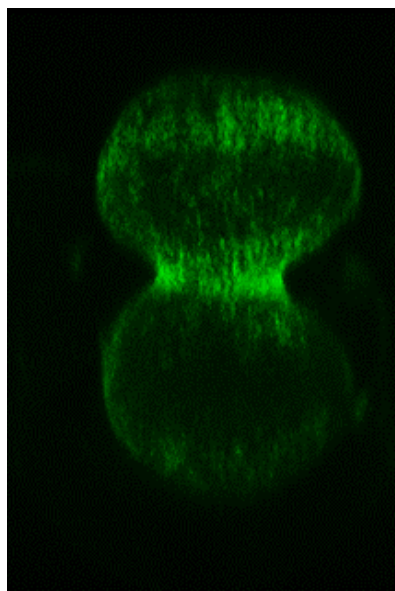
Daniel Riveline^{a*}

- a. *Laboratory of Cell Physics, Strasbourg University, Institut de Génétique et de Biologie Moléculaire et Cellulaire, Strasbourg - France*

* riveline@unistra.fr

Cell phenomena are traditionally explained by molecular activation pathways. Signaling networks are indeed playing key roles in cell fate, for example in motility, division and death. However these switching events at the nanometer scale fail to provide satisfactory explanations for their microscopic read-outs which are at the micrometer scale. Our approach consists of trying to bridge this gap of three orders of magnitude in scales. We take cell biology tools for performing experiments on individual cells and we develop and analyze cell phenomena with condensed matter physics methods and frameworks.

I will present examples illustrating this approach: i/ the cell *ratchet*, ii/ the constriction of a physiological ring made of molecular motors - the *cytokinetic ring*; and iii/ epithelial elongation.



Quantum solitons as radiating black holes

Charles W. Robson*, Leone Di Mauro Villari, and Fabio Biancalana

Institute of Photonics and Quantum Sciences, Heriot-Watt University, Edinburgh EH14 4AS, UK

* email: cwr1@hw.ac.uk

For many years it has been known that integrable equations have associated with them non-trivial geometries [1]. Each of these equations, such as the nonlinear Schrödinger equation (NLSE), the Korteweg-de Vries (KdV), the sine-Gordon, induces a metric having rich properties, and these can be used to study lower dimensional gravitational systems.

In recent years, quantum thermal emission by solitons has been studied as an analogue of Hawking radiation from a black hole [2]. In this work we derive a metric induced by the moving soliton solution to the NLS equation and find that it contains a radiating horizon with a Hawking temperature. Interestingly this metric, although generated by a linearly moving soliton in (1+1) dimensions has striking formal similarities to that of the Kerr metric, which describes rotating black holes in four dimensions.

We also present new results on the thermodynamics of the NLS soliton, deriving a “first law” which confirms its Hawking temperature and defines its entropy. Hopefully this work will stimulate further research into both lower dimensional black holes, their analogues in condensed matter and nonlinear optics, and the thermodynamics of solitons.

[1] C. Rogers and W. K. Schief, *Bäcklund and Darboux Transformations: Geometry and Modern Applications in Soliton Theory* (CUP, Cambridge, 2002).

[2] L. D. M. Villari, G. Marucci, M. C. Braidotti, and C. Conti, arXiv:1703.02891v3 (2018).

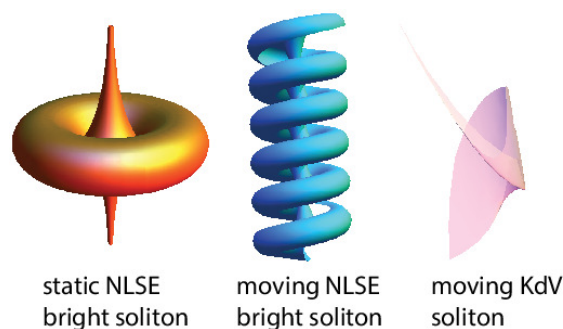


Figure 1: The pseudosurfaces associated with several soliton solutions to integrable equations.

Optical generation of single vortex/anti-vortex pairs in superconductors

A. Rochet^{a,b,c}, W. Magrini^{a,b}, A. Buzdin^{c,d}, Ph. Tamarat^{a,b}, B. Lounis^{a,b}

a. Université de Bordeaux, LP2N, F-33405 Talence, France

b. Institut d'Optique & CNRS, LP2N, F-33405 Talence, France

c. University of Bordeaux, LOMA UMR-CNRS 5798, F-33405 Talence Cedex, France

d. Department of Materials Science and Metallurgy, University of Cambridge, CB3 0FS, Cambridge, United Kingdom

antonine.rochet@institutoptique.fr

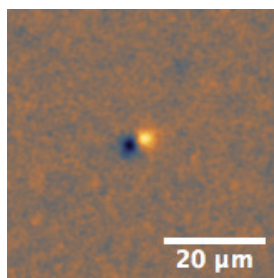


Figure 1 : a) Magneto-optical image of a vortex/anti-vortex pair in a superconducting film of niobium.

We demonstrate the optical generation of single vortex/anti-vortex pairs with a short laser pulse. Combined with the fast and precise optical manipulation of a single vortices [1], this results is promising for the ultrafast optical control of superconducting devices such as Josephson junctions [2].

[1] I. S. Veshchunov, W. Magrini, S. V. Mironov, A. G. Godin, J.-B. Trebbia, A. Bouzdine, Ph. Tamarat, B. Lounis, *Nat. Comm.*, Vol. 7 12801 (2016).

[2] S. Mironov, E. Goldobin, D. Koelle, R. Kleiner, Ph. Tamarat, B. Lounis, A. Bouzdine, *Phys. Rev. B*, Vol. 96 N. 21 (2017).

Integration of a grafted solid-state nanopore chip into a simple to make and use microfluidic system

Jean Roman^{a,b*}, Gilles Patriarche^c, Nathalie Jarroux^a, Juan Pelta^a, Bruno Le Pioufle,^b
and Laurent Bacri^{b,c}

a. Lambe, Univ. d'Évry val d'Essonne, France

b. Satie, ENS Paris-Saclay, France

c. C2N, Univ. Paris-Saclay, France

* jean.roman@univ-evry.fr

Solid-state nanopores have been developed since 2001[1] when the available proteic nanopores like α -hemolysin were proved too wide for DNA sequencing.[2] Modern manufacturing techniques like TEM[3] piercing or dielectric breakdown[4] piercing can indeed lead to pores with under one nanometre radius. However, solid-state nanopore analysis still lack the reliability and reproductibility of proteic nanopores. The very nature of proteic nanopore makes them biocompatible whereas solid-state nanopores, often made of silicium-based materials need further treatment.[5] On another hand, an advantage of solid-state nanopores resides in the durable membrane they are pierced in. These membranes can easily be transported after piercing to perform analysis on the field or in a laboratory. An easy to use fluidic device to handle the nanopore chips is all it take to permit easy nanopore analysis to be done anywhere.

We propose an easy way to reliably graft polymer chains on a nanopore chip to make it biocompatible. Also we developed an easy to use microfluidic chip made in PDMS from a low cost, 3D-printed mold.[6]

- [1] Li et al, Ion-beam sculpting at nanometre length scales, *Nature*, **421**, 166-169 (2001)
- [2] Kazianowics et al, Characterization of individual polynucleotide molecules using a membrane channel, *PNAS*, **93**, 13770-13773 (1996)
- [3] McNally et al, Electro-mechanical unzipping of individual DNA molecules using synthetic sub-2 nm pores, *Nano Lett.*, **8**, 3418-3422 (2010)
- [4] Beamish et al, Precise control of the size and noise of solid-state nanopores using high electric fields, **23**, 405301 (2012)
- [5] Wanunu and Meller, Chemically modified solid-state nanopores, *Nano Lett.*, **6**, 1580-1585 (2007)
- [6] Roman et al, Functionalized Solid-State Nanopore Integrated in a Reusable Microfluidic Device for a Better Stability and Nanoparticle Detection, **9**, 41634-41640 (2017)

Wave transport in heterogeneous media and imaging

Vincent Rossetto^{a*}

a. Univ. Grenoble Alpes / CNRS, LPMMC, Grenoble

* vincent.rossetto@grenoble.cnrs.fr << Vincent Rossetto >>

Waves in heterogeneous media travel in a disordered fashion. An imaging method has been recently designed to take advantage of this disorder [1]. It relies on the average statistics of trajectories in a ideally disordered medium. But disorder in a real medium is far from being ideal and the fluctuations of the medium hinder the accuracy of the imaging method. In this talk, I will show that such fluctuations are quite large but can be controlled to some extent.

This work is based on radiative transfer theory and the resolution of a simplified version of the Boltzmann equation. Exact solutions exist in one and two dimensions thanks to the analogy with a persistent random walk [2].

The imaging method is based on the local time of the persistent random walk [3]. The local time depends on the Green's functions but is randomly distributed and also has fluctuations that will aggravate the fluctuations of the radiative transfer Green's functions.

- [1] Rossetto, Margerin, Planès and Larose, *Locating a weak change using diffuse waves: Theoretical approach and inversion procedure*, *J. Appl. Phys.* **109**, 034903 (2011)
- [2] Rossetto, *Space-time domain velocity distributions in isotropic radiative transfer in two dimensions*, *J. Phys. A: Math. Theor.* **50**, 165001 (2017)
- [3] Rossetto, *Local time in diffusive media and applications to imaging*, *Phys. Rev. E* **88**, 022103 (2013)

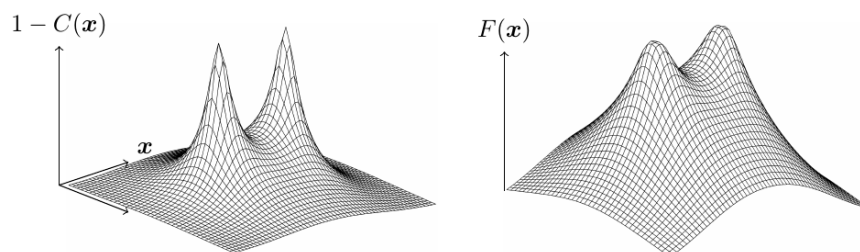


Figure 1: Left: resolution kernel. The two maxima correspond to the positions of a source and a receiver. Right: fluctuations of the resolution kernel. The fluctuations are large and become relatively larger away from the source and the receiver.

Cooperative magnetic phenomena in artificial spin systems

N. Rougemaille,^{a*} Y. Perrin,^a I. A. Chioar^a, V.-D. Nguyen^a, M. Hehn^b, D. Lacour^b, F. Montaigne^b, A. Locatelli^c, T. O. Montes^c, B. Santos Burgos^c and B. Canals^a

a. CNRS and Univ. Grenoble Alpes, Inst NEEL, F-38000 Grenoble, France

b. Univ. de Lorraine and CNRS, Inst Jean Lamour, F-54506 Vandoeuvre les Nancy, France

c. Elettra-Sincrotrone, AREA Science Park, 34149 Basovizza, Trieste, Italy

* nicolas.rougemaille@neel.cnrs.fr

Complex architectures of nanostructures are routinely elaborated using bottom-up or nanofabrication processes. This technological capability allows scientists to engineer materials with properties that do not exist in nature, but also to manufacture model systems permitting the exploration of fundamental issues in condensed matter physics. One- and two-dimensional frustrated arrays of magnetic nanostructures are one class of systems for which theoretical predictions can be tested and revisited experimentally [1,2]. These systems have been the subject of intense research in the last few years and allowed the investigation of a rich physics, including the study of the extensively degenerate ground-state manifolds of spin ice systems, the evidence of new magnetic phases in purely two-dimensional lattices, and the observation of pseudo-excitations involving classical analogues of magnetic monopoles.

This talk aims at providing two examples of two-dimensional frustrated arrays of magnetic nanostructures, in which the low-energy physics of two exotic Ising systems was probed. The first example is related to the seminal six vertex model and shows that a scan through the phase diagram of this model can be achieved experimentally, provided that the artificial spin system is designed appropriately [3]. In particular, the symmetric point of the square ice is recovered, and signatures of an algebraic Coulomb spin liquid are observed. The second example refers to a recent proposal [4], the fragmentation of magnetization [4-7], in an Ising kagome model. The magnetic configurations we image in a thermally active artificial system [5] reveal the fingerprints of this fragmentation process, which corresponds to a splitting of the spin degree of freedom into two independent sectors. The first sector is identified as an incipient antiferromagnetic crystal of an all-in/all-out spin configuration, despite the ferromagnetic nature of the system, in which spins carry 1/3 of their total magnetic moment. The second sector corresponds to a diffuse organization of the remaining (2/3 and 4/3) fragmented spins.

- [1] M. Tanaka et al., J. Appl. Phys. 97, 10J710 (2005)
- [2] R. F. Wang et al., Nature 439, 303 (2006)
- [3] Y. Perrin et al., Nature 540, 410 (2016)
- [4] M. E. Brooks-Bartlett et al., Phys. Rev. X 4, 011007 (2014)
- [5] B. Canals et al., Nat. Commun. 7, 11446 (2016)
- [6] S. Petit et al., Nat. Phys. 12, 746 (2016)
- [7] E. Lefrancois et al., Nat. Commun. 8, 209 (2017)

On the use of aptamer microarrays as a platform for the exploration of human prothombin/thrombin conversion

Yoann Roupioz^{a*}, Camille Daniel^a, Ferial Melaïne^a and Arnaud Buhot^a

a. Univ Grenoble Alpes, CNRS, CEA, INAC-SyMMES, 38000 Grenoble, France

* yoann.roupioz@cea.fr

Although the selection of aptamers has been described 25 years ago, the use and application of these RNA or DNA sequences in biosensing devices is significantly described since less than a decade. Microarrays are particular biosensors with multiple probes that are generally used for parallel and simultaneous detection of various targets. In this talk, we present microarrays functionalized with aptamer probes in order to follow up the different biomolecular interactions with a major enzyme, the thrombin protein, involved in the complex coagulation cascade. Several DNA based aptamers are used along with DNA control strands to simultaneously follow the interactions of a single sample with several probes. More precisely, thanks to the label-free Surface Plasmon Resonance imaging, we are able to monitor *in situ* and in real-time several events of the coagulation cascade: interactions of thrombin with DNA aptamers (two different sequences are followed), the differential binding of these aptamers with the prothrombin and last but not least, the enzymatic transformation of prothrombin into thrombin, catalyzed by the factor Xa. We are also able to appraise the influence of other biochemical factors and their corresponding inhibiting or enhancing behaviors on thrombin activation. Our study not only opens the door for the development of a complete microarray-based platform for the whole coagulation cascade analysis, but also for novel drug screening assays in pharmacology. On a more general point of view, the combination of such a label-free and user-friendly optical approach should significantly help in the use of aptamer microarrays for much wider applications.

References:

- [1] Daniel, C.; Melaine, F.; Roupioz, Y.; Livache, T.; Buhot, A., Real time monitoring of thrombin interactions with its aptamers: Insights into the sandwich complex formation. *Biosensors & bioelectronics* **2013**, *40* (1), 186-192.
- [2] Daniel, C.; Roupioz, Y.; Gasparutto, D.; Livache, T.; Buhot, A., Solution-phase vs surface-phase aptamer-protein affinity from a label-free kinetic biosensor. *PLoS one* **2013**, *8* (9), e75419.
- [3] Daniel, C.; Roupioz, Y.; Livache, T.; Buhot, A., On the use of aptamer microarrays as a platform for the exploration of human prothrombin/thrombin conversion. *Analytical biochemistry* **2015**, *473*, 66-71.

Classical analogue of an interstellar travel through a hydrodynamic wormhole

Léo-Paul Euvé^a et Germain Rousseaux^{a*}

a. Institut Pprime CNRS Université de Poitiers ISAE-ENSMA, 11 Boulevard Marie et Pierre Curie, 86962 Futuroscope

* germain.rousseau@univ-poitiers.fr

The classical theory of space-time, namely general relativity, suggests but does not demonstrate the existence of so-called wormholes allowing for interstellar journeys. Alternative proposals such as quantum gravity theories are developed nowadays to allow for wormhole travels by assuming hypothetical trans-Planckian effects at tiny scales. Here we show experimentally that analogue traversable and bidirectional wormholes exist in hydrodynamics following a suggestion by Wheeler. Using a water channel, we sent free surface waves on a countercurrent in an analogue gravity setup aiming at showing that hydrodynamic wormhole travels are controlled by a cascade of dispersive scales including surface tension effects: the capillary wavelength plays the role of a Planckian scale below which long gravity waves are transformed into short capillary waves that are able to move at speeds higher than the “flow” of space-time. Whereas our results do not apply to putative astrophysical wormholes per se, we anticipate that they will trigger new ideas to explore quantum gravity physics. [1].

[1] L.-P. Euvé, and G. Rousseaux, Classical analogue of an interstellar travel through a hydrodynamic wormhole (PRD Kaleidoscope Select), Physical Review D, **96** (6), 064042-1/15 (2017).

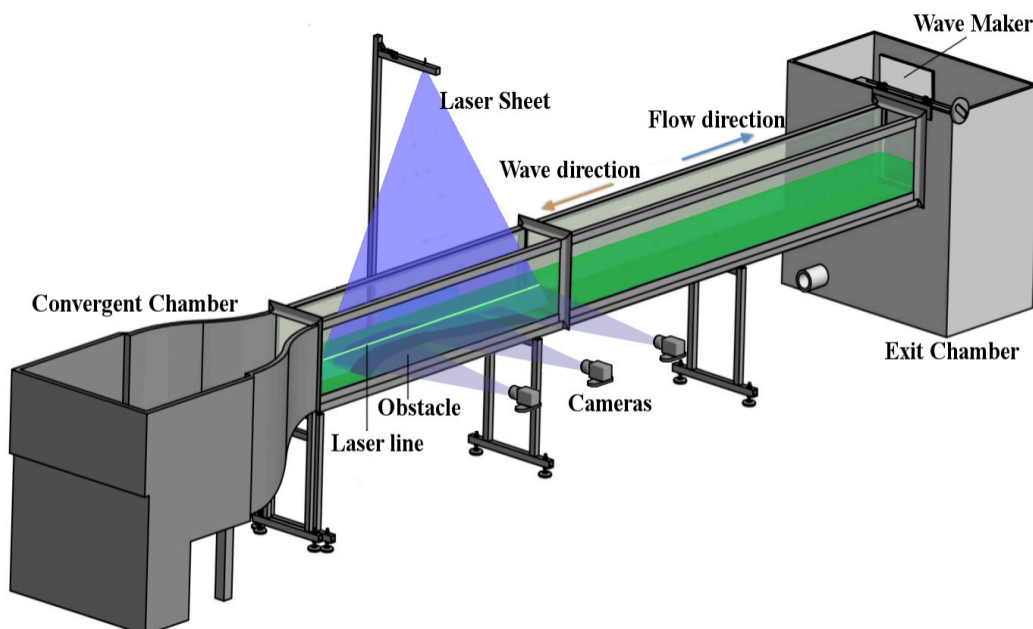


Figure 1: Water channel in which a current circulates over a bottom obstacle. The velocity gradients play the role of an effective space-time for free surface waves, which propagate analogously to light waves in the curved space-time induced by a gravitational mass.

Evidence and modeling of mechanoluminescence in a novel transparent glass particulate composite

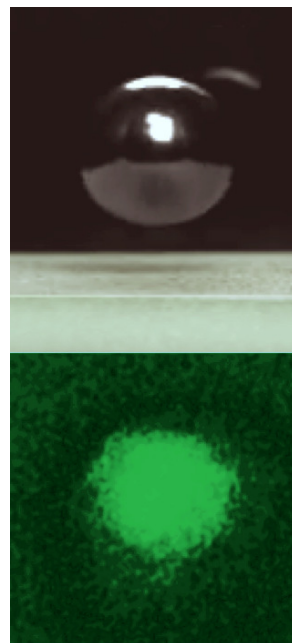
Tanguy Rouxel^{a*}, Marion Dubernet^a, Yann Gueguen^a, Patrick Houizot^a,
Emilie Bruyer^{a,b}, Xavier Rockefelte^b

- a. Département Mécanique et Verres, IPR, UMR UR1-CNRS 6251, Université de Rennes 1, Campus de Beaulieu, 35042 Rennes Cedex, France
- b. Chimie Théorique, Sciences Chimiques Rennes, UMR UR1-CNRS 6226, Université de Rennes 1, Campus de Beaulieu, 35042 Rennes Cedex, France

Mechanoluminescence of a transparent glass-matrix particulate composite with $\text{SrAl}_2\text{O}_4:\text{Eu,Dy}$ particles (SAOED) was observed in compression, torsion and hydrostatic loading. Experiments show the linear dependence of the mechanoluminescence intensity with the mechanical power. A rheological model is proposed, based on the physics of delayed processes (in analogy to viscoelasticity), and on the electron trapping and de-trapping processes.

- [1] M. Dubernet, Y. Gueguen, P. Houizot, F. Célarié, J.C. Sangleboeuf, H. Orain, and T. Rouxel, "Evidence and modelling of mechanoluminescence in a transparent glass particulate composite", *Appl. Phys. Lett.*, **107** 151906 (2015)
- [2] T. To, F. Célarié, C. Roux-Langlois, A. Bazin, Y. Gueguen, H. Orain, M. Le Fur, V. Burgaud, T. Rouxel, "Fracture toughness, fracture energy and slow crack growth of glass as investigated by the Single-Edge Pre-cracked Beam (SEPB) and Chevron- Notched Beam (CNB) methods", *Acta Mater.*, 146 1-11 (2018).

Figure 1 : Emission de lumière au moment de l'impact d'une bille sur une plaque de verre contenant des particules SAOED.



Swimming in foam

Q. Roveillo ^{a*}, J. Dervaux ^a, L. Seuront ^b, and F. Elias ^{a,c}

a. Laboratoire Matière et Systèmes Complexes, Université Paris Diderot, France

b. Laboratoire d'Océanologie et de Géosciences, Wimereux, France

c. Université Pierre et Marie Curie – Sorbonne Université, France

* quentin.roveillo@univ-paris-diderot.fr

Inspired by the problematic of the trapping of planktonic organisms in marine foams [1], we measured the sedimentation dynamics of a motile micro-algae in a laboratory-generated foam. A liquid foam is made of air bubbles separated by a continuous network of liquid microchannels. Initially the liquid is equally distributed along the height of the foam. Then during the experiment it drains in time out of the foam under the effect of gravity and capillarity. If present in the liquid phase, solid particles are either advected downwards by the flow or trapped in the foam, depending on their size and concentration [2]. We use a model single-cell algae, *Chlamydomonas reinhardtii* [3]. The algae is homogeneously incorporated in the liquid phase of a foam, buoyant on top of its liquid phase and we measured the temporal evolution of the number of algae released from the foam in the underlying liquid. *C. reinhardtii* is bi-flagellate, thus motile. We investigated the effect of motility on the transport of algae through the foam, using motile and non-motile (dead) *C. reinhardtii*, and we show that motile algae are more likely than non-motile to remain trapped in the foam.

[1] L. Seuront, D. Vincent, J.G. Mitchell, *J. of Marine Systems* 61, 2006 p. 118 (2006)

[2] B. Haffner et.al., *J. Colloid Interface Sci.* 458, 200-208 (2015).

[3] M. Polin et.al., *Science*, 325, p. 487 (2009)

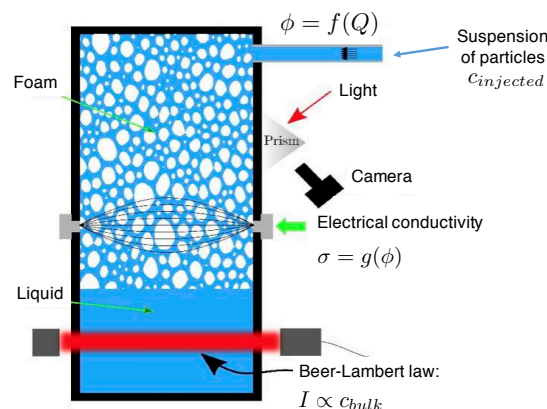


Figure 1: Diagram of the experimental setup

High field transport properties of high mobility 2DEG at the LaAlO₃/SrTiO₃ interface

K. Rubi^{a*}, M. Yang^a, B. kerdia^a, K. Han^b, S. Zeng^b, M. Pierre^a, Ariando^b, M. Goiran^a and W. Escoffier^a

- a. Laboratoire National des Champs Magnetiques Intenses (LNCMI-EMFL), CNRS-UGA-UPS-
INSA, 143 Avenue de Rangueil, 31400 Toulouse, France
b. Department of Physics and NUSNNI-Nanocore, National University of Singapore, Singapore
117411

* rubi.km@lncmi.cnrs.fr

The formation of a two-dimensional electron gas (2DEG) at the interface between two insulators SrTiO₃ (STO) and LaAlO₃ (LAO) is among the most intriguing findings in oxide electronics. While the gate tunable superconductivity [1] and spin orbit coupling [2] at this interface are well studied, no clear consensus is reached on the quantum oscillations due to the limitation of applied magnetic field. We have investigated the quantum transport of a high mobility 2DEG at LAO/STO interface under high magnetic field (55T). The Shubnikov-de Haas (SdH) oscillations in longitudinal resistance (R_{xx}) show a clear monotonic dependence with varying the gate voltage/carrier density (see Fig. 1), despite a one order of magnitude discrepancy between the carrier concentrations estimated from the Hall resistance and the SdH oscillation's frequency [3]. Interestingly, the Landau fan diagram is non-linear implying the presence of many sub-bands derived from the Ti:3d orbitals (d_{xy} , d_{xz} and d_{yz}) of STO and/or sub-band spin-splitting at the Fermi energy in the band structure. The substantial shift in the amplitude and frequency of the oscillations observed with varying back-gate voltage allows investigating the complex band structure of this 2DEG.

[1] A. Joshua *et al.*, Nature Comm. **3**, 1129 (2012); J. Biscaras *et al.*, Phys. Rev. Lett. **108**, 247004(2012).

[2] A. D. Caviglia *et al.*, Phys. Rev. Lett. **104**, 126803 (2010); M. Ben Shalom *et al.*, Phys. Rev. Lett. **104**, 126802 (2010); Z. Zhong *et al.*, Phys. Rev. B **87**, 161102(R) (2013).

[3] M. Yang *et al.*, App. Phys. Lett. **109**, 122106 (2016).

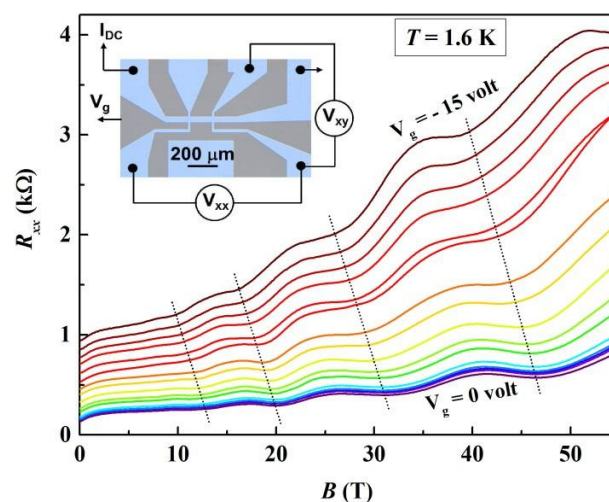


Figure 1. The magnetic field dependence of longitudinal resistance (R_{xx}) with varying back-gate voltage. The dot lines are guides for the eye. The inset shows an optical micrograph of LAO/STO device.

Moving as one?

Collective steps in molecular motor assemblies

J.-F. Rupprecht^{a,*}, J. Prost^{a,b}, M. P. Sheetz^{a,c}.

- a. Mechanobiology Institute, National University of Singapore, 5A Engineering Drive 1, 117411 (Singapore).
- b. Laboratoire Physico Chimie Curie, Institut Curie, PSL Research University, CNRS UMR168, 75005 Paris, France.
- c. Department of Biological Sciences, Columbia University, New York, New York 10027, USA.

* mbijr@nus.edu.sg

Cells sense the rigidity of their environment through local pinching – just as you would do with your finger and thumb when you want to know if something is soft or rough. Such rigidity sensing is perturbed in most cancer cells, which spread and grow on soft environment – while normal cell would not.

Healthy cells rely on myosin II motor assemblies – which contract over bundles of polymers called actin – to pinch their environment. Recent high resolution experiments performed on such myosin assemblies are challenging the current understanding of molecular motor force generation [1]. These experiments show that:

- (1) myosin II motors are surprisingly efficient, exerting forces an order of magnitude larger than the commonly accepted 3pN/motor value obtained through in vitro experiments, and
- (2) that the actomyosin contractions occur through 2.5nm steps, which correspond to half of the actin period (5nm).

By developing a new look on a molecular motor toy model, called two-state model [2], we show that we can explain both experimental observations. In particular, we explain why efficient motors necessarily contract in a step-wise fashion, with 2.5nm steps, while weak motors do not exhibit such steps - thus rationalizing the specificity of motor contractions implied in rigidity-sensing compared to previous in vitro observations.

[1] J. Lohner, J.-F. Rupprecht, Junqiang Hu, N. Mandriota, M. Saxena, J. Hone, D. Pitta de Araujo, O. Sahin, J. Prost, M. Sheetz, bioRxiv <https://doi.org/10.1101/296400>

[2] F. Julicher, A. Ajdari, J. Prost, *Modeling molecular motors*. Reviews of Modern Physics, **69**, 4 (1997).

**VITREOUS SILICA UPON MECHANICAL LOADS AND LASER IRRADIATION:
THE VIBRATIONAL MODES TREATMENT AND RAMAN ANALYSIS**

Nikita S. Shcheblanov^a, Mikhail E. Povarnitsyn^b, Anne Tanguy^c, and Nadège Ollier^a

- a. Laboratoire des Solides Irradiés CEA-CNRS, Ecole polytechnique, F-91128 Palaiseau, France
- b. Joint Institute for High Temperatures, RAS, 13 Bld. 2 Izhorskaya str., Moscow 125412, Russia
- c. Laboratoire LAMCOS, INSA de Lyon, Bat. Jacquard 27 av. Jean Cappelle, F-69621 Villeurbanne Cedex, France

ABSTRACT

We perform a simulation of vitreous silica to explore the sensitivity to mechanical loads and laser irradiation, and, especially, an irreversible densification is considered. We rely on Raman spectroscopy, and we also present partial and total vibrational densities of states. To reveal the structure of the vibrational spectrum, the characteristics of vibrational modes in different frequency ranges are investigated using a mode-projection approach at different symmetries. We consider the main experimental bands, and relate them to a detailed description of the vibrations. Finally, we compare our Raman and VDOS spectra with experimental measurements.

Physico-chemical characterization of a steel thin sheet during cold rolling

K..Slimani^{a,b}, A.Grairia^a, H.Bendjamaa^a,

a. Research Center in Industrial Technologies CRTI, P.O.Box 64, Cheraga 16014
Alger,Algeria

b. *Laboratory for shaping metal materials University Badji Mokhtar PB12, Annaba 23000*

E-mail: khairo23s@gmail.com

ABSTRACT

The aim of this work is the characterization of shaping processes by plastic deformation of thin sheets. For that we took the sample of types A9M after stripping and after each tandem rolling mill stand, . This identification required a large experimental work ,after knowing the chemical composition ;some tensile tests were carried out in the axes and off-axis, in addition metallographic allows to observe the effects of hardening and a rolling texture.

the accuracy of modeling will depend on the reliability of the law of behavior and friction. The results of experimental part are used for identification of the behavior law.

Keywords: characterization - metallographic - tensile tests -Modeling - rolling.

In what follows, we present the micrographs obtained.

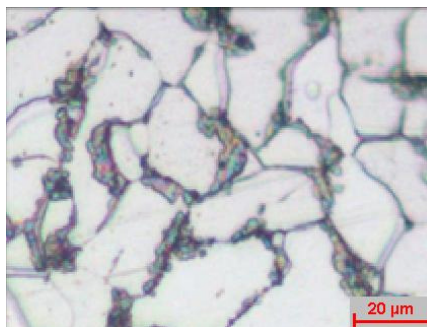


FIG. 1 : Micrography before rolling
Structure ferrito- perlitic

Modeling thermoelectric transport coefficients of multicomponent solid solutions

Maximilien Saint-Cricq^{a*}, Ambroise van Roekeghem,^a and Natalio Mingo^a

a. Université Grenoble Alpes, CEA LITEN, 38000 Grenoble, France

* maximilien.saintcricq@cea.fr

We describe two approaches to compute the Seebeck coefficient (or thermopower) and the electrical resistivity of the Nickel-based alloys containing Cr, Si and small amounts of Al, Co, Fe, Mn, Mg, Cu, P and C.

We first benchmark the applicability of the Gorter-Nordheim law to describe the experimental measurements of those multicomponent alloys. We find a good agreement between the calculated and the measured values of the Seebeck coefficient with a deviation of less than 2.5 %.

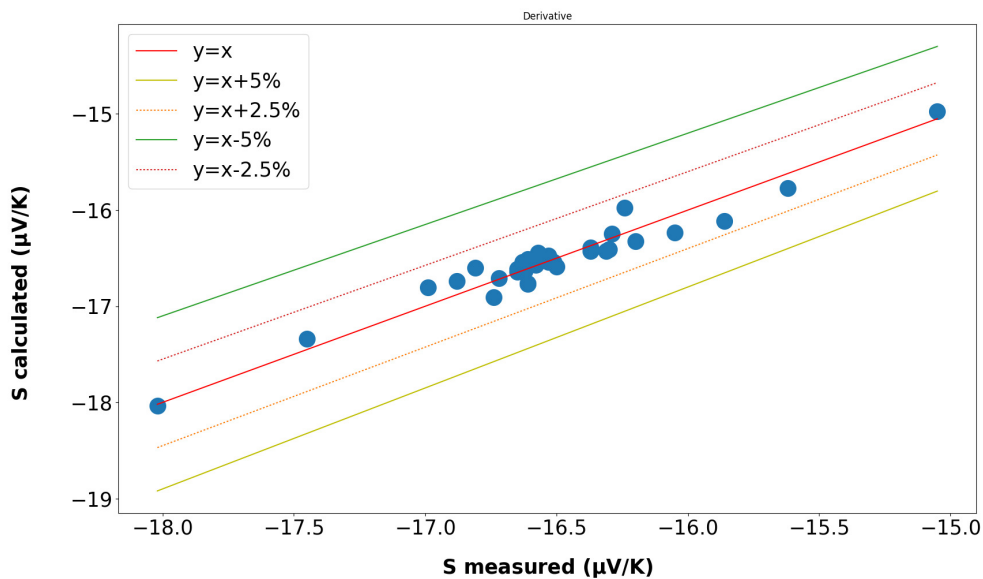


Figure 1: Calculated Seebeck vs. measured Seebeck

Then, we present some preliminary results of the thermopower and the electrical resistivity directly calculated with an *ab initio* method, using the Density Functional Theory (DFT) within the Local Density Approximation (LDA), called the Korringa-Kohn-Rostoker Green's function method in the Coherent Potential Approximation (KKR-CPA)^[1].

[1] Swihart, J. C., Butler, W. H., Stocks, G. M., Nicholson, D. M. and Ward, R. C. First-Principles Calculation of the Residual Electrical Resistivity of Random Alloys. Phys. Rev. Lett. 57, 1181–1184 (1986)

Magnetic fluctuations in BaFe_{2-x}Ni_xAs₂ superconductors

M.Saint-Paul^{a,b}, C.Guttin^{a,b}, A. Abbassi^c, Zhao-Sheng Wang^{a,b,d,1}, Huiqian Luo^d,
Xingye Lu^d, Cong Ren^d, Hai-Hu Wen^{d,e}, K.Hasselbach^{a,b*}

- a. Université Grenoble Alpes, Institut Néel, F-38042 Grenoble France
- b. CNRS, Institut Néel, F-38042 Grenoble France
- c. Faculté des Sciences et Techniques, Université Abdelmalek Essaâdi, Tanger Morocco
- d. Beijing National Laboratory for Condensed Matter Physics, Institute of Physics, Chinese Academic of Science Beijing 100190 China.
- e. National Laboratory for Solid State Microstructures, Department of Physics Nanjing University 210093 Nanjing, China.

* klaus.hasselbach@neel.cnrs.fr Institut Néel F-38042 Grenoble France.

¹ Present address High Magnetic Field Chinese Academic of Science Hefei Anhui 230031 China.

We report the behavior of the radiofrequency response of BaFe_{2-x}Ni_xAs₂ in the antiferromagnetic and superconducting states. At radiofrequencies (10 MHz to 1 GHz) the temperature dependence of the surface impedance $Z=R+jX$ was measured which yields the temperature dependence of the complex conductivity $\sigma_1-j\sigma_2$ in the

$$Z = R + jX = \sqrt{\frac{j\mu_0\omega}{\sigma_1 - j\sigma_2}}$$

superconducting and magnetic states:

R and X differ from each other in the superconducting and magnetic states [1]. The unusual temperature dependence of the real part σ_1 of the electronic conductivity found around the superconducting phase transition $T_C \sim 16$ K are attributed to magnetic fluctuations. The establishment of a magnetic order at $T_M \sim 21$ K results in marked decrease of the scattering of electronic carriers [2]. A similar behavior of the conductivity has been observed in DyNi₂B₂C compound which exhibits superconductivity coexisting with magnetic order [1]. The real part of the conductivity σ_1 represents the loss related to the normal carriers. The imaginary part of the conductivity σ_2 is related to the London penetration depth. The complex permeability $\mu = \mu_0(1 + j\omega\tau_{mag})$ in the ordered magnetic state below T_M is attributed to a relaxation time τ_{mag} . A complex permeability is algebraically equivalent to a Drude type conductivity $\sigma_1 - j\sigma_2 = (\sigma_{1cor} - j\sigma_{2cor}) / (1 + j\omega\tau_{mag})$

where $\sigma_{1cor}-j\sigma_{2cor}$ is the corrected conductivity. σ_{1cor} takes into account the total dissipation of the system. σ_{2cor} is the measure of the superfluid density in the system and should be =0 at $T > T_C$. Below T_M the enhancement of σ_{1cor} is attributed to the increase of the electron scattering time when local magnetic order sets in.

[1] Durga P. Choudury, H. Srikanth, S. Sridhar, and P. C. Canfield Phys. Rev. B **58**, 14490 (1998).

[2] M. Saint-Paul, C. Guttin, A. Abbassi, Zhang-Sheng Wang, Huiqian Luo, Xingye Lu, Cong Ren, Hai-Hu Wen, and K. Hasselbach Solid State Commun **267**, 48 (2017)..

Equation of state and thermal-like behavior in a confined granular suspension

N. Sakai^{a,b,*}, F. Lechenault,^a S. Moulinet^a and M. Adda-Bedia^{a,c}

- a. Laboratoire de Physique Statistique, Ecole Normale Supérieure, 24 rue Lhomond 75005 Paris
 b. HH Wills Physics Lab., University of Bristol, Tyndall Avenue, BS8 1TL Bristol
 c. Laboratoire de Physique, ENS Lyon, 46 allé d'Italie, F-69364 Lyon Cedex 07

* nariaki.sakai@bristol.ac.uk

We experimentally investigate the stationary sedimentation of an assembly of buoyant cylinders in a rotating Hele-Shaw cell. The resulting tunable centripetal force allows exploring various states of the system, from a dispersed liquid state to a hexagonally packed state. The phenomenology of the liquid state is remarkably thermal-like: we uncovered an equation of state relating pressure, density through an effective temperature, valid in the whole range of physical parameters we investigated. The "thermal" fluctuations comes from the energy injected by the buoyancy, and this effective temperature takes a thermodynamic signification when the energy injection rate is small *i.e.* close to equilibrium, as the ratio between fluctuations and compressibility. This relation is supported by the existence of a large deviation function on the density, and in particular implies that correlations on density are short-ranged *i.e.* extensivity holds in the system, and there is a one-to-one relation between density fluctuations its mean.

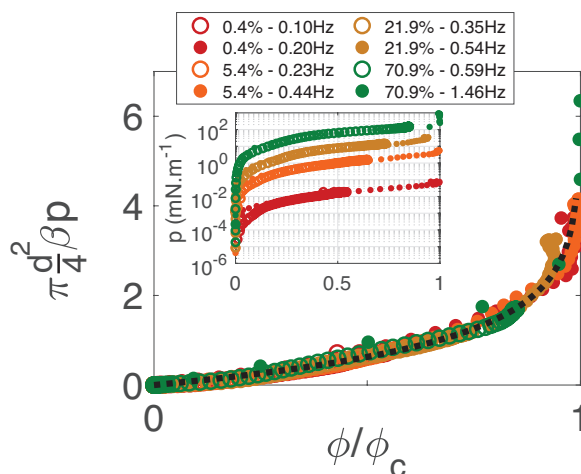


Figure 1: Equation of state between normalized osmotic pressure $\pi \frac{d^2}{4} \beta p$ and normalized packing fraction ϕ/ϕ_c - where ϕ_c is the close packed density $\phi_c = \frac{\pi}{\sqrt{12}}$ - for selected rotation rates and density contrasts between grains and solvent. The black dotted line corresponds to the analytical expression of the equation of state $y = -\phi_c \log(1 - \phi/\phi_c)$. The inset shows the non-normalized pressure in semi-log scale.

Nanoscale analyses of axial III-V nanowires for solar cells

O. Saket¹, H. Chalermchai¹, A. Ali¹, V. Piazza¹, F. H. Julien¹, S. Collin¹, A. Cattoni¹, F. Oehler¹, J.-C. Harmand¹, M. Tchernycheva¹

¹ C2N sites Orsay et Marcoussis, UMR9001 CNRS, Université Paris Sud, Université Paris Saclay

Email: omar.saket@u-psud.fr*, maria.tchernycheva@u-psud.fr

The record in photovoltaic conversion efficiency is detained by multi-junction solar cells based on III-V semiconductors. However, the wide adoption of these devices is hindered by their high production cost, to a large extent due to the expensive III-V substrates. As an alternative, a hybrid geometry has been proposed [LaPierre JAP 2011], which combines a 2D Si bottom cell with a III-V nanowire top cell in a tandem device. This approach, which may reach theoretical efficiencies of approx. 34%, requires smaller amounts of expensive III-V materials compared to conventional III-V tandem cells and benefits from the nanowire light trapping effects.

In this work, we report the fabrication and nanoscale characterization of nanostructures for solar cells: namely, axial GaAsP p-n junction nanowires. Nanowires are grown by gallium-assisted molecular beam epitaxy using Be and Si as doping sources. The composition (probed by EDX and cathodoluminescence) was adjusted to tune the bandgap toward the optimal value for a III-V-on-Si tandem cell (approx. 1.7 eV). Local I-V characteristics and electron beam induced current (EBIC) microscopy under different biases are used to probe the electrical properties and the generation pattern of individual nanowires. The doping concentrations and the minority carrier diffusion lengths were extracted from the EBIC generation profiles (see figure 1). The effect of an epitaxial GaP passivating shell on the optical and generation properties was assessed.

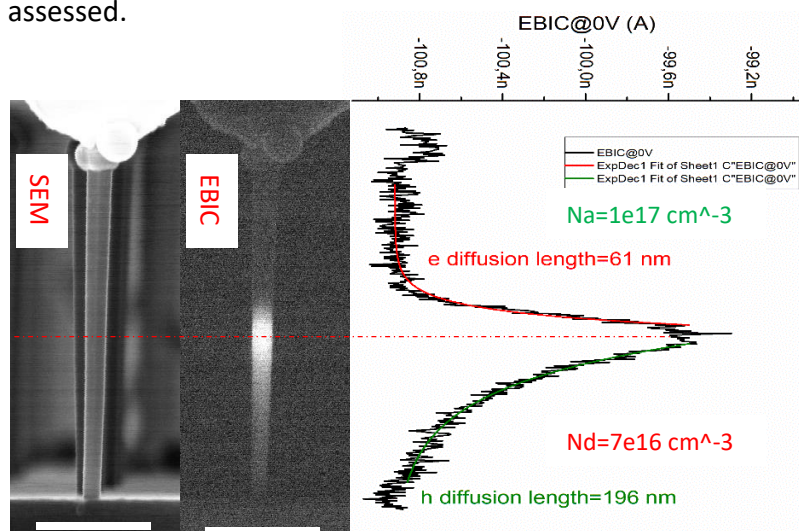


Figure 1: EBIC map of a single GaAsP NW containing an axial p-n junction and the corresponding SEM image at $V_{bias}=0V$

LaPierre, JAP, **110**, 014310, 2011) and Bu 34.3 % (Bu et al., APL, **102**, 031106, 2013).

A bright electron source produces UV light

Evelyne Salançon^{a*}, Laurent Lapena^a, Victoria Tishkova^a & Roger Morin^a

a. Aix Marseille Université, CNRS, CINaM, UMR 7325, campus de Luminy-case 913, 13288 Marseille cedex 9

* salancon@cinam.univ-mrs.fr

Electron emission from an insulating crystal (celadonite) deposited on a carbon surface [1,2,3] follows a Fowler-Nordheim law up to a threshold field $F_t \sim 5V/\mu m$. An emission process based on the nanostructure created in between the carbon surface and the insulator will be first presented. It explains why Fowler-Nordheim emission, requiring some V/nm , is possible even with a low applied field of about some $V/\mu m$.

Above F_t departure from the Fowler-Nordheim law takes place (smaller increase of current vs field). An ultraviolet light is then detected by various materials fluorescence (glass, MACOR...). The UV source is characterized by projection microscopy. It is shown that its location is that one of the electron point source and its size is submicrometric (same order of the crystal dimensions $\sim 500nm$). The detected light intensity vs the voltage difference between a pure Fowler Nordheim $I(V)$ characteristic and the measured $I(V)$ characteristics follows a cube root law.

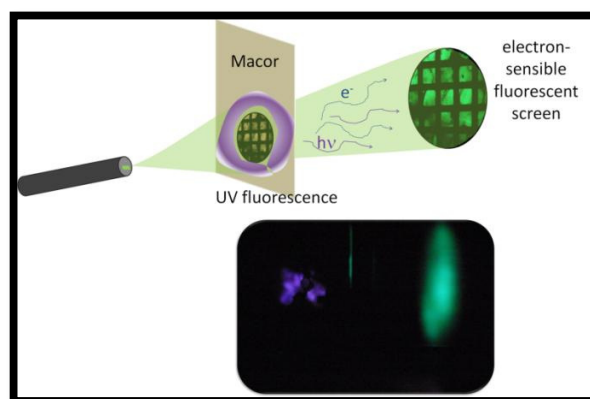


Figure 1: Scheme of electron and UV emissions from an insulating crystal deposited at the apex of a carbon wire.

1. E. Salançon, R. Daineche, O. Grauby, and R. Morin, JVST B 33, 030601 (2015)
2. R. Daineche, A. Degiovanni, O. Grauby, and R. Morin, Appl. Phys Lett. 88, 023101 (2006)
3. J. Rech, O. Grauby, and R. Morin, JVST B 20, 5-9 (2002)

Seebeck coefficient of AuGe thin films for thermoelectric applications in organic nanoscale devices

Chloé Salhanir^a, Philippe Lafarge^a, and Maria Luisa Della Rocca^{a*}

a. Laboratoire MPQ, Université Paris Diderot, Sorbonne Paris Cité, UMR 7162, CNRS.
10, rue Alice Domon et Léonie Duquet, 75205 Paris Cedex 13, France

* Electronic mail: maria-luisa.della-rocca@univ-paris-diderot.fr

We experimentally study the thermoelectric properties of $\text{Au}_x\text{Ge}_{1-x}$ thin film alloys, close to the metal-insulator transition[1], with the goal of obtaining an element with good thermal sensor electrical properties for integration into nanoscale organic devices.

Based on finite element simulations and by taking into account all spurious thermoelectric effects[2], we have revealed a Seebeck coefficient of the thin film alloy very close to that of Au thin films. Simultaneously we have observed good electrical properties of the thin film alloy allowing to use it as a high resolution thermometer.

As a proof of principle, we have demonstrated the possibility to integrate such an element as the top electrode of a large area vertical molecular junction, embedding thin (5–10 nm) molecular layer, device in which the AuGe film simultaneously fulfills the functions of a local heater and thermometer.

[1]Dodson, B. W., McMillan, W. L., Mochel, J. M., & Dynes, R. C.. Metal-insulator transition in disordered germanium-gold alloys. *Physical Review Letters* 46(1), 46. (1981)

[2]Bakker, F. L., Flipse, J., & van Wees, B. J. Nanoscale temperature sensing using the Seebeck effect. *Journal of Applied Physics*, 111(8), (2012)

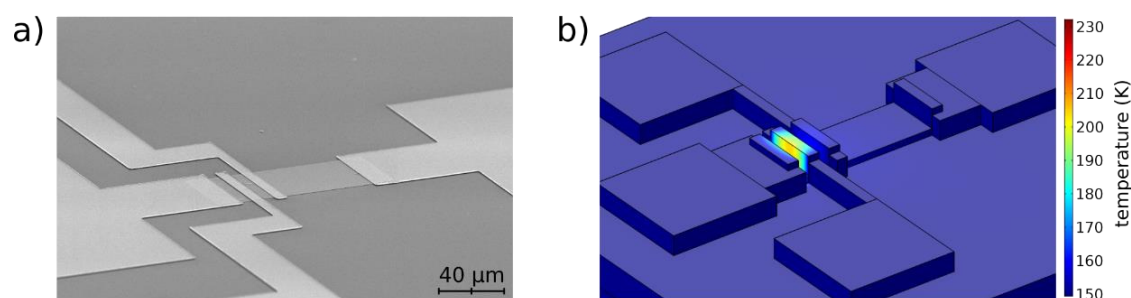


Figure 1 : a) : SEM image of a device intended to measure the Seebeck coefficient of an $\text{Au}_x\text{Ge}_{1-x}$ thin film alloy. b) Simulated three dimensional color plot of the temperature in said sample for an applied voltage V_{ab} of 2V between the a and b contacts at a temperature $T=150$ K of the environment.

Strongly-correlated ultracold bosons in one dimension

Laurent Sanchez-Palencia^{a*}

a. CPHT, Ecole Polytechnique, CNRS, Université Paris-Saclay, Route de Saclay, 91128 Palaiseau, France

* « lsp@cpht.polytechnique.fr »

Reduced dimensions have dramatic effects on the dynamics of many-body quantum systems. For instance, in one dimension, the interactions as well as the interference effects are strongly enhanced compared to higher dimensions. It has fundamental consequences, such as the enhancement of quantum correlations in extreme dilute systems, the fermionization of Bose gases, and the emergence of diverging susceptibilities at characteristic length scales. The latter is responsible for a novel superfluid-insulator transition in infinitely small periodic potentials, known as the pinning transition. Recently, there has been a huge amount of activity in the quantum simulation of such systems with ultracold quantum gases.

In this contribution, I report recent results of ours on Lieb-Liniger bosons subjected to external potentials. On the one hand, I discuss the behaviour of the Tan contact of the Lieb-Liniger gas under harmonic confinement for arbitrary temperature, number of particles, interaction strength, and trap frequency [1]. We show that it can be written as a universal function of only two scaling parameters and derive the scaling function. Importantly, we show that the contact realizes an unequivocal signature of the fermionization effect in the trapped system and provide quantitative evidence that this effect can be extracted from the general behaviour of momentum distributions as measured routinely in experiments. On the other hand, I discuss recent developments on the pinning transition [2]. In particular, we show that the quantum critical line is significantly affected by strong renormalization of the Luttinger parameter induced by an even weak periodic potential. This results are found using exact quantum Monte Carlo calculations and confirmed in quantum simulators realized with ultracold Bose gas with controlled interactions.

[1] H. Yao, D. Clément, A. Minguzzi, P. Vignolo, and L. Sanchez-Palencia, Tan's contact for trapped Lieb-Liniger bosons at finite temperature, *to appear*, arXiv:1804.XXXXX.

[2] G. Boéris, L. Gori, M. D. Hoogerland, A. Kumar, E. Lucioni, L. Tanzi, M. Inguscio, T. Giamarchi, C. D'Errico, G. Carleo, G. Modugno, and L. Sanchez-Palencia, Mott transition for strongly interacting one-dimensional bosons in a shallow periodic potential, *Phys. Rev. A* **93**, 011601(R) (2016).

Thermosensitive and magnetic polymer microgels: structural studies of the volume phase transition by SANS and *in situ* VSANS under magnetic field hyperthermia

O. Sandre^{a*}, G. Hemery^a, A. Brûlet^b, G. Aguirre^c, L. Billon^c, E. Deniau-Lejeune^c

- Laboratoire de Chimie des Polymères Organiques, UMR 5629 CNRS / Univ. Bordeaux / Bordeaux INP, Pessac, France
- Laboratoire Léon Brillouin, UMR12 CNRS/CEA-Saclay, Saclay, France
- IPREM, Equipe de Physique et Chimie des Polymères, UMR 5254 CNRS / Université de Pau & Pays Adour, Pau, France

* olivier.sandre@enscbp.fr

The aim of our work is to study the outer size of biocompatible and thermoresponsive microgels based on oligo(ethylene glycol) methyl ether methacrylate (OEGMA), di(ethylene glycol) methyl ether methacrylate (MEO2MA) and methacrylic acid (MAA) (P(MEO₂MA-co-OEGMA-co-MAA) microgels) and of the corresponding hybrid analogues loaded with iron oxide magnetic nanoparticles (MNPs).^[1] Three different cross-linkers, ethylene glycol dimethacrylate (EGDMA), oligo(ethylene glycol) diacrylate (OEGDA) or N,N-methylenebisacrylamide (MBA) were used for the synthesis of the microgels.^[2] Due to different reactivity ratio of cross-linkers compared to monomers, three different microgel structures differing by their distribution of crosslinks were assumed by macroscopic consumption of the reactants using ¹H NMR. These hypothetical structural differences impacts the swelling-to-collapse transition of these microgels in response to T and pH.^[2]

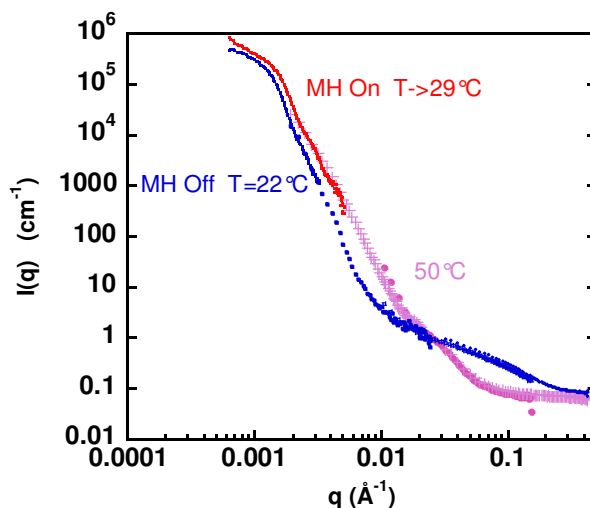


Figure 1 : Merged (V)SANS curves of magnetic microgels crosslinked with MBA and loaded with 5wt% γ -Fe₂O₃ MNPs.

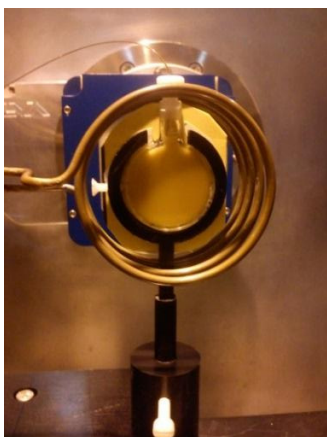


Figure 2: Inductor coil on TPA

A SANS study on the PAXY spectrometer has permitted to investigate the inner structure of these microgels (either core-shell or homogeneous crosslinked spheres) depending on the choice of cross-linker and on temperature. In parallel, a VSANS study on TPA enabled to measure overall size change (*i.e.* gyration radius) vs. temperature, be it varied macroscopically (with a water bath) or by magnetic induction. After the recently reported magnetic field hyperthermia (MFH) combined with DLS,^[3] this novel *in situ* coupling of MH with VSANS is another world-premiere!

[1] M. Boularas, E. Gombart, J-F. Tranchant, L. Billon, M. Save, *Macromol. Rapid Commun.* **36**, 79-83 (2015)

[2] M. Boularas, E. Deniau-Lejeune, V. Alard, J-F. Tranchant, L.

Billon, M. Save, *Polym. Chem.* **7**, 350-363 (2016)

[3] G. Hemery, E. Garanger, S. Lecommandoux, A. Wong, E. Gillies, B. Pedrono, T. Bayle, D. Jacob, O. Sandre, *J. Phys. D.* **48**, 494001 (2015)

Synchrotron X-ray Diffraction Exploration of Growth and Structure in 2D Transition Metal Dichalcogenides

R. Sant^{1,2}, **S. Lisi**^{1,2}, **A. Marty**^{1,3}, **M. Jamet**^{1,3}, **J. Coraux**^{1,2}, **G. Renaud**^{1,4}
roberto.sant@neel.cnrs.fr

¹Université Grenoble-Alpes, Grenoble, France

²CNRS, Inst. Néel, Grenoble, France

³CEA, INAC-SP2M, Grenoble, France

⁴CEA, INAC-MEM, Grenoble, France

Two-dimensional transition metal dichalcogenides (TMDCs) host unique phenomena related to their dimensionality and they are considered for a variety of optoelectronic applications. However, the growth of crystalline epitaxial TMDC layers over large surfaces in view of large-scale (opto)electronic-grade quality is a major challenge. The moderate structural quality of the 2D TMDCs achievable up to date hinders access to their intrinsic properties and limits device performance. As in the case of graphene, an in-depth study of the growth mechanisms is expected to solve these issues. We aim to explore the nature of the epitaxy, which is crucial to eventually achieve large single-crystalline TMDC domains or even full layers. For that purpose we rely on fine *in-situ* diagnostics of the structure based on synchrotron X-ray surface diffraction. Thanks to this technique, high resolution characterization can be performed down to the single layer level, and this can be done in real time, during growth or thermal treatments. We used the INS2 instrument installed at the BM32 CRG/IF beamline at ESRF. Our study is focused on structural features that are expected to have key influence over the (opto)electronic properties, noteworthy strain in three dimensions, mosaic spread, domain size, superstructures, and thickness. Our detailed structural analysis also sheds light on the still-open question about the nature of the interaction between the TMDC layers and the substrate surface, which a priori comprises a van der Waals contribution and a certain covalent character. In the presentation, we will show the specificities of the INS2 instrument, the methods of analysis and the first results obtained from our investigations started in October 2016 on two prototype TMDC systems: single layer PtSe₂, obtained by selenization of a Pt(111) single crystal surface, and single layer MoS₂, grown by molecular beam epitaxy on Au(111). Both materials grow highly oriented on the respective substrates, exhibit highly-ordered superstructures, and have various degrees of strain related to heteroepitaxial stress.

Cooling a Bose gas by three-body losses

Max Schemmer^{a*}, Isabelle Bouchoule,^a

a. Laboratoire Charles Fabry, Institut d'Optique, CNRS, Université Paris Sud 11, 2 Avenue Augustin Fresnel, F-91127 Palaiseau Cedex, France

* maximilian.schemmer@institutoptique.fr << corresponding author >>

The lifetime of Bose-Einstein condensates is limited by three-body recombination processes, which amount to three-body losses. These losses are typically associated with a heating. Here I present the first demonstration of cooling by three-body losses in a 1D Bose gas in the quasi-condensate regime, using an atom chip experiment. While three-body losses continuously reduce the density of the system the temperature T drops up to a factor of four.

To compare with theory, we extended the recent theoretical description of one-body losses in a homogeneous gas [1] to arbitrary j-body losses and to inhomogeneous gases. For 3-body losses occurring in a harmonically confined 1D quasi-condensate, we find that the ratio $k_B T / (mc^2)$ is expected to converge to 0.7, with c the speed of sound and m the atom mass. This ratio for our experimental data is close to this asymptotic value all along the observed time-evolution. We took different sets of data, corresponding to different effective 1D interaction strength g and different linear densities n . The dimensionless 1D interaction parameter $\gamma = mg / (\hbar^2 n)$ spans more than two orders of magnitude over the different sets of data, while the ratio $T / (mc^2)$ stay close to its asymptotic value of 0.7 (see Fig.1).

[1] Grišins, P., et al.. Degenerate Bose gases with uniform loss. Physical Review A, 93(3), 033634.

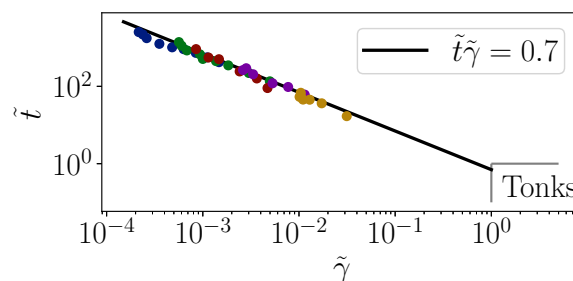


Figure 1: The thermodynamic properties of a 1D Bose are characterized by γ and the dimensionless temperature $t = \hbar^2 k_B T / (mg^2)$. The experimental data collapses on the line $t\gamma = 0.7$, which correspond to $T / (mc^2) = 0.7$.

Linking electronic transport through a spin crossover thin film to the molecular spin state using X-ray absorption spectroscopy operando techniques

Filip Schleicher^{a,b,*}, Michał Studniarek^b, Kuppusamy Senthil Kumar^b, Etienne Urbain^b, Kostantine Katcko^b, Jinjie Chen^c, Timo Frauhammer^c, Marie Hervé^c, Ufuk Halisdemir^b, Lalit Mohan Kandpal^b, Daniel Lacour^a, Alberto Riminucci^d, Loic Joly^b, Fabrice Scheurer^b, Benoit Gobaut^e, Fadi Choueikani^e, Edwige Otero^e, Philippe Ohresser^e, Jacek Arabski^b, Guy Schmerber^b, Wulf Wulfhekel^{c,f}, Eric Beaurepaire^b, Wolfgang Weber^b, Samy Boukari^b, Mario Ruben^{b,f}, Martin Bowen^b

- a. Université de Lorraine, CNRS, IJL, F-54000 Nancy, France
- b. IPCMS UMR 7504 CNRS, Université de Strasbourg, 23 Rue du Loess, BP 43, 67034 Strasbourg Cedex 2, France
- c. Physikalisches Institut, Karlsruhe Institute of Technology, Wolfgang-Gaede-Str. 1, 76131 Karlsruhe, Germany
- d. ISMN-CNR, Via Gobetti 101, 40129 Bologna, Italy
- e. Synchrotron SOLEIL, L'Orme des Merisiers, Saint-Aubin - BP 48, 91192 Gif-sur-Yvette, France
- f. Institute of Nanotechnology, Karlsruhe Institute of Technology (KIT), Hermann-von-Helmholtz-Platz 1, 76344 Eggenstein-Leopoldshafen, Germany

* filip.schleicher@univ-lorraine.fr

One promising route toward encoding information is to utilize the two stable electronic states of a spin crossover molecule. While this property is clearly manifested in transport across single molecule junctions, evidence linking charge transport across a solid-state device to the molecular film's spin state has thus far remained indirect. To establish this link, we deploy materials-centric and device-centric operando experiments involving X-ray absorption spectroscopy. We find a correlation between the temperature dependencies of the junction resistance and the Fe spin state within the device's [Fe(H₂B(pz)₂)₂(NH₂-phen)] molecular film. We also factually observe that the Fe molecular site mediates charge transport. Our dual operando [1] studies reveal that transport involves a subset of molecules within an electronically heterogeneous spin crossover film. Our work confers an insight that substantially improves the state-of-the-art regarding spin crossover-based devices, thanks to a methodology that can benefit device studies of other next-generation molecular compounds.

Language: English.

[1] Studniarek, M.; Halisdemir, U.; Schleicher, F.; Taudul, B.; Urbain, E.; Boukari, S.; Hervé, M.; Lambert, C.-H.; Hamadeh, A.; Petit-Watelot, S.; et al. Probing a Device's Active Atoms. *Adv. Mater.* 2017, 29 (19), 1606578.

Quantum Simulation of Hawking Radiation with Surface Acoustic Waves

R. P. Schmit^{a*}, B. G. Taketani,^b and F. K. Wilhelm^a

- a. Theoretical Physics, Saarland University, Campus, 66123 Saarbrücken, Germany
- b. Departamento de Física, Universidade Federal de Santa Catarina, 88040-900, Florianópolis, SC, Brazil

* raphael.schmit@lusi.uni-sb.de

In 1975, using quantum field theory in curved space-time, S. Hawking predicted black holes to emit thermal radiation. Since the experimental observation from an actual black hole is challenging, analogue systems have gained more and more attention in the verification of this concept. We propose an experimental set-up consisting of two adjacent piezoelectric semiconducting layers, one of them carrying dynamic quantum dots (DQDs), and the other being p-doped with an attached gate on top, which introduces a space-dependent layer conductivity. The propagation of surface acoustic waves (SAWs) on the latter layer is governed by a wave equation with an effective metric. In the frame of the DQDs, this metric is equivalent to that of a two dimensional non-rotating and uncharged black hole with an apparent horizon for SAWs. Analogue Hawking radiation appears in form of phonons. We show that for a GaAs piezoelectric the Hawking temperature is in the mK-regime.

- [1] R. P. Schmit, B. G. Taketani, F. K. Wilhelm, Quantum Simulation of Hawking Radiation with Surface Acoustic Waves, arXiv preprint arXiv:1804.04092 (2018)

Pairing in inhomogeneous and mesoscopic systems: cold atoms, metallic clusters, nuclei.

Peter Schuck^{a*}

a. LPMMC, Grenoble

* schuck@grenoble.cnrs.fr

Different aspects of pairing in finite size quantum systems will be presented.

i) Cold atoms in harmonic traps. Gap as a function of radius and temperature is discussed. It will be shown that the Local Density Approximation is not valid when approaching the critical temperature.

ii) Superconducting metallic grains show an *increase* of the gap with *decreasing* size before superconductivity breaks down due to the Anderson criterium.

iii) In the outer crust of neutron stars there are still isolated superfluid nuclei. Going deeper into the crust, it happens that the nuclei spill out neutrons which form a gas of superfluid itinerant neutrons. It will be shown that close to the spill out (overflow) point the gap becomes strongly quenched.

STM-induced light emission: from molecular LED to subnanometric optical microscopy.

Guillaume Schull*

Institut de Physique et Chimie des Matériaux de Strasbourg, UMR 7504
(CNRS - Université de Strasbourg), Strasbourg, France Remplacez ceci par la première

* schull@unistra.fr

The electric current traversing the junction of a scanning tunneling microscope (STM) may generate a local emission of light. During the last years, we have used this method to study the intrinsic luminescence properties of individual molecules. This work has progressed in two directions. On one side we have used the ability of the STM to manipulate matter with atomic-scale precision to form single-molecule light emitting devices [1]. Composed by individual molecular wires suspended between the tip and the sample of the STM (see figure), these devices generate an emission of light whose color, intensity and bandwidth can be controlled with high precision [2,3]. On the other side, we used the intrinsic resolution of the STM to performed sub-molecularly resolved vibronic spectroscopy of molecules separated from a metallic surface by a thin insulating layers [4]. Together with other recent reports [5,6], this result constitutes an important step towards photonic measurements with atomic-scale resolution.

- [1] G. Reecht et al., Phys. Rev. Lett. 112, 047403 (2014)
- [2] M.C. Chong et al., Phys. Rev. Lett. 116, 036802 (2016)
- [3] M.C. Chong et al., Nanoletters 16, 6480 (2016)
- [4] B. Doppagne et al., Phys. Rev. Lett. 118, 127401 (2017)
- [5] Y. Zhang et al. Nature 531, 623 (2016)
- [6] H. Imada et al., Nature 538, 364 (2016)

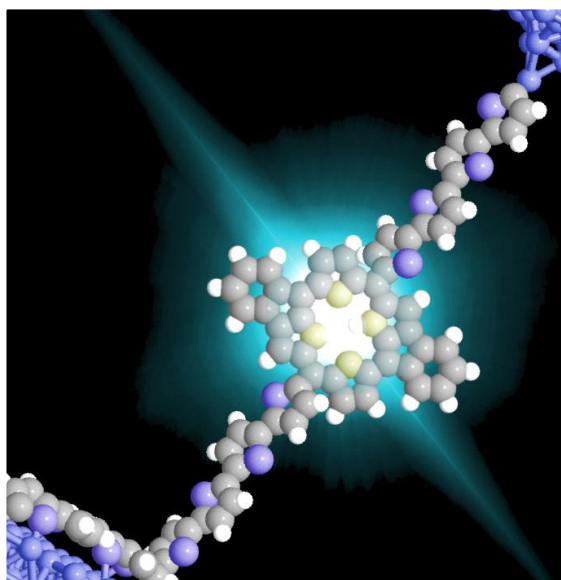


Figure : Artistic view of a single-molecule optoelectronic device operated with a scanning tunnelling microscope.

Cavitation events in a liquid confined by a porous media

Chiara Scognamiglio^{a,b*}, Xavier Noblin^b and Carlo Massimo Casciola^a

- a. Dipartimento di Ingegneria Meccanica e Aerospaziale, Università degli studi di Roma La Sapienza, Via Eudossiana 18 00184 Roma, Italia
- b. Institut de Physique de Nice (INPHYNI), UMR 7010 UNS/UCA/CNRS. Parc Valrose, 06108 Nice Cedex 2, France.

* scognamiglio.chiara1@gmail.com

Cavitation bubbles are extraordinary, albeit small, objects that play a determinant role in countless processes, inside natural [1] and artificial [2] systems. The present study focuses on the nucleation and dynamics of cavitation bubbles in a confined liquid. It relies on a device made of micrometric volumes of water encapsulated by a hydrogel, poro-elastic and hydrophilic material mimicking plant tissues. Water evaporation across the hydrogel pores results in a remarkable pressure reduction in the liquid, that will eventually break into a cavitation bubble. A dedicated optical and acoustic set-up has been developed to perform imaging and acoustic measurements. Indeed, previous studies showed that confined bubbles oscillate at high frequency emitting ultrasounds with a frequency being order of a few MHz [3]. We were able to identify the acoustic signature of a confined bubble and characterize its parameters (resonant frequency and damping rate) as a function of the confinement size. The dynamics is even more intriguing if water is confined in an array of small hydrogel cavities. Water cavities, separated one from the other by hydrogel walls, are close enough to interact in a unique fashion. Cavitation in one volume can trigger other nucleation events in the neighboring cavities, causing cavitation propagation. We will present acoustic signatures in case of multiple cavitation events, giving insights on the possible mechanism underlying the propagation of cavitation.

[1] X. Noblin, N. Rojas, J. Westbrook, C. Llorens, M. Argentina, and J. Dumais, The fern sporangium: a unique catapult., *Science*, vol. 335, no. 6074, p. 1322, 2012.

[2] T. D. Wheeler and A. D. Stroock, "The transpiration of water at negative pressures in a synthetic tree," *Nature*, vol. 455, no. 7210, pp. 208–212, 2008.

[3] O. Vincent, P. Marmottant, S. R. Gonzalez-Avila, K. Ando, and C.-D. Ohl, "The fast dynamics of cavitation bubbles within water confined in elastic solids," *Soft Matter*, vol. 10, no. 10, pp. 1455–1461, 2014.

Coherent backscattering of weakly interacting ultracold atoms

Thibault Scoquart^{a*}, Nicolas Cherroret,^a Dominique Delande^a

a. Laboratoire Kastler Brossel, Sorbonne Université, CNRS, ENS-Université PSL, Collège de France, 4 Place Jussieu, 75005 Paris, France

* thibault.scoquart@lkb.upmc.fr

We study the momentum-space dynamics of a weakly interacting quantum gas of bosons propagating in a spatially disordered medium. Specifically, we focus on the impact of weak interactions on the time evolution of the Coherent Backscattering (CBS) peak [1]. For a non-interacting gas initially prepared as a plane wave state $|\mathbf{k}_0\rangle$ in a random potential, CBS usually manifests itself as an interference peak around the backscattering direction of the momentum distribution [2]. When weak interactions are present, the evolution is governed by the Gross-Pitaevskii equation for the condensed, disordered Bose gas.

Recent simulations suggest that interactions have three main effects on the CBS peak. At very short times first, they prevent the CBS peak from reaching its maximum value of twice the height of the diffusive background. Then on a longer time scale, interactions mimic a decoherence mechanism and make the CBS peak contrast slowly decay in time (Fig. 1). Finally, at very long times, interactions are expected to thermalize the whole momentum distribution. The study of these effects will give some insight on how the interactions affect phase coherence and the energy distribution of quantum gases in disordered environments.

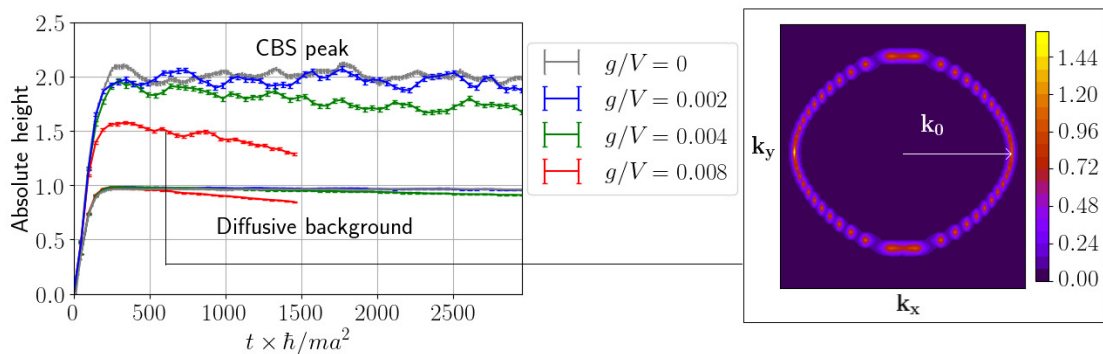


Figure 1: Left : Time evolution of the CBS peak and the diffusive background amplitudes in momentum space for various values of the interaction energy scale g/V (V is the volume of the system). We use a delta-correlated disorder of strength $V_0 = 0.2 \times \hbar^2/ma$, and $k_0 = \frac{\pi}{2a}$ such that $k_0 l \sim 100$. the result is averaged over 3000 realizations of the disorder. Right : Density plot of the momentum distribution at time $t = 600 \times \hbar/ma^2$ (a is the lattice spacing).

[1] N. Cherroret et al., Phys. Rev. A **85**, 011604 (2012).

[2] F. Jendrzejewski et al., Phys. Rev. Lett. **109**, 195302 (2012).

Towards strain-coupled optomechanics with rare-earth doped crystals

S. Seidelin^{a,e*}, N. Galland^a, N. Lucic^b, S. Piccolomo^b, H. Alvarez-Martinez^b, R. Le Targat^b, A. Ferrier^{c,d}, J.-F. Motte^a, B. Fang^b, P. Goldner^c, Y. Le Coq^b

- a. Université Grenoble Alpes and CNRS, Institut NEEL, F-38042 Grenoble,
- b. LNE-SYRTE, Observatoire de Paris, Université PSL, CNRS, Sorbonne Université, 61 avenue de l'Observatoire 75014 Paris
- c. Université PSL, Chimie ParisTech, CNRS, Institut de Recherche de Chimie Paris, 75005, Paris,
- d. Sorbonne Université, 75005, Paris, France
- e. Institut Universitaire de France, 103 Boulevard Saint-Michel, F-75005 Paris, France

* signe.seidelin@neel.cnrs.fr

An exciting challenge of modern physics is to investigate the quantum behavior of a bulk “material” object - for instance a mechanical oscillator - placed in a non-classical state. One major difficulty relies in interacting with the mechanical object without perturbing with its quantum behavior. An approach consists of exploiting a hybrid quantum system consisting of a mechanical oscillator coupled to an atom-like object, and interact via the atom-like object. A particularly appealing coupling mechanism between resonator and “atom” is based on material strain. Here, the oscillator is a bulk object containing an embedded artificial atom (dopant, quantum dot, ...) which is sensitive to mechanical strain of the surrounding material. Vibrations of the oscillator result in a time-varying strain field that modulates the energy levels of the embedded structure. We have recently suggested to use rare-earth doped crystals for strain-coupled systems [1]. More concretely, we are currently studying an yttrium silicate (Y₂SiO₅) crystal containing a triply charged europium ion (Eu³⁺), which is optically active. The reason behind this choice stems from the extraordinary coherence properties of this dopant, combined with its high strain-sensitivity: the Eu³⁺ in an Y₂SiO₅ matrix has an optical transition with the narrowest linewidth known for a solid-state emitter [2], and the transition is directly sensitive to strain [3]. We have successfully fabricated mechanical resonators (see figure1), designed and set up the experiment, and achieved a signal-to-noise ratio compatible with the planned measurements [4]. We have recently obtained measurements of the frequency sensitivity the europium ions of uniaxial stress applied to the bulk crystal, and are currently starting to investigate the resonator shown in figure 1.

[1] K. Mølmer, Y. Le Coq and S. Seidelin, Dispersive coupling between light and a rare-earth ion doped mechanical resonator, *Phys. Rev. A* 94, 053804 (2016)

[2] R. Yano, M. Mitsunaga, and N. Uesugi, Ultralong optical dephasing time in Eu³⁺:Y₂SiO₅, *Optics Letters*, 16, 1884 (1991)

[3] M. J. Thorpe et al., Frequency stabilization to 6 x10⁻¹⁶ via spectral-hole burning, *Nature Photonics*, 5, 688 (2011)

[4] O. Gobron et al, *Optics Express*, 15539, 25 (2017)

Gate-tunable superconductivity in the AlOx/SrTiO3 heterostructure

Shamashis Sengupta^{a*}, Emilie Tisserond^b, Florence Linez^c, Miguel Monteverde^b, Tobias Rodel^a, Anil Murani^b, Philippe Lecoeur^c, Thomas Maroutian^c, Claire Marrache-Kikuchi^a, Andrés Santander-Syro^a, and Franck Fortuna^a

- a. Centre de Sciences Nucléaires et de Sciences de la Matière, Univ. Paris-Sud, CNRS/IN2P3, Université Paris-Saclay, 91405 Orsay, France
- b. Laboratoire de Physique des Solides, Univ. Paris-Sud, CNRS, Université Paris-Saclay, 91405 Orsay, France
- c. Centre de Nanosciences et de Nanotechnologies, Univ. Paris-Sud, CNRS, Université Paris-Saclay, 91405 Orsay, France

* shamashis.sengupta@csnsm.in2p3.fr

SrTiO₃-based two-dimensional electron gases (2DEGs) have led to important discoveries [1,2] about superconductivity in low dimensions, such as the observation of pairing interactions without superconductivity [3] and density-of-states features resembling the pseudogap in cuprates [4].

We have devised a method for the facile realization of a 2DEG by the creation of oxygen vacancies (Rodel et al., *Advanced Materials* 28,1976 (2016)). The deposition in ultra-high vacuum of a thin layer of metallic Al on SrTiO₃ leads to the creation of a 2DEG due to the withdrawal of oxygen atoms from the surface by the reducing agent Al (which turns into insulating AlO_x).

Transport experiments show that the 2DEG is superconducting with a critical temperature of 320 mK. The critical parameters (temperature and field) are tunable with the gate voltage, leading to a 'superconducting dome' in the phase diagram. The possibility of continuously varying the carrier density allows us to study different equilibrium and non-equilibrium features characterizing the electronic phases. Results of some recent experiments will be presented.

[1] Reyren et al., *Science* 317, 1196 (2007)

[2] Cavaglia et al., *Nature* 456, 624 (2008)

[3] Cheng et al., *Nature* 521, 196 (2015)

[4] Richter et al., *Nature* 502, 528 (2013)

L'intermittence dans les modèles de dynamo turbulente, quel moment prédit le seuil de l'instabilité?

Kannabiran Seshasayanan^{a*}, François Pétrélis^b

- a. Service de Physique de l'État Condensé, CEA, CNRS UMR 3680, Université Paris-Saclay, CEA Saclay, 91191 Gif-sur-Yvette, France
- b. Laboratoire de Physique Statistique, École Normale Supérieure, CNRS UMR 8550, Université Paris Diderot, Université Pierre et Marie Curie, 24 rue Lhomond, 75005 Paris, France

* kannabiran.seshasayanan@cea.fr

L'effet dynamo explique l'existence du champ magnétique (B) dans la terre et d'autres objets astrophysiques. L'instabilité dynamo est engendrée par le mouvement d'un fluide conducteur. La plupart des théories sur l'effet dynamo sont faites pour un écoulement laminaire. Mais les dynamos de laboratoire ou dans la nature sont engendrées par un écoulement fortement turbulent.

Un modèle analytique qui prend en compte les fluctuations turbulentes a été proposé par Kazantsev [1]. Au même moment Kraichnan [2] a développé un modèle similaire pour le problème de l'advection d'un scalaire passif. Le modèle de Kazantsev considère un champ de vitesse qui est un bruit blanc et a une distribution Gaussienne. Les études sur ce modèle considèrent uniquement les prédictions pour le moment d'ordre 2 (l'énergie du champ magnétique).

On revisite ce problème en supposant une séparation d'échelle entre l'écoulement et le champ magnétique, ce qui permet d'écrire une équation pour le champ magnétique à grande échelle. Les équations sont analogues à celles d'une particule brownienne et il apparaît naturellement la puissance injectée par la force aléatoire sur la particule. À l'aide de résultats de la théorie des grandes déviations obtenus dans le problème de particule brownienne [3] on peut trouver la distribution du champ magnétique pour le problème linéaire. On montre que le taux de croissance des différents moments $\langle B^n \rangle$ est une fonction nonlinéaire de n . Cela implique que différents moments du champ magnétique prédisent un seuil différent.

Ensuite, on utilise les simulations numériques pour résoudre le problème nonlinéaire. On montre que c'est le seuil prédit par la croissance du moment d'ordre 0^+ (le log de B) du problème linéaire qui donne le vrai seuil pour le problème nonlinéaire complet. En particulier, le moment d'ordre 2 sous-estime le seuil. On a vérifié ce résultat pour différents exemples d'écoulements.

- [1] A. P. Kazantsev, Enhancement of a magnetic field by a conducting fluid, Sov. Phys. JETP, 26, 1031–1034, (1968).
- [2] R. H. Kraichnan, Small-Scale Structure of a Scalar Field Convected by Turbulence, Phys. Fluids, 11, 5, 945–953, (1968).
- [3] J. Farago, Injected Power Fluctuations in Langevin Equation, J. Stat. Phys., 107, 781, (2002).

Phase locked loop operation of spin torque oscillators

M. Kreissig,¹ P. Sethi,² S. Wittrock,³ A. Litvinenko,² C. Murapaka,² K. Merazzo-Jaimes,² E. Jimenez-Romero,² J. Hem,² R. Lebrun,³ A. Jenkins,⁴ L. Vila,² M. C. Cyrille,⁵ R. Ferreira,⁴ P. Bortolotti,⁶ V. Cros,³ F. Ellinger,¹ and U. Ebels²

1. Technische Universität, Dresden, Germany
2. Univ. Grenoble Alpes, CEA, CNRS, INAC, SPINTEC, F-38000 Grenoble, France
3. Unité Mixte de Physique CNRS, Thales, Univ. Paris-Sud, Université Paris-Saclay, Paris, France
4. International Iberian Nanotechnology Laboratory (INL), Braga, Portugal
5. CEA, LETI, F-38000 Grenoble, France
6. THALES TRT, Palaiseau, France

Through spin polarized transport properties spintronic devices provide microwave functions that are of interest for wireless communication schemes. These functions include microwave signal generation (DC-to-RF converter), modulation and frequency selective microwave signal detection (RF-to-DC converter). In this presentation we discuss the signal generation using spin torque oscillators (STO) within a phase locked loop (PLL) [1, 2]. A phase locked loop is used (i) to provide a variable output frequency from a stable fixed frequency oscillator and (ii) to improve the phase noise of a frequency tuneable oscillator of lower performance. In order to provide a flexible design of the constituting rf components, to decrease losses and reduce noise, and to realize a first step towards compact system design, we have fabricated hybrid phase locked loops on 0.18 μm BiCMOS. The PLL's frequency divider, loop filter and voltage-current converter were designed for two types of STOs: vortex devices emitting in a frequency range of 0.1-1GHz and uniform magnetized devices emitting in the 1-10 GHz range. PLLs were assembled on two different PCBs with appropriate signal amplification and DC current source to adapt to different power levels and operation condition. Results will be presented for magnetic tunnel junction devices with $RA \approx 2\Omega\mu\text{m}^2$ and TMR of 50-100%. The Polarizer Pol is an in-plane magnetized synthetic antiferromagnet and the free layer is made of CoFeB2/Ta0.2/FeNi(t) with thickness $t=7\text{nm}$ for vortex devices and $t=2\text{nm}$ for uniform devices. The PLL of vortex devices shows a reduction of phase noise of -50dBc at 100kHz offset frequency in a bandwidth of 2MHz. The corresponding free running parameters are $f=337\text{MHz}$, $\Delta f=100\text{kHz}$ and $P=1\mu\text{W}$. For uniform devices ($f=4.2\text{GHz}$, $\Delta f=15\text{MHz}$ and $P=100\text{nW}$) temporarily locking is also demonstrated within a bandwidth of 1MHz. The frequency of the oscillator clearly follows the PLL target frequency, while the phase noise reduction is not yet complete due to instabilities of the free running signal. Besides phase noise reduction we also demonstrate the possibility to shift the PLL output frequency through variation of frequency division which gives prospect to use the PLL for frequency shift keying. Further improvements of PLL operation such as locking via a field line will be discussed. The achieved results are a first step towards integration of spin torque oscillators for microwave applications.

Acknowledgements

The work has been supported in part by the FP7 program ICT MOSAIC 317950. Financial support is acknowledged from the French space agency CNES for CM and PS, from the First-TF consortium for SW and from ERC MagiCal 669204 for AL and UE.

References

- [1] M. Kreißig *et al.*, 2017 *IEEE 60th International Midwest Symposium on Circuits and Systems (MWSCAS)*, Boston, MA, 2017, pp. 910-913; doi: 10.1109/MWSCAS.2017.8053072
- [2] S. Tamaru, *et al.*, *Applied Physics Express* **5**, 053005, (2016).

A sensor to measure flow rate in individual nanopore

P. Sharma^a, J. F. Motte,^b F. Fournel^c B. Cross^a, E. Charlaix^a et C. Picard^{a*}

a. Univ. Grenoble Alpes, CNRS, LIPhy, 38000 Grenoble, France

b. Univ. Grenoble Alpes, CNRS, Grenoble INP, Institut Néel, 38000 Grenoble, France

c. CEA, LETI, MINATEC, 38054 Grenoble, France

* cyril.picard@univ-grenoble-alpes.fr

Nanopore based applications have benefited from significant instrumental development in order to measure physical quantities associated to flow and transport at the nanoscale. Electrical current, for instance, can now be measured through a single nanochannel with commercial apparatus. Flow rate, on the other hand, is a quantity that is both central when dealing with flows and still notoriously difficult to be measured experimentally at the scale of an individual nanometric confinement. The best commercial flow rate sensor gives the ability to measure flow rates of the order of 10 nL/min that remain three decades larger than those typically expected in a single nanopore. A few approaches exist though to probe such small flow rates but indirectly and in specific configurations only [1]. We show in this communication that minute flow rate can be directly measured accumulating liquid over time within a compliant membrane whose deflection is precisely measured by means of strain gages [2]. A demonstrative sensor based on this approach cover three decades of flow rates ranging from 1 pL.min⁻¹ to 1 nL.min⁻¹. Such a versatile sensor works independently of the nature of the liquid, the origin of the flow, and the geometry of the confinement. The capabilities of the sensor are illustrated with the measurement of flow rate through benchmark micro capillaries and through a single conical nanopore within a 1 micron thick silica membrane that opens new possibilities for the study of electro-osmosis in strong confinement.

- [1] E. Secchi, S. Marbach, A. Nigués, D. Stein, A. Siria, and L. Bocquet, Massive radius-dependent flow slippage in carbon nanotubes, *Nature*, **537**, 7619, 210-213, (2016).
 [2] C. Picard, E. Charlaix, P. Sharma, Dispositif et procédé de mesure de débit d'un liquide, demande de brevet d'invention N° 1851804 (2017).

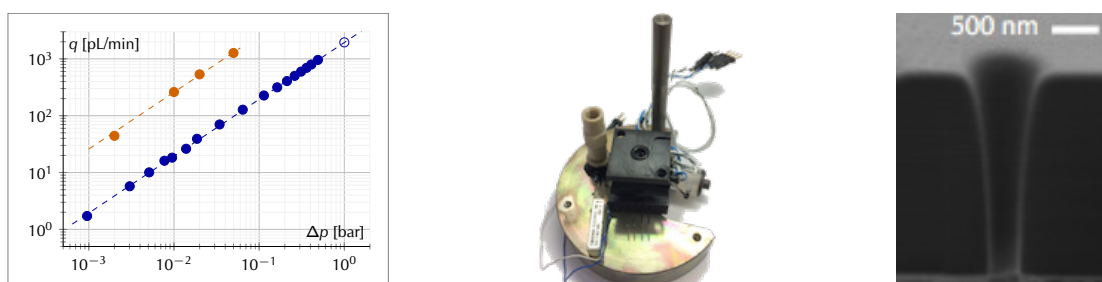


Figure 1: Measured flow rate through calibrated capillaries (left), picture of the flow rate sensor (center) and a transmembrane nanopore studied with the sensor (right).

NMR investigation of classical kagome magnets

R. K. Sharma^{a,*}, R. Hénaff^a, B. Koteswararao^b, P. L. Paulose^c, H. Luetkens^d, C. Baines^d, and E. Kermarrec^{a,*}

- a. Laboratoire de Physique des Solides, Univ. Paris Sud, Bât. 510, 91405 Orsay
- b. Faculty in Physics, Indian Institute of Technology Tirupati
- c. Department of Condensed Matter Physics and Materials Science, TIFR, Mumbai
- d. Laboratory for muon spectroscopy, Paul Scherrer Institut, Villigen

* ramender.sharma@u-psud.fr, edwin.kermarrec@u-psud.fr

Kagome magnets are the archetype of frustration in two dimensions [1]. While significant efforts have been devoted to the study of the $S=1/2$ *quantum* kagome antiferromagnet, the ground state and the unconventional spin dynamics of *classical* kagome magnets are far from being completely understood, and the scarcity of relevant compounds prevents progress on the experimental side.

Here, we investigate the low temperature magnetic properties of the layered monodiphosphates family $\text{Li}_9\text{M}_3(\text{P}_2\text{O}_7)_3(\text{PO}_4)_2$ with $\text{M}=\text{Fe}^{3+}$ ($S=5/2$) and Cr^{3+} ($S=3/2$) [2]. The isostructural materials crystallize in the hexagonal space group P-3c1 with magnetic ions forming a lattice of regular corner sharing triangles in the crystallographic ab -plane (Fig. 1a & b). Thermodynamic measurements reveal an energy scale of $\sim 10\text{K}$ for the exchange interactions, with frustration effect resulting in a lower temperature onset of a ferromagnetic order for $\text{Li}_9\text{Cr}_3\text{P}_8\text{O}_{29}$ at 2.3K and of an antiferromagnetic order at 1.2K for $\text{Li}_9\text{Fe}_3\text{P}_8\text{O}_{29}$ (Fig. 1c). We further carry out ^{31}P NMR local probe measurements on $\text{Li}_9\text{Fe}_3\text{P}_8\text{O}_{29}$ to get more insight into the static susceptibility and the spin dynamics. The NMR spin susceptibility reveals the development of anisotropic short-range correlations. The $1/T_1$ spin-lattice relaxation rate shows a critical divergence at 1.2K and evidence strong fluctuations in the correlated paramagnetic regime, presumably linked to the existence of predicted local zero energy modes.

[1] P. Mendels and F. Bert, *Comptes Rendus Physique* **17**, 455-470(2016).

[2] S. Poisson *et al.* *J. Solid State Chem.* **138**, 32 (1998).

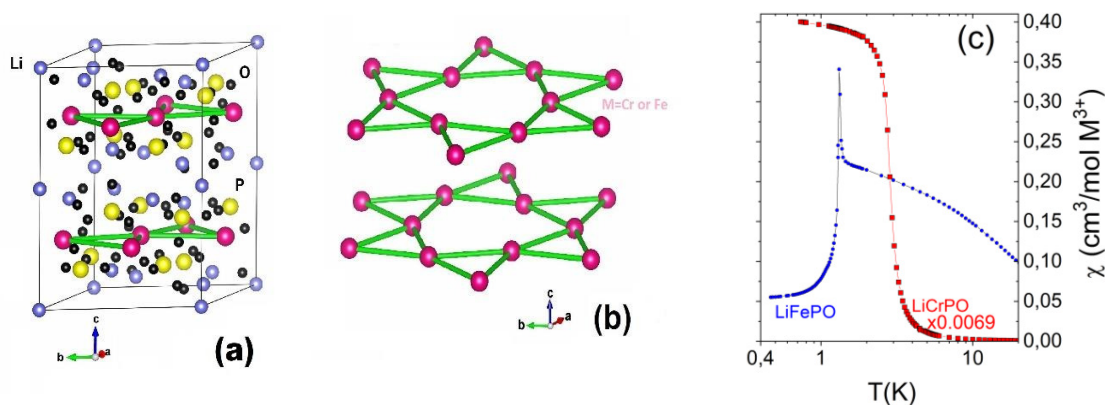


Figure 1 : (a) A depiction of a unit cell of $\text{Li}_9\text{M}_3\text{P}_8\text{O}_{29}$ ($\text{M}=\text{Cr}, \text{Fe}$). (b) M^{3+} ions form a network of corner sharing triangles in the crystallographic ab -plane. (c) Magnetic susceptibilities (χ) measured for the polycrystalline samples of $\text{Li}_9\text{Fe}_3\text{P}_8\text{O}_{29}$ (blue circles) and for $\text{Li}_9\text{Cr}_3\text{P}_8\text{O}_{29}$ (Red squares) with an applied field of $H=100$ Oe.

Experimental signatures of emergent quantum electrostatics in $\text{Pr}_2\text{Hf}_2\text{O}_7$

R. Sibille^{a*}, N. Gauthier,^a H. Yan,^b M. Ciomaga Hatnean,^c J. Ollivier,^d B. Winn,^e G. Balakrishnan,^c M. Kenzelmann,^a N. Shannon,^b and T. Fennell^a

- a. Paul Scherrer Institute, 5232 Villigen PSI, Switzerland
- b. Okinawa Institute of Science and Technology, Onna-son, Okinawa 904-0495, Japan
- c. Physics Department, University of Warwick, Coventry, CV4 7AL, UK
- d. Institut Laue-Langevin, CS 20156, 38042 Grenoble Cedex 9, France
- e. Neutron Scattering Division, Oak Ridge National Laboratory, Tennessee, USA

* romain.sibille@psi.ch

Magnetic systems with competing interactions often adopt exotic ground states, which can be relevant to study new physics in quantum matter. A recurrent ingredient to stabilize such phases is geometrical frustration, such as in pyrochlore oxides where rare-earth magnetic moments decorate a lattice of corner-sharing tetrahedra. An unusual spin liquid appears for example in the pyrochlore $\text{Ho}_2\text{Ti}_2\text{O}_7$, which features a classical spin ice short-range correlated state. A local constraint – the 2-in-2-out ice rule acting on each tetrahedron – leads to a manifold of degenerate ground states in which the spin correlations give rise to emergent magnetostatics [1]. Spin flips violating the ice rule generate magnetic monopole excitations, a mobile magnetic charge regarded as a quasiparticle carrying half of the dipole moment. A quantum analogue of the spin ice state is predicted to be a quantum spin liquid formed through the coherent superposition of spin ice configurations [2]. Remarkably, this dynamical ground state leads to emergent electrostatics. In $\text{Pr}_2\text{Hf}_2\text{O}_7$, the single-ion ground state doublet [3] has a dipole moment of about $2.4\mu_B$ and, perpendicular to it, electric quadrupoles that allow quantum tunneling between the in and out states of the dipole [4]. A correlated ground state with macroscopic indications of spin ice correlations forms below 0.5 K [3]. The experimental structure factor has pinch points – a signature of a classical spin ice – that are partially suppressed, as expected in the presence of quantum dynamics [5]. Moreover, a continuum of magnetic excitations is observed in inelastic neutron scattering, which relates to the monopoles of spin ices that become quantum-coherent fractionalized excitations – akin to the spinons found for instance in quantum spin chains.

- [1] Fennell, T. et al. Magnetic Coulomb Phase in the Spin Ice $\text{Ho}_2\text{Ti}_2\text{O}_7$. *Science* **326**, 415 (2009).
- [2] Gingras, M. J. P. & McClarty, P. A. Quantum spin ice: a search for gapless quantum spin liquids in pyrochlore magnets. *Rep. Prog. Phys.* **77**, 056501 (2014).
- [3] Sibille, R. et al. Candidate quantum spin ice in the pyrochlore $\text{Pr}_2\text{Hf}_2\text{O}_7$. *Phys. Rev. B* **94**, 024436 (2016).
- [4] Onoda, S. & Tanaka, Y. Quantum Melting of Spin Ice: Emergent Cooperative Quadrupole and Chirality. *Phys. Rev. Lett.* **105**, 047201 (2010).
- [5] Sibille, R. et al. Experimental signatures of emergent quantum electrostatics in $\text{Pr}_2\text{Hf}_2\text{O}_7$. *Nature Physics* 10.1038/s41567-018-0116-x (2018).

Doping inhomogeneity in GaN and Al_xGa_{1-x}N nanowires

Alexandra-Madalina Siladie^{a*}, Fabrice Donatini^b, Gwénoél Jacopin^{a,b}, Lynda Amichi^a, Catherine Bougerol^b, Eric Robin^a, Nuria Garro^c, Ana Cros^c, Julien Pernot^b and Bruno Daudin^a

- a. Univ. Grenoble Alpes, CEA, INAC, F-38000 Grenoble, France
- b. Univ. Grenoble Alpes, CNRS, Institut Néel, F-38000 Grenoble, France
- c. Institute of Material Science, University of Valencia, P.O. Box 22085, Valencia, Spain

* alexandra-madalina.siladie@cea.fr

UV Light emitting diodes (LEDs) are nowadays gaining particular attention due to their potential for replacing mercury lamps currently used for sterilization and water disinfection applications. Due to the bandgap tuning possibility, Al_xGa_{1-x}N ternary alloy is the main candidate for such devices. Planar structure LEDs having a low internal efficacy due to a high density of extended defects and limited doping for high AlN molar fraction combined to a low light extraction efficacy, Al_xGa_{1-x}N nanostructures such as nanowires (NWs) could be a realistic alternative with respect to their 2D counterparts due to their advantage of plastically relaxing the strain during growth, coupled with an improved solubility limit of Si dopants [1] and an eased light extraction coming from their particular morphology.

Material and doping homogeneity are nevertheless not easy to control in nanowires. Indeed, Atom Probe Tomography, Energy Dispersive X-ray and Raman spectroscopy performed on GaN pn junctions grown by PA-MBE have shown that both n-type and p-type dopants, namely Si and Mg, respectively, exhibit an inhomogeneous radial distribution, with dopant incorporation upper limits attaining 10²¹ atoms/cm³ at the periphery, higher than in 2D layers[1][2]. The full control of electrical transport properties of NW-based devices implies taking into account these peculiarities of dopant physics in NWs. However, quantitative determination of doping levels by standard techniques such as Hall effect or SIMS measurements is inherently difficult. To overcome this limitation, Electron Beam Induced Current (EBIC) experiments have been performed providing information on the quality of materials and allowing to extract the electrical parameters of the junction, assessing wire to wire inhomogeneous p-n junction space charge region (SCR) distribution.

[1] Z. Fang, E. Robin et al, Nano Lett. 15 (10) (2015), 6794–6801

[2] A.M. Siladie, L. Amichi et al, Nanotechnology 29 (25) (2018)

[3] Z. Fang, F. Donatini et al, Nanotechnology 29 (2018)

Local magnetic fields to explore novel behaviors in frustrated and quantum magnetism

Virginie Simonet^{a*}

a. Institut Néel, CNRS–Université Grenoble Alpes, F-38000 Grenoble, France

* virginie.simonet@neel.cnrs.fr

The complexity embedded in condensed matter fertilizes the discovery of new states of matter, enriched by ingredients like frustration, low-dimensionality or quantum fluctuations. Illustrating examples in magnetic systems are quantum spin liquids in spin chains or 2-dimensional frustrated materials or spin ices in 3-dimensional pyrochlore compounds. They support fractionalized excitations, for example the magnetic charges in spin ices, also called monopoles, or the spinons in quantum spin liquids. To explore the phase diagrams of this rich physics, external parameters are commonly used such as magnetic or electric fields, pressure or doping effects.

Here I will take an alternative route with two selected studies where another driving parameter, a local staggered field, can change drastically the properties of the systems. The first example deals with spin ice physics in a pyrochlore iridate material where the local field is created by one magnetic sublattice on the other one. This well-defined non-collinear field leads to a fragmentation of the magnetization, a new state of matter where the magnetic moment fragments into an ordered part and a persistently fluctuating one [1]. The second example concerns a spin chain compound with anisotropic magnetic moments. In this case, an internal staggered field is generated from the anisotropic response of the magnetic moments to the application of an external uniform magnetic field. This staggered magnetic field produces a quantum phase transition where the magnetic excitations characterizing the ordered phases on both sides of the transition are two different types of competing topological objects [2].

- [1] E. Lefrançois et al., Magnetic charge injection in spin ice: a new way to fragmentation, *Nature Communications* **8**, 209 (2017)
- [2] Q. Faure, et al., Topological quantum phase transition in the Ising-like antiferromagnetic spin chain $\text{BaCo}_2\text{V}_2\text{O}_8$, to appear in *Nature Physics*

Thermal transport in suspended graphene

Priyank Singh^{*a}, Swati Achra^a, Michele Lazzeri^b, Laetitia Marty^a and Nedjma Bendiab^a

a. Univ. Grenoble Alpes, CNRS, Grenoble INP, Institut Néel, 38000 Grenoble, France

b. IMPMC, CNRS-UPMC, Paris, France

* priyank.singh@neel.cnrs.fr

Thermal physics is one of the central topics of interest in physics from fundamental and application point of views. As a matter of fact, the need to control the heat loss in devices makes its important to learn about the fundamentals of heat generation and transport. On the other hand, in the race of miniaturizing the electronic devices, low dimensional materials, due to their enhanced electrical properties, have become one of the lead candidates. From practical restrictions, these materials are always supported by a substrate, hence the study of thermal transport in such materials remains a topic of debate with measured thermal conductivities ranging from 600 to 5000 W/mK. Theory predicts that the single phonon picture for heat transfer fails up to high temperature in graphene (cite Bonini). Decoupling 2D materials from the supporting substrate has proven a promising approach to address this debate (cite Balandin). Raman scattering gives direct access to the phonons of the systems hence it has advantage over electrical measurements.

We propose to study the thermal transport in suspended graphene and other low dimensional materials using Raman scattering measurements with a 2-laser approach : one for excitation and one as a non invasive Raman probe. In order to settle down to a robust conclusion, we plan to compliment the results from Raman scattering with electrical and opto-mechanical measurements. We will present our strategy and preliminar results.

[1]. Alexander A. Balandin , *Nature Materials* **10**, 569–581 (2011)

o a
l g
u e
m s
e

Next-Generation Pb-free Photovoltaics: All-inorganic Perovskite to Kesterite

Vijay Singh, Ambroise van Rookeghem, and Natalio Mingo

CEA-Liten, Grenoble, France

Vijay.singh@cea.fr

Photovoltaic (PV) systems, which convert sunlight into either electrical or chemical energy, constitute a promising renewable energy source. Current state-of-the-art PV systems based on perovskites -typically metal-organic halides- have reached impressive performance with record efficiencies rising from 4% to 22% in less than a decade. But most perovskites contain lead, raising environmental concerns, and questions regarding the materials' long-term stability also remain. This is indeed a big hurdle to commercialize these perovskites. In this talk, I will discuss the atomic and electronic structure of *Pb-free* all-inorganic perovskite and kesterites materials for next-generation PV applications. I will also discuss our machine learning model to predict the stability of 1568 kesterites. To elucidate the electronic, magnetic, optical and chemical bonding properties of these materials, we have employed first-principles density functional theory. The phononic properties (i.e. lattice dynamics) were investigated using first principles density functional perturbation theory and a direct, supercell force-constant approach. To treat anharmonic effects beyond perturbation theory, we have used our inhouse code. This talk will illustrate how theoretical results can highlight physical materials properties that might be important for the development of the next generation PV materials.

Magnetic Order and Lattice Instabilities in $\text{Ni}_2\text{Mn}_{1+x}\text{Sn}_{1-x}$ Heusler based Magnetic Shape-Memory Alloys

Vijay Singh^{a*}, Ambroise van Roekeghem^a, S. K. Panda^b, Natalio Mingo^a, and Indra Dasgupta^c

- a. CEA, LITEN, 17 Rue des Martyrs, 38054 Grenoble, France
- b. Centre de Physique Théorique, Ecole Polytechnique, CNRS UMR 7644, Université Paris-Saclay, 91128 Palaiseau, France
- c. Department of Solid-State Physics, Indian Association for the Cultivation of Science, Jadavpur, Kolkata 700032, India

* vijay.singh@cea.fr << corresponding author >>

The magnetic correlations in the austenite phase and the consequent martensitic transition in inverse magnetocaloric alloys, $\text{Ni}_2\text{Mn}_{1+x}\text{Sn}_{1-x}$, have been a matter of debate for decades. We conclusively establish using *ab initio* phonon calculations that the spin alignment of excess Mn at the Sn site (Mn_{Sn}) with the existing Mn in the unit cell in the high temperature cubic phase of Ni-Mn-Sn alloy is ferromagnetic (FM), and not ferrimagnetic (FI), resolving a long lasting controversy. Using first principles density functional perturbation theory (DFPT), we observe an instability of the TA_2 mode along the Γ -M direction in the FM phase, very similar to that observed in the prototypical ferromagnetic shape memory alloy (FSMA) Ni_2MnGa . This specific instability is not observed in the FI phase. Further finite temperature first principles lattice dynamics calculations reveal that at 300 K the FM phase becomes mechanically stable, while the FI phase continue to remain unstable providing credence to the fact that the high-temperature phase has FM order. These results will be primordial to understand the magneto-structural properties of this class of compounds.

Implementation of Scattering matrix formalism at optical analogues

Vyome Singh^{*}, Friedrich Koenig

SUPA, University of St Andrews, School of Physics & Astronomy, St Andrews, KY16 9SS

*vs28@st-andrews.ac.uk

Any stationary scattering process is completely described by the scattering matrix, S . The scattering matrix relates the incoming states to the outgoing states. The scattering matrix formalism is used in many fields of physics such as quantum mechanics, optics, electronics and quantum field theory. In this poster we discuss different numerical ways to compute the S matrix to find a numerically stable and efficient way, without invoking approximations such as the JWKB approximation. We discuss the T-Matrix algorithm, S-Matrix algorithm [1] and the generalised scattering coefficients [2]. Performance and efficiency of each algorithm is analysed and presented. Analogue Optical Event horizons created by a pulse travelling in a fiber were first proposed and demonstrated in 2008 [3]. Spontaneous emission have been studied in detail from a travelling refractive index step [4] but an in depth understanding of the strength of emission from pulses remains to be demonstrated. Here, we implement the scattering formalism at optical analogues created by pulse travelling in a fiber. We treat the pulse as a stationary scatterer and compute a corresponding scattering matrix describing the system. We formulate a general scattering matrix equation, to be solved numerically. This makes it possible to calculate the strength of spontaneous vacuum emission from a pulse. Our formalism can be used in other scattering problems which encounter numerical instabilities and/or problems with convergence.

[1] D. Y. K. Ko and J. R. Sambles, "Scattering matrix method for propagation of radiation in stratified media: attenuated total reflection studies of liquid crystals," *J. Opt. Soc. Am. A* 5, 1863-1866 (1988)

[2] Weng Cho Chew, *Waves and Fields in Inhomogeneous Media*, IEEE press, 1995

[3] T.G. Philbin, C. Kuklewicz, S Robertson, S Hill, F Koenig, U Leonhardt, "Fiber-Optical Analog of the Event Horizon," *SCIENCE* Vol 319, Issue 5868, 2008 : 1367-1370

[4] M. Jacquet and F. König: "Quantum vacuum emission from a refractive index front" *Phys. Rev. A* 92, 023851 (2015)

Thermal Conductivity Measurements on Highly-Dense Forest of Nanowires

D.Singhal^{a,b,c,*}, J. Paterson^{b,c}, E. Chavez-Angel^e, D. Tainoff^{b,c},
J. Jaramillo-Fernandez^e, M. Ben-Khedim^{b,c,d}, P. Gentile^a, L. Cagnon^{b,c}, D. Bourgault^{b,c},
C.M. Sotomayor-Torres^{e,f}, D. Buttard^{a,b} and O. Bourgeois^{b,c}

- a. Univ. Grenoble Alpes, CEA INAC-Pheliqu- SiNaPS, F-38000 Grenoble, France
- b. Universit Grenoble Alpes, Grenoble, France
- c. Institut Néel, CNRS, 25 Avenue des Martyrs, 38042 Grenoble, France
- d. Technology R&D, STMicroelectronics, 13106 Rousset, France
- e. ICN2, CSIC and BIST, Campus UAB, Bellaterra 08193 Barcelona, Spain
- f. ICREA, Passeig Lluís Companys 23, 08100 Barcelona, Spain

* dhruv.singhal@neel.cnrs.fr << corresponding author >>

Thermal conductivity in semiconductors is dominated by phonons that have a broad spectral distribution at room temperature. The rate of Umklapp processes dominates the phonon scattering at room temperature; it scales with ω^2 (ω is the phonon frequency). This implies that low frequency acoustic phonons will have longer mean free path that can be reduced by rational incorporation of phonon scattering elements. For instance, when the dimensions of the material are comparable to the mean free path of the phonons, the thermal conductivity drops down significantly due to surface scattering mechanism. In this work, we have fabricated an array of nanowires (silicon and various bismuth telluride) in nanoporous alumina templates with very high nanowire density ($\approx 10^9/cm^2$). We have employed 3ω method and Raman thermometry to extract the thermal conductivities of the nanowires. Both methods are often employed with a simplified approximation and this, in turns, brings several limitations on its applicability especially in the case of thin nanoporous material. For using it in our case in 3ω method, we have developed a model using an analytical solution of 2D heat conduction on a multilayer system to extract the thermal conductivity of the whole array of nanowires embedded in porous alumina which is an anisotropic film. Fitting of the experimental data with the model considering all the different layers on the sample is done to extract the correct value of thermal conductivities of the embedded nanowires. The variation in thermal conductivities as a function of temperature (ranging from 80 K to 350 K) has been obtained. The results are correlated with the geometry (roughness) and composition of the nanowires. High-resolution TEM imaging along with the compositional analysis with EDX gives an insight of the variation in phonon transport. The difference in thermal conductivities between nanowire and bulk is significant in silicon showing a strong confinement effect in silicon. A thermal conductivity around 10 W/mK is observed in 60 nm diameter nanowires. The thermal conductivity is reduced with the reduction in nanowire diameter, which shows stronger confinement in thinner silicon nanowires. Comparison of the thermal conductivity in between silicon and ternary alloys of Bi_2Te_3 with reduction in dimensions is clearly interpreted. By analysing the different parameters (Seebeck effect, electrical conductivity etc.), it can be seen that the array of highly-doped thin nanowires of silicon would result in highly-efficient building blocks for innovative thermoelectric devices.

Intra- and interlayer optical transitions at **K** points of multilayers of transition metal dichalcogenides

A.Slobodeniuk^{a*}, L.Bala^b, C.Faugeras^a, M.Molas^{a,b}, K.Nogajewski^{a,b},
M.Bartos^a, K.Watanabe^c, T.Taniguchi^c and M. Potemski^a

- a. Laboratoire National des Champs Magnétiques Intenses, CNRS-UGA-UPS-INSA, Grenoble, France
- b. Institute of Experimental Physics, Faculty of Physics, University of Warsaw, Warszawa, Poland
- c. National Institute for Materials Science, Tsukuba, Japan

* artur.slobodeniuk@lncmi.cnrs.fr

We study the optical transitions in **K** valleys of few-layer 2H stacked transition metal dichalcogenide (TMDC) crystals encapsulated in hBN medium. The description of such processes is based on the effective Hamiltonians derived as an extension of the 7-band **kp** model for a multilayer case [1,2]. The Hamiltonians are considered up to quadratic in momentum **k** terms to incorporate the magnetic field effects in TMDC [3,4].

We focus on the bi- and trilayers as the simplest representatives of even- and odd-layered systems. The classification of their bands and eigenstates in **K** points is done with respect to the crystals' symmetry (bilayer possesses an in-plane mirror symmetry, while trilayer has an inverse symmetry). It allows to define the two types of optical transitions in TMDC -- intra- and interlayer ones, and obtain the optical selection rules for both cases. The latter is used to analyze the behaviour of excitons (which are formed due to above-mentioned transitions) in the presence of magnetic field. We examine the optical spectra of both systems, demonstrate the good agreement between theory and experiment and extract the model parameters of few-layer TMDC.

Finally, we discuss the experimental manifestations of intra- and interlayer excitons in few-layer TMDC.

- [1] A. Kormányos et al., 2D Mater. 2, 022001 (2015)
- [2] G.-B. Liu et al., Chem. Soc. Rev. 44, 2643 (2015)
- [3] M. R. Molas et al., Nanoscale 9, 13128 (2017)
- [4] Z. Gong et al., Nat. Commun. 4, 2053 (2013)

Proximity magneto-resistance calculations on graphene induced by magnetic insulators

Daniel A. Solis^{a*}, Ali Hallal^a, Xavier Waintal^b, Mairbek Chshiev^a

a. Univ. Grenoble Alpes, CNRS, CEA-INAC, Grenoble, France.

b. Univ. Grenoble Alpes, INAC-SPSMS/ CEA, INAC-SPSMS, Grenoble, France.

* daniel.solislerma@cea.fr

Graphene has been attracting great interest due to its fascinating characteristics for development of graphene-based devices in several fields. When it is placed on top of a magnetic insulator, it can acquire spin polarization [1]. The mechanism behind this phenomenon is known as proximity effect resulting from the hybridization of graphene's p_z orbitals with those of the neighboring magnetic material. Evidence of this effect is the emergence of exchange splitting in the graphene band structure reported experimentally [2,3] and theoretically [1,4]. Here we demonstrate the existence of proximity magnetoresistance (PMR) effect in graphene considering magnetic insulator proximity cases reported in Ref. [4]. The PMR calculations were performed using KWANT package, for yttrium iron garnet (YIG), cobalt ferrite (CFO), and two europium chalcogenides EuO and EuS [4]. The system studied consisted of two identical proximity induced magnetic regions of width W , length L and separated a distance d of a graphene sheet, with its ends connected to two leads. We found significant PMR (up to 100%) values defined as a relative change of graphene conductance with respect to parallel and antiparallel alignment of two proximity induced magnetic regions. Namely, for high Curie temperature (T_c) CFO and YIG insulators which are particularly important for applications, we obtained 22% and 77% at room temperature, respectively. For low T_c chalcogenides, EuO and EuS, the PMR is 100% in both cases, as shown in Figure 1. We also found that the PMR is robust with respect to the device dimensions as well as the edge termination of graphene. Our findings show that it is possible to explore spin polarized currents in graphene with no direct injection through magnetic materials. We acknowledge EU Programme Graphene Flagship.

[1] H. X. Yang, A. Hallal, D. Terrade, X. Waintal, S. Roche, and M. Chshiev, Phys. Rev. Lett. 110, 046603 (2013).

[2] P. Wei, S. Lee, F. Lemaitre, L. Pinel, D. Cutaia, W. Cha, F. Katmis, Y. Zhu, D. Heiman, J. Hone, et al. Nat. Mater. 15, 711 (2016).

[3] J. C. Leutenantsmeyer, A. A. Kaverzin, M. Wojtaszek, and B. J. van Wees, 2d. Mater. 4, 1 (2016).

[4] A. Hallal, F. Ibrahim, H. Yang, S. Roche, and M. Chshiev, 2d. Mater. 4, 025074 (2017).

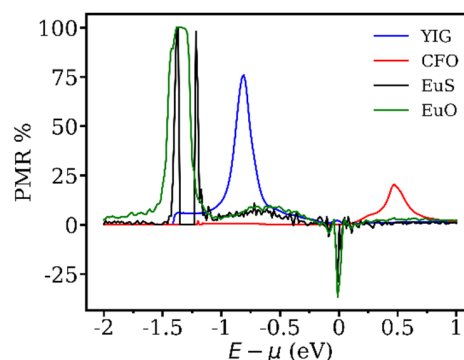


Figure 1: For a system of $L = 36.4$ nm, $W = 29.5$ nm and $d = 1.5$ nm, PMR curves for YIG, CFO, EuS and EuO smeared using $T=300$ K, 300 K, 16 K and 70 K respectively.

Analogue physics with exciton-polaritons

Dmitry Solnyshkov^{a*}, Guillaume Malpuech,^a

a. Institut Pascal, PHOTON-N2, Université Clermont Auvergne, CNRS, 4 Avenue Blaise Pascal, 63178 Aubière Cedex, France.

* dmitry.solnyshkov@uca.fr

Exciton-polaritons are a versatile solid-state platform providing large opportunities for simulating various physical phenomena. These quasiparticles appear from the strong coupling of excitons and photons in microcavities [1]. The excitonic part provides strong non-linear interaction and thermalization, whereas the photonic part brings a small effective mass and a possibility to create complicated potentials. Quantum fluids of exciton-polaritons [2] are routinely created either by condensation with a reservoir or by direct optical injection by a coherent laser. Such fluids extend the possibilities of studying analogue effects.

The analogue physics in polariton condensates has been developing in several directions. Effective magnetic monopoles have been predicted and observed experimentally [3,4]. Analogue black holes and wormholes were predicted [5], and crucial steps towards their observation have been taken [6]. Topological insulators for polaritons can be seen as analogs of solid-state systems [7] or as a base for optical devices [8]. An array of polariton condensates allows to simulate the XY model [9]. Finally, the analog of the formation of topological defects in the primordial Universe via the Kibble-Zurek mechanism can be studied in a zigzag chain of pillar microcavities [10].

- [1] A.V. Kavokin, J.J. Baumberg, G. Malpuech, and F.P. Laussy, *Microcavities* (Oxford Science Publications, Oxford, 2017)
- [2] I. Carusotto, and C. Ciuti, *Quantum fluids of light*, *Rev. Mod. Phys.* **85**, 299 (2013)
- [3] D.D. Solnyshkov, H. Flayac, and G. Malpuech, *Stable magnetic monopoles in spinor polariton condensates*, *Phys. Rev. B* **85**, 073105 (2012)
- [4] R. Hivet et al, *Half-solitons in a polariton quantum fluid behave like magnetic monopoles*, *Nature Physics* **8**, 724 (2012)
- [5] D. D. Solnyshkov, H. Flayac, and G. Malpuech, *Black holes and wormholes in spinor polariton condensates*, *Phys. Rev. B* **84**, 233405 (2011)
- [6] H.S. Nguyen et al, *Acoustic Black Hole in a Stationary Hydrodynamic Flow of Microcavity Polaritons*, *Phys. Rev. Lett.* **114**, 036402 (2015)
- [7] A. Amo and J. Bloch, *Exciton-polaritons in lattices: A non-linear photonic simulator*, *Comptes Rendus Physique* **17**, 934 (2016)
- [8] D.D. Solnyshkov, O. Bleu, G. Malpuech, *Topological optical isolator based on polariton graphene*, *Appl. Phys. Lett.* **112**, 031106 (2018)
- [9] N.G. Berloff et al, *Realizing the classical XY Hamiltonian in polariton simulators*, *Nature Materials* **16**, 1120 (2017)
- [10] D.D. Solnyshkov, A.V. Nalitov, and G. Malpuech, *Kibble-Zurek Mechanism in Topologically Nontrivial Zigzag Chains of Polariton Micropillars*, *Phys. Rev. Letters* **116**, 046402 (2016)

Playing with the Redox Potentials in Ludwigite Oxyborates: Fe₃BO₅ and Cu₂MBO₅ (M = Fe, Mn and Cr)

Jonas Sottmann^{a*}, Lucie Nataf^b, Laura Chaix^c, Valérie Pralong^a, Christine Martin^a

- a. NormUniv, ENSICAEN, UNICAEN, CNRS, CRISMAT, 14000 Caen, France
- b. Synchrotron Soleil, Saint-Aubin BP 48, 91192 GIF-SUR-YVETTE CEDEX, France
- c. Laboratoire Léon Brillouin, UMR 12, LLB-Saclay, 91191 GIF-SUR-YVETTE Cedex, France

* Jonas.Sottmann@ensicaen.fr

Lithium ion batteries (LIBs) play an important role in powering portable electronics and electric vehicles, and are considered as serious candidates for grid applications. Borates and oxyborates have been proposed as attractive electrode materials with high energy density and safety. Ludwigite oxyborates represent an interesting new class of conversion-type electrode materials for LIBs [1].

Fe₃BO₅ shows a first lithiation capacity of 678 mAhg⁻¹ (~6.5 Li). Very low voltage polarizations for conversion-type reactions (300 and 440 mV) are observed for the two reversible redox couples at ~1.3 and ~1.8 V which give rise to a stable capacity of 345 mAhg⁻¹ between 0.75 and 3.0 V. *Ex-situ* X-ray diffraction and *operando* X-ray absorption spectroscopy show that Fe₃BO₅ is almost completely converted to iron metal nanograins embedded in a lithia matrix during the initial lithiation and that subsequent cycling takes place between amorphous or nanocrystalline Fe-based phases.

In Cu₂MBO₅ (M = Fe, Mn and Cr) the trivalent transition metals are found to be electrochemically active in addition to copper but at lower voltages causing a large spread in redox potentials. When limiting the voltage range to the Cu²⁺/Cu⁰ redox couple (at ~2.4 V) the best performance in terms of voltage polarization and reversible capacity is obtained for Cu₂FeBO₅. Annealing of Cu₂FeBO₅ in a reducing atmosphere at low temperatures (~250 °C) - yielding a composite of Cu₂FeBO₅/Fe₃BO₅/Cu in nanostructural state - [2] is identified as new a means to improve the first cycle reversibility.

[1] V. Pralong, B. Le Roux, S. Malo, A. Guesdon, F. Lainé, J.F. Colin, C. Martin, Electrochemical Activity in Oxyborates toward Lithium. *J. Solid State Chem.*, **255**, 167 (2017).

[2] C. Martin, A. Maignan, A. Guesdon, F. Lainé, O.I. Lebedev, Topochemical Approach for Transition-Metal Exchange Assisted by Copper Extrusion: from Cu₂FeBO₅ to Fe₃BO₅. *Inorg. Chem.*, **56**, 2375 (2017).

Funding: ANR-16-CE08-0007-02 BORA-BORA

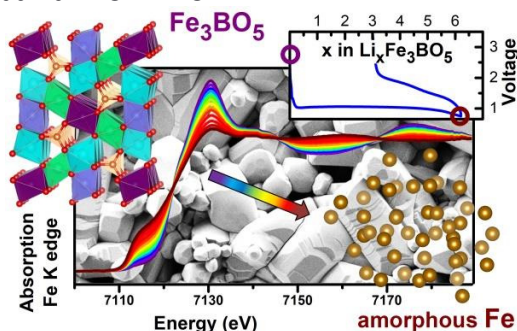


Figure 1 : Illustration of the first lithiation of Fe₃BO₅ resulting in amorphous iron surrounded by lithia (consisting of Li₃BO₃ and Li₂O). The reaction was followed by *operando* XANES and *ex-situ* XRD.

Linear photoresponse in nanowires with GaN/AlN heterostructure

Maria Spies^a, Jakub Polaczyński^a, Akhil Ajay^b, Dipankar Kalita^b, Jonas Lähnemann^b, Bruno Gayral^b, Martien I. den Hertog^a, and Eva Monroy^b

a. University Grenoble-Alpes, CNRS, Institut Néel, Grenoble, France
 b. University Grenoble-Alpes, CEA, INAC, Grenoble, France

* maria.spies@neel.cnrs.fr

Nanowire-based photodetectors are promising candidates for flexible electronics, and on-chip optical interconnects. In the UV spectral region, GaN is a natural candidate for spectrally-selective photodetectors. However, a general feature of nanowire (NW) photoconductors (also for other material systems such as ZnTe, ZnO, InP, CuO or GaAs) is that the output photocurrent scales sublinearly with the input laser power, limiting applications requiring the quantification of the radiant fluence [1,2].

We show that for GaN nanowire photodetectors with embedded AlN heterostructures the dependence of the output photocurrent on the input laser power can be linear for those nanowires with a diameter below a certain threshold (80 nm in our design). This limit corresponds to the total depletion of the nanowire stem due to the Fermi level pinning at the sidewalls. We explain the nonlinearity in partially depleted nanowires as due to a nonlinear variation of the diameter of their central conduction channel under illumination. We compare our experimental results with theoretical calculations, which provide a view of the electric fields within the structure and into surface effects. From this comparison we can explain the behavior of the photocurrent and its dependence on the nanowire diameter [3].

References

- [1] M. Spies *et al.*, Nano Lett. **17**, 4231 (2017).
 [2] F. González-Posada, *et al.*, Nano Lett. **12**, 172 (2012).
 [3] M. Spies *et al.*, Nanotechnology (2018) (10.1088/1361-6528/aab838).

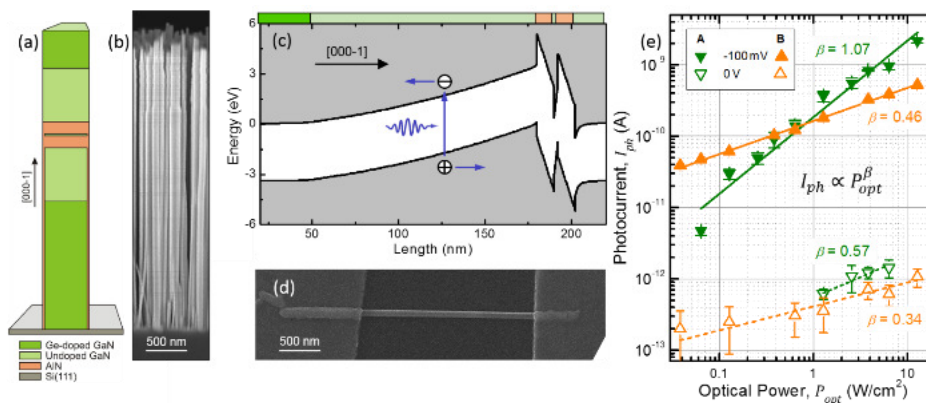


Figure 1. (a) Scheme, (b) SEM image and (c) band diagram of the heterostructured NWs. (d) SEM image of a contacted single NW. (e) Typical photoresponse of NWs with a diameter <80 nm (**A**) and >80 nm (**B**) under bias and at zero bias. Under reverse bias, **A** nanowires are linear ($\beta \approx 1$) whereas **B** nanowires are sublinear ($\beta < 1$).

Kardar-Parisi-Zhang universality in the phase distributions of one-dimensional exciton-polaritons

Davide Squizzato, Léonie Canet, and Anna Minguzzi
Univ. Grenoble Alpes and CNRS, LPMMC, F-38000 Grenoble

Exciton-polaritons under driven-dissipative conditions exhibit a condensation transition [1] which belongs to a different universality class than equilibrium Bose-Einstein condensates. Recently it was shown that the long-distance physics of the phase-dynamics is ruled by the Kardar-Parisi-Zhang equation and a numerical verification was given in (1+1)dimensions [2, 3]; however, the experimental accessibility of the KPZ mapping is still under debate. In this talk we present some recent results we get by numerically solving the generalized Gross-Pitaevskii equation with realistic experimental parameters. We show that one-dimensional exciton-polaritons display fine features of KPZ dynamics beyond the scaling exponents, i.e. their phase distribution follows the Tracy-Widom form predicted for KPZ growing interfaces. We moreover evidence a crossover to the stationary Baik-Rains statistics, recently observed also in turbulent liquid-crystals experiments [4]. We finally show that these features are unaffected on a certain timescale by the presence of a smooth disorder often present in experimental setups, in agreement with theoretical predictions [5]. This analysis suggests new experimental protocols for the observation of KPZ properties in exciton-polaritons.

-
- [1] J. Kasprzak *et al.*, *Nature* **443**, 409 (2006).
 - [2] K. Ji, V. N. Gladilin, and M. Wouters, *Phys. Rev. B* **91**, 045301 (2015).
 - [3] L. He, L. M. Sieberer, E. Altman, and S. Diehl, *Phys. Rev. B* **92**, 155307 (2015).
 - [4] K. A. Takeuchi, *Phys. Rev. Lett.* **110**, 210604 (2013).
 - [5] D. Squizzato, L. Canet, and A. Minguzzi, arXiv 1712.03709 (2017).

Large voltage tuning of Dzyaloshinskii-Moriya Interaction: a route towards dynamic control of skyrmion chirality.

Titiksha Srivastava,^{a*} Marine Schott,^{a, b} Roméo Juge,^a Viola Křížáková,^b Mohamed Belmeguenai,^c Yves Roussigné,^c Anne Bernard-Mantel,^b Laurent Ranno,^b Stefania Pizzini,^b S. M. Chérif,^c A. Stachkevitch,^c Stéphane Auffret,^a Olivier Boulle,^a Gilles Gaudin,^a Mair Chshiev,^a Claire Baraduc,^a and Hélène Béa^a

- a. Univ. Grenoble Alpes, CEA, CNRS, Grenoble INP[†], INAC-Spintec, 38000 Grenoble, France, [†] Institute of Engineering Univ. Grenoble Alpes
 b. Univ. Grenoble Alpes, CNRS, Néel Institute, F-38042 Grenoble, France
 c. Laboratoire des Sciences des Procédés et des Matériaux, Univ. Paris 13 Nord, Villetaneuse, France

* titiksha.srivastava@cea.fr

Electric control of magnetism is a pre-requisite for efficient and low power spintronic devices. More specifically, in heavy Metal/Ferromagnet/Insulator heterostructures, voltage gating has been shown to locally and dynamically tune magnetic properties like interface anisotropy and saturation magnetization [1,2]. However its effect on interfacial Dzyaloshinskii-Moriya Interaction (DMI) [3], which is crucial for the stability of magnetic skyrmions, has been challenging to achieve and therefore has not been reported yet for ultrathin films.

Here, we demonstrate 140% variation of DMI with electric field in sputter deposited Ta/FeCoB/TaOx trilayers through Brillouin Light Spectroscopy (BLS). We further show a monotonic variation of DMI and skyrmionic bubble size with electric field by polar-Magneto-Optical-Kerr-Effect microscopy. Our experiments show an unprecedented electric field efficiency for DMI $\beta_{\text{DMI}} = 700\text{fJ/Vm}$. The efficient DMI manipulation with voltage thus establishes an additional degree of control over skyrmions and spin orbitronic based devices. We anticipate through our observations that a sign reversal of DMI with electric field is possible, leading to a chirality switch. This dynamic engineering of DMI lays the foundation towards programmable skyrmion based memory or logic devices.

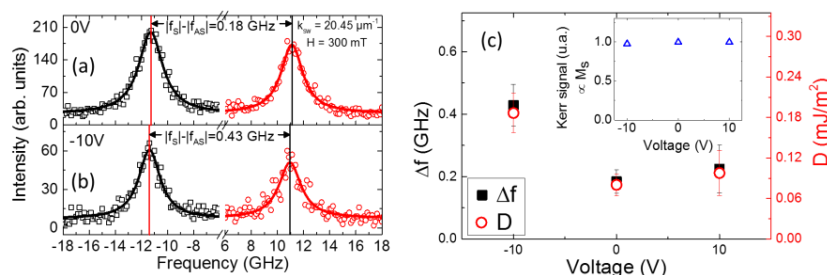


Figure 1: BLS spectra (open symbols) and Lorentzian fits (lines) measured under 0V (a) and -10V (b). The frequency difference Δf changes by 140% at -10V. (b) Variation of frequency difference Δf and deduced interfacial DMI as a function of applied voltage.

- [1] P.-J. Hsu, A. Kubetzka, A. Finco, N. Romming, K. vonBergmann, R. Wiesendanger, Electric-Field-Driven Switching of Individual Magnetic Skyrmions. *Nat. Nanotech.*, **12**, 123 (2016)
 [2] M. Schott et al., The Skyrmion Switch: Turning Magnetic Skyrmion Bubbles on and off with an Electric Field. *NanoLett.*, **17**, 3006 (2017)
 [3] U. K. Robler, A. N. Bogdanov, and C. Pfleiderer, Spontaneous skyrmion ground states in magnetic metals. *Nature* **442**, 797 (2006)

Development of Highly Sensitive Scanning Thermal Probe (S_{Th}M) for Nanoscale Thermometry

Rahul Swami^{a,b}, Gwénaëlle Julié^{a,b}, Simon Le Denmat^{a,b}, Jean-François Motte^{a,b},
Séverine Gomès^c, Pierre-Olivier Chapuis^c, and Olivier Bourgeois^{a,b}

- a. Université Grenoble Alpes, Grenoble, France
- b. Institut Néel, CNRS, 25 Avenue des Martyrs, 38042 Grenoble, France
- c. CETHIL, INSA, Campus de la Doua, 69100 Villeurbanne, France

* rahul.swami@neel.cnrs.fr << corresponding author >>

The realisation of thermal transport in micro and nanoscale devices has become important for the development of novel electronic and thermal devices. Over many years, various thermal measurement techniques have been developed, but precise thermal measurement at small length scale is still difficult to achieve. Therefore, there is currently a growing need for new experimental tools with high sensitivity to study temperature and thermal conductivity at low dimensions. In this respect, new instruments have to be developed to fill those requirements. The Scanning Thermal Microscopy (S_{Th}M) is one of them. This instrument consists in using an Atomic Force Microscopy (AFM) environment and in having a probe equipped with a highly sensitive thermometer. Here we propose to use resistive thermometry based on niobium nitride (NbN) as developed at Institut Néel, to functionalize a thermometer at the apex of the AFM tip. This NbN based thermometer has shown temperature coefficient of resistance (TCR) up to $(1.2 \times 10^{-2} K^{-1})$ at room temperature, a value ten times higher than currently existing resistive thermometer on S_{Th}M probes. This will allow strong improvements of the thermal sensitivity of S_{Th}M. Also, a proper thermal design of the cantilever will also lead to an improvement of the technique. Indeed, currently available cantilevers have not been fully optimized, which results in significant thermal losses in S_{Th}M probes. We will show how we optimize the deposition of a NbN thermometer on AFM probes (S_{Th}M probes) for nanoscale quantitative thermal measurements. The perspectives rely on demonstration of the new capabilities of this new resistive S_{Th}M probe on micro and nanostructured materials and systems.

How does temperature affect the conformation of single DNA molecules below melting temperature?

Catherine Tardin^{a*}, Annaël Brunet^{a,b}, Laurence Salomé^a, Philippe Rousseau^c,
Nicolas Destainville^b, Manoel Manghi^b

- a. Institut de Pharmacologie et de Biologie Structurale, Université de Toulouse, CNRS, UPS, France
- b. Laboratoire de Physique Théorique (IRSAMC), Université de Toulouse, CNRS, Toulouse, France
- c. Laboratoire de Microbiologie et Génétique Moléculaires (LMGM), Centre de Biologie Intégrative (CBI), Université de Toulouse, CNRS, UPS, France

* tardin@ipbs.fr

The double stranded DNA molecule undergoes drastic structural changes during biological processes such as transcription during which it opens locally under the action of RNA polymerases. Local spontaneous denaturation could contribute to this mechanism by promoting it. Supporting this idea, different biophysical [1-3] studies have found an unexpected increase in the flexibility of DNA molecules with various sequences as a function of the temperature, which would be consistent with the formation of a growing number of locally denatured sequences. Here, we take advantage of our capacity to detect subtle changes occurring on DNA by using high throughput tethered particle motion to question the existence of bubbles in double stranded DNA under physiological salt conditions through their conformational impact on DNA molecules ranging from several hundreds to thousands base pairs [4]. Our results strikingly differ from previously published ones, as we measure a bending modulus that remains stable with temperature as expected for intact double stranded DNA.

[1] Forties, R.A., Bundschuh, R. and Poirier, M.G. The flexibility of locally melted DNA. *Nucleic Acids Res.*, **37**, 4580–4586 (2009)

[2] Geggier, S., Kotlyar, A. and Vologodskii, A. Temperature dependence of DNA persistence length. *Nucleic Acids Research*, **39**, 1419–1426 (2011).

[3] Driessen, R.P.C., Sitters, G., Laurens, N., Moolenaar, G.F., Wuite, G.J.L., Goosen, N. and Dame, R.T. Effect of Temperature on the Intrinsic Flexibility of DNA and Its Interaction with Architectural Proteins. *Biochemistry*, **53**, 6430–6438 (2014).

[4] Brunet, A., Salomé, L., Rousseau, P., Destainville, N., Manghi, M. and Tardin, C. How does temperature impact the conformation of single DNA molecules below melting temperature? *Nucleic Acids Res.*, [10.1093/nar/gkx1285](https://doi.org/10.1093/nar/gkx1285) (2017).

Photoémission induite par laser de nanopointes de diamant : mécanismes de conduction et dynamique temporelle.

Olivier Torresin^{a*}, Mario Borz^b, Julien Mauchain^a, Ivan Blum^b, Angela Vella^b and Benoît Chalopin^a

- a. Laboratoire Collisions Agrégats Réactivité, Université Toulouse 3, CNRS
b. Groupe de Physique des Matériaux, Université de Rouen, INSA Rouen, CNRS

* torresin@irsamc.ups-tlse.fr

Nous présentons des résultats expérimentaux sur l'émission statique et induite par laser femtoseconde de nanopointes de diamant, matériau attractif pour l'émission de champ du fait de la possibilité d'avoir une électroaffinité négative [1]. En émission statique le courant d'émission combine une conduction à l'intérieur de la pointe (conduction de Poole-Frenkel) et une émission de champ à l'interface entre la pointe et le vide (émission de Fowler-Nordheim) [2]. À l'aide d'un modèle électrique simple [3], nous pouvons reproduire fidèlement la dépendance, en fonction de la tension appliquée V_{DC} , du courant d'émission et de la chute de tension ΔV qui apparaît le long de la pointe.

Le comportement de l'émission induite par laser d'une nanopointe de diamant est complètement différent de celle d'une pointe métallique. L'intensité du courant présente une saturation au-delà d'une certaine intensité laser. La chute de tension ΔV est aussi modifiée, et s'explique par une extinction de la barrière tunnel à l'interface entre le diamant et le vide. Enfin, des mesures résolues en temps montrent que sous illumination laser, l'émission statique disparaît et les électrons sont émis durant un temps très court autour de l'impulsion laser. Après l'impulsion laser femtoseconde, l'émission statique met quelques centaines de microsecondes avant de réapparaître, contrairement au cas d'une pointe métallique où l'émission statique entre impulsions est instantanée et n'est pas perturbée par le passage de l'impulsion.

- [1] J. Van der Weide et al., *Negative-electron-affinity effects on the diamond (100) surface*, Phys. Rev. B **50**, 5803 (1994)
[2] V. I. Kleshch et al., *Single Crystal Diamond Needle as Point Electron Source*, Scientific Reports **6**,35260 (2016)
[3] O. Torresin et al., *Voltage drop and conduction mechanisms in diamond nanoemitters*, soumis.

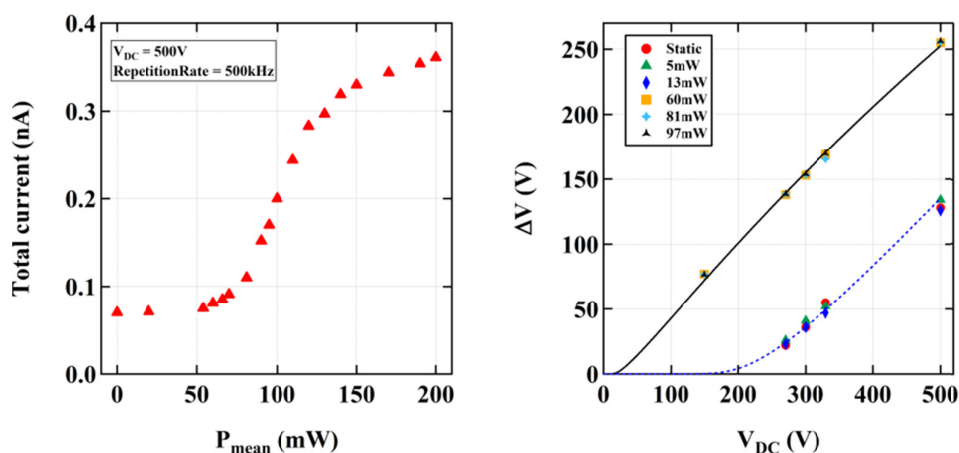


Figure 1: Gauche : Courbe du courant total d'émission en fonction de la puissance moyenne du laser. Droite : Mesure de la chute de tension ΔV en fonction de V_{DC} pour une émission statique et laser à différentes puissances moyennes du laser.

Robustness of a gel marble

Victor Tabouillot^a, Anne-Laure Biance^{*a}, Osvanny Ramos^a, Elise Lorenceau^c and Carole Planchette^b

- a. ILM, CNRS et Université de Lyon, Villeurbanne, France
- b. TU Graz, Graz, Austria
- c. LiPhy, CNRS et Université Grenoble-Alpes, France

* anne-laure.biance@univ-lyon1.fr

Reversible encapsulation of liquid materials is a technical challenge in many applications as for the transport and controlled delivery of active ingredients. In contrast to most state-of-the-art processes, capillary adsorbed solid particles can achieve a chemical-free encapsulation by forming dense rafts which isolate the liquid from its surrounding. The robustness of such liquid marbles against coalescence have been well established and depends on the particle size, the smaller particles being the less robust [1,2]. On the contrary, when a droplet impact on a solid surface with large particles, the smaller the particles, the better the coating [2]. In this work, we report some experiments on the robustness of carbopol gel marbles, which exhibit an intermediate behavior between solid and liquid. A new strategy to create such marbles is proposed, and the effect of the material yield stress on the marble robustness is apprehended.

[1] Coalescence of armored interface under impact, C. Planchette, A.-L. Biance, O. Pitois and E. Lorenceau, *Phys. Fluids*, 25, 042104 (2013).

[2] Rupture of granular rafts: effects of particle mobility and polydispersity, C. Planchette, E. Lorenceau, A.-L. Biance, *soft matter*, accepted (2018)

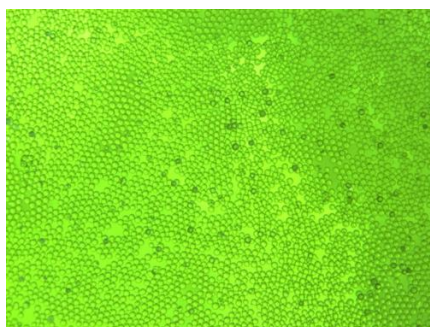


Figure 1 : Granular beads (85 μm) at the surface of a liquid gel.

Semiconductor nanowires : elaboration, analyses and applications

Maria Tchernycheva^{a*}

a. C2N-CNRS, Université Paris-Sud, Université Paris Saclay, 91405 Orsay, France

* maria.tchernycheva@u-psud.fr

Semiconductor nanowires are nano-objects with a high aspect ratio and a sub-micrometre diameter (Fig. 1 (a) and (b)). These nanomaterials are intensively studied as promising building blocks of future photonic and electronic devices (e.g. transistors, sensors, photovoltaic converters, light emitting diodes, photodetectors...). They are also unique systems to study fundamental physical phenomena at the nanoscale. The nanowires exhibit unique optical and electrical properties stemming from their anisotropic geometry, high surface-to-volume ratio, and carrier confinement.

The nanowires can be fabricated either by a top-down or a bottom-up approach. The main advantage of the bottom-up nanowire synthesis is the possibility to reduce the object dimensions disregarding the limitations imposed by the lithographic techniques while preserving lateral surface flatness.

In this talk, the elaboration, characterization and applications of bottom-up semiconductor nanowires will be discussed. We will first discuss the nanowire epitaxy and different structures that can be obtained. We will then present some nanoscale characterization techniques allowing to get access to the nanowire physical parameters. Finally, we will focus on the nanowire optoelectronic applications with a special attention to light emission and energy harvesting. In particular, mechanically flexible nanowire light emitting diodes will be highlighted (Fig. 1 (d) and (e)).

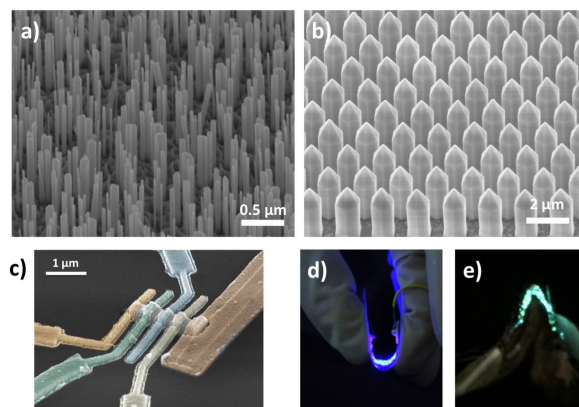


Figure 1 : SEM images of (a) – self-assembled and (b) – organized GaN nanowires; (c) nanowire with multiple electrical contacts; (d) bleu and (e) green flexible nanowire light emitting diodes

Anomalous lattice dynamics in $\text{La}_{2-x}\text{Sr}_x\text{CuO}_{4+y}$ (LSCO): The role of static or mobile dopants

T. Tejsner^{a,b*}, M. Boehm,^a A. Piovano^a, A. ȚuȚeanu^{a,b}, L. Udby^b

a. Institut Laue-Langevin, 38000 Grenoble, France

b. Niels Bohr Institute, University of Copenhagen, DK-2100 Copenhagen, Denmark

* tejsnertb@ill.fr

The cuprate $\text{La}_{2-x}\text{Sr}_x\text{CuO}_4$ (LSCO) is an interesting model system for high-temperature superconductivity (HTSC) due to its relatively simple crystal structure and differences in the superconducting transition as function of Sr and Oxygen doping. Hole-doping with Sr^{2+} creates a superconductor where the superconducting transition temperature T_c varies monotonically with doping. Doping with highly mobile, excess O^{2-} by contrast, results in a bulk superconductor separated into two unique phases: 1) An optimally doped, bulk superconducting phase ($T_c = 40\text{K}$)[1] with low pinning[2] and a 2) long-range modulated antiferromagnet with period ≈ 8 similar to the striped cuprates[3].

While both optimally doped LSCO and LSCO+O appear to have similar superconducting properties, the specific role of the dopant ions on a microscopic scale is still unknown. Recently, an anomaly in the Cu-O bond stretching phonon was found to correlate with T_c in Sr-doped LSCO, indicating a coupling to a novel charge mode possibly related to stripes[4,5]. In order to distinguish between a lattice effect driven by the superconducting transition or a lattice anomaly introduced by Sr doping, we concentrated our research on samples that are strongly underdoped in terms of Sr ($x \leq 0.06$), but optimally superconducting ($T_c = 40\text{K}$) due to excess Oxygen. Our preliminary measurements with $x = 0.06$ shows a phonon anomaly with similar strength to optimally doped LSCO as reported in literature[6]. Expanding on these results, we will measure the phonon anomaly in LCO+O in spring this year and compare our experimental results with DFT calculations.

- [1] Mohottala, H. E., et al, Nature Materials, 5(5), 377–382 (2006)
- [2] Mohottala, H. E., et al, Physical Review B, 78(6), 64504 (2008)
- [3] Udby, L., et al, Physical Review Letters, 111(22), 227001 (2013)
- [4] Park, S. R., et al, Physical Review B, 89(2), 20506 (2014)
- [5] Reznik, D. Physica C: Superconductivity, 481 (2012)
- [6] Tejsner, T. et al, Manuscript in preparation (2018)

Ballistic thermal transport in two-dimensional MoSe₂ lattices

Nicolas Morell^a, Slaven Tepsic^a, Antoine Reserbat-Plantey^a, Andrea Cepellotti^b, Marco Manca^c, Andreas Isacsson^d, Xavier Marie^c, Francesco Mauri^e, Adrian Bachtold^a

- a. ICFO-The institute of photonic sciences, Av. Carl Friedrich Gauss, 3, Castelldefels (Barcelona), Spain.
- b. University of California at Berkeley, LeConte Hall 366, Berkeley (California),USA.
- c. INSA, 135 Avenue de Rngueil, Toulouse, France.
- d. Chalmers University of Technology, Gothenburg, Sweden.
- e. Università di Roma La Sapienza, Pizzale Aldo Moro 5, Roma, Italy.

E-mail: slaven.tepsic@icfo.es

The conduction of heat in two-dimensional lattices features striking phenomena that have attracted considerable interest from a basic science point of view and for technological applications. The thermal conductance of monolayer materials have been extensively studied with Raman and electrical measurements. However, the thermal transport properties of monolayers remain highly debated. Here, I will discuss a new method to study thermal transport in two-dimensions based on opto-mechanical measurements. These measurements are possible because suspended MoSe₂ monolayers form mechanical resonators that feature high quality factors and can be probed with low laser power [1]. We measure both the thermal conduction Fig.1a and the heat capacity Fig.1b of suspended MoSe₂ monolayers. These measurements reveal ballistic transport of heat when lowering temperature. The new measurement method opens avenues in thermal transport of low-dimensional systems.

[1] Nicolas Morell, Antoine Reserbat-Plantey, Ioannis Tsioutsios, Kevin G. Schadler, Francois Dubin, Frank H. L. Koppens, and Adrian Bachtold, NanoLetters 16, 5102-5108 (2016)

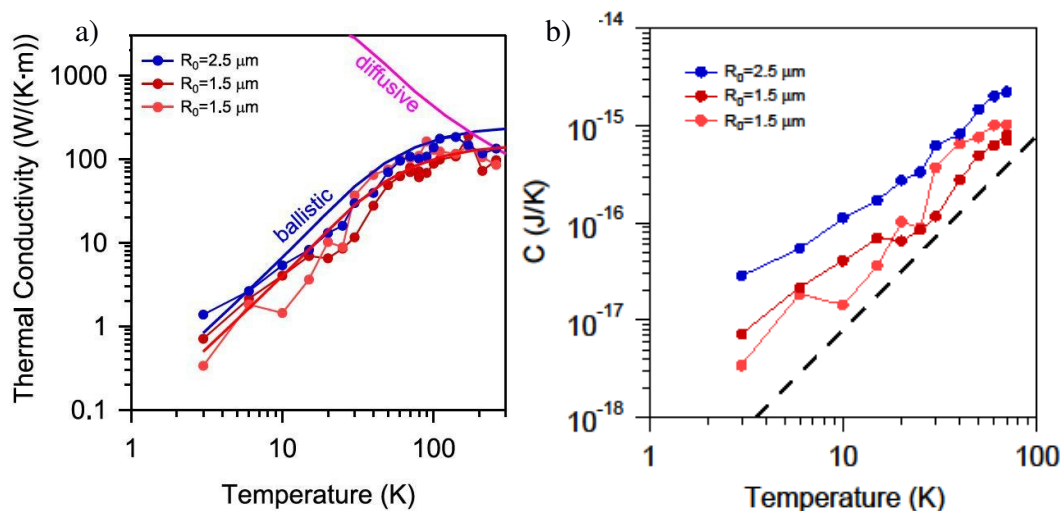


Figure 1 : (a) Thermal conductivity and (b) Heat Capacity versus temperature of single layer MoSe₂ showing ballistic thermal transport regime below 100K.

Intraneuronal transport measurement by tracking the optical non-linear response of nanoparticles

F. Terras *, Q.-L. Chou, G. Allard, F. Marquier, M. Simonneau et F. Treussart

Laboratoire Aimé Cotton, CNRS, Univ. Paris-Sud, ENS Paris-Saclay and Université Paris-Saclay, 91405 Orsay, France.

* feriel.terras@u-psud.fr

Brain diseases involve a large network of genes displaying subtle changes in their expression. Abnormalities of intraneuronal transport have been linked to genetic risk factors found in patients but current techniques cannot detect minor changes. Our team has developed a sensitive method relying on spontaneous internalization and subsequent single particle tracking of fluorescent nanodiamonds in endosomes of mouse hippocampal neurons in 2D cultures. This method is able to detect slight alterations of intraneuronal transport in neurons from transgenic mouse models displaying a genetic risk factor of a neuropsychiatric disease [1].

The extent of this technique to more realistic and complex 3D neuronal network can benefit from the use of non-linear crystals that can be excited in the near-infrared spectral window in which tissue are transparent, allowing to study intraneuronal transport in deep tissues. We will present our first results regarding the tracking of translation and rotational motion of endosomes in 2D-cultures using non-linear nanocrystals displaying second harmonic response detected by fast scanning 2-photon excited microscopy (Fig.1).

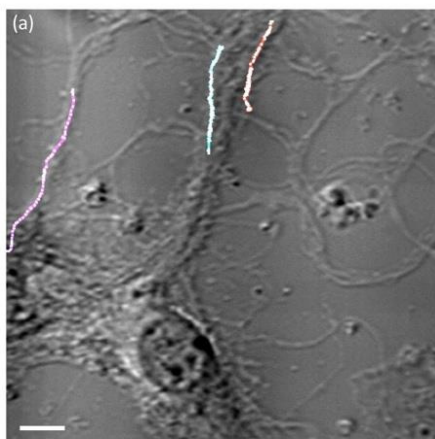


Figure 1: Tracking of second harmonic generation (SHG) of non-linear crystals of KTiPO_4 (KTP, size ≈ 140 nm) internalized inside 2D-cultures of mouse cortical neurons. Dotted contrast image of a neuron overlapped with 3 representative trajectories of nanoKTP. 2-photon microscope of *France Life Imaging PIMPA* platform (Orsay), $\lambda_{\text{exc}}=890$ nm, laser power ≈ 1 mW, SHG detection filter: 448 ± 20 nm. Scale bar: 10 μm .

[1] S. Haziza, *et al.*, « Fluorescent nanodiamond tracking reveals intraneuronal transport abnormalities induced by brain-disease-related genetic risk factors, » *Nat. Nanotech.* **12**, 322 (2017).

Analogue Hawking radiation in BECs: recent results regarding the black-hole laser effect

Manuele Tettamanti^{a,b*}

a. Università degli studi dell'Insubria, Como

b. INO-CNR BEC Center, Trento

* m.tettamanti8@uninsubria.it

In recent years physicist J. Steinhauer made important progresses in the field of sonic black holes created in Bose-Einstein condensates; in particular, in two different works published on Nature Physics, he claimed to have observed the analogue of the black-hole laser effect and of the Hawking radiation (the famous radiation predicted in 1974 by S.Hawking which causes black holes to “evaporate”). Starting from the first of these two works [1], we developed few numerical simulations in order to further test J. Steinhauer's claims, reaching substantially different conclusions [2] which were later supported by independent studies by another team [3]. Furthermore, these results triggered a new work which has recently lead to the demonstration that the effects seen in the experiment are unrelated to hydrodynamical instabilities (and thus to the black-hole laser effect).

[1] J. Steinhauer, Nature Phys. **10**, 864 (2014)

[2] M. Tettamanti, S. L. Cacciatori, A. Parola, I. Carusotto, EPL **119** 50002 (2017)

[3] Y.-H. Wang, T. Jacobson, M. Edwards, C. W. Clark, Phys. Rev. A **96**, 023616 (2017)

Chirality effects in the magnetism of ultrathin films

André THIAVILLE

Laboratoire de Physique des Solides, CNRS UMR 8502, Université Paris-Sud,
Bâtiment 510, Centre universitaire, 91405 Orsay, France

andre.thiaville@u-psud.fr

The magnetism of condensed matter differs from that of atoms by the so-called exchange interactions, which couple spins of neighboring atoms and produce collective phenomena. The exchange is typically ferromagnetic or antiferromagnetic, giving rise to a variety of magnetic orders. In addition, the atomic structure of condensed matter leads to magnetic anisotropy, with easier and harder directions along which a sample can be magnetized. Finally, magnetic moments interact at long distances by the magnetic field they create, the driving force for the zoo of domain structures, which can be observed, and explain the magnetization vs. field loops any particular sample. In the presence of a surface or interface, as experimentally studied in the last 35 years, all these interactions are modified so that ultrathin magnetic films can be seen as synthetic new magnetic materials [1].

In this context, I will discuss the latest discovered magnetic interaction at an interface, namely another form of the exchange interaction that favors non-collinear magnetic structures, with a definite chirality. The numerous observed consequences of this interaction will be presented. One group of effects modifies the physics of magnetic domain walls (see an example in Fig. 1). Another group of effects leads to small magnetic domains with topological properties, known as skyrmions [2].

[1] E. du Trémolet de Lacheisserie, D. Gignoux, M. Schlenker (Eds.), *Magnetism* (Springer, New York, 2005)

[2] F. Hellman, et al., Interface-induced phenomena in magnetism, *Rev. Mod. Phys.* **89**, 025006 (2017)

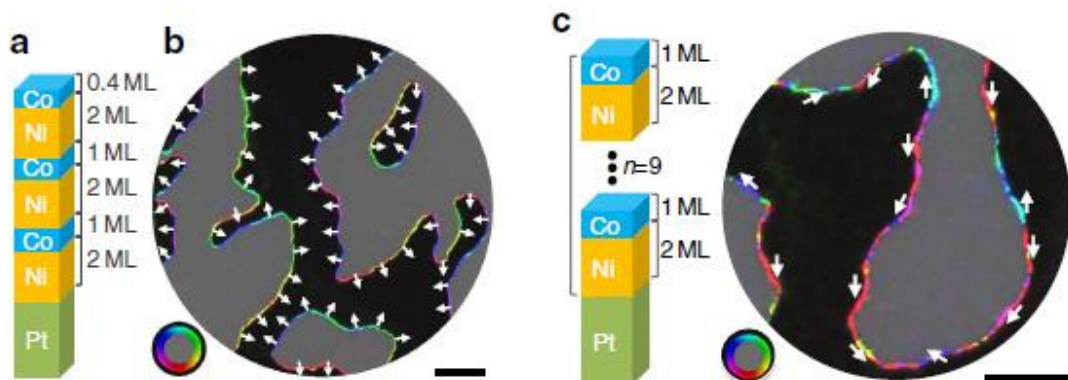


Figure 1 : Imaging of magnetic domain walls by spin-polarized low energy electron microscopy, showing change of structure as thickness increases (G. Chen et al., *Nat. Commun.* **4** :2671 (2013)).

Variational Ansätze for frustrated quantum magnetism: reconstructing correlations, entanglement and the sign structure

Jérôme Thibaut^{a*}, Fabio Mezzacapo,^a and Tommaso Roscilde^a

a. Laboratoire de physique de l'ENS de Lyon

* jerome.thibaut@ens-lyon.fr

Exotic quantum spin states stabilised by magnetic Hamiltonians are fundamentally characterised by their correlation/fluctuations properties, and by their entanglement pattern - namely by the properties which are completely missed at the mean-field level. The sign problem in quantum Monte Carlo generally leaves us without unbiased numerical approaches to reconstruct the above properties of models of quantum frustrated magnetism for large ($N \gg 10$) systems. A general strategy to circumvent this fundamental difficulty is offered by the variational approach, which is at the core of the most successful algorithms to study frustrated quantum magnetism; namely, the density-matrix renormalisation group approach — which variationally optimises matrix-product states — and its generalisations, which optimise so-called tensor-network states. Such states, while very powerful, are fundamentally limited in their entanglement content by the number of variational parameters (the so-called bond dimension), and their optimisation becomes very complex in dimension $d=2$ and higher (implying the contraction of a d -dimensional tensor network). Here we propose an alternative strategy to the variational study of frustrated quantum magnetism, based on a class of wavefunctions called entangled-plaquette states ^[1] or correlator-product states ^[2]. Such states have a very transparent structure in terms of correlations, which can be made to be scale invariant and therefore reproduce faithfully the structure at quantum critical points; they can be efficiently optimised using Monte Carlo techniques; and they can accommodate for an arbitrary amount of entanglement with a polynomial number of variational parameters. Most importantly, our recent progress shows us that, by complexifying the wavefunction coefficients, we can variationally reconstruct their correct sign structure, biased uniquely by the form of the Ansatz - something which is generally considered to be hard in frustrated magnetism [Becca, Sorella in ^[3]]. We demonstrate the power of our variational Ansatz in the paradigmatic case of the J1-J2 Heisenberg chain, whose quantum phase transition is correctly reproduced, as well as its intricate sign structure induced by the appearance of incommensurate spin correlations.

[1] F. Mezzacapo et al, New Journal of Physics, 11, 083026 (2009)

[2] H. Changlani et al., Phys. Rev. B 80, 245116 (2009)

[3] J.Chalker, Introduction to frustrated magnetism (Springer, 2011)

Study of structural change in amorphous phase-change materials' thin films by Pair Distribution Function

R. Tholapi¹, M. Gallard^{1,2}, M.-I. Richard^{1,3}, C. Mocuta², N. Burle¹, S. Escoubas¹, C. Guichet¹, L. Fellouh⁴, M. Bernard⁴, R. Chahine⁴, P. Kowalczyk⁴, C. Sabbione⁴, A. André⁴, F. Hippert⁵, P. Noé⁴ and O. Thomas¹

¹ Aix-Marseille Université, CNRS, IM2NP UMR 7334, Campus de St-Jérôme, 13397 Marseille, France

² Synchrotron SOLEIL, l'Orme des Merisiers, Saint-Aubin-BP 48, 91192 Gif-sur-Yvette, France

³ ID01/ESRF, The European Synchrotron, 71 rue des Martyrs, 38043 Grenoble, France

⁴ Université Grenoble Alpes, CEA-LETI, MINATEC campus, 17 rue des Martyrs, 38054 Grenoble, France

⁵ LNCMI, CNRS-UGA-UPS-INSA, 25 rue des Martyrs, 38042 Grenoble, France

ABSTRACT

Phase-change materials (PCMs, e.g. GeTe) and PCM memories are now considered as the most promising technology among new emerging resistive memory technologies to replace the Flash technology [1-2]. Nevertheless, one of the major issue of PCM memories is the drift of the resistance of PCM amorphous (a-)phase upon ageing. This so-called resistance drift phenomenon is related to attributed to a structural relaxation and can lead to memory failure and has limited up to now the development of Multi-Level Cell PCM memories. Understanding the structural changes occurring during drift of a-PCM is thus of paramount importance. A very recent work by Noé *et al.* reported structural changes in the drifted a-phase of GeTe thin films by means of X-ray absorption spectroscopy [3]. This first experimental evidence of a structural relaxation in a-GeTe thin films revealed an increase in Ge-Ge homopolar bonds during drift which is opposite to currently proposed theoretical models [4]. In that context, a total scattering technique like Pair Distribution Function (PDF) analysis is needed for understanding both short and long range structural information during drift in GeTe samples.

In this work, we attempt to measure the small structural changes occurring in the amorphous phase of PCM thin films by using PDF at ID31 the high-energy beamline of the ESRF. For this purpose, 500 nm-thick GeTe films capped with SiO₂ protective layer were deposited on SiO₂ substrates and drifted by means of annealing at various temperature below the crystallization temperature. Annealing were performed either *ex-situ* at different temperature for different time duration and *in-situ* by isothermal annealing during PDF acquisition. All PDF data were acquired at 80 KeV in both reflection and transmission geometries. During *in-situ* measurements, samples were kept at constant temperatures until changes in the total scattering structure function are detected. These small changes correspond to changes in interatomic distances, nature and coordination number in the amorphous GeTe phase during drift. Finally, the role of such structural changes and their probable implication on the resistance drift will be discussed. In addition, we also demonstrate that reliable PDFs can be obtained from thin films deposited on amorphous substrates which to date are scarcely investigated [4].

This work is funded by ANR within ANR SESAME ANR-15-CE24-0021 project.

REFERENCES

1. Raoux, S., Xiong, F., Wuttig, M., & Pop, E. 2014. MRS Bulletin, 39(8), 703–710.
2. Wuttig, M., & Yamada, N. Nature Materials, 6(11), 824–832 (2007).
3. Noé, P., Sabbione, C., Castellani, N., Veux, G., Navarro, G., Sousa, V., Hippert, F., D'Acapito, F. *J. Phys. D*, 49(3) (2015).
4. P. Noé, C. Vallée, F. Hippert, F. Fillot, and J. Y. Raty, *Semicond. Sci. Technol.* 33, (2018).
5. Jensen, K. M, *et al. IUCrJ*, 2(5), 481–489 (2015).

How to fill any nanopipettes and to determine their aperture size!

Bernard TINLAND^{a*} & *Evelyne SALENÇON*^a

a. Aix-Marseille Université, CNRS, CINaM UMR 7325, 13288 Marseille, France

* tinland@cinam.univ-mrs.fr

We describe a dynamic micro-distillation technique that can be used to fill all nanopipettes whatever their shape or aperture size. First, nanopipettes are filled with pure water that is later replaced with the desired electrolyte via electro-migration. Electrical measurements are used to check that filling is complete.

Nanopipette aperture sizes up to 25 nm are determined using a method based on the Poiseuille law. Pressure is applied to the backside of a liquid plug placed in the widest end of the nanopipette, resulting in an air pressure tank with an aperture at the very tip of the nanopipette. Measuring the velocity of the liquid meniscus gives the air flow and thus is related to the aperture size. Aperture size determinations are in good agreement with SEM estimations.

Both methods are simple, efficient, relatively fast and cheap.

[1] B. Tinland, E. Guirleo (Salançon), patent WO 2013079874 A1, "Method and device for filling nanopipettes via dynamic microdistillation"

[2] E. Salançon & B. Tinland, Filling nanopipettes with apertures smaller than 50nm: dynamic micro-distillation submitted to the Beilstein Journal of Nanotechnology (2018).

[3] E. Salançon & B. Tinland, Measuring liquid meniscus velocity to determine size of nanopipette aperture, *J. Colloid Interface Sci.*, **392**, 465–469 (2013)

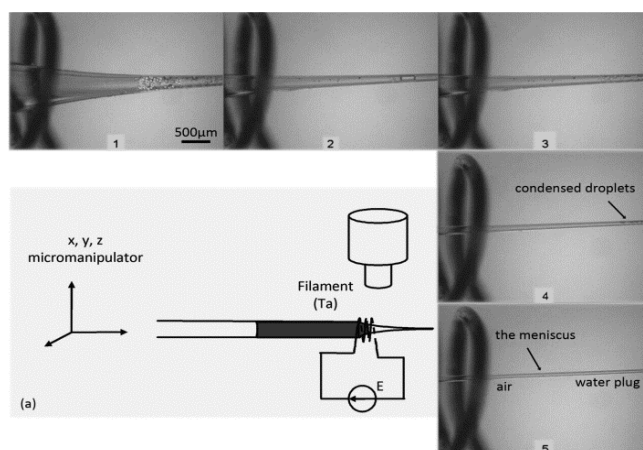


Figure 1 (a) The nanopipette is loaded with water up to its millimeter-to-micrometer region and then inserted into a tantalum loop heated by Joule effect. (1) The heated filament brings the water to boil inside the capillary; water re-condenses further on the cold wall of the nanopipette. (2) The nanopipette is moved to heat the part where the water has re-condensed as droplets. (3) The droplets are boiled again and water is re-condensed further on the next cold part of the nanopipette. (4) The process is repeated. (5) The water is re-condensed at the very end of the tip; the meniscus formed by the water plug and coming from the tip is visible under the optical microscope.

Microscopic theories vs kinematic constraints in frustrated magnets

Bruno Tomasello^{a*}

a. Institut Laue-Langevin, CS 20156, Cedex 9, 38042 Grenoble, France

tomasello@ill.eu

The concept of emergent quasi-particles is ubiquitous in condensed matter systems, most prominently in the effective description of low-temperature excitations. The variety of such excitations is rich in frustrated magnets. This is due mainly to strong-correlations that are enhanced by complex geometric constraints on the atomic constituents. The distinction between quantum-mechanical vs classically-effective degrees of freedom is crucial for a realistic description of measured properties, in particular for timescales. In this talk I will summarise a few groundbreaking point of views which represent a step forward in analysing the emergence of spin-dynamics rare-earth magnets. To allow a discussion of interest for both experimentalists and theorists I will refer to pyrochlore oxides and garnet systems.

Non-shallow water waves on a vortex: A model for dispersive fields around rotating black holes

Theo Torres^{ab*}

- a. School of Mathematical Sciences, University of Nottingham, University Park, Nottingham, NG7 2RD, UK.
- b. Centre for the Mathematics and Theoretical Physics of Quantum Non-Equilibrium Systems, University of Nottingham, NG7 2RD, UK.

* theo.torresvicente@nottingham.ac.uk

Shallow water waves scattering on a draining and rotating potential flow constitute the analogue of a rotating black hole. In such a spacetime, it has been shown theoretically that, at low frequency, waves can extract energy from black holes. Such a process is known as superradiance. Our recent observation of this effect in an experiment at the University of Nottingham [1] suggests that superradiance persists beyond the shallow water regime. In this talk, I will briefly present the experiment we conducted and I will extend some features of analogue rotating black holes to the dispersive regime. Especially I will focus on light rings and quasi-normal modes. This presentation is based on [2]

- [1] T. Torres, S. Patrick, A. Coutant, M. Richartz, E. W. Tedford, and S. Weinfurtner, *Nature Phys.* 13, 833 (2017), arXiv:1612.06180 [gr-qc].
- [2] T. Torres, A. Coutant, S. Dolan, and S. Weinfurtner, (2017), arXiv:1712.04675 [gr-qc].

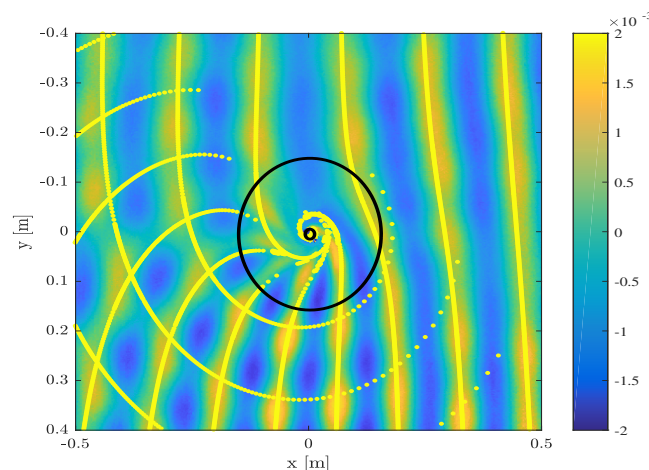


Figure 1: Comparison between eikonal wavefront computed numerically and experimental data from [2]. The bright yellow dots represent the eikonal wavefront reconstructed from the phase along the rays. The two black circles are the unstable orbits. The colorbar represents the amplitude of the wave in metres.

2- Révolution dans les Phénomènes de Nucléation : Transition du 1^{er} ordre et surchauffe de la phase verre au-dessus de T_m

Robert F. Tournier^{ab}

a- Univ. Grenoble Alpes, Inst. Néel, F-38042, Grenoble cedex 9, France,

b- CNRS, inst. Néel, F-38042, Grenoble cedex 9, France,

*robert.tournier@neel.cnrs.fr

L'équation classique complète de la nucléation [1] prévoit, non seulement l'existence de germes de nucléation au-dessus de la température de fusion T_m mais aussi la fusion endothermique de toute phase surchauffée au-delà de sa température de formation. Un cristal surchauffé et protégé contre la fusion de surface, fond à une température très supérieure à T_m . L'existence d'une température de surchauffe T_{n+} de la phase vitreuse doit être envisagée si sa formation est accompagnée par une transition du 1^{er} ordre (un peu cachée et spéciale [2]) [3]. Cet exposé a pour objectif de démontrer l'existence de ces deux phénomènes dans des alliages liquides et des verres surchauffés avec deux exemples : $Zr_{41.2}Ti_{13.8}Cu_{12.5}Ni_{10}Be_{22.5}$ (Vit 1) et l'eau amorphe.

Un taux de surfusion critique est relié à un taux de surchauffe critique des alliages liquides : $Zr_{52.5}Cu_{17.9}Ni_{14.6}Al_{10}Ti_5$ (Vit 105) [4] and Co-B [5] au-dessus de leur température de cristallisation. Une faible chaleur latente est aussi détectée pour Co-B et $Fe_{71.2}B_{24}Y_{4.8}Nb_4$ [6]. Il s'agit, dans ces deux cas, de la température de fusion T_{n+} de germes de nucléation de la phase vitreuse. Pour observer une transition complète, il faut partir du verre et chauffer le liquide au-dessus de T_m sans le cristalliser. Une fusion de $Zr_{41.2}Ti_{13.8}Cu_{12.5}Ni_{10}Be_{22.5}$ (Vit 1) est alors observée et accompagnée par la chaleur latente prédite à T_{n+} [4,7]. La transition du 1^{er} ordre à $T_{K2} = 601$ K en dessous de $T_g = 625$ K augmente la température de Kauzmann de $T_{K1} = 519$ K à $T_{K2} = 601$ K parce que l'enthalpie irréversible de la phase vitreuse disparaît au-dessus de T_m . La température de Kauzmann (116 K) de l'eau amorphe ne change pas car la transition du 1^{er} ordre se produit à $T_{LL} = 228.5$ K. La chaleur latente devrait être exothermique au cours du refroidissement à travers le no man's land et égale à $2222 \text{ JK}^{-1}\text{mol}^{-1}$ tandis qu'elle est quasiment nulle au cours du chauffage à cause de la contribution de la phase amorphe (de signe contraire) à $T_{LL} = 228.5$ K au-dessus de $T_g = 136.6$ K [8-10]. Le calcul des températures T_{K1} et T_{K2} montre que la transition du 1^{er} ordre devrait exister dans la plupart des verres. Il faut donc rechercher une température de fusion au-dessus de T_m .

[1] R.F. Tournier, JMC2018, Compléter l'équation classique de la nucléation et prédire les propriétés thermodynamiques des verres.

[2] T. Kirpatrick, D. Thirumalai, Phys. Rev. A: At. Mol. Opt. Phys. **31**, 939 (1985).

[3] R.F. Tournier, Chem. Phys. Lett. **665**, 64-70 (2016).

[4] S. Mukherjee, Z. Zhou, J. Schroers, W.L. Johnson, and W.K. Rhim, Appl. Phys. Lett. **84**, 5010-5012 (2004).

[5] Y. He, J. Li, J. Wang, H. Kou, E. Beaugnon. Appl. Phys. A. **123**, 391 (2017).

[6] Q. Hu, H.C Sheng, M.W. Fu, X.R. Zeng, J. Mat. Sci. **49**, 6900-6006 (2014).

[7] S. Wei, F. Yang, J. Bednarcik, I. Kaban, O. Shuleshova, A. Meyer & R. Busch, Nature Commun. **4**, 2083 (2013).

[8] R.F. Tournier, Chem. Phys. **500**, 45-53 (2018).

[9] M. Oguni, S. Maruyama, K. Wakabayashi, A. Nagoe, Chem. Asian J. **2**, 514 (2007).

[10] S. Maruyama, K. Wakabayashi, and M. Oguni, AIP Conf. Proc. **708**, 675 (2004).

Chemical arrangement and surface effects in CoAu nanoparticles

F. Tournus^{a*}, O. Loiselet^a, K. Sato^b and O. Stephan^c

- Institut Lumière Matière, UMR5306 Université Lyon 1-CNRS, Université de Lyon, 69622 Villeurbanne cedex, France
- Institute for Materials Research, Tohoku University, Sendai 980-8577, Japan
- Laboratoire de Physique des Solides (UMR CNRS 8502), Université Paris Sud, Campus Paris Saclay, 91405 Orsay, France

* florent.tournus@univ-lyon1.fr

Nanoparticles associating a noble metal and a ferromagnetic metal are appealing from a magneto-plasmonics point of view, in addition to the problematics of magnetic anisotropy tailoring (interface anisotropy, phase transformation) and of nanoalloy original geometries. Because Co and Au are immiscible in the bulk phase, and since fcc cobalt and gold have highly different cell parameters, chemically separated structures (core-shell type) are expected for nanoparticles.

We have studied CoAu cluster assemblies, with a diameter between 3 and 10 nm, prepared by low energy cluster beam deposition (LECBD) where nanoparticles are formed in out-of-equilibrium conditions by laser vaporization, then deposited on a substrate under ultrahigh vacuum conditions and protected by a capping layer (amorphous carbon, to avoid oxidation). The nanoparticles' structure and chemical arrangement (see figures) have been investigated by HRTEM, STEM-HAADF and STEM-EELS before and after annealing (2h around 500°C). As prepared particles are found to be inhomogeneous (as deduced from EELS measurements), with interatomic distances always corresponding to pure gold, and they appear to be surrounded by a shell of lighter HAADF intensity which rapidly transforms upon electron beam exposure in STEM. After annealing, a phase separation is observed and CoAu nanoparticles adopt a core-shell structure where, as observed by HRTEM (with a clearly visible difference of inter-plane distances between Co and Au regions), STEM-HAADF and STEM-EELS, an off-centered cobalt core is surrounded by a gold shell (see figure). These results shed light on the atomic-scale behavior of the Co-Au nanoalloy.

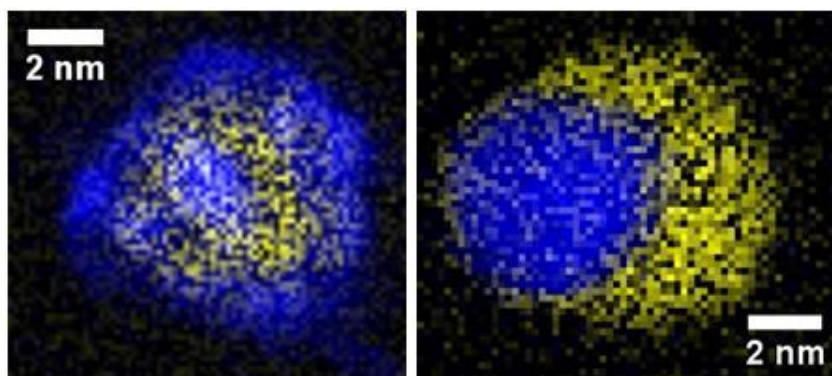


Figure 1: Chemical map from STEM-EELS measurements (Co in blue and Au in yellow), for a CoAu nanoparticle before (left) and after (right) annealing. A core shell geometry is obtained after annealing while Co is rather at the surface for as-prepared particles.

Structure and properties of Co-Ag nanoparticles: towards nano-systems combining magnetic and plasmonic features

F. Tournus^{a*}, O. Loiselet^a, J. Bellessa^a, V. Dupuis^a, and O. Stephan^b

- a. Institut Lumière Matière, UMR5306 Université Lyon 1-CNRS, Université de Lyon, 69622 Villeurbanne cedex
 b. Laboratoire de Physique des Solides (UMR CNRS 8502), Université Paris Sud, Campus Paris Saclay, 91405 Orsay

* florent.tournus@univ-lyon1.fr

The combination of plasmonic and magnetic properties in a single nano-system, which is needed for magneto-plasmonic purposes, may be achieved with nanoparticles made of a noble metal and a transition metal. In the case of cobalt and silver, the two elements are immiscible and we expect that the noble metal will go to the surface. However, nano-alloys can have specific behaviors and thus offer original possibilities. Moreover, for small nanoparticles, the surface and interface with the environment is of course crucial ((interface anisotropy, phase transformation), and thermodynamic equilibrium is not necessarily reached.

We have studied Co-Ag bi-metallic nanoparticles (cf. figure), in a small size domain (diameter lower than 10 nm), with the aim of relating the structure at the atomic and nanometer scale and both the magnetic and plasmonic properties. The particles are prepared by Low energy cluster beam deposition (LECBD), where preformed particles are softly deposited under vacuum and diluted in a matrix [1,2]. The use of an alumina dielectric matrix, of particular interest for optical properties, has strong repercussions on the structures (chemical arrangement) and the magnetic properties, which are very different from those met in an amorphous carbon matrix. While a plasmonic resonance can be measured from optical absorption measurements in Al_2O_3 , plasmonic features can also be observed using Electron Energy Loss Spectroscopy (EELS) measurements acquired with Scanning Transmission Electron Microscopy (STEM). It has thus been possible to cartography different plasmon modes (in particular surface modes) for Co-Ag particles capped by an amorphous carbon layer. From these various investigations, we also find that Co-Ag and Co-Au particles display a much distinct behavior.

[1] V. Dupuis et al., Physical Chemistry Chemical Physics **17**, 27996-28004 (2015)

[2] V. Dupuis et al., Journal of Nanoparticle Research, In press

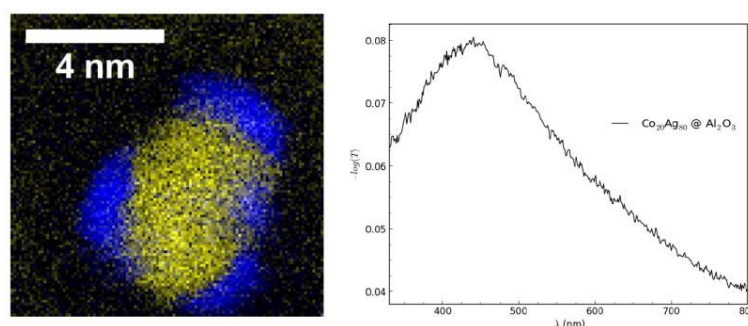


Figure 1: (Left) Chemical map (Co in blue, Ag in yellow) obtained from STEM-EELS measurements for a CoAg nanoparticle embedded in carbon. (Right) Transmission spectrum for a thin film of $\text{Co}_{20}\text{Ag}_{80}$ nanoparticles diluted in Al_2O_3 . The peak around 450 nm corresponds to the localized surface plasmon resonance of the Co-Ag nanoparticles.

Organization and magnetic properties of mass-selected FePt nanoparticles deposited on epitaxially grown graphene on Ir(111)

F. Tournus^{a*}, P. Capiod^a, L. Bardotti^a, A. Tamion^a, O. Boisron^a, C. Albin^a, V. Dupuis^a, G. Renaud^b, and P. Ohresser^c

- Institut Lumière Matière, UMR5306 Université Lyon 1-CNRS, Université de Lyon, 69622 Villeurbanne cedex
- CEA, Institut Nanosciences et Cryogénie, Service de Physique des Matériaux et Microstructures, Nanostructures et Rayonnement Synchrotron, 17 Avenue des Martyrs, F-38054 Grenoble, Cedex 9
- Synchrotron SOLEIL, L'Orme des Merisiers, BP48, Saint-Aubin, 91192 Gif-sur-Yvette

* florent.tournus@univ-lyon1.fr

The FePt alloy, when chemically ordered in the L_{10} phase, is among the magnetic materials displaying the highest magnetic anisotropy constant. Therefore it is a perfect candidate for ultra-high density magnetic storage applications, provided nanoparticles can be prepared in such a high anisotropy phase and organized in a 2D array. One path of bottom-up elaboration following a physical route consists in using template surfaces with specific sites regularly distributed. Such a 2D lattice can be obtained with the moiré (hexagonal lattice of 2.5 nm cell parameter) displayed by a graphene layer epitaxially grown on a Ir(111) surface [2]. For the first time, we have characterized the organization and the magnetic properties of FePt nanoparticles on such a moiré pattern.

FePt/graphene/Ir(111) samples have been prepared using Low Energy Cluster Beam Deposition of preformed size-selected FePt nanoparticles (around 2 nm diameter). We will discuss the organization of such particles on specific sites of the moiré lattice, as determined by grazing incidence x-ray scattering measurements (cf. figure) [3]. The deposited nanoparticles are sensitive to the moiré pattern and we find that the resulting organization can be preserved up to temperatures around 700 °C. Using X-ray Magnetic Circular Dichroism measurements (cf. figure), we will report a clear evolution of the magnetic properties of the FePt nanoparticles induced by annealing (anisotropy modification, interface effects between FePt and the graphene...), while the particles keep their individuality (no layer formation is observed).

[1] P. Andreatza et al., Surface Science Reports **70**, 188 (2015)

[2] A. T. N'Diaye et al., New Journal of Physics **10**, 043033 (2008)

[3] S. Linas et al., Scientific Reports **5**, 13053 (2015)

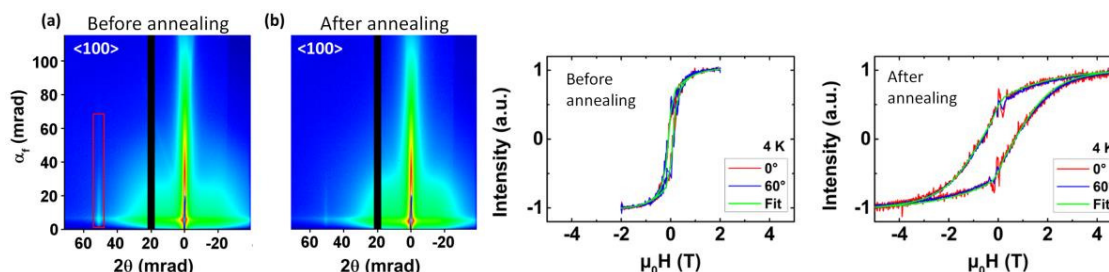
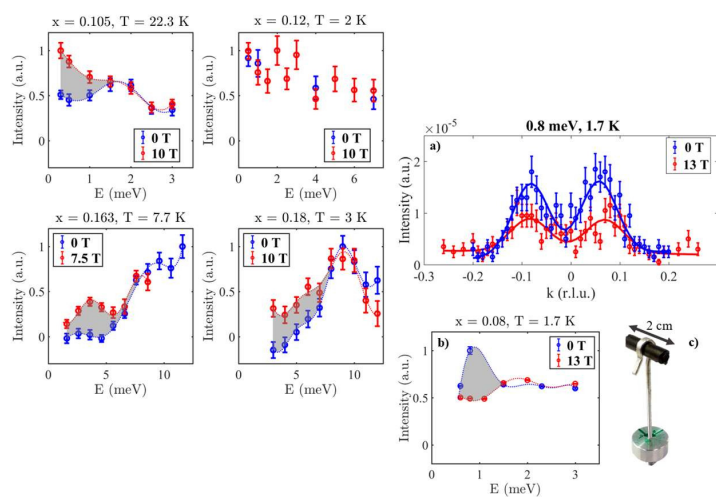


Figure 1: (left) GISAXS measurements displaying a correlation peak, signature of the coherent organization of FePt nanoparticles on the moiré lattice. (right) Hysteresis loops, from XMCD measurements, before and after annealing of the FePt nanoparticles, where a large increase of the anisotropy constant is visible.



Engineering symmetries in the waveguide lattices

Lavi K Upreti^{a*}, Marco Marciani,^a and Pierre Delplace^a

a. École Normale Supérieure de Lyon, 46 Allée d'Italie, 69007 Lyon, France

* lavi-kumar.upreti@ens-lyon.fr

Periodically driven systems have specific boundary states with no counterpart in static systems. These states appear in the quasi-energy spectrum of finite size samples, that encodes the phase accumulation of a state after its evolution over one period of drive.

We investigate the non-trivial topological properties of 1D periodically driven systems and their experimental realization in photonics. As for static systems, the existence of topological properties in 1D requires some extra symmetry, such as chiral or particle-hole. We show how to implement these symmetries by adjusting the drive, and propose different arrays of evanescently coupled waveguides that realize the optical analog. In such devices, propagation of the predicted topological boundary modes could be directly observed by fluorescence.

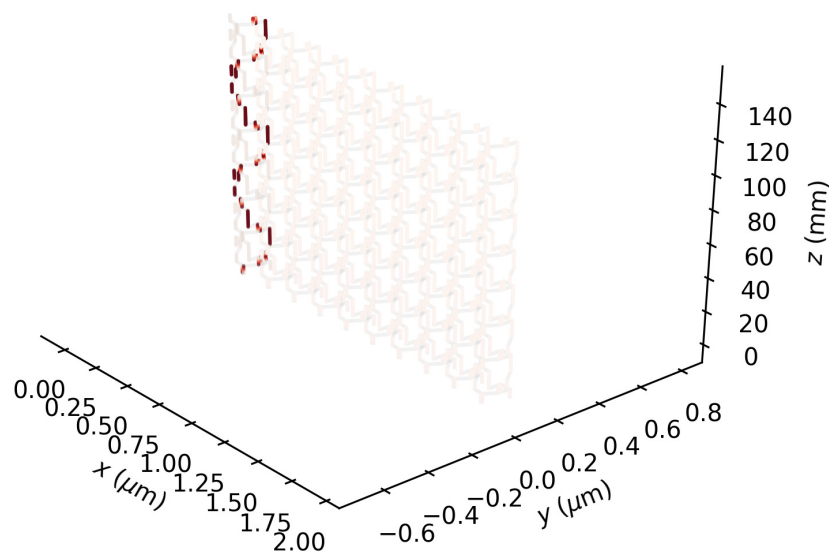


Figure 1: Wave guide propagation for topological phase at the boundaries

Bosonic Double Ring Lattice Under Artificial Gauge Fields

Nicolas Victorin^{a*}, Frank Hekking,^{a†} and Anna Minguzzi^a

a. Univ. Grenoble Alpes, CNRS, LPMMC, F-38000 Grenoble, France

* << nicolas.victorin@lpmmc.cnrs.fr >>

We consider a system of weakly interacting bosons confined on a planar double lattice ring subjected to two artificial gauge fields. We determine its ground state by solving coupled discrete non-linear Schrödinger equations at mean field level. At varying inter-ring tunnel coupling, flux and interactions we identify the vortex, Meissner and biased-ladder phases also predicted for a bosonic linear ladder by a variational Ansatz. We also find peculiar features associated to the ring geometry, in particular parity effects in the number of vortices, and the appearance of a single vortex in the Meissner phase. We show that the persistent currents on the rings carry precise information on the various phases. Finally, we propose a way of observing the Meissner and vortex phases via spiral interferogram techniques.

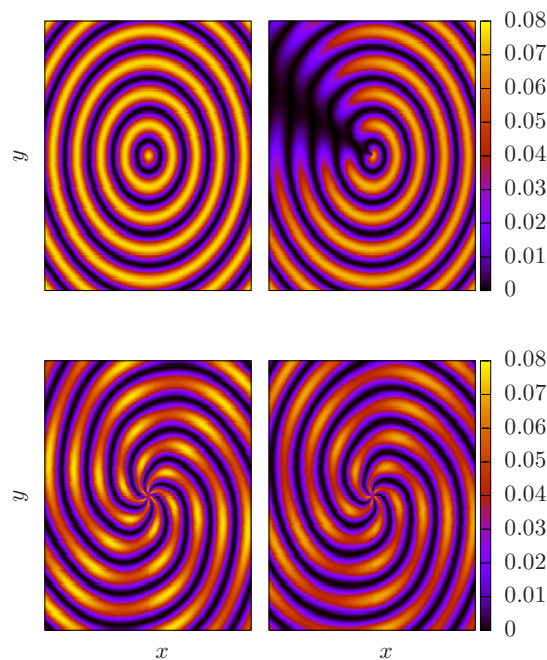


Figure 1: Spiral interferogram in the Meissner phase (upper panels), and in the vortex phase (lower panels) showing the parity effect of the total flux Φ on the number of vortices.

Thermal conductivity measurements of a 200 μ m-thick Silicon wafer between 0.3K and 2K

Yaser Vaheb, Sebastian Volz and Jay Amrit

The *in-plane* thermal conductivity of a slab of Si wafer is measured between 0.3K and 2K. The sample dimensions are 25 mm x 6 mm x 200 μ m. The thermal conductivity varies by two orders of magnitudes and it shows a deviation from the bulk T^3 -behavior. Temperature dependent mean free paths can account for the thermal conductivity.

Poster presentation

Static strain tuning of quantum dots embedded in a photonic wire

D. Tumanov¹, N. Vaish¹, H.A. Nguyen¹, Y. Curé², J.-M. Gérard², J. Claudon²,
F. Donatini¹, J.-Ph. Poizat¹

¹ Université Grenoble-Alpes, CNRS, Institut Néel, France

² Université Grenoble-Alpes, CEA, INAC-PHELIQS, France

Email : jean-philippe.poizat@neel.cnrs.fr

Epitaxial semiconductor quantum dots (QDs) embedded in nanophotonic structures are very efficient single photon sources [1]. However their use in quantum information protocols involving more than two sources has been hindered by the dispersion in energy of different QDs. QD energy tuning can be achieved using temperature, electric field, or material strain. In this work, we used strain to statically tune the QDs embedded within a photonic waveguide.

Our system consists of InAs QDs embedded within a GaAs photonic wire as a waveguide featuring very efficient single photon collection efficiency [1]. Four years ago, these photonic structures were used in our team as mechanical oscillator to demonstrate strain-mediated optomechanical coupling [2,3]. Owing to its off-centered position within the nanowire circular cross-section, the quantum dot strained as the wire is bent. This strain alters the quantum dot energy levels [2] and therefore the spectral position of the photoluminescence lines.

In the present work [4], we used strain to statically tune the semiconductor band gap (up to 25 meV) of QDs embedded in a photonic waveguide. As opposed to our previous work [2,3], the strain is produced statically using a nanomanipulator enabling the realization of bright and broadly tunable quantum light sources. Moreover, owing to the strong transverse strain gradient generated in the structure, we can relatively tune two QDs located at different locations in the waveguide and bring them in resonance, opening the way to the observation of collective effects such as superradiance.

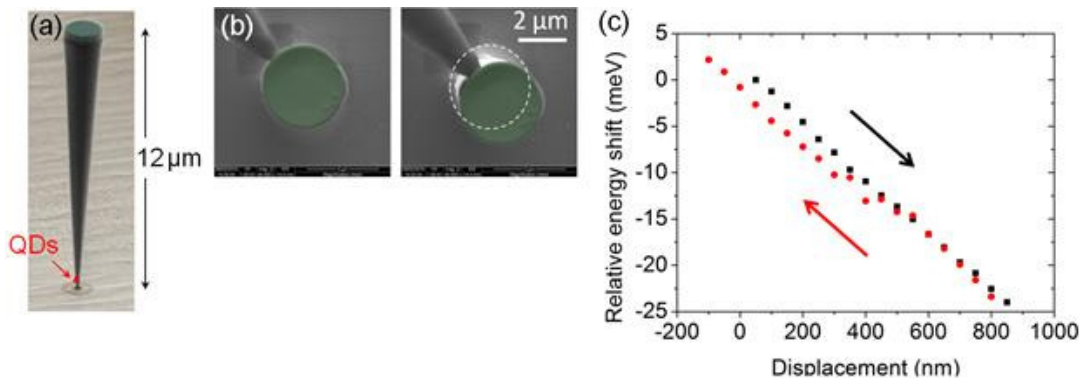


Fig. (a) Tilted scanning electron microscope (SEM) view of the GaAs photonic waveguide. (b) SEM top view showing the top facet of a waveguide displaced by the tip of a nanomanipulator. (c) Relative energy shift as a function of the displacement of nanomanipulator tip.

References

- [1] M. Munsch et al, Phys. Rev. Lett 110, 177402 (2013).
- [2] I. Yeo, et al, Nat. Nano 9, 106 (2014).
- [3] P.L. de Assis et al, Phys. Rev. Lett. 118, 117401 (2017).
- [4] D. Tumanov et al, Appl. Phys. Lett. 112, 123102 (2018).

Dynamics of highly excited electrons in 3D and quasi-2D semiconductors: theory and experiments.

J. Sjakste^{a*}

a. Ecole Polytechnique, Laboratoire des Solides Irradies, CNRS UMR 7642, CEA-DSM-IRAMIS, Université Paris-Saclay, F91128 Palaiseau cedex, France,

* jelena.sjakste@polytechnique.edu

Understanding hot carrier dynamics is crucial for the development of photovoltaic and optoelectronic devices. Electron scattering by phonons is one of the major processes that determine the relaxation dynamics of hot carriers. Recently, we have developed a computational method, based on density functional theory and on interpolation of the electron-phonon matrix elements in Wannier space, for the calculation of the electron-phonon coupling in polar materials [1]. This method allowed us to successfully interpret the dynamics of hot electron relaxation in bulk GaAs, in excellent agreement with time- and angle- resolved photoemission experiment by the group of K. Tanimura (University of Osaka, Japan). We have demonstrated, for the relaxation of hot carriers in GaAs, the existence of two distinct relaxation regimes, one related with the momentum, and the other with energy relaxation [2]. Interestingly, the energy relaxation times become faster at lower energies [3].

Furthermore, we will present our new results on hot electron relaxation dynamics in InSe, a layered semiconductor material that presents high potential for optoelectronic devices. We compare *ab initio* results to recent time-resolved ARPES experiments performed in our laboratory by the group of L. Perfetti [4]. We argue that highly mobile electrons accumulating in valleys 0.7 eV above the conduction band minimum could be easily extracted from a multilayer flake of InSe. The hot carriers pave a viable route to the realization of below-bandgap photodiodes and Gunn oscillators. These technologies are well established in III-V semiconductors and may find a natural implementation in layered chalcogenides.

[1] J. Sjakste, N. Vast, M. Calandra, and F. Mauri, Phys. Rev. B 92, 054307 (2015)

[2] H. Tanimura, J. Kanasaki, K. Tanimura, J. Sjakste, N. Vast, M. Calandra, F. Mauri, Phys. Rev. B 93, 161203(R) (2016)

[3] J. Sjakste, N. Vast, G. Barbarino, M. Calandra, F. Mauri, J. Kanasaki, H. Tanimura, K. Tanimura Phys. Rev. B 97, 064302 (2018).

[4] Z. Chen, C. Giorgetti, J. Sjakste, R. Cabouat, V. Veniard, Z. Zhang, A. Taleb-Ibrahimi, E. Papalazarou, M. Marsi, A. Shukla, J. Peretti, and Luca Perfetti, *Ultrafast electrons dynamics reveal the high potentials of InSe for hot carriers optoelectronics*, submitted, 2018.

Hydrodynamic heat transport regime in bismuth: a theoretical viewpoint

Nathalie Vast^{a*}, Maxime Markov^a, Jelena Sjakste^a, Giuliana Barbarino^a, Giorgia Fugallo^b, Lorenzo Paulatto^c, Michele Lazzeri^c, Francesco Mauri^d

- École Polytechnique, Laboratoire des Solides Irradiés, CNRS UMR 7642, CEA-DSM-IRAMIS, Université Paris-Saclay, F91128 Palaiseau cédex.
- CNRS, LTN UMR 6607, PolytechNantes, Université de Nantes, F44306 Nantes cédex
- Sorbonne Universités, UPMC Université Paris 06, CNRS UMR 7590, MNHN, IRD UMR 206, Institut de Minéralogie, de Physique des Matériaux et de Cosmochimie, 75005 Paris
- Dipartimento di Fisica, Università di Roma La Sapienza, I-00185 Roma, Italy

* nathalie.vast@polytechnique.edu

Currently, a lot of attention is devoted to the study of phonon-based heat transport regimes in nanostructures. Of particular interest is the hydrodynamic regime, in which a number of fascinating phenomena such as Poiseuille's phonon flow and second sound occur, and where temperature fluctuations are predicted to propagate as a true temperature wave of the form $e^{i(k \cdot r - \omega t)}$. Together with solid helium and NaF, bismuth is one of the rare materials in which second sound has been experimentally observed, and regimes of heat transport vary with the increase of the (yet cryogenic) temperature: from heat transport via ballistic phonons, to the regime of Poiseuille's flow with second sound, to the diffusive (Fourier) propagation [1].

In this work [2,3], a major advance consists of accounting for the phonon repopulation by the normal phonon-phonon processes in the framework of the exact variational solution of the Boltzmann transport equation, coupled to the ab initio description of anharmonicity: three-phonon collisions turn out to be particularly strong at low temperatures and lead to the creation of new phonons in the direction of the heat flow (normal processes), which enhance the heat transport. This induces time and length scales over which heat carriers behave collectively and form a hydrodynamic flow that cannot be described by independent phonons with their own energy and lifetime.

Our exact calculations predict the occurrence of this Poiseuille phonon flow between ≈ 1.5 and ≈ 3.5 K, in a sample size of 3.86 and 9.06 mm, consistent with the experimental observations. Hydrodynamic heat flow characteristics are given for any temperature: heat wave propagation length, drift velocity, and Knudsen number. We finally discuss a Gedanken experiment allowing us to assess the presence of a hydrodynamic regime in any isotopically pure bulk material.

Support from the DGA, the Chaire Énergie of the École Polytechnique, the program NEEDS Matériaux, and from ANR-10-LABX-0039-PALM (Project Femtonic) is gratefully acknowledged. Computer time was granted by École Polytechnique through the LLR-LSI Project and by GENCI.

[1] V. Narayanamurti and R. Dynes. Observation of Second Sound in Bismuth, *Phys. Rev. Lett.* **28**, 1461 (1972).

[2] M. Markov, J. Sjakste, G. Barbarino, G. Fugallo, L. Paulatto, M. Lazzeri, F. Mauri, and N. Vast. Same title as above, *Phys. Rev. Lett.*, **120**, 075901 (2018).

[3] M. Markov, J. Sjakste, G. Fugallo, L. Paulatto, M. Lazzeri, F. Mauri and N. Vast. Nanoscale mechanisms for the reduction of heat transport in bismuth, *Phys. Rev. B* **93**, 064301 (2016).

Interphase and domain wall motion in Ferroelectric Films as probed by in-situ X-ray Diffraction during Electrical Biasing

N. Vaxelaire^{a*}, B. Allouche^a,

a. Univ. Grenoble Alpes, CEA, LETI, DTSI, SCMC, F-38000 Grenoble.

*nicolas.vaxelaire@cea.fr

Piezoelectric and ferroelectric thin films are ubiquitous in many applications such as sensors, actuators, pyroelectric devices or advanced memories. The case of polycrystalline thin films is particularly complex and delicate to model. Several effects (i.e. interface, substrate clamping, grain boundary, stress) affect the behavior of the domains at the local scale and by consequence impose the film macroscopic response.

It will be shown in this communication how in-situ X-ray diffraction during electrical biasing (DC or AC mode) offers unique information to address these complex behaviors at different scales. The case of the prototypal Pb (Zr₄₈, Ti₅₂) O₃ or PZT films will be discussed. These films at the morphotropic phase boundary (MPB) are composed of two textured ferroelectric phases (one tetragonal and the other rhombohedral). It has been observed that interphase boundary motion is the predominant effect during the biasing. A strong heterogeneity from grain to grain and as a function of the depth in the film has also been observed [1].

Our results are based a combination of synchrotron beamtimes as well as results from our in-situ lab source based setup [2]. Finally, the ability to image ferroelastic domains by coherent diffraction techniques (or CBDI) will be discussed.

[1] Vaxelaire et al *Jour. of Appl. Phys.* **120**, 104101(2016)

[2] Allouche *in preparation*

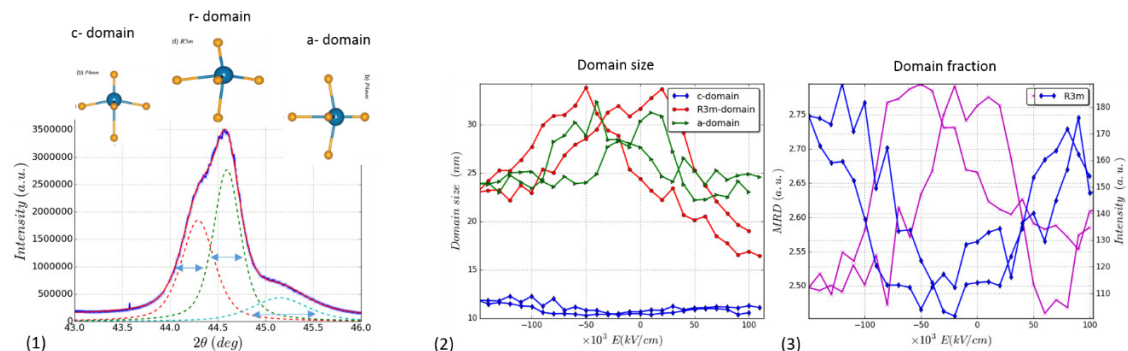


Figure 1: A diffraction peak (1) is recorded for each bias where the contribution of three domain variants is quantified. The FWHM (related in first approximation to the domain size) (2) and the intensity of the 3 variants (3) (related to domain fraction) present a typical butterfly shape as a function of the electrical field.

Quantum computing with silicon and germanium

M. Veldhorst

QuTech and Kavli Institute of Nanoscience, TU Delft

m.veldhorst@tudelft.nl

Semiconductor quantum dots constitute a promising platform for quantum computation. Two decades after the seminal proposals by Loss and DiVincenzo, impressive results have been obtained, including the initialization, readout, and coherent control of single electron spins. Silicon has become the leading material as it can be isotopically purified, thereby removing a nuclear spin bath, such that qubits can be defined with extremely long coherence times.

I will present our latest efforts on silicon quantum computing. These include operation at elevated temperatures for hot-qubit operation, enabling to integrate classical electronics on the same chip for scalability and superior control. Moving forward, I will discuss our vision to increase the number of qubits toward that is needed for practical quantum information.

I will also present our parallel efforts on germanium. Starting from high-mobility quantum wells, we fabricate quantum dot and induce superconductivity for the creation of novel quantum devices. We find remarkably low charge noise, while we observe ballistic gate-tunable supercurrents that extend over micrometers.

[1] L. Petit, J.M. Boter, H.G.J. Eenink, G. Droulers, M.L.V. Tagliaferri, R. Li, D.P. Franke, K.J. Singh, J.S. Clarke, R.N. Schouten, V.V. Dobrovitski, L.M.K. Vandersypen, M. Veldhorst, Spin lifetime and charge noise in hot silicon quantum dots, arXiv:1803.01774

[2] R. Li, L. Petit, D.P. Franke, J.P. Dehollain, J. Helsen, M. Steudtner, N.K. Thomas, Z.R. Yoscovits, K.J. Singh, S. Wehner, L.M.K. Vandersypen, J.S. Clarke, M. Veldhorst, arXiv:1711.03807

[3] J. Helsen, M. Steudtner, M. Veldhorst, S. Wehner, Quantum error correction in crossbar architectures, Quantum Science and Technology 2018.

[4] M.L.V. Tagliaferri, P.L. Bavdaz, W. Huang, A.S. Dzurak, D. Culcer, M. Veldhorst, Impact of valley phase and splitting on readout of silicon spin qubits, arXiv:1803.01811

[5] N.W. Hendrickx, D.P. Franke, A. Sammak, M. Kouwenhoven, D. Sabbagh, L. Yeoh, R. Li, M.L.V. Tagliaferri, M. Virgilio, G. Capellini, G. Scappucci, M. Veldhorst, Gate-controlled quantum dots and superconductivity in planar germanium, arXiv:1801.08869

Investigation of optical properties of non-metallic materials under high electric DC field using ultrafast laser assisted Atom Probe Tomography

A. Vella^{1*}, L. Venturi¹, E.P. Silaeva¹, L. Arnoldi¹, J. Houard¹, B. Deconihout¹, L. Rigutti¹, A. Obraztsov^{2,3}

¹ GPM UMR 6634, Université de Rouen, Avenue de l'Université, 76801, BP12, 76801 Saint Etienne du Rouvray

² Department of Physics, M. V. Lomonosov Moscow State University, Moscow 119991, Russia

³ Department of Physics and Mathematics, University of Eastern Finland, Joensuu 80101, Finland

*angela.vella@univ-rouen.fr

In laser assisted Atom Probe Tomography (APT) atoms from a nanometric needle-shape sample are removed one by one in a well-controlled way, thanks to the combined action of a high electric field and a laser pulse [1].

In the case of non-metallic samples, the high DC electric field was predicted to penetrate into the sample inducing clusters evaporation and reducing the control of the evaporation process. These predictions are invalidated by the experimental results and the recent nice APT images obtained on non-metallic samples [2].

Here we report on the process of the DC field screening at the tip surface. Experimental results using filed ion microscopy (FIM) as shown in Fig 1 (a) and theoretical results considering high filed charge activation processes, are presented and discussed [3].

Then we discuss the effect on the DC field on diamond needles containing color centers. The photoemission of these centers is studied using a micro-photoluminescence (- PL) system (Fig 1 b). The application of a high electrostatic field at the apex of monocrystalline diamond nanoscale needles induces an energy splitting of the photoluminescence lines of color centers [2]. The splitting of the zero-phonon PL line of the NV⁰ defect (Fig 1c) has been studied as a function of the voltage applied to the tip. We prove that the DC field induced a tensile stress up to 7 GPa and can be used to perform piezo-spectroscopy of nanoscale systems by electrostatic field regulation.

[1] Gault, B. *et al.* Design of a femtosecond laser assisted tomographic atom probe. *Rev. Sci. Instrum.* **77**, 43705 (2006).

[2] Kelly, T. F. & Larson, D. J. Atom Probe Tomography 2012. *Annu. Rev. Mater. Res.* **42**, 1–31 (2012).

[3] Silaeva, E. P. *et al.* Do dielectric nanostructures turn metallic in high electric dc fields? *Nano Letters* **14** (11), 6066-6072 (2014)

[4] L. Rigutti, *et al.*, Optical Contactless Measurement of Electric Field-Induced Tensile Stress in Diamond Nanoscale Needles. *Nano Lett.*, **17** (12), 7401-7409, 2017.

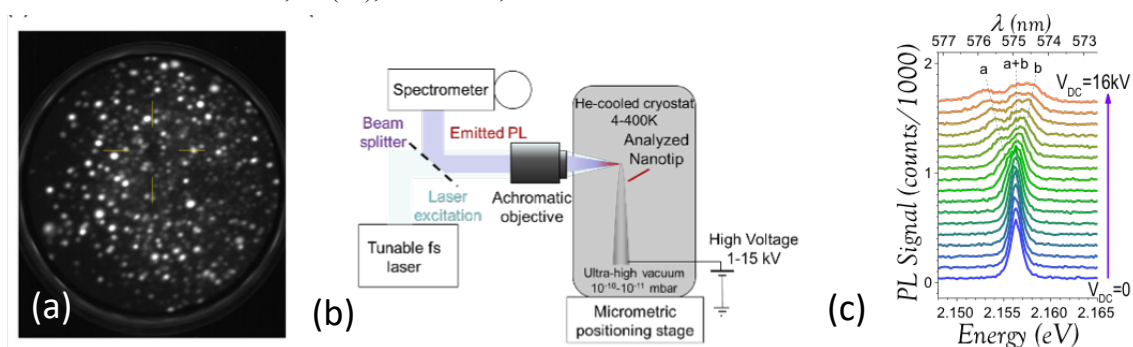


Figure 1. (a) FIM image of Diamond samples, at 50 K with 10–5 mbar of Ne as imaging gas. (b) μ -photoluminescence system. (c) Optical study of the NV⁰ ZPL as function of the applied bias.

Effects of confinement and symmetries on the electrical manipulation of semiconductor spin qubits

B. Venitucci^{a*}, L. Bourdet^a, D. Pouzada^a and Y.M. Niquet^a

a. University Grenoble Alpes, CEA, INAC-MEM, L_Sim, 38000 Grenoble, France

* benjamin.venitucci@cea.fr

The electrical manipulation of spins based on intrinsic spin-orbit coupling (SOC) allows for compact and scalable, micromagnet-free designs of semiconductor qubits. In this talk, we discuss some aspects of the physics of SOC in semiconductor qubits, using a versatile formulation of electrically-driven spin manipulation based on a generalized g -matrix [1].

We illustrate our discussion with a hole spin qubit on silicon-on-insulator (SOI). Fig. 1(a) shows a model for such a qubit device. The hole is localized under a front gate on top of a silicon nano-wire, and is manipulated by a radio-frequency (RF) modulation on that gate resonant with the Zeeman splitting between the “up” and “down” spin states. The shape of the hole wave function can further be manipulated with a substrate back gate. The Rabi frequency (number of spin rotations per second) computed in this device is plotted on Fig. 1(b) as a function of the back gate voltage [2]. It shows two prominent peaks separated by a dip. We show how these trends result from strong confinement and from the bias-dependent symmetries of the hole wave functions. We discuss the implications of these results for the design of both electron and hole semiconductor qubits, and highlight the options to enhance the Rabi frequency and/or reduce the sensitivity of the qubits to charge noise.

[1] A. Crippa *et al.*, Electrical Spin Driving by g -Matrix Modulation in Spin-Orbit Qubits, Phys. Rev. Lett. **120**, 137702 (2018).

[2] Simulation are performed using the tight-binding and $\mathbf{k} \cdot \mathbf{p}$ methods.

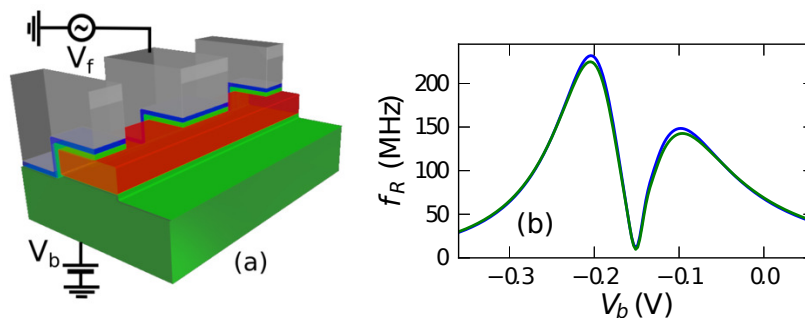


Figure 1: (a) 3D representation of qubit device on SOI (V_f : front gate voltage, V_b : back gate voltage, Red: silicon nanowire, Green: SiO₂, Blue: HfO₂, Gray: metallic gate). (b) Calculated Rabi frequency versus back gate voltage V_b at $V_f = -0.1$ V [$\mathbf{k} \cdot \mathbf{p}$ calculation to all orders in the magnetic field (green), or to first-order within the g -matrix formalism (blue)]. The RF amplitude on the front gate is 1 mV and the magnetic field is 1 T.

Quantum transport in MoS₂ mono and multilayer

Venkateswarlu Somepalli^{a*}, Javad Vahedi^a, Andreas Honecker^a, Didier Mayou^{b,c}, et
Guy Trambly de Laissardière^a

- a. Laboratoire de Physique théorique et Modélisation, Université de Cergy-Pontoise and CNRS (UMR 8089), 95302 Cergy-Pontoise, France
- b. Université Grenoble Alpes, Inst NEEL, F-38042 Grenoble, France
- c. CNRS, Inst NEEL, F-38042 Grenoble, France

* somepalli.venkateswarlu@u-cergy.fr

In spite of many recent studies of electronic structure in TMD and similar transition metal dichalcogenides, there are very few works on quantum transport in these new 2D materials. To study quantum transport, taking into account realistic scattering effects, we have developed a tight-binding model for MoS₂ mono and multilayer in agreement with previous studies [1]. Calculated tight-binding bands are close to usual DFT calculations [2] for states around the gap, in particular to our calculations performed using ABINIT software [3]. Tight-binding model allows to compute quantum diffusion in the framework of the Kubo-Greenwood formula by using a polynomial expansion in real space ([4] and Refs. therein). Calculations are performed on samples containing up to a few 10⁶ atoms, which corresponds to typical sizes of about one micrometer square and allows to study systems with elastic mean free length of the order of few hundred nanometers. Elastic scattering events due to static defects (vacancies, substitution of atoms) [5] are taken into account in the Hamiltonian, and the effects of inelastic scattering by phonons at finite temperature are treated through a Relaxation Time Approximation. This approach allows to calculate microscopic conductivity and mobility of charge carriers around the gap. We also address quantum corrections that may occur at low temperature.

- [1] E. Ridolfi, D. Le, T. S. Rahman, E. R. Mucciolo and C. H. Lewenkopf, A tight-binding model for MoS₂ monolayers, *J. Phys.: Condens. Matter* **27**, 365501 (2015)
- [2] J. K. Ellis, M. J. Lucero, G. E. Scuseria, The indirect to direct band gap transition in multilayered MoS₂ as predicted by screened hybrid density functional theory, *Appl. Phys. Lett.* **99**, 261908 (2011); E. S. Kadantsev, P. Hawrylak, Electronic structure of a single MoS₂ monolayer, *Solid State Comm.* **152**, 909 (2012)
- [3] X. Gonze et al., First-principles computation of material properties: the ABINIT software project, *Comp. Mat. Sci.* **25**, 478 (2002). <https://www.abinit.org>
- [4] G. Trambly de Laissardière and D. Mayou, Conductivity of Graphene with Resonant and Nonresonant Adsorbates, *Phys. Rev. Lett.* **111**, 146601 (2013)
- [5] S. Dubey et al., Weakly Trapped, Charged, and Free Excitons in Single-Layer MoS₂ in the Presence of Defects, Strain, and Charged Impurities, *ACS Nano* **11**, 11206 (2017)

Out-of-equilibrium quantum magnetism and thermalization in a spin-3 dipolar lattice system

L. Vernac^{a,b,*}, S. Lepoutre^{a,b}, J. Schachenmayer^c, L. Gabardos^{a,b}, B. Zhu^d, B. Naylor^{a,b}, E. Maréchal^{a,b}, O. Gorceix^{a,b}, A. M. Rey^d, B. Laburthe-Tolra^{a,b}

- a. Université Paris 13, Sorbonne Paris Cité, Laboratoire de Physique des Lasers, F-93430, Villetaneuse, France
- b. CNRS, UMR 7538, LPL, F-93430, Villetaneuse, France
- c. CNRS, UMR 7504, IPCMS; UMR 7006, ISIS; and Université de Strasbourg, Strasbourg, France
- d. JILA, NIST and Department of Physics, University of Colorado, Boulder, USA

* laurent.vernac@univ-paris13.fr << corresponding author >>

Understanding quantum thermalization through entanglement build-up in isolated many-body systems addresses fundamental questions on how unitary dynamics connects to statistical physics. These studies also constitute a novel way to investigate strongly correlated quantum systems. A promising pathway is being opened by ultracold atomic systems featuring internal levels that can be initialized in pure states and coherently evolved with controllable long-range interactions. Experiments have been limited so far to small systems (hundreds or fewer particles), or to dilute disordered molecular ensembles. In contrast, magnetic atoms offer a unique possibility to investigate truly macroscopic and well-ordered arrays of spins [1].

We report experimental study of the dynamics and approach towards thermal equilibrium of a pure macroscopic ensemble of spins initially tilted compared to the magnetic field, under the effect of dipole-dipole interactions [2]. The experiment uses a unit filled array of $\approx 10^4$ chromium atoms in a three dimensional optical lattice, realizing the spin-3 XXZ Heisenberg model. We monitor the population of the seven spin components after a collective rotation of an initially polarized ensemble, as a function of the angle between the initial coherent state with respect to the magnetic field. We find that the approach to thermal equilibrium is increasingly driven by quantum correlations as the angle approaches $\pi/2$. The quantum dynamics is benchmarked by comparison with an improved numerical quantum phase-space method [3] which also enables us to compute the dynamics of the Renyi entanglement entropy. Although the measurements only allow us to reconstruct the entropy generated by the diagonal components of the average local density matrix, the excellent agreement with simulations supports entanglement build-up and the corresponding approach to local thermal equilibrium, and provides a first benchmark of our experiment as a quantum simulator.

- [1] A. de Paz, et al, Probing spin dynamics from the Mott insulating to the superfluid regime in a dipolar lattice gas, *Phys. Rev. A* **93**, 021603(R) (2016)
- [2] S. Lepoutre et al, arXiv:1803.02628 (2018)
- [3] J. Schachenmayer, A. Pikovski, and A. M. Rey., Many-Body Quantum Spin Dynamics with Monte Carlo Trajectories on a Discrete Phase Space, *Phys. Rev. X* **5**, 011022 (2015)

Gate-defined quantum point contact in high mobility graphene

Louis Veyrat^{a*}, Katrin Zimmermann,^a Anna Jordan,^a Frederic Gay,^a Kenji Watanabe,^b Takashi Taniguchi,^b Zheng Han,^a Vincent Bouchiat,^a Hermann Sellier,^a Benjamin Sacépé,^a

a. Univ. Grenoble Alpes, CNRS, Institut Néel, F-38000 Grenoble, France

b. National Institute for Materials Science, 1-1 Namiki, Tsukuba 306-0044, Japan

* louis.veyrat@neel.cnrs.fr

Since its discovery a decade ago, graphene has opened the field of 2D materials and is still of great importance for fundamental and applied physics. In particular, its gapless linear energy dispersion gives access to the new physics of Dirac fermions. However, the absence of gap is also detrimental to the engineering of advanced nanostructures. Indeed, nano-patterning in most two dimensional electron gases relies on electrostatic gating to tailor the electron gas, or the guiding of edge channels in the quantum Hall regime, by depleting the electron gas underneath them. In graphene, electrostatic gating only creates p-n junctions, that are highly transparent due to Klein tunneling. This impairs the development of devices, and especially of quantum point contacts, which are an important tool for many quantum transport studies (quantum Hall interferometry, shot noise experiment, etc...). Even in the quantum Hall regime, the fact that the $N=0$ Landau level is shared between electrons and holes prevents from getting quantized transport through a constriction. This limitation can however be overcome, by using high mobility heterostructures, where all degeneracies can be lifted with holes and electrons edge channels physically separated.

Here we present the magnetic field dependence of a gate-defined constriction in high mobility graphene heterostructures. At low magnetic field, transport is characterized by ballistic Fabry-Pérot resonances in the n-p-n cavity created by the top-gates and no quantization is observed. Specific graphene properties can be evidenced through the study of these oscillations, such as graphene Berry phase, evidenced by a typical phase shift. Upon increasing the magnetic field, Fabry-Pérot oscillations vanish and are replaced by Landau levels oscillations in the constricted region. In the quantum Hall regime, spin and valley degeneracies are lifted, and the transport happens through the constriction. In this regime, we demonstrate the gate-tunable selective transmission of integer and fractional quantum Hall edge channels through the quantum point contact, and the possibility to fully pinch-off the constriction [1]. This gate control of the edge channel transmission opens the door to quantum Hall interferometry and electron quantum optics experiments in graphene.

[1] Zimmermann et al., Nature Communications 8, 14983 (2017)

Ultrafast Thermo-Optical Dynamics of Plasmonic Nanoparticles

VIALLA Fabien^a, MAIOLI Paolo^a, CRUT Aurélien^a, GANDOLFI Marco^b,
MEDEGHINI Fabio^a, BANFI Francesco^b, VALLÉE Fabrice^a
and DEL FATTI Natalia^a

- a. iLM – Institut Lumière Matière, UMR5306 CNRS, Université Claude Bernard Lyon 1, Bâtiment Kastler 10 rue Ada Byron, 69622 Villeurbanne CEDEX, France
b. I-LAMP - Interdisciplinary Laboratories for Advanced Materials Physics, Università Cattolica del Sacro Cuore, Brescia I-25121, Italy

* fabien.vialla@univ-lyon1.fr

Femtosecond time-resolved optical spectroscopy is emerging as a precious tool for investigating the ultrafast thermal dynamics of nanostructures [1]. In this context, connecting the ultrafast optical response after pulsed excitation to the correct thermal energy flow is of key importance for quantitative extraction of thermal parameters – such as the interfacial resistance and the local environment thermal conductivity – from experiments.

We present here full thermo-optical models relating transient spectroscopy measurements, performed on metal nanoparticles in dielectric media, to the thermal dynamics of both the nanoparticle and its local environment [2]. When put in relation with experimental results [3, 4], this understanding allows to selectively probe the environment thermal dynamics using specific wavelengths (see Figure), and extract the interfacial thermal resistance. We further extend the analytical case of small nanospheres embedded in a homogeneous matrix to arbitrarily complex geometries, sizes and inhomogeneous environments using a finite element approach.

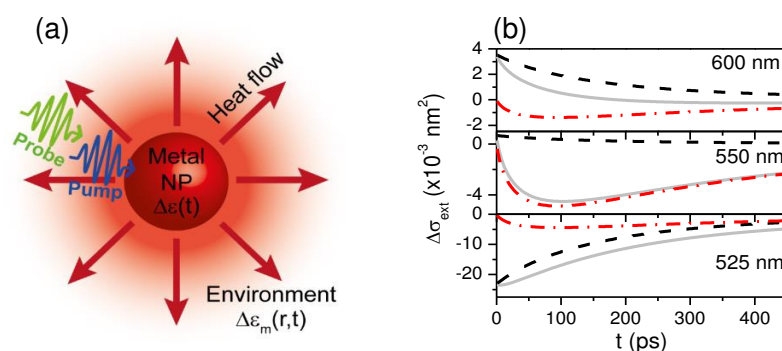


Figure: Computed thermo-optical dynamics of gold nanospheres (10 nm in diameter) immersed in ethanol. (a) Schematic representation. (b) Ultrafast cross-section transients $\Delta\sigma_{\text{ext}}(\lambda_{\text{pr}}, t)$, as function of probe wavelength and pump-probe delay. The complete signal (grey solid lines) is directly given by the sum of the particle (black dashed lines) and the environment (red dash-dotted) contributions.

- [1] Cahill, D. G., Braun, P. V., Chen, G., Clarke, D. R., Fan, S., Goodson, K. E., Keblinski, P., King, W. P., Mahan, G. D., Majumdar, A., et al. *Appl. Phys. Rev.*, 1, p. 11305 (2014).
[2] Gandolfi, M., Crut, A., Medeghini, F., Stoll, T., Maioli, P., Vallée, F., Banfi, F., Del Fatti, N., submitted (2018).
[3] Juvé, V., Scardamaglia, M., Maioli, P., Crut, A., Merabia, S., Joly, L., Del Fatti, N., Vallée, F., *Phys. Rev. B*, 80, p. 195406 (2009).
[4] Stoll, T., Maioli, P., Crut, A., Rodal-Cedeira, S., Pastoriza-Santos, I., Vallée, F., Del Fatti, N., *J. Phys. Chem. C*, 119, p. 12757 (2015).

Engineering of excitonic complexes in van der Waals heterostructures

Fabien Violla^{a*}, M. Massicotte^b, P. Schmidt^b, and F.H.L. Koppens^b

- a. iLM – Institut Lumière Matière, UMR5306 CNRS, Université Claude Bernard Lyon 1, Bâtiment Kastler 10 rue Ada Byron, 69622 Villeurbanne CEDEX, France
- b. ICFO - Institut de Ciències Fòniques, The Barcelona Institute of Science and Technology, Castelldefels, Barcelona 08860, Spain

* fabien.violla@univ-lyon1.fr

Opto-electronic properties of transition metal dichalcogenides (TMDs) are largely governed by coulomb-mediated many body interactions stemming from quantum confinement and reduced screening. This results in the emergence, upon light excitation, of tightly bound electron-hole complexes stable even at room temperature. Furthermore, integration of TMDs in van der Waals heterostructures allows to engineer those quasiparticles. The recent maturity reached by the nanofabrication of these heterostructures now offers a unique platform to study original physics in low-dimensional systems.

In this talk, I will give an overview of our recent studies based on spectrally- and temporally-resolved measurements of the photoluminescence and photocurrent originating from TMDs integrated in several devices with different designs. The fine tuning of the electrostatics achieved using local gates leads to the characterization and manipulation of the excitonic complexes generated in mono- [1], multi- [2] and heterolayers [3] of TMDs. By contacting the TMDs with graphene layers, we can probe the complexes dissociation dynamics and follow the subsequent intra- [1] or interlayer [2,4] transport of the free charges. Overall we extract important insights on the photophysics of these low-dimensional systems and identify guidelines for future fundamental and technological opto-electronic applications based on TMD.

- [1] M. Massicotte, F. Violla *et al.*, Dissociation of 2D excitons in monolayer WSe₂, *Nature Communications* 9, 1633 (2018)
- [2] M. Massicotte, P. Schmidt, F. Violla *et al.*, Picosecond photoresponse in van der Waals heterostructures, *Nature Nanotechnology* 11, 42-46 (2016)
- [3] F. Violla *et al.*, submitted
- [4] M. Massicotte, P. Schmidt, F. Violla *et al.*, Photo-thermionic effect in vertical graphene heterostructure, *Nature Communications* 7, 12174 (2016)

Introduction to ferroics and current trends

Nathalie Viart^{a*}

- a. Institut de Physique et Chimie des Matériaux de Strasbourg (IPCMS), UMR 7504 CNRS, Université de Strasbourg, 23 rue du Lœss BP 43, 67034 Strasbourg, France

* viart@unistra.fr

The term « ferroic » was introduced by Aizu approximately 50 years ago with the emerging conscience of a possibility to unify the vision of ferromagnetic, ferroelectric and ferroelastic materials. It describes materials which are characterized by the existence of an order parameter and show switchable properties under an external stimulus.

During the last decade, ferroics, and in particular those presenting multiple orders, i.e. multiferroics, have been the focus of an intense interest. This is due to the fact that they provide new opportunities to tackle crucial societal issues such as low energy data manipulation and storage.

A topical issue addresses the conditions for the existence of order, which intrinsically rely on symmetry considerations. The possibility to find new ferroic materials has been recently significantly revisited, and interesting paths have arisen, in particular *via* interface engineering.

The characterization of ferroics, and especially the elucidation of their domain structure, has also received special attention, and considerable experimental efforts have been developed to achieve characterization at different scales in complex structures.

This general introduction to the thrilling world of ferroics will therefore aim at giving a state of the art panorama addressing the present quest for new ferroics, the advanced characterization methods and the clever use of their properties for cutting-edge devices. Most of the examples will be given among oxide ferroics presenting magnetic and/or electric ordering.

Transport investigation of two-dimensional materials for topological superconductivity

Florian Vigneau^{a*}, Raisei Mizokuchi^a, Ludovic Desplanque^b, Dante Colao Zanuz^a, Romain Maurand^a, François Lefloch^a, Maurand^a Maksym Myronov^c, Xavier Wallart^b, Giordano Scappucci^d, Silvano De Franceschi^a

- a. CEA, INAC-PHELIQS, 17 Rue des Martyrs, F-38000 Grenoble, France
- b. Université Lille, CNRS, Centrale Lille, ISEN, Univ. Valenciennes, UMR 8520 - IEMN, Lille, F-59000, France
- c. Department of Physics, The University of Warwick, Coventry CV4 7AL, United Kingdom
- d. QuTech and Kavli Institute of Nanoscience, Delft University of Technology Lorentzweg 1, 2628 CJ Delft, Netherlands

* Florian.VIGNEAU@cea.fr

We develop in the following experimental investigations of two material candidates to achieve topological superconductivity: SiGe heterostructures and InAs/GaSb bilayers.

Ge one-dimensional nanowires with large spin-orbit could host robust helical states and form very good contacts with metals and superconductors. Starting from nominally undoped SiGe/Ge/SiGe quantum-well heterostructures grown by reduced pressure chemical vapor deposition, we fabricated quantum wires through a top-down approach. One-dimensional (1D) ballistic hole transport was clearly revealed by conductance quantization at 0.3 K [Fig. 1a] [1]. Next, we fabricated Ge 2DHG device with aluminum contacts to realize Josephson field effect transistors (JoFET) by proximity effect. Measurement at 16 mK revealed a gate tunable supercurrent for channel length up to 800nm [Fig. 1b].

It has been predicted that InAs GaSb heterojunctions can be turned into a topological regime showing the quantum spin Hall behavior due to unusual band alignment. However, despite that edge states transport has been probed experimentally, uncertainties remain about the topological nature of this material. We present here preliminary results on fabrication and transport measurement of InAs/GaSb bilayers. Our objective is to conclude about their topological nature by searching for edge states and channel length independent conductance quantization in a diversity of sample geometries.

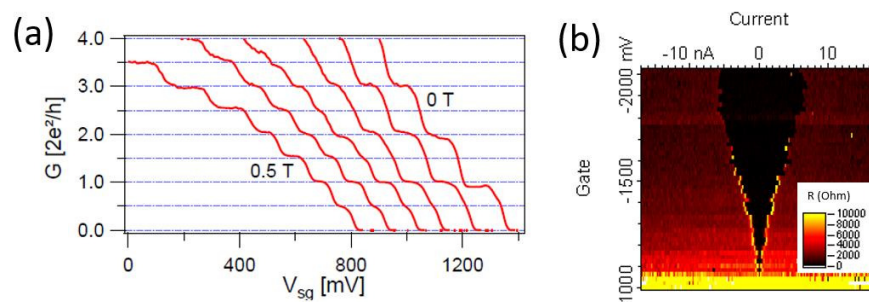


Figure 1: (a) Conductance measurement versus gate voltage of 1D ballistic Ge hole gas under out-of-plane magnetic field. (b) Resistance measurement of Ge JoFET versus current and gate voltage showing a superconducting transition.

[1] R. Mizokuchi et al., "Ballistic one-dimensional holes with strong g-factor anisotropy in germanium" arXiv:1804.04674.

Electrical and biocompatibility properties of different soft intra-cortical implant designs

Paul Villard^{a,b,*}, Fannie Darlot^{a,b}, Jean-marie Mayaudon^{a,b}, Cyril Zenga^{a,b}, Anne Quesnel-Hellmann^{a,b}, Lionel Rousseau^c, Blaise Yvert^{a,b}, Gaelle Piret^{a,b}

- a. Braintech Lab, INSERM U1205, 2280 rue de la piscine, 38400 Saint Martin d'Hères, France
- b. Université Grenoble Alpes, Grenoble, France
- c. ESYCOM, ESIEE-Paris, Cité Descartes, 2 Boulevard Blaise Pascal, 93160 Noisy-le-Grand

* paul.villard@inerm.fr

Neuroengineering more efficient neural interfaces is crucial to develop better clinical rehabilitation solutions and for neural network exploration. Most of current intra-cortical implants are stiff and generate mechanical strain that results in complex cellular responses and instabilities in neural signal recording. Designing soft intra-cortical neural implant with a high density microelectrode array has therefore become essential to faithfully record several neural units overtime and to facilitate for instance, brain computer interface performances and the study of memory and plasticity. We developed a soft SU-8 polymer neural implant with 64 nanostructured gold or platinum 20 μ m electrodes and vary the design of the 2mm deep intra-cortical part of the implant. Leads were either 50 μ m, 20 μ m or 11 μ m wide with a straight or a wavy shape. We then evaluated the impact of different designs on electrical properties of the implant. In vivo biocompatibility tests in rodents were performed and astrocytes, microglia and cell density were analyzed around the different implant lead types.

Artificial trees to investigate nanoscale capillary effects

Olivier Vincent^{a*} & Abraham Stroock^b

- a. Institut Lumière Matière, UMR 5306 CNRS & Université Lyon 1, 10 rue Ada Byron, 69622 Villeurbanne, France
 - b. Cornell University, Robert Frederick Smith School of Chemical and Biomolecular Engineering, 120 Olin Hall, Ithaca, NY 14853, USA
- * olivier.vincent@univ-lyon1.fr

Trees evolved efficient ways to transport water (sap) from their roots to their leaves, based on passive transpiration at the leaf level. The driving force for the flow is the capillary (negative) pressure associated with confined, curved liquid-vapor interfaces and can reach massive magnitudes due to the nanoscale character of the confinement.

Inspired by plants, we developed silicon-based microplatforms able to generate tunable capillary pressures down to approximately -100MPa, which we used to study a variety of nanoscale capillary phenomena, including cavitation [1], drying-induced flows [2], capillary condensation and spontaneous imbibition flows [3].

In this presentation, I will show that the analysis of these dynamic responses to large capillary stresses allows to get precise measurements of the behavior of highly confined liquids and can be used both as tool for the study of nanoscale fluid physics and as a method to handle liquids in a controlled way for lab-on-chip applications. I will also discuss flow enhancement possibilities based on ideas from the vascular anatomy of plants.

[1] O. Vincent, D.A. Sessoms, E.J. Huber, J. Guioth, A.D. Stroock, Drying by cavitation and poroelastic relaxations in porous media with macroscopic pores connected by nanoscale throats, *Physical Review Letters* **113**, 134501 (2014)

[2] O. Vincent, A. Szenicer and A.D. Stroock, Capillarity-driven flows at the continuum limit, *Soft Matter* **12**, 6656-6661 (2016)

[3] O. Vincent, B. Marguet and A.D. Stroock, Imbibition triggered by capillary condensation in nanopores, *Langmuir* **33**, 7, 1655-1661 (2017)

NMR study of CDW order in $\text{YBa}_2\text{Cu}_3\text{O}_y$ under hydrostatic pressure

Igor Vinograd^{a,*}, Rui Zhou^a, Hadrien Mayaffre^a, Steffen Krämer^a, Ruixing Liang^{b,c},
Walter N. Hardy^{b,c}, Douglas A. Bonn^{b,c} and Marc-Henri Julien^a

a. LNCMI Grenoble, France

b. UBC, Vancouver, Canada

c. CIFAR, Toronto, Canada

* igor.vinograd@lncmi.cnrs.fr

We address the question whether the enhancement of the superconducting T_c in $\text{YBa}_2\text{Cu}_3\text{O}_y$ with the application of hydrostatic pressure is due to the suppression of a competing charge-density-wave ordered (CDW) phase as proposed by Cyr-Choinière et al. [1]. Using a BeCu clamp cell and Daphne oil as the pressure medium we apply 1.9 GPa (19 kbar) to a very clean $\text{YBa}_2\text{Cu}_3\text{O}_y$ single crystal with an oxygen concentration $y = 6.56$ ($p = 0.109$) and increase its T_c from 60.5 K at 0 GPa to 66.5 K.

We have performed ^{17}O -NMR measurements under hydrostatic pressure and studied its effect on the 2D short-ranged CDW as well as the 3D long-ranged CDW in high magnetic fields. Since hydrostatic pressure enhances T_c and the critical field H_{c2} the main effect is a higher onset field towards the long-range CDW order which emerges when CDW patches inside and around vortex cores start to overlap [2]. Neither CDW phase appears to be strongly affected by the applied pressure. This is confirmed by the fact that a negative sign of the Hall effect in $\text{YBa}_2\text{Cu}_3\text{O}_y$ ($p=0.11$) [3] as well as slow quantum oscillations in $\text{YBa}_2\text{Cu}_4\text{O}_8$ [4] persist under moderate pressures. On the other hand these results are in conflict with two recent X-ray diffraction studies that find a complete suppression of charge order at 10 to 15 kbar [5-6].

[1] O. Cyr-Choinière, D. LeBoeuf, S. Badoux, S. Dufour-Beauséjour, D. A. Bonn, W. N. Hardy, R. Liang, N. Doiron-Leyraud, L. Taillefer, Suppression of charge order by pressure in the cuprate superconductor $\text{YBa}_2\text{Cu}_3\text{O}_y$: Restoring the full superconducting dome, arXiv.1503.02033 (2015).

[2] T. Wu, H. Mayaffre, S. Krämer, M. Horvatić, C. Berthier, P. L. Kuhns, A. P. Reyes, R. Liang, W. N. Hardy, D. A. Bonn and M.-H. Julien, Emergence of charge order from the vortex state of a high-temperature superconductor, Nat.Comm. **4**, 2113 (2013)

[3] C. Putzke, J. Ayres, J. Buhot, S. Licciardello, N. E. Hussey, S. Friedemann and A. Carrington, Charge Order and Superconductivity in Underdoped $\text{YBa}_2\text{Cu}_3\text{O}_{7-\delta}$, Phys. Rev. Lett. **120**, 117002 (2018)

[4] C. Putzke, L. Malone, S. Badoux, B. Vignolle, D. Vignolles, W. Tabis, P. Walmsley, M. Bird, N. E. Hussey, C. Proust and A. Carrington, Inverse correlation between quasiparticle mass and T_c in a cuprate high- T_c superconductor, Science Adv. **2**, 3 (2016)

[5] S. Souliou, H. Gretarson, G. Garbarino, A. Bosak, J. Porras, T. Loew, B. Keimer and M. Le Tacon, Rapid suppression of the charge density wave in $\text{YBa}_2\text{Cu}_3\text{O}_{6.6}$ under hydrostatic pressure, Phys. Rev. B **97**, 020503 (2018)

[6] H. Huang, H. Jang, T. Nishizaki, Y. Lin, J. Wang, J. Ying, J. S. Smith, C. Kenney-Benson, G. Shen, W. Mao, C.-C. Kao, Y.-J. Liu and J.-S. Lee, Direct observation of a critical role of structural disorder in superconducting YBCO under high pressure, arXiv:1710.02769 (2018)

Twins Percolation for Qubit Losses in Topological Color Codes

D. Vodola,^a D. Amaro,^a M.A. Martin-Delgado,^b M. Müller,^a

^a*Department of Physics, Swansea University, Singleton Park, Swansea SA2 8PP, United Kingdom.*

^b*Departamento de Física Teórica I, Universidad Complutense, 28040 Madrid, Spain.*

Quantum information is the generalisation of the classical information theory to quantum systems. If for a classical computer the bits are the fundamental units, quantum computers are built on an analogous concept, the quantum bits currently implemented in different physical systems (atoms, ions, molecules) due to recent experimental advances in the control of cold and ultra-cold gases. However, these experimental setups are so delicate that qubits can be corrupted by environmental noise and even be completely lost from the apparatus resulting in the partial or total loss of the information there memorised. In this talk, we will consider how losses can affect a particular class of quantum code (the so-called color codes). We introduce a protocol for dealing with losses and we show that checking whether the logical information is still recoverable is equivalent to a generalized percolation process.

Photo-response mechanisms in ferroelectric Ba(Sn,Ti)O₃ solid solutions

H. Volkova^{a*}, P. Gemeiner^a, B. Wague^b, B. Vilquin^b, J. Guillot^c, D. Lenoble^c, F. Karolak^a, C. Bogicevic^a, N. Chauvin^b, R. Solanas^d, C. Frontera^d, I. Fina^d, F. Sanchez^d, B. Dkhil^a, I. C. Infante^b

- a. Laboratoire SPMS CNRS-UMR8580 CentraleSupélec, Université Paris-Saclay, Gif-sur-Yvette 91190, France
- b. Institut des Nanotechnologies de Lyon CNRS-UMR5270 ECL INSA UCBL CPE, Villeurbanne 69621, France
- c. Luxembourg Institute of Science and Technology, Materials Research and Technology Department, Belvaux 4422, Luxembourg
- d. Institut de Ciència de Materials de Barcelona (ICMAB-CSIC), Campus UAB, Bellaterra, 08193, Barcelona, Spain.

* halyna.volkova@centralesupelec.fr

In the framework of photoinduced (photovoltaic and photocatalytic) applications, ferroelectrics because of their internal electric dipole order are expected to favor charge separation. For solar cells, it could be possible to overcome the theoretical efficiency limit of p-n junction by using ferroelectrics, owing to their shift current flowing through them under illumination in short-circuit conditions, if optical and electronic properties are optimised [1]. Understanding how to improve these properties by chemical substitution is essential in view of new and more efficient devices exploiting light.

In this work, we focus on environmentally friendly BaTiO₃-based systems. In Ba(Sn_xTi_{1-x})O₃ solid solutions the electron mobility can be improved by Sn substitution, which would introduce Sn 5s 5p orbitals in the conduction band [2]. Our study of different Ba(Sn_xTi_{1-x})O₃ compositions in ceramic form showed the band gap increase by ~0.35 eV for intermediate compositions. The phase diagram of this system includes different polar arrangements, from ferroelectrics to relaxors. We used spectroscopic techniques (Raman and X-ray Photoelectron spectroscopy) to explain the band gap increase by local distortions structure due to disordered dipole state in relaxor phase. Such distortions can change the chemical bonding by narrowing the conduction band, and thus alternate the band gap and conductivity.

We further study the photo-response of Ba(Sn_xTi_{1-x})O₃ ceramics under lasers of different energy. From our measurements, it is possible to discriminate between pyro-current, transient component due to emptying of intrabandgap states, and steady intrinsic photocurrent. By fitting the photo-response of different compositions with this model, we make quantitative analysis of components, including the time-dependent recombination processes. Further, we study the charge trapping by distortion-related defects using ultraviolet-photoluminescence spectroscopy. We confront these two experiments and electric characterization with previous spectroscopic studies of local chemical environment. Our aim is to describe how the balance between different processes of photo-response is related to potential photovoltaic efficiency of Ba(Sn_xTi_{1-x})O₃.

[1] C. Paillard et al., Photovoltaics with ferroelectrics: Current status and beyond. *Adv. Mat.* 28(26), 5153-5168 (2016)

[2] B. G. Kim, J.Y. Jo, and S.W. Cheong, Hybrid functional calculation of electronic and phonon structure of BaSnO₃. *J. Solid State Chem.* 197, 134–138 (2013)

Etude de la densité électronique expérimentale de YTiO_3 dans ses différentes phases magnétiques

Ariste Bolivard Voufack^{a*}, Iurii Kibalin^a, Nicolas Claiser^a, Zeyin Yan^b, Saber Gueddida^a, Jean-Michel Gillet^b, Béatrice Gillon^c, Claude Lecomte^a, Florence Porcher^{a,c}, Yoshiharu Sakurai^e, Hiroshi Sakurai^d, Mohamed Souhassou^a

- a. CRM2, Institut Jean Barriol, Université de Lorraine et Centre National de la Recherche Scientifique, Vandœuvre-lès-Nancy, BP70239, 54506, France
- b. Laboratoire SPMS, UMR 8580, Centrale Supélec, 91190 Saint-Aubin, France
- c. Laboratoire Léon Brillouin, CEA, Centre National de la Recherche Scientifique, CE-Saclay, 91191 Gif-sur-Yvette, France
- d. Graduate School of Science and Technology, Gunma University, 1-5-1 Tenjin-cho, Kiryu, Gunma 376-8515, Japan
- e. Japan Synchrotron Radiation Research Institute, SPring-8, 1-1-1 Kouto, Sayo, Hyogo 679-5198, Japan

*ariste-bolivard.voufack@univ-lorraine.fr

La pérovskite du titane d'yttrium YTiO_3 est un isolant de Mott et présentant une transition de phase paramagnétique-ferromagnétique à 29 K [1]. Le magnétisme du matériau est lié à l'électron non apparié du titane ($3d^1$) ce dernier est en coordination octaédrique légèrement déformée, allongée le long de l'axe vertical (z). Dans le cadre du projet ANR MTMED nous nous sommes intéressés à l'étude de ce matériau magnétique, en combinant la diffraction des rayons X et des neutrons polarisés pour modéliser la densité électronique résolue en spin. La densité électronique a été déterminée dans les deux phases à l'aide d'un modèle développé au laboratoire [2, 3].

Les résultats de ces travaux montrent, que la densité électronique expérimentale n'est pas la même entre les deux phases étudiées. Quant à la densité de spin, les résultats de cette étude montrent que la densité de spin est localisé sur les orbitales d_{xz} et d_{yz} de l'atome de titane en bon accord avec les calculs de type DFT et la diffraction magnétique des rayons X [4].

- [1]. J. R. Hester, K. Tomimoto, H. Noma, F. P. Okamura and J. Akimitsu, Electron density in YTiO_3 , *Acta Cryst. B* 53, 739—744, (1997).
- [2]. M. Deutsch, B. Gillon, N. Claiser, J.-M. Gillet, C. Lecomte and M. Souhassou "First spin-resolved electron distributions in crystals from combined polarized neutron and X-ray diffraction experiments," *IUCrJ*, 194—199, (2014).
- [3]. M. Deutsch, N. Claiser, S. Pillet, Y. Chumakov, P. Becker, J.-M. Gillet, B. Gillon, C. Lecomte and M. Souhassou, experimental determination of spin-dependent electron density by joint refinement of X-ray and polarized neutron diffraction data," *Acta Cryst. A* 68, (2012).
- [4]. I. Kibalin, Z. Yan, A. B. Voufack, S. Gueddida, B. Gillon, A. Gukasov, F. Porcher, A. M. Bataille, F. Morini, N. Claiser, M. Souhassou, C. Lecomte, J.-M. Gillet, M. Ito, K. Sakurai, Y. Sakurai, C. M. Hoffmann and X. P. Wang, Spin density in YTiO_3 : Joint refinement of polarized diffraction and magnetic x-ray diffraction data leading to insights into orbital ordering, *Phys. Rev. B* 96, 054426, (2017).

Fine structure of phonon replicas and exciton-phonon interaction in the strong coupling regime in hexagonal boron nitride

T. Q. P. Vuong^{*}, G. Cassabois, P. Valvin, B. Gil

Coulomb, UMR 5221 CNRS-Université de Montpellier, 34095 Montpellier, France

Corresponding author : vuongquynhphuong90@gmail.com

Hexagonal boron nitride (h-BN) is a wide bandgap semiconductor promising for applications in deep UV that raises many interests of scientists in this material. The recently publication of Cassabois *et al.* [1] shows the experimental evidence by photoluminescence (PL) for the indirect bandgap of h-BN, with phonon replicas and an indirect exciton transition in PL spectrum that was confirmed by polarization-resolved PL [2]. In our work, we focus on understanding the intrinsic optical and electronic properties of h-BN in deep ultraviolet which are determined by the lattice vibrations. Firstly, we show that the fine structure of the emission spectrum in h-BN arises from the phonon replicas (at T point) associated with the overtones of the interlayer shear mode (at zone center). We present the excellent agreement of the theoretical fit with the emission spectrum above 5.7 eV (Fig.1), obtained under the convolution of a cumulative Gaussian broadening as a function of overtones index. The only varying parameter is the group velocity for each phonon branch, thus controlling the intrinsic properties of h-BN [3]. Secondly, we prove for the first time that h-BN provides a text-book example for the strong coupling regime of the exciton-phonon interaction due to: (i) The line-shape has a Gaussian profile in contrast to the weak coupling regime with Lorentzian lines and (ii) the linewidth increases as \sqrt{T} in contrast to the weak coupling regime with a linear increases with temperature following the theoretical predictions of Toyozawa [4].

[1] G. Cassabois et al, Nature Photonics, **10**, 262-266 (2016).

[2] Vuong et al, 2D Materials, **4**, 011004 (2017).

[3] Vuong et al, Physical Review B, **95**, 045207 (2017).

[4] Y. Toyozawa, Progr. Theor. Phys. 20, 53 (1958).

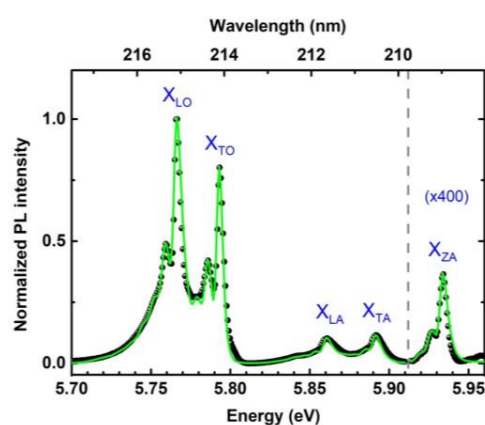


Figure 1 : Photoluminescence spectrum of h-BN at 8K includes experimental data (symbol) and theoretical fit (green line).

Dynamical Features of Escape Flows using Coulombs Friction Model

Julian Weninger^{a*}, T. Metivet^{b,a}, and P. Peyla^a

a. Univ. Grenoble Alpes, CNRS, LIPhy, 38000 Grenoble, France

b. Institut de Recherche Mathématique Avancées, 67000 Strasbourg, France

* Julian Weninger <<j.weninger@stud.uni-heidelberg.de>>

Evacuating crowded areas through bottlenecks can be a crucial issue during escape panics. The development of clogs at a constriction is a commonly observed phenomenon for dense and impatient crowds, but also in colloidal suspensions and granular materials [1]. As a result the flow is intermitted and the evacuation time increases drastically, which is known as the faster-is-slower effect [2].

Simulations usually base on individuals moving at a desired speed within the crowd and interacting with one another via normal compression, tangential friction and further social forces [2,3]. We propose to replace the tangential compression-spring model to simulate sliding friction [2] with the more physical Coulomb Model. The bodies are hence subject to a tangential friction force proportional to the exerted normal force and behave collectively once in a regime of static friction. This approach can help to understand the characteristics of clogging and allows to determine the importance of friction in such situations.

- [1] I. Zuriguel, D. R. Parisi, R. C. Hidalgo, C. Lozano, A. Janda, P. A. Gago, J. P. Peralta, et. al. Clogging transition of many-particle systems flowing through bottlenecks. *Scientific Reports*, 4, 1–8. (2014)
- [2] D. Helbing, I. Farkas, and T. Vicsek, Simulating dynamical features of escape panic. *Nature*, 407(6803), 487–490. (2000)
- [3] T. Metivet, L. Pastorello, and P. Peyla, How to push one's way through a dense crowd, *Europhysics Letters* (in press, 2018)

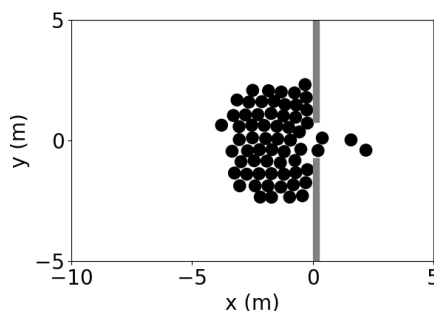


Figure 1: Sketch showing pedestrians evacuating a room through a door, that imposes a constriction.

Resummation of diagrammatic series with zero convergence radius for a strongly correlated Fermi gas

Riccardo Rossi^{a,b}, Takahiro Ohgoe^c, Kris Van Houcke^a et Félix Werner^{d*}

- a. Laboratoire de Physique Statistique, Ecole Normale Supérieure, Sorbonne Université, Université Paris Diderot, CNRS, Paris Sciences et Lettres, Paris, France
- b. Center for Computational Quantum Physics, The Flatiron Institute, New York, USA
- c. Department of Applied Physics, University of Tokyo, 7-3-1 Hongo, Bunkyo-ku, Tokyo 113-8656, Japan
- d. Laboratoire Kastler Brossel, Ecole Normale Supérieure, CNRS, Sorbonne Université, Collège de France, Paris Sciences et Lettres, Paris, France

* werner@lkb.ens.fr

Making accurate predictions for strongly correlated fermions is a long-standing theoretical challenge. A new approach is being developed since 10 years. All connected Feynman diagrams are sampled efficiently up to a certain order N_{\max} using diagrammatic Monte Carlo algorithms. Convergence of the diagrammatic series for $N_{\max} \rightarrow \infty$ was observed in several interesting situations for fermions on a lattice or frustrated spins. Here we consider a continuous-space model, where the series diverges strongly (the convergence radius is zero), and there is no small parameter in the strongly correlated regime. Nevertheless, we obtain accurate results by resumming the series using a conformal-Borel transformation that incorporates the large-order behavior and the analytic structure in the Borel plane, which we obtain by the instanton approach [1]. The specific model we consider is the unitary Fermi gas, a model of non-relativistic fermions in 3 space dimensions. We compare with ultracold-atom experimental data for the equation of state and the contact parameter.

- [1] R. Rossi, T. Ohgoe, K. Van Houcke, F. Werner, arXiv:1802.07717
- [2] M. J. H. Ku, A. Sommer, L. W. Cheuk, and M. W. Zwierlein, *Science* **335**, 563 (2012).

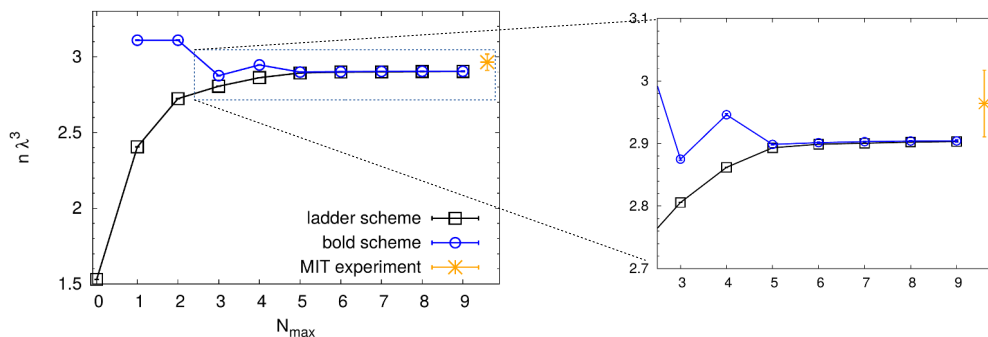


Figure 1: Theory-experiment comparison for the equation of state (dimensionless density $n\lambda^3$, here at zero chemical potential). Open squares and circles: resummed diagrammatic series up to order N_{\max} for two diagrammatic schemes, star: experimental data [2].

Architecture and Co-Evolution of Allosteric Materials

Le Yan^a, Riccardo Ravasio^b, Carolina Brito^c, and Matthieu Wyart^{b*}

- a. Kavli Institute for Theoretical Physics, University of California, Santa Barbara, USA
- b. Physics institute, EPFL, Lausanne, Switzerland
- c. Instituto de Física, Universidade Federal do Rio Grande do Sul, Porto Alegre RS, Brazil

* matthieu.wyart@epfl.ch

We introduce a numerical scheme to evolve functional materials that can accomplish a specified mechanical task. In this scheme, the number of solutions, their spatial architectures and the correlations among them can be computed. As an example, we consider an "allosteric" task, which requires the material to respond specifically to a stimulus at a distant active site. We find that functioning materials evolve a less-constrained trumpet-shaped region connecting the stimulus and active sites and that the amplitude of the elastic response varies non-monotonically along the trumpet. As previously shown for some proteins, we find that correlations appearing during evolution alone are sufficient to identify key aspects of this design. Finally, we show that the success of this architecture stems from the emergence of soft edge modes recently found to appear near the surface of marginally connected materials. Overall, our *in silico* evolution experiment offers a new window to study the relationship between structure, function, and correlations emerging during evolution.

PNAS **114**, 2526-2531 (2017)

Nanometer-scale active thermal devices for thermal microscopy probe calibration

Jun Yin^{a,*}, Tianqi Zhu^a, Di Zhou^a, Thierno Moussa Bah^a, Stanislav Didenko^a, Severine Gomes^b, Olivier Bourgeois^c, Didier Pellerin^d, Emmanuel Dubois^a and Jean-François Robillard^a

a. Univ. Lille, CNRS, Centrale Lille, ISEN, Univ. Valenciennes, UMR 8520-IEMN, F-59000 Lille, France

b. Centre for Energy and Thermal Sciences, Lyon (CETHIL)-CNRS, INSA, UCBL, Campus La Doua LyonTech, Lyon, France

c. Institut NEEL, CNRS-UJF, 25 rue des Martyrs, 38042 Grenoble, France

d. CSInstruments, 2 rue de la Terre de Feu, 91940 Les ULIS, France

*Jun.Yin@isen.iemn.univ-lille1.fr

Heat transfer in micro and nanoscale materials or devices gains more and more attention due to increasing thermomechanical issues and the dependence of many phenomena involving an Arrhenius-type law on local temperature [1]. Scanning Thermal Microscopy (SThM) is a technique derived from Atomic Force Microscopy (AFM) where a thermal sensor is located on the probe [2,3]. This technique allows the thermal characterization in nanoscale a reality. However, many challenges still remain as among which the sensitivity of the SThM probe and its quantitative calibration [4,5].

In this work, dedicated micrometer devices are designed in order to provide ultimately flat surfaces and thermally active samples which are suitable for the characterization and calibration of SThM probes. The design includes as well various characterization platforms, such as Van der Pauw measurement, 4-point electrical resistance measurement and 3-omega measurement in order to better control various sample properties. Finite Element Modeling (FEM) was used to simulate the device, so as to understand the impact of critical factors to our samples and determinate the final fabrication dimensions at different parts.

The first device was completed by using ion implantation in the top layer of a silicon-on-insulator (SOI) substrate to create conductive channels that will be used as resistive elements for heat generation. The narrow conductive channels are down to 20 or 40 nm wide, fabricated via electron-beam lithography. Some preliminary characterizations, such as IR camera and Raman thermometry, will be tried to test its functionalities.

This work was supported by the French government through the National Research Agency (ANR) under project TIPTOP ANR-16-CE09-0023 and by the French RENATECH network.

[1] D. G. Cahill, K. Goodson, and A. Majumdar, Thermometry and thermal transport in micro/nanoscale solid-state devices and structures. *J. Heat Transfer* **124**, 223 - 241 (2002).

[2] M. Nonnenmacher, and H. K. Wickramasinghe, Scanning probe microscopy of thermal conductivity and subsurface properties. *Appl. Phys. Lett.* **61**, 168 (1992).

[3] A. Majumdar, Thermal imaging using the atomic force microscope. *Appl. Phys. Lett.* **62**, 2501 (1993).

[4] F. Menges, et al., Temperature mapping of operating nanoscale devices by scanning probe thermometry. *Nat. Commun.* **7**,10874 (2016).

[5] Y. F. Ge, et al., Topography-free sample for thermal spatial response measurement of scanning thermal microscopy. *Journal of Vacuum Science & Technology B* **33**, 06FA03 (2015).

Nanoscale manipulation of coherent electron waves from a nano-tip

Hirofumi Yanagisawa,

Ludwig-Maximilians University, D-85748 Garching, Germany

Email: hirofumi.yanagisawa@mpq.mpg.de

In this presentation, we will overview our work on laser-induced electron emission from a tungsten tip. In particular, we will focus on optical control of electron emission sites on a scale of nanometers and their application for optical control of Young's electron interference.

Illuminating a sharp metallic tip with femtosecond laser pulses produces spatially and temporally confined electron pulses by plasmonic effects at the tip apex [1]. We have found that these plasmonic effects induce asymmetric electron emissions from the tip apex as schematically shown in Fig. 1. They also allow one to select the electron emission sites on a nanometer scale by changing the laser polarization [2]. Using this technique, we can manipulate electron emissions within their coherence time and area, which then enables us to control coherent electron emission in time and space. In a demonstration, we realized optical control of Young's electron interference [3]. The interference emerged between the two adjacent electron beams. The intensity of the interference could be successfully controlled by changing the laser polarization and intensity. The underlying physics that drove the interference was revealed by measuring the energy spectra [4, 5] and also by simulating the temporal evolution of the electron waves by solving a two-dimensional time-dependent Schrödinger equation [3]. Using a site-selective coherent electron source, we expect to create time-resolved electron holography with a possible time resolution in attoseconds.

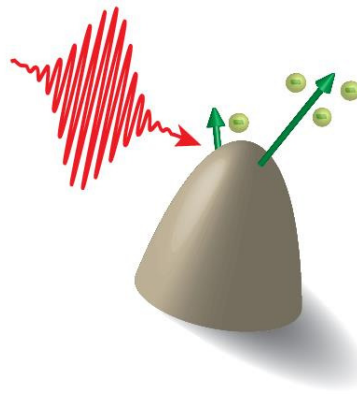


Figure 1: A schematic diagram of the laser-induced field emission.

References

1. P. Hommelhoff, *et. al.*, Phys. Rev. Lett. **96**, 077401 (2006).
2. H. Yanagisawa, *et. al.*, Phys. Rev. Lett. **103**, 257603 (2009).
3. H. Yanagisawa, *et al.* Sci. Rep. **7**, 12661 (2017).
4. H. Yanagisawa, *et al.* Phys. Rev. Lett. **107**, 087601 (2011).
5. H. Yanagisawa, *et al.* Sci. Rep. **6**, 35877 (2016).

Magneto-transport properties of BaNiS₂ and BaCoS₂ under high pressure up to 10 GPa

Hancheng Yang^{a*}, Yannick Klein^a, and Andrea Gauzzi^a

- a. Institut de Minéralogie, de Physique des Matériaux et de Cosmochimie (IMPMC), Sorbonne Université, CNRS, IRD, MNHN, 4 place Jussieu 75005 Paris, France

* Hancheng.yang@upmc.fr

During the 1990s, the quasi-2D BaCo_{1-x}Ni_xS₂ system ($x = 0$ to 1) has been topic of numerous studies due to its similarity with high- T_C superconducting materials. Its structure consists of electronically active Co(Ni)S sheets sandwiched between BaS layers. The relation between magnetism and transport properties in BaCo_{1-x}Ni_xS₂ is quite complex and not yet understood. As an illustration, the mother compound ($x = 0$) exhibits a paramagnetic to antiferromagnetic transition at $T_N \sim 300$ K, but without any transition in the transport properties [1]. On the other hand, when doped with Ni, the system undergoes a metal–insulator transition (MIT) at $x \sim 0.22$ [1]. A systematic study on the two end members of the series (BaNiS₂ and BaCoS₂) should help to unveil the mechanism of the MIT.

The control of the bandwidth and band-filling are two traditional ways to understand and manipulate the MIT. Experimentally, the bandwidth control can be achieved by applying a high pressure that may provide a tool to adjust the magnetic properties simultaneously.

In that respect, we have carried out magneto-transport measurements under high pressure up to 10 GPa on high quality single-crystals of BaNiS₂ and BaCoS₂. The resistance is measured down to a temperature of 2 K and under magnetic fields of up to 9 T. Only BaCoS₂ shows an MIT. BaNiS₂ keeps a metallic behavior, except at the lowest temperature where a weak localization is found. The results presented are interpreted with a Debye model.

[1] L. S. Martinson, J. W. Schweitzer, and N. C. Baenziger, *Phys. Rev. Lett.* **71**, 125 (1993).

Hierarchical assembled nanostructured electrodes based on transition metal chalcogenides for next generation secondary batteries

M.-R. Zamfir^{a,*}, M. Ezzedine^a, L. Sacco^a, I. Florea^a, C. - S. Cojocaru^a

^aLPICM, CNRS, Ecole Polytechnique, Université Paris-Saclay, 91128, Palaiseau

* mihai-robert.zamfir@polytechnique.edu

Transition metal dichalcogenides (TMDCs) pose as potential candidates for applications in the area of energy storage due to their layered structure (with the general formula MX_2 , in which a layer consists of a sheet of transition metal atoms (M) bonded to two adjacent sheets of chalcogen atoms ($X = S, Se$ or Te)), high surface area and electrochemical properties [1]. Depending on the chemical composition TMDCs can be used either as cathode or anode material exhibiting theoretical specific capacities larger than the commercially available graphite anode or transition layered metal oxides [2]. At the same time their large interlayer van der Waals gaps allow the intercalation of Li ions (or larger size Na ions) in the structure alleviating the large volume expansion presented in alloying type materials. However due to their low electronic conductivity the cycling performances are poor [3].

In this work we have developed hierarchical assembled nanostructured electrodes based on carbon nanotubes (CNTs) carpets used as current collectors decorated with TMDC nanomaterials using simple scalable techniques. The role of the CNTs is: i) increasing the specific electrode surface area ii) insuring the fast charge transfer and iii) to promote good crystallinity of the deposited active material. The functionalization of vertically aligned CNT by TMDs offers an unprecedented opportunity for their use in energy storage devices. These hierarchical architecture electrodes, due to their unique combination of redox chemistry, rapid ionic-transport channels, short-distance interactions between charge carriers, as well as between carriers and ions, and their earth-abundance, will play a key role in the successful implementation in the area of next generation rechargeable batteries.

[1] L. Peng, et al. *Adv Energy Mat.* 6 (2016) 1600025

[2] H. Hwang, et al. *Nano Lett.* 11 (2011) 4826

[3] W.Y. Li, et al. *J. Mater. Chem.* 22 (2012) 14864

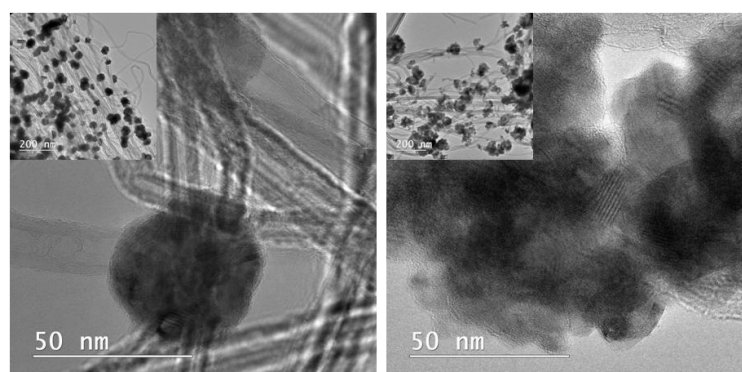


Figure 1: HR-TEM analysis of functionalized CNTs with transition metal nanoparticles and the morphological and structural changes after thermal sulfurization.

Fabrication of large-scale free-standing Si membrane using laser ablation

Zhou Di*, Flavie Braud, Arun Bhaskar, Quentin Theret, Emmanuel Dubois and Jean-Francois Robillard

Univ. Lille, CNRS, Centrale Lille, ISEN, Univ. Valenciennes, UMR 8520 – IEMN, Lille, France

* di.zhou@iemn.univ-lille1.fr

Energy conversion based on thermoelectric effect is a topic of renewed interest in material science. In order to achieve high conversion efficiency, good thermoelectric materials are expected to exhibit high figure-of-merit zT , i.e. low thermal conductivity, high electrical conductivity and large Seebeck coefficient. Free-standing crystalline silicon membranes are therefore very promising objects, due to the important Seebeck coefficient of silicon and the opportunity to decouple thermal transport and electrical conductivity in these low-dimensional structures [1,2,3].

Typical processes for Si membranes suspension come from the Micro-Electro Mechanical Systems (MEMS) technologies. They rely on either: i) Cavities opening from the front side of SOI wafer and suspension thanks to XeF_2 dry etching or ii) backside wet etching. The complete fabrication cycles are usually long and have several difficulties such as low density of integration and two-sides alignment [4]. In this work, we have developed a method to fabricate Si membranes by laser ablation of the handle wafer from the backside which suppresses several lithography steps and enable short-loop prototyping to obtain large-scale (mm scale) membranes with even thinner thickness and arbitrary shapes. This suspension process opens a way for fast engineering of functional devices such as: sensors, energy scavengers and micro-batteries.

This work has received funding from the European Research Council under the European Community's Seventh Framework Programme (FP7/2007/2013) ERC Grant Agreement no.338179. This work was also supported by the French government through the National Research Agency (ANR) under program PIA EQUIPEX LEAF ANR-11-EQPX-0025 and partly supported by the French RENATECH network.

- [1] G. Pennelli and M. Macucci, High-power thermoelectric generators based on nanostructured silicon, *Semicond. Sci. Technol.* **31**, 054001 (2016)
- [2] J-K. Yu, S. Mitrovic, D. Tham, J. Varghese and J. R. Heath, Reduction of thermal conductivity in phononic nanomesh structures, *Nature nanotechnology* **5**, (2010)
- [3] M. Haras, V. Lacatena, F. Morini, J.-F. Robillard, S. Monfray, T. Skotnicki and E. Dubois Thermoelectric energy conversion: How good can silicon be?, *Materials Letters* **157**, 193 (2015)
- [4] M. Haras, V. Lacatena, T. M. Bah, S. Didenko, J.-F. Robillard, S. Monfray, T. Skotnicki and E. Dubois, Fabrication of thin-film Silicon membranes with phononic crystals for thermal conductivity measurements, *IEEE Electron Device Letters*, **37**, 1358 (2016)

Tuning spin-charge interconversion with confinement in ultrathin Bi/Ge(111) films

C. Zucchetti,^{a,b*} M.-T. Dau,^b F. Bottegoni,^a C. Vergnaud,^b T. Guillet,^b A. Marty,^b C. Beigné,^b A. Picone,^a A. Calloni,^a G. Bussetti,^a A. Brambilla,^a L. Duò,^a F. Ciccacci,^a P. K. Das,^c J. Fujii,^c I. Vobornik,^c M. Finazzi,^a and M. Jamet^b

- a. LNESS-Dipartimento di Fisica, Politecnico di Milano, 20133 Milano, Italy
- b. Univ. Grenoble Alpes, CEA, CNRS, Grenoble INP (Institute of Engineering Univ. Grenoble Alpes), INAC-Spintec, 38000 Grenoble, France
- c. CNR-IOM Laboratorio TASC, 34149 Trieste, Italy

* carlo.zucchetti@polimi.it

Spin-charge interconversion (SCI) phenomena have attracted a large interest in nowadays spintronics, since they represent an essential step towards the design and engineering of spintronic devices [1]. In this respect, the scalability down to the nanometer scale and the integrability with opto-electronic and spintronic devices are important features that drive the choice of the SCI platform [2]. Here, we investigate SCI in ultrathin Bi films epitaxially grown on Ge(111) as a function of the Bi thickness t . We use x-ray diffraction and scanning tunneling microscopy to obtain a clear picture of the morphology and crystallography of the system. Through spin- and angle-resolved photoemission we show that spin-polarized surface states crossing the Fermi level are present. Then, we directly probe the charge-to-spin conversion by detecting with magneto-optical Kerr effect the electrically-induced spin accumulation in Bi, and the spin-to-charge conversion by generating a spin current in the system with either optical or ferromagnetic resonance driven spin injection. We recover large SCI signals in the thickness range ($1 < t < 3$ nm) characterized by the presence of small Bi nanocrystals. We observe that the conversion efficiency drastically decreases as t increases, when the Bi islands start to percolate. Since bulk SCI is small, the conversion is mainly related to the Rashba-Edelstein effect associated with electron transport in the spin-polarized surface states. In this frame, we tentatively explain the observed thickness dependence of SCI by reminding that the Bi conductivity can be strongly affected by quantum confinement effects [3]. In the high confinement conditions realized in the Bi nanoislands obtained for $1 < t < 3$ nm, the bulk resistivity is assumed to be high enough to electrically disentangle the upper and lower Bi surfaces, which otherwise would give rise to opposite contributions to SCI conversion that tends to cancel out, drastically decreasing the net SCI signal. Our results indicate that quantum size effects might be exploited as a tool to tune SCI and investigate a very rich spin-physics [4].

- [1] J.-C. Rojas-Sanchez, et al., Spin-to-charge conversion using Rashba coupling at the interface between non-magnetic materials. *Nat. Comm.* **4**, 2944 (2013)
- [2] S. Caprara, Spin-to-charge current conversion, *Nat. Mater.* **15**, 1224 (2016)
- [3] Z. Zhang, et al., J. Electronic transport properties of single-crystal bismuth nanowire arrays, *Phys. Rev. B* **61**, 4850 (2000)
- [4] C. Zucchetti, et al., submitted to *Nat. Phys.*

IN6-SHARP: towards a new cold neutron spectrometer at ILL. Illustration of the potentialities of QENS to probe the dynamics of Ionic liquids in bulk and under 1D nanometric confinement.

J.-M. Zanotti^{a*}, Q. Berrod^a, F. Ferdeghini^a, P. Judeinstein^a, J. Dijon^b,
S. Petit^a, B. Homatter^a, S. Rodrigues^a, P. Lavie^a

- a. Laboratoire Léon Brillouin (CEA-CNRS), Université Paris-Saclay,
91191 Gif-sur-Yvette, France
b. CEA/DRT/LITEN/DTNM, CEA Grenoble, 38054 Grenoble, France

* jmzanotti@cea.fr

Following the agreement to strengthen [the Franco-Swedish cooperation in the field of neutron scattering](#), the Laboratoire Léon Brillouin ([LLB](#)) is involved in the construction of an inelastic neutron time-of-flight (INToF) spectrometer. After the announcement of the Orphée reactor shutdown in 2019, the project originally planned at Saclay has been transferred to the Laue Langevin Institute ([ILL](#), Grenoble). This renaissance takes the form of a [CRG A](#) contract concluded on September 29 2017 between the [DRF](#) of the CEA, the [INP](#) of the CNRS, and the ILL. This new [SHARP](#) (Spectromètre Hybride Alpes Région Parisienne) project consists in a complete rebuilding of the [IN6](#) secondary spectrometer: sample environment, time-of-flight chamber and detection. This talk will start by an update on the project.

We will then illustrate the potentialities of Quasi-Elastic Neutron Scattering (QENS) in the study of Ionic liquids (ILs). ILs are pure solutions of charged organic molecules with no solvent. These molecular electrolytes show a property original for a pure liquid: they self-organize in nanometric fluctuating aggregates [1]. When probed at the macroscopic scale, ILs behave as highly dissociated (*i.e.* strong) electrolytes [2] while, at the molecular scale, they show clear characteristics of weak ionic solutions [3]. In this talk, we report a multi-scale analysis that sheds new light on these apparently at odd behaviors [4,5]. We then address the conductivity of electrolytes directly relevant to the field of electrochemical storage systems: ILs charged with lithium salts. We show that these electrolytes confined in composite polymer CNT (Carbon NanoTube) membranes show a drastic and unprecedented increase in ionic conductivity: we report conductivity gains by a factor up to 50 compared to the bulk analogues. Such CNT membranes are a possible route to boost the transport properties and hence the specific power of lithium batteries [6,7].

On a more neutron technical ground, this talk will illustrate on the practical case of the multiscale dynamics of a bulk IL, the RRM (Repetition Rate Multiplication) method [8] on INToF spectrometers. With this setting, successive wavelength bands are selected within each of the incident neutron pulses, resulting in an extended mapping of the (Q, ω) space. As this will be a routine mode on INToF instruments at the [European Spallation Source](#) (ESS), a take-home message will be that, to take full advantage of the ESS potentialities, it is time to get hands-on practice in this new method.

- [1] Hayes, R., Warr, G. G. & Atkin, R. Structure and Nanostructure in Ionic Liquids. *Chem. Rev.* 115, 6357–6426 (2015).
[2] Lee, A. A., Vella, D., Perkin, S. & Goriely, A. Are Room-Temperature Ionic Liquids Dilute Electrolytes? *J. Phys. Chem. Lett.* 6, 159–163 (2015).
[3] Gebbie, M. A., Dobbs, H. A., Valtiner, M. & Israelachvili, J. N. Long-range electrostatic screening in ionic liquids. *Proc. Natl. Acad. Sci.* 112, 7432–7437 (2015).
[4] Ferdeghini, F. et al. Nanostructuring of ionic liquids: impact on the cation mobility. A multi-scale study. *Nanoscale* 9, 1901–1908 (2017).
[5] Quentin Berrod et al. Ionic Liquids: evidence of the viscosity scale-dependence. *Sci. Rep.* 7, (2017).
[6] Berrod, Q. et al. Enhanced ionic liquid mobility induced by confinement in 1D CNT membranes. *Nanoscale* 8, 7845–7848 (2016).
[7] Berrod, Q., Ferdeghini, F., Judeinstein, P. & Zanotti, J.-M. Nanocomposite membranes for electrochemical devices. Patent WO 2016151142 A1. (2016).
[8] Mezei, F. Multi-wavelength data collection strategies in inelastic neutron scattering. *Phys. B Condens. Matter* 385–386, Part 2, 995–999 (2006).

Poster CPR3: Investigation of the aging mechanism in Silicon-based lithium-ion batteries by operando scattering techniques

Diana Zapata Dominguez^{a*}, Christopher Berhaut^b, Samuel Tardiff^a, Stéphanie Pouget^a, David Aradilla^b, Sandrine Lyonnard^b

- a. University Grenoble Alpes, CEA, INAC, MEM, F-3800 Grenoble, France
 b. University Grenoble Alpes, CEA, INAC, SYMMES, F-3800 Grenoble, France
 *diana.zapatadominguez@cea.fr

Lithium ion batteries are one of the best solutions for energy storage firstly due to the lighter weight of the lithium conferring high energy density. This also enables the flexibility in design and the portability that facilitates the use in several applications ranging from mobile devices to automobile market. In the research for materials that can reversibly host or release large quantities of lithium ions, it has been realized that silicon offers interesting possibilities because of its high theoretical capacity (3579 mAh/g) and natural abundance, compared to the usual commercial electrode, graphite (372 mAh/g). However, silicon suffers large volume expansion upon the insertion-disinsertion of the lithium ions, which results in the continuous formation of solid electrolyte interphase (SEI), leading to Li trapping and capacity loss. This continuously happen, leading to irreversible capacity and electrical contact loss.

One way of limiting volume expansion is using silicon nanoparticles, where the small size enables Li transportation and strain relaxation. These nanoparticles can also be embedded into a matrix to form a composite electrode, where the Si nanoparticles are embedded in a matrix. This strategy is expected to reduce SEI formation and mitigate volume changes, therefore reducing the capacity loss. However, the mechanism of the aging and the impact of the battery function on the structure of the composite electrode are not well known.

We address this problematic performed non-intrusive operando characterization of Si-Nps composite anodes by combining synchrotron wide-angle X-ray scattering (WAXS) [1] and small angle X-ray scattering (SAXS) (fig 1a, b.) to probe simultaneously the nanoscale morphology of the nanoparticles and their atomic structure. We compared the behavior of Si-Nps anodes and composite Si-graphite anode, cycle at different C rates. By analyzing the width, position and intensity of the diffracted peaks, coupled to the small angle variations and the applied voltage, we could thus evidence the reversible and irreversible changes occurring during the lithiation and delithiation processes.

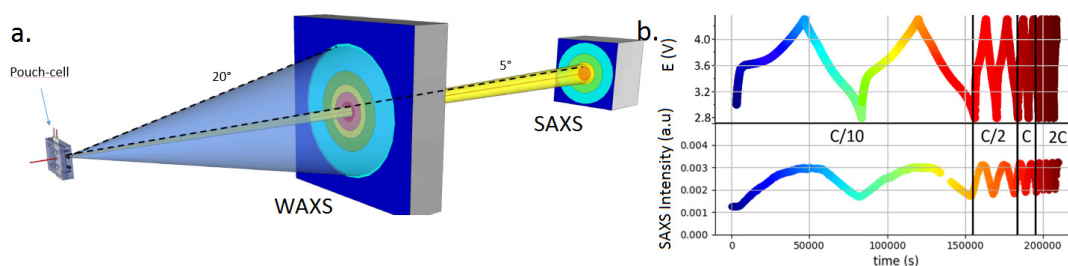


Figure 1: a. Scheme of the Operando WAXS and SAXS experiments. b. Evolution of the SAXS intensity integrated of the composite electrode over the q -range $4 \times 10^{-2} \text{ \AA}^{-1}$ - 9×10^{-2}

[1] S. Tardiff et al, Operando Raman Spectroscopy and Synchrotron X-ray Diffraction of Lithiation/Delithiation in Silicon Nanoparticle Anodes, ACS Nano **11**, 11306 (2017)

***In situ* switching of ferroelectric nanodomains probed by X-ray nanodiffraction**

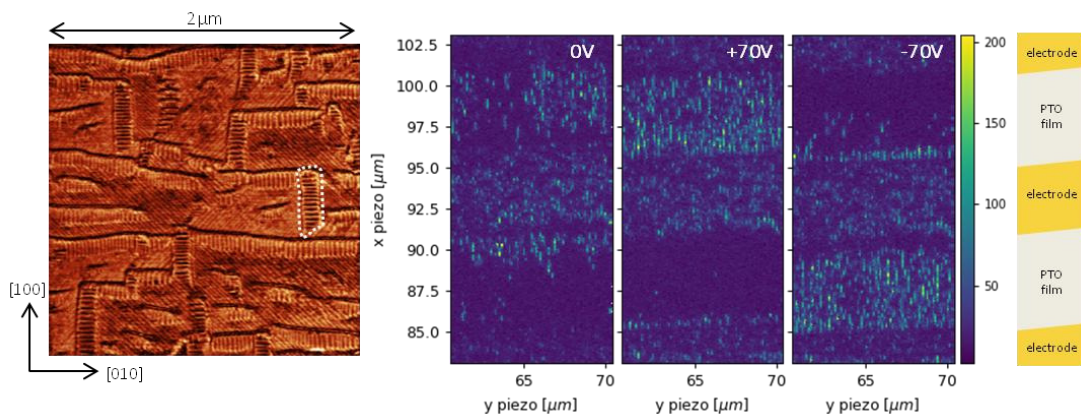
E. Zatterin^{a,b*}, M. Hadjimichael^b, S. J. Leake^a, and P. Zubko^b

- a. London Centre for Nanotechnology and Department of Physics and Astronomy, University College London, London WC1H 0HA, United Kingdom
 b. ESRF - The European Synchrotron, 71 Avenue des Martyrs, Grenoble 38000, France
 *corresponding author : edoardo.zatterin@esrf.fr

The promise of novel domain-wall based nanoelectronic devices has recently motivated much work concerning strain-engineered ferroelectrics with dense ferroelastic domain structures [1]. Certain thin film systems display an hierarchal organization, whereby ferroelastic domains arrange in distinct “superdomain” bundles [2]; the behavior of these superdomain structures under device- like conditions is still unclear.

Here we employ Scanning X-ray NanoDiffraction (SXND) [3] to investigate in-situ the response of an hierarchal ferroelectric thin film to in-plane applied electric field via a set of interdigitated electrodes deposited on its surface. We use PbTiO₃ (PTO) // KTaO₃ (KTO) thin films as a prototype system for this study due to the peculiar mixture of in-plane and out-of-plane domain bundles that PTO exhibits at the value of misfit strain resulting from deposition onto KTO substrates.

A typical piezoresponse microscopy image depicting the domain structure of a 62nm thick PTO//KTO thin film is shown on the left side of the figure below. In-plane a_1a_2 domain bundles are visible as diagonal stripes; out-of-plane ac bundles appear instead as horizontal and vertical “ladders” – an individual bundle is marked by a white dotted line. The right side of the Figure shows a SXND map (20x5 μ m) displaying the distribution of ac domains as a function of applied voltage on the same PTO//KTO film. The map covers an area where both the interdigitated electrodes and the film’s surface in between those is visible, as the schematic on its right illustrates. The migration of one variant of ac bundles from one trench to the adjacent one due to the switching of the field lines direction under the inversion of the applied voltage polarity can be seen. Other kinds of bundles show different behavior which can also be visualized analogously, and based on these findings we propose to interpret this intricate domain structure and its response to in-plane electric field. We further demonstrate the value of SXND as a tool to investigate in-situ the structure of ferroelectric thin films to external stimuli.



- [1] Martin, L.W, et al. (2017) Nature Reviews Materials, 2(2), p.16087
 [2] Damodaran, A.R., et al. (2017) Journal of Physics: Condensed Matter, 28(26), p.263001
 [3] Chahine, G. A., et al. (2014) J. Appl. Cryst. 47, 762–769

Competition between the antiferromagnetic phase and the superconducting phase and the effect of the Magnetic Fluctuations in the underdoped $\text{BaFe}_{2-x}\text{Ni}_x\text{As}_2$.

A. Abbassi^{a,c}, M.Saint-Paul^b, C.Guttin^b, M.R. Britel^c, R. Dkiouak^a, Z-Sheng Wan^{b,d}, Huinqian Luo^d, X. Lu^d, Cong Ren^d, Hai-Hu Wen^{d,e} and K. Hasselbach^b.

^a Faculté des Sciences et Techniques de Tanger, BP 416 Tanger, Université Abdelmalek Essaâdi, Morocco.

^b Université Grenoble Alpes, Institut Néel, F-38042 Grenoble ; CNRS, Institut Néel, F-38042 Grenoble France.

^c Laboratoire des Technologies Innovantes, ENSAT, UAE, BP 1818 Tanger, Morocco.

^d Institute of Physics and National Laboratory for Condensed Matter Physics, Chinese Academy of Sciences, P.O Box 603, Beijing 100190, People's Republic of China.

^e National Laboratory for solid State Microstructures, Department of Physics, Nanjing University, 210093 Nanjing, People's Republic of China.

* corresponding author, E-mail: abdellatif1966@hotmail.com

We report a comparison between the results obtained by two different measurements of the temperature and RF frequency dependence. The results of the relative change of the ultrasonic attenuation and the electrical conductivity show respectively the competition between the antiferromagnetic and superconducting states and the effect of magnetic fluctuations in the underdoped superconducting $\text{BaFe}_{2-x}\text{Ni}_x\text{As}_2$.

These results concern the measurement of the surface impedance in the underdoped superconducting $\text{BaFe}_{2-x}\text{Ni}_x\text{As}_2$ crystal with $x = 0.07$ in the $5 < T < 30\text{K}$ temperature range using the Ultrasound technique and the radiofrequency reflection technique by induction using impedance and network analyzers in the frequency range 10 MHz–1.5 GHz.

The ultrasound measurements were performed on superconducting $\text{BaFe}_{1.93}\text{Ni}_{0.07}\text{As}_2$ crystals. The elastic constants C_{33} and C_{44} for the underdoped crystal show a large softening related to the structural phase transition at high temperatures. Anomalies in the sound velocity and the ultrasonic attenuation have been found at the superconducting phase transition $T_c = 17\text{K}$

A similar behavior was observed by the magnetic induction measurements. With our two measurement technics, we observed and highlighted the transition to the superconducting state of the underdoped sample. Strong anomalies are observed along the antiferromagnetic phase before reaching the superconducting state. The succession of variations in the two phases, confirms the competition between them.

The establishment of the antiferromagnetic order at $T_N \sim 50\text{K}$ gives rise to anomalous an increase of electron scattering time. The increase of the real conductivity σ_1 in the superconducting state is attributed to a rapid decrease of the σ_1 quasiparticle scattering time. This result gives evidence of coexistence of superconductivity and antiferromagnetism.

The conductivity σ_1 increases with decreasing temperature below T_c . A similar behavior was coarsely observed in the measurement LC resonant circuit.

The large anomalies in the elastic constants C_{33} and C_{44} modes and the unusual temperature dependence of the real part σ_1 of the electronic conductivity found around the superconducting phase transition $T_c \sim 16\text{K}$ are attributed to magnetic fluctuations. The establishment of a magnetic order at $T_M = 21\text{K}$ results in a marked decrease of the scattering of electronic carriers.

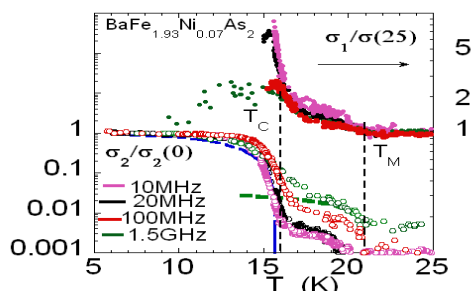


Figure. 1 Temperature dependence of the real $\sigma_1/\sigma(25)$ (filled symbols) and imaginary $\sigma_2/\sigma_2(0)$ (open symbols) parts of the electronic conductivity, $\sigma(25)$ is the conductivity at 25 K for the underdoped $\text{BaFe}_{1.93}\text{Ni}_{0.07}\text{As}_2$.

**The Effect of Series Resistance on Electrical Characterization in Schottky
Au- μ -polycrystalline silicon**

**H. Ayed^{a,b,*}, L.Mahdjoubi^b, L Béchiri^b, M. Benabdeslem^b, N.Benslim^b
and T Mohammed-Brahim^c**

^aUniversité Larbi Mehani Tebessa 12000, Algérie.

^bLaboratoire Cristaux et Couches Minces, Faculté des Sciences, Dpt de physique ¹(LESIMS),
Université Badji Mokhtar BP.12 Annaba, 23000, Algérie.

^cGM-IETR, Université RENNES I, 35042 Rennes Cedex, France.

E-mail : ayedhamida24@gmail.com

ABSTRACT

Polycrystalline silicon, obtained by crystallisation of amorphous deposited silicon films, is usually columnar with grain boundaries perpendicular to the film surface. The electrical transport properties may be different in the parallel and perpendicular to the surface directions consequently. Most of characterisation techniques of polysilicon lead to the knowledge of the parallel (or coplanar) properties. However, some of polysilicon devices as photovoltaic solar cells need the knowledge of the properties perpendicular to the surface.

Schottky Au-Polysilicon diodes are successfully realised in this work. The diffusion potential is around 1.3 eV as determined from Capacitance – Bias C-V characteristics. Electrical characteristics of Au/poly-Si Schottky barrier diodes are analysed by current-voltage (I–V) and capacitance voltage (C–V) techniques at room temperature. The electronic parameters such as ideality factor, barrier height and average series resistance are determined. The barrier height 1.87eV obtained from the C–V measurements is higher than that of the value 0.97eV obtained from the I–V measurements. The series resistance RS and the ideality factor n are determined from the $\ln(I)/dV$ plot. The depth profile of the apparent doping is deduced from these measurements. Its behaviour leads to the expected experimental profile. Moreover, the diode admittance measurements versus the frequency and the temperature at different biases show the possibility to use this device to characterise the electrical quality of the polysilicon.

Superfluidity and coherence in uniform two-dimensional Bose gases

J.L. Ville, R. Saint-Jalm, E. Le Cerf, P.C.M. Castilho, M. Aidelsburger, S. Nascimbene, J. Dalibard, J. Beugnon*

a. Laboratoire Kastler Brossel, Collège de France, CNRS, ENS-PSL University, Sorbonne Université, 11 Place Marcelin Berthelot, 75005 Paris

* beugnon@lkb.ens.fr

In uniform two-dimensional systems symmetry breaking phase transitions, like Bose-Einstein condensation for an assembly of bosons, are forbidden. Nevertheless, a topological phase transition of Kosterlitz-Thouless type can take place at low temperature. Below this critical temperature a superfluid phase appears and the phase coherence of the system presents quasi-long range order.

In our team we have developed an experimental apparatus allowing us to trap and manipulate uniform two-dimensional clouds of ultracold weakly interacting bosons in arbitrary geometries [1,2]. In this talk, I will first present recent results describing the characterization of the superfluid behavior of the system thanks to the measurement of the speed of second sound. I will also describe measurements of phase coherence decay with distance between particles.

[1] J.L. Ville, T. Bienaimé, R. Saint-Jalm, L. Corman, M. Aidelsburger, L. Chomaz, K. Kleinlein, D. Perconte, S. Nascimbène, J. Dalibard, and J. Beugnon, *Loading and compression of a single two-dimensional Bose gas in an optical accordion*, Phys. Rev. A. **95**, 013632 (2017).

[2] M. Aidelsburger, J.L. Ville, R. Saint-Jalm, S. Nascimbène, J. Dalibard, and J. Beugnon, *Relaxation dynamics in the merging of N independent condensates*, Phys. Rev. Lett. **119**, 190403 (2017).

Organic spintronics

S. Boukari

Université de Strasbourg, CNRS, Institut de Physique et Chimie des Matériaux de
Strasbourg, UMR 7504, F-67000 Strasbourg
samy.boukari@ipcms.unistra.fr

To ensure the long-term progress of information technology, radically new concepts, materials and processing methods are required to circumvent the limitations of traditional electronics. Spin electronics, or spintronics, adds a new spin degree of freedom to conventional charge-based electronics. By injecting, transporting, controlling and detecting spin-polarized currents, new spin-based devices can be obtained, including spin valves (magnetoresistive devices), spin-FETs (field-effect transistors with spin-polarized source and drain), spin-LEDs (spin-polarized light-emitting diodes), and quantum bits for quantum computation and communication.

Separately, organic electronics offers the advantages of low-cost materials and processing, the tuning of electronic properties by simple chemical routes to build multifunctional devices, and self-organization. In a more long-term perspective, organic electronics at the nano- or molecular scale will exploit intriguing electric properties of nanoscopic objects down to single molecules in electric circuits.

For instance, the spin-polarized hybridization resulting from the adsorption of molecules on ferromagnetic metals, which is called an organic spinterface [SAN11], can lead to a high spin polarization (~100%) even at room temperature [DJE16], and in turn promotes giant magnetoresistance, high tunneling magnetoresistance (up to 10000 % !) or tunneling anisotropic magnetoresistance [BAR15, BAR16]. The recently reported ability to electrically modulate the magnetism of the organic spinterface [STU17], which drives its spintronic properties, represents an important first building block within a conceptual proposal to develop active molecular spinterfaces [CIN17].

Recently, as another consequence of interface properties, it appeared that an organic layer can induce an effective exchange field on ferromagnetic layers, either i) due to the presence of spin chains in the molecular layer [BAR15, GRU15] -- a mechanism similar to exchange bias in inorganic materials -- or ii) due to spin frustration induced at the interface [RAM13]. The latter case is a new effect, not yet not fully understood, specific to organic materials and unknown with inorganic materials, in that it occurs with nominally non-magnetic molecules.

[BAR15] Barraud *et al.* Phys. Rev. Lett. **114** (2015) 206603.

[BAR16] Barraud *et al.* Dalton Trans **45** (2016) 16694.

[CIN17] Cinchetti *et al.* Nat. Mater. **16** (2017) 507.

[DJE16] Djeghloul *et al.* J. Phys. Chem. Lett. **2016**, 7, 2310.

[GRU15] Gruber *et al.* Nature Mater. **14** (2015) 981.

[RAM13] Raman *et al.* Nature **493** (2013) 509.

[SAN11] Sanvito, *Chem. Soc. Rev.* **40** (2011) 3336.

Microstructural investigation of nickel deposits obtained by pulsed current

Amel Boukhouiete^{a*}, Juan Creus^b

- a. Laboratoire de Métallurgie Physique et Propriété des Matériaux (LM2PM) Faculté des sciences, Université Badji-Mokhtar, 23 000 Annaba, Algeria.
- b. Laboratoire des Sciences de l'Ingénieur pour l'Environnement (LaSIE), CNRS-FRE 3474, Université de La Rochelle, Avenue Michel Crépeau, 17042 La Rochelle, France

* « amelboukhouiete@yahoo.fr »

The synthesis of nickel by pulse electrodeposition has attracted much attention during the last decades. Pulse electrodeposition has been reported to improve the deposition process and deposit properties such as porosity [1], ductility [2], hardness [3] and surface roughness [3]. It has been reported that pulse plating strongly modifies the properties, the structure, the surface morphology and the macroscopic characteristics of nickel coatings. In the present research nickel deposits were produced by pulse current electrodeposition from Watts bath. The optimization of the conditions of deposition was established and the influence of pulse parameters, on the grain size, surface morphology and crystal orientation was determined. The morphology of the coatings was characterised by observations in scanning electronic microscopy (SEM). X-ray diffraction in symmetric mode was also used to evaluate the structure and principal crystallographic orientations of the deposits. The results obtained, showed that the development in pulsed induced a marked improvement in the morphology and grain refinement.

[1] I Popov, D. N. Keca, B.I. Vuksanovic, *Journal of Applied Electrochemistry* 7 (1977) 185

[2] C. J. Raub, A. Knodler, *Plating and Surface Finishing* 65 (9)(1978) 32.

[3] J. Puipe, F. Leaman, *Theory and Practice of Pulse Plating*, AESF Publication, Orlando, 1986

Investigation of disordered systems using Total scattering: introduction to the method and experimental techniques

Michela Brunelli^{a*}

- a. Dutch-Belgian Beamline DUBBLE at the ESRF – 71, av. des Martyrs CS 40220 38043
Grenoble Cedex 9

* brunelli@esrf.fr

Structural disorder and/or nano-scale structures are found in many technologically relevant modern materials, such as batteries, catalysts, and guest storage systems. Understanding this disorder is often key to understanding the functional materials properties. While traditional Bragg crystallography is only sensitive to the long-range ordered structure, diffuse scattering features between the Bragg peaks contain information on the local atomic structure. Hence, a combined analysis of Bragg and diffuse contributions to the powder diffraction data provides a versatile approach to probe and characterize these structures.

In powder diffraction, Pair-Distribution Function (PDF) analysis of Total Scattering data is the method for going beyond classical crystallographic analysis by providing quantitative information about local as well as meso-structure, because is sensitive to local static and dynamic disorder. It based on the Fourier transformation of diffraction data into real-space [1, 2].

In this talk, the main characteristics of Total Scattering and its domain of application will be presented. Particular emphasis will be devoted to the experimental implementation of the technique, both for X-ray and neutron powder diffraction.

[1] T. Egami, and S.J.L. Billinge, *Underneath the Bragg peaks: Structural Analysis of Complex Materials* (Pergamon Materials Series, V. 7: Oxford, 2003)

[2] H.E. Fischer, A.C. Barnes, and P.S. Salmon, *Neutron and x-ray diffraction studies of liquids and glasses*, *Rep. Prog. Phys.* **69**, 233–299 (2006)

Table Ronde : Recherche et Innovation en entreprise et emploi des docteurs

Animateur de la table-ronde : C. Chapelier

(co-fondateur d'AITAP, l'association des doctorants du CEA-Grenoble)

Organisateurs : P.E. Wolf * (Comité d'Organisation des JMC),
A. Fontaine (SFP et Fondation Nanoscience)

* pierre-etienne.wolf@neel.cnrs.fr

Dans le monde entier, le doctorat, plus haut diplôme de l'enseignement supérieur, est valorisé aussi bien dans les entreprises que dans le monde académique. Dans les entreprises, les diplômés sont en particulier recherchés pour leur expérience en conduite de projets innovants et pour leur capacité à travailler en équipe. Ainsi, un débouché important pour nos docteurs est la recherche et l'innovation au sein d'entreprises, en France et au-delà. Cette session, plus particulièrement orientée vers les doctorant(e)s qui participeront aux journées, sera l'occasion de faire un point sur la situation.

Dans une première partie, des docteurs travaillant au sein d'entreprises de différentes natures (grands groupes, start-ups, etc.), apporteront leur témoignage. En se basant sur leur expérience personnelle, ils expliqueront (entre autres) comment ils ont trouvé leur emploi, quelles sont les compétences qu'ils ont mises en avant, lesquelles leur servent encore aujourd'hui, en quoi ils estiment que leur thèse les a formés à leur métier actuel, ou quelles différences ils voient entre le milieu académique et le milieu de l'entreprise en matière de recherche au quotidien.

La seconde partie aura lieu sous forme de table ronde, au cours de laquelle les intervenants précédents et quelques représentants d'entreprises répondront aux questions de l'auditoire.

Intervenants prévus et leur spécialité :

M. Frédéric Boeuf - *ST Microelectronics* [Photonique sur Silicium]

M. Emmanuel Dufour - *Rolls Royce* [instrumentation et contrôle] (à confirmer)

M. Jeremy Patarin - *Rheonova* [rhéologie pour l'industrie]

Mme Pamela Rueda - *Aledia* [affichage par LEDs]

(en duo avec M. Philippe Gilet, fondateur de la start-up)

M. Ahmad Sultan - *Sofradir* [détection pour l'infrarouge]

Certains des participants seront présents sur des stands lors des JMC. Ils accueilleront avec plaisir les personnes qui souhaiteraient discuter de possibilité d'emploi dans leurs entreprises.

Twisted graphene layers under heterostrain

L. Huder^a, A. Artaud^{a,b}, T. Le Quang^a, G. Trambly de Laissardière^c, A. G. M. Jansen^a, G. Lapertot^a, C. Chapelier^a and V. T. Renard^{a*}.

- a. Université Grenoble Alpes/CEA, INAC-PHELIQS, F-38000 Grenoble, France
- b. Université Grenoble Alpes, CNRS, Inst. NEEL, F-38000 Grenoble, France
- c. Laboratoire de Physique Théorique et Modélisation, Université de Cergy-Pontoise-CNRS, F-95302 Cergy-Pontoise, France

* vincent.renard@cea.fr << corresponding author >>

Stacking layered materials is a very powerful method to tailor their optical and electronic properties. The properties not only depend on the choice of materials to be stacked but also on the details of the relative arrangement of the layers. For instance, the rotation between the layers has been used to tune the energy of van Hove singularities in twisted graphene layers [1] or to observe the Hofstadter butterfly pattern in graphene on h-BN [2,3]. An even more impressive demonstration of the possibilities offered by precise tuning of the relative arrangement is the recent observation of correlated insulating and superconducting behaviour in magic angle twisted graphene layers[4,5].

Besides rotation, van der Waals stacking offers another possibility to adjust the relative arrangement of the layers: individual stretching of the layers (so-called heterostrain). In the present contribution we will expose scanning tunnelling measurements exploring this possibility in twisted graphene layers[6]. We will show that uniaxial stretching of one layer by only 0.36% with respect to the other layer can dramatically affect the electronic properties of twisted graphene layers with low rotation angle. The amount of heterostrain is determined by a detailed Fourier analysis[7]. With such a low level of heterostrain, we observe a pronounced peak in the density of states at the Dirac energy which we attribute to the emergence of a flat band similar to that observed at magic angles. The strain-induced modification of the band structure could therefore prove useful for the study of the recently discovered correlated electron physics in carbon materials. More generally heterostrain opens up new possibilities for straintronics with 2D materials.

- [1] G. Li *et al.* Observation of Van Hove singularities in twisted graphene layers *Nature Phys.* **6** 109 (2009)
- [2] G. Li *et al.* Cloning of Dirac fermions in graphene superlattices *Nature* **497** 594 (2013)
- [3] C. R. Dean *et al.* Hofstadter's butterfly and the fractal quantum Hall effect in moiré superlattices *Nature* **497**, 598 (2013)
- [4] Y. Cao *et al.* , Unconventional superconductivity in magic-angle graphene superlattices *Nature*, London (In press)
- [5] Y. Cao *et al.* , Correlated insulator behaviour at half-filling in magic-angle graphene superlattices *Nature*, London (In press)
- [6] L. Huder *et al.* *Phys. Rev. Lett.* (In press)
- [7] A. Artaud *et al.* *Sci.Rep.* **6**, 25670 (2016)

Strong nanomechanical softening signature induced by memristive charge accumulation in suspended monolayer MoS₂

Julien Chaste^{1*}, Imen Hnid¹, Ali Madouri¹, Alan Durnez¹, Xavier Lafosse¹, Meng-Qiang Zhao², A.T. Charlie Johnson², R. Braive^{1,3}, Abdelkarim Ouerghi¹

¹ Centre de Nanosciences et de Nanotechnologies, CNRS, Univ. Paris-Sud, Université Paris-Saclay, C2N – Marcoussis

² Department of Physics and Astronomy, University of Pennsylvania, 209S 33rd Street, Philadelphia, Pennsylvania 19104 6396, United States

³ Université Paris Diderot, Sorbonne Paris Cité, 75207 Paris Cedex 13, France

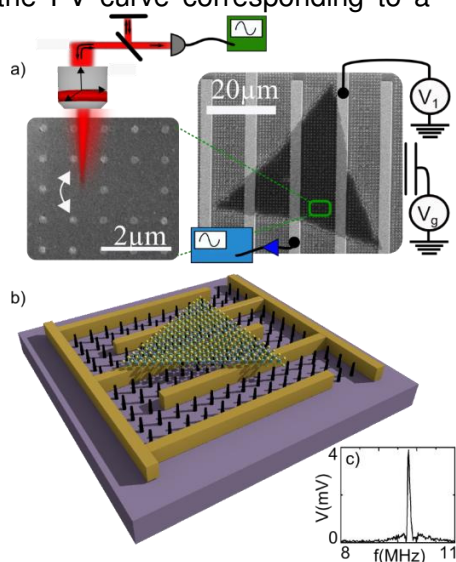
Abstract

The new 2D transitions metal dichalcogenide (TMDs) as MoS₂ represents ideal material for multiple purposes. MoS₂ is promising for electronic transistor and fundamentals phenomena such as superconductivity or valleytronic. It is a rich platform for optoelectronic; excitonic effects have high binding energy, strain engineering can induce a high tunability of the band gap itself. Moreover, MoS₂ transit between different crystalline phase (2H-1T) making this material interesting for memristive devices and energy storage.

Nanomechanical systems have been at the heart of recent physic discoveries of importance, from the detection of cosmic gravitational waves to the sensitivity record for detection of mass or force. It is a recent and almost universal probe of condensed matters issues and quantum mechanics. Since 2007, the emergence of suspended atomically thin materials, with the largest geometrical aspect ratio which can be obtained, brought new insight in nanomechanical resonators with very low mass and spring constant, high elongation resistance, high frequency-tuning and especially strong mechanical non-linearities. A high potential release in MoS₂ for nanomechanics. It opens new experimental perspectives by measuring unique intrinsic properties when transduced into the mechanical motion. We propose to focus on unexpected electrical behaviors measured in our samples^{1,2}: a strong photodoping under illumination and a hysteretic loop in the I-V curve corresponding to a memristive effect. We use the sensitivity of our mechanical MoS₂ membrane as a non-conventional probe to explore deeply these intriguing behaviors and we have seen a strong effect of softening due to the non-linear charge of the devices.

Figure 1 We explore these topics within unique sample geometry of a suspended single layer membrane of the MoS₂ embedded in a nano-opto-electro-mechanical system (NOEMS)

1. Chaste, J. *et al.* Intrinsic Properties of Suspended MoS₂ on SiO₂/Si Pillar Arrays for Nanomechanics and Optics. *ACS Nano* (2018). doi:10.1021/acsnano.7b07689
2. Chaste, J. *et al.* Nanostructures in suspended mono- and bilayer epitaxial graphene. *Carbon* **125**, 162–167 (2017).



Sensing the Influence of Resveratrol on the BSA Adsorption on Gold Nanoparticle Through Solid-State Nanopore

Diego Coglitore^{a*}, Nicoletta Giambianco^a, Agn  Kizalait ^a, Pierre Eugene Coulon^b, Benoit Charlot^c, Jean-Marc Janot^a and S bastien Balme^a

a. Institut Europ en des Membranes, UMR5635, Universit  de Montpellier CNRS ENSCM, Place Eug ne Bataillon, 34090 Montpellier, France

b. Laboratoire des Solides Irradi s,  cole polytechnique, Universit  Paris-Saclay, Route de Saclay, 91128 Palaiseau Cedex, France

c. Institut d'Electronique et des Syst mes, Universit  de Montpellier, 34095 Montpellier Cedex 5, France

* diego.coglitore@umontpellier.fr

Nanoparticles are increasingly considered in nanomedicine providing new solutions due to their unique physico-chemical properties. Together with other therapeutic agents, they can be formulated in a single hybrid nanocomposite, incorporating both diagnostic and therapeutic functions, leading to the so-called theranostic system¹.

Gold nanoparticles are one of the most promising candidate for theranostic applications. They are widely studied and employed as imaging agent for diagnosis, imaging and monitoring, but also in the treatment of malignant diseases and drug delivery systems².

Bovine serum albumin has been widely employed for the studies on protein-nanoparticle interaction and it is often used for the stability of gold nanoparticles suspensions. Gold nanoparticles, covered by bovine serum albumin BSA and loaded with different kind of antibiotics, have proved to be effective drug carriers, enhancing the antibacterial activity³.

The use of resveratrol (RESV) as a drug has attracted interest among researchers for its antioxidant and chemical cancer inhibition activities. The increase of drug delivery application involving resveratrol leads to the need of a deep understating of its interaction with drug carriers, as gold nanoparticles, and proteins present in the biofluid of interest⁴.

Through a combination of experimental techniques, we studied the interaction between gold nanoparticles, bovine serum albumin and resveratrol. We initially evaluated the gold nanoparticle aggregation, and the subsequent impact of the BSA and the resveratrol, by surface plasmon resonance spectroscopy and dynamic light scattering. We investigated the mechanism of interaction at the single-molecule level using solid-state nanopore technology for sensing the nanoparticle-protein corona complex and comprehend the influence of the resveratrol on the protein adsorption onto the particle surface. We pursued the investigation at the single-molecule level by fluorescence correlation spectroscopy, particularly suitable technique when the size of the nanoparticle approaches the protein dimension. The translocation through the solid-state nanopore revealed different species in presence or absence of resveratrol, revealing the desorption, in NaCl, of the BSA from the nanoparticle when the polyphenol is involved. Clearly from our results, the resveratrol plays an important role, making the BSA adsorption reversible in presence of salt.

[1] T. Lammers, S. Aime, W. E. Hennink, G. Storm, and F. Kiessling, Theranostic nanomedicine, *Accounts of Chemical Research* 44, 1029(2011)

[2] T. S. Hauck, A. A. Ghazani, and W. C. W. Chan, Assessing the effect of surface chemistry on gold nanorod uptake, toxicity, and gene expression in mammalian cells, *Small* 4, 153(2008)

[3] S.H. Brewer, W.R. Glomm, M.C. Johnson, M.K. Knag, S. Franzen, Probing BSA binding to citrate-coated gold nanoparticles and surfaces, *Langmuir* 21, 9303(2005)

[4] S. Cao, D. Wang, X. Tan, and J. Chen, Interaction between trans-resveratrol and serum albumin in aqueous solution, *Journal of Solution Chemistry* 38, 1193(2009)

Composition and morphology of composite materials by ptychographic X-ray computed tomography

J. C. da Silva^{a*}, L. Bloch,^{a,b} A. Pacureanu,^a Y. Yang,^a A. Diaz,^c M. Holler,^c N. Blanc,^d N. Boudet,^d J.-L. Hazemann,^d A. Menzel,^c J. A. van Bokhoven,^{b,c} et P. Cloetens^a

- a. European Synchrotron Radiation Facility, Grenoble, France
- b. Institute for Chemical and Bioengineering, ETH Zürich, Switzerland
- c. Paul Scherrer Institut, Villigen, Switzerland
- d. Institut Néel, Grenoble, France

* E-mail: jdasilva@esrf.fr

The properties of functional composite materials are heavily affected by the arrangement of the different material phases within their 3D structure. The ability of visualizing their structures with high sensitivity and nanometric spatial resolution can improve the engineering of these composites. We show that ptychographic X-ray computed tomography (PXCT) is the key imaging technique to reconstruct quantitative 3D images of the complex-value refractive index of those heterogeneous materials in such a critical length scale[1-5]. Those 3D images can be processed later to extract the localization of the different material phases, the intermaterial pore space[1,2], and the composition of each constituent material of the composite without the need of spectroscopic measurements in certain cases[3,4]. At ESRF, PXCT is available at ID16A beamline. We present here the analysis of the structure of technical catalysts bodies for the oil industry at different lifetimes[1,2], the quantitative characterization of the hydration products of cement pastes[3,4], and the morphological structures of the interface metal-polymer aiming at improving the welding of metals for aerospace industry[5]. We will also quickly discuss the possibilities of the use of coherent beams at CRG beamlines of ESRF.

- [1] J. da Silva et al., ChemCatChem 7, 413-416 (2015).
- [2] J. Ihli et al., Nat. Communications 8, 809 (2017).
- [3] J. da Silva et al., Langmuir 31, 3779-3783 (2015).
- [4] A. Cuesta et al., J. Phys. Chem. C 121, 3044-3054 (2017).
- [5] J. Haubrich et al., Appl. Surf. Sci. 433, 546-555 (2018).

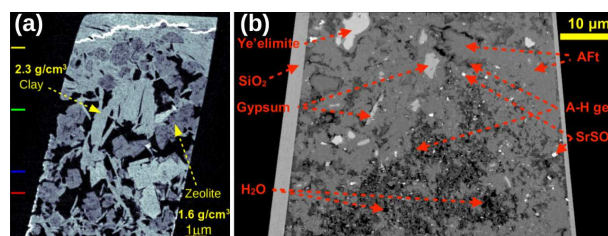


Figure 1: Examples of characterization of heterogeneous materials by PXCT: (a) Catalyst bodies for oil industry[1] and (b) hydrated eco-cement paste[4].

Quantum horizon for silicon nanoelectronics

Silvano De Franceschi^{a*}

a. University Grenoble Alpes & CEA, INAC-PHELIQS, F-38000 Grenoble, France.

* silvano.defranceschi@cea.fr

Silicon transistors are the building blocks of modern microelectronics. We carry billions of them in our pockets every day. Following decades of uninterrupted development, transistors have gotten smaller and smaller, yet the physics laws governing their operation remain largely classical.

Under extreme conditions such as the very low temperatures, however, the switching efficiency of silicon transistors can drastically improve enabling the possibility of realizing electronic circuits with reduced power consumption. At the same time, quantum phenomena become prominent opening the possibility to turn transistors into devices capable of encoding elementary bits of quantum information, so-called qubits, through the spin state of localized electronic charges.

In Grenoble, the Quantum Silicon Group (<https://www.quantumsilicon-grenoble.eu>) which gathers physicists and engineers from different institutions (UGA, CEA, and CNRS), is exploring these opportunities. I will present our research progress in this fascinating and challenging area. Special emphasis will be given to the most relevant results and questions at the fundamental physics level.

The wiggly cosmic string as a waveguide model for propagating massless and massive fields

Frankbelson dos S. Azevedo^{a*}, Fernando Moraes^b, Francisco Mireles^c, Bertrand Berche^d and Sébastien Fumeron^d.

- a. Dynamique et Symétrie, and Collège Doctoral \mathbb{L}^4 for Physics of Complex Systems, Laboratoire de Physique et Chimie Théoriques, UMR Université de Lorraine - CNRS 7019, 54506 Vandœuvre les Nancy, France
- b. Departamento de Física, Universidade Federal Rural de Pernambuco, 52171-900, Recife, PE, Brazil
- c. Centro de Nanociencias y Nanotecnología, Universidad Nacional Autónoma de México, Apdo. Postal 14, 22800 Ensenada B.C., Mexico
- d. Dynamique et Symétrie, Laboratoire de Physique et Chimie Théoriques, UMR Université de Lorraine - CNRS 7019, 54506 Vandœuvre les Nancy, France

* dossanto2@univ-lorraine.fr << corresponding author >>

We examine the effect of a wiggly cosmic string for both massless and massive particle propagation along the string axis. We show that the wave equation that governs the propagation of a scalar field in the neighborhood of a wiggly string is formally equivalent to the quantum wave equation describing the hydrogen atom in two dimensions. We further show that the wiggly string spacetime behaves in an appropriate limit as a gravitational waveguide in which the wave modes propagate with quantized frequencies that depend on the mass, string energy density, and string tension. We propose an analogy with an optical fiber, defining an effective refractive index likely to mimic the cosmic string effect in the laboratory.

Etude du bruit de capteurs de champ à base de jonctions tunnel magnétiques

S.Dounia^{a,b*}, M.Mouchel^a, J.Chidress^a, J.Alvarez-Herault^a, K.Mackay^a

I.L.Prejbeanu^b, et C.Baraduc^b.

a. Crocus-Technology, 5, Place Robert Schuman, F-38054 Grenoble, France

b. Univ. Grenoble Alpes - CNRS - CEA, INAC-SPINTEC, F-38000 Grenoble, France

* sdounia@crocus-technology.com

Dans l'objectif de détecter des champs de plus en plus faibles avec des composants de plus en plus petits, les capteurs de champ magnétique à base de jonctions tunnel magnétiques constituent un choix attrayant. Deux caractéristiques sont importantes pour déterminer la qualité des capteurs : la sensibilité exprimée en %/mT représentant l'intensité du signal mesuré en fonction du champ appliqué sur le dispositif (plus élevée est la sensibilité, meilleur est le dispositif) et la densité spectrale de bruit permettant de quantifier le bruit du dispositif à une fréquence donnée.

Le travail présenté ici est une étude de ces caractéristiques sur des jonctions tunnel uniques de différentes formes (circulaires et elliptiques), tailles et épaisseurs de couches magnétiques.

L'évolution de la résistance des jonctions avec le champ magnétique (courbe R-H) montre un comportement accidenté (en escalier), indicateur de la présence de défauts dans les couches magnétiques. Par ailleurs, l'étude de la densité spectrale de bruit à basse fréquence en fonction du champ montre clairement une corrélation entre la sensibilité et le bruit : les sauts de résistance associés au comportement « en escalier » sont accompagnés par une augmentation du bruit (Fig1a).

Une étude du nombre de sites de piégeage en fonction de la taille et du volume magnétique a été réalisée et a montré que les défauts sont volumiques et que l'impact de chaque défaut est réduit lorsque le nombre de ces défauts augmente (piégeage moins effectif).

La nature du bruit a également été investiguée. L'étude montre que pour de faibles valeurs de sensibilité, seuls des bruits en $1/f$ sont présents, signe d'un grand nombre de fluctuateurs. Lors des sauts de résistance, on observe la présence de bruits Lorentziens d'énergie plus élevée indiquant la présence de fluctuateurs à deux niveaux (Fig1b).

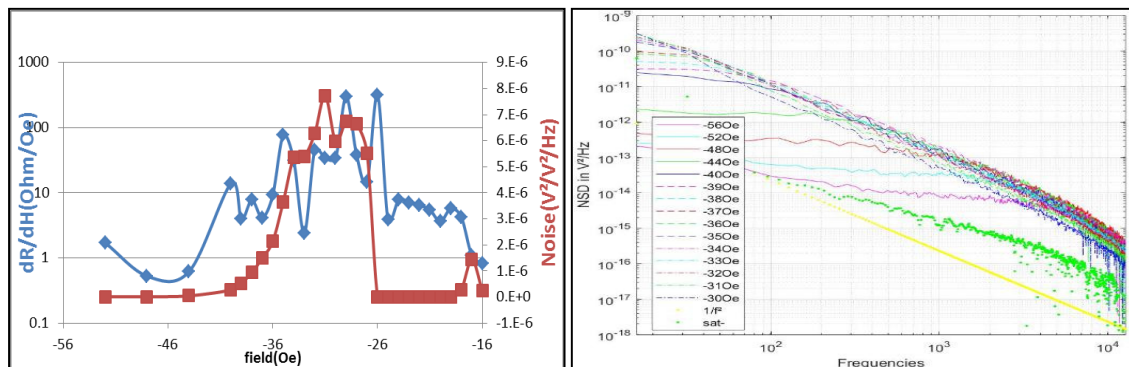


Figure 1 : a) Evolution de la sensibilité dR/dH et du bruit avec le champ, b) Densité spectrale de bruit pour différentes valeurs de champ.

Phonon thermometry below 1 K temperatures

D. Cattiaux^{a*}, X. Zhou^{a,b}, R.R. Gazizulin^a, A. Luck^a, A.D. Fefferman^a, E. Collin^a

a. Université Grenoble Alpes, CNRS Institut Néel, BP 166, 38042 Grenoble cedex 9, France

b. Institut d'Electronique, de Microélectronique et de Nanotechnologie (IEMN), Univ. Lille et CNRS, 59000 Lille, France

* dylan.cattiaux@neel.cnrs.fr

The study of genuine quantum effects in the motion of a mechanical object requires in the first place to cool it down to its quantum ground state. For structures resonating up to 100 MHz, this requires sub-milliKelvin temperatures to be reached.

In order to measure on-chip the phonon temperature of a nano electromechanical systems (NEMS), we have used a circuit based on an optomechanical scheme where a long mechanical resonator is coupled to a microwave cavity. We demonstrate the ability of our device to be actively cooled or amplified. Focusing on this second phenomenon we resolved the parametric instability in order to extrapolate the mode temperature of our nanoscale beam at zero optical antidamping effect. This essentially realizes an in-built parametric amplifier.

The experimental cell is installed in a nuclear demagnetization cryostat able to reach temperatures below 1 mK. Even if active amplification is performed, the main goal is to exhibit the limits of brute force cooling of nanosized objects within a standard microwave setup.

Supraconductivité non conventionnelle dans la famille κ -(BEDT-TTF)₂X

C. Essghaier^{a*}, P. Auban-Senzier^a, C.R. Pasquier^a et C. Mezière^b

- a. Laboratoire de Physique des Solides, UMR 8502 CNRS, Université Paris-Sud, 91405 Orsay, France
 b. Laboratoire MOLTECH-Anjou, CNRS, Université d'Angers, 49045 Angers (France)

* Chaima.essghaier@u-psud.fr

Nous présentons de nouvelles signatures expérimentales de supraconductivité de type d dans les sels de transfert de charge organiques quasi bidimensionnels de la famille κ -(BEDT-TTF)₂X (T_c environ 10K) où X est l'un des anions suivants : X=Cu(NCS)₂, H₈Cu[N(CN)₂]Br et D₈Cu[N(CN)₂]Br. Dans cette famille, la supraconductivité est à la limite de la transition entre l'isolant Mott et le métal et émerge d'une phase antiferromagnétique.

Dans cette présentation, nous présenterons les caractéristiques de conductance différentielle des jonctions N-(I)-S en fonction de la température, du champ magnétique et des axes cristallographiques. Ces jonctions ont été créées à l'aide de la technique dite "spectroscopie à point de contact *soft*". Les pics de conductance à tension nulle apparaissent en dessous de la température critique (fig1). Les résultats sont en accord avec de récentes et par STM qui soutiennent une image de supraconductivité de type d avec des fluctuations de spin comme mécanisme d'appariement [1].

Ces résultats sont renforcés par une analyse plus complète de l'évolution des résistivités dans le plan et hors plan en fonction de la température et du champ magnétique.

[1] D. Guterding et *al*, Phys. Rev. Lett **116**, 237001 (2016)

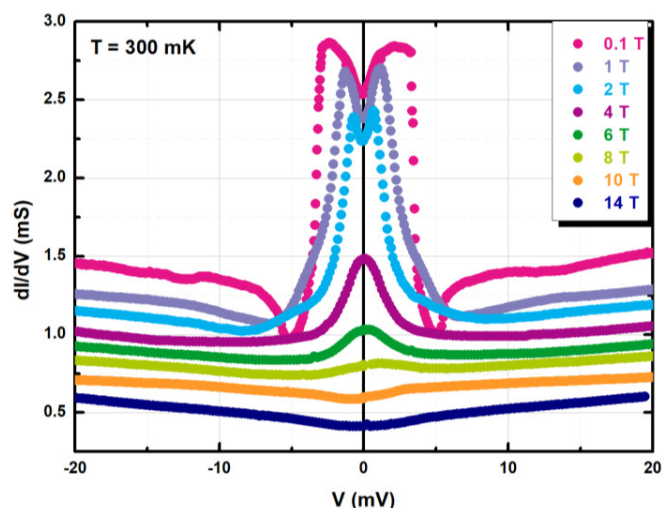


Figure 1 : Caractéristiques de la conductance différentielle à des champs magnétiques allant de 0.1T à 14T pour une température fixe T=300 mK.

Etude par ultrasons de supraconducteurs à base de lanthane en champs magnétiques intenses

Mehdi Frachet,^{a,b,*} David Le Boeuf,^a Siham Benhabib,^a Cyril Proust,^a Jérôme Debray^c

- a. Laboratoire National des Champs Magnétiques Intenses, Grenoble/Toulouse
- b. Université Grenoble Alpes
- c. Institut Néel, Grenoble

* correspondance to : mehdi.frachet@lncmi.cnrs.fr

Lanthanum based cuprate superconductors are highly correlated electrons systems well-know for their structural, magnetic, charge and superconducting instabilities. In underdoped compound (i.e. for doping less than optimal for superconductivity) a dip in the onset temperature for superconductivity T_c , centered at $p \sim 0.125$, occurs, know as the "*1/8 problem*". While the origin of this dip is still under debate, most of the experimental evidence in $La_{2-x}Sr_xCuO_4$ (LSCO) seems to point toward a competition with frozen magnetism¹ whose onset temperature is higher when superconducting T_c is lower.

In order to further investigate the relationship between magnetism and superconductivity we have performed measurements of ultrasonic velocity and attenuation in LSCO. Around $p=1/8$, several anomalies are observed in the sound velocity and attenuation, associated with superconductivity and magnetic freezing. The competition between the two orders parameters is tuned with a magnetic field which enhances magnetic correlations at the expense of superconductivity².

[1] M. H. Julien, Physica B 329-333 (2000) 693.

[2] J. Chang, et al., Phys. Rev. B 78 (2008) 104525.

Dépendance en déformation uniaxiale de la température de transition de l'ordre supraconducteur et de l'ordre de charge dans le cuprate YBCO

Mehdi Frachet,^a Siham Benhabib,^a Benjamin Borgnic,^a David Le Boeuf,^{a*} Cyril Proust,^a

a. Laboratoire National des Champs Magnétiques Intenses (CNRS,UJF,UPS,INSA), Grenoble-Toulouse, France

* correspondance to << david.leboeuf@lncmi.cnrs.fr >>

Nous avons étudié la dépendance en déformation uniaxiale ϵ_i de la température critique supraconductrice T_c dans le cuprate YBCO à différents dopages grâce à des mesures de vitesse du son. Nous nous sommes concentrés sur la dépendance en déformation dans le plan CuO_2 , selon l'axe a, $dT_c/d\epsilon_1$, et b, $dT_c/d\epsilon_2$, de la maille orthorhombique de YBCO. Ces 2 quantités ont une dépendance en dopage complexe et montrent une anisotropie de la dépendance en déformation uniaxiale de la température critique supraconductrice. Nous comparons ces pentes $dT_c/d\epsilon_i$ avec celles mesurées à la transition vers l'ordre de charge 3D uniaxial observé à fort champ magnétique [1]. Une anisotropie similaire à celle observée à la transition supraconductrice est observée à cette transition ordre de charge. Ces observations sont naturellement interprétées comme provenant d'une compétition entre ordre supraconducteur et ordre de charge, contrôlée par la déformation uniaxiale.

[1] T. Wu *et al.* Nature **477** 191 (2011)

A microscopic insight onto phonon dynamics and thermal transport in disordered systems

Valentina M. Giordano

Institute Lumiere Matiere, University of Lyon and CNRS, Villeurbanne, France

* valentina.giordano@univ-lyon1.fr

Despite disordered systems have long been at the focus of scientific research, a microscopic understanding of many peculiar features, marking the difference between disordered and ordered systems, is still missing. Many are such properties, which still give rise to a lively debate, such as the nature of the glass transition, the microscopic mechanisms leading to the physical aging, the origin of disorder-specific vibrational and thermal anomalies...

Recent advanced synchrotron-related experimental techniques, able to capture the vibrational and relaxational properties of liquids and glasses down to a microscopic lengthscale and over typical times ranging from ps to s, have clearly shown the need of a multiscale investigation for significantly advancing the understanding of the physics of glasses.

Vibrational properties indeed will clearly depend on the probed lengthscale, the disorder starting to play a role only when the wavelength becomes comparable to the inter-atomic distance. Similarly, relaxational processes will be active or frozen depending on the comparability between the experimental probing time and the relaxation time.

In this lecture I will revise our experimental investigations of the last 10 years, based on top of the art synchrotron radiation techniques, allowing to probe different time and lengthscales, and identify the different dynamical regimes, and the corresponding key players determining vibrational and thermal properties in disordered systems.

Films de Langmuir d'oxyde de graphène, de liquides ioniques et des systèmes mixtes

H. Ibrahim^{a,b*}, N. Bonatout^{a,b}, F. Muller^{b,c}, P. Fontaine^d, I. Gascon^e, M. Goldmann^{a,d}

- a. Institut des NanoSciences de Paris, Sorbonne Universités, CNRS-UMR 7588, 75005 Paris, France E-mail: helen.ibrahim@insp.upmc.fr
- b. LICORNE, ECE Paris Ecole d'Ingénieurs, Immeuble POLLUX, 75015 Paris, France
- c. LLB, CEA Saclay, 91191 Gif-sur-Yvette, France
- d. Synchrotron SOLEIL L'Orme des Merisiers, Saint Aubin, 91192 Gif-sur-Yvette, France
- e. Physical Chemistry Department and Instituto de Nanociencia de Aragón, Universidad de Zaragoza, 50018 Zaragoza, Spain

Le stockage de l'énergie électrique constitue un problème majeur pour les applications. Les batteries possèdent une durée de vie limitée, étant sensibles à la corrosion de leurs électrodes¹. L'une des alternatives proposées est celle des supercondensateurs à base de liquides ionique (LI) et graphène². Cependant, ces supercondensateurs ne parviennent pas actuellement à stocker suffisamment d'énergie³. Dans ce contexte, l'étude de l'interface graphène ou oxyde de graphène (GO)/LI est primordiale. Nous avons choisi la procédure des films de Langmuir pour élaborer une telle interface.

Nous avons commencé par étudier l'organisation des films purs de GO et LI à l'interface air-eau. Nous avons démontré par réflectivité des rayons X (XRR) et diffraction des rayons X d'incidence rasante (GIXD) que le GO s'auto-assemble à l'interface air-eau en une bicouche de feuillets liées par des molécules d'eau. La monocouche en contact avec l'eau est parallèle et la couche supérieure est formée par des feuillets texturées⁴.

Nous avons ensuite choisi l'lpz-2 comme LI (présentant un cycle de Pyrazolium comme cation et Chlorure comme ion) car il est l'un des rares LI capables de former un film stable à l'interface air-eau. Nous avons observé par XRR et GIXD l'organisation d'une monocouche désorganisée d'lpz-2 à basse pression de surface et d'une triple couche organisée en colonnes à des pressions plus élevées.

Actuellement, nous commençons l'étude des films mixtes de ces deux composantes. Les résultats de Microscopie à angle Brewster (BAM) suggèrent une ségrégation verticale des deux composantes. De même, les résultats de XRR, GIXD et de la fluorescence des rayons X de surface montrent un changement de structure de l'lpz-2 en présence du film d'oxyde de graphène. Ce système semble donc un bon candidat pour l'étude de l'interface GO/LI.

[1] J. Vetter, Ageing mechanisms in lithium-ion batteries, *Journal of Power Sources* **147.1-2** 269–281(2005).

[2] S.Y. Toh, Graphene Production via Electrochemical Reduction of Graphene Oxide: Synthesis And Characterization, *chemical engineering journal*, **251**, 422-434 (2014).

[3] R. Raccichini, The role of graphene for electrochemical energy storage, *Nature materials* **14.3** 271–279 (2015).

[4] N. Bounatout, How exfoliated graphene oxide nanosheets organize at the water interface: evidence for a spontaneous bilayer self-assembly, *Nanoscale* **9**, 12543-12548 (2017)

Anisotropy of the electronic g-factor in the hidden order state of URu₂Si₂ revealed by quantum oscillations

Gaël Bastien^{a,b}, Dai Aoki^{a,c}, Jean-Pascal Brison^a,
Gerard Lapertot^a, Jacques Flouquet^a, Georg Knebel^{a,*}

- a. Univ. Grenoble Alpes, CEA, INAC-Pheliqs, F-38000 Grenoble, France
b. Present address : IFW Dresden, Institute for Solid State Research, Helmholtzstraße 20, 01069 Dresden, Germany
c. IMR, Tohoku University, Oarai, Ibaraki 311-1313, Japan

* georg.knebel@cea.fr

The "hidden order" state in the heavy-fermion compound URu₂Si₂ that develops below $T_0 = 17.5$ K is still under debate despite several decades of research after its discovery. An important characteristic of the hidden order state is the strong Ising-type anisotropy of the magnetic properties of the quasiparticles. We re-investigated the g-factor anisotropy of the quasiparticles in URu₂Si₂ macroscopically by detailed measurements of the superconducting upper critical field H_{c2} and microscopically by Shubnikov-de Haas experiments. From the angular dependence of the amplitude of the Shubnikov de Haas oscillations we determine the anisotropy of the g-factor for the α , β and γ Fermi surface pockets. Both techniques show a strong g factor anisotropy between the c axis and the basal plane. The Shubnikov-de Haas oscillations shows an additional anisotropy in the basal plane for the α Fermi surface pocket. The β branch shows a non-linear Zeeman splitting leading to a reduction of the observed g-factor anisotropy under magnetic field.

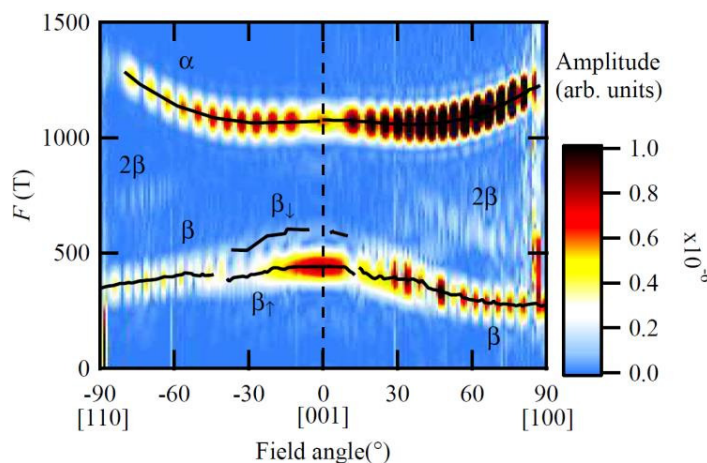


Figure 1: FFT spectra of quantum oscillations at $T=22\sim mK$ in the field range from $12\sim T$ to $15\sim T$ as a function of angle for S2. The color code corresponds to the amplitude of the FFT spectra.

Magneto-active substrates for local mechanical stimulation of living cells

C. M. Bidan^a, M. Fratzl^{b,c}, A. Coullomb^a, P. Moreau^a, A. H. Lombard^{a,*}, I. Wang^a, T. Boudou^d, N. M. Dempsey^b, M. Balland^a, T. Devillers^b and A. Dupont^a

a. Univ. Grenoble Alpes, CNRS, LIPhy, 38000 Grenoble, France

b. Univ. Grenoble Alpes, CNRS, Grenoble INP, Institut Néel, 38000 Grenoble, France

c. Univ. Grenoble Alpes, CNRS, Grenoble INP, G2Elab, 38000 Grenoble, France

d. Univ. Grenoble Alpes, CNRS, Grenoble INP, LMGP, 38000 Grenoble, France

* alain.lombard@univ-grenoble-alpes.fr

The cellular response to an external mechanical stimulation has been investigated with various static and dynamic systems, so far limited to global deformations or to local stimulation through discrete substrates. To apply local and dynamic mechanical constraints at the single cell scale through a continuous surface, we have developed and modelled magnetoactive substrates made of magnetic micro-pillars embedded in an elastomer. Constrained and unconstrained substrates are analysed to map surface stress resulting from the magnetic actuation of the micro-pillars and the adherent cells. These substrates have a rigidity in the range of cell matrices, and the magnetic micro-pillars generate local forces in the range of cellular forces, both in traction and compression. As an application, we followed the protrusive activity of cells subjected to dynamic stimulations. Our magneto-active substrates thus represent a new tool to study mechanotransduction in single cells, and complement existing techniques by exerting a local and dynamic stimulation, traction and compression, through a continuous soft substrate. The coupling of the magneto-active substrates with FRET-based biosensors reporting in live the biochemical activity of Rho-GTPases will allow studying mechanotransduction with spatio-temporal correlations between mechanical and biomechanical signals.

- [1] *Magneto-active substrates for local mechanical stimulation of living cells*, C. M. Bidan¹, M. Fratzl^{2,3}, A. Coullomb¹, P. Moreau¹, A. H. Lombard^{1,*}, I. Wang¹, T. Boudou⁴, N. M. Dempsey², M. Balland¹, T. Devillers² and A. Dupont¹, *Scientific Reports* (2018 8 :1464)

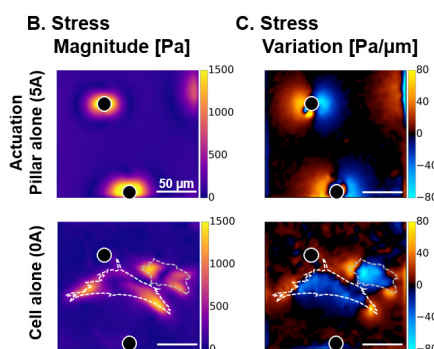


Figure 1: Stress maps in TFM with and without cells

Quantum transport in deformed dice lattice

Lassaad Mandhour*, Farah Bouhadida, et Ameni Daboussi

a. Laboratoire de Physique de la Matière Condensée, Département de Physique, Faculté des Sciences de Tunis, Université Tunis El Manar, Campus Universitaire 1060 Tunis, Tunisia

* lassaad.mandhour@istmt.utm.tn << corresponding author >>

Graphene, a single sheet of carbon atoms forming a honeycomb lattice (HCL). The T_3 or dice lattice presents the same structure as HCL with an additional site at the center of each hexagon. The corresponding band structure presents the same one as HCL with an additional flat band at the Dirac point. An uniaxial strain on the T_3 lattice induce a moving and a deformation of Dirac cones. At moderate deformation, the dispersion relation remain linear in all direction but for a suitable strong strain, the two Dirac points merge into a single one and a gap opens. This merging of Dirac points signals a topological transition from a semi-metallic to an insulating phase. We study theoretically the effect of the uniaxial strain on the quantum transport in the dice lattice. We focus on the transmission across a potential barrier perpendicular to the strain axis, on the conductivity as well as on the shot noise. Particularly, for an energy equal half the barrier height, the barrier becomes totally transparent (the super Klein tunneling [1]) at moderate deformation and becomes nearly opaque when the two Dirac points merge.

[1] D.F. Urban, D. Bercioux, M. Wimmer and W. Häusler, Phys. Rev. B **84**, 115136 (2011).

[2] F. Piéchon, J.-N. Fuchs, A. Raoux, and G. Montambaux, J. Phys.: Conf. Ser. **603**, 012001 (2015).

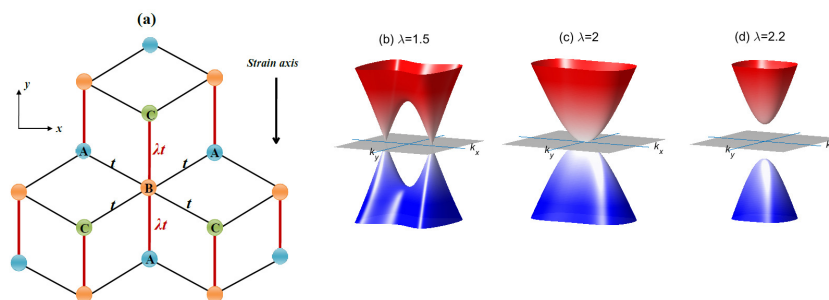


Figure 1: (a) Strained dice lattice. There are three sites A,B and C in each unit cell. The hopping amplitude connecting B to C and B to A is λt along the strain axis (red thick lines) and t (black thin lines) in the other directions. (b-d) The energy spectrum of the Strained dice lattice for three values of the strain parameter λ . For $\lambda = 2$ the low energy dispersion is linear in the k_y direction and quadratic in the k_x direction (the T_3 semi-Dirac model [2]).

Quantum transport in a ballistic shifted bilayer graphene

Lassaad Mandhour* et Ameni Daboussi

a. Laboratoire de Physique de la Matière Condensée, Département de Physique, Faculté des Sciences de Tunis, Université Tunis El Manar, Campus Universitaire 1060 Tunis, Tunisia

* lassaad.mandhour@istmt.utm.tn << corresponding author >>

Two graphene layers generally stack over the common AB or Bernal stacking configuration. Recently, it has been reported that a stacking defects can occur in natural and synthetic graphene bilayer systems. Stacking defaults (or shift) of a bilayer graphene turn the low-energy band structure into pairs of Dirac cones [1]. Here we theoretically investigate how a shift between the two layers of a bilayer graphene could affect the quantum transport. Starting from the four-band energy hamiltonian, we report a calculation of the conductivity and the Fano factor F in shifted bilayer graphene within the Landauer-Büttiker approach. Then we discuss the effect of the stacking default and the orientation of the Dirac cones on the pseudo-diffusive regime ($F = 1/3$) [2] around the neutrality point. We found that the range of energies which this pseudo-diffusive regime holds can be suppressed for a specific stacking default.

- [1] A. Daboussi, A. L. Mandhour, J.N. Fuchs and S. Jaziri, Phys. Rev. B **89**, (2014) 085426.
 [2] J. Tworzydło, B. Trauzettel, M. Titov, A. Rycerz, and C. W. J. Beenakker, Phys. Rev. Lett. **96**, 246802 (2006).

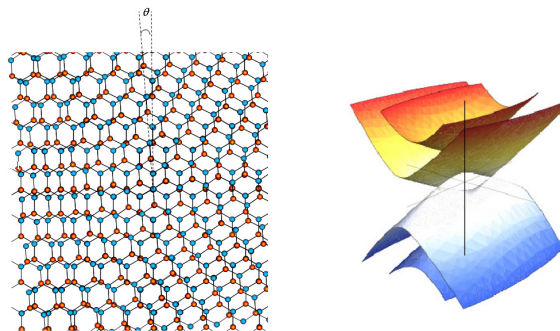


Figure 1: Left: The twisted bilayer graphene is an example of shifted bilayer graphene. Right: energy band structure of the twisted bilayer graphene.

Observation et caractérisation de nano objets vibrants

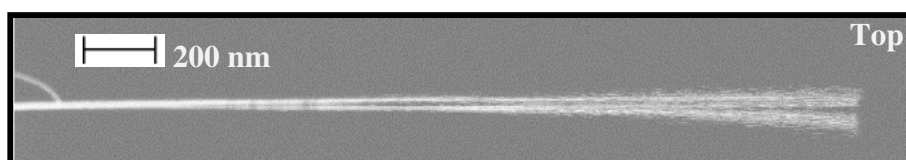
S. Pairis^{a,*}, F. Donatini^a, M. Hocevar^{a,b}, D. Tumanov^{a,b}, N. Vaish^{a,b}, J. Claudon^c,
J.-P. Poizat^{a,b} and P. Verlot^d

- a. Univ. Grenoble Alpes, CNRS, Grenoble INP, Institut Néel, F-38000 Grenoble, France
- b. CNRS, Inst. NEEL, "Nanophysique et semiconducteurs" group, 38000 Grenoble, France
- c. Univ. Grenoble Alpes, CEA, INAC, PHELIQS,
Nanophysique et semiconducteurs Group, F-38000 Grenoble, France
- d. Université Claude Bernard Lyon 1, UCBL,
Domaine Scientifique de La Doua, 69622 Villeurbanne, France

* sebastien.pairis@neel.cnrs.fr

Le microscope électronique à balayage est un outil de choix pour l'observation des nano objets et nanostructures. Couplé à des systèmes d'analyses, il est couramment employé pour effectuer des caractérisations chimiques (EDS ou WDS) et de texture cristallographique (EBSD). Il peut être également utilisé comme un véritable instrument de mesures physiques en enregistrant et en analysant les signaux provenant de ses détecteurs habituellement dédiés à l'imagerie.

La présentation portera sur l'observation des oscillations mécaniques dans des micro et nanostructures de diamètres inférieurs à 50 nm - nano-fils de carbone et nano-piliers de semi-conducteur InAs - ainsi que sur la méthode de mesure de leur fréquence de vibrations à partir de la détection des électrons secondaires. La présentation sera complétée par des simulations de Monte-Carlo sur ces nano objets [1]. Cette méthode originale offre la possibilité de contrôler de nombreux types de structures micro et nano-électromécaniques, dont la détection du mouvement est impossible optiquement en raison de la limite de diffraction de la lumière.



Vibration d'un nano fil de carbone (SE)

[1] : H. Demers, N. Poirier-Demers, A. Réal Couture, D. Joly, M. Guilmain, N. de Jonge, and D. Drouin. (2011). "Three-dimensional electron microscopy simulation with the CASINO Monte Carlo software." Scanning 33(3): 135-146.

Etude par simulations du rôle de la géométrie et des défauts sur les propriétés de conduction électrique des nanopores.

Fabien Picaud^{a*}, et Jérémy Bentin^a

- a. Laboratoire de Nanomédecine, Imagerie et Thérapeutiques, Université de Bourgogne-Franche-Comté, 16 route de Gray, 25000 Besançon

* fabien.picaud@univ-fomte.fr

La nanofluidique est de nos jours un domaine en pleine extension par les propriétés uniques de transport qui apparaissent dans ces milieux nanoscopiques où le confinement des particules est ultime [1]. Différents nanopores ont récemment vu le jour et ont été étudiés en profondeur par les expérimentateurs et les courbes caractéristiques « courant/tension » appellent souvent au questionnement quant à la réalité physique des phénomènes mis en jeu [2]. La simulation par dynamique moléculaire apparaît alors comme un outil indispensable permettant d'aller scruter plus en détails ce qu'il peut se dérouler au sein même du nanopore.

Nous proposons dans cette étude de montrer quelques résultats de simulations ayant permis de comprendre comment, dans des nanotubes de carbone, les courants courant/tension pouvaient varier de droite pure à des courbes activées [2]. En effet, la présence de défaut de charges sur la surface du nanotube de carbone engendre une barrière de potentiel à franchir pour les ions ralentissant leur progression normale jusqu'à un seuil de potentiel suffisant pour retrouver un comportement naturel.

Puis nous continuerons nos explorations en discutant les premiers résultats visant à simuler le comportement de nanopores coniques hydrophobes de différentes sections. Bien qu'étudiés expérimentalement depuis quelques années, les simulations de tels systèmes restent rares. Nous montrerons notamment que le rôle de la charge de surface, même minime, peut être crucial dans l'obtention d'un courant et que les premières simulations apparaissant plutôt encourageantes pour la poursuite de nos études [3].

[1] « Nanopores and Nanochannels: From Gene Sequencing to Genome Mapping », S. Howorka et al., ACS Nano (2016), 10, 9768

[2] "Voltage-activated transport of ions through single-walled carbon nanotubes", Yazda et al, Nanoscale (2017), 9, 11976

[3] "Unexpected ionic transport behavior on hydrophobic and uncharged conical nanopore", S. Balme et al. Faraday Discussion, in press (2018)

Field induced Fermi surface instabilities in UPd_2Al_3

Alexandre Pourret^{a*}, Georg Knebel^a, A. Gourgout^a, G. Bastien^a, D. Aoki^b,
G. Seyfarth^c, I Sheikin^c, J. Flouquet^a

- a. Univ. Grenoble Alpes, CEA, INAC, PHELIQS, F-38000 Grenoble, France
b. Institute for Materials Research, Tohoku University, Oarai, Ibaraki, 311-1313, Japan
c. Laboratoire National des Champs Magnétiques Intenses (LNCMI), CNRS, Univ. Grenoble Alpes, 38042 Grenoble, France

* alexandre.pourret@cea.fr

Fermi surface (FS) instabilities, such as Lifshitz transitions, which have been neglected in mean field theories has recently been mentioned as a driving force to modify the ground-state properties in correlated electron systems such as cuprates, pnictides and heavy fermion materials. Due to the strong quasiparticle renormalization, the latter possess flat bands close to the Fermi level. These flat bands are extremely sensitive to external parameters such as doping, pressure or magnetic field. In particular, field induced Lifshitz transitions have been identified in an increasing number of systems [1,2]. I will present recent thermoelectric power (TEP) measurements in the antiferromagnetic superconductor UPd_2Al_3 . A succession of anomalies appears at low temperature as a function of magnetic field below the metamagnetic transition (which occurs at $H_M=18\text{T}$), see Fig. 1. We can attribute the different anomalies to complex topological changes occurring in the FS. Additionally, we observe a sudden change of sign in the TEP and in the Hall coefficient at H_M from the AF state to the polarized paramagnetic (PPM) state. The appearance of large TEP quantum oscillations in the PPM state indicates a strong FS reconstruction above H_M due to the unfolding of the electronic bands.

[1] A. Pourret, et al., J. Phys. Soc. Jpn. 82, 053704 (2013)

[2] G. Bastien, et al., Phys. Rev. Lett. 117, 206401 (2016)

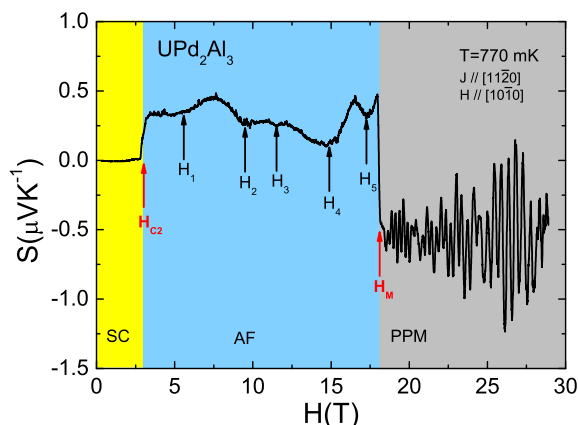


Figure 1: Field dependence of the thermoelectric power at $T = 770$ mK.

Faisceaux d'ions Ar non-focalisés (BIB) pour l'analyse EBSD 3D à grand volume.

V. Richard^a, T. Hosman^b,

- a. Gatan France - ROPER SCIENTIFIC SAS, Evry France
- b. Gatan, Inc, Pleasanton USA.

Le polissage par faisceaux d'ions non focalisé (BIB) permet d'obtenir efficacement des données EBSD 3D sur des zones de plusieurs mm² en raison de la taille de son faisceau. L'utilisation d'ions Argon de faible énergie entraînent très peu d'endommagements à la surface de l'échantillon à l'issue de la coupe et permet d'obtenir une excellente analyse EBSD.

Le système utilisé, l'IPrep II de Gatan, permet l'automatisation de la préparation des coupes (de quelques dizaines à plusieurs centaines de nanomètres) et l'acquisition des cartographies EBSD dans le MEB. Le passage de l'échantillon entre le polisseur ionique et le MEB / EBSD est entièrement automatique et géré par un automate. Un support spécifique permet le transfert de l'échantillon de manière reproductible de la zone de préparation au MEB, des algorithmes spécifiques de mise au point automatique et de repositionnement sont ensuite utilisés pour aligner et focaliser l'échantillon avant l'acquisition EBSD.

Au cours de cette conférence, nous montrerons des résultats obtenus sur différents types d'échantillons : métallurgiques (acier dual-phase (DP), alliage de cuivre, ...) et géologiques. Cette technique a permis par exemple d'estimer pour les aciers dual-phase la répartition en 3D de la martensite dans l'échantillon. Comme la martensite joue un rôle important dans les propriétés mécaniques de ces aciers, il est important de la localiser et de la distinguer de la ferrite.

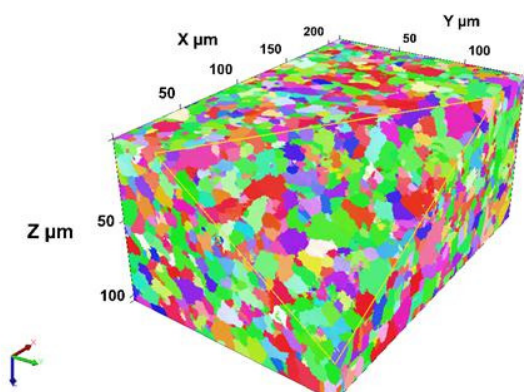


Figure 1 : Dual-phase (DP) steel : 3D reconstruction of EBSD x IPF data acquired using automated SSBIB tomography. The volume is 213x141x 103 μm³ with 0.5x0.5x0.7 μm³ voxels. Milling used 8 keV Argon ions at 5° incidence for 7 minutes per slice, followed by EBSD acquisition of 20 minutes per slice. L. Kestens, H. Pirgazi, Ghent University.

Finite temperature aspect ratio of Bose gas

S. Kouidri^{a*}

a. Department of Physics, University of Saida, 20000 Saida, Algeria

* kouidris@yahoo.fr << S. Kouidri >>

We perform a comparative study of the aspect ratio at finite temperature for a Bose gas with contact interactions. We use both the Hartree-Fock Bogoliubov Popov (HFB-P) approximation and the Generalized Hartree-Fock Bogoliubov approximations (GHFB) which includes the anomalous thermal average. We calculate the radius of the condensate density in Thomas-Fermi limit as function of condensed fraction.

[1] S. Kouidri, Aspect ratio Bose gas variation via condensed fraction, article in preparation.

Cavitation et confinement

Panayotis Spathis^{a*}, Victor Doebele^a, Hermann Böttcher^a, Fabien Souris^a, Laurent Cagnon^a, Annie Grosman^b, Isabelle Trimaille^b, Etienne Rolley^c, Joël Puibasset^d, et Pierre-Etienne Wolf^a

- a. Institut Néel, CNRS/UGA, UPR2940, Grenoble
- b. INSP, CNRS/UPMC, UMR 7588, Paris
- c. LPS-ENS, CNRS/Univ. Paris Diderot/UPMC, UMR 8550, Paris
- d. Interfaces, Confinement, Matériaux et Nanostructures, CNRS et Université d'Orléans, UMR 7374, Orléans

* panayotis.spathis@neel.cnrs.fr

La cavitation joue un rôle central dans de nombreux domaines. Cependant, la Théorie Classique de la Nucléation (TCN), qui décrit les conditions d'apparition de la cavitation homogène dans un fluide massique, n'a pu être vérifiée quantitativement que dans peu de systèmes. Par ailleurs, l'influence d'un confinement sur la cavitation homogène reste débattue, plusieurs expériences récentes ayant donné des résultats contradictoires.

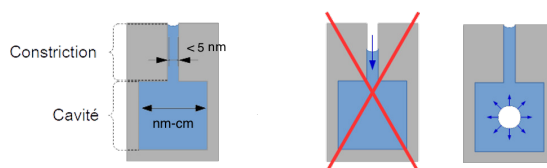


Figure 1: Schéma des pores étudiés. Le faible diamètre des constriction (< 5 nm) permet, en diminuant la pression du gaz extérieur, d'atteindre les conditions de cavitation dans la cavité (de taille modulable entre quelques nm et le cm) avant que la constriction ne se vide.

Dans cet exposé, nous décrivons comment le projet CAVCONF devrait éclairer la situation. D'une part, nous utilisons des fluides cryogéniques (hélium et azote) et la technique d'arbre synthétique développée à l'Université de Cornell (USA) [1] pour tester les prédictions de la TCN pour la cavitation homogène. D'autre part, nous étudions l'influence du confinement en utilisant des membranes poreuses d'alumine et de silicium contenant des pores en forme de bouteille d'encre. Enfin, nous cherchons à vérifier une idée théorique récente, qui est, que dans des cavités de petit volume, la conservation de la masse bloque la cavitation. Nous présenterons nos premiers résultats.

- [1] Wheeler et Stroock, The transpiration of water at negative pressures in a synthetic tree, Nature 455, 208 (2008).
- [2] Vincent, Dynamique de bulles de cavitation dans de l'eau micro-confinée sous tension. Application à l'étude de l'embolie dans les arbres, Thèse UGA, (2012)

Ce travail est soutenu par l'ANR dans le cadre du projet CAVCONF.

Table-Ronde : Peer review au 21e siècle

Martina Knoop^a, Bart Van Tiggelen^{b*}, Agnès Henri^c, et Jean Daillant^d

- a. PIIM (UMR 7345), CNRS/Aix-Marseille Université
- b. LPMMC, UMR 5493, CNRS/Université de Grenoble Alpes, Grenoble
- c. EDP Sciences, Les Ulis.
- d. Société Civile Synchrotron SOLEIL, CEA/CNRS, Gif-sur-Yvette.

* contact : bart.van-tiggelen@lpmmc.cnrs.fr

La Commission Publications de la SFP propose une séance sur l'évaluation par les pairs (« Peer Review ») des publications scientifiques. Le *Peer Review* fait partie du quotidien de chaque physicien, que ce soit en tant qu'auteur ou rapporteur. Aujourd'hui, la pratique traditionnelle pour publier un article de physique commence souvent par le dépôt du « preprint » sur ArXiv donc sans filtre de qualité, suivi par la soumission à une revue académique qui organise la relecture, souvent anonyme, par des pairs avant publication. Le *Peer Review* est considéré comme indispensable pour maintenir la qualité scientifique de nos publications, la carte de visite de nos travaux.

Mais le système actuel semble à bout du souffle et obsolète. Ya-t-il trop de rapports à rédiger ? Les rapporteurs sont-ils sur-sollicités ? Leurs rapports sont-ils trop souvent biaisés ? La publication des grandes découvertes est-elle ralentie ou bloquée par les pairs-concurrents ?

Cette séance permettra d'échanger sur les problèmes d'éthique, de science, et d'organisation liés au *Peer Review* pour en proposer une modernisation. Faut-il publier les rapports ? Divulguer le nom du rapporteur ? Remplacer le *Peer Review* par un blog sur le Web ?

Nous invitons tous les adhérents de la SFP et les congressistes des JMC ayant une activité de *Peer Review* à renseigner une enquête qui alimentera les échanges du mercredi 29 août à Grenoble. [LIEN vers l'enquête](#).

Transport sous un gradient de température dans les fluides complexes: le piston de Rayleigh

Simon Villain-Guillot^{a,*} et Alois Würger^a

a. LOMA - Laboratoire Onde Matière d'Aquitaine, Université de Bordeaux

* simon.villain-guillot@u-bordeaux.fr

La **thermophorèse et de l'effet Soret** permettent de comprendre le transport dans les fluides complexes dont le contrôle est un challenge important en biotechnologie et en microfluidique. Dans un gradient de température, on observe un mouvement des solutés. La vitesse de transport, via le coefficient de diffusion qui apparait dans la relation phénoménologique d'Onsager $= -D_T \nabla T$, dépend du soluté considéré. Ce qui permet par exemple de séparer des espèces dans un micro canal.

Comme modèle pour ce problème, nous avons regardé l'exemple du **piston de Rayleigh** : dans un cylindre, un piston mobile, supposé adiabatique, (représentant le soluté comme une macro particule sans structure interne) fluctue du fait des collisions avec les deux gaz qu'il sépare. Même si les pressions dans les deux réservoirs semi infinis sont égales, i.e. même s'il y a équilibre macroscopique, dès que les températures sont différentes, le système est hors équilibre et acquiert une vitesse moyenne non nulle, proportionnelle au gradient ∇T .

Le piston se comporte ainsi comme un **rectificateur des fluctuations ou du mouvement Brownien**. Par conséquent, il existe un transfert thermique entre les deux gaz, alors même que le piston est adiabatique (il n'a pas de degré de liberté interne pouvant conduire la chaleur). Ce flux thermique est à l'origine d'un flux d'entropie que nous avons calculé, associé au travail de la « force généralisée ».

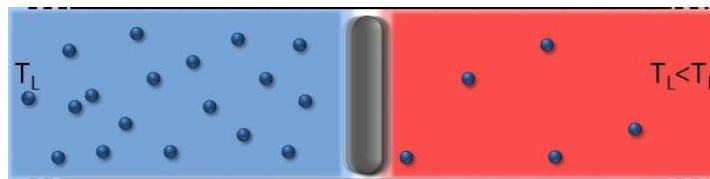


Figure 1 : Le piston de Rayleigh séparant dans un canal unidimensionnel deux gaz à des températures et/ou des pressions différentes.

Comparative study of mechanical and structure properties of geopolymer matrices incorporated by nano-silica, nano-alumina and nano-zinc

Z. Zidi^a, M. Ltifi^{b,c}, Z.Ben Ayadi^a and L.El Mir^{a,d}

- a. Laboratory of Physics of Materials and Nanomaterials Applied at Environment, College of Sciences in Gabes, Tunisia
- b. Al-Imam Mohammad Ibn Saud Islamic University, College of Engineering, Department of Civil engineering, Riyadh, Saudi Arabia
- c. Al Manar University, National Engineering School of Gabes, Department of Civil engineering, Gabes, Tunisia
- d. Al-Imam Mohammad Ibn Saud IslamicUniversity, College of Sciences, Department of Physics, Riyadh, SaudiArabia

Corresponding Author: Zidizoo18@gmail.com

Abstract:

This work aims to study the effect of nano-silica, nano-alumina and nano-zinc on structural and mechanical properties of geopolymer matrix. The composite is produced by metakaolin, alkaline solution constant L/S ratio 0.55. The products is investigated by XRD, XRF, FTIR, SEM, UV/VIS and compressive strength test. The result show that nano-alumina increased more the mechanical and structural properties of geopolymer than nano-silica and nano-zinc. From FTIR spectra, we find that amorphous structure and geopolymer gel content are increased for the all nanoparticles but nano-alumina is more effective than other oxides. Dense structure as also observed in SEM investigation. Same results are also seen on physicals properties.

Key words: geopolymer, nano-silica, nano-alumina, nano-zinc, mechanical properties, structure properties

Liste des auteurs

Ababou Soraya, 212
Aballe Lucia, 250
Abbassi Abdelatif, 427
Abbassi Abdellatif, 522
Ablett James, 116
Abramovici Gilles, 5
Abushammala Haneen, 6
Achra Swati, 451
Adda Coline, 242
Affouard Frederic, 357
Agnus Guillaume, 323
Aguirre Garbiñe, 433
Ahufinger Veronica, 386
Ait Oukaci Kousseila, 1
Ait-Hellal Fatima, 391
Ajejas Fernando, 2
Alba-Simionesco Christiane, 347
Albaret Tristan, 176, 245
Albert Mathias, 7, 58
Albertini David, 179
Alberto Riminucci, 436
Albigès-Rizo Corinne, 173
Albin Clément, 481
Alibart Fabien, 8
Alkurdi Ali, 3
Allègre Olivier, 19
Allain Clémence, 404
Allard-Trippé Gaele, 470
Allouche Billal, 489
Alonzo Mathieu, 141
Alzina Francesc, 209
Amand Thierry, 108
Amara Mohamed, 343
Amichi Lynda, 449
Amico Luigi, 379
Amine Chloé, 54
Amissé Anthony, 4, 109
Amo Alberto, 9, 10
Amrit Jay, 485
Andreazza Pascal, 11, 382, 393
Andreazza-Vignolle Caroline, 11, 382, 393
Anelli Andrea, 152
Anfray Valentin, 12
Antonenko D., 147
Aoki Dai, 72
Appert Estelle, 284
Aprà Agostino, 109
Aqdim Said, 148
Arabski Jacek, 436
Aradilla David, 520
Arbouet Arnaud, 233
Arcizet Olivier, 328
Ardavan Arzhang, 225
Ariando Ariando, 422
Arjmand Tabassom, 302
Arras Rémi, 13
Arrighi Pablo, 14
Artaud Alexandre, 15, 529
Artioli Alberto, 267
Attané Jean-Philippe, 319, 361
Audouard Alain, 264
Auffeves Alexia, 16, 259, 344
Auffret Stéphane, 181
Avriller Rémi, 17
Ayari Anthony, 120, 209
Ayed Hamida, 523
Aymonier Cyril, 18
Ayrat Thomas, 12, 19
Azzini Stefano, 298

Böhm Martin, 482
Böttcher Hermann, 139, 140, 551
Béa Hélène, 462
Babich Danylo, 242
Baboux Nicolas, 57, 179
Bachtold Adrian, 469
Bachtold, Adrian, 360
Bacri Laurent, 415
Bahri Mounib, 25
Bai Xiaofei, 20
Baillin Xavier, 284
Bain Nicolas, 26
Baines Christopher, 447
Bakangura Erigene, 27
Baldim Victor, 45
Balestro Franck, 28, 50
BALIBAR, Sébastien, 360

Ballet Philippe, 361
 Ballou Rafik, 88, 105, 312
 Baltz Vincent, 181
 Bannenberg Lars, 338
 Bano E, 367
 Baraduc Claire, 462
 Barbarino Giuliana, 488
 Bardin Fabrice, 97
 Bardotti Laurent, 481
 Barnes Jean, 254
 Barnes Jean-Paul, 145
 Baron Thierry, 214, 277
 Barraud Clément, 279
 Barraud Sylvain, 109, 287
 Barredo Daniel, 129
 Barresi David, 21, 22
 Barthélemy Quentin, 29, 30
 Bartok-Partay Livia, 31
 Bartolo Denis, 346
 Bartos Miroslav, 161
 Basile Audoly, 32
 Basko Denis, 190
 Bassani Franck, 214, 284
 Bastie Pierre, 316
 Bath Jonathan, 225
 Baudelet François, 116
 Baudin Emmanuel, 33
 Bauerle Christopher, 4, 109, 150, 348
 Baulin Oriane, 34
 Baum Markus, 35
 Bazaliy Yaroslaw, 400
 Beaurepaire Eric, 436
 Beauvois Ketty, 36
 Beigné Cyrille, 183, 320, 518
 Bellaiche Laurent, 138
 Bellec Matthieu, 58
 Bellessa Joel, 480
 Bellon Ludovic, 170
 Bellot Gaetan, 37
 Belmeguenai Mohamed, 462
 Belzig Wolfgang, 172
 Benabdeslem M, 38
 Bendiab Nedjma, 395, 451
 Benhabib Siham, 538, 539
 Benoit Magali, 78
 Benslim Nouredine, 39
 Bentin Jérémy, 40, 547
 Benton Owen, 243
 Benzo Patrick, 194
 Berciaud Stéphane, 298, 371
 Bergen Lorenz, 105
 Berger Claire, 128
 Berhanu Michael, 41
 Berhaut Christopher, 520
 Bermudez David, 42
 Bernand-Mantel Anne, 462
 Bernard Mathieu, 474
 Bernert Marie, 43
 Bernier Nicolas, 229
 Bernon Simon, 44
 Berret Jean-François, 45
 Berrod Quentin, 519
 Bertet Patrice, 121
 Berthier Claude, 281
 Bertin Eric, 46
 Bertran François, 117
 Bertrand Benoit, 4, 109, 256
 Bescond Marc, 188
 Besga Benjamin, 328
 Besland Marie-Paule, 242
 Besombes Lucien, 60
 Beugnon Jerome, 524
 Beutier Guillaume, 47
 Beznasiuk Daria, 48, 49
 Bharadwaj Karthik, 114, 289, 383
 Biancalana Fabio, 309, 413
 Biance Anne-Laure, 466
 Biard Hugo, 50
 Bienaimé Tom, 201
 Bieniek Bjoern, 83
 Biermann Silke, 291
 Bihi Ilyesse, 51
 Billiot Gérard, 287
 Billon Laurent, 433
 Blanc Nils, 532
 Bleuse Joël, 169, 267
 Blinder Rémi, 281
 Bloch Jacqueline, 52
 Bloch Leonid, 532
 Bluet Jean-Marie, 3
 Blum Ivan, 310
 Bochkarev Anton, 53
 Bocquet L., 352
 Bocquet Lydéric, 77
 Bodiguel Hugues, 221
 Boehm Martin, 468
 Bohuslavskyi Heorhi, 109
 Bohuslavsky Heorhii, 4, 287
 Boire Adeline, 54
 Boisron Olivier, 481
 Bonnefoy Maxime, 55
 Bonnet Romeo, 279

Bordet Pierre, 126, 127
 Borgnic Benjamin, 539
 Boronat, Jordi, 360
 Bortolotti Paolo, 296
 Borz Mario, 56, 310
 Bossy Jacques, 316
 Bottegoni Federico, 183, 518
 Bouard Chloé, 319
 Bouaziz Jordan, 57
 Bouchiat Vincent, 495
 Boudet Nathalie, 532
 Boudinar Naouam, 23
 Bougerol Catherine, 145, 254, 449
 Boughdad Omar, 58
 Bouhallab Saïd, 59
 Boukari Hervé, 60
 Boukari Samy, 436, 525
 Boukhouiete Amel, 526
 Boulle Olivier, 250, 462
 Bourdarot Frederic, 61
 Bourdet Léo, 62, 109, 492
 Bourgeois Olivier, 211
 Bourrier Antoine, 63
 Bousquet Jessica, 64
 Boutefnouchet Abdelatif, 24
 Boutu Willem, 65
 Bowen Martin, 436
 Boya R., 352
 Brûlet Annie, 433
 Braithwaite Daniel, 66
 Braive Rémy, 339
 Bramato Alberto, 201
 Brambilla Alberto, 518
 Briand Emrick, 248
 Brihuega I., 146
 Brisset François, 67
 Browaeys Antoine, 129
 Brubach Jean-Blaise, 105, 276
 Brun-Cosme-Bruny Marvin, 68
 Brunelli Michela, 527
 Brunet Annael, 464
 Buda-Prejbeanu Liliana, 250, 313
 Bugnet Matthieu, 69
 Buhler Eric, 70
 Buhot Arnaud, 71
 Buhot Jonathan, 72
 Buisson Olivier, 73, 114, 289, 383
 Burdin Sébastien, 72
 Bureau Lionel, 74
 Burle Nelly, 474
 Buset Pablo, 331
 Bussetti Gianlorenzo, 518
 Bustarret Etienne, 64
 Butté Raphael, 145
 Buzdin Alexander, 414
 Cécile Naud, 114, 289, 383
 Cadete Santos Aires Francisco J., 69
 Cagnon Laurent, 139, 140, 551
 Calloni Alberto, 518
 Calvo Florent, 78
 Camarero Julio, 2
 Camosi Lorenzo, 377
 Campillo Clément, 79
 Canals Benjamin, 15
 Canepari Marco, 80
 Canero-Infante Ingrid, 138
 Canet Leonie, 461
 Cano Andres, 81
 Cantat Isabelle, 82, 251
 Capiod Pierre, 481
 Capponi Sylvain, 281
 Carbogno Christian, 83
 Cario Laurent, 242
 Carlin Jean-François, 145
 Carlos Sabín, 84
 Carrete Jesús, 85
 Cartellier Alain, 282
 Caruso Giuseppe Mario, 233
 Carusotto Iacopo, 86
 Casanove Marie-José, 13
 Casanove Marie-Jose, 194
 Casciola Carlo Massimo, 440
 Cassabois Guillaume, 509
 Castellani Niccolo, 229
 Castiella Marion, 194
 Castillo Gustavo, 41
 Casula Michele, 87, 116, 264
 Cathelin Vadim, 88, 312
 Cavassilas Nicolas, 188
 Cayla Hugo, 89
 Cazayous Maximilien, 72
 Cazorla Maxime, 97
 Cepellotti Andrea, 469
 Cercellier Hervé, 90
 Ceriotti Michele, 152
 Chérif Salim-Mourad, 462
 Chaboussant Gregory, 338
 Chaix Laura, 75
 Chamard Virginie, 91
 Champel Thierry, 92
 Chandesris Dominique, 93
 Chanrion Emmanuel, 348

Chaouche Mouna, 94
 Chapel Jean Paul, 95
 Chapelier C., 146
 Chapelier Claude, 15, 320, 528, 529
 Chapon Laurent, 88, 312
 Chapuis Pierre-Olivier, 3, 209, 378
 Charitat Thierry, 96
 Charlaix Elisabeth, 110, 282, 446
 Charlot Benoit, 97
 Chaste Julien, 530
 Chauveau Jean-Michel, 286
 Chaves Dayane, 250
 Chemmi Houria, 375
 Chen Jinjie, 436
 Chen Yani, 395
 Chennevière Alexis, 27, 99
 Chernozatonskii Leonid, 274
 Cherroret Nicolas, 441
 Chervy Thibault, 298
 Chigarev Nikolay, 138
 Chirtoc Mihai, 216
 Chong Michael, 371
 Chou Qiao-Ling, 470
 Chouahda Zohra, 76
 Choueikani Fadi, 436
 Chrafi Younes, 98
 Christoulaki Anastasia, 27, 99
 Chshiev Mairbek, 222, 457, 462
 Ciccacci Franco, 518
 Ciliberto Sergio, 100
 Citro Roberta, 363
 Clément Jean-François, 101
 Claiser Nicolas, 508
 Claudon Julien, 49, 169, 259, 267, 486
 Cloetens Peter, 532
 Coasne Benoit, 102, 221, 249
 Coati Alessandro, 11, 227, 382
 Cobian Manuel, 245
 Cobo Saioa, 395
 Coglitore Diego, 531
 Coilhac Clothilde, 211
 Cojocar Costel-Sorin, 345
 Colao Zanuz Dante, 499
 Colin Claire, 126, 127, 312
 Collet Eric, 103
 Collin Eddy, 272
 Colonna Jean-Philippe, 378
 Combe Nicolas, 78
 Compagno Enrico, 104
 Comtet Jean, 77
 Consonni Vincent, 284
 Constable Evan, 105
 Constant Eric, 120
 Coraux Johann, 15
 Cordier Yvon, 286
 Cornelius Thomas, 106, 275
 Corraze Benoit, 242
 Cottin-Bizonne Cecile, 265
 Couder Yves, 234
 Coupier Gwennou, 107
 Courtade Emmanuel, 108
 Courtois Herve, 128, 147, 190, 303
 Crepet Agnes, 132
 Crepieux Adeline, 285
 Creuze Jérôme, 11
 Crippa Alessandro, 4, 109
 Croguennec Thomas, 59
 Cros Ana, 449
 Cros Vincent, 296
 Cross Benjamin, 110, 446
 Cuello Gabriel, 111, 357
 Cugliandolo Leticia, 112
 Curé Yoann, 267
 Cure Yoann, 486
 Cuvelier Damien, 113
 D'acapito Fransesco, 229
 D'astuto Matteo, 115, 116
 D. Osterkryger Andreas, 169
 Débarre Delphine, 74
 Da Costa Gérald, 310
 Da Silva Barbosa Jéssica Fernanda, 121
 Da Silva Julio, 532
 Dahlem Franck, 241
 Dai Ji, 117
 Daimon Hiroshi, 13
 Dal Pont Stefano, 118
 Dalmas De Reotier Pierre, 122, 123
 Damay Françoise, 88, 312
 Dang Suzanne, 124
 Daniel Lacour, 436
 Dappe Yannick, 320
 Dar S. A., 352
 Darcheville Marie, 125
 Darie Celine, 126, 127
 Darlot Fannie, 500
 Das Pranab, 518
 Dassonneville Remy, 172, 289, 383
 Dau Minh Tuan, 183, 320, 518
 Daudin Bruno, 206, 449
 David Olivier, 236
 David Philippe, 15
 David Sylvain, 214

Davies Heather, 74
 Dawid Alexandre, 149
 De Assis Pierre-Louis, 259
 De Brion Sophie, 105
 De Cecco Alessandro, 128
 De Corato Marco, 235
 De Franceschi Silvano, 4, 109, 256, 287, 499, 533
 De Heer Walter A., 128
 De Leseleuc Sylvain, 129
 De Palo Stefania, 363
 De Riz A., 130
 Dean Cory, 408
 Debray Jérôme, 538
 Decorse Claudia, 105, 258, 338
 Dehnen Stefanie, 263
 Delagrang Raphaëlle, 131
 Delair Thierry, 132
 Delamarre Amaury, 188
 Delande Dominique, 441
 Delaroche Fabien, 310
 Delas Tim, 132
 Delhay Gabriel, 212
 Della Rocca Maria Luisa, 279
 Della Rocca Maria-Luisa, 431
 Delord Tom, 133
 Delplace Pierre, 134
 Demaille Dominique, 227
 Den Hertog Martien, 135, 277
 Deniau-Lejeune Elise, 433
 Deniz Dogukan, 128
 Denoyel Renaud, 375
 Dervaux Julien, 421
 Descamps Marc, 119
 Desplanque Ludovic, 499
 Destaing Olivier, 173
 Destainville Nicolas, 464
 Deudon Catherine, 127
 Deutsch Maxime, 338
 Dhesi Sarnjeet, 250
 Di Dio Mario, 363
 Di Mauro Villari Leone, 413
 Di-Felice Daniela, 320
 Diaz Ana, 532
 Dichiarra Anthony, 323
 Diény Bernard, 313
 Dijon Jean, 519
 Disseix Pierre, 270
 Djekoun Abdelmalik, 136
 Djellouli Adel, 107
 Djeridi Henda, 107
 Dkhil Brahim, 137, 138
 Dobson Phillip, 209
 Doebele Victor, 139, 140, 551
 Dollet Benjamin, 141, 221
 Donatini Fabrice, 449, 486
 Dornsiepen Eike, 263
 Dos S. Azevedoa Frankbelson, 534
 Douliez J-Paul, 142
 Douliez Jean-Paul, 374
 Doumouro Joris, 143
 Dounia Salim, 535
 Draxl Claudia, 83
 Drevillon Jérémie, 218
 Duò Lamberto, 518
 Dubois Emmanuelle, 99
 Ducci Sara, 144
 Duchet Maxime, 120
 Dufouleur Joseph, 278
 Dumur Etienne, 172
 Duong Quynh, 285
 Duperray Alain, 74
 Dupont Maxime, 281
 Dupuis Veronique, 480, 481
 Durand Christophe, 145, 254
 Dutreix C., 146
 Dutta Bivas, 147, 303
 Dutta Sujeet, 347
 Dylan Cattiaux, 536
 Ebbesen Thomas, 298
 Ebels Ursula, 239, 296
 Edlbauer Hermann, 150
 Egger Reinhold, 246
 El Amri Nouha, 74
 El Kacimi Amine, 155
 El Sachat Alexandros, 209
 Elezgaray Juan, 151
 Elias Florence, 421
 Elkaim Eric, 126
 Elouard Cyril, 344
 Engel Edgar, 152
 Epicier Thierry, 69, 245
 Er-Rouissi Yassine, 148
 Escoffier Walter, 380, 422
 Escoubas Stéphanie, 474
 Espel Joël, 149
 Essafi Karim, 243
 Essghaier Chaima, 537
 Estevez-Torres Andre, 153, 200
 Euvé Léo-Paul, 154, 419
 Eymery Joël, 155, 156
 Eymery Joel, 145, 254

Ezzahri Younes, 218
 Ezzouch Rami, 4, 109

 Förtsch Andre, 177
 Fabien Souris, 139
 Fabreges Xavier, 157
 Fabregue Damien, 34
 Faccio Daniele, 309
 Faez Rahim, 302
 Faist Jerome, 286
 Falcon Eric, 41
 Fan Arcara Victor, 160
 Fanni Juranyi, 35
 Faugeras Clement, 161
 Fauqué Benoît, 162
 Fauré Marie-Claude, 404
 Faure Quentin, 158
 Fauve Stephan, 163
 Fava Mauro, 164
 Favier Benjamin, 196
 Fefferman Andrew, 272
 Feinberg Denis, 104, 165, 166
 Fellouh Leila, 474
 Ferdeghini Filippo, 519
 Ferrando Riccardo, 11, 382
 Ferreira Ricardo, 296
 Fève Gwendal, 264
 Feyer V., 320
 Filhol Alain, 316
 Finazzi Marco, 518
 Fischer Henry, 312
 Flahaut Emmanuel, 395
 Flentje Hanno, 348
 Flindt Christian, 331
 Florea Ileana, 167, 345
 Florens Serge, 190, 199, 289
 Flurin Emmanuel, 168
 Foerster Michael, 250
 Fogliano Francesco, 328
 Foldyna Martin, 356
 Fonda Emiliano, 227
 Fons Romain, 169, 267
 Fontaine Alain, 528
 Fontaine Quentin, 201
 Fontana Alex, 170
 Forestier Guillaume, 181
 Foret Marie, 171
 Foroughi Farshad, 172, 289, 383
 Fortuna Franck, 117, 443
 Fossard Frederic, 345
 Fourcade Bertrand, 173
 Fournel Franck, 446

 Fourneret Eric, 174
 Frachet Mehdi, 538, 539
 Fragneto Giovanna, 93
 Francois Rieutord, 35
 Frangou Lamprini, 181
 Franke Katharina J., 190
 Frantzeskakis Emmanouil, 117
 Frauhammer Timo, 436
 Frederic Mila, 280
 Freulon Vincent, 264
 Frick Bernhard, 347
 Fruchart O., 130
 Fu Li, 159
 Fu Yu, 361
 Fuchs Jean-Noël, 175
 Fugallo Giorgia, 488
 Fujii Jun, 518
 Fullerton Eric, 323
 Fusco Claudio, 176

 Géhanne Pierre, 213
 Gérard Jean-Michel, 169, 259, 267, 486
 Gaffuri Pierre, 184, 185
 Gagliardi Luca, 186
 Galand Marina, 187
 Galarneau Anne, 375
 Galas Jean-Christophe, 200
 Gallais Yann, 72
 Gallard Manon, 178, 474
 Gallois-Garreignot Sébastien, 378
 Galvani Benoit, 188
 Gambarelli Serge, 181, 361
 Ganguly Rini, 189
 Gaona-Reyes Jose, 42
 Garbin Valeria, 235
 Garcia Barriocanal Javier, 387
 Garcia Corral Alvaro, 190
 Garcia Leo, 110
 Garcia-Corral Alvaro, 303
 Garcia-Ojalvo Jordi, 244
 Garnier Léo, 191
 Garnier Philippe, 282
 Garreau Yves, 11, 227, 382
 Garro Nuria, 449
 Gaspard Jean-Pierre, 192, 193
 Gassenq Alban, 214
 Gatel Christophe, 194
 Gaudet Jonathan, 258
 Gaudin Gilles, 250, 462
 Gauffre Fabienne, 195
 Gaulin Bruce, 258
 Gautier Brice, 179

Gautier Eric, 169
 Gauzzi Andrea, 264, 515
 Gay Amélie, 196
 Gay Frederic, 495
 Gay Maxime, 320
 Gayral Bruno, 145
 Geim A. K., 352
 Geiselman Johannes, 149
 Genet Cyriaque, 298
 Genot Anthony, 197
 Genovese Luigi, 156
 Gentile Pascal, 214, 277
 Genuist Yann, 267, 335
 Georgiou Rafaella, 198
 Gerard Valentin, 180
 Gheeraert Nicolas, 199
 Ghiringhelli Luca, 83
 Giermanska Joanna, 95
 Gigliotti James, 128
 Gil Bernard, 509
 Gilles Bruno, 114
 Gines Guillaume, 200
 Ginot Félix, 265
 Giordano Valentina, 540
 Girard Armelle, 345
 Giraud Romain, 278
 Gladii Olga, 181
 Glazov Mikhail M., 108
 Glorieux Quentin, 201
 Gloter Alexandre, 202
 Gobaut Benoit, 436
 Godfrin Clément, 203
 Goerbig Mark Oliver, 204
 Goiran Michel, 380
 Goldmann Michel, 404
 Gomès Séverine, 209
 Gomes Sèverine, 3
 Gomez Ana Cristina, 182
 Gonzàles-Herrero H., 146
 Gonzalez Miguel, 384
 Gordillo, Maria Carmen, 360
 Gorni Tommaso, 116
 Gouillart Emmanuelle, 205
 Goujon Céline, 127
 Goujon Celine, 126
 Grandjean Nicolas, 145
 Gravier Sébastien, 34
 Gregersen Niels, 169
 Grosman Annie, 139, 140, 551
 Gruart Marion, 206
 Gruber Manuel, 207
 Guézo Sophie, 212
 Guan Nan, 254
 Gudin Adrian, 2
 Guehenneux Thomas, 208
 Guen Eloïse, 3, 209
 Gueron Sophie, 210
 Guerrero Ruben, 2
 Guichard Wiebke, 289, 383
 Guichet Christophe, 474
 Guillemoles Jean-François, 188
 Guillemot Loïc, 323
 Guillet Thomas, 183, 518
 Guillou Hervé, 211
 Guisset Valérie, 15
 Gulans Andris, 83
 Gusakova D., 130
 Gusev Vitali E., 138
 Hénaff Robin, 447
 Hétet Gabriel, 133
 Haboucha Adil, 310
 Haddad Sonia, 220
 Haddou Marie, 95
 Hadji Celine, 221
 Haffner Thibault, 214
 Halisdemir Ufuk, 436
 Hallal Ali, 222, 457
 Hallegot Philippe, 215
 Hamaoui Georges, 216
 Hamdani Khalida, 217
 Han Zheng, 495
 Hansen Thomas, 116
 Harazi Maxime, 317
 Hasselbach Klaus, 427
 Hautier Geoffroy, 223
 Hayward Rosie, 224
 Hazemann Jean-Louis, 532
 Hebert Clement, 219
 Hekking Frank, 386
 Helmi Seham, 225
 Hemery Gauvin, 433
 Henn Francois, 226
 Hennes Marcel, 227
 Henri Agnès, 552
 Herbert Eric, 228
 Hervé Marie, 436
 Herve Armande, 218
 Hideur Ammar, 310
 Hierro Adrián, 286
 Hinkov Borislav, 286
 Hippert Françoise, 229, 474
 Hirsch Lionel, 230

Hocevar Moira, 48, 335
 Hocevar Moira, 49
 Hofmann Oliver, 83
 Holdsworth Peter, 231
 Holler Mirko, 532
 Homatter Benoit, 519
 Hone James, 408
 Honecker Andreas, 493
 Horisberger Roland, 232
 Horny Nicolas, 216
 Horvatic Mladen, 281
 Hosokawa Shinya, 263
 Houard Jonathan, 310
 Houdellier Florent, 233
 Hrabec Ales, 213
 Hu Yiran, 128
 Hu Yue, 128
 Huang Qiushi, 248
 Hubert Maxime, 234
 Huc Vincent, 345
 Huder Loic, 320, 529
 Huerre Axel, 235, 251
 Hugues Etienne, 236
 Hugues Maxime, 286
 Hungria Teresa, 13
 Hussey Nigel, 72
 Hutin Louis, 4, 109, 256, 287

 Ibrahim Helen, 541
 Idlahcen Said, 310
 Ignacio Maxime, 238
 Inglebert Mehdi, 74
 Isacson Andreas, 469
 Isoard Mathieu, 237
 Iurchuk Vadym, 239

 Jérôme Richard, 211
 Jacobsen Karsten, 83
 Jacopin Gwénolé, 206, 449
 Jacquet Maxime, 266
 Jalabert Thomas, 240
 Jaloustre Lucas, 241
 Jamet Matthieu, 183, 320, 518
 Janod Etienne, 242
 Jansen A, 529
 Jansen Louis, 287
 Jaubert Ludovic, 243
 Je Soong-Geun, 250
 Jean Daillant, 552
 Jedynak Maciej, 244
 Jehl Xavier, 4, 109, 287
 Jenkins Alex, 296

 Jensen Kaare, 141
 Jeudy Vincent, 213
 Jiménez-Ruiz Monica, 357
 Jollivet Arnaud, 286
 Joly Laurent, 159
 Joly Loïc, 436
 Joly-Pottuz Lucile, 245
 Jomard François, 64
 Jonas Alain M., 290
 Jonckheere Thibaut, 246
 Jonnard Philippe, 247, 248
 Jordan Anna, 495
 Jouault Nicolas, 27, 99
 Joulain Karl, 218
 Jouneau Pierre-Henri, 361
 Judeinstein Patrick, 249, 392, 519
 Juge Roméo, 250, 462
 Jugovac M., 320
 Juhin Amélie, 116
 Julien François, 254, 286
 Jullien Marie-Caroline, 251
 Junay Alexandra, 212
 Jussiau Etienne, 252
 Juvé Vincent, 138

 König Jürgen, 147
 Křižáková Viola, 462
 Kandpal Lalit, 436
 Kaoui Badr, 51
 Kapoor Akanksha, 114, 254
 Katcho Nebil A., 253
 Katcko Kostatine, 436
 Katsnelson M. I., 146
 Keerthi A., 352
 Kellay Hamid, 255
 Kerdi Banan, 380, 422
 Kerjuan Adèle, 173
 Kermarrec Edwin, 258, 281, 447
 Kettler Jan, 259
 Khabthani Jouda, 260
 Khasanov Rustem, 258
 Kheng Kuntheak, 261
 Kibalin Iurii, 508
 Kihal Amel, 262
 Kim Yun Ji, 256
 Klee Benjamin, 263
 Klein Holger, 126, 127
 Klein Thierry, 64
 Klein Thorsten, 409
 Klein Yannick, 264, 515
 Klembt Sebastian, 409
 Klongvessa Natsuda, 265

Klotz Stefan, 116
 Knebel Georg, 542
 Knoop Martina, 552
 Kodjikian Stéphanie, 127
 Koenig Friedrich, 266
 Koleski Goce, 257
 Korb Jean-Pierre, 375
 Kotal Saptarshi, 267
 Kotbi Mohammed, 268
 Koteswararao Bommiseti, 447
 Kowalczyk Philippe, 229, 474
 Kramer Roman, 114, 354
 Kremer Geoffroy, 269
 Kreyder Geoffrey, 270
 Krueger Peter, 208
 Krupko Yuriy, 172
 Kshirsagar Aseem Rajan, 271
 Kubala Björn, 147
 Kukreja Roopali, 323
 Kumar Sumit, 272
 Kumigashira Hiroshi, 117
 Kuppusamy Senthil, 436
 Kurkjian Hadrien, 273
 Kuroda Shinji, 60
 Kvashnin Dmitry, 274

 Lömker Patrick, 117
 Lépine Bruno, 212
 Lépine Franck, 120
 Lévy Laurent, 354
 Labat Stephane, 275
 Labau Sébastien, 284
 Labousse Matthieu, 234
 Labracherie Valentin, 278
 Lafarge Philippe, 279, 431
 Laflorencie Nicolas, 280, 281
 Lafuente-Sampietro Alban, 60
 Lahaye Thierry, 129
 Lainé Antoine, 77
 Lallart Adeline, 282
 Lamard Nathalie, 239
 Lançon Frédéric, 156
 Lancry Matthieu, 307
 Lang Sascha, 283
 Langer Juergen, 239
 Lannoo Michel, 188
 Lapertot Gérard, 72, 529
 Larionov Konstantin, 274
 Larré Pierre-Élie, 58
 Lassagne Benjamin, 108
 Launois Pascale, 343
 Lauraux Florian, 275

 Lausecker Clément, 284
 Lavagna Mireille, 285
 Lavie Pascal, 519
 Lazzeri Michele, 451, 488
 Le Biavan Nolwenn, 286
 Le Bolloc'h David, 5
 Le Caer Sophie, 276
 Le Fèvre Patrick, 117
 Le Goff Anne, 51
 Le Guen Karine, 248
 Le Guevel Loïck, 287
 Le Marchand Gilles, 116
 Le Pioufle Bruno, 415
 Le Quang T., 320
 Le Quang Toai, 529
 Le-Denmat Simon, 241
 Lebœuf David, 538, 539
 Lebert Blair, 116
 Lecoeur Philippe, 138, 323, 443
 Lee Mihee, 13
 Lefebvre Denis, 286
 Lefloch François, 499
 Lefmann Kim, 482
 Lefort Ronan, 347
 Lefrançois Emilie, 88, 312
 Legagneux Pierre, 288
 Legendre Murielle, 126, 127
 Leger Sebastien, 172, 289, 383
 Lejay Pascal, 88, 312
 Lejman Mariusz, 138
 Lemaitre Matthieu, 290
 Lemoine Asseline, 11, 382
 Lenz Benjamin, 291
 Leocmach Mathieu, 265
 Leonhardt Ulf, 292
 Leonov Andrei, 338
 Lepetit Marie-Bernadette, 293, 294
 Lepoittevin Christophe, 127
 Levitz Pierre, 375
 Lhotel Elsa, 88, 105, 312
 Liao Lei, 295
 Liao Yuanyuan, 276
 Lienhard Vincent, 129
 Lilette Emmanuel, 19
 Linez Florence, 443
 Lippmaa Mikk, 13
 Litvinenko Artem, 296
 Liu M., 194
 Liu Xiaoqing, 95
 Livet Frédéric, 297
 Locatelli Andrea, 250

Loiseau Annick, 345
 Loiselet Ophelliam, 479, 480
 Lombard Alain, 543
 Lorchat Etienne, 298, 371
 Lorcy Dominique, 242
 Lorenceau Elise, 221, 282, 466
 Lorenzo Jose Emilio, 299
 Louf Jean-François, 141
 Lounis Brahim, 414
 Lubeck Sven, 83
 Lucchesi Christophe, 3
 Ludwig Arne, 150, 348
 Luetkens Hubertus, 447
 Lugstein Alois, 277
 Luisier Mathieu, 300
 Luong Minh Anh, 277
 Lyonnard Sandrine, 520

 Müller Martina, 117
 Méasson Marie-Aude, 72, 368
 Médard François, 270
 Ma Lei, 128
 Ma Tianji, 301
 Maccarini Marco, 306
 Maccherozzi Francesco, 250
 Magrini William, 414
 Mahfoudhi Mohamed, 307
 Maignan Antoine, 308
 Maitland Calum, 309
 Majidi Danial, 302, 303
 Makita Kenji, 60
 Mallet Pierre, 320
 Malomed Boris, 379
 Malpuech Guillaume, 458
 Malyshev Eugene, 97
 Mammez Marie-Hélène, 310
 Manca Marco, 108, 469
 Mancini Lorenzo, 254
 Mandhour Lassaad, 544, 545
 Manghi Manoel, 311, 464
 Mangin-Thro Lucile, 312
 Mansueto Marco, 313
 Mantovani Mattia, 172
 Maréchal Manuel, 249
 Marcenat Christophe, 64
 Marchalot Julien, 251
 Marciani Marco, 314
 Mariano Antonio Lorenzo, 315
 Mariano Lorenzo, 387
 Marie Xavier, 108, 469
 Markov Maksim, 488
 Marmeggi Jean-Claude, 316

 Marmottant Philippe, 107, 141, 317
 Maroutian Thomas, 318, 323, 443
 Marquier François, 470
 Marrache-Kikuchi Claire, 443
 Martin Nicolas, 304, 338
 Martin Simon, 179
 Martin Thierry, 246
 Martinez Eugénie, 214
 Martins Cyril, 291
 Marty Alain, 183, 319, 320, 518
 Marty Laëtitia, 395
 Marty Laetitia, 451
 Masenelli Bruno, 57
 Masenelli-Varlot Karine, 245
 Massoud Antonin, 3
 Massouras Maryam, 321
 Mathieu Christian, 322
 Matzen Sylvia, 138, 323
 Maurand Romain, 4, 109, 499
 Mauri Francesco, 469, 488
 Maurice Jean-Luc, 356
 Mayaffre Hadrien, 281
 Mayaudon Jean Marie, 500
 Mayaudon Jean-Marie, 324
 Mayou Didier, 260, 493
 Mazaleyrat Estelle, 325
 Mcgraw Joshua, 326
 Menezes Roberta, 200
 Meng Bo, 286
 Mentès Tevfik, 250
 Menzel Andreas, 532
 Merabia Samy, 159, 327
 Mercier De Lépinay Laure, 328
 Mercone Silvana, 329
 Merminod Simon, 41
 Meschke Matthias, 147
 Mesples Florie, 141
 Metivet Thibaut, 305, 510
 Metzdorff Rémi, 330
 Meunier Frederic, 69
 Meunier Tristan, 109, 150, 256, 348, 361
 Mhanna Ramona, 347
 Mi Shuo, 331
 Micha Jean-Sébastien, 332
 Michel Claire, 58
 Michelin Sebastien, 333
 Michelini Fabienne, 188
 Micoulaut Matthieu, 334
 Mier González Cristina, 335
 Mihailovic Martine, 270
 Mikolasek Mirko, 336

Mingo Natalio, 337
Minguzzi Anna, 379, 386, 409, 461, 484
Miralles Vincent, 251
Miranda Rodolfo, 2
Mirebeau Isabelle, 338, 381
Misbah Chaouqi, 74
Missaoui Ahmed, 260
Mizokuchi Raisei, 499
Mladek Bianca, 149
Mock-Joubert Maxime, 132
Mocuta Christian, 474
Modica Giuseppe, 339
Mokdad Julia, 340
Molas Maciej, 161
Molho Pierre, 341
Monceau Pierre, 342
Monet Geoffrey, 343
Monroy Eva, 48
Monsel Juliette, 344
Montéléon Pierric, 229
Montenegro-Johnson Thomas, 333
Montes Bajo Miguel, 286
Montes L, 367
Monteverde Miguel, 443
Montiel Xavier, 72
Moorthi Kanagaraj, 368
Moréac Alain, 347
Moreira Da Silva Cora, 345
Morell Nicolas, 469
Moretti Simone, 377
Morfin Isabelle, 384
Morfin, Pascal, 360
Morillo Joseph, 78, 194
Morin Alexandre, 346
Morineau Denis, 347
Mortemousque Pierre-Andre, 348
Mortensen Jens, 83
Morvan Alexis, 349
Mossa Stefano, 350
Motte Jean-François, 446
Mottet Christine, 351, 393
Mousseau Fanny, 45
Moutaux Eve, 97
Mouterde T., 352
Muñoz-Rojas David, 353
Munsch Pascal, 116
Murani Anil, 443
Murapaka Chandrasekhar, 296
Murr Beshara, 17
Myronov Maksym, 499
Nacenta Jorge, 354
Nara Kaori, 200
Naud Cécile, 172
Ngo Eric, 356
Ngono Frédéric, 357
Nguyen Hoai Anh, 486
Nguyen Thuy, 358
Niño Miguel Angel, 2
Nicolas Alexandre, 355
Nicolas Louis, 133
Niguès Antoine, 77
Niquet Yann-Michel, 109, 492
Noël Paul, 181, 319, 361
Noblin Xavier, 359, 440
Noe Pierre, 229, 474
Nogajewski Karol, 161
Nogues Gilles, 335
Noirez Laurence, 249, 347
Noury, Adrien, 360
Nysten Bernard, 290
Ohgoe Takahiro, 511
Ohresser Philippe, 436, 481
Oikonomou Evdokia, 45
Oitmaa Jaan, 243
Ollier Nadège, 307, 424
Ollivier Jacques, 312
Olshanii Maxim, 379
Orignac Edmond, 363
Orlova Anna, 281
Otero Edwige, 436
Othmen Zied, 364
Ott Frédéric, 362
Oukhaled Abdelghani, 365, 369
Ouladdiaf Bachir, 316
Ouldali Hadjer, 366, 369
Overbury Steven, 69
Pépin Catherine, 72
Pacureanu Alexandra, 370, 532
Paduan-Filho Armando, 281
Paillard Charles, 138
Paineau Erwan, 343
Pairis Sébastien, 546
Panayanthatta N, 367
Pappas Catherine, 338
Parette Georges, 381
Parra Lopez Luis Enrique, 371
Patel Sheena, 323
Paterson Jessy, 372
Patriarche Gilles, 373
Pauc Nicolas, 214, 277
Paul Huillery, 133

Paulatto Lorenzo, 264, 488
 Pauliac-Vaujour Emmanuelle, 155
 Paulose P. L., 447
 Paulus Benedict, 263
 Pavloff Nicolas, 237
 Pawbake Amit, 368
 Payen Christophe, 127
 Peña Garcia Jose Antonio, 377
 Pedurand Richard, 170
 Pekola Jukka, 147, 303
 Pelletier Jean-Marc, 34
 Pelta Juan, 369
 Peltonen Joonas, 147, 303
 Perisanu Sorin, 120
 Perna Paolo, 2
 Pernot Julien, 449
 Perrard Stéphane, 234
 Perro Adeline, 374
 Peter Sebastian C., 368
 Petit Dominique, 375
 Petit Sylvain, 105, 258, 312, 376, 519
 Petkovic Aleksandra, 405
 Petrelis Francois, 444
 Peyla Philippe, 177, 510
 Pham Tuong, 319
 Pic Axel, 378
 Picard Cyril, 446
 Picaud Fabien, 40, 547
 Pickard Chris, 152
 Picone Andrea, 518
 Picot Pierre, 276
 Piero Naldesi, 379
 Pierre Mathieu, 380, 422
 Pierre-Louis Olivier, 186
 Pierron-Bohnes Véronique, 381
 Pigeau Benjamin, 328
 Piguet Fabien, 369
 Pilgrim Wolf-Christian, 263
 Pillonnet Gaël, 287
 Piovano Andrea, 468
 Pirart Jérôme, 382
 Piraux Luc, 290
 Piret Gaëlle, 324
 Piret Gaelle, 500
 Pistolesi Fabio, 17
 Pizzini Stefania, 2, 250, 462
 Plaçais Bernard, 264
 Plaçais, Bernard, 360
 Planat Luca, 172, 289, 383
 Planchette Carole, 466
 Plapp Mathis, 238
 Plazanet Marie, 384
 Plochocka Paulina, 385
 Pochet Pascal, 320
 Poggioli A. R., 352
 Pohle Rico, 243
 Poizat Jean-Philippe, 259, 486
 Polian Alain, 116
 Polo Gomez Juan, 379, 386
 Poloni Roberta, 271, 315, 387
 Pons Antonio J., 244
 Porcher Florence, 347
 Potemski Marek, 161
 Pouget Stephanie, 520
 Pourret Alexandre, 548
 Pouzada Daniel, 492
 Povarnitsyn Mikhail, 424
 Prain Angus, 309
 Prejbeanu Ioan, 313
 Prejbeanu Ioan-Lucian, 239
 Prieto Rafael, 378
 Proust Cyril, 388, 538, 539
 Proust Martin, 383
 Prudkovskiy Vladimir, 128
 Pucci Carlotta, 95
 Pucci Giuseppe, 389
 Puertas Javier, 172
 Puertas Martinez Javier, 289, 383
 Pugat Pierre, 390
 Puibasset Joël, 551
 Puibasset Joel, 391–393
 Purcell Stephen, 120
 Putero Magali, 474
 Querré Madec, 242
 Quesnel-Hellmann Anne, 324, 500
 Quilliet Catherine, 107
 Réveret François, 270
 Raba Matthias, 399
 Rabkin Eugen, 275
 Raetz Samuel, 138
 Rafai Salima, 177
 Rahimpour Soleimani Hamid, 302
 Rajkumar Ravishkrishnan, 209
 Ralko Arnaud, 397
 Ramazashvili Revaz, 400
 Ramos Osvanny, 466
 Ramzan Akif, 327
 Ranno Laurent, 462
 Raty Jean Yves, 229
 Ravaine Valérie, 374
 Ravelosona Dafiné, 323

Ravy Sylvain, 394
 Raymond Stephane, 401
 Rea Brice, 395
 Rebiscoul Diane, 35
 Rech Jérôme, 246
 Redon Stephane, 402, 403
 Rego Tomas, 404
 Reichert Benjamin, 251, 405
 Renahy David, 209
 Renard Denis, 54, 396
 Renard V., 146
 Renard Vincent, 320, 529
 Renaud Gilles, 320, 481
 Renault Olivier, 320
 Renucci Pierre, 108
 Renversade Loïc, 332
 Repain Vincent, 406
 Reserbat-Plantey Antoine, 469
 Respaud Marc, 194
 Revenant Christine, 407
 Rhyner Reto, 300
 Ribeiro Palau Rebeca, 408
 Richard Marie-Ingrid, 474
 Richard Maxime, 259, 344, 409
 Richard Vincent, 549
 Richter Ralf, 74
 Ries Lucie, 410
 Ristivojevic Zoran, 405
 Ritter Clemens, 258
 Riveline Daniel, 411
 Robach Odile, 332
 Robert Cedric, 108
 Robert Julien, 88, 105, 312, 397
 Robillard Jean-Francois, 412, 513, 517
 Robin Eric, 214, 277, 449
 Robson Charles, 413
 Roca I Cabarrocas Pere, 356
 Roch Nicolas, 289, 383
 Rochet Antonine, 414
 Rodière Pierre, 399
 Rodrigues Sylvain, 519
 Roedel Tobias, 443
 Rohart Stanislas, 213
 Rojas Sanchez Juan Carlos, 398
 Rojo Romeo Pedro, 57
 Rolley Etienne, 139, 140, 551
 Roman Jean, 415
 Rondelez Yannick, 200
 Rossetto Vincent, 416
 Rossi Riccardo, 511
 Rougemaille Nicolas, 417
 Roupioz Yoann, 418
 Rousseau Lionel, 324, 500
 Rousseau Philippe, 464
 Rousseaux Germain, 419
 Roussel Hervé, 284
 Roussigné Yves, 462
 Rouxel Tanguy, 420
 Rouzière Stephan, 343
 Roveillo Quentin, 421
 Roy Pascal, 105
 Roy Pascale, 276
 Royal Guy, 395
 Rozenberg Marcelo, 242
 Ruben Mario, 436
 Rubi Km, 422
 Rueff Jean-Pascal, 116
 Ruello Pascal, 138
 Rupin Matthieu, 317
 Rupperecht Jean-Francois, 423
 Sabbione Chiara, 229, 474
 Sacépé Benjamin, 495
 Sacuto Alain, 72
 Sahoo Shaon, 285
 Saint-Cricq Maximilien, 426
 Saint-Paul Michel, 427
 Sakai Nariaki, 428
 Saket Omar, 429
 Salançon Evelyne, 430
 Salem Bassem, 214, 277, 284
 Salençon Evelyne, 475
 Salhani Chloé, 431
 Salomé Laurence, 464
 Salomon Damien, 156
 Saminadayar Laurent, 64
 Sanchez-Palencia Laurent, 432
 Sandre Olivier, 132, 433
 Sanquer Marc, 4, 109, 287
 Sant Roberto, 434
 Santander-Syro Andrés, 117, 443
 Santos-Cottin David, 264
 Sarigiannidou Eirini, 284
 Sato Kazuhisa, 479
 Saudou Frederic, 97
 Sauvage Michele, 227
 Saverro-Torres Williams, 319
 Scappucci Giordano, 499
 Schützhold Ralf, 283
 Schatz Christophe, 95, 132
 Scheffler Matthias, 83
 Schemmer Maximilian, 435
 Scheurer Fabrice, 436

Schleicher Filip, 436
 Schmaus Disier, 248
 Schmerber Guy, 436
 Schmit Raphael, 437
 Schott Marine, 462
 Schott Michel, 404
 Schuck Peter, 438
 Schull Guillaume, 371, 439
 Scognamiglio Chiara, 440
 Scoquart Thibault, 441
 Seeger Lopes Rafael, 181
 Seidelin Signe, 442
 Sellier Hermann, 495
 Semina Marina, 108
 Sengupta Shamashis, 443
 Seshadri Saranath, 48
 Seshasayanan Kannabiran, 444
 Sethi Pankaj, 296, 445
 Seuront Laurent, 421
 Shannon Nic, 243
 Sharma Preeti, 446
 Sharma Ramender, 258, 447
 Shcheblanov Nikita, 424
 Sheikin Ilya, 399
 Shpyrko Oleg, 323
 Sibille Romain, 448
 Siladie Alexandra-Madalina, 449
 Silke Hampel, 278
 Simonet Virginie, 88, 105, 312, 450
 Simonneau Michel, 470
 Singh Priyank, 451
 Singh Rajiv, 243
 Singh Vijay, 452–454
 Singhal Dhruv, 455
 Siria A., 352
 Siria Alessandro, 77
 Sistani Masiar, 277
 Sjakste Jelena, 487, 488
 Skvortsov Mikhail, 147
 Slimani Kheireddine, 425
 Slobodeniuk Artur, 161, 456
 Smail Kouidri, 550
 Snyman Izak, 289
 Solal Francine, 212
 Solana Mathias, 64
 Solis Lerma Daniel, 457
 Solnyshkov Dmitry, 270, 458
 Songmuang Rudeesun, 241
 Sorokin Pavel, 274
 Sotomayor Torres Clivia, 209
 Sottmann Jonas, 459
 Souris Fabien, 140, 551
 Sousa Ricardo, 239
 Spagnoli Sylvie, 384, 404
 Spathis Panayotis, 139, 140, 551
 Spies Maria, 460
 Squizzato Davide, 461
 Srivastava Titiksha, 462
 Stéphane Auffret, 250
 Stachkevitch Andreï, 462
 Stauffer Douglas, 245
 Steffens Paul, 482
 Stellhorn Jens, 263
 Stepanov Petr, 169, 409
 Stephan Odile, 479, 480
 Stephan Olivier, 317
 Stoliar Pablo, 242
 Stoof Henk, 295
 Straessle Thierry, 116
 Strange Mikkel, 83
 Strasser Gottfried, 286
 Stroock Abraham, 504
 Studniarek Michal, 436
 Suard Emmanuelle, 126
 Suchet Daniel, 188
 Sugiyama Masakazu, 188
 Sunaga Masahiro, 60
 Swami Rahul, 463
 Szabo Aron, 300
 Tabouillot Victor, 466
 Takada Shintaro, 150
 Taketani Bruno, 437
 Taly Valérie, 200
 Tamarat Philippe, 414
 Tamayo-Arriola Julen, 286
 Tamion Alexandre, 481
 Tang Hao, 194
 Tanguy Anne, 176, 424
 Taniguchi Takashi, 108, 161, 298, 408, 495
 Tardiff Samuel, 520
 Tardin Catherine, 464
 Tarrat Nathalie, 194
 Tchernycheva Maria, 254, 467
 Tejsner Tim, 468, 482
 Tepsic Slaven, 469
 Terras Ferial, 470
 Tettamanti Manuele, 471
 Theodoly Olivier, 251
 Thiaville André, 213, 472
 Thibaut Jérôme, 473
 Thill Antoine, 276
 Thirion C., 130

Tholapi Rajkiran, 474
 Thomas Candice, 361
 Thomas Oliver, 474
 Thomas Olivier, 275
 Thygesen Kristian Sommer, 83
 Tinland Bernard, 475
 Tisserond Emilie, 443
 Tomasello Bruno, 476
 Tonon Xavier, 316
 Torres Theo, 477
 Torresin Olivier, 465
 Tournier Robert, 478
 Tournus Florent, 479–481
 Toussaint J.-C., 130
 Trambly De Laissardière Guy, 260, 493, 529
 Tranchant Julien, 242
 Treussart François, 470
 Tricot Sylvain, 212
 Trimaille Isabelle, 139, 140, 551
 Trombotto Stephane, 132
 Tsvirkun Daria, 74
 Tumanov Dmitrii, 486
 Turban Pascal, 212
 Turberfield Andrew, 225
 Turmaud Jean-Philippe, 128
 Tutueanu Ana Elena, 468, 482

 Udagawa Masafumi, 243
 Udby Linda, 468
 Ulrich Olivier, 332
 Upreti Lavi, 483
 Urbain Etienne, 436
 Urbaszek Bernhard, 108
 Urdampilleta Matias, 4, 109, 348

 Vaheb Yaser, 485
 Vahedi Javad, 493
 Vaillon Rodolphe, 3
 Vaish Nitika, 259, 486
 Valvidares Manuel, 2
 Valvin Pierre, 509
 Van Bokhoven Jeroen, 532
 Van Der Wurff Erik, 295
 Van Houcke Kris, 511
 Van Oosten Dries, 295
 Van Tiggelen Bart, 552
 Van Zanten David, 190
 Vandewalle Nicolas, 234
 Varela Maria, 2
 Varma Akhil, 333
 Vast Nathalie, 487, 488
 Vaudel Gwenaëlle, 138

 Vaxelaire Nicolas, 489
 Veldhorst Menno, 490
 Vella Angela, 310, 491
 Venitucci Benjamin, 492
 Venkateswarlu Somepalli, 493
 Verdier Claude, 74
 Vergara, Jorge, 360
 Vergnaud Céline, 183, 320, 518
 Verheijen Marcel, 49
 Verhille Gautier, 196
 Vernac Laurent, 494
 Verseils Marine, 264
 Vesperini Doriane, 51
 Veuillen Jean-Yves, 320
 Veyrat Louis, 278, 495
 Vialla Fabien, 496, 497
 Viart Nathalie, 498
 Vickridge Ian, 248
 Victorin Nicolas, 484
 Vidal Franck, 227
 Vidal Julien, 175
 Vigneau Florian, 499
 Vignolles David, 264
 Vila Laurent, 181, 239, 296, 319, 361
 Villain-Guillot Simon, 553
 Villard Paul, 500
 Vilquin Bertrand, 57, 501–503
 Vincent Olivier, 504
 Vincent Pascal, 209
 Vinet Maud, 4, 109, 256, 287
 Vinograd Igor, 505
 Vinter Borge, 286
 Vlad Alina, 227
 Vobornik Ivana, 518
 Vodola Davide, 506
 Vogel Jan, 2, 250, 377
 Volkova Halyna, 507
 Volz Sebastian, 485
 Voufack Ariste, 508
 Vuong Phuong, 509

 Würger Alois, 553
 Waintal Xavier, 457
 Wallart Xavier, 499
 Walter Philippe, 248
 Wang Weixi, 356
 Wang Zhanshan, 248
 Warot-Fonrose Bénédicte, 13, 194
 Watanabe Kenji, 108, 161, 298, 408, 495
 Weaver John, 209
 Weber Sebastien, 233
 Weber Wolfgang, 436

Wen Haidan, 323
 Weng Xiaorong, 227
 Weninger Julian, 510
 Werner Félix, 511
 Wernsdorfer Wolfgang, 50
 Whitney Robert, 252
 Wieck Andreas, 150, 348
 Wilhelm Frank, 437
 Willart Jean-François, 119
 Willart Jean-Francois, 357
 Winkelmann Clemens, 147, 190, 303
 Winkelmann Clemens B., 128
 Wolf Pierre-Etienne, 139, 140, 391, 528, 551
 Wrona Jerzy, 239
 Wruss Elisabeth, 83
 Wu Meiyi, 248
 Wu Zili, 69
 Wulfhekel Wulf, 436
 Wyart Matthieu, 512

Yan Zeyin, 508
 Yanagisawa Hirofumi, 514
 Yang Hancheng, 264, 515
 Yang Ming, 422
 Yang Yang, 532
 Ybert Christophe, 265
 Yin Jun, 513
 Yukawa Ryu, 117
 Yvert Blaise, 43, 324, 500

Zadorin Anton, 200
 Zahnd Gilles, 319
 Zamborlini G., 320
 Zamfir Mihai-Robert, 516
 Zamoum Redouane, 285
 Zanolli Jean-Marc, 392, 519
 Zapata Dominguez Diana, 520
 Zatterin Edoardo, 521
 Zazunov Alex, 246
 Zeng Shengwei, 422
 Zenga Cyril, 500
 Zhang Changjian, 408
 Zhang Yuan, 209
 Zheng Yunlin, 227
 Zhou Di, 517
 Zhou Xin, 272
 Zhu Rui, 339
 Zidi Zeineb, 554
 Zimmermann Katrin, 495
 Zimmermann Walter, 177
 Zucchetti Carlo, 183, 518
 Zuo Peng, 126



Les exposants



Heure	Lundi 27 Août	Mardi 28 Août	Mercredi 29 Août	Jeudi 30 Août	Vendredi 31 Août
8:30		Plénière (8:30-9:20) Amphi Weil	Plénière - Prix Ancels Amphi Weil	Plénières (8:30-10:20) Amphi Weil	Mini-Colloques (8:30-10:00) Galerie des Amphis
9:00		H. Kellay Plénière - Prix Holweck (9:20-10:20) Amphi Weil	S. Duccl (8:30-9:30) E. Collet (9:30-10:30)	S. De Franceschi (8:30-9:20) I. Cantat (9:30-10:20)	MIMB3, MMH2, MPS1, MPS2, MPS4, MPS7, PMQ1, PMQ3, PMQ4, PMQ7
9:30		M. Galand Exposants (10:20-10:50) Amphi Weil	Pause café Galerie des Amphis	Pause café Amphi Weil	Pause café (10:00-10:30) Galerie
10:00		Pause café (10:50-11:30) Galerie Amphis	Tables rondes parallèles (11:00-12:30) - Docteurs, Innov & Indus Amphi 9 - Peer review 21 ^e siècle Amphi 10	Table ronde (11:00-12:30) Egalité des Chances Amphi Weil	Mini-Colloques (10:30-12:00) Galerie des Amphis
10:30	(10:30-13:00) Accueil & Inscriptions Galerie des Amphis	Semi-Plénières (11:30-12:20) Galerie des Amphis	Déjeuner (12:30-14:00) Galerie des Amphis ou Restaurant Barnave	Déjeuner (12:30-14:00) Galerie des Amphis ou Restaurant Barnave	Plénière (12:15-13:05) Amphi Weil
11:00		M. O. Goerbig, L. Hirsch, D. Riveline Déjeuner (12:30-14:00)	Semi-Plénières (14:00-14:50) Galerie des Amphis	Semi-Plénières (14:00-14:50) Galerie des Amphis	A. Thivaille Amphi Weil
11:30		Semi-Plénières (14:00-14:50) Galerie des Amphis	Mini-Colloques (15:00-16:30) Galerie des Amphis	Mini-Colloques (15:00-16:30) Galerie des Amphis	CPR4, MMH2, MPS1, MPS2, MPS4, MPS7, PMQ1, PMQ3, PMQ4
12:00		L. Bureau, S. Guéron, V. Simonet Mini-Colloques (15:00-16:30) Galerie des Amphis	Mini-Colloques (15:00-16:30) Galerie des Amphis	Mini-Colloques (15:00-16:30) Galerie des Amphis	Clôture (13:05-13:30) Amphi Weil
12:30		CPR1, MIMB1, MIMB4, MIMB5, MPS3, MPS8, OPS1, PMQ5, PMQ6, PMQ8	CPR3, MCPG1, MIMB2, MMH3, MPS9, MPS10, OPS1, PMQ5, PMQ6, PMQ8	CPR2, MCPG1, MIMB2, MIMB3, MPS1, MPS5, MPS6, OPS2, PMQ2, PMQ7	
13:00		Pause café Galerie des Amphis	Pause café Galerie des Amphis	Pause café Galerie des Amphis	
14:00		Pause café (15:00-16:20) Amphi Weil (ou Galerie Amphis)	Mini-Colloques (17:00-18:30) Galerie des Amphis	Mini-Colloques (17:00-18:30) Galerie des Amphis	
15:00		Plénière (16:20-17:10) Amphi Weil	Mini-Colloques (17:00-18:30) Galerie des Amphis	Mini-Colloques (17:00-18:30) Galerie des Amphis	
16:00		Plénière (14:00-14:50) Amphi Weil	Pause café Galerie des Amphis	Pause café Galerie des Amphis	
16:30		Pause café (15:00-16:20) Amphi Weil (ou Galerie Amphis)	Mini-Colloques (17:00-18:30) Galerie des Amphis	Mini-Colloques (17:00-18:30) Galerie des Amphis	
17:00		Pause café Galerie des Amphis	Mini-Colloques (17:00-18:30) Galerie des Amphis	Mini-Colloques (17:00-18:30) Galerie des Amphis	
17:30		Mini-Colloques (17:00-18:30) Galerie des Amphis	Mini-Colloques (17:00-18:30) Galerie des Amphis	Mini-Colloques (17:00-18:30) Galerie des Amphis	
18:00		Semi-Plénières (17:40-18:30) Galerie des Amphis	CPR3, MCPG1, MIMB2, MIMB5, MIMH3, MPS6, MPS9, MPS10, OPS1, PMQ2, PMQ5, PMQ6, PMQ7, PMQ8	CPR2, CPR4, MIMB3, MMH2, MPS5, MPS6, OPS2, PMQ1, PMQ2, PMQ4, PMQ7	
18:30		B. Audoly, E. Janodi, G. Schull Déplacement vers le musée	Posters & dégustation (18:30-21:00) Galerie des Amphis	Posters & dégustation (18:30-20:30) Galerie des Amphis	
19:00		Cocktail (19:00-20:30) Musée de Grenoble	Banquet (19:00-22:30) Restaurant Le Téléferique	Prix posters (20:30) Amphi 1	